

SOC 7002

MEMORIE

della Società Italiana
di Scienze Naturali
e del Museo Civico
di Storia Naturale di Milano

Volume XXXVII - Fascicolo I

**CRISTIANO DAL SASSO &
SIMONE MAGANUCO**

***SCIPIONYX SAMNITICUS*
(THEROPODA: COMPSOGNATHIDAE)
FROM THE LOWER CRETACEOUS
OF ITALY**

**Osteology, ontogenetic assessment,
phylogeny, soft tissue anatomy,
taphonomy and palaeobiology**

MILANO MAGGIO 2011

MCZ
LIBRARY
AUG 15 2011
HARVARD
UNIVERSITY

pm	premaxilla premaxillare	srsf	sinusoidal ridge of supratemporal fossa cresta sinusoidale della fossa sopratemporale
pm1-5	premaxillary teeth 1-5 denti premaxillari 1-5	ss	sagittal suture sutura sagittale
pmfo	premaxillary foramina forami premaxillari	stfe	supratemporal fenestra fenestra sopratemporale
pmfv	premaxillary process of vomer processo premaxillare del vomere	subn	subnarial process of nasal processo sottonasale del nasale
po	postorbital postorbitale	subpm	subnarial process of premaxilla processo sottonasale del premaxillare
pop	paroccipital process processo paroccipitale	suppm	supranarial process of premaxilla processo sopranasale del premaxillare
popp	postorbital process of parietal processo postorbitale del parietale	tnep	transverse nuchal crest of parietal cresta nucale trasversale del parietale
popsq	postorbital process of squamosal processo postorbitale dello squamoso	trso	transverse ridge of supraoccipital cresta trasversale del supraoccipitale
pppt	posteromedial process of pterygoid processo posteromediale dello pterigoide	v	vomer vomere
ppsq	parietal process of squamosal processo parietale dello squamoso	vcd	entrance of vena capitis dorsalis ingresso della vena dorsale del capo
pqf	paraquadrate foramen forame paraquadrate	vfect	ventral fossa of ectopterygoid fossa ventrale dell'ectopterygoide
pra	prearticular prearticolare	vmaf	ventral margin of adductor fossa margine ventrale della fossa degli adduttori
prf	prefrontal prefrontale	vppal	vomer process of palatine processo vomerale del palatino
prfe	promaxillary fenestra fenestra promaxillare	vppt	vomer process of pterygoid processo vomerale dello pterigoide
pro	prootic prootico	wmfe	osseous wall of maxillary fenestra parete ossea della fenestra mascellare
prs	promaxillary strut puntello promaxillare		Axial skeleton / Scheletro assiale
pt	pterygoid pterigoide	asil	articular surface for ilium superficie articolare per l'ileo
ptaq	pterygoid ala of quadrate ala pterigoidea del quadrato	assr	articular surface for sacral rib superficie articolare per la costola sacrale
ptect	pterygoid process of ectopterygoid processo pterigoide dell'ectopterygoide	ati	atlantal intercentrum intercentro dell'atlante
ptpal	pterygoid process of palatine processo pterigoide del palatino	atn	atlantal neupophys neurapofisi dell'atlante
ptppv	pterygopalatine process of vomer processo pterigo-palatino del vomere	axi	axial intercentrum intercentro dell'epistrofeo
q	quadrate quadrato	axns	axial neural spine spina neurale dell'epistrofeo
qapt	quadrate ala of pterygoid ala quadratica dello pterigoide	C	cervical vertebra vertebra cervicale
qcsq	quadrate cotyle of squamosal cotilo quadratico dello squamoso	Ca	caudal vertebra vertebra caudale
qh	quadrate head testa del quadrato	caaf	caudal articular facet faccetta articolare caudale
qj	quadratojugal quadratojugale	cac	caudal centrum centro caudale
qjqc	quadratojugal contact of quadrate contatto quadratojugale del quadrato	cana	caudal neural arch arco neurale caudale
qjpsq	quadratojugal process of squamosal processo quadratojugale dello squamoso	cap	capitulum capitello
rarp	retroarticular process processo retroarticolare	cc	cervical centrum centro cervicale
rrm	rostral ramus of maxilla ramo rostrale del mascellare	cg	costal groove solco costale
sa	surangular soprangolare	clp	craniolateral process processo craniolaterale
sbtfe	subtemporal fenestra fenestra sottotemporale	cons	concavity of the neural spine concavità della spina neurale
scl	scleral plates placche della sclera	Cr	cervical rib costola cervicale
snf	subnarial foramen forame sottonasale	craf	cranial articular facet faccetta articolare craniale
so	supraoccipital sopraoccipitale	crpr	cranial process processo craniale
sofe	suborbital fenestra fenestra sottorbitale	csga	cranial chevron-shaped gastralium gastralium craniale a forma di V
sp	splenic spleniale	ctw	capitulotubercular web membrana capitello-tubercolare
spfe	subsidiary palatal fenestra fenestra palatale sussidiaria	D	dorsal vertebra vertebra dorsale
sq	squamosal squamoso	dc	dorsal centrum centro dorsale

Elenco delle Memorie della Società Italiana di Scienze Naturali e del Museo Civico di Storia Naturale di Milano

Volume I

- I - CORNALIA E., 1865 - Descrizione di una nuova specie del genere *Felis*: *Felis jacobita* (Cern.). 9 pp., 1 tav.
 II - MAGNI-GRIFFI F., 1865 - Di una specie d'*Hippolais* nuova per l'Italia. 6 pp., 1 tav.
 III - GASTALDI B., 1865 - Sulla rievacuazione dei bacini lacustri per opera degli antichi ghiacciai. 30 pp., 2 figg., 2 tavv.
 IV - SEGUENZA G., 1865 - Paleontologia malacologica dei terreni terziarii del distretto di Messina. 88 pp., 8 tavv.
 V - GIBELLI G., 1865 - Sugli organi riproduttori del genere *Verrucaria*. 16 pp., 1 tav.
 VI - BEGGIATO F. S., 1865 - Antracotero di Zovencedo e di Monteviale nel Vicentino. 10 pp., 1 tav.
 VII - COCCHI I., 1865 - Di alcuni resti umani e degli oggetti di umana industria dei tempi preistorici raccolti in Toscana. 32 pp., 4 tavv.
 VIII - TARGIONI-TOZZETTI A., 1866 - Come sia fatto l'organo che fa lume nella lucciola volante dell'Italia centrale (*Luciola italica*) e come le fibre muscolari in questo ed altri Insetti ed Artropodi. 28 pp., 2 tavv.
 IX - MAGGI L., 1865 - Intorno al genere *Aeolosoma*. 18 pp., 2 tavv.
 X - CORNALIA E., 1865 - Sopra i caratteri microscopici offerti dalle Cantaridi e da altri Coleotteri facili a confondersi con esse. 40 pp., 4 tavv.

Volume II

- I - ISSELLA A., 1866 - Dei Molluschi raccolti nella provincia di Pisa. 38 pp.
 II - GENTILLI A., 1866 - Quelques considérations sur l'origine des bassins lacustres, à propos des sondages du Lac de Come. 12 pp., 8 tavv.
 III - MOLON F., 1867 - Sulla flora terziaria delle Prealpi venete. 140 pp.
 IV - D'ACHIARDI A., 1866 - Corallari fossili del terreno nummulitico delle Alpi venete. 54 pp., 5 tavv.
 V - COCCHI I., 1866 - Sulla geologia dell'alta Valle di Magra. 18 pp., 1 tav.
 VI - SEGUENZA G., 1866 - Sulle importanti relazioni paleontologiche di talune rocce cretacee della Calabria con alcuni terreni di Sicilia e dell'Africa settentrionale. 18 pp., 1 tav.
 VII - COCCHI I., 1866 - L'uomo fossile nell'Italia centrale. 82 pp., 21 figg., 4 tavv.
 VIII - GAROVAGLIO S., 1866 - *Manzonina cantiana, novum Lichenum Angiocarporum generis propositum atque descriptum*. 8 pp., 1 tav.
 IX - SEGUENZA G., 1867 - Paleontologia malacologica dei terreni terziarii del distretto di Messina (Pteropodi ed Eteropodi). 22 pp., 1 tav.
 X - DÜRER B., 1867 - Osservazioni meteorologiche fatte alla Villa Carlotta sul lago di Como, ecc. 48 pp., 11 tavv.

Volume III

- I - EMERY C., 1873 - Studi anatomici sulla *Vipera Redii*. 16 pp., 1 tav.
 II - GAROVAGLIO S., 1867 - *Thelopsis, Belonia, Weittenwebera et Limboria, quatuor Lichenum Angiocarporum genera recognita iconibusque illustrata*. 12 pp., 2 tavv.
 III - TARGIONI-TOZZETTI A., 1867 - Studi sulle Cocciniglie. 88 pp., 7 tavv.
 IV - CLAPAREDE E. R. e PANCERI P., 1867 - Nota sopra un Alciopide parassito della *Cydippe densa* Forsk. 8 pp., 1 tav.
 V - GAROVAGLIO S., 1871 - *De Pertusartis Europae mediae commentatio*. 40 pp., 4 tavv.

Volume IV

- I - D'ACHIARDI A., 1868 - Corallari fossili del terreno nummulitico dell'Alpi venete. Parte II. 32 pp., 8 tavv.
 II - GAROVAGLIO S., 1868 - *Octona Lichenum genera vel adhuc controversa, vel sedis prorsus incertae in systemate, novis descriptionibus iconibusque accuratissimis illustrata*. 18 pp., 2 tavv.
 III - MARINONI C., 1868 - Le abitazioni lacustri e gli avanzi di umana industria in Lombardia. 66 pp., 5 figg., 7 tavv.
 IV - (Non pubblicato).
 V - MARINONI C., 1871 - Nuovi avanzi preistorici in Lombardia. 28 pp., 3 figg., 2 tavv.

NUOVA SERIE

Volume V

- I - MARTEORELLI G., 1895 - Monografia illustrata degli uccelli di rapina in Italia. 216 pp., 46 figg., 4 tavv.

Volume VI

- I - DE ALESSANDRI G., 1897 - La pietra da cantoni di Rosignano e di Vignale. Studi stratigrafici e paleontologici. 104 pp., 2 tavv., 1 carta.
 II - MARTEORELLI G., 1898 - Le forme e le simmetrie delle macchie nel piumaggio. Memoria ornitologica. 112 pp., 63 figg., 1 tav.
 III - PAVESI P., 1901 - L'abbate Spallanzani a Pavia. 68 pp., 14 figg., 1 tav.

Volume VII

- I - DE ALESSANDRI G., 1910 - Studi sui pesci triasici della Lombardia. 164 pp., 9 tavv.

Volume VIII

- I - REPOSSI E., 1915 - La bassa Valle della Mera. Studi petrografici e geologici. Parte I. pp. 1-46, 5 figg., 3 tavv.
 II - REPOSSI E., 1916 (1917) - La bassa Valle della Mera. Studi petrografici e geologici. Parte II. pp. 47-186, 5 figg., 9 tavv.

- III - AIRAGHI C., 1917 - Sui molari d'elefante delle alluvioni lombarde, con osservazioni sulla filogenia e scomparsa di alcuni Proboscidiati. pp. 187-242, 4 figg., 3 tavv.

Volume IX

- I - BEZZI M., 1918 - Studi sulla ditterofauna nivale delle Alpi italiane. pp. 1-164, 7 figg., 2 tavv.
 II - SERA G. L., 1920 - Sui rapporti della conformazione della base del cranio colle forme craniensi e colle strutture della faccia nelle razze umane. (Saggio di una nuova dottrina cranioologica con particolare riguardo dei principali crani fossili). pp. 165-262, 7 figg., 2 tavv.
 III - DE BEAUX O. e FESTA E., 1927 - La ricomparsa del Cinghiale nell'Italia settentrionale-occidentale. pp. 263-320, 13 figg., 7 tavv.

Volume X

- I - DESIO A., 1929 - Studi geologici sulla regione dell'Albena (Prealpi Bergamasche). pp. 1-156, 27 figg., 1 tav., 1 carta.
 II - SCORTECCI G., 1937 - Gli organi di senso della pelle degli Agamidi. pp. 157-208, 39 figg., 2 tavv.
 III - SCORTECCI G., 1941 - I rettori degli Agamidi. pp. 209-326, 80 figg.

Volume XI

- I - GUIGLIA D., 1944 - Gli Specidi italiani del Museo di Milano (*Hymen*). pp. 1-44, 4 figg., 5 tavv.
 II-III - GIACOMINI V. e PIGNATTI S., 1955 - Flora e Vegetazione dell'Alta Valle del Braulio. Con speciale riferimento ai pascoli di altitudine. pp. 45-238, 31 figg., 1 carta.

Volume XII

- I - VIALI V., 1956 - Sul rinoceronte e l'elefante dei livelli superiori della serie lacustre di Leffe (Bergamo). pp. 1-70, 4 figg., 6 tavv.
 I - VENZO S., 1957 - Rilevamento geologico dell'anfiteatro morenico del Garda. Parte I: Tratto occidentale Gardone-Desenzano. pp. 71-140, 14 figg., 6 tavv., 1 carta.
 III - VIALI V., 1959 - Ammoniti sinemuriane del Monte Albena (Bergamo). pp. 141-188, 2 figg., 3 tavv.

Volume XIII

- I - VENZO S., 1961 - Rilevamento geologico dell'anfiteatro morenico del Garda. Parte II. Tratto orientale Garda-Adige e anfiteatro atesino di Rivoli veronese. pp. 1-64, 25 figg., 9 tavv., 1 carta.
 II - PINNA G., 1963 - Ammoniti del Lias superiore (Toarciano) dell'Alpe Turati (Erba, Como). Generi *Mercaticeras*, *Pseudomercaticeras* e *Brodiaea*. pp. 65-98, 2 figg., 4 tavv.
 III - ZANZUCCHI G., 1963 - Le Ammoniti del Lias superiore (Toarciano) di Entratico in Val Cavallina (Bergamasco orientale). pp. 99-146, 2 figg., 8 tavv.

Volume XIV

- I - VENZO S., 1965 - Rilevamento geologico dell'anfiteatro morenico frontale del Garda dal Chiese all'Adige. pp. 1-82, 11 figg., 4 tavv., 1 carta.
 II - PINNA G., 1966 - Ammoniti del Lias superiore (Toarciano) dell'Alpe Turati (Erba, Como). Famiglia *Dactyloceratidae*. pp. 83-136, 4 tavv.
 III - DIENI L., MASSARI F. e MONTANARI L., 1966 - Il Paleogene dei dintorni di Orsei (Sardagna). pp. 13-184, 5 figg., 8 tavv.

Volume XV

- I - CARETTO P. G., 1966 - Nuova classificazione di alcuni Briozoi pliocenici, precedentemente determinati quali Idrozoi del genere *Hydractinia* Van Beneden. pp. 1-88, 27 figg., 9 tavv.
 II - DIENI L. e MASSARI F., 1966 - Il Neogene e il Quaternario dei dintorni di Orsei (Sardagna). pp. 89-142, 8 figg., 7 tavv.
 III - BARBIERI F., IACCARINO S., BARBIERI F. e PETRUCCI F., 1967 - Il Pliocene del Subappennino Piacentino-Parmense-Reggiano. pp. 143-188, 20 figg., 3 tavv.

Volume XVI

- I - CARETTO P. G., 1967 - Studio morfologico con l'ausilio del metodo statistico e nuova classificazione dei Gasteropodi pliocenici attribuibili al *Murex brandaris* Linneo. pp. 1-60, 1 fig., 7 tabb., 10 tavv.
 II - SACCHI VIALI G. e CANTALUPPI G., 1967 - I nuovi fossili di Gozzano (Prealpi piemontesi). pp. 61-128, 30 figg., 8 tavv.
 III - PIGORINI B., 1967 - Aspetti sedimentologici del Mare Adriatico. pp. 129-200, 13 figg., 4 tabb., 7 tavv.

Volume XVII

- I - PINNA G., 1968 - Ammoniti del Lias superiore (Toarciano) dell'Alpe Turati (Erba, Como). Famiglie *Lytoceratidae*, *Nannolytoceratidae*, *Hammatoceratidae* (excl. *Phymatoceratidae*) *Hildoceratidae* (excl. *Hildoceratinae* e *Bouleiceratinae*). pp. 1-70, 2 tavv. n.t., 6 figg., 6 tavv.
 II - VENZO S. e PELOSIO G., 1968 - Nuova fauna di Ammonoidi dell'Anisico superiore di Lenna in Val Brembana (Bergamo). pp. 71-142, 5 figg., 11 tavv.
 III - PELOSIO G., 1968 - Ammoniti del Lias superiore (Toarciano) dell'Alpe Turati (Erba, Como). Generi *Hildoceras*, *Phymatoceras*, *Paroniceras* e *Frechiella*. Conclusioni generali. pp. 143-204, 2 figg., 6 tavv.

Volume XVIII

- I - PINNA G., 1969 - Revisione delle ammoniti figurate da Giuseppe Meneghini nelle Tavv. 1-22 della «*Monographie des fossiles du calcaire rouge ammonitique*» (1867-1881). pp. 5-22, 2 figg., 6 tavv.

Cristiano Dal Sasso & Simone Maganuco

***Scipionyx samniticus* (Theropoda: Compsognathidae)
from the Lower Cretaceous of Italy**

Osteology, ontogenetic assessment, phylogeny,
soft tissue anatomy, taphonomy and palaeobiology

MCZ
LIBRARY
AUG 15 2011
HARVARD
UNIVERSITY

Volume XXXVII - Fascicolo I

Maggio 2011

CREDITI DELLE ILLUSTRAZIONI

La maggior parte delle immagini pubblicate in questa monografia è tutelata da diritti d'autore pertinenti ai fotografi, disegnatori e artisti che le hanno realizzate, e/o alle istituzioni cui appartengono i soggetti illustrati. Tali immagini, pertanto, non possono essere utilizzate a fini commerciali senza previo permesso scritto dei titolari dei diritti d'autore.

Date le limitazioni di spazio imposte dalle didascalie bilingui, i nomi degli autori delle foto e dei disegni sono qui elencati in ordine alfabetico, seguiti dai numeri delle figure; i nomi degli autori delle ricostruzioni artistiche sono elencati separatamente, preceduti dai numeri delle pagine.

Roberto Appiani, © Soprintendenza per i Beni Archeologici di Salerno, Avellino, Benevento e Caserta: 9, 19B, 23, 28A, 31A, 35A, 40A, 43A, 49, 55, 87, 97, 103, 116, 125, 126, 127, 128, 129B, 136B, 137, 145, 146B, 159, 164A.

Roberto Appiani & Leonardo Vitola, © Soprintendenza per i Beni Archeologici di Salerno, Avellino, Benevento e Caserta: 10, 21, 115, 156.

Marco Auditore, © Museo di Storia Naturale di Milano: 5, 8A, 10, 22, 24, 25A, 25B, 26, 29, 33, 36B, 37, 38, 41, 50, 53, 56, 60, 62, 64, 67, 68, 73, 76, 81, 88, 98, 109, 111, 112, 114, 117, 173, 174, 175, 176, 178A, 182, 186.

Armando Cioffi, © Soprintendenza per i Beni Archeologici di Salerno, Avellino, Benevento e Caserta / Fondazione Ospedale Maggiore di Milano: 32, 92, 101, 148.

Cristiano Dal Sasso: 2, 7B, 20.

Cristiano Dal Sasso, © Soprintendenza per i Beni Archeologici di Salerno, Avellino, Benevento e Caserta / Museo di Paleontologia dell'Università di Napoli "Federico II": 15.

Cristiano Dal Sasso & Simone Maganuco: 34.

Cristiano Dal Sasso & Simone Maganuco, © Soprintendenza per i Beni Archeologici di Salerno, Avellino, Benevento e Caserta: 8B, 8D, 8F, 8G, 11, 27, 28B, 30, 31B, 31C, 35B, 36A, 39, 40B, 42, 43B, 45, 46, 48, 51, 52, 54, 57, 58, 59, 61, 65, 69, 70, 72, 74, 75, 77, 78, 79, 82, 83, 84, 86, 89, 90, 93, 95, 96, 99, 100, 102B, 104, 105, 106, 107, 108, 122, 123, 124, 130, 131, 133, 134, 135, 136A, 138A, 138B, 140, 142, 147, 150A, 152, 154, 155, 158, 160, 162, 163, 164B, 166, 167, 168, 172, 177, 178B, 179, 180, 184.

ILLUSTRATION CREDITS

Most images used in this publication are copyrighted by the authors of the photographs, drawings, or artworks, and/or by the institutions which the illustrated subjects belong to. Therefore, they may not be used for commercial purposes without prior written permission of the copyright holders.

Due to space limitations for the bilingual figure captions, the names of the authors of photographs and drawings are listed in alphabetical order, followed by the figure numbers; the names of the authors of the artworks are listed separately, preceded by the page numbers.

Fritz Huchzermeyer: 110.

Simone Maganuco: 85, 113.

W. Scott Persons, IV: 160C.

Stefano Scali: 1.

Giorgio Teruzzi: 6, 18, 19A, 150B, 151, 183.

Leonardo Vitola, © Soprintendenza per i Beni Archeologici di Salerno, Avellino, Benevento e Caserta: 8C, 8E, 8H, 12, 14B, 44, 47, 63, 66, 71, 80, 91, 94, 102A, 129A, 138C, 141, 146A, 153, 161, 165, 185A.

Leonardo Vitola, © Soprintendenza per i Beni Archeologici di Salerno, Avellino, Benevento e Caserta / Museo di Paleontologia dell'Università di Napoli "Federico II": 14 A, 14C, 14D.

Michele Zilioli, © Soprintendenza per i Beni Archeologici di Salerno, Avellino, Benevento e Caserta / Museo di Storia Naturale di Milano: 13, 118, 119, 120, 121, 132, 139, 143, 144, 149, 157, 169, 170, 171, 181, 185B, 185C.

269: © Marco Auditore & Arianna Nicora

270: © Davide Bonadonna

271: © Paolo Cinquemani

272: © Fabio Pastori

273: © Renzo Zanetti

274: © Loana Riboli

275: © Fabio Fogliazza

276: © Lukas Panzarin

277: © Tullio Perentin

278: © Troco

© 2011 Società Italiana di Scienze Naturali
Museo Civico di Storia Naturale di Milano
Corso Venezia, 55 - 20121 Milano

In copertina: *Scipionyx samniticus* in grandezza naturale, nella porzione di Plattenkalk autentico.
Life-size *Scipionyx samniticus*, and the authentic portion of Plattenkalk embedding it.

Registrato al Tribunale di Milano al n. 6694
Direttore responsabile : Anna Alessandrello
Grafica editoriale: Michela Mura

Stampa: Litografia Solari, Peschiera Borromeo - Maggio 2011

ISSN 0376-2726

*Quando lanatura viene alla generatiō delle/pietre essa genera una qualita
domore viscioso/il quale col suo secharsi congele inse co chedē/tro allui
sirinchiude enōli converte inpietra/ma li cōserua dentro asse nella forma
che elli ha trovati...*

Leonardo da Vinci

Quando la natura crea le pietre genera una specie di umore vischioso che
asciugandosi congela ciò che racchiude in se stesso e non trasforma tutto in pietre
ma conserva ciò che racchiude nella forma trovata...

When nature creates stones she generates a type of viscous humour that upon
drying freezes within it whatever is found, not transforming those things into
stone but conserving them in the form with which they were found....

Cristiano Dal Sasso & Simone Maganuco

Scipionyx samniticus (Theropoda: Compsognathidae)

from the Lower Cretaceous of Italy

Osteology, ontogenetic assessment, phylogeny, soft tissue anatomy, taphonomy and palaeobiology

Abstract – This monograph provides a detailed account of the remarkably preserved holotype of the theropod dinosaur *Scipionyx samniticus* uncovered in the Lower Cretaceous (Albian) of Pietraroja, southern Italy. We describe the geological setting of the only known specimen and give a short description of the lithology and stratigraphy of this famous, fossil-rich locality. Macroscopic and microscopic observations, as well as chemical analysis of the sediment embedding the fossil, has allowed better estimation of its position within the stratigraphic series of the outcrop. An overview of the depositional environments hypothesised by previous authors for the Pietraroja fossils is presented, although the taphonomical study of *Scipionyx* suggests that this specimen was buried in a single, rapid event by a turbidite. We also include palaeoenvironmental and palaeogeographic data commented in the light of the Cretaceous dinosaur record of the Periadriatic region, focusing in particular on the central and southern Italian tracksites and their palaeobiogeographical significance.

Part I is dedicated to the osteology of the specimen. The major cranial novelties described include the identification of formerly unrecognised braincase bones, and reinterpretation of palatal and mandibular elements, which lead to better understanding of their topology. Other relevant cranial features of the specimen are 5 premaxillary teeth, a sinusoidal ridge of the supratemporal fossa with frontoparietal contact, a distally squared descending process of the squamosal, lower tooth row extending farther back than the upper row, and the absence of an external mandibular fenestra. Among the relevant postcranial skeletal features described are fan-shaped dorsal neural spines with beak-like ligament attachments, hair-like cervical ribs, dorsal ribs with cup-like sternal attachments, gastralia with peculiar morphology and pathology, carpus composed of only two stacked, well-ossified bones, manual digit III longer than digit I, a cranially notched iliac preacetabular blade and a distally squared ischial obturator process.

We then expound on the immaturity of the specimen – which was probably less than three weeks old at the time of death – as suggested by a long list of juvenile characters, such as the presence of a frontoparietal fontanelle, a short and deep antorbital region, tooth replacement not yet started, peculiar scarred bone surfaces, non-sutured girdle elements and closure of the neurocentral sutures not yet started in any vertebra. At the end of this part, we give a phylogenetic analysis of Coelurosauria (90 taxa, 360 characters), evaluating also the ontogeny-related characters that identify *Scipionyx* as a basal member of a monophyletic Compsognathidae, which results to be more derived than Tyrannosauroidae.

Part II is on the superbly preserved internal organs and soft tissues of *Scipionyx samniticus*. The preserved internal tissues include axial ligaments, axial and appendicular articular cartilage, neck muscles and connective tissue, part of the trachea, oesophageal remains, traces of the liver and other blood-rich organs, the entire intestine, mesenteric blood vessels and pelvic and hindlimb muscles. External soft tissues are beautifully represented by the horny manual claws. Most of the soft tissues can be easily identified by their ochre colour, whereas other organic remains are preserved as thin films that are visible under ultraviolet-induced fluorescence (UV). Scanning electron microscopy (SEM) analyses have revealed an exceptional three-dimensional preservation of the soft tissues and astonishing information at a cellular and even subcellular level, such as the sarcomere-related banded pattern observable within every single muscular myofibre. SEM element microanalysis has also confirmed the haematic origin of the reddish macula formerly referred to the liver. On the other hand, it has been established that the remains or imprints purported by some authors to be of the diaphragmatic muscles are, in fact, a calcite nodule of amorphous microstructure, inconsistent with the preservation of other muscle tissue in this specimen. This evidence, and other anatomical observations on bones and soft tissues, deny the hypothesis of an hepatic-piston assisted breathing mechanism in *Scipionyx*. The exceptional preservation of labile soft tissue indicates that, after death, the carcass of this theropod hatchling was subjected to very little decay and rapid authigenic mineralisation in the presence of a high concentration of phosphates. We examine this process in the taphonomy section of this monograph.

Part III focuses on the functional morphology and the palaeobiology of *Scipionyx samniticus*. Outstandingly, the degree of preservation of the soft tissues has permitted an analysis of the relative position of the food remains in the digestive apparatus and, thus, reconstruction of a feeding chronology for this specimen, an insight that is usually impossible to obtain for fossil vertebrates. In fact, *Scipionyx*'s gut has been found to contain alloigenous bones from a lepidosaurian reptile in the stomach region, lizard-like polygonal squamae in the duodenum, fish scales in the rectum, and a variety of tiny remains in several points of the intestine. This is compelling evidence that *Scipionyx* fed on both lizards and fish. Finally, remarks on the digestive physiology and respiratory physiology of *Scipionyx*, inferred from the internal organs and their osteological correlates, close the monograph.

The amount and detail of information gained from this single specimen make the Pietraroja Plattenkalk a unique fossil locality. In contrast to the Chinese Jehol Group, which is a lacustrine/volcanic freshwater deposit that has preserved dinosaurs with delicate integumentary structures, such as filaments, feathers and bristles, the Italian shallow marine Lagerstätte has preserved internal organs. This is unprecedented not only for a dinosaur, but also for any other Mesozoic terrestrial vertebrate.

Key words: Theropoda, Compsognathidae, soft tissue preservation, Lower Cretaceous, Pietraroja Plattenkalk, Italy.

Riassunto – Questa memoria monografica descrive in dettaglio il dinosauro teropode *Scipionyx samniticus*, proveniente dal Cretaceo inferiore (Albiano) di Pietraroja (Benevento). L'inquadramento geologico dell'olotipo, che è straordinariamente ben conservato allo stato fossile e rappresenta tuttora l'unico esemplare conosciuto di questa specie, è qui richiamato con una breve trattazione della litologia e della stratigrafia della celebre località fossilifera. Lo studio del sedimento in cui giace il fossile, condotto a livello macroscopico e microscopico e comprendente anche l'analisi della sua composizione chimica, ha permesso di identificare con buona appros-

simazione la posizione dell'esemplare all'interno della serie stratigrafica del giacimento. Sebbene lo studio tafonomico di *Scipionyx* suggerisca che questo esemplare sia stato sepolto da una torbide in un singolo e rapido evento, viene presentata una panoramica dei possibili ambienti di deposizione ipotizzati da altri autori per i fossili di Pietraraja. Vengono qui portati anche dati paleoambientali e paleogeografici, commentati alla luce della documentazione fossile riguardante i dinosauri nel Cretaceo della regione periadriatica, con particolare attenzione ai giacimenti di impronte dell'Italia centro-meridionale, e alla loro importanza paleobiogeografica.

L'intera osteologia dell'esemplare viene qui revisionata e descritta osso per osso (Parte I). Nel cranio, le più importanti novità consistono nell'identificazione di un maggior numero di ossa della scatola cranica; gli elementi del palato e della mandibola sono stati reinterpretati e la loro topologia è ora più chiara. Le caratteristiche più importanti del cranio sono: 5 denti premaxillari, una cresta sinusoidale presente sul margine della fossa sopratemporale a livello del contatto frontoparietale, un processo discendente dello squamoso che termina con una estremità squadrata, la fila dei denti inferiori che si estende in direzione caudale più della fila dei denti superiori, l'assenza della finestra mandibolare esterna. Rilevanti caratteri scheletrici postcraniali sono: le spine neurali delle vertebre dorsali espanse a forma di ventaglio e con attacchi dei legamenti a forma di becco, le costole cervicali filiformi, gli attacchi delle costole sternali, la morfologia dei gastralia e la condizione patologica di alcuni di essi, il carpo composto soltanto da due ossa ben ossificate e impilate una sull'altra, il terzo dito della mano più lungo del primo, la lama preacetabolare dell'ileo che porta una incisura craniale, il processo otturatore dell'ischio squadrato in direzione distale.

L'imaturità dell'esemplare, che al momento della morte aveva probabilmente meno di tre settimane, è confermata da una lunga lista di caratteri giovanili, come la presenza della fontanella frontoparietale, la regione antorbitale corta, la sostituzione dei denti non ancora iniziata, la particolare tessitura solcata delle ossa, gli elementi dei cinti non suturati e la chiusura della sutura neurocentrale non ancora iniziata in alcuna vertebra.

L'analisi filogenetica dei Coelurosauria (360 caratteri analizzati in 90 taxa), in cui si è tenuto conto anche dei caratteri legati all'ontogenesi, pone *Scipionyx* come membro basale dei Compsognathidae, che risultano un clade monofiletico e più derivato dei Tyrannosauroidae.

Una sezione specifica di questa memoria (Parte II) è riservata alla descrizione degli organi interni e di diversi altri tessuti molli, che nell'olotipo di *Scipionyx samniticus* sono conservati in modo incomparabile. Tra i tessuti interni che sono fossilizzati vi sono legamenti intervertebrali, cartilagini articolari dello scheletro assiale e appendicolare, muscoli e connettivi del collo, parte della trachea, residui dell'esofago, tracce del fegato e di altri organi ricchi di sangue, l'intero intestino, vasi sanguigni mesenterici, muscoli del cinto pelvico, degli arti posteriori e della coda. I tessuti esterni sono superbamente rappresentati dagli artigli cornei, ancora presenti sulle ultime falangi delle dita delle mani. In gran parte i tessuti molli conservati nell'olotipo di *Scipionyx samniticus* sono visibili ad occhio nudo, grazie al colore ocra che ben li distingue dal bruno scuro delle ossa. Altri resti organici sono conservati sotto forma di sottili pellicole, che possono essere viste solo in fluorescenza indotta da luce ultravioletta (UV). Con esami dettagliati al microscopio elettronico a scansione (SEM), il nostro studio dimostra che in questo fossile risalente a 110 milioni di anni fa i tessuti molli non sono semplici impronte, ma sono mineralizzati in tre dimensioni, con una fedeltà di conservazione eccezionale, che raggiunge livelli cellulari e talvolta subcellulari (per esempio, all'interno di ogni singola miofibrilla muscolare è conservata la struttura a bande dei sarcomeri). La microanalisi degli elementi al SEM ha confermato l'origine ematica della macchia rossastra precedentemente attribuita al fegato. Per contro, i residui o impronte di muscoli diaframmatici presunti da alcuni autori in realtà appartengono ad un nodulo di calcite, che a livello microscopico mostra una struttura amorfa, non compatibile con la conservazione degli altri tessuti muscolari di *Scipionyx*. Questa evidenza, unita ad altre osservazioni anatomiche sulle ossa e sui tessuti molli, smentisce l'ipotesi di una meccanica respiratoria assistita da pistone epatico (una soluzione fisiologica che caratterizza i coccodrilli odierni).

La conservazione eccezionale di tessuti molli molto delicati indica che, dopo la morte, la carcassa del teropode neonato subì una decomposizione molto limitata e una rapida mineralizzazione autigena, in presenza di una alta concentrazione di fosfati. Questo processo è esaminato in una sezione dedicata alla tafonomia dell'esemplare.

Questa monografia indaga anche sulla morfologia funzionale e sulla paleobiologia di *Scipionyx samniticus* (Parte III), grazie a resti di cibo che nei primi esami dell'esemplare non erano stati notati. La conservazione dei tessuti molli consente di ricostruire perfino una cronologia della dieta del piccolo dinosauro, attraverso la posizione relativa dei resti alloigeni contenuti nel suo apparato digerente: un dato impossibile da ricavare per quasi tutti gli organismi fossili. I visceri di *Scipionyx* contengono: nella regione dello stomaco, le ossa della cavaglia di un rettile lepidosauro; nel duodeno, lembi di pelle composta da squame poligonali riferibili ad un rettile lacertiforme; nel digiuno, un ammasso di vertebre che probabilmente appartengono ad un piccolo pesce; nel retto, scaglie di un pesce più grande; in diversi punti dell'intestino, una varietà di altri resti più minuti. Pertanto abbiamo una prova evidente che *Scipionyx* si nutriva sia di piccoli rettili sia di pesci, e che questi ultimi rappresentavano un cibo abituale.

La monografia si chiude con alcune considerazioni sulla fisiologia digestiva e respiratoria di *Scipionyx*, suggerite dallo studio degli organi interni e dei loro correlati osteologici. La quantità di informazioni e i dettagli che queste hanno fornito, grazie allo studio di un singolo esemplare, fanno del Plattenkalk di Pietraraja un sito paleontologico unico al mondo. A differenza dei giacimenti cinesi appartenenti al Jehol Group (depositi di origine lacustre/vulcanica che conservano dinosauri fossilizzati con strutture tegumentarie delicate quali filamenti, penne e setole), il Lagerstätte marino italiano ha permesso la conservazione di tessuti molli all'interno del corpo di un organismo fossile mai visti in precedenza, non solo in un dinosauro, ma anche in qualsiasi altro vertebrato terrestre mesozoico.

Parole chiave: Theropoda, Compsognathidae, conservazione dei tessuti molli, Cretaceo inferiore, Plattenkalk di Pietraraja, Italia.

INTRODUCTION

Scipionyx samniticus abruptly entered the limelight when, on the occasion of its formal naming, it made the cover of *Nature* (Dal Sasso & Signore, 1998a). Since then, it has attracted not only the interest of vertebrate palaeontologists but also popular imagination throughout the world. In fact, the *Scipionyx* fossil is a striking, articulated, juvenile coelurosaur with a unique combination of osteological characters and superbly fossilised soft tissues. The latter render *Scipionyx* one of the best preserved dinosaurs known, and a unique specimen within the fossil record of Mesozoic vertebrates.

Scipionyx samniticus was the first dinosaur fossil body unearthed in Italy; thus, its discovery was a major event in the history of Italian palaeontology. In fact, Italy was considered to be devoid of dinosaur remains until this conviction was overturned by a striking series of finds consisting mainly of fossilised prints (for longer accounts, see Dal Sasso, 2001, 2003, 2004). Following a first find in the Dolomites (Mietto, 1988), more dinosaur trackways were discovered later at Lavini di Marco, in the Veneto region of northern Italy (Leonardi & Lanzinger, 1992). Thereafter, a number of Triassic (Norian) and Jurassic

(Hettangian to Pliensbachian) tracksites have been found in the mid-eastern Alps (for a complete list, see Leonardi & Mietto, 2000; Nicosia *et al.*, 2005; D’Orazi Porchetti *et al.*, 2008; Leonardi, 2008). Moreover, Cretaceous (Apertian to Santonian) dinosaur tracks have been uncovered in central and southern Italy, mainly in the Latium and Apulia regions (Andreassi *et al.*, 1999; Gianolla *et al.* 2000a, 2000b, 2001; Nicosia *et al.* 2000a, 2000b, 2007; Conti *et al.*, 2005; Sacchi *et al.*, 2006, 2009; Petti *et al.* 2008a, 2008b).

In addition to *Scipionyx*, the skeletal remains of three kinds of non-avian dinosaurs have been found so far in Italy. Two of them belong to new, possibly endemic, taxa that inhabited regions of the Periadriatic Domain during Jurassic (Sinemurian) and Cretaceous (Campanian) times: one taxon is represented by fragmentary bones of a large theropod that were collected in a commercial quarry in Saltrio (Lombardy region, northern Italy) – this specimen, still not named officially, has been described only preliminarily (Dal Sasso, 2001, 2003, 2004); the second taxon is represented by six specimens, one of which almost complete, of the hadrosauroid *Tethyshadros insularis*, unearthed at Villaggio del Pescatore, near the town of Trieste, in north-eastern Italy (Dalla Vecchia, 2009). The presence of a third kind of dinosaur is documented by a single bone found encased in the eroded wall of a cave from the Cretaceous (Cenomanian) of Capaci (Palermo, Sicily): recently examined *in situ* in cross-section, this bone is the midshaft of a leg from a medium-large theropod (Garilli *et al.*, 2009). Given the continuous and frequent rate of these recent finds, the dinosaur record in Italy is expected to increase rapidly in the near future.

Uniquely, the footprints and skeletal remains of Italian dinosaurs were preserved in coastal marine deposits. These finds indicate a peculiar palaeogeography and demonstrate that the model of Bahama-like small islands proposed for the region is no longer consistent with the presence of medium-large dinosaurs, which could survive only in terrestrial ecosystems. As documented by the wide temporal range of the dinosaur-bearing Italian outcrops (Avanzini *et al.*, 2000; Dalla Vecchia, 2001; Dal Sasso, 2001, 2002, 2003, 2004; Nicosia *et al.*, 2007; Sacchi *et al.*, 2009), Mesozoic Italy might have, in actual fact, emerged several times and quite extensively (see Palaeogeography, this volume).

The story of the discovery of the *Scipionyx* fossil is original in itself (for a detailed account, see Dal Sasso,

2001, 2004). In the spring of 1981, Giovanni Todesco unearthed a fossil reptile that was rather unusual for the marine outcrop of Pietraroja (Province of Benevento, southern Italy). The collector cleaned the fossil as well as he could and stored it in the basement of his house. It remained there until 1993, when Todesco showed it to professional palaeontologists, who identified the tiny reptile, as a dinosaur. The popular magazine *Oggi* dubbed the dinosaur “Ciro” (a typical Neapolitan name) in an article they published on it. In accordance with Italian law, the specimen was handed over to the superintendence of the site of provenance i.e., the Soprintendenza per i Beni Archeologici di Salerno, Avellino, Benevento e Caserta, where it is still housed. The specimen was first presented in a brief note (Leonardi & Teruzzi, 1993) and later in a current publication (Leonardi & Avanzini, 1994). Subsequently, a rough examination was conducted, in that the fossil had still not been fully prepared, and the results described in an unpublished degree thesis (Signore, 1995). In 1994, the Museo di Storia Naturale di Milano (MSNM) obtained official permission to properly prepare and study the fossil. It was only during this preparation work, performed in Salerno by Sergio Rampinelli (a collaborator at the palaeontology laboratory of the MSNM) and one of the authors of this monograph (CDS), that the extraordinary degree of preservation of the specimen’s soft tissue was fully realised. This later became the main focus of the paper published in *Nature* on its formal description (Dal Sasso & Signore, 1998a).

The present monograph, concisely introduced by Dal Sasso & Maganuco (2009), is the most complete publication existing to date on *Scipionyx samniticus*. Extensive re-examination of the specimen was possible thanks to the Soprintendenza per i Beni Archeologici di Salerno, Avellino, Benevento e Caserta (SBA-SA), which placed the fossil on loan to the MSNM from December 2005 to October 2008. The research laboratories at the MSNM, and those of collaborators, provided technical support that was appropriate to the importance of the specimen. In particular, SEM analysis carried out at the MSNM provided remarkable evidence of the exceptional level of the soft tissue preservation. Given that no other single dinosaur fossil is known to preserve such a quantity of previously unknown anatomical features, this monograph is duly devoted to a detailed description of the unique osteology, ontogenetic stage, phylogeny, soft tissue anatomy, taphonomical history and palaeobiology of *Scipionyx samniticus*.

GEOLOGICAL SETTING

The locality

The village of Pietraroja (Benevento Province) sits near the top of a 970 m high carbonate relief, called “Civita di Pietraroja”, that rises almost vertically from the plain adjacent to the eastern margin of the Matese Mountains (central southern Italian Apennines) roughly 70 km north-east of Naples (Figs. 1-2). The Lower Cretaceous levels, assigned to the Lower Albian on the basis of foraminiferal biozonology (Bravi & Garassino, 1998; Carannante *et al.*, 2006), crop out at the “Le Cavere” locality, just above the village 41°20’52.18”N, 14°32’53.33”E. (The geographi-

cal coordinates 45°77’43.1”N, 24°82’22.8”E reported in recent papers on Pietraroja fossils [Evans *et al.*, 2004; 2006] are markedly wrong, as they refer to a locality in central Romania).

Excavations in the fine-grained marine limestones have been in progress, albeit intermittently, for more than 150 years. During this time, the site has yielded a rich assemblage of plants, invertebrates and vertebrates, including fishes, amphibians and reptiles (e.g. Bravi, 1994, 1999; Bravi & Garassino, 1998; Barbera & Macuglia, 1991; Dal Sasso & Signore, 1998a; Evans *et al.*, 2006).

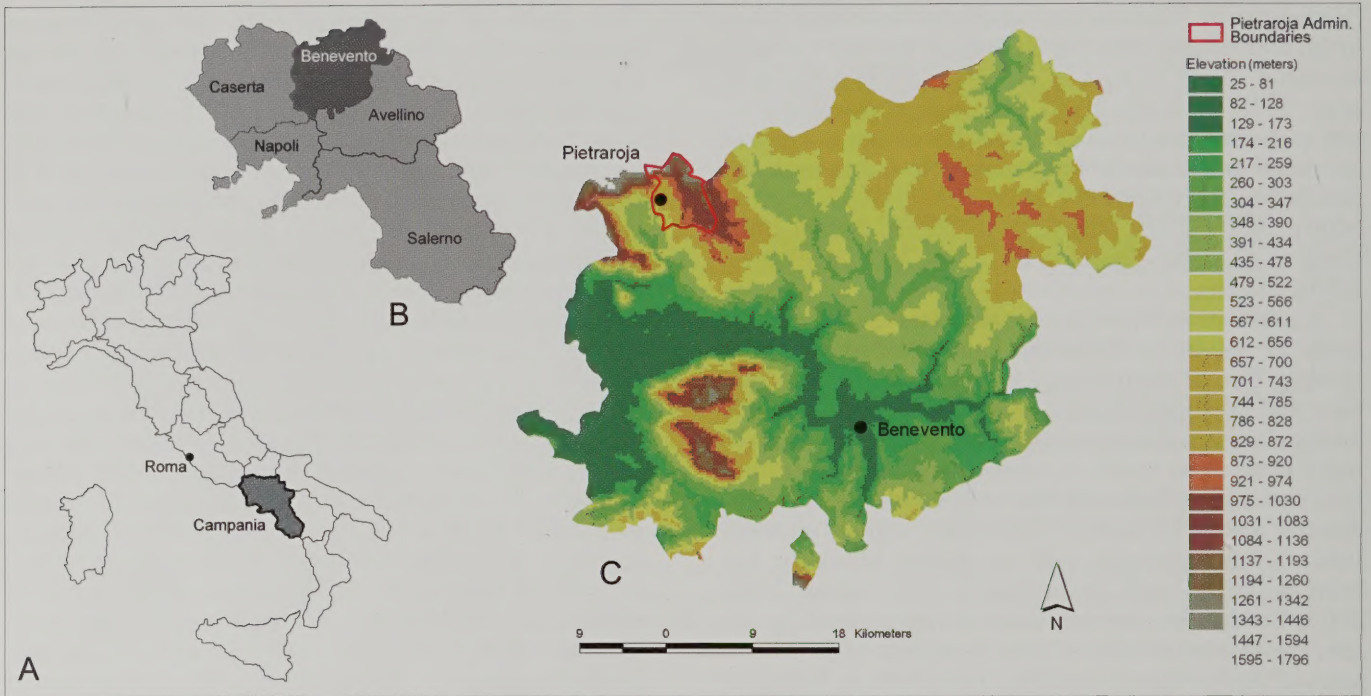


Fig. 1 - Geographic location of Pietraraja. A) map of Italy; B) map of the Campania region and its provinces; C) physical map of the Benevento province and the municipality of Pietraraja.

Fig. 1 - Posizione geografica di Pietraraja. A) mappa dell'Italia; B) mappa della regione Campania e delle sue province; C) mappa fisica della provincia di Benevento e del comune di Pietraraja.



Fig. 2 - The north-western slope of the "Civita di Pietraraja" and the outcrop of "Le Cavere" (centre right). Part of the fossiliferous site was fenced off after the discovery of the little dinosaur (arrow).

Fig. 2 - La scarpata nord-ovest della "Civita di Pietraraja" e l'affioramento de "Le Cavere" (a destra). Parte del sito fossilifero è stata cintata dopo la scoperta del piccolo dinosauro (freccia).

Historical background

The limestones of Pietraroja have been known for their beautifully preserved fossils since the nineteenth century. The palaeontological richness of the outcrop was mentioned for the first time in 1798 by Breislak (Fig. 3), but scientific studies began only much later and focused immediately upon the plentiful number of fossil fishes, called “ittioliti” (Italian for ichthyoliths), which emerged from the calcareous rocks. Between 1851 and 1866, Costa

(1851, 1853-1864, 1865, 1866) described the “Calcarei ad Ittioliti di Pietraroja” in a series of volumes superbly illustrated with lithographic prints in the typical style of the period (Fig. 4). The term “Calcarei ad Ittioliti di Pietraroja” was slightly modified into “calcarei selciferi ed ittiolitiferi di Pietraroja” (Catenacci & Manfredini, 1963), which has been used frequently to indicate that geological formation. A formal name has not been validated, yet (Petti, pers. comm., 2010). Here we use the term Plattenkalk *sensu* Carannante *et al.* (2006).



Fig. 3 - “Physical topography” of north-western Campania, represented in a three-dimensional style. Pietraroja (circle), which is located some 70 km NE of Naples, is labelled here with the ancient toponym Pietra Roja. (After Breislak, 1798).
 Fig. 3 - “Topografia fisica” della Campania nord-occidentale, rappresentata con un aspetto tridimensionale. Pietraroja (area cerchiata), che si trova circa 70 km a nord-est di Napoli, è qui nominata con l’antico toponimo Pietra Roja. (Da Breislak, 1798).



Fig. 4 - Lithography illustrating *Belonostomus crassirostris* and other fossil fishes unearthed from the Pietraraja Plattenkalk in the nineteenth century. (After Costa, 1853-1864).

Fig. 4 - Litografia del diciannovesimo secolo che illustra *Belonostomus crassirostris* e altri pesci fossili del Plattenkalk di Pietraraja. (Da Costa, 1853-1864).

The age of these limestones – considered to be Jurassic – was a subject of debate up to the end of nineteenth century, when Bassani (1885) re-examined the fossil fishes collected by Costa and confirmed their Cretaceous affinity. The deposit was studied in the 1900's by D'Erasmus (1914, 1915) and D'Argenio (1963), but generally there was less interest than in the previous century. In more recent times, research has been carried out by the Università di Napoli "Federico II", which in 1982, in cooperation with the Museo di Scienze Naturali di Torino, conducted excavations in the Le Cavere locality (Bravi, 1987, 1988, 1994). After the *Scipionyx* fossil came to light, a small quarry was opened in 2001 by the MSNM, under the aegis of the Soprintendenza per i Beni Archeologici di Salerno, Avellino, Benevento e Caserta. Today, the fossiliferous outcrop of Pietraraja is protected by a fence and is a geo-palaeontological park.

Geological framework

The central-southern Italian Apennines are a thrust-and-fold belt that originated during the Late Tertiary from the deformation of the continental margin of the Adria Plate. This plate is interpreted as being either an independent Cretaceous unit or part of the Africa Plate (Channel *et al.*, 1979). The Matese Mountains are part of the Simbruini-Ernici-Matese structural unit (Patacca

& Scandone, 2007), that is made of 3-4 km thick Mesozoic carbonate platform deposits topped with Tertiary carbonates and terrigenous sediments (D'Argenio *et al.*, 1973). During the Miocene, deformation piled the Matese onto more external (eastern) domains; subsequent uplift occurred from the latest Pliocene to the Pleistocene and brought the Matese to its present elevation (Carannante *et al.*, 2006).

In the Early Cretaceous, the present-day Pietraraja area was part of a shallow-water carbonate domain (Abruzzese-Campana Platform) which developed in tropical-subtropical climatic conditions (D'Argenio, 1976). Although the regional palaeoceanography of the continental margin to which Pietraraja belonged is still debated, the stratigraphic context and evolution of the Abruzzese-Campana Platform is well-assessed (D'Argenio *et al.*, 1973). As for other carbonate domains of the Southern Tethyan Margin, predominantly shallow lagoonal conditions prevailed during the Early Cretaceous. Beginning with the Late Aptian-Early Albian, margin retrogradation and broad tectonic uplifts took place, with the establishment of more open marine conditions, including deeper margins connecting the shelf to the basin areas (Vigorito *et al.*, 2003; Carannante *et al.*, 2004). According to these authors, between the Middle Aptian and Early Albian the southeastern sectors of the Matese Mountains were downfaulted, leading to the development of a narrow eastward-facing channelised carbonate margin.

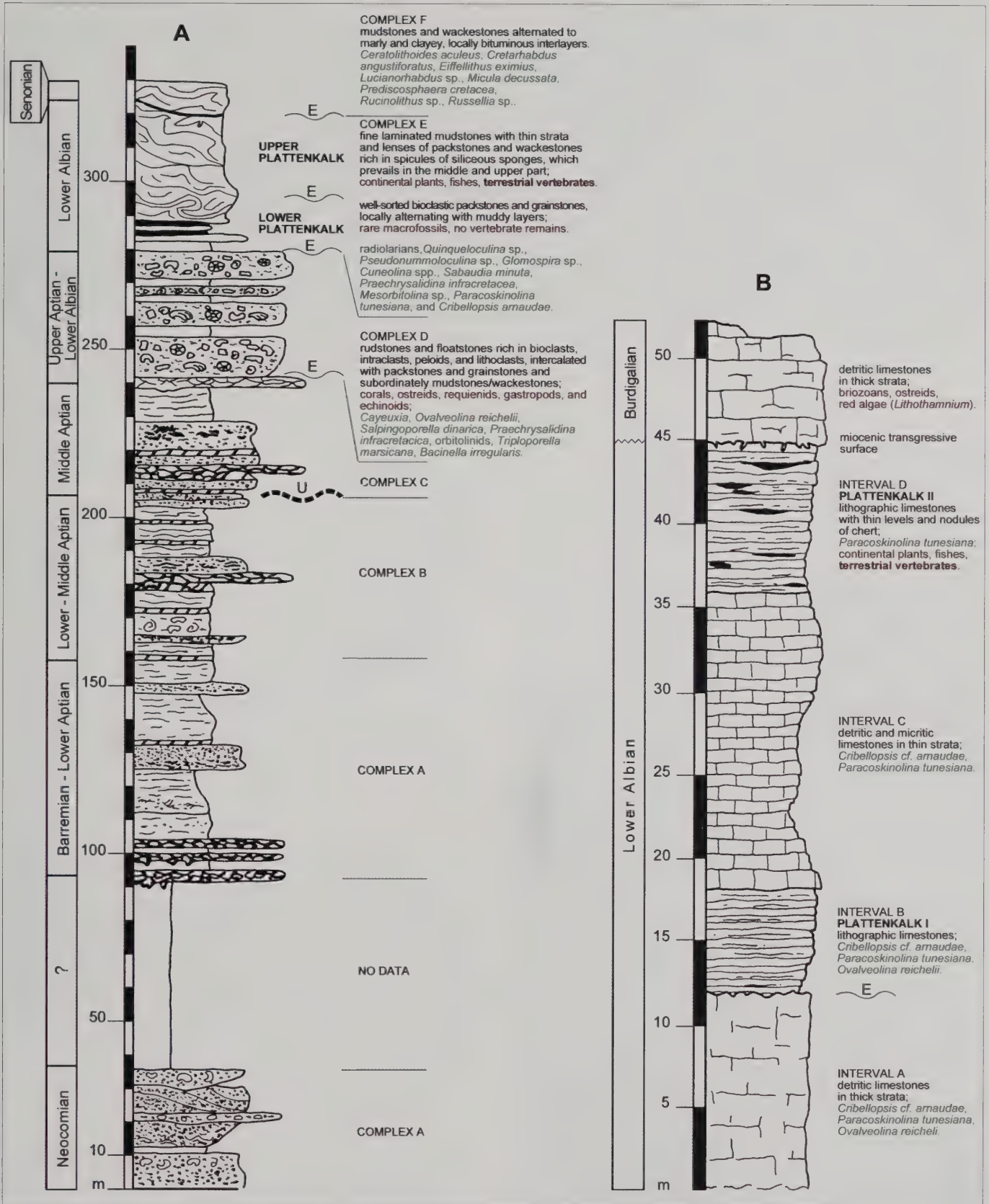


Fig. 5 - A) lithostratigraphic column of the Cretaceous succession of Pietraraja, according to Carannante *et al.* (2006); B) stratigraphic sequence of the north-eastern side of the "Civita di Pietraraja", according to Bravi & Garassino (1998). Plattenkalk I and II in B roughly correspond to lower and upper Plattenkalk in A. Abbreviations: U) unconformity; E) erosional surfaces. Microfossils in green, macrofossils in brown. (Modified from the mentioned authors).

Fig. 5 - A) colonna litostratigrafica della successione cretacea di Pietraraja, secondo Carannante *et al.* (2006); B) sequenza stratigrafica del versante nord-orientale della Civita di Pietraraja, secondo Bravi & Garassino (1998). I livelli denominati Plattenkalk I e Plattenkalk II in B corrispondono approssimativamente ai livelli denominati lower Plattenkalk e upper Plattenkalk in A. Abbreviazioni: U) discordanza; E) superfici di erosione. Microfossili in verde, macrofossili in marrone. (Dagli autori citati, modificate).

Lithology, stratigraphy and sedimentology

The Cretaceous succession of Pietraraja, which is about 340 m thick, includes two well-stratified Plattenkalk horizons (Fig. 5). According to Carannante *et al.* (2006), each Plattenkalk presents distinct fining and thinning upward trends with a detritic basal layer. The lower Plattenkalk is averagely coarser and is characterised by the occurrence of frequent benthonic foraminifera-rich grainstones and packstones: it is relatively poor in macrofossils and, to date, no vertebrate remains have been reported from this interval. Above this is a second Plattenkalk horizon, with a depth of 8-9 m. The thickness of the upper Plattenkalk increases to the southwest, reaching a maximum of some 15 m at the Le Cavere outcrop, which is the source of the major fossil finds. The upper Plattenkalk is averagely finer when compared with the lower one, as it is mostly composed of fine laminated mudstones (Fig. 6). In the middle and upper part of this interval there is a prevalence of mudstones with thin strata and lenses of packstones and wackestones rich in spicules of siliceous sponges. Locally, chert lenses and nodules, as well as bituminous and coprolite-rich beds, are also found. The trend of the layers is about N-S leading eastward, with an average dip around 20°. This trend



Fig. 6 - A section of the upper Plattenkalk series, outcropping at Le Cavere a few metres north of the point where *Scipionyx* was likely collected.

Fig. 6 - Una sezione della serie superiore del Plattenkalk, affiorante a Le Cavere pochi metri a nord del punto in cui è stato raccolto *Scipionyx*.

is almost identical to that of the lower Plattenkalk, except for a “flute-beak” termination, where it becomes more slanted (Bravi & Garassino, 1998).

Carannante *et al.* (2006) recently dated the Pietraraja Plattenkalk as Lower Albian on the basis of its microfossil assemblage, which includes *Bacinella irregularis*, *Glomospira* sp., *Cuneolina* aff. *pavonia*, *Praechrysalidina infracretacea*, *Nummuloculina* sp., *Thaumatoporella* sp., *Debarina* sp., *Ovalveolina reichelii*, *Sabaudia minuta*, orbitolinids, miliolids and textularids. This fits well with previous biostratigraphic data provided by Bravi & De Castro (1995) and Bravi & Garassino (1998), who recorded the following association: *Quinqueloculina* sp., *Pseudonummoloculina* sp., *Glomospira* sp., *Cuneolina* sp., *Sabaudia minuta*, *Praechrysalidina infracretacea*, *Mesorbitolina* sp., *Paracoskinolina tunesiana* and *Cribellopsis arnaudae*. Furthermore, D’Argenio (1963) and Catenacci & Manfredini (1963) reported planktonic foraminifers, tentatively referred to as *Praeglobotruncana* sp., from the upper portion of the Plattenkalk.

Analysis of selected samples from the Pietraraja Plattenkalk conducted by Carannante *et al.* (2006) has led to the recognition of three main microfacies:

Biolithoclastic packstone/grainstone microfacies (1) - this occurs as strata or lenses a few centimetres thick. It makes up most of the lower Plattenkalk, but occurs also in the upper Plattenkalk. Components are mainly carbonate intra- and/or lithoclasts, benthic foraminifers as well as green algae, rudists, corals and thin-shelled bivalves. Microfossil assemblages likely include a mixture of fossils of various ages, from Aptian to Lower Albian (Bravi & Garassino, 1998), and show a conspicuous contribution from the demolition of older deposits.

Spicule-rich packstone/wackestone microfacies (2) - this occurs as 0.005-0.1 m thick lenses, laminae and/or continuous strata dominating the lower-middle portions of the upper Plattenkalk. Siliceous and rare carbonate sponge spicules are the main components, together with subordinate radiolarians. Rare planktonic foraminifers have been also reported (Catenacci & Manfredini, 1963; D’Argenio, 1963).

Thinly laminated mudstone microfacies (3) - this makes up most of the upper portion of the upper Plattenkalk. The deposits are an alternation of several-tens-of-micrometers-thick light havana and ash-grey carbonate muddy laminae. Locally, thin marly, cherty and rare dark grey clay layers alternate with calcareous laminae. Microfossils are absent or rare and consist mainly of sponge spicules.

Stratigraphic position of *Scipionyx*

According to the person who found the fossil (Todesco, pers. comm., 1993), *Scipionyx* was collected at a point of the Le Cavere quarry that, based on the present-day topography, falls into the lower-right quarter of the fenced-off area of the outcrop (Fig. 7). More precisely, the discovery site is located to the right of the entrance gate and some 7-9 m from the paved road (once a gravel one). Todesco also has stated (pers. comm., 2010) that the layer from which *Scipionyx* came from outcropped some 50-80 cm higher than the present stepping (bottom) layer, but in any case at an elevation below the level of the



Fig. 7 - A) orthophotograph of Pietraraja, and the fenced-off area (black arrow) of Le Cavere north of the village; B) western view of the Le Cavere quarry, showing the probable point where *Scipionyx* was collected (red arrow). Scale bar = 100 m.
 Fig. 7 - A) ortofotografia di Pietraraja e dell'area cintata de Le Cavere, a nord del paese (freccia nera); B) vista da ovest della cava de Le Cavere, con indicazione del probabile punto in cui è venuto alla luce *Scipionyx* (freccia rossa). Scala metrica = 100 m.

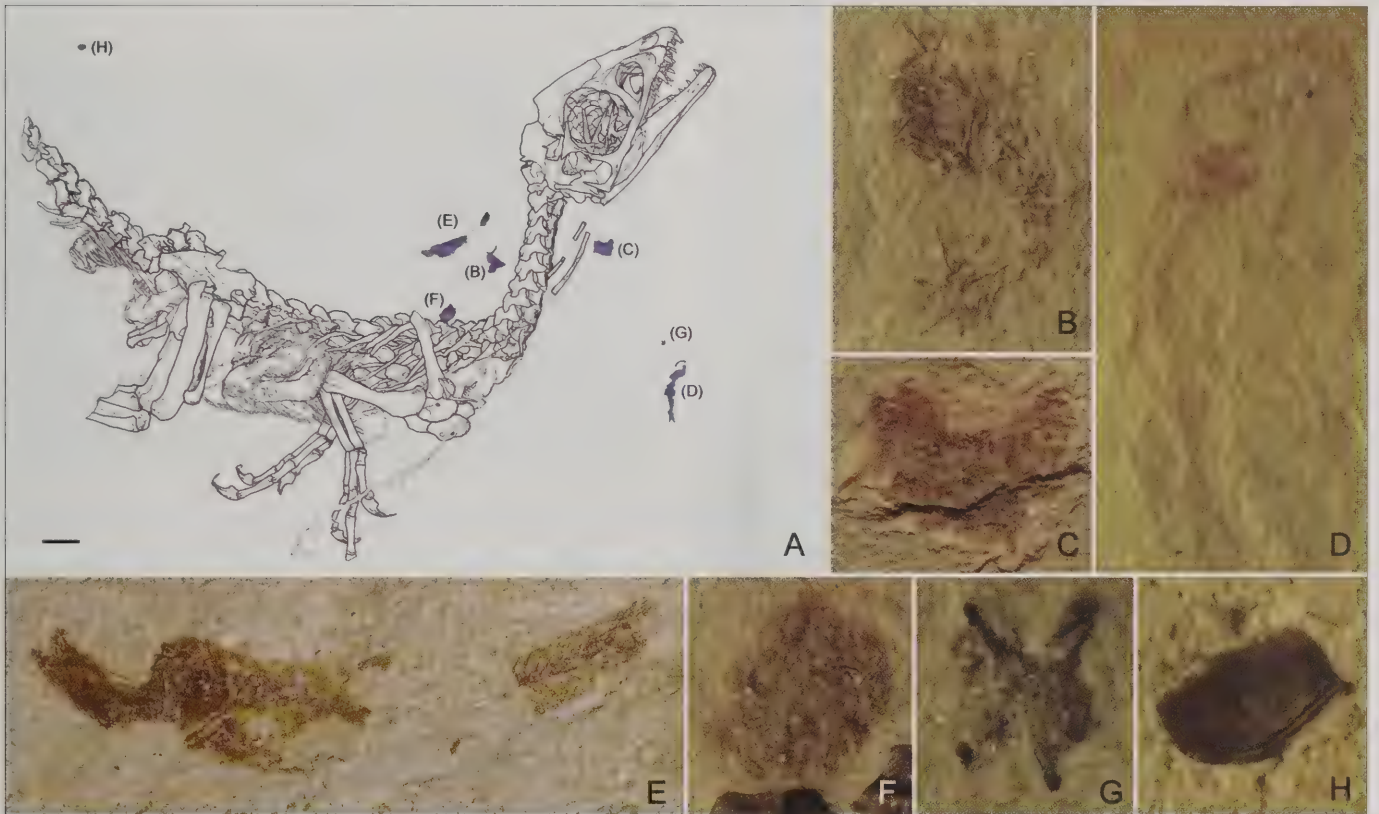


Fig. 8 - A) position of the fish remains co-occurring with *Scipionyx samniticus*; B-F) close-ups of five clupeomorph fishes (*Clupavus* sp.); G) indeterminate vertebra; H) isolated *Notagodus*-like scale. Scale bar = 10 mm.
 Fig. 8 - A) posizione dei resti di pesci associati allo scheletro di *Scipionyx samniticus*; B-F) particolari di cinque pesci clupeomorfi (*Clupavus* sp.); G) vertebra indeterminata; H) squama isolata di un pesce simile a *Notagodus*. Scala metrica = 10 mm.

road. The same layer produced several fish remains, such as pycnodontiform jaws and *Diplomystus*-like fins (Todesco, pers. comm., 1993). Incidentally, the remains of 5 clupeomorph fish (*Clupavus* sp.) are embedded within the slab containing *Scipionyx*. These are preserved to various degrees, from fully articulated to scattered bone clusters (Fig. 8). One isolated scale – referable to a larger species of fish, possibly the semionotiform *Notagodus* – is located 22 mm above the distalmost tip of the dinosaur's tail (Fig. 8). In our opinion, the position of this layer, as well as the contents of the slab, are consistent with the lower-

middle series of the upper Plattenkalk (*sensu* Carannante *et al.*, 2006). Nevertheless, to confirm this, and to more precisely correlate the fossil with the known stratigraphy of Pietraraja, we analysed the lithological and sedimentological aspects of the slab that contains *Scipionyx*. The artificial puzzle created by the various pieces of slabs originating from different layers, which were assembled around and under the specimen (Figs. 9-10), and the elimination of the overlying layers during the preparation of the fossil, rendered the search for the authentic embedding layer tricky.



Fig. 9 - The artifactual puzzle of slabs assembled around the specimen, highlighted under ultraviolet light by the bright fluorescence of the glue used (lightest blue).

Fig. 9 - Il mosaico di lastre assemblate attorno all'esemplare, evidenziato in luce ultravioletta dalla forte fluorescenza del collante impiegato (azzurro più chiaro).



Fig. 10 - Distinction between the authentic bedding layer of *Scipionyx* (outlined in black) and the slabs added by the collector (shaded in grey). See also cover page. Samples of sediment (red dots) were carefully taken from the original layer, along a section of the granular bed (ochre yellow areas) once covering the dinosaur.

Fig. 10 - Distinzione tra lo strato originario in cui giace *Scipionyx* (delimitato dalle linee nere) e le lastre aggiunte dal raccoglitore (velate di grigio). Si veda anche la foto di copertina. I campioni di sedimento (punti rossi) sono stati prelevati con attenzione dallo strato originario, lungo una sezione del livello granulare (zone giallo ocra) che prima ricopriva il dinosauro.

Macroscopic aspect of the embedding sediment -

After mechanical preparation, the sediment of the bed immediately underlying and partially containing the fossil *Scipionyx* became the most exposed one. In other words, the sediment seen surrounding the specimen does not represent the whole layer that originally contained the fossil, but only a portion of it, as most of it was removed to bring to light the fossil like a bas-relief. The exposed sediment is mostly fine-grained, but shows some textural inhomogeneities in the form of localised accumulations of larger-grained sediment. The latter is dominant in the overlying bed, which, as we infer from the fossil's thickness, gave a major contribution to encompassing it. Luckily, patches of this sediment remain at some distance from the fos-

silised bones of the dinosaur: 40-50 mm above the dinosaur's pelvis; 15 mm above the skull; 10 mm below the left forearm and the right knee. There, the larger grains surface in three very oblique, almost longitudinal, sections of the bed, which on macroscopic examination appear as grey-dotted granular halos (Fig. 11). We examined three samples of the section nearest to the fossil (Fig. 10) with optical and scanning electron microscopy.

Cross sections (10-15 mm thick) of the original sequence of layers embedding and underlying *Scipionyx* are visible along a couple of adjacent cracks that delimit the sediment surrounding the forearms and the pectoral and abdominal sides of the dinosaur. Dense, alternating light and dark laminations thinner than 1 mm can be seen there (Fig. 12). These laminations are similar to the light Havana and ash-grey laminae that characterise the fish-rich layers (Dal Sasso & Maganuco, pers. obs., 2003-2010 on historical and recently collected specimens), and are consistent with microfacies (2) and (3) described by Caranante *et al.* (2006).

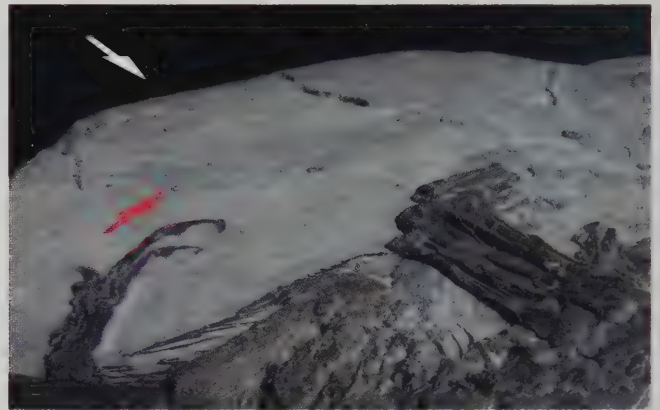


Fig. 11 - Grazing view of the granular bed that was sampled and examined under scanning electron microscopy (red arrow). The white arrow indicates the point of view of the cross-section shown in Fig. 12.

Fig. 11 - Vista radente del livello granulare campionato ed esaminato al microscopio elettronico a scansione (freccia rossa). La freccia bianca indica la posizione della sezione mostrata in Fig. 12.



Fig. 12 - Exposed cross-section of the original slab of Plattenkalk embedding *Scipionyx*, and a supporting slab added by the collector (shaded in grey). The red arrow points to the bed examined in Fig. 13; the white arrow indicates the left manus of *Scipionyx*. Scale bar = 1 mm.

Fig. 12 - Sezione esposta della lastra originaria di Plattenkalk che racchiude *Scipionyx* e di una lastra di supporto aggiunta dal raccoglitore (velata di grigio). La freccia rossa indica il livello esaminato in Fig. 13; la freccia bianca indica la mano sinistra di *Scipionyx*. Scala metrica = 1 mm.

Microscopic aspect and chemical composition of the embedding sediment - Under the light microscope, the original sediment embedding *Scipionyx* has two main components: a fine-grained (0.01-0.03 mm), white matrix, probably composed of carbonates; and a medium-grained (0.10-0.26 mm), vitreous, brown substrate, possibly siliceous clasts, that according to Torricelli (pers. comm., 2010) are more or less fragmented sponge spicules (Fig. 13B). Based on the classification of Dunham (1962), this sediment can be defined as an intermediate between packstone and wackestone in that it is matrix-supported but consisting in more than 10% grains, some of them in contact.

SEM element microanalysis of the three samples of sediment confirmed that the fine-grained matrix is composed of calcium carbonate, thus it can be defined as a micrite (Fig. 13A-B); in contrast, the larger grains are composed of silica, thus they are likely the fragmented spicules of siliceous sponges (Fig. 13B-C). The low aluminium peak indicates a secondary terrigenous component (clay minerals). Worthy of note is the total absence of phosphorus, one of the main elements in the chemical composition of the fossil. That means that the abundant phosphorus preserved in *Scipionyx* does not come from the depositional environment but derives from the decay of the carcass. This is a very important datum, which will be dealt with in more detail in the section dealing with soft-tissue taphonomy.

Both the texture and chemical composition of our samples of sediment fit well with the description of microfacies (2), the “spicule-rich packstone/wackestone microfacies” (Carannante *et al.*, 2006). Microfacies (2) “largely dominate[s] the lower-middle portions of the upper Plattenkalk”, providing good sedimentological evidence that *Scipionyx* comes from one of those layers. In our opinion, and according to Torricelli (pers. comm., 2010), the probable presence of microfacies (3) in the bed underlying *Scipionyx*, as well as in other stratigraphically adjacent layers, strengthens, rather than contradicts, that

conclusion. Indeed, the thin strata and spicule-rich lenses of packstones and wackestones typically intercalate with mudstones in the lower and middle parts of the upper Plattenkalk (Carannante *et al.*, 2006). At the same time, the layers embedding *Scipionyx* cannot pertain to microfacies (1) because none of our samples is grain supported (*sensu* Dunham, 1962), and no foraminifers, algae, coral or bivalve fragments are present.

Other observations lead us to exclude another stratigraphic portion of the Pietraraja outcrop: without doubt, *Scipionyx* does not come from the uppermost series of the upper Plattenkalk. In 2001, fieldwork was conducted by the MSNM, in collaboration with the SBA-SA, to investigate the fossil contents of the uppermost strata of the upper Plattenkalk at the Le Cavere locality. Samples collected just a few meters from the point where *Scipionyx* was uncovered, from the top of the series to a depth of 3 meters, were numbered as a continuous series of 20 levels and were analysed in parallel by two sedimentology laboratories. Almost all these layers turned out to be dominated by microfacies (3) as described by Carannante *et al.* (2006): very fine mudstone, with absent to rare microfossils. In fact, palynology and calcareous nannoplankton analysis revealed these layers to be completely sterile (Torricelli, pers. comm., 2007; Maffioli, pers. comm., 2009).

Depositional environment

The exceptional degree of preservation of the fossil vertebrates from Pietraraja results from peculiar depositional conditions. The relatively small size of the specimens, the rapid sedimentation of fine-grained sediments in a subaqueous environment, and the scarcity or absence of oxygen, are among the physical parameters that allowed the exceptionally fine fossilisation of bones and soft tissues in this site (see also Soft Tissue Taphonomy).

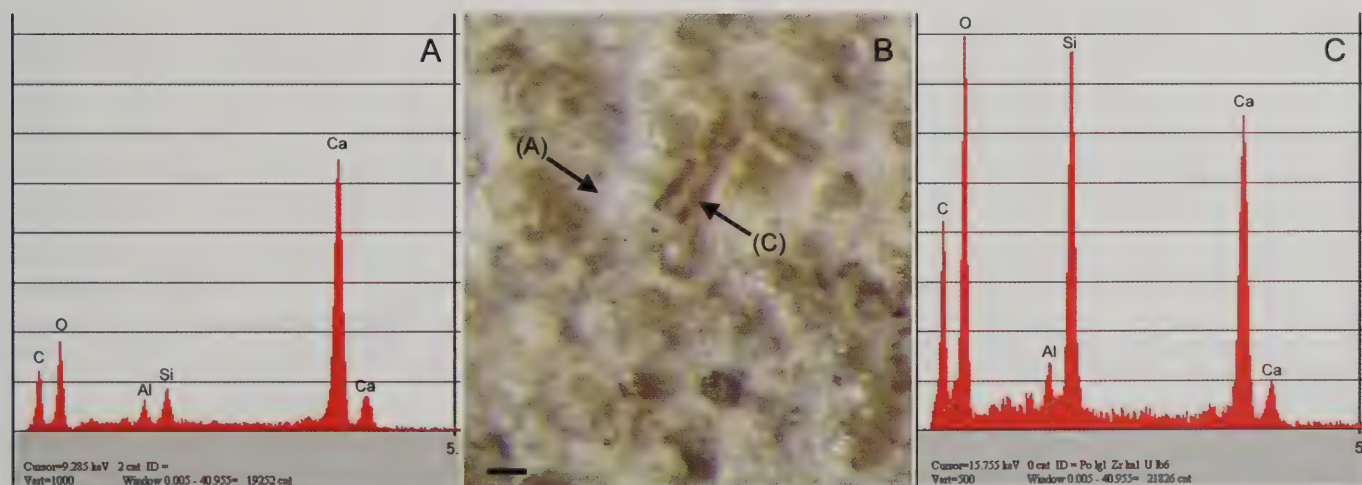


Fig. 13 - Close-up of the sampled granular bed seen under the optical microscope, and SEM element microanalysis of its two main components. A) elemental spectrum of the fine-grained matrix (white areas in B), composed of calcium carbonate; C) elemental spectrum of the medium-grained clasts (brown-coloured inclusions in B), composed of fragmented spicules of siliceous sponges. Note the absence of phosphorus, which is one of the main components of the *Scipionyx* fossil. Scale bar = 0.1 mm.

Fig. 13 - Particolare al microscopio ottico di un campione del livello granulare e microanalisi degli elementi (al SEM) delle sue due componenti principali. A) spettro degli elementi della matrice a grana fine (bianca in B), composta da carbonato di calcio; C) spettro degli elementi dei clasti di grana media (marroni in B), che sono frammenti di spicole di spugne silicee. Si noti l'assenza di fosforo, che invece è uno dei componenti principali del fossile di *Scipionyx*. Scala metrica = 0,1 mm.

Fossil-rich Plattenkalks have been documented from shallow lagoonal to relatively deep basinal settings, so there is still great uncertainty on the depositional environment that created the Pietraraja Plattenkalk. On this point, three distinct models have been proposed.

Lagoon model - According to some authors (D'Argenio, 1963; Bravi & Garassino, 1998), the Pietraraja Plattenkalk was laid down close to a coastal area, in a very shallow lagoonal environment that was frequently isolated from the open sea but subject to tidal influence and occasional storms. "Apparent cyclicity in the lithotype distribution" (Bravi & Garassino, 1998), inferred from the graded horizons in most layers of the upper Plattenkalk, led to hypothesise that sediment deposition was linked to the rhythm of tides and storms which reached the lagoons and poured the finer sediments of the surrounding above-sea-level areas into them. Those instantaneous microturbiditic events alternated with more or less prolonged intervals of sedimentary starvation, that Bravi & Garassino (1998) attribute to isolation of the basins from the open sea – these periods would have caused overheating and dystrophic conditions in the waters of the lagoons. The presence of bioturbations in the Pietraraja limestone suggests that oxygen was not entirely lacking on the seabed, whereas several layers particularly rich in fish and coprolites document mass mortality events. According to this model, films of algae and bacteria would have been the most probable origin of the fine laminations seen in these layers.

According to D'Argenio (1963), putative mud cracks, cracked chips and gas pits in some Plattenkalk layers indicate occasional emersions. However, Bravi & Garassino (1998) did not find any certain sign of the drying of sediments in the same stratigraphic series. On the other hand, the latter authors regard the abundance of sponge spicules in several layers as not necessarily linked to a deep depositional environment, since sponge colonies can develop also in very shallow water. According to Bravi & Garassino (1998), strong overheating of the waters of the Pietraraja lagoons, probably occurring when they came close to the limit of emersion, is proven by certain layers of the upper Plattenkalk that are literally carpeted with bivalves, all lying with the valves open upwards and still articulated at the umbones. The lack of evaporitic minerals, expected to be present in overheated coastal lagoons, is explained by occasional freshwater contribution. In this perspective, the exceptional integrity of the vertebrate fossils is linked to calm lagoonal waters, and the random bone dispersion of disarticulated skeletons is linked to bioturbation rather than to currents. Conversely, the mutilation of some carcasses and the dorsally arcuate position of many fish, caused by putrefaction gases in the abdominal cavity, are linked to flotation. From this, it is inferred that the depth of the basins was limited, because putrefaction gases might not expand the abdomen of dead fish at higher pressures (Bravi & Garassino, 1998). In any case, *Scipionyx* suffered a different fate: floating carcasses never reach the bottom intact, so we can definitely conclude that the little dinosaur was drawn down to the bottom rapidly, and just as rapidly buried.

Slope/shallow basin model - Contrary to the authors above, Catenacci & Manfredini (1963) believe that depo-

sition of the Pietraraja Plattenkalk took place in a coastal strip which ran between the margin of the platform and the deepest sediments of the opposite basin (Molise-Sannitica depression). The transitional nature of this environment is inferred by sedimentological and stratigraphic observations, including a lateral "flute-beak" transition from reefoidal to plattenkalk deposits. This type of depositional environment would have been subjected to recurrent bathymetric variations causing the irregular alternation of semicontinental-lagoonal conditions and open-sea conditions. The authors explain in this way the presence of very different organisms and lithotypes (amphibians, reptiles and crustaceans on one side; radiolarians, sponge spicules, fishes and chert on the other). Such "alternation" of very different domains seems, however, very unlikely.

Freels (1975) hypothesised that the Pietraraja Plattenkalk was deposited in a submarine erosion basin characterised by low-energy and reducing conditions towards the sea bottom (stagnation-type deposits *sensu* Seilacher, 1970). From the geometry of the Plattenkalk bodies, and from the way in which they overlap the adjacent carbonate platform facies, Freels (1975) estimated the Pietraraja basin to have been about 60 m deep and 1 km wide. The filling of the basin would have been due to suspension currents developing at the margin of the basin and carrying materials derived from the adjacent depositional environments. Evidence of such suspension currents would be provided by slumpings at the borders of the Plattenkalk and by gradation of some layers of the Plattenkalk itself. Consistent with this hypothesis, the structures that D'Argenio (1963) interpreted as caused by sediment drying would be ascribed, rather, to subaqueous shrinkage.

Submarine channel model - Both models above appeared inadequate in that, according to some researchers, they failed to take into account all the sedimentological and palaeontological features of the Pietraraja Plattenkalk. A new model was therefore proposed more recently by Carannante *et al.* (2006). According to this, the Pietraraja Plattenkalk sequences are not shallow lagoonal deposits or intra-platform basin-fill, but deposits of a submarine channel (referred to as the Pietraraja Channel) that document a major transgressive event. In particular, the lower Plattenkalk and the fine-grained, fossil-rich upper Plattenkalk are interpreted as representing, respectively, channel-fill and abandon deposits, which followed previous coarse-grained channel-fill sequences as a response to the demise of the channel as a sedimentary conduit. Carannante *et al.* (2006) support this model with a number of observations. First of all, these authors note that the Pietraraja Plattenkalk is arranged within a relatively narrow, east-dipping incision, and is confined laterally by coarse biointraclastic deposits and by a sharp erosive surface. Secondly, both the lower and the upper Plattenkalk consist in moderately to well-sorted deposits. It is improbable that these could form in upper subtidal to intertidal lagoonal settings like those proposed by D'Argenio (1963) and Bravi & Garassino (1998); rather, they usually originate from carbonate turbidites. Palaeocurrent measurements have been reported to be documented in the two Plattenkalks by scours, groove marks, oriented grains and ripples, and to indicate sediment transportation always towards the east. However, Carannante *et al.* (2006) did not find any evidence for multi-directional or bi-directional

flows or for turbidite ponding, that characterise wave-dominated and tide-dominated shallow-water environments and small intraplatform basins. Therefore, it is likely that microfacies (1) derives from eroded submarine sediments that were re-arranged mainly as turbidites or bottom current-related deposits; microfacies (2) derives from primary deposition from bottom currents and turbidites; and microfacies (3) originates from deposition of low-density, muddy turbidites. According to this model, we deduce that *Scipionyx* was buried in a single, rapid event by a turbidite.

The fossils of Pietraraja range from the beautifully preserved *Scipionyx* to very poorly preserved and unidentifiable skeletal remains. According to Carannante *et al.* (2006), these features can be recognized both at outcrop scale and over a small area of a single bed, and may mean that the carcasses came from different places and were subjected to different transportation processes. Moreover, the fossils seem to increase in dimension moving from the borders of the inferred Pietraraja Channel towards the axis. This spatial arrangement may derive from the kind of transportation that was able to drag or carry large carcasses only over limited distances.

Carannante *et al.* (2006) also observe that the invertebrate fauna assemblage is very poor compared to the vertebrate one. It is unlikely that this could have been caused by a taphonomic artefact, because the exoskeleton of most of the site's invertebrate taxa would have rendered them more resistant than the vertebrates to decay. As a matter of fact, Bravi & Garassino (1998), while supporting the lagoon model, describe the decapod crustacean assemblage of Pietraraja as having "a not particularly good state of preservation": in fact, only 17 of the 29 studied specimens could be given a confident systematic ascription. A very similar conclusion was reached a century ago on different decapod specimens by D'Erasmus (1914, 1915).

According to Carannante *et al.* (2006), and *contra* other authors (D'Argenio, 1963; Bravi & Garassino, 1998), the bioturbation index of the site is very low, most traces being ascribed to *repichnia*, with no evidence of *domichnia* or *pascichnia*. This observation is consistent with a shallow, anoxic surface very close to the water-sediment interface. Anoxic to suboxic conditions at the seafloor fit well with the occurrence of calcareous or marly bituminous layers. They also explain the very scarce benthic invertebrates, and a curious lack of nematodes, annelids or any other "worm", which in any marine biocoenoses (including lagoons) are quite abundant. Also, according to Carannante *et al.* (2006) the finding of very small bivalves preserved with open but still connected valves cannot be interpreted as a mass-death event caused by overheating water (Bravi & Garassino, 1998); rather, this is another typical feature of anoxia, given that only under this condition does the hinge ligament not decompose – thus keeping the two valves conjoined – and the adductor muscles relax – opening the bivalves up.

Another interesting point is the strong presence of durophagous fish coupled with the almost complete absence of possible prey. If the site represents a thanatocoenosis, as previously thought, then a large number of shelled invertebrates, or at least of corals, should be present. On the contrary, a large part of the fish fauna is composed from pelagic predators, like *Belonostomus* and at least two species of ichthyodectid fishes (Signore *et al.*, 2005). So, the

faunal assemblage of Pietraraja likely represents a mixture of organisms originating from different types of environment, but certainly not from a lagoonal one. Summing up, Carannante *et al.* (2006) concluded that the fossils of the Pietraraja Plattenkalk represent a taphocoenosis and an obruption deposit (*sensu* Bottjer *et al.*, 2002; Martin, 1999). This scenario is also supported by the scarcity of terrestrial animals and the complete absence of insects, which are found in fossil lagoons from the Carboniferous onwards. Since there is no sedimentological evidence of a fluvial contribution, it is conceivable that the terrestrial taxa were drawn into the basin during exceptional events, such as storms and hurricanes. Whether *Scipionyx* drowned or died from other causes, remains impossible to say.

In our opinion, further work (especially in the field) is needed to evaluate the models above. For example, some crucial information supporting the model of Carannante *et al.* (2006), such as the lack of ichnofossils and the size-related distribution of body fossils on the surface of the strata, are based on observations made on a quite limited sampling area, which was "too small to offer conclusive evidence" (Signore, 2004). In addition, as admitted by Signore (2004), who co-authored the paper of Carannante *et al.* (2006), this sampling area was excavated rapidly because of an urgency to terminate the building of the basement of a water reservoir.

In the taphonomic study of *Scipionyx* we actually noticed some difference from the Solnhofen fossils (see Soft Tissue Taphonomy). In particular, the well-documented evidence that phosphorus is limited to the body of *Scipionyx* (i.e., not present in the sediment) has lead us to prefer a depositional environment of relatively shallow, open marine waters, rather than a lagoon where phosphates deriving from organic activity would have more easily accumulated. Although in a lagoon some additional factors – such as reduced vertical water remix and seasonal overheating – might favour low oxygen levels on the sea bed (Bravi & Garassino, 1998), anoxia is not at all limited, nor linked, to "closed" and/or shallow basins. Rather, it is worth to mention that in aquatic settings under normal conditions (i.e., open waters), the oxic-anoxic boundary may be at, or even above, the sediment-water interface, and that under water, most decay of carcasses is usually anaerobic (Briggs, 2003). For sure, the complete and rapid burial of *Scipionyx* in a relatively soft, muddy substrate at a single depositional event would have been conducive in greatly increasing the chances of soft tissue preservation, in saving the carcass from violent crushing, and in permitting subsequent slow, plastic, diagenetic compaction.

The fossil assemblage and palaeoenvironment

Since the site was first reported more than two centuries ago (Breislak, 1798), hundreds of fossils have been recovered from Pietraraja. The biodiversity of the site, revealed by the number of taxa found there (e.g., Fig. 14), indicates that the depositional basin was surrounded by a variety of natural settings. Below, we give a concise list of the flora and fauna so far described.

Microfossils - The site contains a significant quantity of radiolarians and spicules from siliceous sponges. Their abundance is documented also indirectly by the chert lay-

ers and nodules derived from the accumulation and natural processing of the skeletal remains of these organisms. Benthic macroforaminifers are also found in the lower and upper Pietraraja Plattenkalks. These include orbitolinids, alveolinids, miliolids and agglutinated foraminifers (Catenacci & Manfredini, 1963; D'Argenio, 1963; Bravi & De Castro, 1995; Bravi & Garassino, 1998; Carannante *et al.*, 2006; for a list of all taxa, see Lithology, Stratigraphy And Sedimentology). Planctonic foraminifers (*Praeglobotruncana* sp.) are rarer. Some layers are rich in calcareous algae (Dasycladaceae).

Plants - Fossil plants are very rare, but they are very useful palaeoenvironmental indicators. The lower portion of the upper Plattenkalk includes laminated horizons that are richer in bitumen than the regular layers and that often contain remains of terrestrial plants (Bravi & Garassino, 1998). At least two kinds of gymnosperms are represented at Pietraraja: the Cheirolepidiaceae and the Bennettitales. The former consist of loose branches belonging to the araucaria-like conifer *Brachyphyllum*; the Bennettitales are represented by abundant disarticulate foliage belonging to the genus *Podozamites*, which shows some resemblance with extant cycads. The first fossil fern, referred to the genus *Phlebopteris* (Matoniaceae), was recently reported (Bartirromo *et al.*, 2006).

Based on the different palaeobiology of these taxa, we can hypothesise the gross distribution of the vegetation with respect to the depositional basin. Probably, bennettitaleans and ferns flourished in proximity to the seashore, whereas cheirolepidiaceans, capable of inhabiting more arid settings, grew further inland. The leathery leaves of the cheirolepidiaceans, and the other strategies against evotranspiration exhibited by these plants, suggest that some 110 million years ago the Pietraraja region had a warm, dry climate for most of the year.

Invertebrates - The invertebrate records are abundant and include a dozen mollusc species, such as Nerineidae gastropods (Bravi, 1994; Marramà, pers. comm., 2007), undetermined bivalves (Bravi, 1999) and Hoplitaceae ammonites of the genus *Trochleicerus*. The presence of these taxa confirms the age of the Pietraraja Plattenkalk (Barbera & La Magna, 1999). Echinoderms are rare (Fig. 14A) and represented only by small-sized Asteroidea and Ophiuroidea (Bravi, 1999; Freels, 1975). Interestingly, 3 brand new taxa of decapod crustaceans were described by Bravi & Garassino (1998): the penaeid *Micropenaeus tenuirostris*, the caridean *Parvocaris samnitica* (Fig. 14B) and the thalassinid *Huxleyecaris beneventana*. A possible palaemonid was mentioned by Signore (2004). Other fossil specimens, which have not yet been examined in de-



Fig. 14 - A snapshot of the fossil biodiversity at Pietraraja: A) an indeterminate sea star; B) a decapod crustacean (*Parvocaris samnitica*); C) a pycnodontid fish (*Ocloedus costai*); D) a guitarfish (*Rhinobatus obtusatus*). Not to scale.

Fig. 14 - Esempi di biodiversità tra i fossili di Pietraraja: A) una stella marina indeterminata; B) un crostaceo decapode (*Parvocaris samnitica*); C) un pesce picondonte (*Ocloedus costai*); D) un pesce chitarra (*Rhinobatus obtusatus*). Proporzioni non rispettate.

tail, indicate the presence of astacid crayfish (Bravi, 1999; Marramà, pers. comm., 2007).

Fishes - Fishes are the most abundant and diversified fossil vertebrates at Pietraraja: at least 20 species belonging to 12 suprageneric taxa of cartilaginous and bony fishes have been recognised (for a complete list, see Bravi, 1999). Most coprolites, which abound in some layers of the upper Plattenkalk, can be referred to fish.

The Osteichthyes are represented by basal neopterygians (Holostei) and more derived neopterygians (Teleostei). The former include three extinct suprageneric taxa: the Pycnodontiformes (Fig. 14C), to which the genera *Paleobalistum* (D'Erasmus, 1914, 1915) and *Ocloedus* (Poyato-Ariza & Wenz, 2002) belong, have a disk-shaped, laterally flattened body, well-adapted for swimming in narrow reefs, and typical dome-shaped crushing teeth, which allowed them to feed on hard-shelled molluscs and corals. The Macrosemiiformes were small bony fish that were very common in the Cretaceous oceans of the world; at Pietraraja they are represented by *Notagogus pentlandi*, a species with a peculiar dorsal fin composed from two closely spaced lobes (Bravi, 1994). The Semionotiformes include the genus *Lepidotes*, the members of which were covered by very robust, diamond-shaped ganoid scales and are regarded as freshwater forms.

At least six suprageneric teleostean taxa are represented at Pietraraja. The Aspidorhynchiformes, such as *Belonostomus crassirostris* (Costa, 1853-1864), were slender-bodied pelagic predators – similar to extant needlefish – equipped with a long rostrum and pointed teeth. The Ichthyodectiformes, open-water predators of even larger size, are represented by the genus *Chirocentrites* and by a second ichthyodectid (Signore *et al.*, 2005) recently referred to the genus *Cladocycclus* (Signore *et al.*, 2006). Other predatory teleosteans include the elopomorph *Anaethalion* and the possibly endemic pholidophoriform *Pleuropholis decastroi* (Bravi, 1988), which is regarded a freshwater-brackish form. Another species known only in this locality is the ionoscopiform *Ionoscopus petrarajiae* (Costa, 1853-1864). The Clupeomorpha are represented by two genera: *Diplomystus*, an unspecialised form with a very convex abdomen – related to present-day sardines – and *Clupavus*, which is one of the smallest and most abundant fishes in the Pietraraja outcrop. The Chondrichthyes are represented by a fossil guitarfish, *Rhinobatus obtusatus* (Costa, 1853-1864), of which the only specimen so far recovered is remarkably articulated and well-preserved, skin remains included (Fig. 14D). This is a rare case, as the cartilaginous skeletons of the Chondrichthyes have much less chance of becoming fossilised than their bony teeth and scales.

As stated above, the submarine channel model would more easily explain the downstream occurrence of species belonging to quite different settings located at higher elevations (open sea/reef/lagoon/brackish/freshwater). In the lagoon hypothesis, on the other hand, one could assume that fish inhabiting open, deep waters reached the lagoon sporadically during catastrophic events.

Tetrapods - Although the upper Plattenkalk of Pietraraja is historically renowned for its well-preserved ichthyofauna, some tetrapods, including amphibians and reptiles,

had also been found before the discovery of *Scipionyx*. The amphibians are represented by a single specimen, the Batrachian *Celtesaurus megacephalus* (McGowan, 2002), belonging to the Albanerpetontidae – an extinct group distantly related to extant salamanders. Leathery skin, well-ossified skeletal elements, and solidly built girdles and limbs, indicate that albanerpetontids were primarily land-dwelling animals (McGowan & Evans, 1995).

Lepidosauromorph and archosauromorph reptiles are represented, respectively, by sphenodontian and squamate lizards, and by still undescribed crocodylomorphs. The Sphenodontia of Pietraraja include two different taxa, represented by two single specimens: the first one (Fig. 15) is *Derasmosaurus pietrarajae* (Barbera & Macuglia, 1988); the second one is still unnamed, but in turn preserves the remains of a small lizard, which was identified and named *Eichstaettisaurus gouldi*, within its abdominal cavity (Evans *et al.*, 2004). Besides *Eichstaettisaurus*, two other Squamata are known from the Pietraraja outcrop: *Chometokadmon fitzingeri* (Costa, 1853-1864), similar in body shape to modern scincids (Fig. 16), was considered for many years a sphenodontian, but is in fact related to the Anguimorpha, as established by a combination of cranial and postcranial characters and recent cladistic analysis (Evans *et al.*, 2006); and *Costasaurus rusconii* (Estes, 1983), represented again by a single specimen, which was a small-bodied, short-limbed animal thought originally to be an amphibian. A fourth lizard taxon awaits description.

The Crocodylomorpha of Pietraraja consist in at least two semi-complete, articulated specimens and in scattered vertebrae that probably pertain to a single Mesoeucrocodylia taxon. A peculiar feature shared by all these remains is their relatively small size, suggesting that these animals did not exceed 1.5 meters in length (Dal Sasso, pers. obs., 2001) – a similar size to extant dwarf crocodiles, dwarf caimans and the Chinese alligator.

The skull fragment that was recently tentatively referred to a juvenile pterosaur (Signore, 2004: fig. 18) must be regarded as such with caution in that it is very similar in shape and size to the lower jaw of *Belonostomus*, an aspidorhynchiform fish collected during the 2001 MSNM fieldwork and very common at Le Cavere (Dal Sasso, pers. obs., 2007; Marramà, pers. comm., 2007).

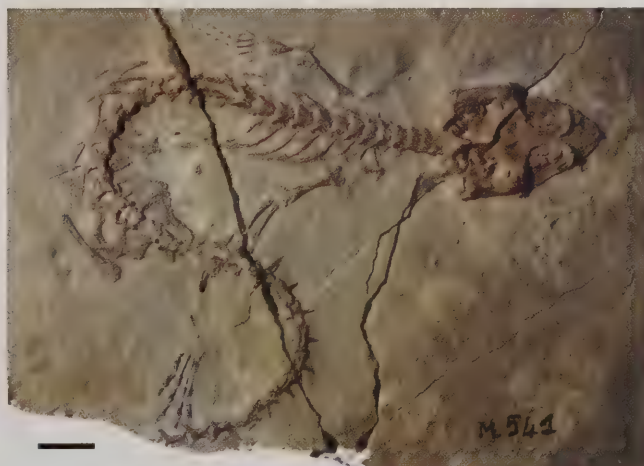


Fig. 15 - The holotype of *Derasmosaurus pietrarajae* (MPN 541), the best preserved sphenodontian from Pietraraja. Scale bar = 10 mm.
Fig. 15 - L'olotipo di *Derasmosaurus pietrarajae* (MPN 541), lo sphenodontide meglio conservato di Pietraraja. Scala metrica = 10 mm.



Fig. 16 - Lithography illustrating the holotype of the squamate *Chometokadmon fitzingeri* (MPN 539) and its integumentary remains, well-preserved on its skull and neck. (After Costa, 1853-1864).

Fig. 16 - Litografia che illustra l'olotipo dello squamato *Chometokadmon fitzingeri* (MPN 539) e i suoi resti di pelle, ben conservati sul cranio e sul collo. (Da Costa, 1853-1864).

Given that marine batrachians have never been reported, *Celtdens* is a truly important palaeoenvironmental indicator. The presence of terrestrial reptiles, along with terrestrial plants and fish genera found also in ancient freshwater settings (e.g., *Lepidotes*, *Pleuropholis*), confirms that dry land with surface freshwater was not far from the depositional basin of Pietraraja. This land must have been quite vast and persistent over time, because only under these conditions would it have been possible to create the ecological balances and complex food chains which had predatory dinosaurs at the top.

Palaeogeography

Palaeogeographical data related to the Albian age support the hypothesis that *Scipionyx* and the other terrestrial fauna of Pietraraja inhabited temporarily isolated lands that probably rose up in the Cretaceous Tethys during the Middle-Upper Aptian tectonic phases (Carannante *et al.*, 2006). Those lands were part of the Adria Plate and of the Periadriatic Domain, the continental margin of the central-western Tethys which included the present-day Adriatic Sea, Italian peninsula, Sicily, northern Tunisia, Malta,

Albania, Montenegro, Bosnia and Herzegovina, Croatia, Slovenia and the Periadriatic orogenic belt (Channel *et al.*, 1979; Zappaterra, 1990).

Cillari *et al.* (2009) have outlined the two main models for the Mesozoic geodynamic evolution of the Adria, which has been considered either an independent microplate or an African Promontory. In the first model, the Ionian Tethys is connected with the Alpine Tethys separating the Periadriatic region from Africa during Jurassic and Cretaceous times (Finetti, 2005). In contrast, the second hypothesis envisages two independent oceanic systems (Alpine Tethys and Ionian Tethys) divided by a continental crustal sector (Channel *et al.*, 1979; Rosenbaum *et al.*, 2004; Stampfli, 2005). In any case, the Periadriatic Domain was a complex puzzle of small units traditionally described as an archipelago of carbonate platforms that was well-separated from both Gondwana and Laurasia (Dercourt *et al.*, 1993, 2000; Yilmaz *et al.*, 1996; Patacca & Scandone, 2004, 2007; Zappaterra, 1990, 1994). These platforms (i.e., the Apenninic Platform, Apulian Platform, Panormide Platform, Adriatic-Dinaric Platform, Kruja Platform, Mirdita Platform and Gavrovo-Tripolitsa Platform) have been interpreted as being similar to the present-day Bahama Banks, and described as small (from

a few hundred to thousands of square kilometres), elongate, emergent islands bordered by large, shallow lagoons and biogenic margins and ramps, and separated by deep pelagic basins (i.e., the Lagonegro-Molise, Sicano, Umbria-Marche and Est Gargano basins, and the Genzana-Greco and Pindos troughs).

Within this scenario, the carbonate platform bearing the present-day Pietraraja – the Apenninic (or Laziale-Abruzzese-Campana) Platform – is assumed to have been separated in Aptian-Albian times from the adjacent Apulian Platform by the Lagonegro-Molise Basin. Evidence of this basin – in the form of a narrow, deep seaway that would have been able to produce isolation – is provided by turbidite and debris-flows deposits containing the macroforaminiferan *Orbitolina texana*, and therefore related to the Late Aptian-Early Albian age (Cati *et al.*, 1989; Zappaterra, 1990, 1994). The Apenninic Platform, not exceeding 250x200 Km in size (Nicosia *et al.*, 2007), can thus be imagined as a small island no larger than the present Sardinia. However, assuming the portion bearing the present-day Pietraraja as having been a distinct subunit (Abruzzese-Campana Platform; see D'Argenio *et al.*, 1973; Carannante *et al.*, 2006), the island could have been even smaller, like Corsica (Dal Sasso 2001, 2004).

In this geographical and environmental framework, the existence of compsognathid theropods and similar small-sized terrestrial vertebrates is acceptable, but the presence of animals such as sauropods and medium-large theropods (Nicosia *et al.*, 2007; see below) would seem to represent a problem. Actually, some sauropods, such as the South American titanosaur *Neuquensaurus australis* (body length 7-9 m, estimated body mass 3,500 kg) and the German basal macronarian *Europasaurus holgeri* (estimated adult body length 6.2 m, body mass 800 kg), reached relatively small adult body sizes (Stein *et al.*, 2010). In particular, the Upper Cretaceous (Maastrichtian) continental formations of the Hațeg Basin of Romania contain an array of relatively small-bodied dinosaur taxa, including the titanosaurian sauropod *Magyarosaurus dacus* (body mass less than 1,000 kg), the basal hadrosaurid *Telmatosaurus* and two species of the noniguanodontian euornithomorph *Zalmoxes*. These, and other taxa such as the Santonian hadrosauroid *Tethyshadros* from Italy (Dalla Vecchia, 2009) and the Hungarian ceratopsian *Ajkaceratops* (Ösi *et al.*, 2010), illustrate that dinosaurs, just like Mediterranean dwarf proboscideans, were not exempt from general ecological principles limiting body size (Stein *et al.*, 2010; and references therein).

Sedimentological evidence for long-lasting exposure of dry land in the Matese area is provided by a stratigraphic gap, which at the maximum amplitude spans from the Albian p.p. up to the Turonian p.p. times, and by vast deposits of bauxite, which also are Lower Albian in age (Bravi & Garassino, 1998; Carannante *et al.*, 2006). Actually, the deposition of the fossiliferous upper Plattenkalk deposits of Pietraraja preceded the Albian regressive event and the formation of the bauxite bedrocks (Carannante *et al.*, 1988).

Evidence from central and southern Italian dinosaur tracksites - Parallel studies of dinosaur tracksites in central and southern Italy – all discovered in recent years (Andreassi *et al.*, 1999; Gianolla *et al.*, 2000a, 2000b, 2001; Nicosia *et al.*, 2000a, 2000b, 2007; Conti

et al., 2005; Sacchi *et al.*, 2006, 2009; Petti *et al.*, 2008a, 2008b; Cillari *et al.*, 2009) – are providing information that may contribute towards a better understanding of the palaeogeography of the region inhabited by *Scipionyx*. These tracksites document the occurrence of a well-developed dinosaur fauna not only in the Apenninic (Laziale-Abruzzese-Campana) Platform, but also in some adjacent carbonate platforms of the Periadriatic Domain (Apulian Platform, Panormide Platform), at least from Tithonian to Santonian times.

As outlined above, most palaeogeographical reconstructions represent the Adria Plate and the Periadriatic Platforms as isolated areas separated from main continental dry lands by deep pelagic basins from the Pliensbachian to the Coniacian – a long interval of about 130 My (Nicosia *et al.*, 2007). Nevertheless, the new palaeontological finds in central and southern Italy indicate that the Periadriatic Platforms were never completely separated by deep seaways (Nicosia *et al.*, 2007). Co-occurrence of analogous dinosaur assemblages in different platforms led also to hypothesise that some sort of geographical connection above sea level existed, at least for certain periods. For example, the Latial ichnosite of Esperia (Petti *et al.*, 2008b) is coeval with the Apulian dinosaur tracksite of Bisceglie (Sacchi *et al.*, 2006), and both show the presence in Aptian times of theropods and sauropods with similar characters. Such faunal affinity was recently interpreted as an evidence of there having been at least temporary land bridges between the Apenninic and the Apulian platforms during the Aptian (Petti *et al.*, 2008b). Under this perspective, the Laziale-Abruzzese part of the Apenninic Platform is considered as having been a promontory of the Apulian main bank, which probably acted as a barrier between the northern Umbria-Marche Basin and the southern Lagonegro-Molise Basin. This suggests that the ancestors of *Scipionyx*, and maybe *Scipionyx* itself, would not have been isolated from the neighbouring platforms for a long time.

Similarly to Sacchi *et al.* (2009), we point out that the present knowledge of dinosaur occurrence in the Italian Periadriatic platforms is surprising and in definite contrast with the idea of a continuous marine environment. The amount of evidence on subaerial emergences – already well-highlighted by a long list of data in a recent paper (Nicosia *et al.*, 2007) – increases considerably when the whole Periadriatic region, including the Istrian Peninsula and Croatia, is considered (Mezga & Bajraktarević, 1999; Dalla Vecchia, 2002, 2009; Mezga *et al.*, 2006, 2007). Thus, a model is needed that takes into consideration the timing of the arrival of dinosaurs in central and southern Italy, their possible immigration route and the possibility for dinosaur assemblages to persist in confined areas. This was attempted by Sacchi *et al.* (2009), using the footprint-bearing Aptian levels at Bisceglie (Apulia, southern Italy), which occur intermittently within exclusively marine successions. The presence of the dinosaur footprints could be explained by two completely different hypotheses: they might represent either the remaining traces – biased by preservation windows – of a long-persisting autochthonous association, or evidence for repeated immigration events that were influenced by a filtering bridge. Analysis of all the available evidence, such as the scattered occurrence of the tracks, the diversity of the dinosaurs, the type of recorded environment, the type of diets, the

absolute and relative dimensions of the track makers and the dimension of the available areas (Sacchi *et al.*, 2009), tends to exclude the presence of a long-lasting coevolved association. It does support, however, the occasional co-occurrence of taxa taking place on account of separate migration events occurring over a period of least 70 million years: in this model, dinosaurs would have been able to immigrate into the carbonate platforms of the Periadriatic area but not to survive there for a time long enough to allow for their co-evolution.

Co-evolution seems to be questioned also by a second example. The Apulian dinosaur ichnocoenoses of Mattinata (Late Jurassic), Borgo Celano (Early Cretaceous) and Altamura (Late Cretaceous) differ from one another but correspond in faunal composition and evolutionary level to age-equivalent dinosaur communities known from Europe, central Asia and North America (Conti *et al.*, 2005). Therefore, it is difficult to accept the hypothesis of a parallel evolution on the mainland and in isolated areas.

In this scenario, the temporary land connections that permitted the dispersal of dinosaurs within the area are considered by Sacchi *et al.* (2009) as real filtering-bridges. The repeated occurrence of the complex biota known to have occurred supports the hypothesis that there were large, directly linked, unstressed biological “reservoirs” that could re-inject plant and animal populations after local extinction events. These ephemeral filtering-bridges, while leaving seaways for the east-west spreading of marine animals, would have allowed “pre-adapted” dinosaurs to reach the Periadriatic platforms in a north-south route. Moreover, repeated connections among the platforms themselves are hypothesised to have possibly acted as a physical and environmental continuum, i.e. as walkways between a land mass and the Periadriatic carbonate platforms during most of the Cretaceous (Sacchi *et al.*, 2009). The same dispersal mechanism is suggested also by Dalla Vecchia (2002, 2009), albeit with another terminology, when he interpreted these ephemeral islands as having been stepping stones for “island hopping” of dinosaurs across the Tethys.

Taking the filtering-bridges model as the most probable, the problem of the dinosaurs’ origin remains open – where did *Scipionyx*, and other Italian dinosaurs of the Cretaceous, come from? The fact that the Periadriatic platforms were certainly bordered to the north by the Ligure-Piemontese Ocean at least until the Turonian (e.g., Mindszenty *et al.*, 1995), places the “homeland” of Italian Cretaceous dinosaurs along the northern margin of Gondwana. For the same reason, putative connections with Laurasia (Evans *et al.*, 2004) or alternative north-south routes via Iberia (Serenio *et al.*, 1994) are very unlikely (Nicosia *et al.*, 2007; Canudo *et al.*, 2009). In fact, current understanding dates the last connection of the Adria Plate to Laurasia – before their ultimate aggregation in the Late Cretaceous – at Jurassic times, during the Bathonian (Schettino & Scotese, 2002).

These constraints gave rise to new palaeogeographical models of the western Tethys (Bosellini, 2002; Dalla Vecchia, 2002, 2005; Conti *et al.*, 2005; Nicosia *et al.*, 2007; Turco *et al.*, 2007; Petti *et al.*, 2008; Sacchi *et al.*, 2009), most of which incorporate a possible filtering bridge between the African continent and the Periadriatic platforms (Fig. 17). Such a hypothesis has been recently refreshed after the description of a titanosaur-like dinosaur track in

the Cenomanian of Sezze (Latina, central Italy), which is part of the Apenninic Platform (Nicosia *et al.*, 2007), and the very recent discovery of a theropod bone in Cenomanian peritidal levels of Capaci (Palermo, Sicily), an area that belongs geologically to the Panormide Platform (Garilli *et al.*, 2009). The geodynamic evolution of the Panormide Platform, as inferred by Zarcone & Di Stefano (2008), as well as the dinosaur fossil record of the region (Petti *et al.*, 2008b; Cillari *et al.*, 2009), is consistent with a crustal sector of land connecting Africa to Adria above sea level, and separating the Ionian Tethys from the Alpine Tethys during most of the Cretaceous period.

Palaeobiogeographical remarks - The palaeogeographical scenario of a variable number of islands arranged in a “string of pearls” between the Gondwanan and Laurasian mainlands was often the basis for explaining some peculiar features of the Cretaceous terrestrial vertebrates found in the Periadriatic region and in other similar domains. The faunas of the region have been described as depauperate (Benton *et al.*, 1997), relict (Signore *et al.*, 2001; Evans *et al.*, 2004), endemic (Grigorescu *et al.*, 1999; Dal Sasso, 2001, 2004) and dwarf (Benton *et al.*, 1997; Jianu & Weishampel, 1999; Dalla Vecchia *et al.*, 2000, 2001; Dal Sasso, 2001, 2004; Dalla Vecchia, 2002, 2009). The presence of dwarf and endemic faunas has been considered as further evidence of life in confined, isolated environment.

The taxon Compsognathidae is a clade of small coelurosaurs presently known from the Late Jurassic and Early Cretaceous. As one can see from the following list, the oldest evidence in the fossil record is from the Late Jurassic of Germany and, possibly, Portugal:

Juravenator starki - Kimmeridgian, Germany (Göhlich & Chiappe, 2006)

Compsognathus longipes - Kimmeridgian, Germany; Tithonian, France (Peyer, 2006)

compsognathid teeth - Kimmeridgian, Portugal (Zinke, 1998)

cf. Aristosuchus - Berriasian, Romania (Benton *et al.*, 1997)

Aristosuchus pusillus - Barremian, England (Naish *et al.*, 2001)

Sinosauropteryx prima - Barremian/Aptian boundary-Aptian, China (Xu & Norell, 2006)

Sinocalliopteryx gigas - ?Barremian/Aptian boundary, China (Xu & Norell, 2006)

Huaxiagnathus orientalis - Barremian/Aptian boundary, China (Xu & Norell, 2006)

Scipionyx samniticus - Albian, Italy (Dal Sasso & Signore, 1998a)

Mirischia asymmetrica - ?Albian, Brazil (Naish *et al.*, 2004)

Scipionyx samniticus was found in an outcrop of Albian age, a time when compsognathids were already differentiated and widespread. Its basal position on the cladogram suggests that *Scipionyx* could represent a relict clade of basal compsognathids that perhaps retained primitive features as a consequence of a separate evolutionary path. Its generally plesiomorphic condition in respect to all other compsognathids, however, might be partly due to the early ontogenetic stage of the only known individual (See Ontogenetic Assessment, Phylogenetic Analysis).

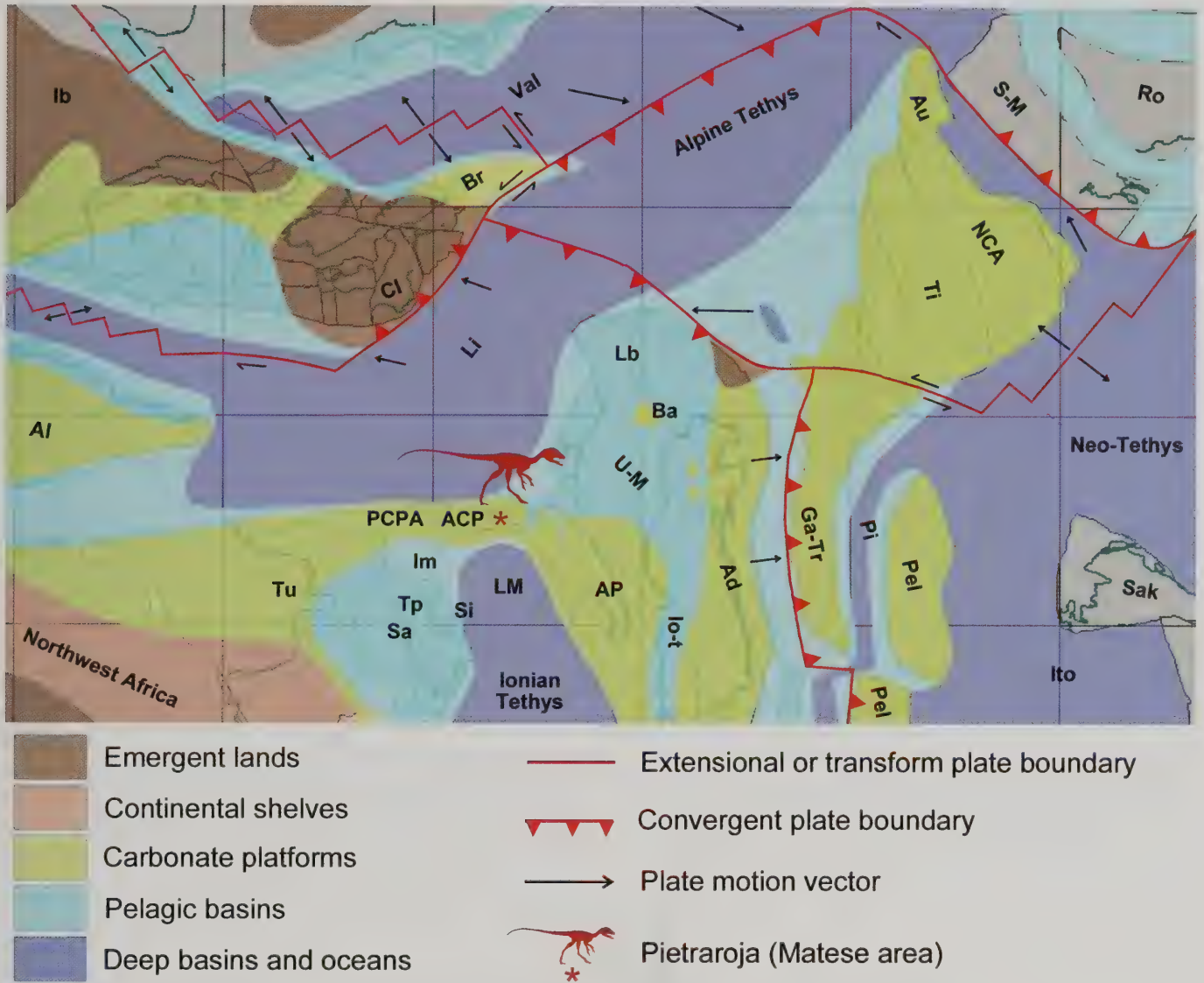


Fig. 17 - Palaeogeographic map of the Periadriatic Domain (the present Central Mediterranean area) in the central-western Tethys, during the Aptian (120 Mya). Abbreviations: ACP Apenninic Carbonate Platform (Laziale-Abruzzese-Campana Platform); Ad Adriatic-Dinaric Platform; Al Algeria; AP Apulian Platform; Au Austroalpine; Ba Bagnolo Platform; Br Briançonnais; Cl Calabria; Ga-Tr) Gavrovo-Tripolitsa Platform; Ib Iberia; Im) Imerese Basin; Io-t) Ionian trough; ITO) Inner Tauride Ocean; Lb) Lombard Basin; Li) Ligure-Piemontese Ocean; LM) Lagonegro-Molise Basin; NCA) Northern Calcareous Alps; PCPA) Panormide Carbonate Platform; Pel) Pelagonian; Pi) Pindos trough; Ro) Rodope; Sa) Saccense Pelagic Plateau; Sak) Sakarya; Si) Sicano Basin; S-M) Serbia-Macedonia; Ti) Titsa; Tp) Trapanese Pelagic Plateau; Tu) Tunisia; U-M) Umbria-Marche Basin; Val) Valais Ocean. (Modified after Turco *et al.*, 2007; Cillari *et al.*, 2009).

Fig. 17 - Carta paleogeografica del Dominio Periadriatico (l'attuale Mediterraneo centrale) nella Tetide centro-occidentale, durante l'Aptiano (120 milioni di anni fa). Abbreviazioni: ACP) Piattaforma Carbonatica Appenninica (Laziale-Abruzzese-Campana); Ad) Piattaforma Adriatico-Dinarica; Al) Algeria; AP) Piattaforma Apula; Au) Austroalpino; Ba) Piattaforma di Bagnolo; Br) Brianzonese; Cl) Calabria; Ga-Tr) Piattaforma di Gavrovo-Tripolitsa; Ib) Iberia; Im) Bacino Imerese; Io-t) Fossa Ionica; ITO) Oceano Interno della Tauride; Lb) Bacino Lombardo; Li) Oceano Ligure-Piemontese; LM) Bacino Lagonegro-Molisano; NCA) Alpi Calcaree Settentrionali; PCPA) Piattaforma Carbonatica della Panormide; Pel) Pelagoniano; Pi) Fossa di Pindos; Ro) Rodope; Sa) Plateau Pelagico Saccense; Sak) Sakarya; Si) Bacino Sicano; S-M) Serbia-Macedonia; Ti) Titsa; Tp) Plateau Pelagico Trapanese; Tu) Tunisia; U-M) Bacino Umbro-Marchigiano; Val) Oceano Vallese. (Modificato da Turco *et al.*, 2007; Cillari *et al.*, 2009).

Studying the Pietraraja herpetofauna, Evans *et al.* (2004) noted that the only known amphibian, the albanerpetontid *Celtesdens*, had its closest relatives in Britain (Berriasian, Purbeck Limestone) and Spain (Barremian, Las Hoyas), and that *Derasmosaurus* is regarded as “one of the last recorded rhynchocephalians from Laurasia” (albeit that southern Italy is a Gondwanan domain). Moreover, the presence of *Eichstaettisaurus* would provide another archaic “Laurasian link” with both Germany (Tithonian, Solnhofen) and Spain (Ber-

riasian, Montsec), suggesting that at Pietraraja “the recovered tetrapod fauna is primarily Laurasian in character” (Evans *et al.*, 2004).

Following Nicosia *et al.* (2007), we remark that that statement points to a problematic connection northwards to Laurasia, which, based on the present palaeogeographical knowledge, is quite unlikely since Jurassic times (see above). Therefore, the conclusion of Evans *et al.* (2004) is evidence of a palaeontological problem. As stated by Xu (2010), “prevailing biogeographical hypotheses of

European isolation seem to be at least partly a product of incomplete fossil sampling” (i.e., too scattered findings or too few known outcrops), “a factor that has bedevilled biogeographical investigations of many dinosaur groups”. The Lagerstätten are rare windows of preservation. Just for that reason, by preserving the delicate remains of small-sized taxa, which elsewhere would not have had the possibility to fossilise in the given time, those exceptional palaeontological sites may induce to infer faunal similarity among distant localities. Those taxa, as the Lagerstätten suggest, might instead have been more spread out. Like other small terrestrial reptiles, compsognathid theropods occur in Solnhofen, Pietraraja, Araripe and Liaoning not because they lived only there, but because, having small delicate skeletons, they had more chance of becoming preserved in the fine sediments that produced those deposits. In fact, from the list above it is inferred that during the Cretaceous, the Compsognathidae might have reached a cosmopolitan distribution: once they appeared, probably in the Middle-Late Jurassic of western Laurasia (Germany, France, ?Portugal), they remained there for a long time (England), and contemporarily they spread up to the western limits of Laurasia (China), moving also to Gondwana lands (Brasil) and to their continental margins (Pietraraja).

Many recent finds – such as the ceratopsian *Ajkaceratops* in Hungary (Ösi *et al.*, 2010), a leptoceratopsid in Sweden (Lindgren *et al.*, 2007), the alvarezsaurid *Albertonykus* in Canada (Longrich & Currie, 2009), the therizinosauroids *Nothronychus* and *Falcarius* in USA (Kirkland & Wolfe, 2001; Kirkland *et al.*, 2005), the centrosaurine ceratopsid *Sinoceratops* in China (Xu *et al.*, 2010), and the reinterpreted Gondwanan, rather than endemic Australian, dinosaurs (Agnolin *et al.*, 2010) – indicate that the biogeography of a number of taxa was in

fact cosmopolitan rather than regional, and demonstrate that any palaeobiogeographical inference must be made with caution.

For all these reasons, we agree with Evans *et al.* (2004) on the relevance of temporal divergence between the taxa from Pietraraja and from other localities more than on their palaeogeographical meaning. For example, the Italian *Eichstaettisaurus* (*E. gouldi*) undoubtedly provides a significant extension to the temporal range of *Eichstaettisaurus*, given that it is separated from the Solnhofen *Eichstaettisaurus* (*E. schroederi*) by a temporal gap of more than 40 million years (Gradstein *et al.*, 2004) and that the morphological differences with *E. schroederi* are minor and do not justify distinction at the generic level (Evans *et al.*, 2004). Although the persistence of fauna under isolating conditions for more than 40 million years seems improbable at best, we agree with Evans *et al.* (2004) that the Pietraraja assemblage may represent a relictual fauna. The central-western Tethys archipelago may explain the relatively archaic character of Early Cretaceous lepidosaurian assemblages, regardless of their ancestors having been Laurasian or Gondwanian, or even cosmopolitan.

Therefore, *Scipionyx samniticus* might have been either an endemic species or simply a more widely spread, Late Jurassic-Early Cretaceous compsognathid stock that had become geographically isolated and relict in the Apennine platform, and maybe in other Periadriatic platforms, too. Insular dwarfism, as previously suggested for *Scipionyx* (Dal Sasso, 2001, 2004) and observed in other dinosaurs (Benton *et al.*, 1997; Jianu & Weishampel, 1999; Dalla Vecchia *et al.*, 2000, 2001; Dalla Vecchia, 2002, 2009; Sander *et al.*, 2006) cannot be ruled out. However, given the averagely small size of compsognathids, this seems an unnecessary survival strategy for the taxon.

MATERIAL

The holotype and only known specimen of *Scipionyx samniticus* is housed at the Soprintendenza per i Beni Archeologici di Salerno, Avellino, Benevento e Caserta with the inventory number SBA-SA 163760. The original slab of fine-grained, grey-yellowish limestone, which at the moment of its find embedded the dinosaur, was collected in at least three broken

pieces. The original adjoining slabs, which probably preserved the distal elements of the hindlimbs and the remaining tail, were unfortunately not collected. The specimen was subsequently completed with other slabs (Figs. 9, 10) collected from the same locality, but originating from different layers (Todesco, pers. comm., 1993).

METHODS

Preparation

In 1993, the fossil appeared lying on a composite slab covered by a layer of sticky vinylic glue (Fig. 18). Just after collecting the specimen, Todesco (pers. comm., 1993) had prepared it roughly with chisels under the naked eye. The abundant glue and some unremoved matrix prevented clear observation of the anatomy of the specimen (Fig. 19A). The specimen also displayed an unusually short, non-segmented and seemingly stiffened tail. This tail was actually an artefact created with polyester resin by the collector (Todesco, pers. comm., 1993).

Restoration and complete preparation of the fragile bones and delicate internal organs involved removal of the

glue and consolidation with proper resin (Paraloid B72). Removal of the false tail revealed a few real tail vertebrae underneath the “connection” point. As mentioned above, these interventions were performed in Salerno between 1994 and 1997, but always entrusted to the Laboratory of Palaeontology of the MSNM.

Scipionyx was properly prepared using only manual mechanical techniques under an optical stereomicroscope (magnification of 10 to 60x). Very small chisels and then increasingly finer steel needles were employed (Fig. 20). In order to avoid damage to, and contamination of, the organic remains, acid preparation was never used. Despite very careful preparation, no integumentary structure, such as scales or protofeathers, were discovered (Dal Sasso, pers. obs., 1993-2010).



Fig. 18 - The Pietraraja theropod in the spring of 1993. Note the artificial tail, nestled in a groove to mimic excavation, and connected to the last preserved caudal vertebra (arrow).

Fig. 18 - Il teropode di Pietraraja nella primavera del 1993. Si noti la coda artificiale, inserita in un solco scavato per simularne l'estrazione, e collegata all'ultima vera vertebra caudale conservata (freccia).

Optical microscopy

To observe the anatomical features in this small-sized specimen, we used a Leica MZ9-5 stereomicroscope equipped with a plan 1.0x lens, 10/20x oculars, and a 0.63 to 6.0 zoom. A Wild Heerbrugg TYP 308700 camera lucida was mounted on top for detailed drawings.

Photographs and drawings

The photographs published in this monograph were taken at different times (1993-2010) with both analog and digital cameras. A camera was mounted on top of the stereomicroscope for close-ups in visible light. Photographs under ultraviolet (UV) light were taken with a digital SLR camera equipped with a UV Hoya filter. Drawings of detailed views were created using a camera lucida; all other drawings were based on printed photographs taken under different (usually opposite) oblique light. Most illustrations were drawn by Marco Auditore, who worked closely with the authors. A complete list of authors of the published photographs and drawings can be found on the title page verso (Illustration Credits).

In all of the original line drawings of *Scipionyx* published herein, bold lines indicate the visible limits of a

given element, thin lines indicate anatomical structures within a given element, and hatched lines indicate the estimated limits of an element overlain by others.

Measurements

Measurements were taken with a digital caliper and a goniometer; micro-measurements were obtained with an optical micrometer. If not specified, length of a given complete/fragmentary element indicates its maximum length, and its height or width or diameter were taken perpendicular to the maximum length. If not specified, diameter refers to both craniocaudal or mediolateral measurements, or to any intermediate plane, according to the exposed view of the given element. Measurements and ratios cited in the text are grouped in Tables 1-3.

UV light analysis

Fossils from some Mesozoic Lagerstätten (Solnhofen, Liaoning) can reveal exceptional morphological details when observed under UV light. Delicate bones, tiny sutures and, in particular, remains of soft body parts that are often poorly discernible or cannot be seen in visible light,

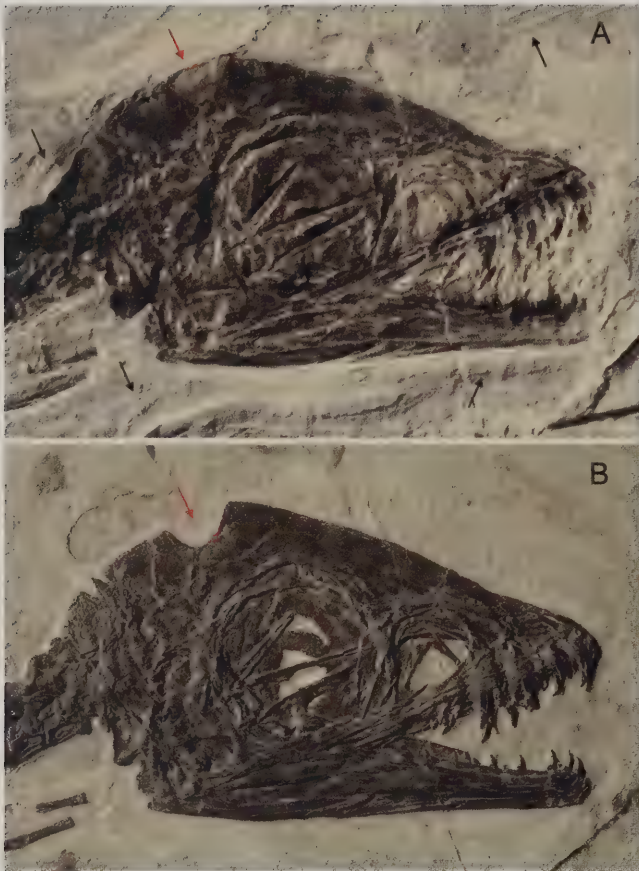


Fig. 19 - The skull of *Scipionyx samniticus* before (A) and after (B) final preparation. Note the U-shaped frontoparietal gap (red arrow), formerly interpreted as damage occurring prior to professional preparation, but actually untouched by the collector's home-made tools (black arrows, scratches made by the tools).

Fig. 19 - Il cranio di *Scipionyx samniticus*, prima (A) e dopo la preparazione finale (B). Si noti lo spazio frontoparietale (freccia rossa), inizialmente imputato ad un danneggiamento precedente alla preparazione finale e invece non toccato dagli strumenti artigianali dello scopritore (solchi indicati dalle frecce nere).

fluoresce conspicuously under filtered UV (e.g. Tischlinger, 2002; Frey *et al.*, 2003; Hone *et al.*, 2010). This technique can be used to show otherwise hidden bony sutures, and to distinguish bones or soft parts from the underlying matrix and from each other.

When examining and photographing *Scipionyx samniticus* under UV light, we obtained very similar and highly informative results. Under black light blue lamps (Philips TL 8W/08 F8 T5/BLB), the bones of *Scipionyx* are opaque brown and the soft tissues fluoresce in colours varying from white-gold to blue-indigo. According to previous studies (e.g., Hone *et al.*, 2010), the variety of colours is caused by a combination of different absorption and reflectance of the various minerals that comprise the specimen and the surrounding matrix. For instance, bones (notably excluding their epiphyses; see Appendicular Articular Cartilages) appear relatively uniform in colour and reflectance, indicating homogeneous preservation; patches of most soft tissues are seen as a bright fluorescence, suggesting that they are phosphatised (Hone *et al.*, 2010). Other tissues, such as the liver remains, fluoresce darkly because of pigment remains (Ruben *et al.*, 1999). Glue, as well as restored parts and other artefacts made by synthetic materials, fluoresce light blue.



Fig. 20 - The restoration and complete preparation of the tiny *Scipionyx* and its delicate internal organs, done entirely under the optical stereomicroscope with manual mechanical techniques, required about 300 hours.

Fig. 20 - Il restauro e la preparazione completa del piccolo *Scipionyx* e dei suoi organi interni sono stati condotti sempre sotto uno stereomicroscopio ottico, con tecniche meccaniche manuali, e hanno richiesto circa 300 ore di lavoro.

CT scan analysis

The specimen was analysed by X-ray computed tomography (CT) at the Radiology Department, Ospedale Maggiore, Milan. The equipment used consisted in a Siemens Somatom Definition Dual Source CT Scanner. The best CT imaging was obtained with a bone algorithm on transverse (axial) slices, with scan parameters 120 kV, 120 mA, and slice thickness of 0.3 mm. Data was exported in DICOM format using eFilm (v. 1.5.3, Merge eFilm, Toronto). Analysis and post-processing were performed by Armando Cioffi, Siemens, Milan. In general, CT scanning did not provide high resolution images of the tiny bones of *Scipionyx*. The extreme mediolateral diagenetic flattening of the specimen was a complicating factor. Nevertheless, this analysis was crucial in the understanding of some obscured features of the skull, the path of the intestinal loops and, especially, the proximal shape of the ischia, which are intimately sandwiched in between the two femoral shafts.

SEM analysis

Scanning electron microscopy (SEM) images and elemental peaks were obtained by analysing microsamples with a Jeol JSM 5610 LV (IXRF Systems Inc.) equipped

with an EDS 500 spectrometer. The instruments are property of the MSNM, and are housed in the Electron Microscope Laboratory of our institute. The microsamples, no more than 0.5-0.7 mm in diameter each, were taken from carefully selected areas of the specimen (see Appendix 7) with the following procedure. The microsamples were obtained mechanically through shallow incisions made with a tiny widia blade. Uplift, rather than a cutting motion, was used in order to favour detachment running as much as possible along the natural lines of separation of the biological structures (for example, the endomysium-sarcolemma of the muscle fibres). A steel point dipped in Plasticine was used to pick up and drop the microsamples immediately onto a double-sided carbon tape adhering to the centre of the SEM sample holders (pin stubs). Most of the microsamples were fixed in a reversed position on the double-sided tape surface in order to expose their “naturally” detached surfaces. This is crucial not only for observing biological elements completely void of artefacts, but also for the element microanalysis. As the spectrometer of the SEM microprobe can analyse only surface layers, it is important to examine the internal surface of freshly fragmented samples to minimise the risk of detecting exogenous contaminants (Schweitzer *et al.*, 2008). Initial screening was performed on uncoated specimens; subsequently, the samples were gold-coated in order to enhance their conductivity to the electrons beamed by the SEM, which produced images with a definitely higher definition. Both SEM analysis and post-processing were performed by Michele Zilioli (MSNM).

Anatomical terms

We refer to the margins and surfaces of the bones according to their orientation *in vivo*, independently of the position they assumed during fossilisation. Following Weishampel *et al.* (2004), we adopt the terminology of the *Nomina Anatomica Veterinaria* (AAVV, 2005) and the *Nomina Anatomica Avium* (Baumel *et al.*, 1993): ventral (towards the belly), dorsal (towards the back), cranial (towards the head), caudal (towards the tail), medial (towards the midline) and lateral (away from the midline). Thus, lateral can also indicate surfaces or structures internal to the bone, exposed by the removal of other, covering bony layers.

In describing head elements, the term cranial was replaced by rostral (towards the tip, or rostrum, of the head), the term cranial having no meaning with respect to the head itself. Proximal (towards the mass of the body) and distal (away from the mass of the body) are used to designate appendages, like segments or elements of a limb, and also regions of the tail (e.g., proximal, middle and distal caudal vertebrae). For the manus, palmar is used to designate the surface directed towards the ground, and dorsal is used for the opposite surface.

Concerning the orientation of the teeth within the jaws, we followed the dental nomenclature specified by Edmund (1969; see also Smith & Dodson, 2003): mesial (the edge of a tooth towards the symphysis or premaxillary midline), distal (the edge away from the symphysis along the tooth row), labial (the surface of a tooth towards the lip or the cheek) and lingual (the surface towards the tongue).

Finally, for vertebrae and ribs we adopted the terms specified by O'Connor (2007), and for vertebral laminae and fossae we followed Wilson (1999); for the gastralia we adopted the terminology of Claessens (2004), whereas we followed Carrano & Hutchinson (2002) in the nomenclature of pelvic and hindlimb muscles. The terminology we used for all other soft tissues is the one that the authors mentioned in the text use in describing homologous elements *in vivo* in extant vertebrates.

Systematic terms

The systematic terms, if not differently indicated, are referred to Senter (2007) and Holtz *et al.* (2004).

Anatomical abbreviations

All anatomical abbreviations used in the text and in the illustrations are listed in alphabetical order in the cover flaps (small font size) and in Appendix 1 (normal font size).

Institutional abbreviations

BSP	Bayerische Staatssammlung für Paläontologie und historische Geologie, München, Deutschland
CEUM	College of Eastern Utah Museum, Price, USA
DINO	Dinosaur National Monument, Jensen, USA
FIP	Florida Institute of Paleontology, Dania Beach, USA
FMNH	Field Museum of Natural History, Chicago, USA
IPFUB	Institut für Geologische Wissenschaften der FU Berlin, Fachbereich Paläontologie, Berlin, Deutschland
IVPP	Institute of Vertebrate Paleontology and Paleoanthropology, Beijing, China
MGI	Mongolian Geological Institute, Ulaanbaatar, Mongolia
ML	Museu da Lourinhã, Portugal
MNHN	Muséum National d'Histoire Naturelle, Paris, France
MPN	Museo di Paleontologia, Napoli, Italia
MSNM	Museo di Storia Naturale di Milano, Milano, Italia
NIGP	Nanjing Institute of Geology and Paleontology, Nanjing, China
NMC	Canadian Museum of Nature, Ottawa, Canada
RTMP	Royal Tyrrell Museum of Palaeontology, Drumheller, Canada
SBA-SA	Soprintendenza per i Beni Archeologici di Salerno Avellino Benevento e Caserta, Salerno, Italia



Fig. 21 - Overall view of the holotype (and only known specimen) of *Scipionyx samniticus*. Scale bar = 20 mm.

Fig. 21 - Vista generale dell'olotipo (e unico esemplare conosciuto) di *Scipionyx samniticus*. Scala metrica = 20 mm.

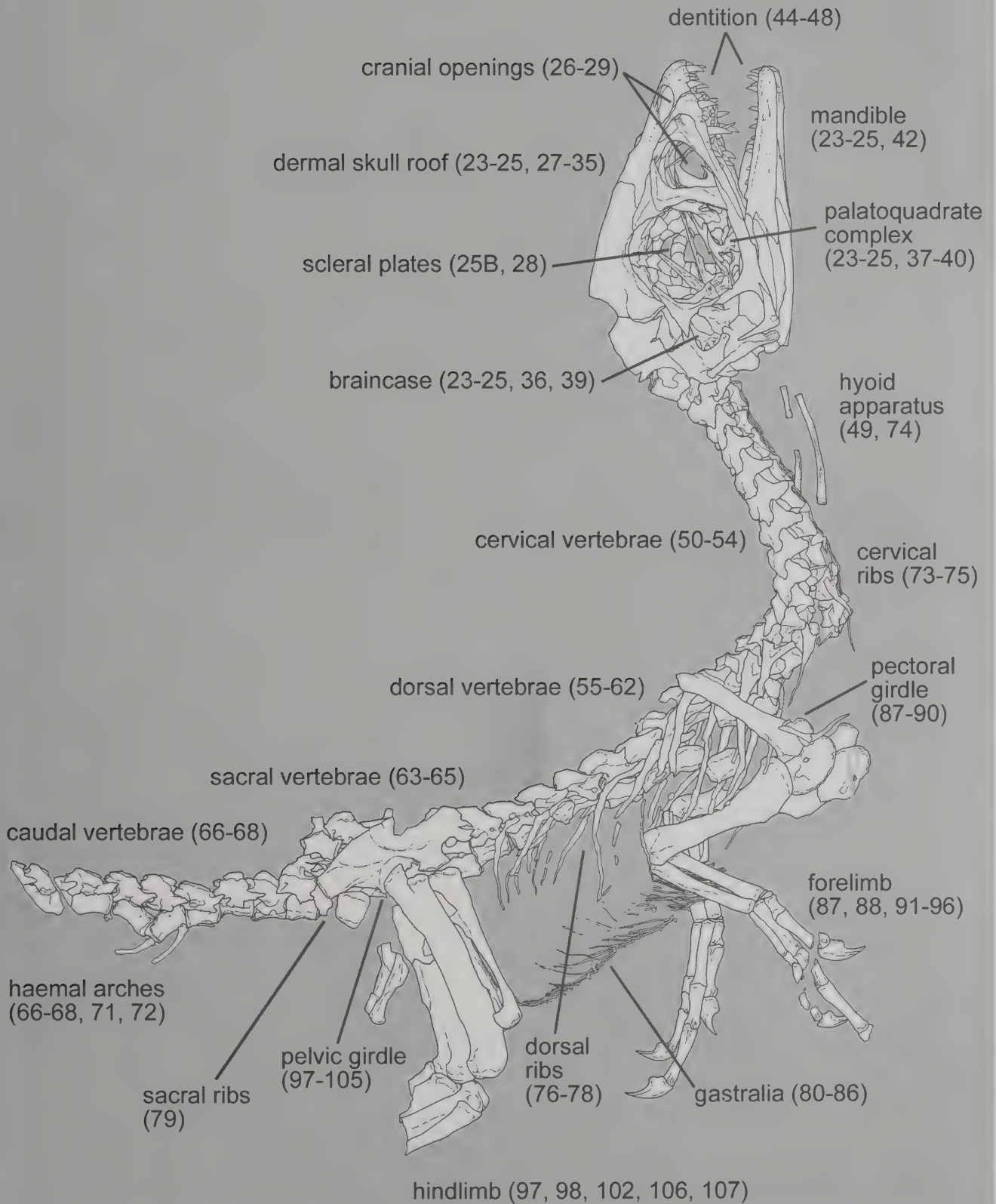


Fig. 22 - Synoptic table of the osteology of *Scipionyx samniticus* (titles of chapters/subchapters for labels, related figures given in brackets). Soft tissues have been omitted from this line drawing.

Fig. 22 - Quadro d'unione dell'osteologia di *Scipionyx samniticus* (nomenclatura conforme ai titoli dei capitoli/sottocapitoli, figure correlate fra parentesi). In questo disegno al tratto sono stati omessi i tessuti molli.



Fig. 23 - Skull and mandible of *Scipionyx samniticus*. Scale bar = 10 mm.

Fig. 23 - Cranio e mandibola di *Scipionyx samniticus*. Scala metrica = 10 mm.

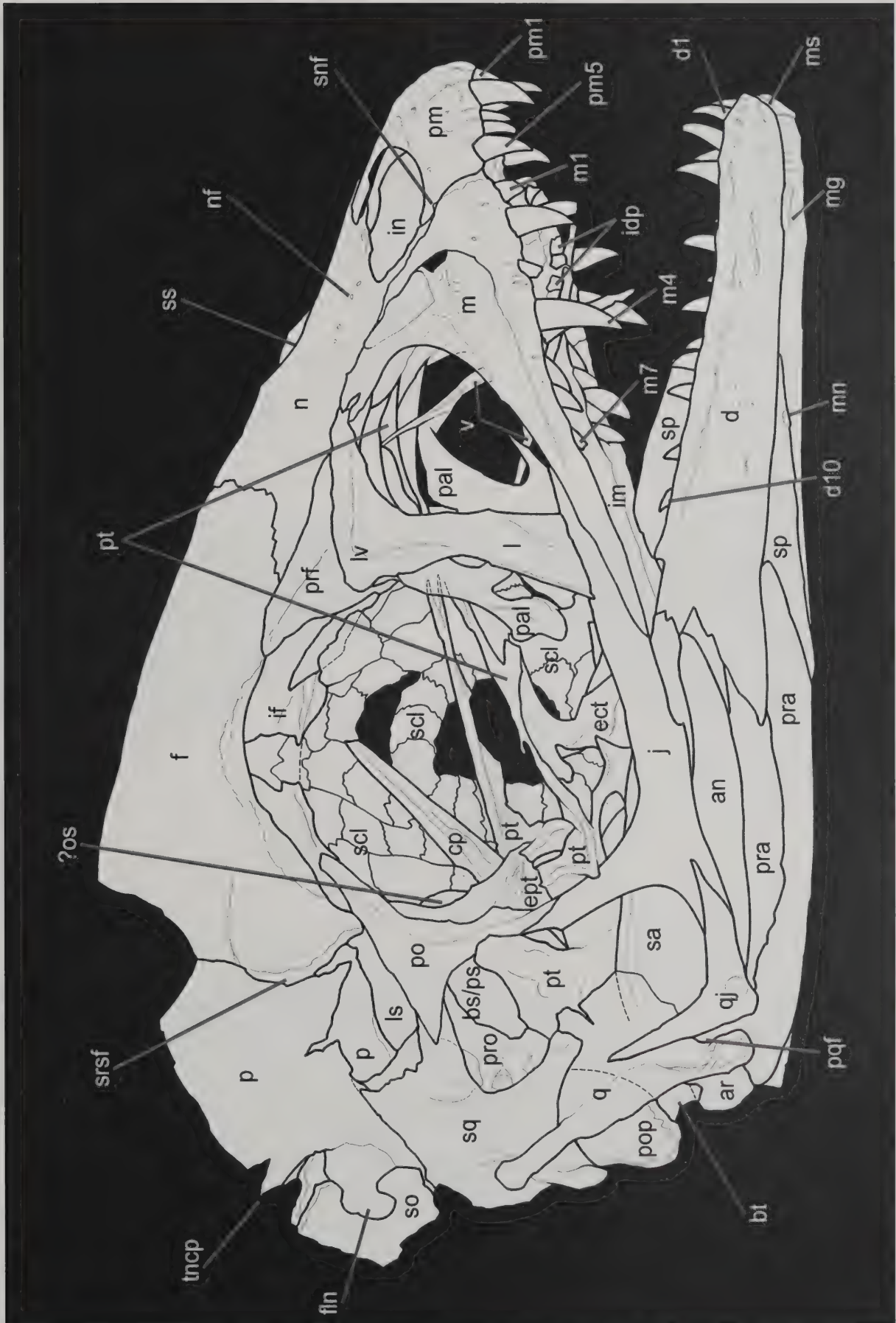


Fig. 24 - Line drawing of the bones illustrated in Fig. 23. Black areas indicate the matrix. See Appendix 1 or cover flaps for abbreviations.
 Fig. 24 - Disegno al tratto delle ossa illustrate in Fig. 23. Lo sfondo nero indica la matrice. Vedi Appendice 1 o risvolti di copertina per le abbreviazioni.

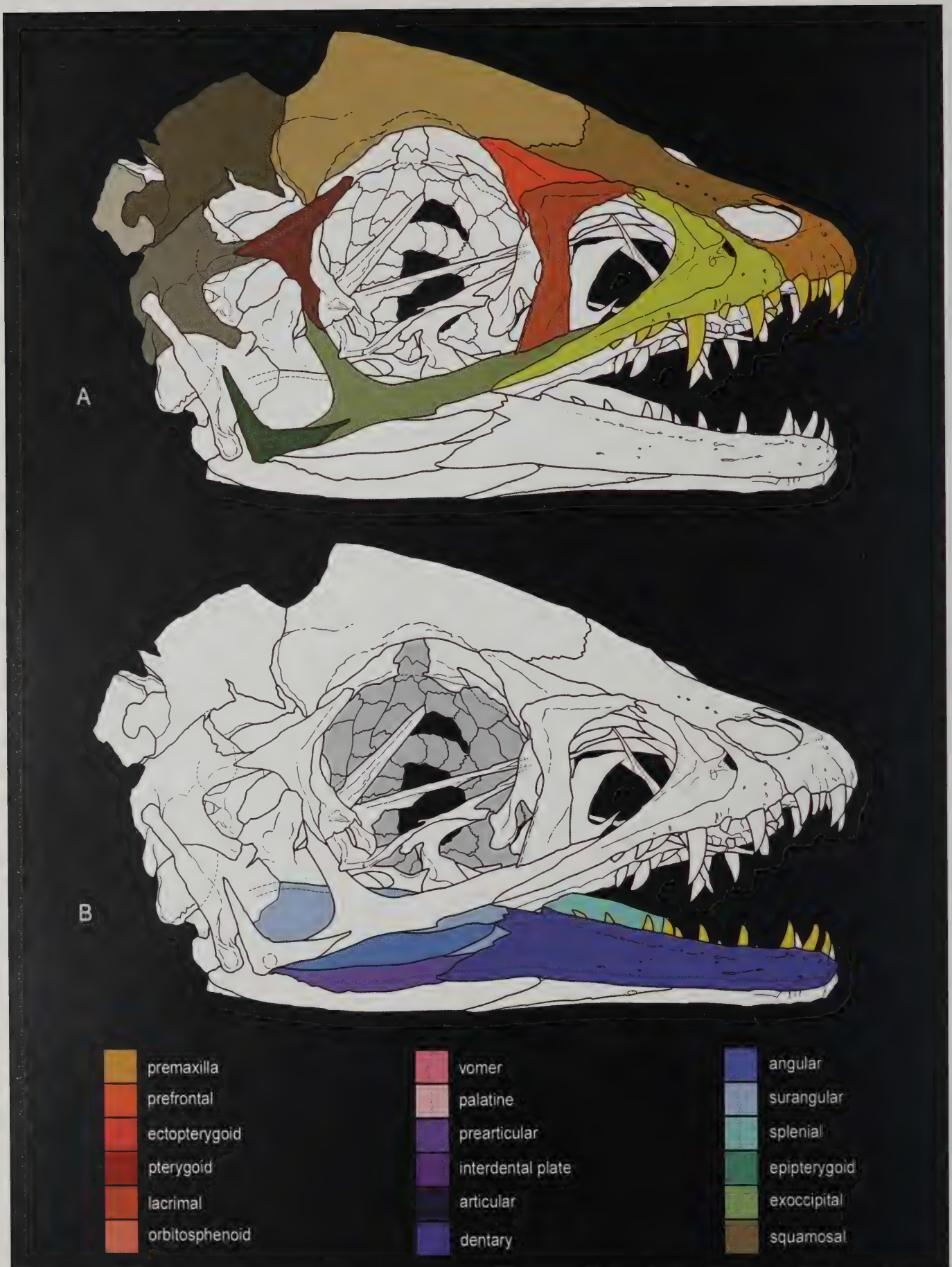


Fig. 25 - Cranial and mandibular bones of *Scipionyx samniticus*. A) right outer elements of the skull; B) scleral plates and right hemimandible. / Ossa del cranio e della mandibola di *Scipionyx samniticus*. A) elementi esterni del lato destro del cranio; B) placche sclerali ed emimandibola destra.



Fig. 25 - Cranial and mandibular bones of *Scipionyx samniticus*. C) right and unpaired inner elements of the skull; D) left elements and indeterminate bones. / Ossa del cranio e della mandibola di *Scipionyx samniticus*. C) elementi interni del lato destro, ed elementi impari del cranio; D) elementi del lato sinistro e ossa indeterminate.

PART I - OSTEOLOGY

Systematic Palaeontology

DINOSAURIA Owen, 1842

SAURISCHIA Seeley, 1887

THEROPODA Marsh, 1881

TETANURAE Gauthier, 1986

COELUROSAURIA von Huene, 1914

COMPSOGNATHIDAE Cope, 1871

SCIPIONYX SAMNITICUS Dal Sasso & Signore, 1998

Type and only species - *Scipionyx samniticus* Dal Sasso & Signore, 1998.

Etymology (Dal Sasso & Signore, 1998a) - “Scipio”, Latin male name, dedicated to Scipione Breislak, the geologist who first described the Pietraraja Plattenkalk, and *Publius Cornelius Scipio* (nicknamed *Africanus*), *consul militaris* of the Roman Army, who fought in the Mediterranean area; and “onyx” (ὄνυξ), Greek for “claw”. “Samniticus”, Latin for “of the *Samnium*”, the ancient name of the region that includes Pietraraja and the Benevento Province. *Scipionyx* should be pronounced “ship-e-ònyx”.

Holotype - Nearly complete, articulated skeleton with fossilised soft tissues, housed in Salerno (Campania), Italy, at the Soprintendenza per i Beni Archeologici di Salerno, Avellino, Benevento e Caserta with inventory number SBA-SA 163760.

Type locality - Le Cavere quarry, Pietraraja, Benevento Province (Campania), Italy: IGM (Istituto Geografico Militare) map sheet 162, III SW-Cusano Mutri, 41°20'52.18"N, 14°32'53.33"E.

Type horizon and age - “Calcarei selciferi e ittiolitiferi di Pietraraja” Fm. (*sensu* Catenacci & Manfredini, 1963), upper Plattenkalk horizon (*sensu* Carannante *et al.*, 2006). Lower Cretaceous, Lower Albian.

Emended diagnosis - Compsognathid theropod with five premaxillary teeth; sinusoidal ridge of supratemporal fossa at frontoparietal contact; descending process of squamosal distally squared; carpus composed by only two stacked, well-ossified bones (radiale and distal carpal 1+2); distal carpal 1+2 lenticular, compressed proximodistally, non-semilunate, and fused, lacking any trace of suture; manual digit III markedly longer (123%) than digit I; cranial concavity of the preacetabular blade of the ilium in lateral view facing cranially and slightly developed; prominent ischial obturator process squared distally.

Remarks - Besides autapomorphic characters, *Scipionyx* shows also a mix of characters, some shared with other compsognathids and/or basal coelurosaurs (see Description for detailed comparisons), and some potentially autapomorphic that might be subject to ontogenetic variation. The elongated dentary, prolonged more caudally than the maxilla, might represent a synapomorphic feature (Currie, pers. obs., 1999) shared with *Juravenator*. A related condition, potentially diagnostic and possibly autapomorphic, is the lower tooth row that extends farther back than the upper tooth row. However, given that: (1) the specimen is immature; (2) both maxilla and dentary might have undergone significant elongation during ontogeny, but it is not clear if they were subjected to positive or negative allometry each with respect to the other; and (3) this probable elongation possibly gave rise to new tooth positions, these characters must be considered with caution until a mature specimen of *Scipionyx* is available. The lack of contact between the quadratojugal and the squamosal might be an autapomorphy of *Scipionyx* among basal coelurosaurs. The absence of an external mandibular fenestra is shared with other compsognathids and a few other basal coelurosaurs. Similar to many compsognathids, *Scipionyx* has dorsal neural spines that are relatively low and significantly expanded craniocaudally, in particular at the mid-top/top, with craniocaudally flat apical margins and beak-like extensions on the cranial and caudal margin of the neural spine, just below the apical margin. In *Scipionyx*, the tip of the ungual phalanx of digit I ends at the level of the distal end of phalanx 1 of digit II, a condition indicated as diagnostic of *Compsognathus* by Peyer (2006). According to this author and to our phylogeny, other compsognathid synapomorphies present in *Scipionyx* are shaft diameter of phalanx I-1 equal/greater than shaft diameter of the radius; manual unguis, especially those of digits II and III, that are weakly curved, short and wide; only slightly inclined dorsal transverse processes; absence of pleurocoels in dorsal vertebrae; and the presence of a proportionally large skull (see Ontogenetic Assessment). Lastly, *Scipionyx* shares with many other compsognathids unserrated rostralmost but serrated lateral teeth, hair-like cervical ribs, an orthopubic pubis, and a pubic foot that lacks a cranial process but has a well-developed caudal process.

OSTEOLOGICAL DESCRIPTION AND COMPARISONS

General features

The skeleton of *Scipionyx* lies on its left side, in nearly complete anatomical articulation (Figs. 21, 22). The specimen measures 237 mm from the tip of the premaxilla to the last (9th) preserved caudal vertebra. The hindlimbs of *Scipionyx* are missing distal to the proximal epipodials, as are most of the tail and the right manual claw II. The *in situ* articulation of the skeleton suggests that the absence of these elements cannot be explained by traumatic *pre mortem* events, nor by taphonomical dispersal conditions (see Skeletal Taphonomy): they

were simply not collected (see Material). The head is upturned relative to the neck, but is not in an opisthotonic condition (see Ostrom, 1978); the jaws are open. Some bones and morphological structures are not exposed, but their outlines are still visible as reliefs where they overlap each other (e.g., left humerus, right paraoccipital process – see hatched lines in figures).

Taxonomic comparisons are made with other compsognathids, basal coelurosaurs and basal forms of more advanced theropods, in order to provide a detailed description useful in elucidating phylogenetic relationships and evolutionary trajectories within Coelurosauria.

SKULL AND MANDIBLE

Scipionyx samniticus has a very large skull – measuring half the length of the presacral vertebral column – with well-developed smooth frontal and nasal bones and a sloping postorbital region; the snout is short and triangular; the orbits are large and rounded, measuring a third of the skull length; and the tooth row consists of sharp, fang-like teeth (Figs. 23-25). No foramina for cranial nerves are visible on the exposed parts of the skull bones.

Most skull bones are preserved in anatomical connection; during diagenesis, the bones of the left side have been shifted 2 mm ventrally with respect to those of the right side, as can be clearly seen in the cranial vault, in the maxillae and in the mandible. This fact has helped interpret some uncertain structures.

The comparatively large skull of *Scipionyx* matches the general compsognathid bauplan, although there are some proportions – most likely linked to the ontogenetic stage of the specimen – that at first glance are reminiscent of birds and ornithomimosaurids. The snout of *Scipionyx*, for example, is comparatively shorter than in most non-avian theropods (Padian, 2004). In the caudal half of the skull, the sloping caudal skull table, and the arrangement and the proportions of the bones as well, are somewhat reminiscent of some ornithomimosaurids (see comparisons below), such as *Garudimimus* (Kobayashi & Barsbold, 2005). These similarities, especially those that appear birdlike, are probably accentuated by the immaturity of the individual, as is the case for *Bambiraptor* (Burnham *et al.*, 2000). Cranial similarities and differences between *Scipionyx* and other

theropods are discussed in the following description of the skull. The characters that can be linked to its ontogenetic stage, such as size and proportions of the skull, are looked at in more detail in the Ontogenetic Assessment section.

Cranial openings (Fig. 26)

Apertura nasi ossea - In *Scipionyx*, the bony nasal opening (*apertura nasi ossea* in formal nomenclature, inappropriately called the “external naris” or simply “naris” in palaeontology) is a drop-shaped opening, rostrocaudally elongated (although not as elongated as in *Sinosauropteryx* and *Huaxiagnathus*), relatively large (as long as the premaxilla) and extending caudally beyond the rostralmost margin of the antorbital fossa. Its inner opening (called the “naris” by most paleontologists) opens rostrally at the level of the distal edge of the third premaxillary tooth and terminates caudally at the level of the distal edge of m2. Rostral to the inner opening, the outer opening (i.e., the rim of the narial fossa) is visible as a depression on the body of the premaxilla, and its mid-caudal outline coincides with that of the inner opening.

The bony nasal opening is clasped in equal halves by the premaxilla (rostrally) and by the nasal (caudally), whose thin subnarial processes prevent the maxilla from bordering the opening. The maxilla is excluded from the opening also in other compsognathids and in other coelurosaurs (e.g., *Caudipteryx*, *Incisivosaurus*, *Archaeopteryx*),

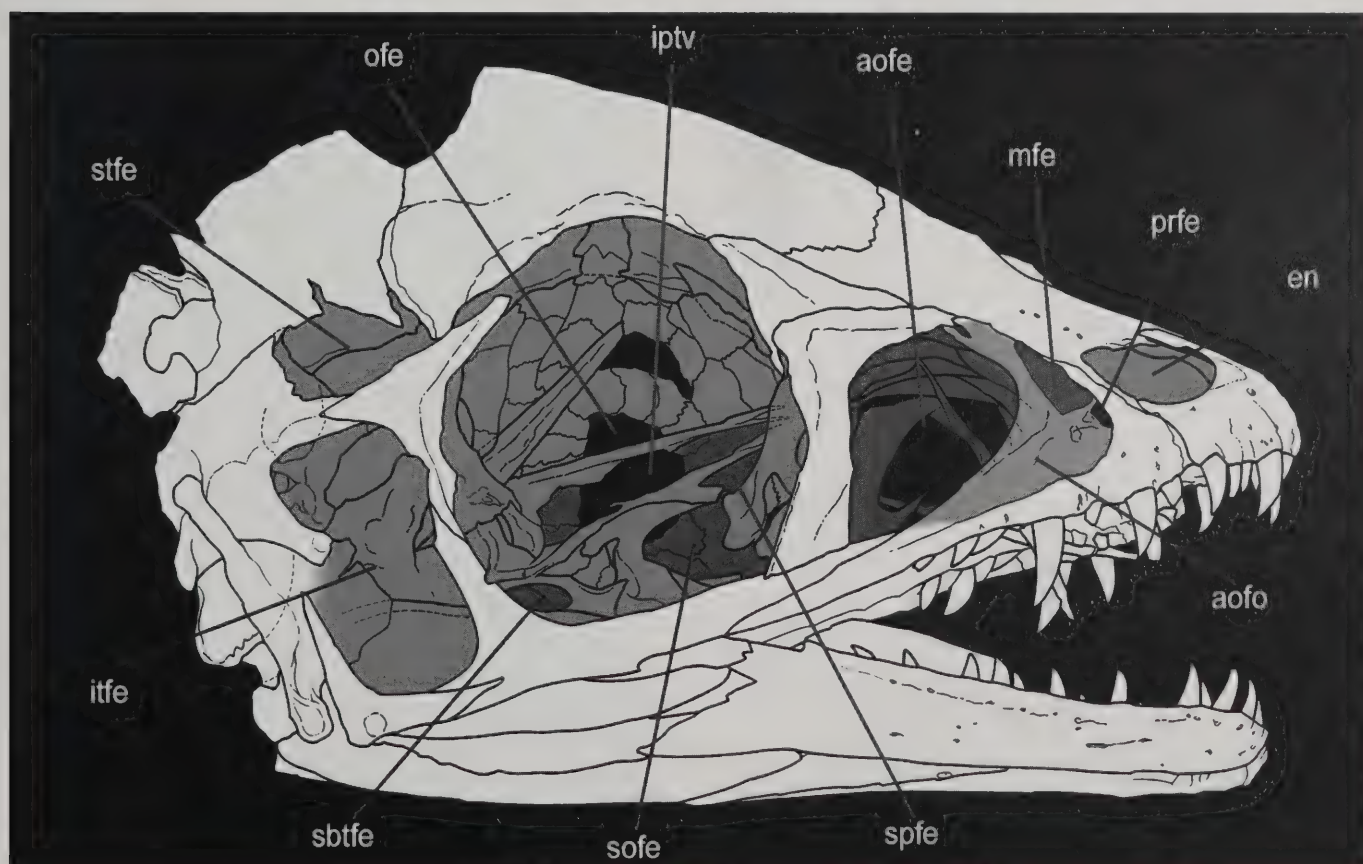


Fig. 26 - Cranial openings of *Scipionyx samniticus*. Black areas indicate the matrix. See Appendix 1 or cover flaps for abbreviations.
Fig. 26 - Apertura del cranio di *Scipionyx samniticus*. Lo sfondo nero indica la matrice. Vedi Appendice 1 o risvolti di copertina per le abbreviazioni.

although the contact between the premaxilla and the nasal occurs differently in each taxon (see Premaxilla). The inner bony nasal opening opens rostrally at the mid-level of the third premaxillary crown in both *Scipionyx* and *Compsognathus* (Peyer, 2006; Ostrom, 1978). Therefore, the rostral margin of the nasal opening in these taxa is caudally retracted with respect to that of *Sinosauropteryx*, *Sinocalliopteryx*, *Huaxiagnathus*, *Juravenator*, *Proceratosaurus*, *Dilong* and *Guanlong*, in which the bone rostral to the opening is as thin as the internarial bar.

Scipionyx is the only compsognathid with partial overlapping between the nasal opening and the antorbital fossa. In *Dilong*, *Ornitholestes* (Osborn, 1916: fig. 1; Rauhut, 2003: fig. 5H) and, possibly, *Huaxiagnathus* (Hwang *et al.*, 2004: fig. 2), the caudal margin terminates where the rostral margin of the antorbital fossa begins. Other coelurosaurs, such as *Proceratosaurus* (Woodward, 1910), *Guanlong* (Xu *et al.*, 2006), *Incisivosaurus* (Xu *et al.*, 2002a), *Sinovenator* (Xu *et al.*, 2002b) and *Archaeopteryx* (Elzanowski, 2002), are more similar to *Scipionyx* in having a large bony nasal opening extending caudally beyond the rostral margin of the antorbital fossa. Both conditions are present in birds (Padian, 2004). This suggests that the condition in *Scipionyx* is not necessarily a consequence of the shortness of the snout due to the ontogenetic stage of the specimen (see Ontogenetic Assessment).

Through the right nasal opening of *Scipionyx*, the supranarial process of the left premaxilla and the medioventral surface of the left ?nasal are visible.

Antorbital fossa - This is a marked, subtriangular depression that includes the antorbital, maxillary and promaxillary fenestrae. The antorbital fossa is surrounded mainly by the maxilla (rostrally and ventrally) and by the lacrimal (caudally and dorsally), with small contributions from the jugal (caudoventral corner) and the nasal (dorso-rostral margin).

Antorbital fenestra - A D-shaped antorbital fenestra occupies most of the antorbital fossa, again with the participation of the lacrimal and the jugal; the remaining margins are entirely formed by the maxillary medial wall of the fossa.

The antorbital fenestra is subequal in length to the orbit in *Juravenator*, *Compsognathus* and *Sinocalliopteryx*, shorter than the orbit in *Sinosauropteryx*, and even shorter in *Scipionyx* (see Ontogenetic Assessment). Thus, the situation in *Scipionyx* is somewhat reminiscent of *Archaeopteryx* (Elzanowski, 2002), birds (Padian, 2004) and the basal oviraptorosaurs *Caudipteryx* (Ji *et al.*, 1998) and *Incisivosaurus* (Xu *et al.*, 2002a). An antorbital fenestra that is shorter than the orbit is also present in some deinonychosaurs, such as *Velociraptor* (Sues, 1977), *Sinornithosaurus* (Xu & Wu, 2001) and the basal troodontid *Jinfengopteryx* (Ji *et al.*, 2005); therefore, this is definitely a widespread condition within the Coelurosauria.

Maxillary fenestrae - The maxillary and the promaxillary fenestrae are situated at the rostral border of the antorbital fossa, with the former dorsal to the latter. They are separated from each other by a promaxillary strut (Fig. 27). Both fenestrae open and face laterally within the maxillary medial wall. Their rostral borders are delimited by the ascending process of the maxilla. The promaxillary

fenestra is small and oval in shape. Its rostral extension may be slightly concealed in its lateral view by the ascending process of the maxilla. The maxillary fenestra has the shape of a subrectangular trapezium. Underlying matrix is visible through the promaxillary fenestra, while the maxillary fenestra has an osseous medial wall (Fig. 27).

The maxillary fenestra in *Sinosauropteryx* and *Compsognathus* is as large as that in *Scipionyx*. In *Juravenator* and *Huaxiagnathus*, it is smaller. The shape and position of the maxillary fenestra varies in compsognathids: *Juravenator*, *Huaxiagnathus*, *Sinosauropteryx* and *Compsognathus* have a rounded maxillary fenestra that is completely enclosed in the centre of the maxillary medial wall of the antorbital fossa. With the possible exception of *Sinosauropteryx*, the fenestra is perforated in these taxa (Currie & Chen, 2001). The maxillary fenestra is perforated in most other theropods, with the exception of some troodontids (Makovicky *et al.*, 2003; Makovicky & Norell, 2004), in which it is closed by a continuous medial wall.

A promaxillary fenestra is also present in most other coelurosaurs, with the exception of most troodontids – among which it was identified only in the basal form *Sinovenator* (Xu *et al.*, 2002b) – and, possibly, in some therizinosauroids (Rauhut, 2003; but see Kundrát *et al.*, 2008). Peyer (2006) reported that *Sinosauropteryx* and *Compsognathus* are the only compsognathids with an identifiable promaxillary fenestra. The promaxillary fenestra of *Scipionyx* is comparable in size but differs in its outline: it resembles more closely that of the basal tyrannosauroid *Dilong* (Xu *et al.*, 2004) in being small, located rostro-ventral to the maxillary fenestra, and confined to the rostral margin of the antorbital fossa. A similar arrangement

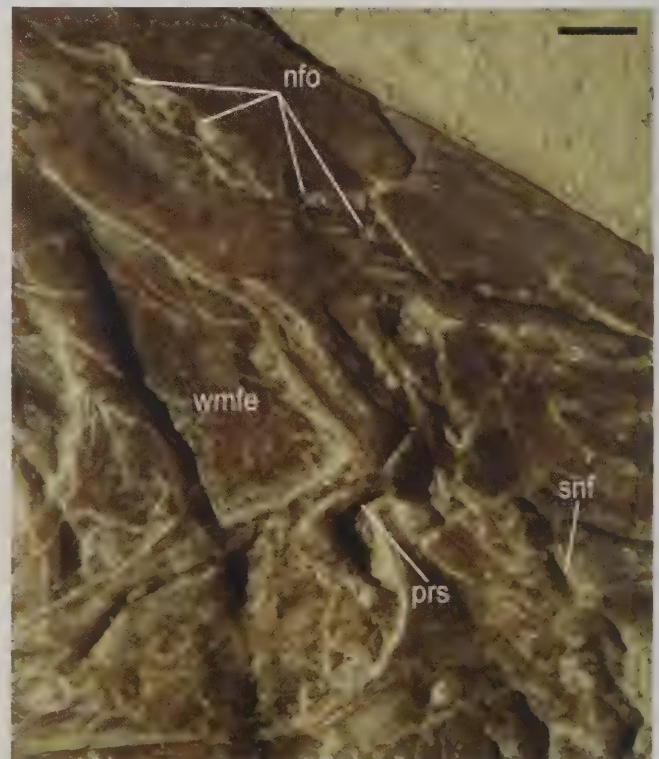


Fig. 27 - Close-up of the right antorbital region of *Scipionyx samniticus*. See Appendix 1 or cover flaps for abbreviations. Scale bar = 1 mm.

Fig. 27 - Particolare della regione antorbitale destra di *Scipionyx samniticus*. Vedi Appendice 1 o risvolti di copertina per le abbreviazioni. Scala metrica = 1 mm.

of the fenestrae, one dorsal to the other, is known for some Ornithomimosauria (Rauhut, 2003: fig. 6E; Makovicky *et al.*, 2004: fig. 6.2B), although, according to Kobayashi & Barsbold (2005), the dorsalmost opening in this taxon would be the promaxillary fenestra.

Orbit - The orbit of *Scipionyx* is circular and larger than the antorbital fossa. It is almost equally bordered by the lacrimal (rostrally), the frontal (dorsally), the postorbital (caudodorsally and caudally) and the jugal (ventrally and caudoventrally). A small contribution of the prefrontal (rostradorsally) is also present.

A large and circular orbit is clearly present in the compsognathids for which the orbital region has been reconstructed, such as *Compsognathus*, *Juravenator* and *Sinosauropteryx*, but also in many other adult theropods that attained a small-to-medium body size, independently of their phylogenetic affinities (e.g., *Eoraptor*, coelophysoids, basal tyrannosauroids, *Ornitholestes*, therizinosauroids, ornithomimosaurids, oviraptorosaurs, deinonychosaurs, alvarezsaurids, Avialae). The frontal and prefrontal contribution to the margin of the orbit in *Scipionyx* is reminiscent of the condition in basal ornithomimosaurids (Barsbold & Perle, 1984; Pérez-Moreno *et al.*, 1994; Kobayashi & Barsbold, 2005: 2A, D), some basal saurischians like *Eoraptor* (Serenó *et al.*, 1993), and in therizinosauroids and *Ornitholestes*. A similar contribution to the margin of the orbit occurs also in the alvarezsaurids (Chiappe *et al.*, 2002), but here the orbit flows caudally into the infratemporal fenestra because of the lack of the postorbital process of the jugal.

Supratemporal fossa - This is a subrectangular depression that comprises the supratemporal fenestra. Usually facing dorsally, it is exposed laterally in *Scipionyx* because of diagenetic crushing of the skull. It extends rostrally up to the frontoparietal suture, and is well-separated from the contralateral fossa, as in *Compsognathus* (Peyer, 2006). The dorsal portion of the parietals, which separates left and right supratemporal fenestrae, is a broad horizontal plate without any trace of a depression, unlike in the majority of theropods (Weishampel *et al.*, 2004). As a consequence, the medial margin of the supratemporal fenestra coincides with that of the fossa.

Supratemporal fenestra - This opening is suboval and bordered by the parietal (medially and rostromedially), the frontal or the postorbital (rostrally, see Postorbital for further comments), the postorbital (laterally) and the squamosal (caudolaterally and caudally).

Whereas the parietal borders most of the supratemporal fenestra in *Scipionyx* and *Compsognathus* (Peyer, 2006), in *Juravenator* it borders the fenestra only for a short, medial tract so that the pre-eminent contribution is made by the frontal (Göhlich & Chiappe, 2006: fig. 2a). Three bones are visible through the supratemporal fenestra: the prootic, the laterosphenoid and the ventral portion of the parietal.

Infratemporal fenestra - This fenestra opens just below the supratemporal fenestra. It is rectangular – the postorbital bar and the ascending ramus of the quadratojugal parallel the quadrate – with four corners formed by the postorbital (rostradorsal), squamosal (dorsocaudal),

quadratojugal (caudoventral) and jugal (ventrorostral). The former hypothesis that the mid-height caudal constriction of this fenestra might be due to a slight rostral displacement of the quadratojugal ramus of the squamosal cannot be ruled out, but in all likelihood the orientation of this ramus is natural. In fact, a comparable mid-height constriction appears to be present, for example, in *Sinosauropteryx* (Currie & Chen, 2001: fig. 3b) and in *Saurornithoides* (Makovicky & Norell, 2004: fig. 9.1), and is also present in other basal tetanurans such as *Allosaurus* and *Monolophosaurus*. In those taxa, as in *Scipionyx*, the squamosal forms most of the protrusion, whereas in tyrannosaurids (Holtz, 2004), and possibly in *Ornitholestes* (Osborn, 1916, fig. 1; Rauhut, 2003, fig. 5H), the infratemporal flange is due to the synapomorphic extension of both the squamosal and the quadratojugal.

Palatal fenestrae - Because of diagenetic distortion of the skull, the following palatal fenestrae have been partially exposed: the rostromedial portion of the subtemporal fenestra, bordered by the ectopterygoid process of the pterygoid, and visible along the caudoventral margin of the orbit; the suborbital fenestra, exposed along the ventrorostral margin of the orbit, bordered by the palatine (rostrally), the pterygoid (medially) and the ectopterygoid (mediocaudally), and reduced in size with respect to the orbit; the subsidiary palatal fenestra, exposed only in its caudal part, clasped by the pterygoid and partly bordered by the pterygoid ramus of the palatine; the internal naris (choana), partly visible in the centre of the antorbital fenestra as a C-shaped opening, bordered by the vomeral and the rostral maxillary processes of the dorsally displaced left palatine; and the interpterygoid vacuity, delimited by the palatal rami of the left and right pterygoid.

Peyer (2006) observed that in *Compsognathus* the rostralateral border of the palatine marked the caudal border of the internal naris. No other details of the palatal fenestrae have been described for compsognathids. Some palatal bones and relative fenestrae are indeed visible in *Sinocalliopteryx* (Ji *et al.*, 2007a) and especially in *Juravenator* (Göhlich & Chiappe, 2006), but they were not described and their shape and margins have not been reconstructed. A subsidiary palatal fenestra (*sensu* Ostrom, 1969; “pterygopalatine fenestra” in Norell & Makovicky, 2004) is present also in tyrannosaurids, ornithomimosaurids, deinonychosaurs (Rauhut, 2003) and in therizinosauroids (Clark *et al.*, 1994).

Foramen magnum - The medialmost third of the straight ventral margin of the right supraoccipital probably bordered the foramen magnum dorsally.

Scleral plates

The bony plates which formed the scleral rings (i.e., the bony reinforcements of the eye balls) occupy most of the orbit of *Scipionyx*. Like many bones of the left side, the left scleral ring has slid a couple of mm ventrally, so that its dorsal arch is now visible at the centre of the orbit. Despite this displacement, it seems to be complete, and its curvature can be followed just below the palatal bones. On the other hand, the right scleral ring is broken into at least 4 arched fragments, each composed of 3 to 5 plates.

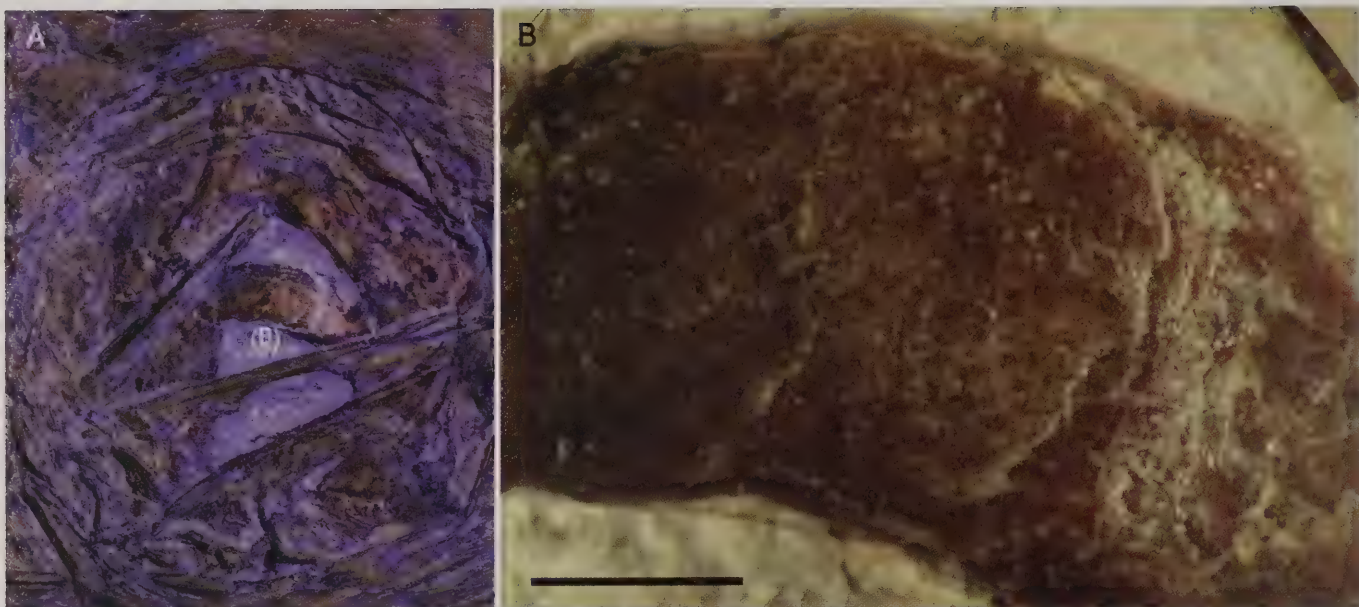


Fig. 28 - The scleral rings of *Scipionyx samniticus*. A) ultraviolet-induced fluorescence highlights the overlapping of the plates. B) close-up, under the optical microscope, of the dorsal arch of the left scleral ring. Scale bar = 1 mm.

Fig. 28 - Anelli sclerali di *Scipionyx samniticus*. A) fluorescenza indotta da luce ultravioletta che evidenzia le sovrapposizioni tra le placche. B) particolare al microscopio ottico dell'arco dorsale dell'anello sclerale sinistro. Scala metrica = 1 mm.

The apparent difference in shape and size of the scleral plates is due to different patterns of superimposition. The plates narrow towards their somewhat irregular or zigzagged contact margins, which are more clearly visible under UV light (Fig. 28A). The exact number of plates that formed each scleral ring cannot be directly determined, but a minimum number of 16 plates can be assumed (each of the 4 fragments of right ring makes up almost a quarter of the ring).

Among compsognathids, *Sinocalliopteryx* had at least 10 scleral elements, in the form of subrectangular to trapezoidal plates (Ji *et al.*, 2007a: fig. 2a-b). Scleral rings are recorded in the Sihetun *Sinosauropteryx*, but they are covered externally by a black substance, possibly representing the decayed retina or iris of the eye (Currie & Chen, 2001). Subrectangular scleral plates with thin, sharp edges were observed in *Sinornithosaurus* (Xu & Wu, 2001). In the holotype of *Garudimimus*, the left side of the skull preserves 11 articulated scleral plates (Kobayashi & Barsbold, 2005). The scleral ring of *Jinfengopteryx* is reported to consist of 12-13 plates (Ji *et al.*, 2005). 24 scleral plates are figured in coelophysoids (Tykoski & Rowe, 2004: fig. 3.2), and 11-12 are reported in *Archaeopteryx* (Elzanowski, 2002). In extant birds (Bellairs & Jenkins, 1960), the number of scleral ossicles varies, ranging from 10 to 18, with 14-15 being the most common numbers.

Dermal skull roof

Premaxilla - The right premaxilla of *Scipionyx* is almost as deep as it is long, tapering rostrally and terminating in a rounded rostral tip (Fig. 29). The rostralmost margin is vertical for only a very short tract and then curves gradually in a dorsocaudal direction, continuing in a caudally directed supranarial process inclined 60° respect to the vertical plane. A similar condition is present in *Juravenator*, *Huaxiagnathus*, *Sinocalliopteryx* and *Compsognathus* (contra Peyer, 2006), but not in *Sinosauropteryx*, where the tip of the snout is truncated, the rostral margin of the premaxilla is vertical and the supranarial process is inclined about 35° caudally to the vertical plane (Currie & Chen, 2001: 2a).

The premaxilla of *Scipionyx* bears five teeth (see Dentition). Several nutritive foramina can be seen on its surface. The premaxillary foramina are larger in *Juravenator* (Göhlich & Chiappe, 2006: fig. 2a), smaller but still well visible in *Sinocalliopteryx* (Ji *et al.*, 2007a: fig. 2a), but absent in *Compsognathus* (Ostrom, 1978; Peyer, 2006).

In *Scipionyx*, the main body of the premaxilla in the subnarial region is as long rostrocaudally as it is high dorsoventrally; thus, it is higher than in *Sinosauropteryx*. The caudal extension of the supranarial and subnarial processes of *Scipionyx* is almost the same, but the former is longer than the latter. As for most theropods, including *Compsognathus* and *Sinosauropteryx*, the subnarial process of *Scipionyx* is narrow and relatively short. The dorsal margin of the subnarial process of the premaxilla borders the external naris ventrally. It contacts the subnarial process of the nasal in a dorsocaudally-to-rostroventrally directed sloping suture, excluding the maxilla from the external nares. In *Juravenator*, however, the longest process is the subnarial one, which forms the entire ventral margin of the naris. In *Sinocalliopteryx*, the supranarial and subnarial rami are even longer, and in *Huaxiagnathus*, the subnarial ramus reaches the level of the rostral margin of the antorbital fossa. In *Scipionyx*, a tiny elliptical hole that may be the subnarial foramen is present along the premaxilla-maxilla suture, just in front of the lanceolate tip of the subnarial process of the nasal (Figs. 27, 29).

The premaxillary-maxillary contact is almost vertical in its ventral half and dorsocaudally directed in its dorsal half. The contact between the two bones is more extensive than in *Juravenator*, and their ventral margins close to the suture are almost horizontal. The maxillary margin is only slightly inclined rostradorsally, and in any case does

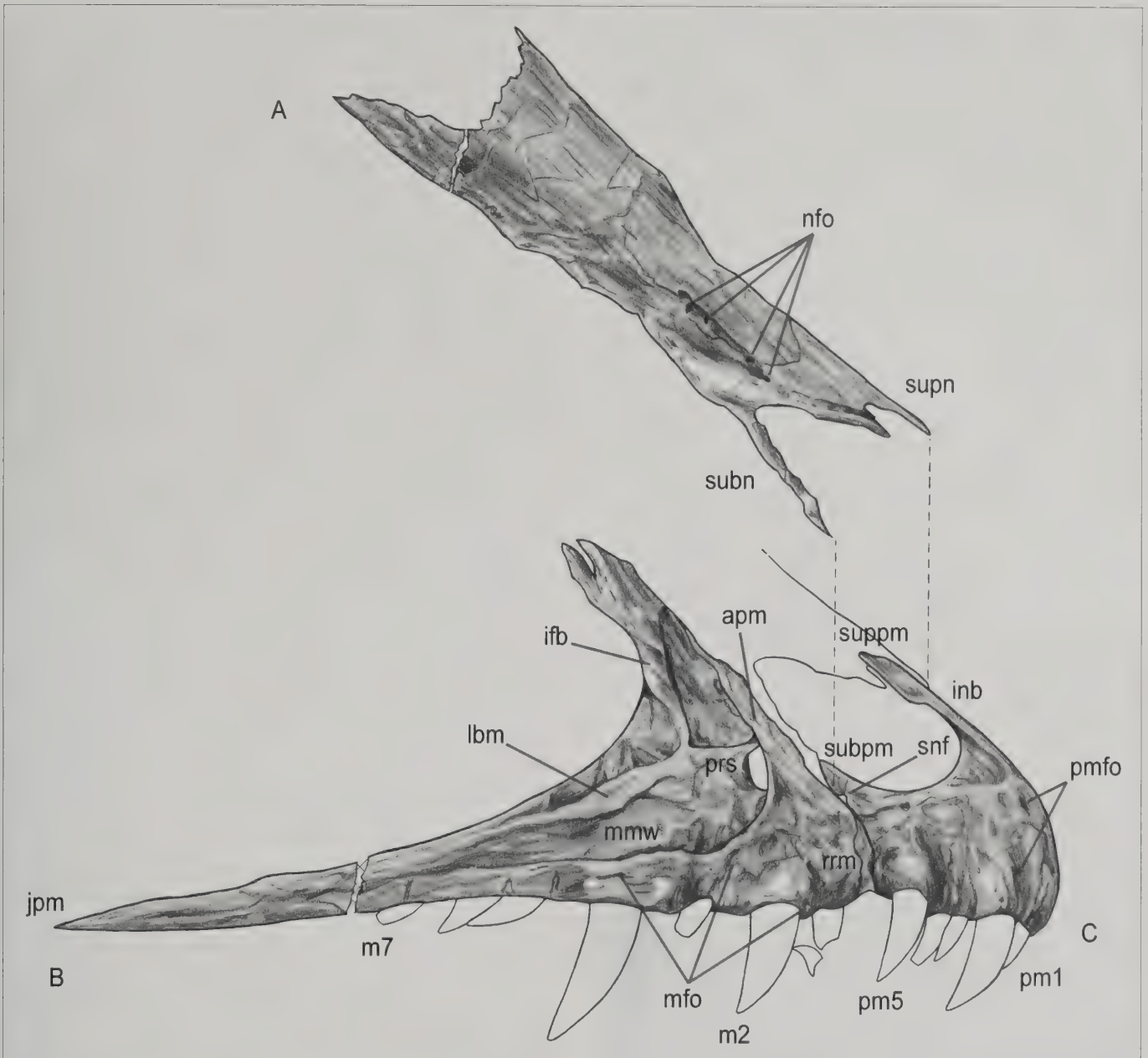


Fig. 29 - Shaded drawings of the right nasal (A), maxilla (B) and premaxilla (C) of *Scipionyx samniticus*, and their sutural contacts. See Appendix 1 or cover flaps for abbreviations.

Fig. 29 - Disegni ombreggiati di nasale (A), mascellare (B) e premaxillare (C) destri di *Scipionyx samniticus*, e loro contatti suturali. Vedi Appendice 1 o risvolti di copertina per le abbreviazioni.

not have the marked ventral notch visible in *Juravenator* (Göhlich & Chiappe, 2006). Judging from the rostral half of the supranarial process, the internarial bar of *Scipionyx* is flattened dorsoventrally. The left premaxilla emerges in medial view only with the supranarial process and a small caudoventral portion.

Maxilla - The maxilla is a triangular bone, notched caudally by the antorbital fenestra and pierced by two smaller fenestrae – the maxillary and the promaxillary fenestrae (Fig. 29). In lateral view, the maxilla seems to develop in two different planes: a portion overhanging laterally, which delimits the antorbital fossa with two rami, one horizontal bearing the tooth row, and one ascending towards the nasal; and a portion lying on a more medial plane, forming the medial wall of the antorbital fossa.

The passage between the two planes is well-marked, even though the antorbital fossa is only slightly depressed below the level of the surrounding bone.

The antorbital fossa is separated from the rest of maxilla by a low, continuous but distinct ridge, as in *Huaxiagnathus* (Hwang *et al.*, 2004) and in a few other theropods (Rauhut, 2003). This ridge is rounded rostrally, then continues caudally ventral to the antorbital fenestra, running parallel to the tooth row. The fossa deepens towards its rostral rim, where it is pierced by the promaxillary fenestra. Whereas the promaxillary fenestra appears as a hole, the maxillary fenestra is not so apparent at first glance because it is paved by an osseous wall that is even more medial than the maxillary medial wall. A similar wall in the fenestra, belonging to the maxilla, was described in some troodontids (Makovicky *et al.*, 2003) and hypothesised to

be present also in *Sinosauropteryx* (Currie & Chen, 2001). In *Scipionyx*, its belonging to the right maxilla, rather than to an unidentified element of the left side of the skull, is supported by the position of both left nasal and left maxilla. These bones, which emerge in other areas, could have invaded the background of the maxillary fenestra with fragments, after breaking into pieces. However, the continuity of the bone that is seen within the fenestra rules out this possibility.

The compression of the medial wall of the maxillary in the rostral portion of the antorbital fossa has forced out a longitudinal bar that would otherwise be visible only in medial view. This bar is rostrocaudally directed and slightly slanting with respect to the ventral margin of the antorbital fossa. It arises in between the promaxillary and maxillary fenestrae in the form of a promaxillary strut, and terminates in correspondence to the ventral margin of the antorbital fenestra. Ventral to this fenestra, the maxilla gradually thins caudally and terminates in an acute triangle which contacts the jugal with an elongated oblique suture.

Rostral to the antorbital fenestra, the ascending process of the maxilla, thinner and lying in a lateral plane, forms a long oblique suture with the subnarial process of the nasal. As mentioned, the maxilla is excluded from the caudal and ventral margin of the external naris by the premaxillary-nasal contact, like in the vast majority of theropods (e.g., Rauhut, 2003).

The dorsorostral margin of the maxilla is slightly concaved for a very brief tract just below the premaxillary-nasal contact (Chiappe, pers. obs., 2006), interrupting its otherwise convex course from the ascending process to the ventral margin. In our opinion, this concavity is homologous to the more evident one that in most theropods marks the transition between the ascending ramus and the rostral ramus. Therefore, contrary to Holtz *et al.* (2004) and Peyer (2006), the rostral ramus is not lost in *Scipionyx*: the bone possessing the primitive simple convex curve is strongly reduced or, more probably, not yet fully developed on account of the immaturity of the specimen. Thus, the rostral ramus of *Scipionyx* is poorly developed and shorter rostrocaudally than it is high dorsoventrally. This is contrary to what is seen in *Juravenator* and *Compsognathus*, and even more so in *Huaxiagnathus* and *Sinocalliopteryx*, which are similar to the other coelurosaurs in having a maxillary rostral ramus that is rostrocaudally as long as, or longer than, it is long dorsoventrally. According to Holtz *et al.* (2004), this condition is one of the diagnostic characters of generalised coelurosaurs, although it is present also in some basal non-coelurosaurian tetanurans.

The antorbital fenestra is delimited rostrally by a portion of the maxillary medial wall, the interfenestral bar (*pila interfenestralis*). This bar separates the antorbital fenestra from the maxillary fenestra. In *Scipionyx*, the maxillary medial wall is not low and subparallel to the tooth row as in *Compsognathus* (Peyer, 2006); rather, it gradually rises up rostrorodorsally to form the interfenestral bar, where it is tall half the height of the antorbital fossa, as is often the case in theropods. As the dorsalmost portion of the maxillary medial wall has been slightly covered by the flattening of the nasal during diagenesis, the antorbital and maxillary fenestrae seem to be bordered by the nasal, too. The nasal possibly participates in forming the antorbital fossa, but is excluded from the antorbital fenestra by the sutural contact between the bifurcating caudal extremity

of the interfenestral bar of the maxilla and the horizontal ramus of the lacrimal (see Nasal).

Above the dentigerous margin, the lateral surface of the maxilla is pierced by numerous nutritive foramina, as in *Sinocalliopteryx* and *Sinosauropteryx* (Currie & Chen, 2001). In contrast, the alveolar ramus in *Compsognathus* (Ostrom, 1978; Peyer, 2006) is devoid of large nutrient foramina. The right tooth row bears 7 teeth, with m1 resulting slightly procumbent because of the very faint slope of the rostral portion of the tooth row towards the premaxillary-maxillary contact; six teeth are preserved on the left maxilla (see Dentition).

As it can be inferred by the position of its ventral margin, which terminates rostrally at the level of the right m1, the left maxilla slid ventrally along the premaxillary-maxillary suture more than the left premaxilla did, creating a step between the two bones. Thanks to this sliding, the medial surface of the left maxilla is exposed in two areas (Fig. 25D): inside the right antorbital fenestra, where the left interfenestral bar is visible, paralleling the counterlateral element; and below the dentigerous margin of the right maxilla. In the latter area, along the medial side of the left maxilla, at least 5 distinct interdental plates emerge, regularly spaced, between maxillary teeth 2-7 (Fig. 30). They are not fused to each other, so they do not form a continuous lamina, nor do they seem fused to the maxilla. They are rather large and bulky, sticking out with respect to the medial margin of the maxilla, and change shape according to the shape of the interdental gaps, the rostralmost being subrectangular and the caudalmost subtriangular. Large, triangular unfused interdental plates are present in both German and French *Compsognathus* (Peyer, 2006). Unfused interdental plates of variable shape but somewhat comparable to those of *Scipionyx*, are described in the basal dromaeosaurid *Sinornithosaurus* (Xu & Wu, 2001). The interdental plates of *Archaeopteryx* resemble those of *Scipionyx* in being distinctly separated from the medial margin of the maxillary bone and widely separated from one another, although they change in shape in an opposite manner, the rostral ones being subtriangular and the caudal ones being subrectangular (Elzanowski, 2002). Unfused interdental plates are present also in the Tyrannosauridae (Currie *et al.*, 2003), but not in some basal tyrannosauroids such as *Tanycolagreus* (Carpenter *et al.*, 2005a).



Fig. 30 - Close-up of the dentigerous margin of the maxillae of *Scipionyx samniticus*, showing teeth attachments and interdental plates. Scale bar = 1 mm. See Appendix 1 or cover flaps for abbreviations.

Fig. 30 - Particolare del margine dentigero dei mascellari di *Scipionyx samniticus*, in cui sono visibili le attaccature dei denti e le placche interdentali. Scala metrica = 1 mm. Vedi Appendice 1 o risvolti di copertina per le abbreviazioni.

Nasal - The nasal is a long and narrow wedge-shaped plate of bone, with parallel medial and lateral margins and a smooth surface. Because the skull was crushed, the right nasal appears flattened, with lateral and dorsal surfaces in one plane.

Rostrally, the nasal diverges to clasp the back of the external naris. In addition, the supranarial process splits rostrally clasping, in turn, the caudal tip of the premaxilla. The subnarial process is hardly visible, on account of its thinness and some parallel microfractures in the surrounding bones, but appears to be long, very thin and with a lanceolate process (Fig. 29). The subnarial process is thin also in *Compsognathus* and in *Juravenator* (thinner than reconstructed in Göhlich & Chiappe [2006: figs. 2a-b]), although not as thin as in *Scipionyx*.

Dorsal to the maxillary fenestra, at mid-height of the bone, the surface of the nasal is pierced by 4 small, oval, rostrocaudally aligned, almost equidistant foramina (Figs. 27, 29). They might have served as passages for branches of the superior nasal artery or led into internal pneumatic chambers. A rostrolaterally directed row of at least 3 nutrient foramina is present in the nasal of *Sinosauropteryx* (Currie & Chen, 2001: fig. 3d) just rostral to the vertical ramus of the lacrimal. No foramina have been found in *Compsognathus* (Peyer, 2006).

On account of the compression of the skull and the consequent position of the nasal, the contacts between the maxilla and the nasal, and their contribution to the antorbital fossa, are not completely clear. Certainly, the antorbital fossa does not invade the ventrolateral margin of the nasal, contrary to the condition shown, for example, by the allosauroids (Rauhut, 2003). It is difficult to establish whether the nasal bordered the antorbital fossa or whether it was excluded by a process of the maxilla. The ascending process of the maxilla seems to have a thin appendage that, running caudodorsally along the dorsal margin of the maxillary fenestra, almost reaches the interfenestral bar and might have continued caudally up to the lacrimal.

Caudally, the nasals are so firmly sutured to the frontals that Dal Sasso & Signore (1998a) were unable to identify any nasofrontal suture. Photos at high magnification (Fig. 31A-B) show an interdigitate type, roughly W-shaped nasofrontal suture just dorsal to the lacrimal. In dorsal view, beginning from the midline, this suture runs rostrolaterally for a short way, then becomes transverse; in its second half, it runs caudolaterally towards the prefrontal. A W-shaped nasofrontal suture at the level of the vertical ramus of the lacrimal is found also in *Compsognathus* (Peyer, 2006: fig. 4C), *Sinocalliopteryx* (Ji *et al.*, 1997a: fig. 2b), *Juravenator* (Göhlich & Chiappe, 2006: fig. 2a) and *Huaxiagnathus* (Hwang *et al.*, 2004: fig 2A). In *Sinocalliopteryx* the suture is an inverted W shape.

A thin chip of the left nasal is visible just dorsal to the short exposure of the medial sagittal suture, and a larger piece can be seen through the opening of the external nares (Fig. 25D).

Lacrimal - The stout lacrimal, with a typical inverted L-shape, is among the most robust cranial bones. Equally robust lacrimals can be found only in tyrannosaurids and ornithomimosaurids. *Compsognathus*, *Juravenator*, *Sinosauropteryx* and *Sinocalliopteryx* have an inverted L-shaped lacrimal like *Scipionyx* and the majority of

theropods, including basal coelurosaurians. The lacrimal is T-shaped in the Deinonychosauria, Ornithomimosauria, Oviraptorosauria and in Aves (Rauhut, 2003).

In *Scipionyx*, the vertical ramus is pillar-like, and its base leans against a dorsal sulcus of the jugal. Dorsally, it has a long, straight contact with the prefrontal, separating the antorbital fenestra from the orbit. The caudal margin of the vertical ramus is reinforced by a crest (very thin in the ventral half of the bone and markedly expanded in the dorsal half) which forms the rostral orbital margin.

The horizontal ramus runs rostrally, ventral to the base of the prefrontal, to reach the ventral margin of the nasal and the interfenestral bar of the maxilla. It is shorter than the vertical ramus, a condition probably linked to the ontogenetic stage of the individual (see Ontogenetic Assessment). The horizontal ramus is reinforced by crests which parallel the contact with the prefrontal. Among these crests, the most marked one borders the lacrimal vacuity, a depression located in the corner between the horizontal and the vertical ramus. A smaller foramen opens laterally at the angle between the two rami in *Juravenator* (Chiappe, pers. comm., 2006). Such a foramen is absent in *Scipionyx* even under UV light (Fig. 31A, C).

As in most small-sized theropods, including other compsognathids, there is no evidence of either a supraorbital crest or a lacrimal horn. In species that attained a medium-to-large body size, these structures are often poorly developed in young individuals, and become apparent only in mature individuals (e.g., Madsen, 1976).

A part of the left horizontal ramus seen in medial view and still contacting the extremity of the left maxillary interfenestral bar is visible through the dorsalmost por-

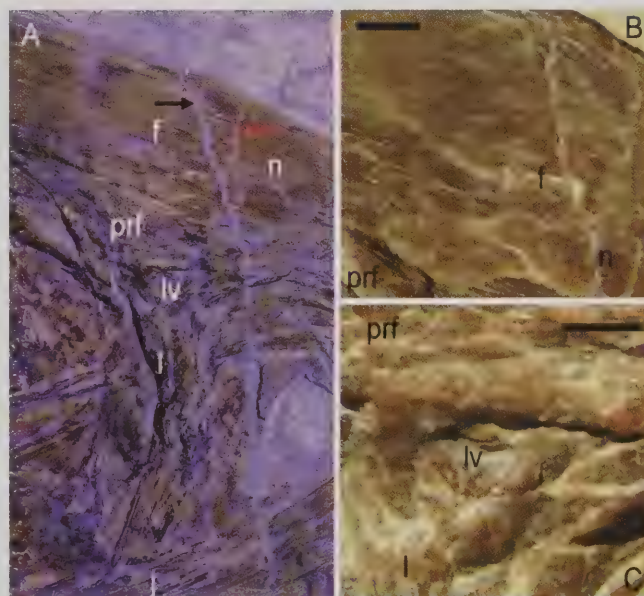


Fig. 31 - Ultraviolet-induced fluorescence photograph (A), and close-ups under visible light (B, C), documenting the position and shape of the nasofrontal suture in *Scipionyx samniticus* (red arrow; black arrow indicates a fracture). Note also the lacrimal vacuity in (A) and (C). Scale bars = 1 mm. See Appendix 1 or cover flaps for abbreviations.

Fig. 31 - Fotografia in fluorescenza indotta da luce ultravioletta (A), e particolari in luce visibile (B, C), che documentano la posizione e l'andamento della sutura nasofrontale in *Scipionyx samniticus* (freccia rossa; la freccia nera indica invece una frattura). Si noti anche la vacuità lacrimale in (A) e (C). Scale metriche = 1 mm. Vedi Appendice 1 o risvolti di copertina per le abbreviazioni.

tion of the antorbital fenestra (Fig. 25D). A piece of the caudoventral portion of the jugal process is sandwiched between the right palatine and the right lacrimal. The thin bar of bone seen paralleling the rostral margin of the right lacrimal at mid-shaft is possibly another fragment of the same lacrimal.

Prefrontal - This is a triangular bone connecting the lacrimal to the nasofrontal complex in close sutural contact. In *Scipionyx*, the prefrontal is well-developed and comparatively large and robust, surpassing the horizontal ramus of the lacrimal in length and, therefore, preventing any contact between the lacrimal and the frontal. In the uncrushed skull, it must have been well-exposed also in lateral view, expanding ventrally to terminate in a small worm-like appendage that still contacts the caudomedial face of the lacrimal. This appendage probably contributed to the rostromedial margin of the orbit, but remained visible in lateral view.

A robust fragment of the left prefrontal is exposed in medial view along the dorsorostral margin of the orbit. It still contacts the ventral surface of the left frontal (see below).

The prefrontal is greatly reduced in basal tetanuran theropods (Holtz *et al.* 2004). A well-developed prefrontal, although less prominent than in *Scipionyx*, is reported in *Sinosauropteryx* (Currie & Chen, 2001), *Compsognathus* (Peyer, 2006) and *Sinocalliopteryx* (Ji *et al.*, 2007a), possibly in *Juravenator* (Göhlich & Chiappe, 2006: fig. 2a), and in a number of coelurosaurids (e.g., some tyrannosauroids, *Ornitholestes*). In therizinosauroids (e.g., Clark *et al.*, 1994; Kundrát *et al.*, 2008) and alvarezsaurids (Serenó, 2001; Chiappe *et al.*, 2002), as well as in some basal coelophyroids, the prefrontal is much larger. The most prominent prefrontals are reported for ornithomimosaurs (e.g., Kobayashi & Lü, 2003: fig. 5B; Makovicky *et al.*, 2004; Kobayashi & Barsbold, 2005: 2a, d). In these animals, they continue ventrally, adhering along the caudomedial face of the lacrimal. Further comments on the size of the prefrontal of *Scipionyx* are given in the Ontogenetic Assessment section.

Postorbital - As in most theropods, the postorbital of *Scipionyx* is triradiate in lateral view. The descending ramus (jugal ramus) is the most developed one. On account of diagenetic crushing, even its contribution to the caudomedial margin of the orbit can be seen. The jugal ramus, however, is more limited in size than was previously considered: in fact, the internal portion of the postorbital, “ipo” in Dal Sasso & Signore (1998a: fig. 4), is reinterpreted here as the right epipterygoid.

The supraorbital ramus is slightly shorter than the jugal ramus, but equally contributes to the orbits. In *Juravenator*, the jugal ramus of the postorbital is even longer than in *Scipionyx*. This contrasts sharply with the condition seen in *Compsognathus* (Peyer, 2006), where the supraorbital ramus is the longest and might have reached forward over the orbit to meet the prefrontal, excluding the frontal from the orbital margin. Looking only at the proportions of these two rami, the postorbital of *Scipionyx* more closely resembles that of ornithomimosaurs (e.g., Kobayashi & Barsbold, 2005). No resemblance is seen with any basal tetanurans, in which the supraorbital ramus is the shortest process of the triradiate postorbital, nor with dromaeosaurids,

in which the dorsal margin of the supraorbital process is directed dorsomedially, not straight rostrally (Norell & Makovicky, 2004).

The caudally directed squamosal ramus is the shortest of the three rami. We cannot exclude the presence of a fourth medial process, which might have contacted the postorbital process of the parietal in the uncrushed skull, excluding the frontal from the margin of the fenestra but not from the fossa, as is the case in *Allosaurus* (Madsen, 1976).

Jugal - The jugal can be divided into the horizontal body, a long flattened bar of bone forming the ventral margin of the orbit and cheek, and the ascending process, caudal to the orbit. The horizontal body terminates rostroventrally in the maxillary process, which forms an oblique suture with the maxilla. Rostrodorsally, it presents a horizontal sulcus accommodating the base of the lacrimal, but it lacks any sublacrimal expansion, like in *Compsognathus* (Peyer, 2006) and *Juravenator* (Göhlich & Chiappe, 2006). *Huaxiagnathus* (Hwang *et al.*, 2004: fig. 2a) has a feeble expansion, whereas *Sinocalliopteryx* (Ji *et al.*, 2007a: fig. 2b) and most theropods (Rauhut, 2003) have a clearly developed sublacrimal expansion.

As pointed out by Dal Sasso & Signore (1998a: fig. 4), the tip of the maxillary process reaches the caudoventral corner of the antorbital fenestra like in many theropods, including *Compsognathus* (Peyer, 2006) and, possibly, *Juravenator* (Göhlich & Chiappe, 2006: fig. 2a). Differently to *Torvosaurus*, *Ornitholestes*, allosauroids and tyrannosauroids, the jugal of *Scipionyx* is devoid of a crescentic depression marking a slight participation of the antorbital fossa.

Caudally, and ventral to the infratemporal fenestra, the horizontal body of the jugal reaches the quadratojugal with a short process that appears bifid because of the superimposition of the pointed apex of that bone. The caudalmost portion is covered by the quadratojugal and, thus, is hardly visible; rather than rod-like, it seems to be “at least twice as tall dorsoventrally as it is wide transversely”, as suggested by Peyer (2006). In fact, the dorsoventral diameter of the quadratojugal process beneath the infratemporal fenestra seems to be naturally twice as long as its mediolateral diameter, the margin of the process being rounded and regular, without any trace of diagenetic compression. The articulated skull of *Scipionyx* shows a condition similar to that of the reconstructed *Compsognathus* (Peyer, 2006: 4B). Detailed comparisons with *Sinosauropteryx* can hardly be made, as the jugal process was generically described as relatively short and high (Currie & Chen, 2001).

The ascending process (postorbital process) is a thin vertical bar that contacts the descending process of the postorbital, separating the orbit from the infratemporal fenestra. In *Scipionyx*, as well as in some other compsognathids (Hwang *et al.*, 2004; Göhlich & Chiappe, 2006; Ji *et al.*, 2007a), it seems to be more robust (i.e., thicker rostrocaudally) than in the reconstructed skull of *Compsognathus* (Peyer, 2006: fig. 4B).

Quadratojugal - The quadratojugal of *Scipionyx* is L-shaped (or hook-shaped), with rami of equal length tapering to simple pointed ends and forming an angle of about 90°. No caudal process is present. The horizontal



Fig. 32 - Computed tomography image of *Scipionyx samniticus*, showing the bones of the left side. The positions of the left (red arrow) and right quadrate (green arrow) reveal that the bump deforming the right quadratojugal is due to the medial condyle of the left quadrate (red arrowhead).

Fig. 32 - Tomografia computerizzata di *Scipionyx samniticus*, mostrante le ossa del lato sinistro. La posizione del quadrato sinistro (freccia rossa) rispetto al destro (freccia verde) rivela che la protuberanza che deforma il quadratojugale destro è causata dal condilo mediale del quadrato sinistro (punta della freccia rossa).

ramus (jugal process) is still firmly sutured to the jugal, whereas the ascending ramus (quadrate process) has lost its medial contact with the quadrate as a consequence of diagenesis. The ascending ramus terminates in a simple tapering point without reaching the descending process of the squamosal. As noted below (see Squamosal), this simple shape is often related to a point contact, at most, with the squamosal.

A quadratojugal similar to that of *Scipionyx* can be seen in *Eoraptor*, *Caudipteryx* and *Sinornithoides* (Russell & Dong, 1993). At least under UV light, a similarly shaped quadratojugal is also present in *Juravenator* (Göhlich & Chiappe, 2006: fig. 2a, *contra* fig. 2b). In the UV picture, the rami are seen tapering to a pointed end, with the jugal ramus clearly accommodated in a forked depression of the jugal. The two rami seem to be of equal length and form a right angle. Unfortunately, the quadratojugal is not well-exposed in the other known compsognathids, limiting the possibility of comparison.

A knob-like, rounded relief is visible in the corner between the two rami (Figs. 23-24). At first glance, it somewhat resembles the cornual process of the jugal visible in *Alioramus* (Brusatte *et al.*, 2009), but it is not part of the quadratojugal. Rather, as shown by CT analysis, this relief is the result of the diagenetic compression of the thin quadratojugal onto the medial condyle of the left quadrate (Fig. 32).

Squamosal - The squamosal of *Scipionyx* is composed of four prominent processes developed in three different planes: dorsal, lateral and caudal (occipital) (Fig. 33). In the dorsal plane, the squamosal is in extensive contact with the parietal medially (parietal process) and borders the supratemporal fenestra rostrally. On account of some crushing, the postorbital process appears to be bifurcated: the upper ramus belongs to the dorsal surface

of the squamosal and borders the caudolateral margin of the supratemporal fenestra; the lower ramus belongs to the lateral surface of the bone and forms the dorsal margin of the infratemporal fenestra. The lateral surface of the squamosal includes also a robust descending process (quadratojugal or paraquadrate process) which terminates in a squared apex and seems to partially reduce the caudal margin of the infratemporal fenestra.

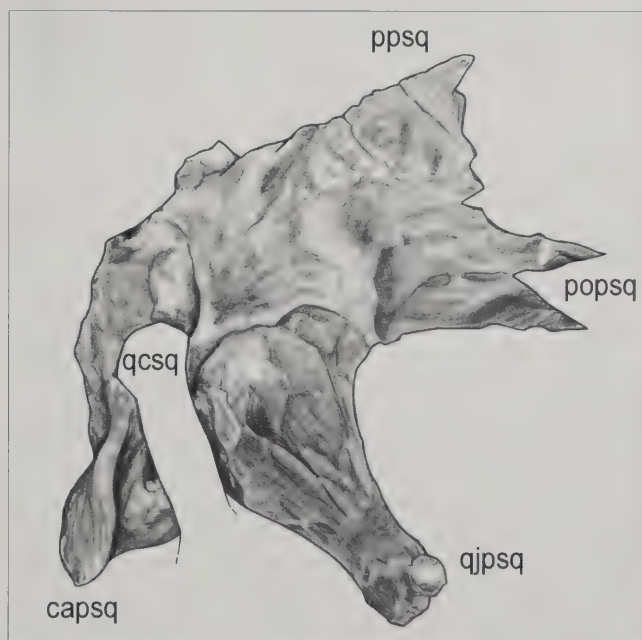


Fig. 33 - Shaded drawing of the right squamosal of *Scipionyx samniticus*, and its tetra-radiate structure. See Appendix 1 or cover flaps for abbreviations.

Fig. 33 - Disegno ombreggiato dello squamoso destro di *Scipionyx samniticus*, con la sua struttura tetra-radiata. Vedi Appendice 1 o risvolti di copertina per le abbreviazioni.

The descending process is probably distorted and might have paralleled the quadrate shaft (but see below) and contacted the ascending process of the quadratojugal in the uncrushed skull. A similar contact occurs in *Jurave-nator* (Göhlich & Chiappe, 2006: fig. 2). If the descending process was naturally formed the way we observe it, in *Scipionyx* the squamosal and quadratojugal did not contact each other. This condition is seen in some basal sau-rischians, such as *Eoraptor* and *Herrerasaurus* (Langer, 2004); in some non-tetanuran theropods, such as *Dilo-phosaurus* and some abelisaurids (Rauhut, 2003); in the advanced Maniraptora, such as the troodontids *Mei* (Xu & Norell, 2004) and *Sinornithoides* (Russell & Dong, 1993); in the dromaeosaurids *Deinonychus* (Ostrom, 1969) and *Sinornithosaurus* (Xu & Wu, 2001); and in birds (Padian, 2004), *Archaeopteryx* included (Elzanowski, 2002). There is a particular similarity between *Scipionyx* and *Herrerasaurus*, as in both genera the descending process of the squamosal terminates in a squared end which expands rostrally within the caudal portion of the infratemporal fenestra. Kobayashi & Barsbold (2005) pointed out that the tip of the ventral process of the squamosal is missing in the ornithomimosaur *Garudimimus*, but it is interesting to note that in both figs. 2 and 3 of Kobayashi & Barsbold (2005) the length and the shape of the process is the same in right and left squamosals. Even if we take into account erosion of the apex on both sides, it is possible that the descending process in *Garudimimus* is almost complete and that it terminated in a squared end that did not contact the quadratojugal. The descending process is rather short and triangular in closely related forms such as *Shenzhou-saurus* (Ji *et al.*, 2003) and *Sinornithomimus* (Kobayashi & Lü, 2003), even if in the latter the squamosal is reached by the very long squamosal process of the quadratojugal.

In *Scipionyx*, irrespective of whether the squamosal and the quadratojugal contacted or not, the quadrate would have been positioned beneath the quadratojugal, resulting more inclined, so that the descending process of the squamosal would have been less inclined with respect to the quadrate than it appears now. For this reason, character 48 has been coded (0) for *Scipionyx* in our phylogenetic analysis.

Caudal to the base of the quadratojugal process, a deep cotyle accommodates the head of the quadrate. Starting from the cotyle, the caudal process of the squamosal is developed caudoventrally, ending in a thin bony crest.

Frontal - The frontal is a large bone with a smooth surface. It is rostrocaudally elongate and widest along the caudal edge, where it forms a distinct postorbital process. As for the nasal, diagenesis has caused the right frontal to appear flattened, its lateral and dorsal sides now lying on the same plane. As described above, the frontal articulates rostrally with the nasal via a thin interdigitate suture. Rostroventrally, it articulates with the prefrontal via a linear suture. The left frontal-prefrontal contact has slid about 2 mm ventrally and is now exposed in medial view, in the dorsalmost area of the orbit. The left frontal, visible as a crescent-shaped surface along the dorsal rim of the right orbit, was wrongly identified as the right “inner (orbital) wall of the frontal” by Dal Sasso & Signore (1998a).

A large U-shaped notch marks the medio-caudal margin of the frontal and the rostromedial margin of the parietal, just medial to the contact between the two bones. It

was formerly thought that this notch was created during the initial preparation of the specimen, when some bone fragments were lost (Fig. 19A). Three-dimensional reconstruction of the skull (Fig. 34) revealed that this notch would have been smaller in the living animal, indicating that part of it has derived from the diagenetic crushing of the hemispheric cranial vault, and that the remnant gap represents, in fact, the still open frontoparietal fontanelle (see Ontogenetic Assessment). The margins of the frontoparietal fontanelle do not appear broken. Likely, the frontoparietal fontanelle acted as a weak point and favoured separation of the frontal and parietal bones during diagenesis.

Ventral to the notch, and up to the postorbital, the frontoparietal suture parallels the margin of a bony ridge having a rugose texture and a sinuous course. This ridge forms the caudolateral end of the frontal and marks the rostral limit of both supratemporal fossa and fenestra. It was previously described as a “transverse postorbital ridge” (Dal Sasso & Signore, 1998a), but should be more properly defined as a “sinusoidal ridge of the supratemporal fossa” (Currie, pers. comm., 1998). A similar structure is considered a diagnostic feature of the dromaeosaurids (Currie, 1995; Barsbold & Osmólska, 1999; Xu & Wu, 2001; Norell & Makovicky, 2004), and was described in troodontids (Makovicky & Norell, 2004) and in the basal tyrannosauroid *Guanlong* (Xu *et al.*, 2006). In all these taxa, the ridge lies in a position more rostral than that in *Scipionyx*, separating the skull table from the excavated caudal tip of the frontal, that participates in the supratemporal fossa. Functionally, this crest might have acted as a supplementary attachment site for the temporal musculature (Holliday, 2009). A sinuous frontoparietal suture is also present in *Compsognathus* (Peyer, 2006), *Sinornithosaurus* (Xu & Wu, 2001) and in the ornithomimosaur *Sinornithomimus*; in the latter taxon it seems associated with a low, rugose ridge (Kobayashi & Lü, 2003: fig. 7B).

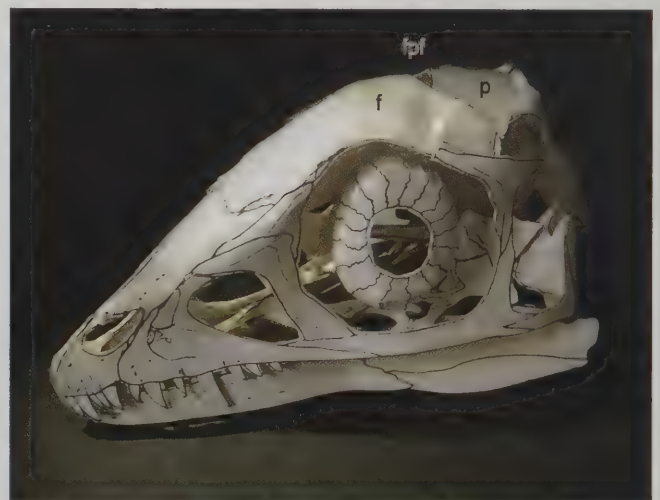


Fig. 34 - Cardboard model of the skull of *Scipionyx samniticus*, showing the frontoparietal notch of the fossil reduced to a narrow space, which is consistent with the fontanelle of a hatchling individual. See Appendix 1 or cover flaps for abbreviations.

Fig. 34 - Modello in cartoncino del cranio di *Scipionyx samniticus*. Con le ossa ricomposte, l'ampia incisura frontoparietale vista nel fossile si riduce ad uno spazio stretto, compatibile con la fontanella di un individuo appena uscito dall'uovo. Vedi Appendice 1 o risvolti di copertina per le abbreviazioni.

Scipionyx resembles most ornithomimosaur (e.g., Kobayashi & Lü, 2003), troodontids (e.g., Ji *et al.*, 2005) and birds (Rauhut, 2003) in having frontals that (1) flare over the orbits up to the frontoparietal suture, where the skull reaches its maximum width, and (2) become domed near the caudal part of the orbit, where the skull forms a flexure between the flat parts of the frontals and the parietals.

In *Scipionyx*, the frontal forms an extensive portion of the dorsal margin of the orbit in lateral view, as does the frontal ramus of the postorbital. In *Compsognathus* (Peyer, 2006), the frontal does not extend beyond the dorso-caudal quarter of the orbit. A condition similar to that of *Scipionyx* can be seen in *Juravenator* and is common in many other unrelated taxa, such as *Eoraptor*, *Coelophysus*, *Nqwebasaurus* (de Klerk *et al.*, 2000), oviraptorosaurs, therizinosauroids, ornithomimosaur (e.g., Kobayashi & Barsbold, 2005; Kobayashi & Lü, 2003) and deinonycho-saur (Xu & Wu, 2001; Barsbold & Osmólska, 1999). Unfortunately, the orbital area is not preserved well enough in other compsognathids.

Parietal - Diagenetic crushing has caused three portions of the parietal of *Scipionyx* to fall on the same plane rather than being exposed in three different views as occurred in life: these are an extended dorsal portion, which is almost flat and lacks any evident sagittal crest; a caudolateral (occipital) portion, which is smaller than the dorsal portion and is slightly concave towards the medial plane; and a ventral portion, partly visible through the upper half of the supratemporal fenestra.

Rostrally, the dorsal portion is still in contact with the sinusoidal ridge of the frontal for most of its length, as first noted by Currie (pers. comm., 1998). Towards the postorbital, it tapers forming a triangular tip, which represents the postorbital process and overhangs the rostral portion of the supratemporal fossa. This tip has lost its contact with the frontal because of crushing of the skull during diagenesis: this opened the parietal like a fan and produced the small crack that can be seen along the dorsal rim of the supratemporal fenestra. As a matter of fact, both crack and contact between the postorbital process of the parietal and the frontal become automatically restored in reconstructing the vault in a three dimensional model. Caudally, the dorsal portion of the parietal is in continuity with the lateral half of the caudolateral portion, whereas in the medial half it has lost its contact with the rostral margin of the supraoccipital, to which it is apparently complementary. The loss of contact is due to crushing, which produced also the crack visible 2 mm rostrally.

Contact with the supraoccipital is still maintained by the caudolateral (occipital) portion of the parietal, which Dal Sasso & Signore (1998a) attributed to the supraoccipital. As mentioned, in the caudal plane this small portion of the parietal forms a medially oriented concavity, the fossa for the *ligamentum nuchae*, and contacts the supraoccipital via an S-shaped suture, which delimits the fossa and is more evident under UV light (Fig. 35). Laterally, the parietal contacts the squamosal through a long, straight suture.

The ventral portion of the parietal appears as a flange below the dorsal portion, terminating ventrally in a clean-cut horizontal suture with the laterosphenoid. The parietal and the laterosphenoid together form the lateral wall of the braincase, and caudally they contact the prootic.

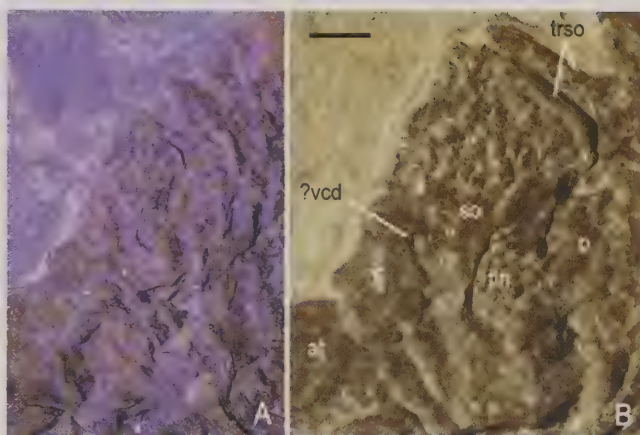


Fig. 35 - Close-ups of the right occipitoparietal region of *Scipionyx samniticus* under ultraviolet-induced fluorescence (A) and visible light (B), documenting the position of the fossa for the *ligamentum nuchae*, and the complex shape of the suture between the supraoccipital and the parietal. Scale bar = 1 mm. See Appendix 1 or cover flaps for abbreviations.

Fig. 35 - Particolari della regione occipitoparietale destra di *Scipionyx samniticus*, in fluorescenza indotta da luce ultravioletta (A) e in luce visibile (B), che documentano la posizione della fossa per il legamento della nuca, nonché il complesso andamento della sutura tra supraoccipitale e parietale. Scala metrica = 1 mm. Vedi Appendice 1 o risvolti di copertina per le abbreviazioni.

In *Scipionyx*, the parietals lack an evident sagittal crest and have only a weakly marked transverse nuchal crest at the angle between the skull roof and the occipital plane. This condition is certainly expected in an immature specimen, but it is noteworthy that it is not necessarily related to the ontogenetic stage, as feebly developed parietal crests are found in adult individuals of small-sized theropods belonging to different groups that are not strictly related to each other, such as the coelophysoids, the compsognathids, the ornithomimosaur (in which the sagittal crest is totally absent; [Makovicky *et al.*, 2004]) and the oviraptorosaurs.

Braincase

The braincase elements are largely obscured by the surrounding bones of the dermal skull roof: stapes, sphenethmoidal and basiptyergoid are entirely invisible. However, some crushed and partly broken elements are visible through the orbital, supratemporal and infratemporal fenestrae.

As for the palate described below, the lack of published descriptions of the braincase in basal coelurosaurians renders it difficult to compare this region and evaluate its eventual taxonomic significance. This is the case, for example, for the tympanic recesses. So, even when extending the comparison to other theropods, we had to base the interpretation of this area on only a few specimens: *Sinraptor* (Currie & Zhao, 1993a), *Sinovenator* (Xu *et al.*, 2002b), *Troodon* (Currie & Zhao, 1993b), *Gallimimus* (Osmólska *et al.*, 1972) and *Majungasaurus* (Sampson & Witmer, 2007).

Supraoccipital - As mentioned above, the supraoccipital has lost contact with the parietal medially. The right supraoccipital begins rostrally with a transverse ridge,

reinforcing the sutural margin, which can be traced as a relief also on the thin portion of the left supraoccipital exposed just rostrally to the right one (Fig. 35). The ridge marks the transition between the dorsal and the occipital plane, the surface of which is marked by a rugose texture for the attachment of the nuchal muscles.

As in the parietal, there is no trace of a sagittal crest close to the midline in the rostralmost portion of the supraoccipital. The lateral margin of the supraoccipital borders on the concavity present on the caudolateral surface of the parietal.

In the holotype of *Scipionyx*, the skull is firmly articulated to the vertebral column, so that the ventralmost portion of the supraoccipital terminates juxtaposed to the neural arch of the atlas. Nevertheless, the ventral margin of the supraoccipital is visible. For a short, medial tract it could represent the dorsal arch of the foramen magnum, whereas the remaining portion could be the exoccipital suture. This uncertainty is due to the fact that the occipital area is not known or not well-described in compsognathids, whereas in some other basal coelurosaurs, such as the basal tyrannosauroid *Guanlong* (Xu *et al.*, 2006), the supraoccipital does not border the foramen magnum.

The supraoccipital of *Scipionyx* closely resembles that of *Allosaurus* (Madsen, 1976: fig. 13) in general shape and mode of contact with the parietal. *Sinocalliopteryx* is the only other compsognathid in which the supraoccipital is well-exposed (Ji *et al.*, 2007a: fig. 2a). It bears a sagittal crest and, according to Ji *et al.* (2007a), it has also a pair of fossae that possibly represent the *fossae ligamenti nuchae*, as is the case in *Velociraptor* (Barsbold & Osmólska, 1999). *Scipionyx* is similar to many basal tetanurans (Holtz *et al.*, 2004) in that these fossae are present on the parietals. A foramen, which by comparison would represent the entrance of the right *vena capitis dorsalis* (e.g., Rauhut, 2003), opens in the wall of the supraoccipital of *Scipionyx*, lateral to the right *fossae ligamenti nuchae* (Fig. 35).

Exoccipital - The exoccipitals of *Scipionyx* are largely hidden by the right squamosal; only the end of the right paraoccipital process can be seen. We are more confident in interpreting the exposed surface as the caudal (occipital), rather than the rostral one, as it is smooth, lacking any rugose texture, is slightly concave and is not marked by an extensive sutural contact with the squamosal.

The exposure of the occipital surface of the paraoccipital process in a skull in lateral view is certainly unusual. However, as the quadrate and the articular region of the mandible are visible in lateral view, rather than being hidden by the quadratojugal, it is apparent that, during diagenesis, deformation of this area of the skull occurred with movement of the bones in a rostral direction. Thus, the lateral end of the paraoccipital process would have been dragged rostrally too. The ridge with rounded margins which borders this element is attributable to the ventral and lateral margins of a paraoccipital process, whereas the outline of the bone visible as a relief underneath the quadrate matches the shape of the dorsal margin.

Prootic - A drop-shaped dimple with a rostrally directed apex is visible in the dorsocaudal corner of the infratemporal fenestra (Fig. 36). This dimple represents the *fenestra ovalis* (the cavity at the bottom of the middle ear,

accommodating the head of the stapes). It is delimited by two small crests, one of which – that ventral to the dimple – is the *crista interfenestralis*. These structures identify the bone which bears them as being the prootic. The presence of what would be the dorsal tympanic recess, which opens dorsally to the *fenestra ovalis*, supports this interpretation. The partly visible recess which opens ventral to the *crista interfenestralis* might be the subotic recess.

Most of these elements were well-illustrated and described in the troodontid *Sinovenator* (Xu *et al.*, 2002b). In *Scipionyx*, the dorsal tympanic recess is directly visible only for a short tract, after which its outline can be traced underneath the squamosal as a depression (Figs. 24, 36B) running up to the supratemporal fenestra, where it surfaces again in the caudoventral corner. This interpretation is consistent with prootic recesses with similar topology, i.e., adjacent to the parietal and laterosphenoid, observed in coelophysoids (Raath, 1985), ornithomimids (Makovicky & Norell, 1998), *Velociraptor* (Barsbold & Osmólska, 1999) and, possibly, *Archaeopteryx* (Elzanowski, 2002). Thus, the prootic of *Scipionyx* extends dorsally and is visible through the supratemporal fenestra, where it forms a vertical suture with the laterosphenoid and the parietal.

Basioccipital-Basisphenoid - Only a small portion of this complex can be seen emerging just ventral to the right paraoccipital process. Based on its size and shape, we interpret this as the right basal tuber.

Basisphenoid-Parasphenoid - The most visible structure of this bone complex is the cultriform process of the parasphenoid. It seems to be complete and oriented rostrorodorsally, crossing the dorsal half of the orbit obliquely. The cultriform process is a straight, slender, rod-like bone that in *Scipionyx*, as in most small theropods (e.g., *Syntarsus*, *Dromaeosaurus*), probably pointed rostrally. Its rostrorodorsal orientation in the fossil is likely an artefact of preservation, as it occurs only in non-coelurosaurian taxa which attained medium to large body size (e.g., *Majungasaurus* and *Allosaurus*). Moreover, in those taxa the cultriform process has a different, plate-like shape (Rauhut, 2003). The simultaneous exposition of both right lateral surface and median ventral sulcus indicates that in *Scipionyx* the cultriform process rotated on its long axis (Currie, pers. obs., 1999). The flat lateral wall and the presence of a ventral sulcus suggest also that the cultriform process of *Scipionyx* had the shape of an inverted V in cross section.

Ostrom (1978) recognised the cultriform process in *Compsognathus* as a double structure with an inverted V-shaped section, after having observed rostral laminae unquestionably continuous with other ventral elements of the braincase. More recently, Xu & Wu (2001) described a triangular cross section in the cultriform process of *Sinornithosaurus*.

As the base of the cultriform process is not visible, it is impossible to ascertain its degree of pneumatization. However, the exposed portion suggests that the cultriform process of *Scipionyx* does not possess a pneumatic bulla as expanded as in troodontids (e.g., Currie & Zhao 1993b).

The cultriform process and the body of the basisphenoid-parasphenoid are two braincase elements that are

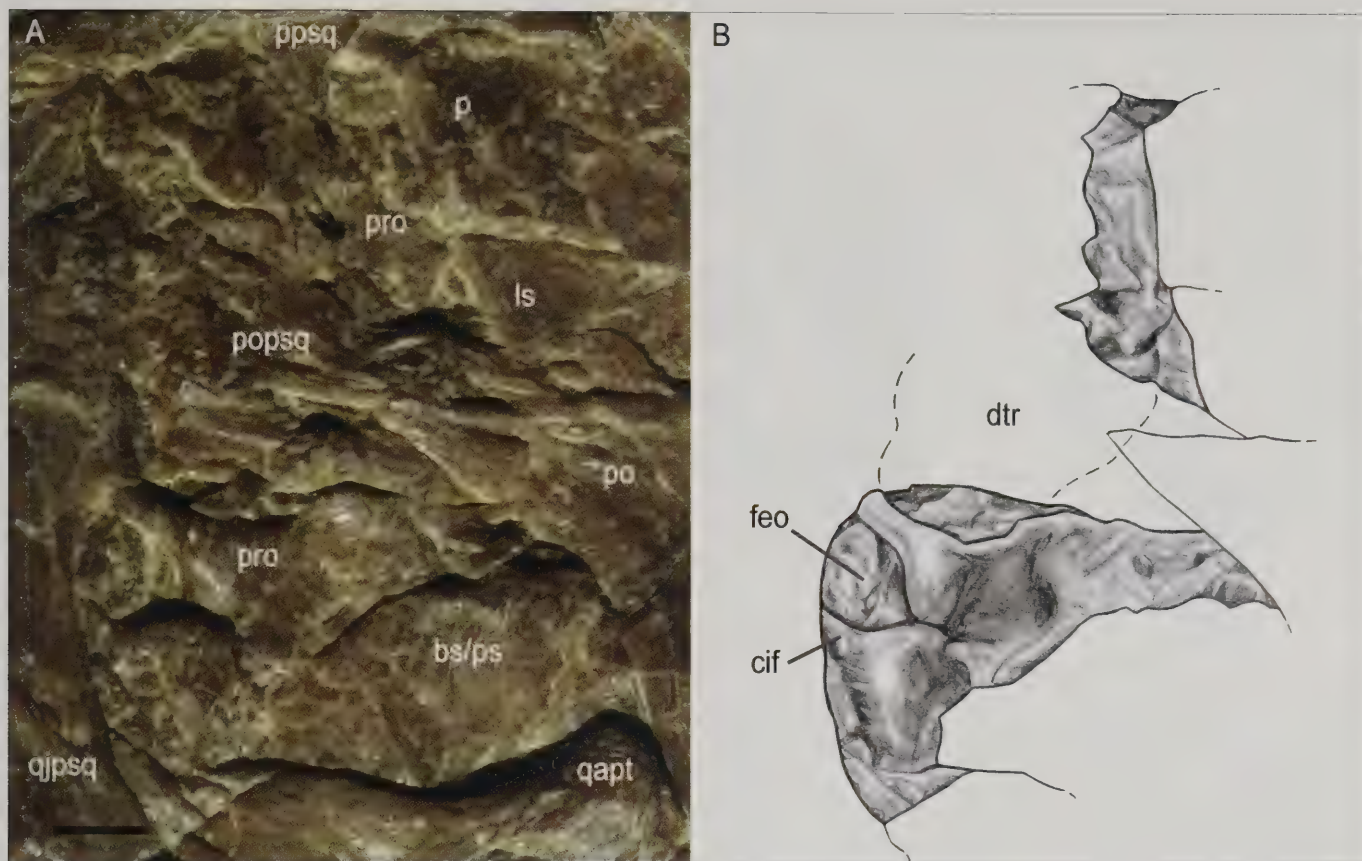


Fig. 36 - Some bones of the braincase of *Scipionyx samniticus* can be seen through the right supratemporal fenestra (A), including the prootic (B). Scale bar = 1 mm. See Appendix 1 or cover flaps for abbreviations.

Fig. 36 - Attraverso la finestra sopratemporale di *Scipionyx samniticus* sono visibili alcune ossa della scatola cranica (A), tra cui il prootico (B). Scala metrica = 1 mm. Vedi Appendice 1 o risvolti di copertina per le abbreviazioni.

usually fused in the archosaurs. Close examination of the area caudal to the postorbital-jugal contact and just ventral to the quadratic ala of the pterygoid reveals a morphological continuity between them also in *Scipionyx*. Moreover, the basisphenoid-parasphenoid complex faces more extensively dorsally to the quadrate ala of the pterygoid, within the infratemporal fenestra.

Laterosphenoid - Within the supratemporal fenestra, a partially covered bone can be seen, dorsally separated from the parietal by a weakly incised horizontal suture. Based on its close relationship with the right parietal, it can be interpreted as the right laterosphenoid. *Contra* Dal Sasso & Signore (1998a: fig. 4), the bone emerging in the dorsal third of the infratemporal fenestra is not the laterosphenoid, but part of the prootic and basisphenoid-parasphenoid complex, as described above.

Orbitosphenoid - Microscopic examination of the element previously identified as the orbitosphenoid by Dal Sasso & Signore (1998a) revealed that it has a laminar structure and texture analogous to scleral plates. That element can now be ascribed, therefore, to the right scleral ring, to which it has also a compatible position. Although it cannot be proven, it is possible that a thin portion of the real orbitosphenoid of *Scipionyx* is visible in the same area, in the form of a splinter of bone previously considered as the rostromedial (inner) wall of the postorbital ("ipo" in Dal Sasso & Signore, 1998a: fig. 4).

Palatoquadrate complex

Vomer - In theropods, the vomers – thin rods of bone located astride the sagittal midline of the palate – are generally indistinguishably fused rostrally (see Ontogenetic Assessment). However, in the holotype of *Scipionyx* they are completely separated and well-exposed (Fig. 37). The right vomer seems to be in contact with the left palatine via a laminar portion of the pterygopalatine process, but it is only superimposed on it. In fact, the right vomer has rotated clockwise up during diagenesis to expose its rostral end (premaxillary process) in-between the m4 teeth, where it overlaps the left vomer (Fig. 30). Because of this rotation, the pterygopalatine end now points dorsally, but remains still aligned with the main body of the bone, showing that the vomer of *Scipionyx* is back straight. The left vomer, which is not so well-preserved, has lost contact with both palatine and pterygoid: facing rostrally between m2 and m4, it runs caudally in a straight line under the crown of m4, re-appearing first between m4 and m5, where it passes below and under the right vomer, and then in the caudoventral corner of the antorbital fenestra, and finally slipping underneath the left palatine (Figs. 25C-D, 30).

Palatine - Both palatines are exposed, the right one within the rostral portion of the orbit, and the left one within the caudal half of the antorbital fenestra. Therefore, the right palatine has shifted dorsocaudally with respect to the position it had in life, together with the whole

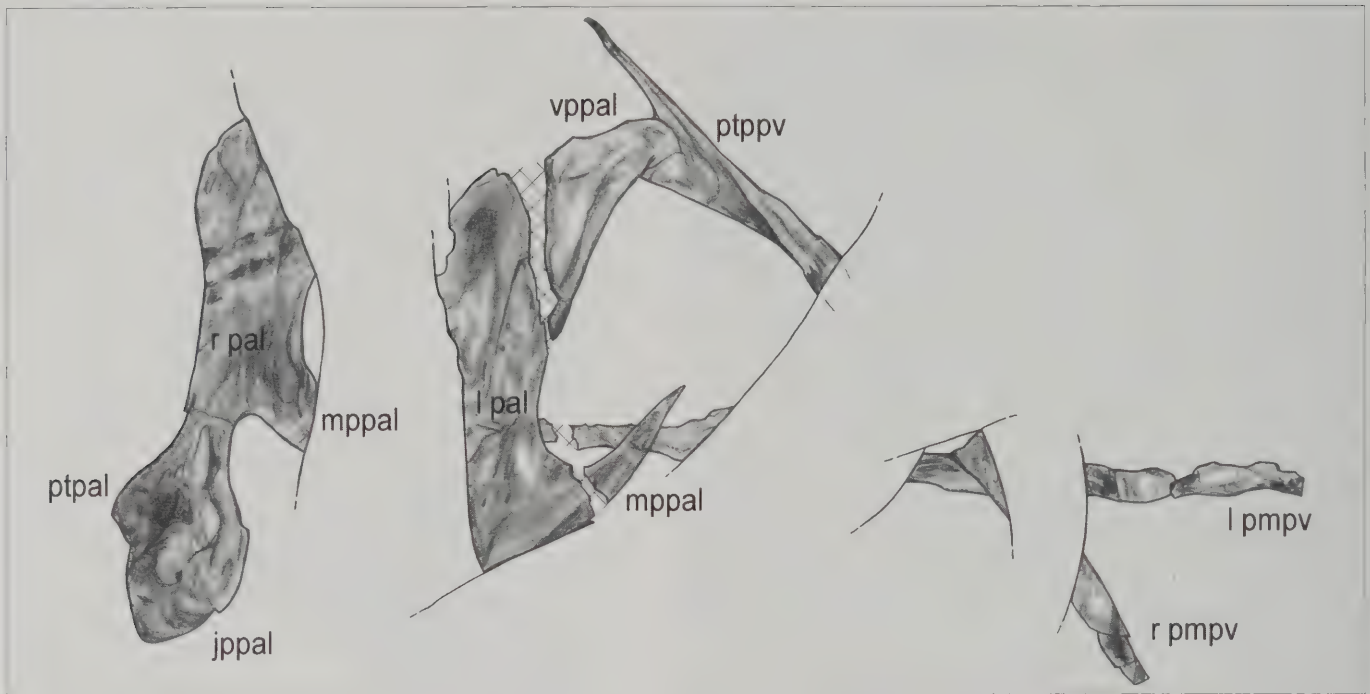


Fig. 37 - Shaded drawing of the palatines and vomers of *Scipionyx samniticus*. See Appendix 1 or cover flaps for abbreviations.

Fig. 37 - Disegno ombreggiato dei palatini e vomeri di *Scipionyx samniticus*. Vedi Appendice 1 o risvolti di copertina per le abbreviazioni.

pterygoid complex, whereas the left palatine has only shifted dorsally. The main body of the palatine (interchoanal bar) terminates dorsally in a margin that is unlike the large, lobate structure of *Allosaurus* (Madsen, 1976). The right lacrimal obscures the maxillary process and the vomeral process of the right palatine. Nevertheless, the shifting of the right palatine has revealed the pterygoid process and the jugal process. Instead, the parts of the left palatine that are visible are the thin maxillary process and the vomeral process, which mark the caudal margin of the choana. Thus, the combined observations on the two palatines demonstrate that these bones are tetradiate in *Scipionyx* (Fig. 37).

A tetradiate palatine (i.e., possessing also a jugal process) is partially exposed also in *Compsognathus* (Peyer, 2006: fig. 4A). Apart from this datum, the other known compsognathids do not show any other detail useful in reconstructing the shape of their palatine.

In *Scipionyx*, the pterygoid-palatine contact is very limited on account of the presence of a subsidiary palatal fenestra. Seemingly, the left palatine contacts the right vomer, which pivoting on the apex of the vomeral process of the palatine, has rotated clockwise. Because of this rotation, part of the vomeropalatine suture cannot be distinguished. Differently to *Allosaurus* (Ji *et al.*, 2003; Norell & Makovicky, 2004) and *Daspletosaurus* (Currie, 2003), the vomeral process is longer than the maxillary process in *Scipionyx*, as is the case in *Majungasaurus* (Sampson & Witmer, 2007), *Sinraptor*, *Shenzhosaurus*, *Deinonychus*, *Velociraptor* and, possibly, *Juravenator* (Göhlich & Chiappe, 2006: fig. 2a).

Within the notch delimited by the maxillary process and the jugal process, some plates of the ?right scleral ring are found. The palatine and the ectopterygoid are not completely separated by the pterygoid, having a point contact at most. This contact is more extensive in *Velociraptor* than in *Scipionyx*, and even more in ornithomimids and

oviraptorosaurs, in which the two bones contact through a long oblique suture (Barsbold & Osmólska, 1999).

Pterygoid - The pterygoid is the longest cranial bone of *Scipionyx*, extending rostrocaudally for about two-thirds of the whole cranial length (Figs. 25C-D, 38). Both right and left pterygoids have markedly shifted dorsally above the plane of the palate. Now their palatal rami, still separated by the interpterygoid vacuity, cross the orbit horizontally, converging rostrally and intersecting beneath the lacrimal: they re-emerge in the dorsal portion of the antorbital fenestra, diverging up to their rostral ends (vomeral processes).

In both pterygoids, the rod-like palatal ramus is well-preserved, whereas the laminar portion formed by the lateral processes directed towards the ectopterygoids and the palatines is preserved and partially visible only in the right pterygoid. It has a rostrolaterally directed horizontal process (caudal palatine process) which, contacting the medial wall of the palatine, delimits two fenestrae: the subsidiary palatal fenestra rostrally and the suborbital fenestra, which is markedly larger, caudally. As mentioned, the subtemporal fenestra is delimited rostrally by another process of the pterygoid (ectopterygoid process), which rises from the caudalmost portion of the palatal ramus and forms an arched bar ventrolaterally directed and contacting the ectopterygoid. In the uncrushed skull, the ventralmost end of this bar, now covered by the jugal, would have projected down from the roof of the mouth, ventral to the jugal, like in many theropods (e.g., Weishampel *et al.*, 2004). At the same level, the ventromedial surface of the arch forming the left ectopterygoid process can be seen between the two palatal rami of the pterygoids. Caudally, the horizontal rod of the right palatal ramus terminates in a pointed caudomedial process (posteromedial process *sensu* Madsen & Welles, 2000: pl.5) which, because of diagenetic compression, is visible as a relief in lateral view, slightly superimposed onto the lateral surface of the jugal.

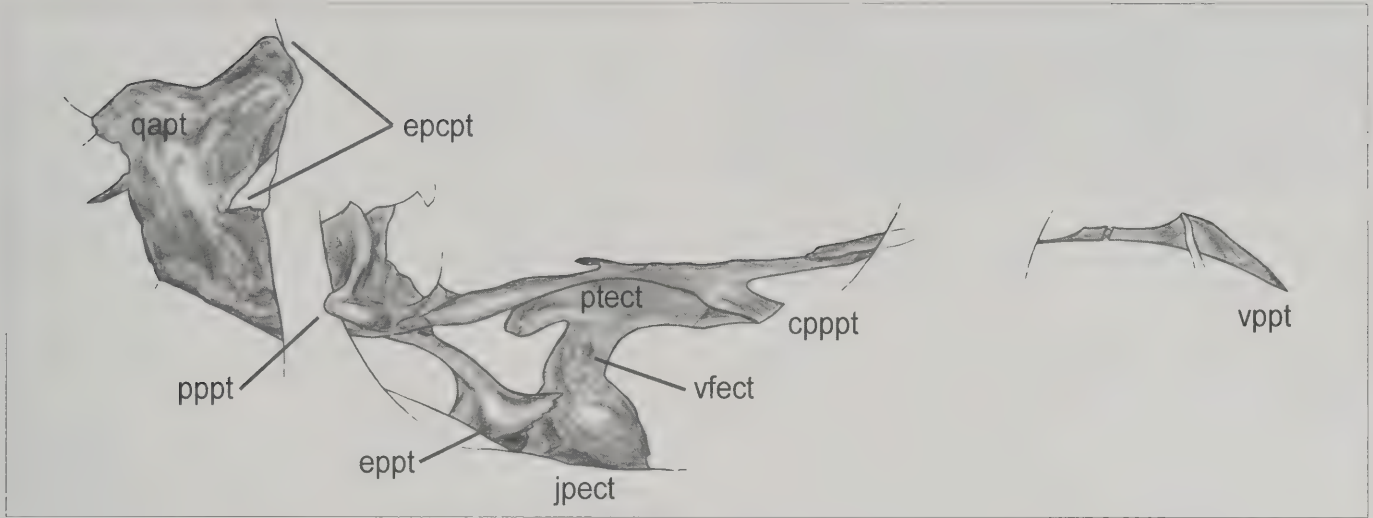


Fig. 38 - Shaded drawing of the right pterygoid and ectopterygoid of *Scipionyx samniticus*. See Appendix 1 or cover flaps for abbreviations.

Fig. 38 - Disegno ombreggiato dello pterigoide ed ectopterigoide destri di *Scipionyx samniticus*. Vedi Appendice 1 o risvolti di copertina per le abbreviazioni.

An abrupt, right-angled change of direction in the caudomedial process of the pterygoid forms a vertical ramus. This vertical ramus is reinforced by a ridge which expands in the postorbital region to form a broad, bony lamina called the quadrate ala, previously interpreted as the basisphenoid ("bs" in Dal Sasso & Signore, 1998a). This ala occupies more than one third of the infratemporal fenestra and contacts the quadrate with a broad, extensive suture.

In the middle of the infratemporal fenestra, the quadrate ala protrudes up to reach a plane more raised laterally than the postorbital-jugal bar, exposing all its thickness and a rostral margin which matches perfectly the outline of the caudal margin of the epipterygoid. This margin, therefore, represents the contact margin between the two bones (Fig. 25C).

Epipterygoid - In lateral view, the epipterygoid of *Scipionyx* has roughly the outline of an isosceles triangle, with the acute apex slightly bent rostrally (Fig. 39). It is fossilised with the caudal margin leaning against the rostromedial (inner) wall of the postorbital, but in the undisturbed skull, as mentioned, it linked the quadrate ala of the pterygoid to the laterosphenoid. Ventrally, the epipterygoid forks into a rostral process, which originally was in continuity with the reinforced rostral ridge of the quadrate ala of the pterygoid, and a caudal process of similar shape and size. In between these processes, the outer surface of the epipterygoid bears a shallow concavity.

This bone was not identified by Dal Sasso & Signore (1998a: fig. 4), who interpreted the dorsal half of the bone as part of the postorbital ("ipo"), leaving the ventral half as an indeterminate bone fragment. The epipterygoid of *Scipionyx* is similar in shape to that of *Allosaurus* (Madsen, 1976) and *Daspletosaurus* (Currie, 2003).

Ectopterygoid - Because of the compression of the skull, the right ectopterygoid of *Scipionyx* exposes mainly its dorsal surface and emerges in the orbit, just below the right pterygoid. They remain in contact through a large, T-shaped pterygoid process (Fig. 38). The same shape and mode of contact can be seen in *Juravenator* (Göhlich & Chiappe, 2006: fig. 2a).

Rostrally, the ectopterygoid borders the caudal margin of the suborbital fenestra and has a point contact with the pterygoid process of the palatine. The contact with the rod of the palatal ramus of the pterygoid is markedly extensive, and more so than in *Sinraptor* (Currie & Zhao,

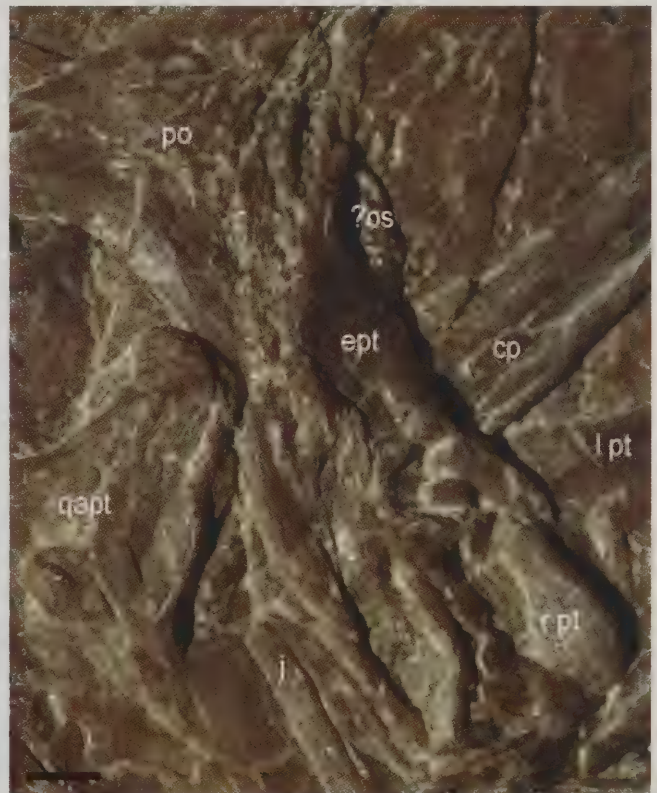


Fig. 39 - Close-up of the right postorbital region of *Scipionyx samniticus*, showing the diagenesis-related protrusion of some elements of the braincase and of the palate above the level of the postorbital bar. Scale bar = 1 mm. See Appendix 1 or cover flaps for abbreviations.

Fig. 39 - Particolare della regione postorbitale destra di *Scipionyx samniticus*. Si noti la protrusione, dovuta alla diagenesi, di alcuni elementi della scatola cranica e del palato al di sopra del livello della barra postorbitale. Scala metrica = 1 mm. Vedi Appendice 1 o risvolti di copertina per le abbreviazioni.

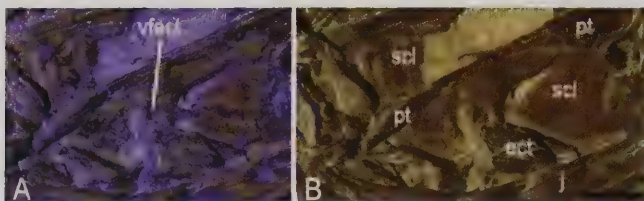


Fig. 40 - Palatal bones of *Scipionyx samniticus* under ultraviolet (A) and visible light (B). Note the extensive contact between the pterygoid and the ectopterygoid. Scale bar = 2 mm. See Appendix 1 or cover flaps for abbreviations.

Fig. 40 - Ossa del palato di *Scipionyx samniticus* in luce ultravioletta (A) e visibile (B). Si noti il contatto prolungato tra lo pterigoide e l'ectopteroide. Scala metrica = 2 mm. Vedi Appendice 1 o risvolti di copertina per le abbreviazioni.

1993a). As in *Sinraptor*, another fenestration is present in *Scipionyx*, between the ectopterygoid process of the pterygoid and the pterygoid process of the ectopterygoid. This is unlike *Dromaeosaurus*, in which a long, continuous suture unites the pterygoid caudally with the ectopterygoid. Besides part of its bulky portion, most of its lateral portion forming the jugal process and its caudoventral corner, which contacted the ventral bar of the pterygoid projecting below the roof of the mouth, are hidden by the jugal. Under UV (Fig. 40A) and properly oriented visible light (Fig. 40B), a shallow circular depression can be seen at the centre of the main body of the ectopterygoid. This depression is consistent with the position of the pneumatic opening, or ventral fossa, which opens ventrally in many theropods (e.g. Currie, 2003: fig. 12).

Quadrate - In lateral view, the quadrate of *Scipionyx* appears as a relatively tall, subvertical pillar with rounded ends (Fig. 41). Actually, it possesses also a remarkable expansion, the pterygoid ala, directed rostromedially and partially covered by the descending process of the squamosal and the ascending process of the quadratojugal. As mentioned, the pterygoid ala consents the pterygoid and the quadrate to be in perfect anatomical continuity, forming the medial wall of the adductor chamber.

The outline of the ventral margin of the pterygoid ala is well-delineated only in proximity of the lateral condyle; rostroventrally, it is hardly distinguishable from the lateral surface of the caudal portion of the mandible because of the similarities in surface texture and the strong diagenetic compression which almost fused the laminar portion of the quadrate onto the surangular. For this reason, part of the pterygoid ala was misinterpreted as the caudal portion of the pterygoid by Dal Sasso & Signore (1998a: fig.4).

The probably single quadrate head is exposed in lateral view within the laterally open quadrate cotyle of the squamosal, slightly caudal to the vertical projection of the quadrate lateral condyle. In fact, during diagenesis the quadrate pivoted on the quadrate cotyle of the squamosal, loosing the connection with the quadratojugal and rotating a little caudally. As a consequence, the quadrate is now faintly inclined rostrally, whereas *in vivo* it was slightly more inclined, based on the position of the quadratojugal which is still articulated to the jugal. According to Rauhut (2003), a rostral inclination of the quadrate occurs in various degrees in spinosaurids, ornithomimosaurids and *Archaeopteryx*.

The caudoventral corner of the lateral condyle presents a rugose, drop-shaped surface which represents the ar-

ticular surface for the quadratojugal, confirming the *post mortem* loss of articulation between the two bones. A little concavity marks the paraquadrate foramen just dorsal to that articular surface; this permitted the passage of neurovasculature between the occiput and the adductor chamber.

No remains of the left quadrate are directly visible in *Scipionyx*. However, as mentioned, the low dome visible under the right quadratojugal (Figs. 23, 42) represents the medial condyle of the left quadrate. This is shown by the deepest parasagittal slices of the CT scan (Fig. 32).

Mandible

The bones of the lower jaw of *Scipionyx* formed two slender, straight and laterally compressed rami united at the rostral ends by a short, weak symphysis. The tooth row of the mandible extends from the symphysis to the level of the caudal border of the antorbital fenestra and, notably, further caudally than the upper tooth row (Figs. 23-25; see also Remarks to the Emended Diagnosis).

Contrary to what appeared to be logical on first examination of the fossil (Dal Sasso & Signore, 1998a), the bones of the mandible protruding most to the right side actually belong not to the right hemimandible but rather to the left. Looking at the mandible in a very oblique right ventrolateral view (Fig. 42), the left mandibular ramus can be seen to stick out from the plane of the slab more than the right

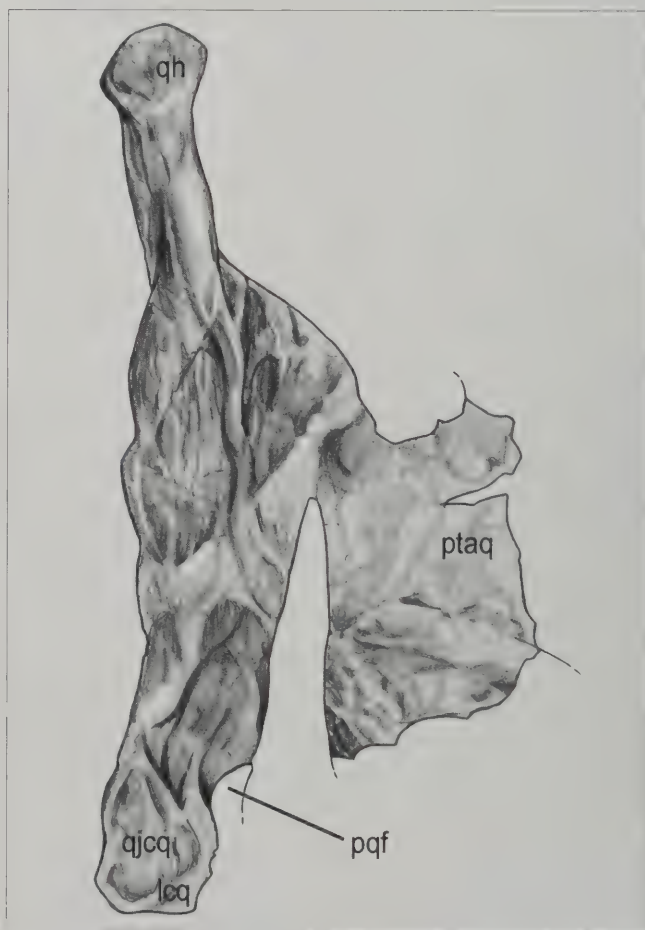


Fig. 41 - Shaded drawing of the right quadrate of *Scipionyx samniticus*. See Appendix 1 or cover flaps for abbreviations.

Fig. 41 - Disegno ombreggiato del quadrate destro di *Scipionyx samniticus*. Vedi Appendice 1 o risvolti di copertina per le abbreviazioni.

one, from only few millimetres caudal to the symphysis backwards. Thus, the left mandibular ramus shifted ventral to the right ramus during diagenesis, and then was crushed in its dorsal half under the right ramus itself; as a consequence, it remained raised in the ventral half. In the end, the bones composing that portion (i.e., left dentary, left splenial and left prearticular) lie on a plane about 0.3 mm higher than that of the counterlateral elements.

Based on what can be seen in both rami, almost all the elements of the lower jaw can be described and reconstructed, at least in part. The only exception is represented by the coronoids, which in *Scipionyx* are covered by the bones of the skull and of the right hemimandible.

Mandibular openings - In lateral view, the mandible of *Scipionyx* lacks any large opening. Contrary to Dal Sasso & Signore (1998a: fig. 4, “emf”) and according to Peyer (2006), there is no external mandibular fenestra: actually, the large depression below the right angular originated from the dorsal displacement of that bone. This depression has brought to light the lateral surface of the right prearticular. There is no external mandibular fenestra also in the lower jaw of the compsognathids *Compsognathus* (Peyer, 2006), *Huaxiagnathus* (Hwang *et al.*, 2004), *Sinosauropteryx* (Currie & Chen, 2001) and *Juravenator* (Göhlich & Chiappe, 2006), or in *Archaeopteryx* (Elzanowski, 2002). According to Peyer (2006), the absence of a mandibular fenestra is an autapomorphy of compsognathids. Interestingly, this opening is reported to be absent or extremely reduced also in the basal tyrannosauroid *Dilong* (Xu *et al.*, 2004).

Evidence for an adductor fossa facing medially in the caudal third of the lower jaw (Fig. 42), and bordered dorsally by the surangular and ventrally by the prearticular, is given by the reinforced margin of the right surangular and the convex rim of the left prearticular.

The Meckelian fossa is not exposed because the splenial, which covers it, is preserved *in situ*; however, obvious

evidence for the presence of the fossa are the Meckelian groove of the dentary and the mylohyoid notch (Meckel notch) of the splenial. As for the latter, we tend to interpret it as a notch rather than as a foramen because it is located close to the ventral margin of the splenial, along its suture with the dentary (see Splenial).

The presence of an internal mandibular fenestra cannot be ascertained because the right dentary obscures the dorsal half of the contact between the left prearticular and the left splenial.

Dentary - The dentary of *Scipionyx* is quite elongate and tapers gradually rostrally, with the ventral and the dorsal edge becoming subparallel. It appears also quite slender, but less so than in *Compsognathus* (Ostrom, 1978), *Huaxiagnathus* (Hwang *et al.*, 2004), *Sinosauropteryx* (Currie & Chen, 2001; Ji *et al.*, 2007b) and *Juravenator* (Göhlich & Chiappe, 2006), because the snout of *Scipionyx* is proportionally less elongate. The bone is almost fully toothed, with a tooth row of 10 teeth.

Rostrally, the right and left dentaries articulate through a short subvertical symphysis, which in life would have been quite weak, as in many theropods, allowing considerable kinesis (Britt, 1991; and references therein). Only the rostral suture can be seen of the symphysis, because the two rami are preserved still in articulation and hide the articular surface. The rostral end of the left dentary does not lie in medial view but, rather, is flattened and deformed for a short tract into a flap lying on the remnants of the left dentary, maintaining its contact with the rostral end of the right dentary. It is unlikely that the symphysis was so firmly sutured to promote distorsion of the right dentary instead of separation of the two rami (see also Skeletal Taphonomy). Thus, the preserved contact between the two rami suggests that the symphyseal region was more U- than V-shaped when seen in occlusal view.



Fig. 42 - A grazing view of the mandibular bones of *Scipionyx samniticus* reveals the uplift of the elements from the left side along their ventral margin, with respect to the same margin of the right hemimandible (follow the two margins from the symphysis, in a caudal direction). See Appendix 1 or cover flaps for abbreviations.

Fig. 42 - Una vista radente delle ossa mandibolari di *Scipionyx samniticus* mostra il sollevamento degli elementi del lato sinistro lungo il margine ventrale, rispetto allo stesso margine dell'emimandibola destra (seguire i due margini in direzione caudale, a partire dalla sinfisi). Vedi Appendice 1 o risvolti di copertina per le abbreviazioni.

Caudally, the right dentary connects with the surangular through a zigzagging suture that, after having formed a dorsal process (intramandibular process *sensu* Currie & Zhao, 1993a), runs obliquely in a caudoventral direction, suturing with the angular in its caudal third. Contrary to many theropods, in which the caudal extension of the dorsal margin of the dentary never goes beyond the level of the caudalmost maxillary tooth (Rauhut, 2003), in *Scipionyx* the dorsal margin of the dentary reaches the level of the rostral portion of the orbit. Other exceptions are *Juravenator*, which seems to be similar to *Scipionyx*, and *Ornitholestes*, in which the dorsal margin of the dentary is even more extended caudally and reaches the vertical projection of the orbital centre.

In lateral view, the right dentary of *Scipionyx* bears two rows of neurovascular foramina, not accommodated along any deep groove: a well-defined row of foramina extends beneath and parallel to the dorsal margin of the dentary; a second, less marked row of foramina extends parallel and just dorsal to the ventral margin of the dentary. In *Compsognathus* (Ostrom, 1978), *Huaxiagnathus* (Hwang *et al.*, 2004: fig. 2A) and, probably, *Juravenator* (Göhlich & Chiappe, 2006: fig. 2a) the foramina are arranged in two parallel rows. Two rows, with the upper one sitting in a groove, are considered to be diagnostic of Dromaeosauridae by some authors (Currie, 1995; Barsbold & Osmólska, 1999; Xu *et al.*, 2001). One row of foramina, emerging within a deep groove, is instead present in the gracile dentary of the basal tyrannosauroid *Coelurus* (Carpenter *et al.*, 2005b). Apart from the two rows of foramina, the external surface of the dentary of *Scipionyx* is almost smooth, with the exception of the thin furrows and pits observed in the bones of many immature individuals, especially embryos and post-hatchlings (see Ontogenetic Assessment).

The medial surface of the left dentary is exposed for all its length. In the rostral end, just caudal to the symphysis, it is markedly wavy, as in *Allosaurus* (Madsen, 1976). From this wavy area, a groove (the Meckelian sulcus) opens and directs caudally, disappearing for a short tract and then reappearing in the splenial.

Supradentary-coronoid - Parallel to the dorsal margin of the right dentary, a thin bony lamina appears as the background of the last four teeth of the mandible. It is hidden ventrally by the right dentary, and caudally by the left maxilla. Its exposed portion has the shape of a rostrocaudally elongate rectangle. During the present study, this bony lamina was initially interpreted as the lateral (inner) surface of the right supradentary, or the medial (outer) surface of the left supradentary. Although those interpretations cannot be ruled out, based on its position and shape we prefer to consider it as the dorsal portion of the right splenial (see below).

Holtz *et al.* (2004) reported that in some tetanurans, such as some tyrannosaurids, allosauroids and dromaeosaurids, the coronoid and the supradentary form a single, continuous bone. Other tetanurans have a small, flat, triangular coronoid, forming the rostradorsal margin of the adductor fossa, and a narrow, band-like supradentary medially overlying the interdental plates along the dorsal portion of the dentary. The bony lamina visible in *Scipionyx* does not match coronoids, neither in shape nor size, as it is definitely too large and rectangular. If it was a supradentary, or a single continuous supradentary-coronoid,

given its length and position it would be either largely incomplete rostrally or the only cranial bone considerably displaced caudally during fossilisation.

Splenial - The size and position of the thin bony lamina mentioned above, emerging dorsal to the caudal half of the right dentary, suggest that it may well represent the dorsal portion of a splenial, as noted also by Audatore (pers. comm., 2010) in making the reconstruction of the skull (see Cranial Reconstruction), and according to the interpretive drawing of the medial side of the lower jaw in *Compsognathus* (Peyer, 2006: fig. 5B). The bony lamina probably represents the disarticulated and dorsally displaced right splenial, rather than the dorsal half of a broken left splenial, in that the ventral portion of the left splenial emerges ventral to the ventral edge of the right dentary and it is still in articulation with the left dentary, without bearing any trace of fracture.

The visible portion of the left splenial has the shape of a low triangle, with the base elongate rostrocaudally and tapering rostrally. The dorsal portion of the putative right splenial terminates rostrally more or less at the same vertical level where the left splenial reaches the horizontal level of the Meckelian groove, marking the point in which the splenial would have probably formed a long, thin rostral extremity, with subparallel margins, composing most of the medial wall of the Meckelian canal.

Reconstructing both hemimandibles, the splenial does not emerge in lateral view along the ventral side of the jaw, contrary to a previous hypothesis (Dal Sasso & Signore, 1998a) that regarded the splenial as the right one, emerging ventrally like in dromaeosaurs (e.g., Makovicky & Norell, 2004). Rostrally to the fracture in the slab which crosses the whole cranium, astride the suture with the dentary, the ventral margin of the left splenial of *Scipionyx* is marked by a concavity corresponding to the mylohyoid notch/foramen (or Meckel's notch/foramen). Because of the imperfect preservation of the bone in that point, it is not possible to establish with certainty whether it is a notch opened towards the dentary, as it seems to be, or a foramen completely enclosed in the splenial, bordered ventrally by a thin splinter of bone lost during the formation of the mentioned fracture. A ventrally facing mylohyoid notch is reported to be present in *Compsognathus* (Peyer, 2006) and in some tetanurans such as *Allosaurus* and *Monolophosaurus* (Rauhut, 2003), whereas in the compsognathid *Sinocalliopteryx* (Ji *et al.*, 2007) and in most theropods (Rauhut, 2003) the foramen is reported to be completely enclosed in the splenial. Caudally, the left splenial contacts the left prearticular via a linear, oblique contact, the former bone slipping under the latter.

Surangular - The surangular forms the entire dorsolateral margin of the mandible caudal to the tooth row. The right surangular of *Scipionyx* is preserved in place, connected to the right dentary via a zigzagging suture. The dorsal margin of the right surangular, delimiting the lower jaw dorsally, is in perfect continuity with that of the dentary. From the contact with the dentary, it disappears for a short tract under the right jugal, then it reappears for 5 mm within the orbit, superimposed on the arched, ventrolaterally directed bar of the right pterygoid, and terminates in the ventral third of the infratemporal fenestra, covering the pterygoid ala of the quadrate. This last tract was pre-

viously ascribed to the pterygoid and the basipterygoid (Dal Sasso & Signore, 1998a: fig. 4). The ventral portion of the right surangular is hidden by the angular, which has moved dorsally.

Although exposed in lateral view, the right surangular shows a morphology typical of its medial side. In fact, the thickened dorsal rim of the surangular, inflected medially and building the dorsal edge of the adductor fossa, has been highlighted as a relief by the diagenetic crushing. A thin splinter of the left surangular is visible ventral to the left prearticular at the caudal end of the mandible (Fig. 42).

Angular - The bone previously interpreted as the right surangular (“sa” in Dal Sasso & Signore, 1998a) actually includes also the right angular. These two bones appear like one element because the latter has moved dorsally, losing its sutural contact with the dentary, and has overlapped the ventral portion of the lateral surface of the right surangular. The identification of the bone as the angular is supported by the fact that its ventral rim neither terminates abruptly nor tapers as a contact margin; rather, it is very smooth (Fig. 42), as expected in a marginal bone, as is the case of the ventral margin of the dentary. The angular appears to taper caudally but it is partially hidden by the jugal-quadratojugal complex, so in this area its shape and mode of contact with the adjacent bones cannot be observed.

Prearticular - Only a portion of the lateral surface of the right prearticular can be seen in *Scipionyx*, i.e., the surface which was in contact with the right angular before the latter moved dorsally. Further support to this interpretation is given by the alignment existing between the ventral margin of the right prearticular and that of the dentary. The fact that the surface of the right prearticular lies in a depressed plane led to misinterpret the depression as a right external mandibular fenestra (“emfe” and “ipa?” in Dal Sasso & Signore, 1998a: fig. 4).

The left prearticular is the most exposed among the bones of the left hemimandible. As it has undergone severe crushing under the cheek and the right hemimandible, it is broken into three pieces, previously interpreted as distinct elements (“an”, “pa”, and “sp” in Dal Sasso & Signore, 1998a: fig. 4). New examination of the alleged sutures between these three pieces in the light of the continuity of their surfaces, which compose a regular dorsoventrally convex margin, and based on the shape of the prearticular in most theropods, suggests that the three pieces belong, in fact, to a single bone, the left prearticular. Such continuity can be clearly seen in medioventral view (Fig. 42). This is confirmed by examination under UV light, which reveals that the splenial-prearticular gap is more open than the space between the three pieces and that it is brighter in colour on account of the gap being filled by a brightly fluorescing fine matrix.

The prearticular in *Scipionyx* can be reconstructed as a rostrocaudally slender, gently arched and dorsoventrally convex bone. As mentioned, the arched bar of the prearticular defines the ventral border of the adductor fossa. Rostrally, the prearticular contacts the splenial in a long, oblique suture. Caudally, the contact with the articular is not easily visible in lateral view, as the latter bone has rotated during diagenesis, exposing its dorsal surface (see below). The mode of contact between the prearticular and

the surangular cannot be seen in *Scipionyx*; however, a thin caudal extension of the dentary can be seen contacting the prearticular in medioventral view.

Articular - Only one articular, preserved in dorsal view, is exposed in *Scipionyx* (Fig. 43). We regard this as the left articular, based on the facts that it lies on the same plane of the caudal end of the left prearticular, both retroarticular process and medial glenoid are exposed with the latter located rostroventral to the former (i.e., rostromedially in the undisturbed skull) and the dorsalmost margin of the former is partly covered by the right basal tuber, a bone which lies close to the medial sagittal plane.

The retroarticular process, known as the attachment site of the *M. depressor mandibulae*, appears shallow, rounded and as long rostrocaudally as the glenoid. Being preserved in dorsal view, it is difficult to compare its shape with that of the caudally tapering retroarticular process of *Sinosauropteryx* (Currie & Chen, 2001) and *Compsognathus* (Peyer, 2006), albeit in *Scipionyx* it seems to be shorter rostrocaudally. A reduced retroarticular process is instead present in basal tyrannosauroids (e.g., Xu *et al.*, 2004; Xu *et al.*, 2006; Carpenter *et al.*, 2005b), ornithomimosaurs (e.g., Kobayashi & Barsbold, 2005) and dromaeosaurids (e.g., Xu & Wu, 2001; Barsbold & Osmólska, 1999).

In *Scipionyx*, the medial glenoid of the mandible is rounded, has a concave surface, and is well-bordered medially by a thick margin that is exposed in dorsomedial view rather than in a full dorsal view, marking a change of plane that occurred during diagenesis. The change of plane is completed at the level of the left prearticular, which reaches the ventral margin of the articular and is exposed in lateral view. The contact with the surangular, the bone which forms the lateral glenoid, is not visible because it is covered by the right quadrate.

Because in theropods the articular is usually bulky and well-developed in all directions, we hypothesise that the bump in the caudoventral corner of the infratemporal fenestra, covered by the pterygoid ala of the quadrate and by the surangular, might reflect the presence underneath of the disarticulated right articular (Fig. 42). Unfortunately, the CT scan analysis performed on the specimen did not help to clarify this detail.

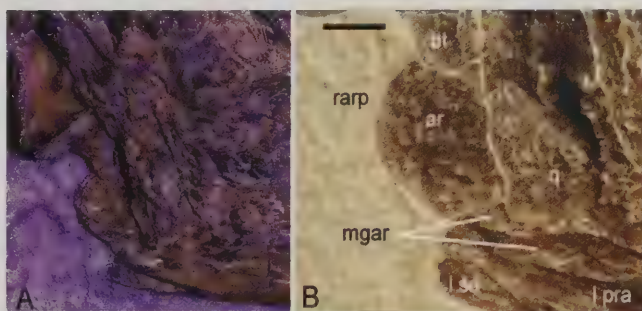


Fig. 43 - Close-up of the caudal mandibular region of *Scipionyx samniticus*. Ultraviolet-induced fluorescence (A) highlights the contour of the right articular (B), which is fossilized in dorsal aspect. Scale bar = 1 mm. See Appendix 1 or cover flaps for abbreviations.

Fig. 43 - *Scipionyx samniticus*, particolare della regione mandibolare caudale. La fluorescenza indotta da luce ultravioletta (A) evidenzia il contorno dell'articolare destro (B), che è fossilizzato in norma dorsale. Scala metrica = 1 mm. Vedi Appendice 1 o risvolti di copertina per le abbreviazioni.

Dentition

The dentition of *Scipionyx* consists of 5 premaxillary, 7 maxillary and 10 dentary teeth (Fig. 44). The teeth are moderate in number (see also Ontogenetic Assessment), pointed and feebly recurved, without constriction at the base of the crown. According to Peyer (2006), the tooth crowns of *Compsognathus* and all other compsognathids are unique among theropods in having a backward “kink” at 2/3 of their height, in being straight along their mid-parts and being expanded at their base. The teeth of *Scipionyx*, except for the largest premaxillary and the rostral dentary ones, which have a similar but only incipient bend, are instead feebly, but regularly recurved. Therefore, in the light of the immaturity of the specimen (see Ontogenetic Assessment), the condition of *Scipionyx* does not support the statement of Makovicky, reported by Peyer (2006), that “this particular tooth shape could be common to juvenile theropods in general, rather than to a unique character of the compsognathids”.

The right and left tooth rows are highly symmetrical in size, shape and position of the crowns. Whereas the first parameter is linked in all likelihood to the very early ontogenetic stage of the individual (i.e., first tooth replacement not yet started - see Ontogenetic Assessment), the different shape of the tooth crowns related to their different position along the jaws indicates a certain degree of heterodonty (see below for more details).

The upper tooth row is completely antorbital in position, ending rostrally to the vertical strut of the lacrimal as in the vast majority of tetanuran theropods, including toothed birds (Rauhut, 2003). As the right and left maxillae are well-exposed, respectively, also in ventrolateral and ventromedial view, we are certain that there are no empty alveoli caudal to the left and right m7. Thus, uniquely, in *Scipionyx* the caudal extension of the lower tooth row is greater than that of the upper one (Figs. 23-24, 25A-B, 25D, 44). This potentially diagnostic character is discussed in Remarks to the Emended Diagnosis. All other compsognathids, and known theropods as well, show the usual condition of a dentary tooth row that is shorter than the maxillary tooth row, independent of their ontogenetic stage.

Premaxillary teeth - *Scipionyx* has 5 premaxillary teeth. This tooth count is confirmed by the integrity of the ventral edge of the right premaxilla, which clearly shows the lateral margins of 5 alveoli, and by the fact that the left premaxilla has moved ventrally, so that the rostralmost tooth visible in the mouth of *Scipionyx* cannot belong to the left tooth row.

The majority of theropods have 4 premaxillary teeth, including the French *Compsognathus* (Peyer, 2006) and *Sinocalliopteryx* (Ji *et al.*, 2007a); this count is usually regarded as the primitive state in theropods (Rauhut, 2003). The premaxillary tooth count is, therefore, comparatively high in *Scipionyx*. One of the three specimens of *Sinosauropteryx* published so far possibly has 5 premaxillary teeth but, given that few theropods have more than 4 teeth in the premaxilla, Currie & Chen (2001) concluded that it is most parsimonious to interpret the fifth tooth as a maxillary tooth morphologically similar to the premaxillary ones. The condition of *Scipionyx* suggests that 5 premaxillary teeth could indeed have been present in some speci-

mens of *Sinosauropteryx*, indicating a certain intraspecific variability for this character. Five premaxillary teeth are reported also in *Allosaurus* (Madsen, 1976) and *Neovenator* (Hutt *et al.*, 1996) among tetanurans, whereas spinosaurids have 6-7 premaxillary teeth (e.g., Dal Sasso *et al.*, 2005). Interestingly, the German *Compsognathus* is reported to have only 3 premaxillary teeth (Ostrom, 1978).

The right premaxillary teeth of *Scipionyx* are all intact, except for the apex of pm1, which has detached and leans against the mesial margin of pm2. With the exclusion of pm5 and the apex of pm2, the left premaxillary teeth are entirely hidden by the right ones. In the space between right pm2 and pm3, the distal and mesial margins of two adjacent left teeth can be seen: they are pm3 and pm4 or, more probably, pm2 and pm3.

The right premaxillary teeth are closely set and are spaced apart from the maxillary ones by a diastema, emphasised by the fact that the pm-m sutural surface does not extend ventrally to the level of the tooth row, creating a shallow ventral concavity between the two bones, similar to the so called “subnarial gap” (Rauhut, 2003; Gauthier, 1986; Welles, 1984). A symmetric diastema is visible in the left tooth row. A slightly enlarged 3rd or 4th dentary tooth, fitting the subnarial gap, is instead reported in coelophysoids and *Dilophosaurus* (Welles, 1984; Colbert, 1989; Rowe, 1989). A long premaxillary-maxillary diastema associated with a very shallow gap appears to be present, although not described, in the German *Compsognathus* (Rauhut, 2003). According to Peyer (2006), however, this space may be occupied by empty alveoli. There is no evidence of a diastema between premaxilla and maxilla in *Sinosauropteryx*, *Sinocalliopteryx*, the French *Compsognathus*, *Juravenator* and *Huaxiagnathus*. Among other coelurosaurids, closely packed premaxillary teeth followed by a diastema and a gap are present in *Dilong* (Xu *et al.*, 2004), whereas a diastema made by a strong lateral excavation of the premaxilla interrupts the otherwise continuous alveolar margin between the premaxilla and the maxilla in *Sinornithosaurus* (Xu & Wu, 2001). In *Scipionyx*, the diastema left an empty space rostral to m1, which permitted m1 to be slightly procumbent.

In *Scipionyx*, pm2 and pm5 are markedly larger than pm1, 3 and 4. Similarly, in *Sinornithosaurus* (Xu & Wu, 2001) pm2 is markedly larger than pm3 and pm4. Pm2 is the longest premaxillary tooth also in both Sihetun specimens of *Sinosauropteryx* (NIGP 127586 and NIGP 127587), although it is not so markedly larger than pm3 and pm4.

The premaxillary teeth of *Scipionyx* are pointed and feebly to moderately recurved especially toward the apexes, where they are more recurved than the maxillary teeth. On the contrary, in *Juravenator* the maxillary teeth are more recurved than the premaxillary ones (Göhlich & Chiappe, 2006). Pm1-4 are oval to suboval in cross-section, and without serrations. Pm5 of *Scipionyx* is transitional in that it is not simply suboval in cross-section (Fig. 45): on the lingual side, it presents two concavities near the carinae, paralleling them. These concavities are absent in the rostralmost teeth. A similarly shaped cross-section is exposed at the broken end of the 2nd left maxillary tooth, whereas from m3 on, the labiolingual compression increases. In *Compsognathus*, the premaxillary teeth are more rounded than the lateral teeth, and completely unserrated, too (Ostrom, 1978; Peyer, 2004). The



Fig. 44 - A potentially diagnostic, and possibly autapomorphic, character of *Scipionyx samniticus* is the lower tooth row that is more extended caudally than the upper tooth row. Heterodonty resembles that of other compsognathids. Note also the symmetrical development of the tooth series in both maxillary rami, which is consistent with tooth-replacement having not yet started (see Ontogenetic Assessment). Left teeth are numbered in black, right teeth in white. Scale bar = 2 mm. See Appendix 1 or cover flaps for abbreviations.

Fig. 44 - La fila dei denti inferiori che si prolunga in direzione caudale più di quella dei denti superiori è un carattere potenzialmente diagnostico e forse autapomorfo di *Scipionyx samniticus*. L'eterodontia ricorda quella di altri compsognatidi. Si noti anche lo sviluppo simmetrico della serie dentaria nei due rami mascellari, che indicherebbe che la prima sostituzione dei denti non era ancora iniziata (vedi Ontogenetic Assessment). Denti sinistri numerati in nero, denti destri in bianco. Scala metrica = 2 mm. Vedi Appendice 1 o risvolti di copertina per le abbreviazioni.

premaxillary teeth of *Compsognathus* are also reported (Peyer, 2004) to be clearly differentiated from the teeth of the maxilla in having parallel mesial and distal borders on the main body, and in being more columnar. The premaxillary teeth are unserrated, expanded labiolingually, and recurved towards the tips also in *Sinosauropteryx* (Currie & Chen, 2001). There is no evidence of either a mesial or distal carina or denticles in the rostralmost premaxillary teeth of many other coelurosaurids, such as *Caudipteryx* (Ji *et al.*, 1998) and the basal deinonychosaurs *Sinornithosaurus* (Xu & Wu, 2001), *Microraptor* (Xu *et al.*, 2000), *Byronosaurus* (Norell *et al.*, 2000) and *Sinovenator* (Xu *et al.*, 2002b). Distal serrations are instead present on the penultimate premaxillary tooth of *Juravenator* (Göhlisch & Chiappe, 2006), whereas *Sinocalliopteryx* is reported to have premaxillary teeth with small serrations on the

lingual side of the distal portions of the 1st and 2nd ones, and on the distal carina of the 4th one (Ji *et al.*, 2007a). In basal theropods (Coelophysidae), both premaxillary teeth and rostralmost dentary teeth are elliptical to nearly circular in cross-section, show little if any curvature and bear few serrations to none at all (Tykoski & Rowe, 2004).

Maxillary teeth - The maxilla of *Scipionyx* bears 7 gently and regularly recurved, fang-like maxillary teeth. A low number of maxillary teeth is reported also in the other compsognathids, except *Compsognathus*, and in a number of other small-sized theropods (for further comparisons and comments about the possible significance of this condition, see the Ontogenetic Assessment section). The maxillary teeth of *Scipionyx* appear more compressed labiolingually than the premaxillary teeth,



Fig. 45 - Close-up of the pair of 5th premaxillary teeth of *Scipionyx samniticus*. Scale bar = 0.5 mm. See Appendix 1 or cover flaps for abbreviations.

Fig. 45 - *Scipionyx samniticus*, particolare del 5° paio di denti premaxillari. Scala metrica = 0,5 mm. Vedi Appendice 1 o risvolti di copertina per le abbreviazioni.

with both labial and lingual sides slightly concave mesiodistally in proximity of the distal carina. As mentioned above, m1 is slightly procumbent, as a consequence of the slightly upturned ventral border of the premaxillary process of the maxilla. As in most theropods, the two m4 are the largest teeth of the upper tooth row (Fig. 44). In *Scipionyx*, they are twice the size of the largest dentary tooth and, thus, appear oversized with respect to the whole tooth series. The last three teeth are the shortest of the maxillary series and are preserved in their natural position: because they are all inclined backwards, the apex of each crown is at a level that is well-caudally beyond the caudal margin of its alveolus. As in the French *Compsognathus* (Peyer, 2006), the maxillary tooth row of *Scipionyx* extends back to the level of the rostralmost tip of the jugal, but does not reach the caudal margin of the antorbital fenestra. Contrary to the premaxillary teeth, the maxillary teeth are well-spaced. The spacing is greater than in *Sinosauropteryx* (Currie & Chen, 2001) and the majority of theropods (e.g., Rauhut, 2003), in which the teeth are relatively closely packed, but narrower than in *Sinocalliopteryx* (Ji *et al.*, 2007a: fig. 2), in which every interdental space approaches two alveolar diameters in length. All the maxillary teeth are preserved in place, fixed in their alveoli. The right crowns are intact, with the exception of m1, the tip of which is detached, rotated about 160° and exposed in lingual view, and of m3 and m7, which lack their apices. The



Fig. 46 - Close-up of the 3rd left maxillary tooth of *Scipionyx samniticus*. The red arrow indicates the best preserved denticles. Scale bar = 0.5 mm. See Appendix 1 or cover flaps for abbreviations.

Fig. 46 - *Scipionyx samniticus*, particolare del 3° dente mascellare sinistro. La freccia rossa indica i denticoli meglio conservati. Scala metrica = 0,5 mm. Vedi Appendice 1 o risvolti di copertina per le abbreviazioni.

left maxillary teeth are also intact, with the exception of m1, which preserves few remains of the mesiolingual surface, and m2, which lacks its apex.

Remarkably, the maxillary teeth are developed symmetrically in the right and left tooth rows (see Ontogenetic Assessment). The only exception is represented by the broken right m3, of which the preserved FABL (fore-aft basal length) is about 70% that of the left m3: even if complete, the right m3 had to be smaller than the left one.

In *Scipionyx*, serrations were previously observed on the distal carina of m2 (Dal Sasso, pers. obs., 1997), but are in fact clearly visible only in the teeth caudal to this one. Serrations are present only on the distal carinae, even if on the left m3 and m4 the mesial carinae appear faintly crenulated rather than smooth. The serrations are composed of simple denticles, perpendicular to the carinae, with parallel sides and slightly rounded tips. On the distal carina of the left m3, the 7 basal denticles are as long as they are high; however, the apical denticles – beginning with the 8th and 9th, which are at mid-height of the crown – become gradually shorter but maintain their length to eventually form a crenulated margin in the apical third of the crown. In m4, the denticles are clearly present up to 3/4 of the height of the distal carina, but appear rather shorter than those of m3. In m6 and m7, the denticles are

inclined towards the apex, are higher than they are long and are spaced more apart. The denticle count per mm, measured on left m3, right m4 and right m6, ranges from 11 to 12. The denticle count per mm in the other compsognathids is discussed in the Ontogenetic Assessment section, as this character is potentially age-related. Concerning the presence of the denticles, in *Compsognathus* (Peyer, 2006) they are first recognised on the m4 and are restricted to the upper third of the distal carina. The caudalmost teeth, however, seem to be devoid of serrations. In *Huaxiagnathus*, maxillary and caudal dentary teeth have fine serrations on their distal carinae only (Hwang *et al.*, 2004). All maxillary teeth of *Sinosauropteryx* and *Juravenator* bear denticles only on their distal carinae. This pattern occurs also in more advanced coelurosaurs, such as *Microraptor* (Xu *et al.*, 2000) and *Sinornithoides* (Russell & Dong, 1993), which, interestingly, represent a basal dromaeosaurid and a basal troodontid, respectively. *Sinocalliopteryx* differs from the other compsognathids, including *Scipionyx*, in having caudal maxillary teeth that are serrated on both carinae (Ji *et al.*, 2007a).

Dentary teeth - Ten well-exposed dentary teeth are in place in the right dentary of *Scipionyx*. Most of the teeth of the left dentary are hidden by the right hemimandible, so no details on the lingual side of the crowns are available: the mesial halves of left d1 and d3 emerge just rostrally to the crowns of the right d1 and d3, whereas only the tips of the left d4 and d5 emerge. Similarly to the upper dentition, the lower tooth row presents a certain

degree of heterodonty: in fact, the first two rostral dentary crowns are oval in cross-section, closely set and without denticles; a third transitional crown bears denticles on the distal carina and is flattened in the distal half; and the remaining caudal ones are moderately compressed laterally, regularly well-spaced, serrated only on the distal carinae and have a distal half of the labial side that is flat to slightly concave (Figs. 47-48). Moreover, as in the maxillary tooth row, the last two crowns of the mandibular series are oblique and shorter, with tips directed caudally.

As in the maxillary teeth, the denticles are simple and perpendicular to the distal carina, with parallel sides and slightly rounded tips. In d3, the denticles are rather short and present only in the basal half of the distal carina (Fig. 47). Caudally to this tooth, the denticles of the distal carina become gradually higher, more widely spaced apart and distributed along a longer portion of the carina, reaching the apex in d7. From the basal half of d7, the height of the denticles surpasses their length (Fig. 48) and they become slightly inclined towards the apex of the crown.

The number of dentary teeth of *Compsognathus* is at least 18 in the German specimen (Ostrom, 1978) and 21 in the French specimen (Peyer, 2006). Denticles are first recognised at the level of the 10th tooth in the latter (Peyer, 2006). *Sinosauropteryx* has 12-15 dentary teeth and, as in *Scipionyx*, the denticles appear from d3 on (Currie & Chen, 2001). A relatively low number of dentary teeth is reported also in a number of other small coelurosaurs (e.g., Sues 1977; Ji *et al.*, 1998; Xu & Wu, 2001; Elzanowski, 2002).



Fig. 47 - Close-up of the left and right rostral dentary teeth of *Scipionyx samniticus*. The red arrow indicates the best preserved denticles. Scale bar = 0.5 mm. See Appendix 1 or cover flaps for abbreviations.

Fig. 47 - *Scipionyx samniticus*, particolare dei denti rostrali destri e sinistri delle ossa dentali. La freccia rossa indica i denticoli meglio conservati. Scala metrica = 0,5 mm. Vedi Appendice 1 o risvolti di copertina per le abbreviazioni.



Fig. 48 - Close-up of the right caudal dentary teeth of *Scipionyx samniticus*. Note the concavity of the distal half of the labial side on each tooth. The red arrows indicate the best preserved denticles. Scale bar = 0.5 mm. See Appendix 1 or cover flaps for abbreviations.

Fig. 48 - *Scipionyx samniticus*, particolare dei denti caudali dell'osso dentale destro. Si noti, su ogni dente, la concavità della metà distale del lato labiale. La freccia rossa indica i denticoli meglio conservati. Scala metrica = 0,5 mm. Vedi Appendice 1 o risvolti di copertina per le abbreviazioni.

In *Scipionyx*, 13 denticles per mm are counted on the right d5 and the right d8, on which the serrations are best preserved. The denticles are higher but narrower at the base than the maxillary ones. A well-preserved caudal dentary tooth of the NIGP 127586 *Sinosauropteryx* specimen is 1.8 mm long and has 10 denticles per mm (Currie & Chen, 2001). Seven denticles per mm are reported in *Huaxiagnathus* (Hwang *et al.*, 2004). In *Sinocalliopteryx*, the teeth are reported to be serrated in the same way as the maxillary ones, these having also mesial denticles. The observations in the Ontogenetic Assessment section about number of teeth and number of denticles per mm in the maxillary tooth row are valid also for the dentary teeth.

Concerning the spacing of the crowns, *Huaxiagnathus* resembles *Scipionyx* in having closely set rostral teeth and well-spaced mid-caudal teeth (Hwang *et al.*, 2004: fig. 2). Instead, the dentary teeth in *Compsognathus* (Peyer, 2006: fig. 5) and *Sinosauropteryx* (Currie & Chen, 2001: fig. 1b) are closely set along the entire tooth row; in *Sinocalliopteryx* (Ji *et al.*, 2007a: fig. 2) alternating large and small crowns, regularly spaced along the entire tooth row, are present.

With respect to the maxillary crowns, the dentary crowns are as short in *Sinocalliopteryx* as they are in *Scipionyx*, but, even if they are similarly inclined caudally in the two species, they are more recurved in *Sinocalliopteryx*. In *Sinosauropteryx*, the dentary teeth curve along their whole length; in *Compsognathus*, the rear edge of the tooth in lateral aspect is almost straight and perpendicular to the jaw, whereas a marked kink is visible in the apical third, where the edge is much recurved.

Finally, the dentition of the deinonychosaurs *Microraptor* and *Sinovenator* (Hwang *et al.*, 2002) is comparable to that of *Scipionyx* only in having unserrated rostral teeth and lateral teeth that are serrated only on the distal carinae, the remaining characters differing markedly.

Heterodonty - Summing up, three morphotypes can be identified in *Scipionyx* (Figs. 44-48). The first morphotype consists in the rostralmost teeth (pm1-3 and d1), which have crowns that appear rounded in cross section and are devoid of carinae. A second morphotype is represented by the transitional teeth (pm5, m1-2 and d2), which have crowns that appear rounded in cross section, although to a lesser degree than the former, and a concave surface close to the unserrated carina (with the mesial one displaced lingually). The

last morphotype includes the lateral teeth (from m3 and d3 on), which have crowns that are more compressed labiolingually and that are more rounded in the mesial half while being more flattened to concave in the distal half and towards the serrated distal carina, which is in turn aligned with the rostrocaudal axis of the tooth row.

The heterodonty of *Scipionyx* is comparable to that of *Sinosauropteryx* (Currie & Chen, 2001), *Huaxiagnathus* (Hwang *et al.*, 2004), *Compsognathus* (Peyer, 2006; Ostrom, 1978) and, possibly, *Ornitholestes* (Bakker, pers. comm., 1998), in having rostral teeth that are rounded in cross section and lacking denticles, and lateral teeth that are more compressed labiolingually and serrated only on the distal carina. Additionally, there is another feature of *Scipionyx* that can be recognised in *Sinocalliopteryx* (Ji *et al.*, 2007a), *Juravenator* (Göhlich & Chiappe, 2006) and *Compsognathus* (Peyer, 2006): caudalmost teeth that have not only the tip, but also the rest of the crown, curving back continuously, and that are smaller and more triangular in lateral view. The variation that led Zinke (1998) to distinguish three morphotypes referred to cf. *Compsognathus* is also consistent with such a heterodonty.

In *Scipionyx*, the size of the rostral teeth is remarkable. Some of the premaxillary teeth are comparable in size to the largest maxillary teeth, whereas the rostral dentary teeth are larger than the more caudal ones. This condition is different to that of the French *Compsognathus*, *Huaxiagnathus* and *Sinocalliopteryx*, in which the premaxillary teeth are smaller than the maxillary teeth and the rostral dentary teeth are as large as the lateral ones; in addition, it is definitely opposite to that of the tyrannosauroids, in which the rostral teeth are markedly smaller than the lateral teeth.

Hyoid apparatus

The preserved elements of the hyoid apparatus consist of a pair of slightly flattened, apically broadened and gently curved rods, identifiable as ceratobranchials I (Fig. 49). They lie ventral to cervical vertebrae 2 and 6, and are still parallel to each other but, *contra* Holtz *et al.* (2004), fossilised caudally of the position they had in life, which would have been in-between the caudal halves of the two hemimandibles (Figs. 21-22). Although at first glance the ceratobranchials I of *Scipionyx* seem disproportionately

large with respect to the postcranial skeleton, their size is appropriate with the size of the skull: in fact, they measure only about half the length of the mandible in most of the dinosaurs in which they are preserved (e.g., *Compsognathus* [Peyer, 2006] and *Proceratosaurus* [Woodward, 1910; Rauhut *et al.*, 2009]).

Contrary to a still persistent common belief, a number of recent studies have demonstrated that ceratobranchials I are not rarely found in association with dinosaur skulls (e.g., Weishampel *et al.*, 2004). Among theropods, a list of the taxa we encountered during this study comprises about 15 genera in which ceratobranchials I are anatomically *in situ*: *Jinfengopteryx* (Ji *et al.*, 2005), *Sinosauropteryx* (Currie & Chen, 2001; Ji *et al.*, 2007b), *Compsognathus* (Ostrom 1978; Peyer, 2006), *Sinornithosaurus* (Xu & Wu, 2001), coelophysoids (Colbert, 1989; Rowe, 1989), *Carnotaurus* (Bonaparte *et al.*, 1990), *Pelecanimimus* (Pérez-Moreno *et al.*, 1994), *Sinornithomimus* (Kobayashi & Lü, 2003), *Caudipteryx* (Ji *et al.*, 1998), *Shuvuuia* (Chiappe *et al.*, 2002),

Sinornithosaurus (Xu & Wu, 2001) and, possibly, *Bambiraptor* (Burnham *et al.*, 2000). In the MGI 100/1001 specimen of *Shuvuuia*, they seem to run just below the pterygoids, almost appressed to their ventral margin and similarly angled (Chiappe *et al.*, 2002: fig. 4.6B).

A displaced ceratobranchial I was described for *Huaxiagnathus* (Hwang *et al.*, 2004), some tyrannosaurids (RTMP 91.36.500) and some deinonychosaurs (Colbert & Russell, 1969; Russell & Dong, 1993). Several authors (e.g. Currie & Zhao, 1993a; Rauhut, 2003; Holtz *et al.*, 2004) reported ceratobranchial I in *Sinraptor dongi*. It seems to us that the alleged ceratobranchial I of *Sinraptor* (Currie & Zhao, 1993a: fig. 12A) does not match the shape of any ceratobranchials I so far described (Weishampel *et al.*, 2004); rather, it strongly resembles the supradytary-coronoid of *Daspletosaurus* in having a pointed rostral end and a distinctly twisted caudal end (Currie, 2003: fig. 35). Therefore, we regard the alleged ceratobranchial I of *Sinraptor* as being a supradytary-coronoid.

POSTCRANIAL AXIAL SKELETON

With the exception of the missing portion of the tail, all the elements of the axial skeleton of *Scipionyx* are preserved, although with slight to moderate *post mortem* damage and deformation (Figs. 21, 22). The vertebral neural arches are still in articulation and the zygapophyses interconnected. Some vertebral centra, especially those that lie at the level of the cervicodorsal transition and in the sacral region, are instead detached from their neural arch and disarticulated from each other. This condition is probably linked to the immaturity of the specimen (see Ontogenetic Assessment) and to the cylindrical shape of the centra, which favoured their mobility (see Skeletal Taphonomy). The ribs, which are still in contact with their respective vertebrae, and the gastralia, which lie almost undisturbed and only slightly fractured by the diagenetic crushing, allow reconstruction of the chest and abdomen, and an estimation of their respective volume (see Palaeobiology).

Vertebrae

In its preserved part, the vertebral column of *Scipionyx* is composed of 37 elements: 23 presacrals, 5 sacrals and 9 caudals. The presacral vertebrae do not vary markedly in length. As in most theropod dinosaurs, the morphological transition of vertebrae from cervical to dorsal is gradual, so much so that their regionalisation can be established only tentatively, mainly basing assumptions on the most apparent regionalisation of the ribs. Taking for certain that there are 23 presacral elements, we consider the first 10 vertebrae to be cervicals, and the remaining 13 to be dorsals, on the basis of the features described below.

A similar vertebral count is reported in many basal neotheropods (e.g., Tykoski & Rowe, 2004; O'Connor, 2007), in basal Tetanurae (Holtz *et al.*, 2004) and in most compsognathids. Regarding the compsognathids, *Compsognathus* (Peyer, 2006) has 23 presacral elements (10 cervicals, 13 dorsals), most likely 5 sacrals and 30 preserved caudals; *Sinosauropteryx* (Currie & Chen, 2001) has 23 presacral elements (10 cervicals, 13 dorsals), probably 5 sacrals and 64 caudals; *Huaxiagnathus*

(Hwang *et al.*, 2004) has 23 presacral elements (10 cervicals, 13 dorsals), an indeterminate number of sacrals (they are covered by the ilia) and 25 preserved caudals; and *Juravenator* (Göhlich & Chiappe, 2006) is reported to have 21-23 presacrals (8-10 cervicals, 13 dorsals), an uncertain number of sacrals and 44 preserved caudals. The only exception may be represented by *Sinocalliopteryx*: Ji *et al.* (2007a) reported 11 cervicals, 12 dorsals, an indeterminate number of sacrals and 49 caudals, but in all likelihood this variation in the cervical count depends on a different interpretation of a transitional vertebra, considered as the last cervical rather than the first dorsal. Even other non-maniraptoran coelurosaurs such as the Tyrannosauroida (Holtz, 2004) and the Ornithomimosauria (Makovicky *et al.*, 2004) have 23 presacrals (10 cervicals, 13 dorsals), although the former taxon presents with a partially sacralised last dorsal, and the latter taxon presents with 5 sacrals in the basal forms *Shenzhousaurus* (Ji *et al.*, 2003) and, probably, *Archaeornithomimus* (Makovicky *et al.*, 2004), but tends to have 6 sacrals in more derived forms. In turn, different and variable vertebral counts characterise the derived coelurosaurs belonging to the Maniraptora (see, for example, Weishampel *et al.*, 2004; and references therein).

Cervical vertebrae - The very well-preserved cervical series emerges in right lateral view with a partial, faint exposition of its dorsal aspect between C2 and C6. The cervical vertebrae appear sharply angled in lateral view, with the cranial articular surfaces elevated dorsally with respect to the caudal surfaces (Figs. 49-50). This offset would have promoted the S-shaped curve typical of most theropods (e.g., Carpenter *et al.*, 2005b; Naish *et al.*, 2001), observed when the articulated cervical column is viewed in lateral view (see also Skeletal Taphonomy). The cervicals of *Scipionyx* have low, rectangular neural spines, prominent zygapophyses, overhanging epiphyses and well-developed transverse processes bearing diapophyses. All parapophyses, set on the cranioventral corner of the centra, are hidden by the heads of the cervical vertebrae.

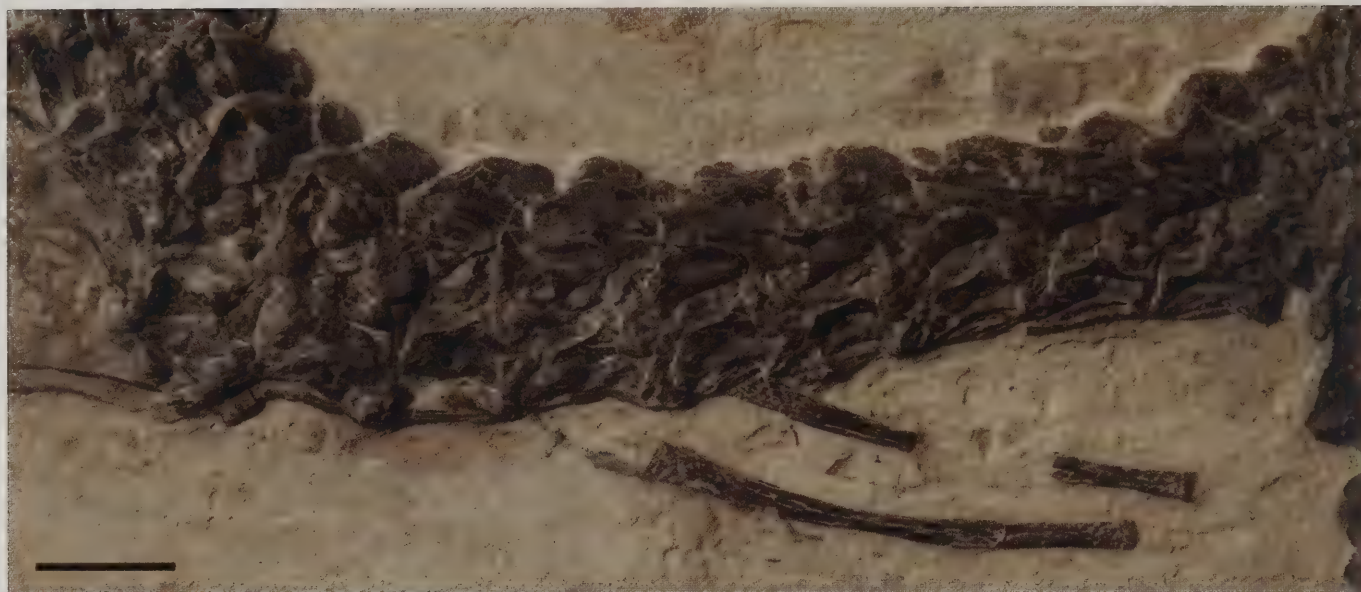


Fig. 49 - Cervical vertebrae, cervical ribs and ceratobranchials I of *Scipionyx samniticus*. Scale bar = 5 mm.

Fig. 49 - Vertebre cervicali, costole cervicali e ceratobranchiali I di *Scipionyx samniticus*. Scala metrica = 5 mm.

As in most theropods, the atlas of *Scipionyx* is composed of the neurapophyses and the intercentrum. The atlantal neurapophysis bears a well-developed, rounded epipophysis, and a short, well-delineated postzygapophysis. Compared to other theropods (e.g., *Majungasaurus* [O'Connor, 2007]; *Deinonychus* [Ostrom, 1969]), the epipophysis of *Scipionyx* seems rather short, as a consequence of the marked dorsoventral development of the neurapophysis, but in any case it projects caudally to the postzygapophysis. The atlas, aligned with the skull, lies in lateral view, whereas the axis is in laterodorsal view. On account of the slight rotation that occurred between the two elements, the atlantal postzygapophysis is not superimposed anymore onto the prezygapophysis of the axis, leaving the articular surface of the latter visible. In fact, contrary to all other zygapophyses, which have articular surfaces lying on the transverse plane, the contact between the atlantal postzygapophysis and the axial prezygapophysis occurs mainly in a sagittal plane. The atlantal intercentrum, which is located ventrally to the axial prezygapophysis and caudally to the caudal margin of the squamosal, probably lost its contact with the neurapophysis, but the presence of the prezygapophysis prevents us from verifying this. The exposed portion is more triangular than rhomboidal in shape and appears to be higher than wide.

Unlike the spines of the following cervicals, the axial neural spine is rather tall and rounded, resembling those of the basal ornithomimosaurs (Kobayashi & Lü, 2003; Kobayashi & Barsbold, 2005). Similar to the other cervical neural spines, it seems compressed mediolaterally rather than flared transversely. The axial epipophysis is large, not pointed, caudally directed and extended beyond the postzygapophysis. Holtz *et al.* (2004) indicate the presence of axial prezygapophyses and well-developed postzygapophyses bearing epipophyses in larger tetanurans, such as the tyrannosauroids, but they do not mention the condition in small forms. According to Rauhut (2003), the character “axis bearing well-developed epipophyses that extend beyond the postzygapophyses” is widespread in Neotheropoda, but among coelurosaur is limited to tyrannosaurids and deinonychosaurs (e.g., Norell

& Makovicky, 2004). In addition, axial epipophysis extending slightly more caudally than the caudal end of the postzygapophysis is reported also in the ornithomimosaur *Sinornithomimus* (Kobayashi & Lü, 2003). In *Scipionyx*, a possible axial pleurocoel (pneumatopore) is the depression visible just caudal to the base of the axial transverse process (Fig. 51). In size and position, it resembles the pleurocoel figured by Madsen (1976: pl. 11M) in *Allosaurus*. Such a pleurocoel is absent in coelophysoids, present in *Ceratosaurus* and the abelisaurids (Tykoski & Rowe, 2004), and often present in the Tetanurae, with the exception, for example, of the megalosaurids (Rauhut, 2003; Holtz *et al.*, 2004). The centrum of the axis of *Scipionyx* is about as long as the centra of the other cervical vertebrae. Similar to its neural arch, also the axial centrum is slightly rotated, appearing in laterodorsal view and exposing the right neurocentral surface. The diapophysis has lost the contact with the tuberculum of its rib, these elements appearing distant from each other. Just below the bifid head of the axial rib, dorsal to the tuberculum and in a cranial direction, emerges a portion of bone which we tentatively refer to as the cranial margin of the axial intercentrum, still connected to the centrum but not yet fused to it (Figs. 50B, 51). A possible sign of the odontoid process of the axis, which is not directly exposed, is the relief under the cranioventral margin of the neural arch and the atlantal intercentrum.

The neural spine of C6 is exposed in dorsal view, emerging vertically from the fossiliferous slab, and showing the absence of a spine table (Fig. 52). The height of the neural spines decreases from C2 to C4; from C5 to C7 the neural spines are equally low but are also elongate craniocaudally; from C8 to C10 they become higher but shorter, as in C3.

In *Compsognathus* (Peyer, 2006), the neural spines are long and very low throughout the entire cervical series. In *Sinosauropteryx* (Currie & Chen, 2001), the cervical neural spines are on average as low as in *Scipionyx* and *Compsognathus*, but are craniocaudally shorter. Based on the published figures, the neural spines of *Juravenator* (Göhhlich & Chiappe, 2006) seem to resemble those of *Scipionyx*. In

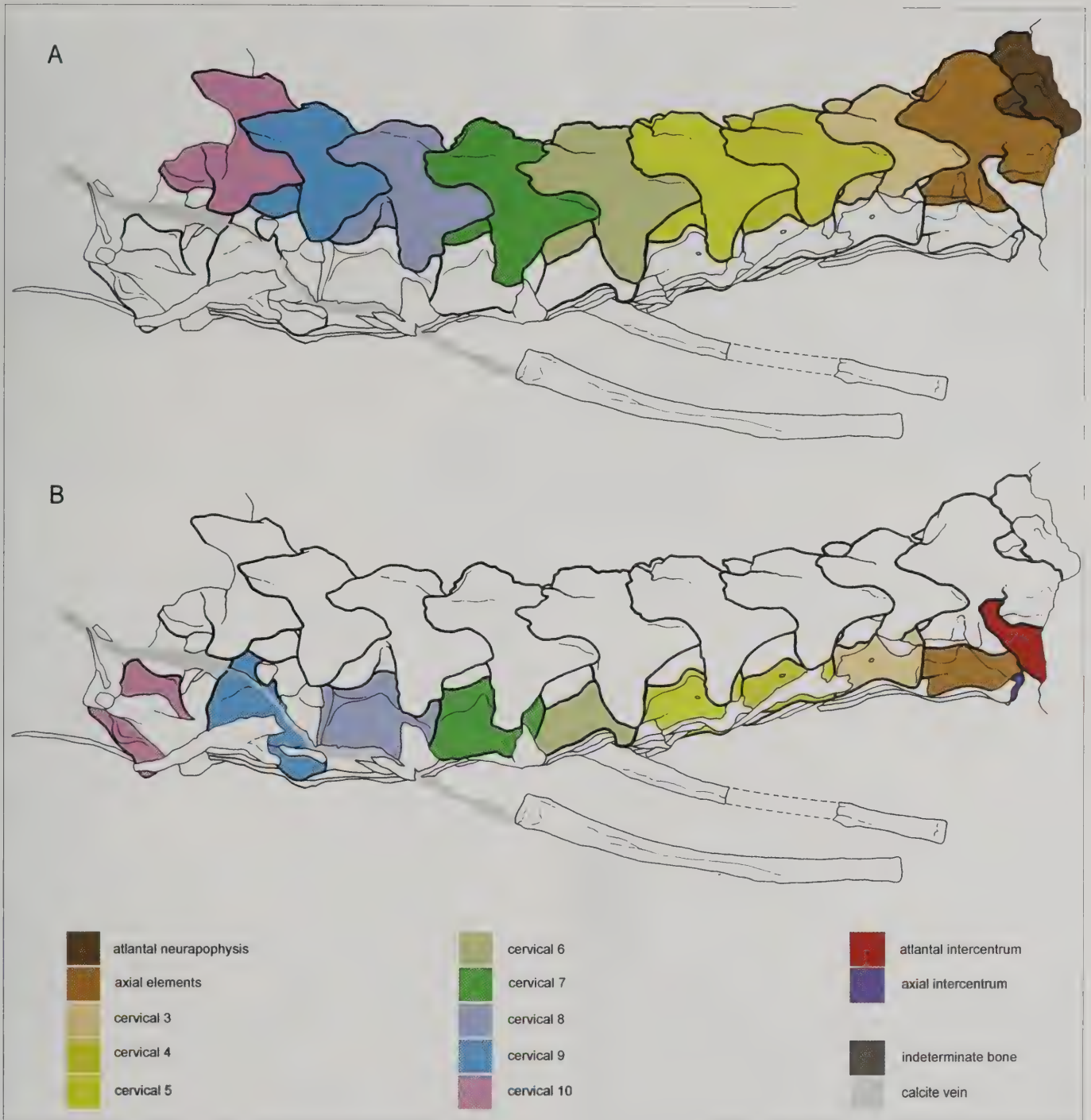


Fig. 50 - Line drawings of the cervical vertebrae of *Scipionyx samniticus*. A) neural arches; B) centra, intercentra.
 Fig. 50 - Disegni al tratto delle vertebre cervicali di *Scipionyx samniticus*. A) archi neurali; B) centri e intercentri.

Huaxiagnathus (Hwang *et al.*, 2004) and *Sinocalliopteryx* (Ji *et al.*, 2007a), the spines are short, and comparatively high and blade-like in the cranial cervicals, whereas they are long and low in the caudal ones. Low neural spines are reported also in other small-sized coelurosaurs such as “*Calamosaurus foxii*” (Naish *et al.*, 2001), *Dilong* (Xu *et al.*, 2004), *Ornitholestes* (in the alleged C4 and C6; the spine of C3 is instead short and tall) and *Coelurus* (in which they extend as long as the arch [Carpenter *et al.*, 2005b]), as well as in the ornithomimosaur (Kobayashi & Barsbold, 2005; Makovicky *et al.*, 2004), in *Nqwebasaurus* (de Klerk *et al.*, 2000) and in derived therizinosauroids and oviraptorosaurs (Kirkland *et al.*, 2005).

In all the post-axial cervical vertebrae of *Scipionyx*, due to the extreme interlocking of the neural arches caused by the backwards bending of the neck (see Skeletal Taphonomy), the postzygapophyses have slid on the prezygapophyses up to the maximum limit of craniocaudal sliding permitted by their articular surfaces. Especially in the cranial and mid cervical arches, the articular surfaces of the prezygapophyses, observed in lateral view, are convex, with the cranial portion flexed ventrally. This flexion gives an indication of the intervertebral mobility in the neck of *Scipionyx* (see Skeletal Reconstruction And ...). The postzygapophyses are stout and rounded, and slightly more pointed in the last three vertebrae. As

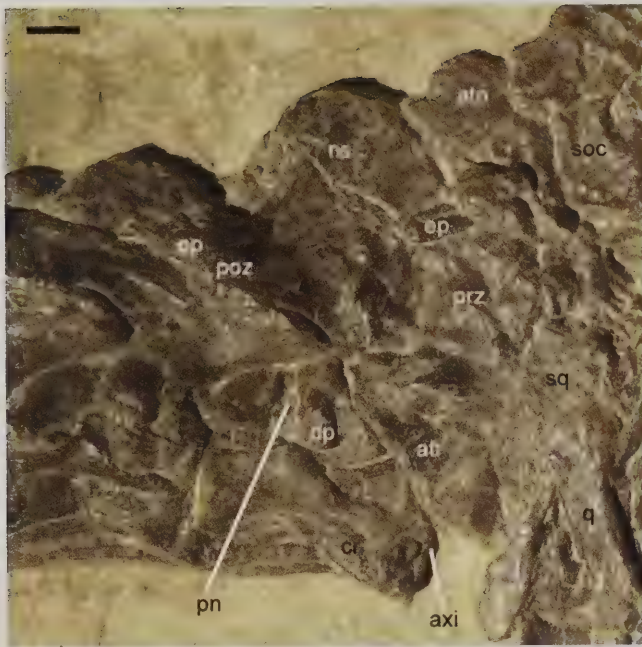


Fig. 51 - Close-up of the atlas and the axis of *Scipionyx samniticus*. Scale bar = 1 mm. See Appendix 1 or cover flaps for abbreviations.

Fig. 51 - Atlante ed epistrofeo di *Scipionyx samniticus*. Scala metrica = 1 mm. Vedi Appendice 1 o risvolti di copertina per le abbreviazioni.

in *Sinosauropteryx* (Currie & Chen, 2001), in *Scipionyx* the prezygapophyses are elongate at the front of the neck. They tend to become gradually shorter at the back, especially between C8 and C10, resulting markedly shorter than the postzygapophyses, which in turn remain constant in length along the whole cervical series. Unlike *Scipionyx*, in *Huaxiagnathus* the prezygapophyses are longer than the postzygapophyses in the cranial cervicals, and the latter apophyses become elongate at the back (Hwang *et al.*, 2004), as occurs in the basal ornithomimosaur *Sinornithomimus* (Kobayashi & Lü, 2003). Also *Compsognathus* (Peyer, 2006) has prezygapophyses that are larger than those of *Scipionyx*, with a more rounded apex than that of the postzygapophyses. In *Scipionyx*, both zygapophyses extend far beyond the ends of their centra, whereas in *Sinosauropteryx* this occurs only in the prezygapophyses (Currie & Chen, 2001). Concerning the ventral flexing of the prezygapophyses, according to Rauhut (2003) the articular surface is more or less straight in non-coelurosaurian theropods, whereas the cranial part of the articular surface is flexed ventrally in *Sinosauropteryx* (Currie & Chen, 2001), *Ornitholestes* (Carpenter *et al.*, 2005b), *Nqwebasaurus* (de Klerk *et al.*, 2000), birds (e.g., *Archaeopteryx*), dromaeosaurids, ornithomimosaur and oviraptorosaurs (Makovicky, 1995). Unlike *Scipionyx*, in *Coelurus* the prezygapophyses are not flexed in the cranial cervical vertebrae, and become slightly flexed only in the caudal ones.

In *Scipionyx*, right and left epiphyses can be seen from C1 to C8, projecting caudally to the postzygapophyses. Apart from the atlas, the vertebra which bears the largest epiphyses is C6; in this vertebra, the apexes of the epiphyses are pointed rather than rounded (Fig. 52). From C6 to C10, the epiphyses become smaller, and in C10 they are no longer clearly recognisable. In *Compsognathus* (Peyer, 2006), small epiphyses are present and

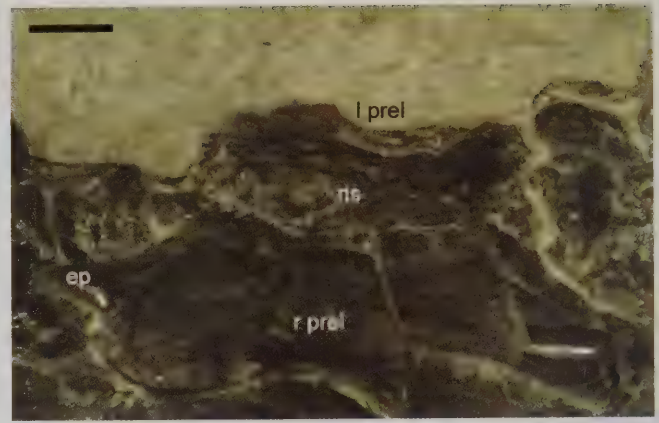


Fig. 52 - Close-up of the neural arch of the 6th cervical vertebra of *Scipionyx samniticus*. Its dorsal aspect shows the absence of a spine table. Scale bar = 1 mm. See Appendix 1 or cover flaps for abbreviations.

Fig. 52 - *Scipionyx samniticus*, particolare dell'arco neurale della 6^a vertebra cervicale. La norma dorsale mostra bene la mancanza di una mensola spinale. Scala metrica = 1 mm. Vedi Appendice 1 o risvolti di copertina per le abbreviazioni.

are placed distally on the postzygapophyses. Small epiphyses are reported also in *Huaxiagnathus* (Hwang *et al.*, 2004). The epiphyses in *Sinosauropteryx* (Currie & Chen, 2001) are represented only in the first few cervicals of NIGP 127586 by low bumps and, unlike in *Scipionyx*, they do not overhang the postzygapophyses caudally, rather, they are oriented more dorsally. Epiphyses similar to those of *Scipionyx* can be seen in the preserved cervicals of *Ornitholestes* (Carpenter *et al.*, 2005b), whereas small epiphyses laterally connected and not overhanging the postzygapophyses caudally are reported in *Nqwebasaurus* (de Klerk *et al.*, 2000).

Concerning the diapophyses, in *Scipionyx* the most apparent change occurs between C2 and C4: in the axis the diapophysis is small and supported by a transverse process ventrally directed; in C3 it increases in size and the transverse process is slightly raised albeit still ventrally directed; in C4, the diapophysis is twice as large as in C2 and the transverse process is longer and even more raised, directed lateroventrally. This pattern is present in most neotheropods, with the exception of some very basal forms (e.g., Welles, 1984; Tykoski & Rowe, 2004) in which the transverse processes and their diapophyses are reduced or absent in C2. In *Scipionyx*, the transverse processes continue to rise gradually from C6 to C10, exposing more clearly the articular surfaces of the diapophyses. The transverse processes become horizontal in the cranialmost dorsal vertebrae (see below).

Along the cervical series, parallel to the shortening of the arch that affected primarily the prezygapophyses, the transverse processes change position also in a craniocaudal direction: they are positioned about midway between the zygapophyses in the cranial and mid cervicals; caudally, they gradually move closer to the prezygapophyses. The lateral protrusion of the transverse processes highlights the presence of prezygodiapophyseal and postzygodiapophyseal laminae, which connect each transverse process with the zygapophyses of that side; a prezygoepiphysal lamina (*sensu* O'Connor, 2007) can be seen, too (Figs. 53-54).

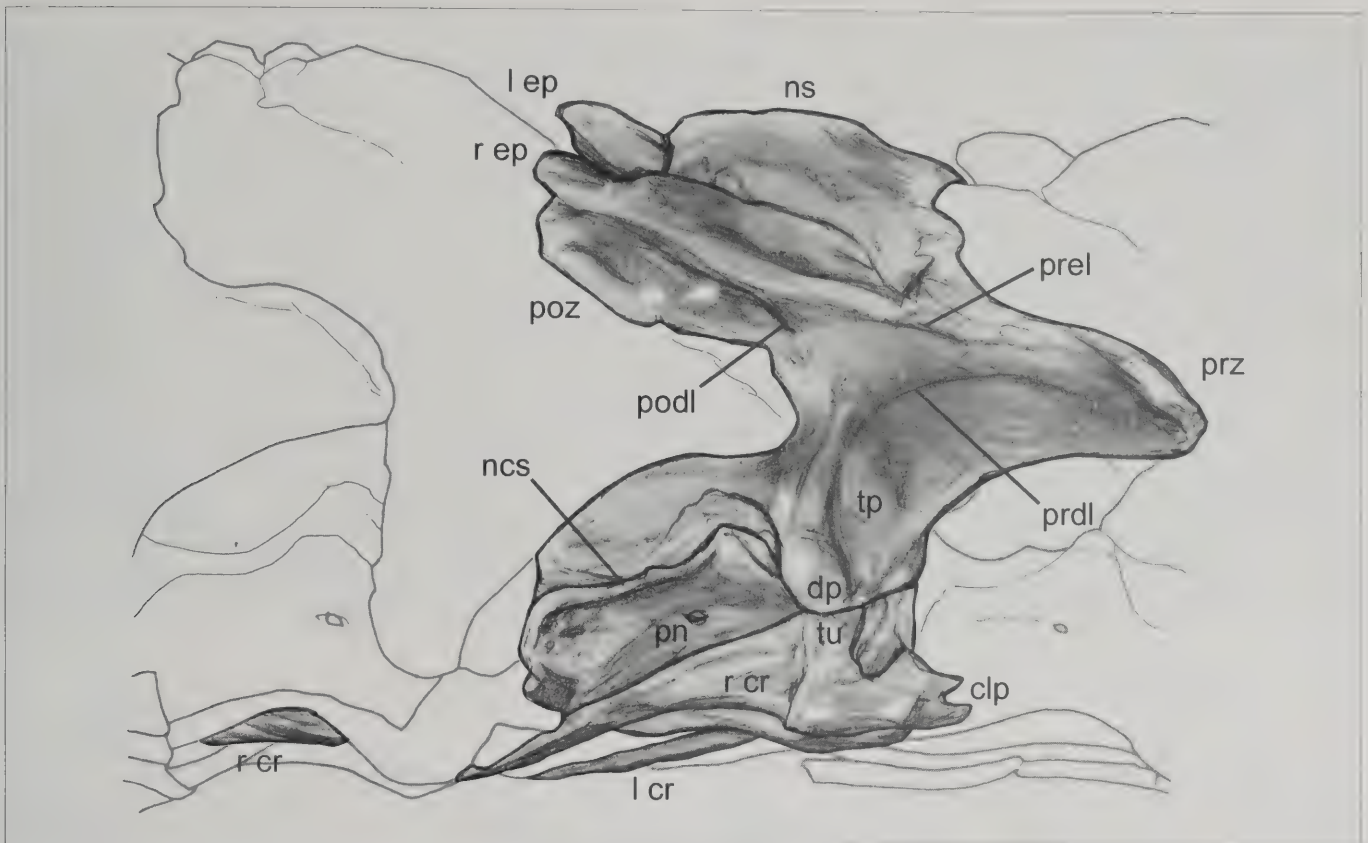


Fig. 53 - Shaded drawing of the 4th cervical vertebra and ribs of *Scipionyx samniticus*. See Appendix 1 or cover flaps for abbreviations.

Fig. 53 - Disegno ombreggiato della 4^a vertebra cervicale di *Scipionyx samniticus* e delle sue costole. Vedi Appendice 1 o risvolti di copertina per le abbreviazioni.

Because of the strict interlocking of the vertebrae, it is difficult to see whether the cervical centra are amphiplatyan or opisthocoelous. However, thanks to a slight uplift of the centrum of C6, the cranial articular surface of this vertebra can be observed. It appears moderately convex, indicating that the cervical vertebrae of *Scipionyx* are moderately opisthocoelous. Thus, *contra* Peyer (2006), the cervical vertebrae of *Scipionyx* are not biconcave. The cervical centra are opisthocoelous also in *Compsognathus* (Ostrom, 1978; Peyer, 2006) and, apparently, in *Sinocalliopteryx* (Ji *et al.*, 2007: fig. 4a). *Sinosauropteryx* is reported to have biconcave cervical vertebrae (Currie & Chen, 2001).

In "*Calamosaurus foxii*" (Naish *et al.*, 2001) and *Ornitholestes* the cervical centra are strongly opisthocoelous, whereas they are amphicoelous in *Coelurus* (Carpenter *et al.*, 2005b). Among basal tyrannosauroids, the cervical vertebrae are opisthocoelous in *Dilong* (Xu *et al.*, 2004) and amphicoelous in *Guanlong* (Xu *et al.*, 2006), the latter being usually considered to be more basal than the former. Strongly opisthocoelous vertebrae are known also in some non-coelurosaur tetanurans, such as the Spinosauroidea and the Allosauroidea (Rauhut, 2003). Opisthocoelous cervical vertebrae are also known in a few Maniraptora, such as the Alvarezsaurids (Perle *et al.*, 1993; Chiappe *et al.*, 1998), even if most of the maniraptoran theropods, including the basal alvarezsaurid *Nqwebasaurus* (de Klerk *et al.*, 2000), tend to have amphicoelous or amphiplatyan centra (e.g., Ji *et al.*, 1998; Norell & Makovicky, 2004; Xu & Norell, 2004; Kirkland *et al.*, 2005).

In *Scipionyx*, the centra of the caudal cervical vertebrae are taller than those of the cranial ones. As in the vast majority of theropods, including other compsognathids (e.g., Currie & Chen, 2001; Ji *et al.*, 2007a), in lateral view the centra are concave ventrally, with articular faces

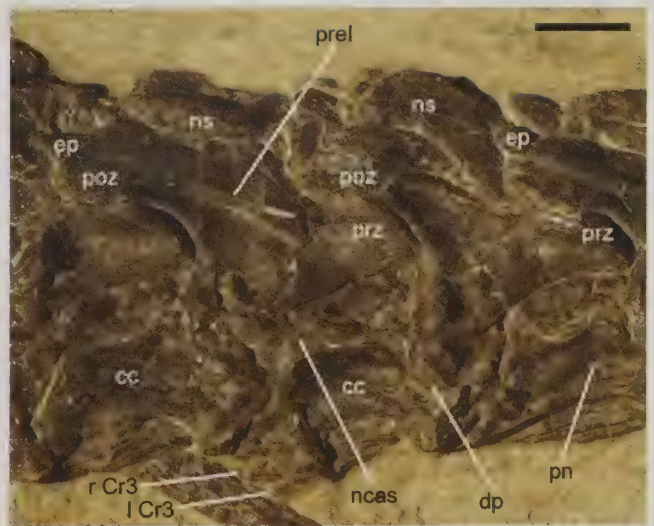


Fig. 54 - Close-up of the 5th and 6th cervical vertebrae (from right to left) and the ends of the preceding ribs of *Scipionyx samniticus*. Scale bar = 2 mm. See Appendix 1 or cover flaps for abbreviations.

Fig. 54 - *Scipionyx samniticus*. Quinta e 6^a vertebra cervicale (da destra a sinistra) e terminazioni delle costole precedenti. Scala metrica = 2 mm. Vedi Appendice 1 o risvolti di copertina per le abbreviazioni.

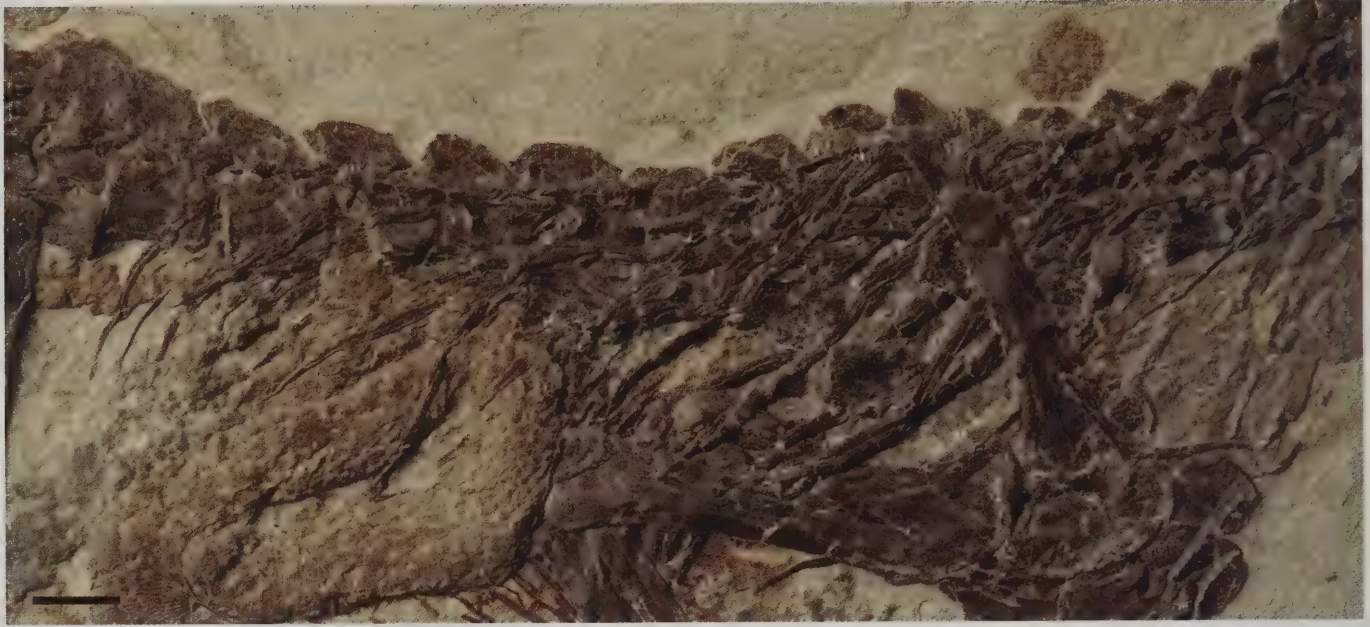


Fig. 55 - Dorsal vertebrae and dorsal ribs of *Scipionyx samniticus*. Scale bar = 5 mm.

Fig. 55 - Vertebre e costole dorsali di *Scipionyx samniticus*. Scala metrica = 5 mm.

parallel but inclined with respect to the long axis of the centrum, not perpendicular, so that in lateral aspect the cranial face is offset well-above the caudal face. The articular surfaces become less oblique towards the end of the cervical series, becoming nearly vertical in the 2nd dorsal centrum. In *Scipionyx*, the length of the cervical centra is on average 5/2 their height; the length of the centra is three times their height in *Compsognathus* (Peyer, 2006). Thus, the cervical centra of the compsognathids are longer than those of juvenile tyrannosaurines and other tyrannosauroids, in which they are as long as or longer than they are tall (Holtz, 2004; Xu *et al.*, 2004), but shorter than those of the therizinosauroids (e.g., Zanno, 2010). In *Scipionyx*, the centra of C6 and C7 are slightly more elongate craniocaudally than the others. This is similar to *Sinosauropteryx* (Currie & Chen, 2001), in which the 6th to 8th cervicals are longer than the cranial ones. The caudalmost cervical centra of *Scipionyx* are not significantly longer than the cranial dorsal elements.

The neurocentral suture is visible on all the cervical vertebrae (see Ontogenetic Assessment). The centra are still connected to their respective arches only in C4 and C6; in C2, C3, C5, C7, C8 and C9, centra and arches are so separated, especially in the caudalmost ones, that the dorsal surface of the centra is often visible.

Small pneumatopores can be seen in the middle of the centra of C3-C5, in the form of single pneumatic foramina (Figs. 53-54). As previously reported by Rauhut (2003; and references therein) and Wedel (2009), in modern birds the pneumatization of the cervical vertebral column during ontogeny starts at the cervical-dorsal transition and then continues cranially and caudally, and in non-avian theropods the pneumatization of the vertebral column probably followed the same ontogenetic pattern. Thus, in *Scipionyx* the finding of the foramina in the cranial half of the cervical series but not in the caudal half is quite unexpected. Single pleurocoels on each side of the centrum have been described for *Compsognathus* (Peyer, 2006), in which they are barely visible, opening just caudal and slightly

ventral to the diapophyses; in *Sinosauropteryx* (Currie & Chen, 2001), in which, as in *Scipionyx*, they open in the cranial half of the series, and more precisely caudodorsal to the parapophysis of the 5th cervical of NIGP 127586, and in the 3rd and 4th cervicals of NIGP 127587; in *Juravenator* (Göhlich & Chiappe, 2006); and more generally in basal Tetanurae (Holtz *et al.*, 2004), including *Dilong* (Xu *et al.*, 2004) and *Nqwebasaurus* (de Klerk *et al.*, 2000). No pleurocoels are present in *Ornitholestes*, whereas they vary in size and number in *Coelurus* (Carpenter *et al.*, 2005b). Two foramina penetrating the lateral surface of the centrum are reported for neoceratosaurs (Tykoski & Rowe, 2004), possibly for the basal tetanuran *Fukuiraptor* (Azuma & Currie, 2000), and, according to Holtz *et al.* (2004), for the juvenile tyrannosauroid *Shanshanosaurus*, some adult therizinosauroids and oviraptorosaurs, and the troodontid *Troodon*.

In *Scipionyx*, the centrum of C10 is detached from the neural arch and has moved ventrally for a distance almost equal to the height of the centrum itself. It has rotated on its craniocaudal axis and has become exposed in a full dorsal view, showing both neurocentral surfaces for their whole length. This view has permitted us to note that the transverse diameter of the centrum is only slightly less than (almost 3/4) its craniocaudal diameter. This vertebra can be considered a transitional vertebra (cervicodorsal), as its rib possesses tuberculum and capitulum that are larger and stouter than those of the preceding cervicals.

Dorsal vertebrae - The boundary between cervical and dorsal vertebrae is defined by an abrupt increase in rib size, affecting especially the capitula. So, as pointed out by Dal Sasso & Signore (1998a), we consider the first dorsal of *Scipionyx* as being the vertebra immediately successive to the one in which the centrum is completely separated from the neural arch (see above). That vertebra, in fact, has a stout diapophysis that is still articulated to its rib through an even stouter tuberculum; the capitulum, although fractured by a calcite vein crossing it, appears

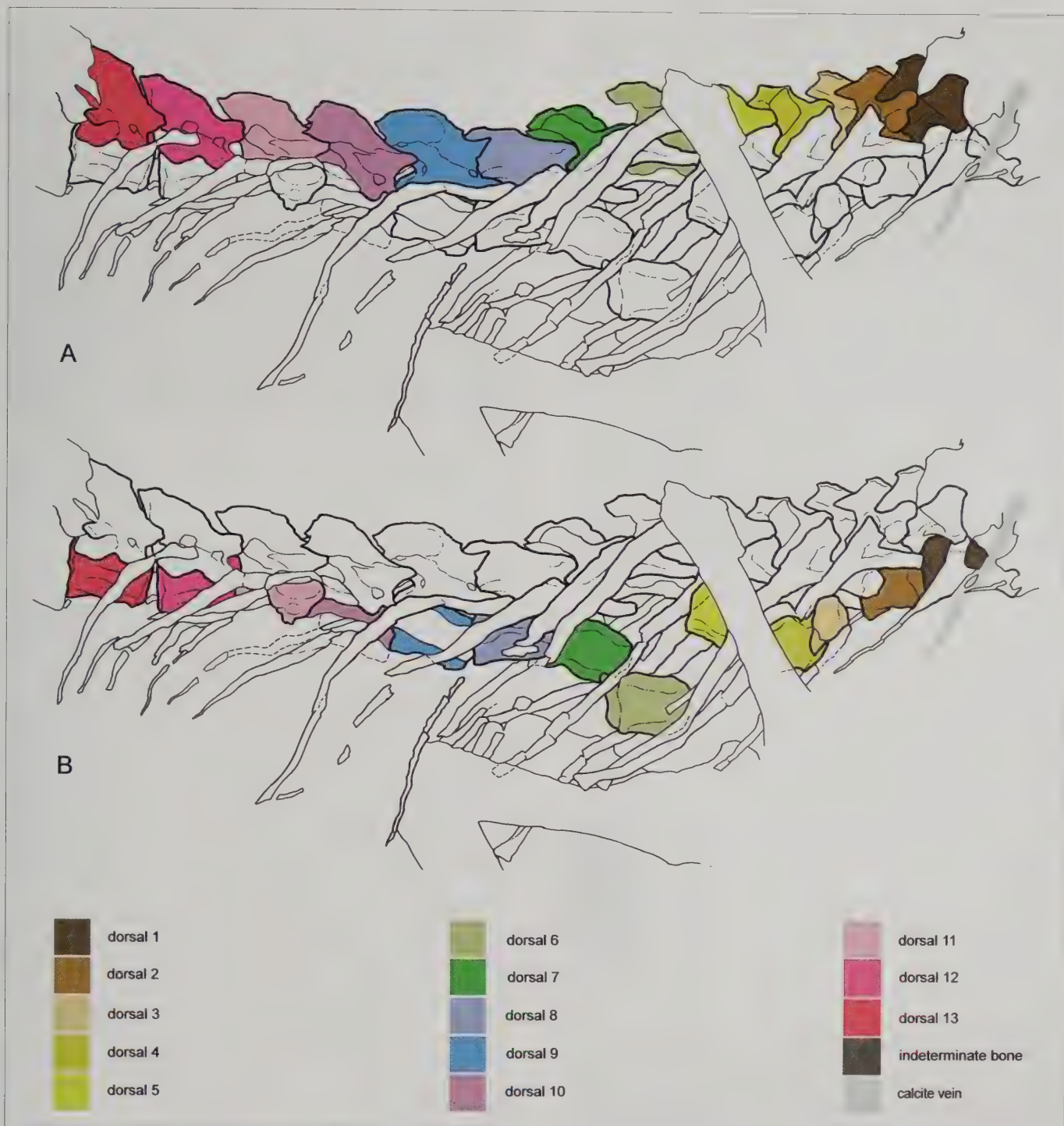


Fig. 56 - Line drawing of the dorsal vertebrae of *Scipionyx samniticus*. A) neural arches; B) centra.
 Fig. 56 - Disegni al tratto delle vertebre dorsali di *Scipionyx samniticus*. A) archi neurali; B) centri.

larger than the preceding ones. At mid-length, however, this rib tapers abruptly, terminating in a thin shaft comparable in size to the cervical ribs. Therefore, the 1st dorsal rib (Dr1) morphologically represents a transitional rib. The 13 dorsal vertebrae of *Scipionyx* are faintly to moderately constricted, not spool-shaped, with neural spines that are low and craniocaudally expanded to an increased degree, and without epipophyses (Figs. 55, 56).

The dorsal vertebrae have maintained anatomical connection and exposure in right lateral view only along the neural arches. D2, although partially covered by the large dichcephalous heads of the right Dr2 and Dr3, is well-

outlined in lateral view, as the centrum and the neural arch are still in articulation. In D2, part of the cranial articular face is also exposed, appearing moderately convex. In D1 and from D3 to D11, the centra have detached from their arches in various ways. In D1, D4 and D8, which lie in almost lateral view, the right neurocentral surface can be seen. Regarding D3, the cranial articular face of its centrum, labelled "h" (humerus) in Dal Sasso & Signore (1998a: fig. 2), is well-exposed. This face, which has rotated not only laterally up to expose the cranial surface, but also anticlockwise as far as to point its ventral margin towards the skull, is convex just like D2. D5, D6, D7

and D9 are exposed in dorsal view, revealing both neurocentral sutural surfaces, and the floor of the neural canal, which appears rather broad, in particular at the level of the pectoral girdle (see also S5, below). In addition, the centra of D6 and D7 have rolled ventrally into the rib cage. The centrum of D6 shows its articular caudal face, but unfortunately it is deformed and consequently not informative. The centrum of D10 also lies in dorsal view, but it exposes only the left neurocentral sutural surface, as the rest of the centrum is covered by the ribs and the intestine. D11 lies in an odd position: the centrum has rotated laterally about a right-angle up to expose the cranial articular face, which is oval just like D3 (5/4 wider than high). At this level of the dorsal series, the articular faces are almost flat, as for the centra of D12 and D13, which in lateral view are slightly spaced from each other. In other compsognathids, the dorsal vertebrae have been described as platycoelous (Peyer, 2006) or amphiplatyan (Hwang *et al.*, 2004), without distinction between cranialmost and caudalmost centra, whereas they are reported to be amphicoelous in some ornithomimosaurs (e.g., Kobayashi & Barsbold, 2005). D12 and D13 are the dorsal vertebrae most clearly exposed in *Scipionyx*, and they still possess a neural arch that is articulated but unfused to the centrum, with the base of the arch forming a bilobed outline marked by a median concavity.

The apexes of the neural spines of the dorsal vertebrae appear faintly expanded transversely. Although the neural arches are exposed mainly in lateral view, these faint transverse expansions are visible at the top of D2, D3 and D6 thanks to a slight distortion of the spine (Fig. 57). Such structures cannot be considered as true spine tables: they simply represent the reinforced, rugose dorsal margins of the spines.

The cranial dorsal vertebrae bear relatively small, trapezoidal neural spines. They are the craniocaudally shortest of the series, being comparable in length to the last cervicals. In *Scipionyx*, beginning from D4, the neural spines arise on the caudal half of the vertebrae, slightly overhanging the succeeding vertebra. A similar pattern can be seen in *Compsognathus* (Peyer, 2006), but already from the 1st dorsal.



Fig. 57 - Close-up of the neural arches of the 2nd and 3rd dorsal vertebra (right to left) of *Scipionyx samniticus*, showing faint transverse expansions going to the left (red arrows) and the right (green arrows) at the top of the neural spines, but no true spine tables. Scale bar = 1 mm.

Fig. 57 - *Scipionyx samniticus*. Particolare degli archi neurali della 2^a e 3^a vertebra dorsale (da destra a sinistra), che mostrano deboli espansioni trasversali, a sinistra (freccie rosse) e a destra (freccie verdi) della sommità delle spine neurali, ma non vere e proprie mensole spinali. Scala metrica = 5 mm.

Unlike non-coelurosaurian tetanurans (e.g., *Allosaurus*) and some coelurosaurs, such as tyrannosauroids (Carpenter *et al.*, 2005a) and ornithomimosaurs (Kobayashi & Barsbold, 2005; Kobayashi & Lü, 2003), in which the neural spines are relatively high, the spinous processes increasing evidently in height throughout the column towards the sacrum (Holtz *et al.*, 2004), in *Scipionyx* the dorsal neural spines are relatively uniformly low and shorter than the centrum, as is the case in *Sinosauropteryx* (Currie & Chen, 2001). In the Italian compsognathid, the caudal dorsal neural spines are also definitely larger and craniocaudally more expanded than the cranial dorsals, especially at mid-top. A similar craniocaudal expansion is found in the other compsognathids (Ostrom, 1978; Currie & Chen, 2001; Hwang *et al.*, 2004; Göhlich & Chiappe, 2006; Peyer, 2006) and was first described as “fan-shaped” (Ostrom, 1978). Subsequently, the term was applied to a variety of forms in literature. As reported by Holtz *et al.* (2004), fan-shaped dorsal neural spines are described also in the basal dinosauromorph *Marasuchus* and in the basal troodontid *Sinovenator*. Later, they were found also in the troodontid *Mei* (Xu & Norell, 2004). In *Marasuchus* (Sereni & Arcucci, 1994) and *Sinovenator* (Xu *et al.*, 2002b), the base of the spine is narrower than the top in lateral view, and the top is slightly convex. The caudal dorsal neural spines are longer craniocaudally at the tip than at the base also in *Elaphrosaurus* (Rauhut, 2003), *Mirischia* (Naish *et al.*, 2004), *Huaxiagnathus* (Hwang *et al.*, 2004), *Sinocalliopteryx* (Ji *et al.*, 2007a) and *Sinosauropteryx* (Chen *et al.*, 1998; Currie & Chen, 2001). The neural spine is craniocaudally expanded also in *Scipionyx* and *Compsognathus* (Peyer, 2006: fig. 2E), but in these two taxa the point of maximum expansion is at mid height, emphasised by the presence of beak-like ligament attachments (see below). As a consequence, the spine appears as a flattened hexagon, inclined caudally. Given these differences, generically fan-like shaped spines should not be considered as a character shared by compsognathids, but rather the simultaneous presence of relatively low spines that are significantly expanded craniocaudally, in particular at the mid-top/top, with craniocaudally flat dorsal margins. This scenario is complicated by the fact that, as reported by Naish *et al.* (2004), the degree of ossification of the dorsal tip and of the cranial and caudal surfaces of the neural spine may increase during ontogeny.

A peculiar feature of the dorsal vertebrae of *Scipionyx* is the presence of beak-like extensions on the cranial and caudal margin of the neural spine, just below the apical margin. They are emphasised dorsally by concavities that mark the craniodorsal and caudodorsal margins of the spine. The cranialmost beak-like extension in *Scipionyx* is preserved on the caudal margin of D6; more clearly exposed are the ones on the cranial and caudal margins of the best preserved neural spines, D9 and D11 (Fig. 58). These extensions were interpreted as hyposphenes-hyantra by Dal Sasso & Signore (1998a), but their proximity to the top of the spine and the strict interlocking of the pre- and postzygapophyses, which eventually obliterate other accessory articulations, allow us to exclude that interpretation. Very similar “hook-like” extensions serving as attachments for the interspinous ligaments were first described by Peyer (2006), who considered them as diagnostic of compsognathids. Peyer (2006) noted their



Fig. 58 - Close-up of the neural arch of the 11th dorsal vertebra of *Scipionyx samniticus*. Note the craniocaudally developed neural spine, which is further expanded by the presence of beak-like attachments for the ligaments. Scale bar = 1 mm. See Appendix 1 or cover flaps for abbreviations.

Fig. 58 - Particolare dell'arco neurale dell'11^a vertebra dorsale di *Scipionyx samniticus*. Si noti la spina neurale sviluppata craniocaudalmente, ulteriormente espansa da attacchi di legamenti a forma di becco. Scala metrica = 1 mm. Vedi Appendice 1 o risvolti di copertina per le abbreviazioni.



Fig. 59 - Close-up of the neural arch of the 1st dorsal vertebra of *Scipionyx samniticus*. Scale bar = 1 mm.

Fig. 59 - Particolare dell'arco neurale della 1^a vertebra dorsale di *Scipionyx samniticus*. Scala metrica = 1 mm.

presence in *Ornitholestes*, *Compsognathus*, *Huaxiagnathus*, *Scipionyx* and *Sinosauropteryx*. Similar structures are also present in *Dilophosaurus*, where they are called "anterior and posterior shoulders" (Welles, 1984). Similar to *Scipionyx*, in *Compsognathus* "hook-like" ligament attachments on the cranial border of the spine can be most easily recognised on mid-caudal dorsal neural spines, in particular in D7, D8, D9 and D11 (Peyer, 2006).

The zygapophyses of the cranial and mid-dorsal vertebrae extend less beyond the ends of their centra than in the cervical vertebrae. In the caudal dorsals (e.g., D12) the postzygapophyses do not extend caudally to the centra at all. The articular surfaces are hardly visible in all zygapophyses except those between D7 and D8. Here, the postzygapophysis of D7 and the successive prezygapophysis of D8 are not strictly in contact and show horizontal articular surfaces.

The transverse processes, visible in most of the dorsals, appear rather short and, especially in the caudal half of the series, slightly oriented caudally. According to Holtz *et al.* (2004) and Peyer (2006), the shortness of the transverse processes is common among Compsognathidae. In *Scipionyx*, the orientation of the transverse processes bearing diapophyses changes abruptly from ventrolateral to lateral between D1 and D2. The orientation is strongly dorsolateral in D7, dorsolateral in D9-D11 and again lateral in D12-D13. Most of the dorsal transverse processes lie, therefore, more or less on the transverse plane, as in *Compsognathus*, *Huaxiagnathus* and more derived maniraptorans (Peyer, 2006).

In D1 (Figs. 59-60), one can see that the diapophysis is clearly buttressed by various pronounced laminae: in a cranial direction by a prezygodiapophyseal lamina, and in a caudal direction by a postzygodiapophyseal and a posterior centrodiapophyseal lamina (*sensu* Wilson, 1999). In

some caudal dorsals (D9, D10, D12 and D13), the cranial laminae, such as the prezygodiapophyseal and the paradiapophyseal lamina, as well as the fossa delimited by them, are more clearly recognisable; in D12, the prezygoparapophyseal lamina can be seen, too (Fig. 61). In D9, a foramen on the bottom of the intrapostzygapophyseal fossa is certainly present (Fig. 62), just like in *Sinraptor* (Currie & Zhao, 1993a).

As is typical of nonavian theropods, the dorsal vertebrae of *Scipionyx* exhibit a dorsal migration of the parapophysis from the cranioventral margin of the centrum to the centre of the neural arch, moving caudally through the series. The wide divergence between tuberculum and capitulum of Dr4 indicates that, although not directly observable, in D4 the migration of the parapophysis on the neural arch has not yet occurred. Similar observations on the successive ribs (see below) suggest that the migration is completed at the level of D6-D7. The migrated parapophyses are directly visible on D9, D10, D12 and D13. More precisely, on D9 and D10 they are located at the cranial base of the arch; on D12, the parapophysis has almost reached the height of the diapophysis; on D13, it is perfectly aligned to the latter (Fig. 56A). At the same time, besides migrating dorsocaudally through the series and approaching the diapophyses, the parapophyses of the caudal dorsal vertebrae are gradually reduced in size (see also Ribs). Unlike *Scipionyx*, in most tetanurans the parapophysis remains below the level of the transverse process even in the caudalmost rib-bearing dorsal vertebra (Rauhut 2003).

In *Scipionyx*, the caudal dorsal centra are slightly longer than the cranialmost ones. The centrum length increases with each additional segment (see Table 1), as occurs also in *Compsognathus* (Peyer, 2006). The latter,



Fig. 60 - Shaded drawing of the 1st dorsal vertebra and the 1st right dorsal rib of *Scipionyx samniticus*. See Appendix 1 or cover flaps for abbreviations.

Fig. 60 - Disegno ombreggiato della 1^a vertebra dorsale e della 1^a costola dorsale destra di *Scipionyx samniticus*. Vedi Appendice 1 o risvolti di copertina per le abbreviazioni.

however, differs from *Scipionyx* in having the 2nd dorsal vertebra with a centrum much shorter than the cervical ones, whereas in *Scipionyx* the cranial dorsals and the cervicals are comparable in length. The dorsal centra of *Scipionyx* are almost parallelepiped-like in shape. Unlike allosaurids, which have a prominent constriction at mid-section of the centra (Holtz *et al.*, 2004), and unlike *Sinosauropteryx*, which has deeply concave sides (Currie & Chen, 2001), the dorsal centra of *Scipionyx* have almost parallel sides when seen in dorsal view and in lateral view. As in *Sinosauropteryx* (Currie & Chen, 2001), in lateral view the concavity of the ventral edge is almost absent in *Scipionyx*, resulting in it being even less marked than in *Compsognathus* (Peyer, 2006). The ventral edges of the cranial dorsal centra are mostly hidden by ribs (D1) and muscular tissue remains (D2). Where the edges emerge, ventral keels and hypapophyses are not visible. In taxa that have well-developed keels and hypapophyses, they are already reduced at the level of D3 (Rauhut, 2003). Thus, in *Scipionyx* the absence of these structures in the cranial face of the centrum of D3 is expected, and not informative of the condition of the preceding vertebrae. Hy-

papophyses are absent in *Compsognathus* (Peyer, 2006). They are present in the cranialmost dorsals of sinraptorids and most Maniraptoriformes (Rauhut, 2003), but not in the basal ornithomimosaur *Garudimimus* (Kobayashi & Barsbold, 2005).

In the mid-caudal dorsal vertebrae of *Scipionyx*, the craniocaudal diameter is 5/3 the dorsoventral diameter, and 5/4 the mediolateral diameter. The caudal dorsal centra are similarly elongate in *Mirischia* (Rauhut, 2003: fig. 27C), on average twice as long as they are tall in *Compsognathus* (Peyer, 2006) and *Huaxiagnathus* (Hwang *et al.*, 2004), and significantly even more elongated in dilo-phosaurids, coelophysoids and ornithomimosaurids (e.g., Kobayashi & Lü, 2003), whereas they are as high as long in *Sinraptor*, *Allosaurus*, *Majungasaurus* (Rauhut, 2003) and *Sinosauropteryx* (Currie & Chen, 2001), or even higher in *Tyrannosaurus* and *Deinonychus* (Rauhut, 2003). Contrary to *Scipionyx*, in many coelurosaurids such as *Coelurus*, *Ornitholestes* (Carpenter *et al.*, 2005b), *Tanycolagreus* (Carpenter *et al.*, 2005a) and *Garudimimus* (Kobayashi & Barsbold, 2005), the centra are reported to be taller than they are wide.

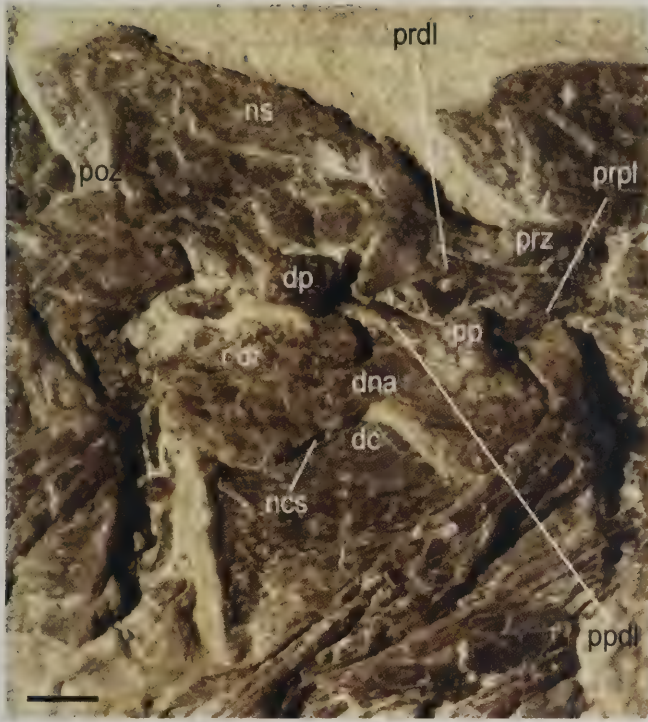


Fig. 61 - Close-up of the 12th dorsal vertebra of *Scipionyx samniticus*. Scale bar = 1 mm. See Appendix 1 or cover flaps for abbreviations.
 Fig. 61 - Dodicesima vertebra dorsale di *Scipionyx samniticus*. Scala metrica = 1 mm. Vedi Appendice 1 o risvolti di copertina per le abbreviazioni.

On the exposed surfaces of the dorsal vertebral centra of *Scipionyx*, no pleurocoels are visible. This is expected, as, according to Holtz *et al.* (2004), the compsognathids differ from most of the other tetanurans in lacking any dorsal pleurocoel. The condition in *Scipionyx*, however, might be influenced by two factors: ontogeny and preservation. Concerning ontogeny, as mentioned above, according to Wedel (2009) the pattern of pneumatization of the vertebrae in the Saurischia seems to reflect that of the extant avian forms, with the phylogenetic trajectory within the group matching what occurs during bird ontogeny. The pneumatization of the cranial dorsals could eventually have occurred later in *Scipionyx*, given that, although not a basal theropod, the specimen is a very immature individual (see Ontogenetic Assessment). Concerning preservation, the exposure in *Scipionyx* of the lateral surface of the centra dorsal and caudal to the parapophyses, where the pleurocoels are usually found, is, unfortunately, very limited, rendering confirmation of their absence difficult. However in D2, which is well-exposed, no pleurocoel can be seen. It is interesting to note that dorsal pleurocoels are entirely absent also in some other taxa that have cervical pleurocoels, such as *Elaphrosaurus*, *Avimimus* (Rauhut, 2003), *Coelurus* (Carpenter *et al.*, 2005b) and the above mentioned *Compsognathus* (Peyer, 2006) and *Sinosauropteryx* (Currie & Chen, 2001), although in the latter genus a problem of preservation cannot be ruled out. In addition, in the Ornithomimosauria (Makovicky *et al.*, 2004) and

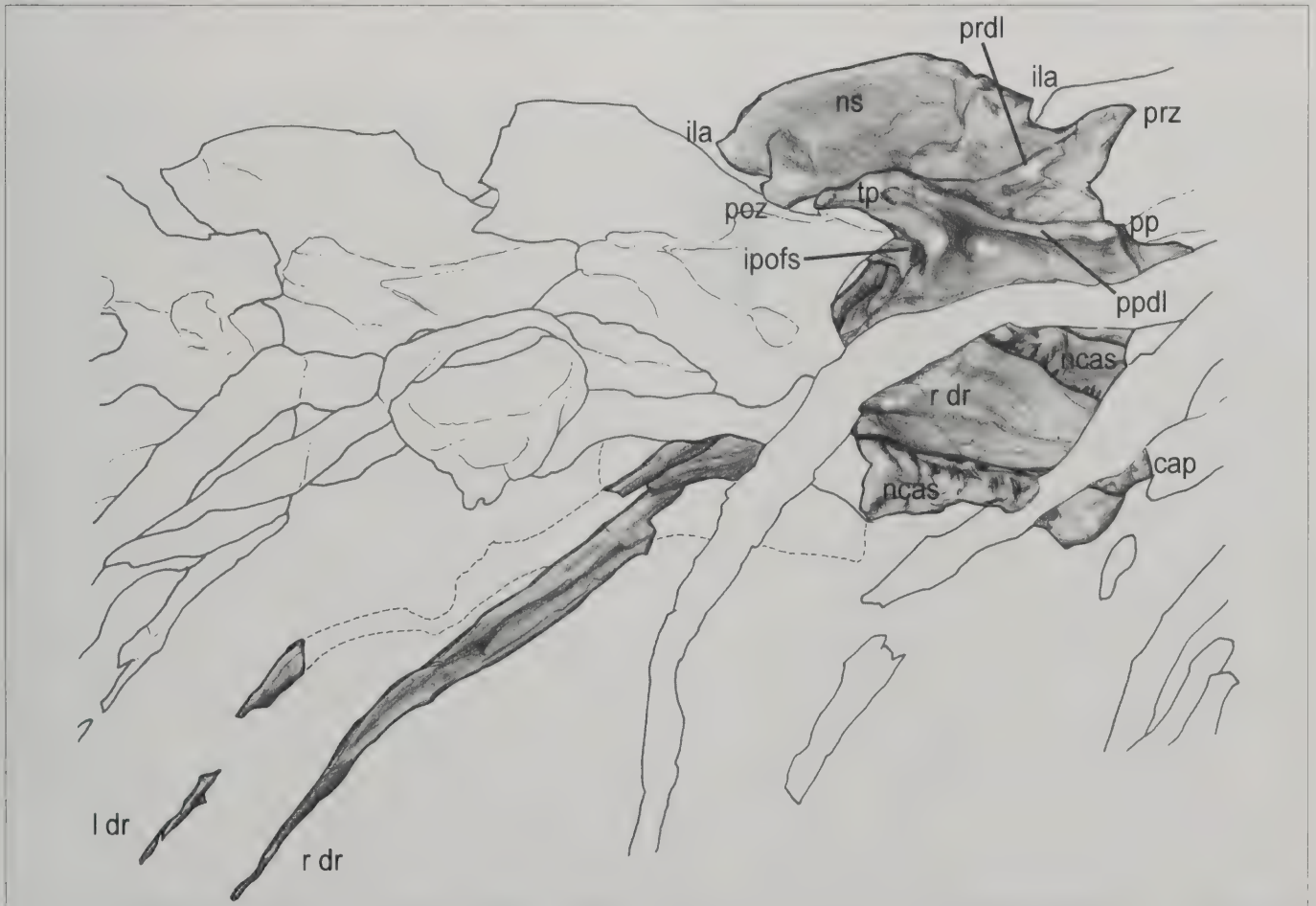


Fig. 62 - Shaded drawing of the 9th dorsal vertebra and ribs of *Scipionyx samniticus*. See Appendix 1 or cover flaps for abbreviations.
 Fig. 62 - Disegno ombreggiato della 9^a vertebra dorsale di *Scipionyx samniticus* e sue costole. Vedi Appendice 1 o risvolti di copertina per le abbreviazioni.

in the Troodontidae (Currie & Dong, 2001, Makovicky & Norell, 2004; Xu & Norell, 2004) only the first one or two dorsal centra are sometimes pneumatic to varying degrees, whereas basal tyrannosauroids (Xu *et al.*, 2004; Carpenter *et al.*, 2005a; Xu *et al.*, 2006) and *Microraptor* (Hwang *et al.*, 2002) are reported to lack pleurocoels/pneumatic foramina.

In *Scipionyx*, the last dorsal vertebra (D13) lacks articulated ribs. However, as both diapophysis and parapophysis are present on its right side, a Dr13 was in all likelihood present. Usually, the last dorsal rib is small and short in theropods. The bony fragment preserved ventral to the centrum may represent a splinter of the right Dr13, lost during preparation, or of the left one, which would emerge between the centrum of the D13 and the intestine (see Ribs).

Sacral vertebrae - In *Scipionyx*, elements belonging to 4 different sacral vertebrae are exposed (Figs. 63-64). S1 is in continuity with the dorsal series, occupying the position it occupied in the undisturbed skeleton. A small portion of a successive centrum, representing S2, can be seen in a space between the elements of the pelvic girdle. The neural arches of the other two exposed vertebrae precede the caudal series. The space between the neural arch of S1 and the penultimate arch matches in size the length of two neural arches. Similarly, based on the length of the centrum of S5, 5 elements are needed to fill the space between the last dorsal and the 1st caudal vertebrae. Thus, the sacrum of *Scipionyx* is composed of 5 vertebrae, and the arches preceding the caudal ones belong to S4 and S5.

Five sacrals (1 dorsosacral, 2 sacrals and 2 caudosacrals) are the usual count for Neotheropoda (Tykoski & Rowe, 2004), and, as mentioned above, this is the number of sacrals preserved in *Compsognathus* (Peyer, 2006). The sacral count is unknown in *Huaxiagnathus* (Hwang *et al.*, 2004), *Sinocalliopteryx* (Ji *et al.*, 2007a) and *Juravenator* (Göhlich & Chiappe, 2006).

S1 is the only sacral vertebra in which the neural arch is still adjacent to its centrum, with the neurocentral suture only slightly open. Because of a slight anticlockwise rotation of the iliac blade, most of the right lateral aspect of S1 is exposed ventral to the ventral margin of the preacetabular ala of the ilium, and cranial to the contact between the ilium and the pubis. The centrum does not show pneumatopores, as for example in *Guanlong* (Xu *et al.*, 2006), and the neural arch, well-dorsal to the neurocentral suture, bears an evident bumpy transverse process. As the latter terminates laterally with a single rugose facet, and no scars are visible on the centrum, we infer that the transverse process and the rib attachments were conjoined in S1. This condition resembles the one of *Tyrannosaurus*, where a single, rugose, bifid facet is seen on a process of the neural arch of S1 (Brochu, 2003) not invading the centrum with its ventral part, contrary to what occurs in *Allosaurus* (Madsen, 1976). Unfortunately, in *Scipionyx* the transverse process facets and rib facets of the successive sacral vertebrae are not exposed, so it is impossible to establish if they are separated and located dorsolaterally and lateroventrally across the neural arch and centrum, as occurs in the above mentioned, well-known, large genera.



Fig. 63 - Sacral vertebrae and ribs of *Scipionyx samniticus*. Scale bar = 5 mm.

Fig. 63 - Vertebre e costole sacrali di *Scipionyx samniticus*. Scala metrica = 5 mm.

In *Scipionyx*, the cranial margin of the centrum of S1 is perfectly aligned to the cranial margin of the iliac blade, just like in the French *Compsognathus* (Peyer, 2006). The exposed tract of the ventral margin appears almost flat. Regarding S2, two small portions emerge: a triangular area, probably corresponding to the craniodorsal portion of the centrum, is visible between the lesser (=anterior) trochanter of the right femur and the pubic peduncle of the right ilium; and the caudodorsal portion of the centrum and the caudoventral base of the neural arch, are visible between the lesser trochanter of the right femur and the cranioventral margin of the acetabulum.

Nothing can be said about S3, as neither the neural arch nor the centrum are exposed. It can be hypothesised that this vertebra is still in place, sandwiched in-between the ilia. In contrast, the elements forming S4 and S5 emerge dorsal and ventral to the postacetabular ala of the right ilium, due to the fact that they are disarticulated and have lost their connection with the ilia. The degree of compression and deformation that occurred in this area of the skeleton renders it difficult to interpret elements and structures belonging to S4 and S5, and to establish in which aspect they became fossilised (Fig. 64). The neural arch of S4, from the top of the spine to its base, can be seen in right lateral view. The ventral margin of the spine leans



Fig. 65 - Close-up of the pelvic region of *Scipionyx samniticus* under properly grazing light, which highlights the presence of a caudal vertebral centrum under the right iliac blade (shadowed relief, and fractures marked by the arrows). Scale bar = 2 mm. See Appendix 1 or cover flaps for abbreviations.

Fig. 65 - Particolare della regione pelvica di *Scipionyx samniticus* in luce radente, che evidenzia la presenza di un centro vertebrale caudale al di sotto della lama iliaca destra (rilievo ombreggiato e fratture indicate dalle frecce). Scala metrica = 2 mm. Vedi Appendice 1 o risvolti di copertina per le abbreviazioni.



Fig. 64 - Line drawings of the bones illustrated in Fig. 63. A) neural arches and ribs; B) centra and indeterminate elements. See Appendix 1 or cover flaps for abbreviations.

Fig. 64 - Disegni al tratto delle ossa illustrate in Fig. 63. A) archi neurali e costole; B) centri ed elementi indeterminati. Vedi Appendice 1 o risvolti di copertina per le abbreviazioni.

against the right ilium and, in its cranial half, is slightly superimposed to the dorsal edge of the iliac blade. The craniodorsal quarter of the neural arch is markedly corrugate, possibly representing the articular surface of the transverse process. Ventral to the arch of the S4, and well-detached from it, the relief of a quadrangular element can be seen, under oblique light, under the right iliac blade (Fig. 65). Both shape and size fit a sacral centrum and, based on its position, it can be referred to S4. The neural arch of S5 is also detached from its centrum. Ventral to the spine, the exposed caudal half is laterally reinforced by a crest. This crest widens ventrally to form a rugose scar that represents the articular surface for the 5th sacral rib. A very similar undescribed crest is visible in the last sacral of *Sinocalliopteryx* (Ji *et al.*, 2007a: fig. 4b). The 5th sacral rib of *Scipionyx* has moved slightly cranially and, together with another element of uncertain attribution, covers the cranial half of the 5th neural arch. The centrum of S5 lies in dorsal view, between the right postacetabular iliac blade and the intestine, exposing a wide neural canal and both neurocentral articular surfaces. The centrum of S5 has flat articular surfaces for the adjacent centra.

Caudal vertebrae - Only 9 proximal vertebrae of the tail of *Scipionyx* are preserved (Figs. 66-67). Presumably, the tail was longer than the skull-presacral length (see Skeletal Reconstruction And...), given that in complete coleurosaurian skeletons, especially in compsognathids, the intact tail is definitely longer than the skull-presacral



Fig. 66 - Caudal vertebrae and haemal arches of *Scipionyx samniticus*. Scale bar = 5 mm.
 Fig. 66 - Vertebre caudali e archi emali di *Scipionyx samniticus*. Scala metrica = 5 mm.

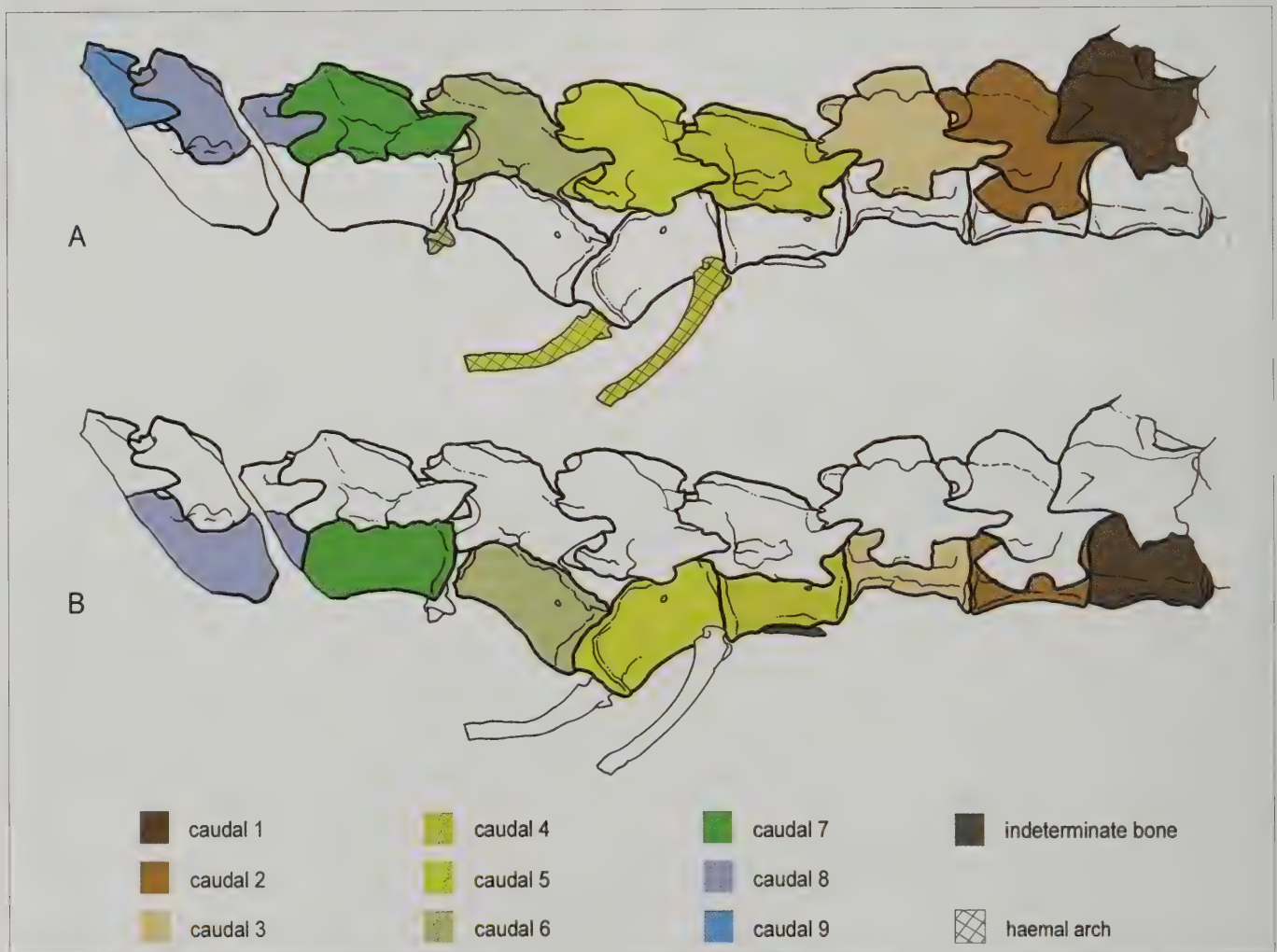


Fig. 67 - Line drawings of the bones illustrated in Fig. 66. A) neural and haemal arches; B) centra and indeterminate bones.
 Fig. 67 - Disegni al tratto delle ossa illustrate in Fig. 66. A) archi neurali ed emali; B) centri e ossa indeterminate.

length, irrespective of the ontogenetic stage (Kobayashi & Lü, 2003). In the preserved series, no transition point is seen, as is demonstrated by the persistence of transverse processes.

The caudal neural spines are markedly low, proximodistally elongate and shorter than the transverse process-

es. They bear well-developed zygapophyseal articulations that overhang their centrum. As in most of the preceding vertebrae, the neural arches are more or less aligned and articulated, but not fused to their centra, so that the neurocentral sutures are open and the centra are detached to varying degrees and variably reoriented. The neural

arches are mainly preserved in lateral view, but the diagenetic compression caused a slight rotation that has partly exposed the left zygapophyses and transverse processes. This laterodorsal exposure is particularly apparent in Ca3 and Ca5 (Fig. 68).

The caudal centra are long and platycoelous, as in *Compsognathus* (Peyer, 2006). From Ca1, which lies in full dorsal view, the centra rotate gradually along the series up to Ca4, which is in lateral view. This variety of views allows to reconstruct many structures (see below), despite the centra of Ca2 and Ca3 being slightly covered ventrally by patches of soft tissue. The centra of Ca5 and Ca6 are no longer aligned along the proximodistal horizontal plane. Their contact has moved so far ventrally that their adjacent articular faces are perpendicular rather than parallel. An oblique fracture, interrupting the slab in which the caudosacral portion of the specimen lies, has truncated both Ca8, of which the proximal half of the centrum and neural arch are preserved, and Ca9, of which the centrum is completely missing and only a proximal portion of the neural arch is preserved.

The neural spines of Ca1 and Ca2 are taller and more rounded than the successive ones. Notably, the proximal end of the spine of Ca1 seems to be in continuity with the caudal end of the spine of S5 (Fig. 69). From Ca3, the neural spines become lower than long, more elongated proximodistally and tilted backwards. The spines are tilted backwards also in *Compsognathus*, but they differ from those of *Scipionyx* in being markedly higher and rectangular in shape (Peyer, 2006). From Ca4, the spines of *Scipionyx* develop a slight concavity at mid-length of the dorsal edge (Fig. 68). However, contrary to *Sinosauropteryx* (Currie & Chen, 2001) and some other theropods (e.g., allosauroids), in *Scipionyx* this concavity does not really separate the neural spine in a proximal emargination (accessory neural spine) and a distal spine, at least in the preserved, proximalmost sequence. Thus, *Scipionyx* presents a condition intermediate between *Sinosauropteryx* and *Compsognathus*, in which not even a slight concavity has been described (Peyer, 2006). Bifid spines are also not reported in other coelurosaur such as *Ornitholestes* and *Coelurus* (Carpenter *et al.*, 2005b).

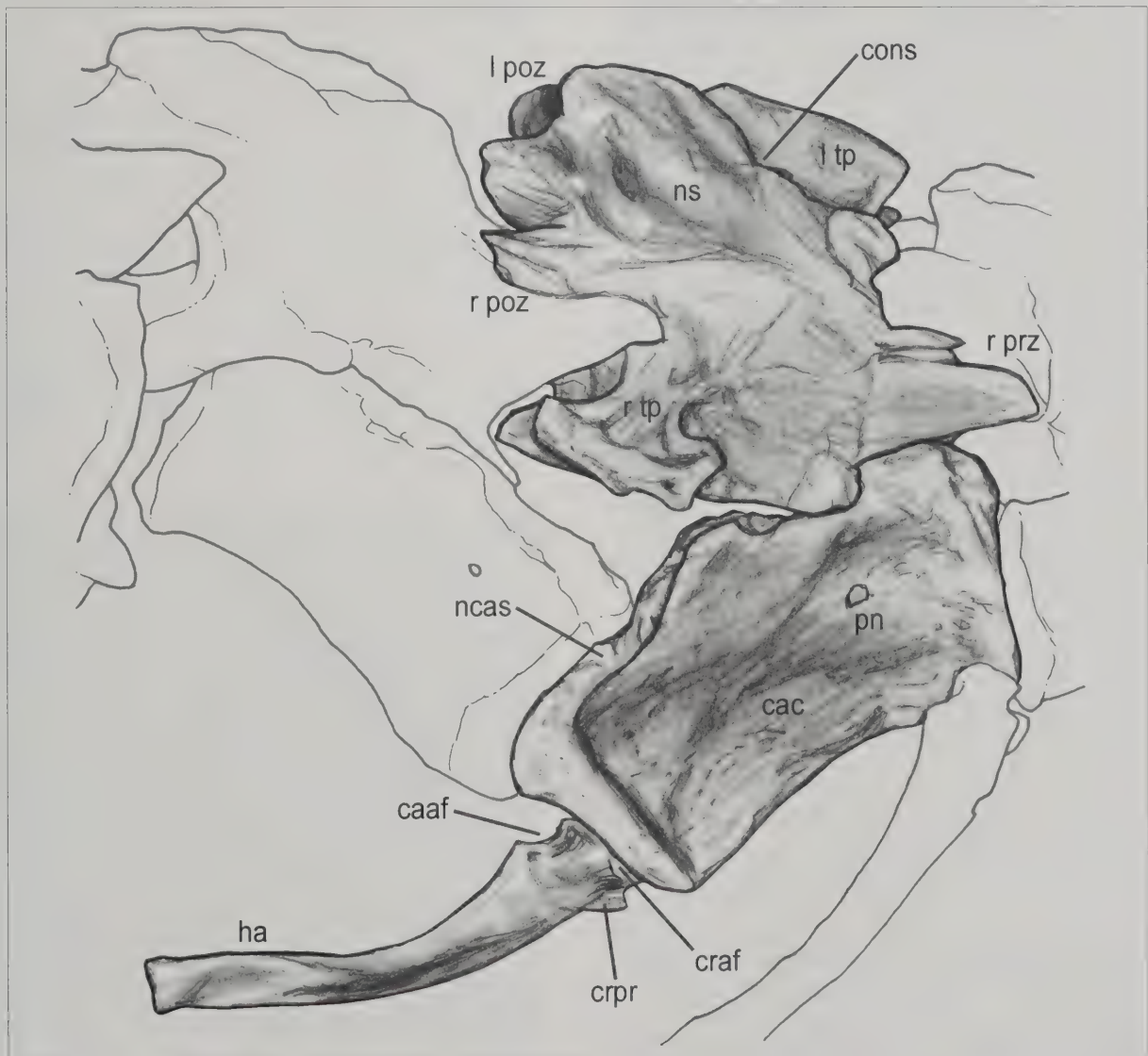


Fig. 68 - Shaded drawing of the 5th caudal vertebra and 5th haemal arch of *Scipionyx samniticus*. See Appendix 1 or cover flaps for abbreviations.

Fig. 68 - Disegno ombreggiato della 5^a vertebra caudale e del 5^o arco emale di *Scipionyx samniticus*. Vedi Appendice 1 o risvolti di copertina per le abbreviazioni.

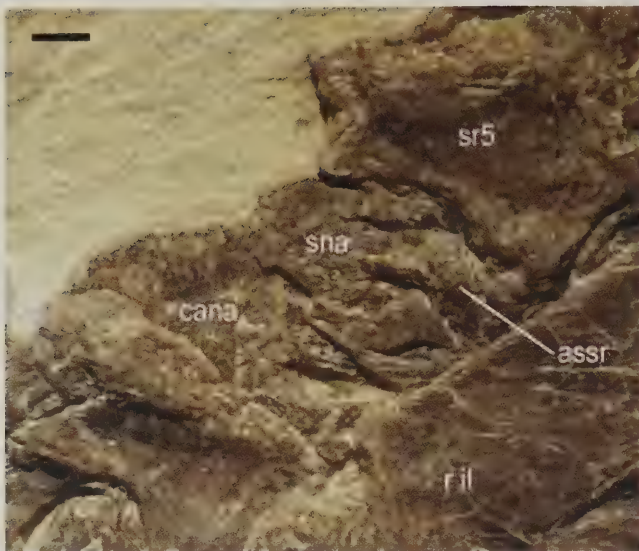


Fig. 69 - Close-up of the caudosacral region of *Scipionyx samniticus*, showing the seemingly fused neural spines of the 5th sacral and 1st caudal vertebra. For asr, see also Fig. 79. Scale bar = 1 mm. See Appendix 1 or cover flaps for abbreviations.

Fig. 69 - Particolare della regione caudosacrale di *Scipionyx samniticus*, con le spine neurali della 5^a vertebra sacrale e della 1^a caudale in apparente contatto suturale. Per asr, vedi anche Fig. 79. Scala metrica = 1 mm. Vedi Appendice 1 o risvolti di copertina per le abbreviazioni.

The passage between the spines and the postzygapophyses is marked by a margin that appears remarkably concave in lateral view (right postzygapophyses), whereas it appears as a ridge subdividing the dorsal surfaces of the postzygapophyses in dorsal view (left postzygapophyses). The zygapophyseal articular surfaces seem to be inclined about 30-45° with respect to the medial sagittal plane.

All the preserved transverse processes are robust and project perpendicularly to the direction of the vertebral column. Along the series they also become slightly inclined distally and seem to be broader laterally than at their base, with more concave proximal and distal margins. No accessory transverse processes, such as those described by Currie & Chen (2001) in the proximal vertebrae of the tail of *Sinosauropteryx*, can be seen in *Scipionyx*. In Ca2, the base of the arch, which is not hidden by the transverse process, distinctly shows its ventral margin. It has a bilobed shape that is more marked than in D12 and D13.

On account of the rotation described above, the floor of the neural canal and the rugose neurocentral articular surfaces of Ca1-Ca3 are visible (Fig. 70). The passage from the neurocentral surfaces to the articular and lateral faces of the centra is abrupt and angled. This, together with the fact that the ventral concavity of the centra is very faint, renders the proximal caudal centra markedly parallelepiped-like (box-like), as in *Compsognathus* (Peyer, 2006), *Juravenator* (Göhlich *et al.*, 2006), *Ornitholestes*, *Coelurus* (Carpenter *et al.*, 2005b), deinonychosaurs (Makovicky & Norell, 2004; Norell & Makovicky, 2004) and basal birds (e.g., Rauhut, 2003). Besides the ventral concavity, the centra of *Scipionyx* ventrally also lack distinct proximal and distal pedicels for the articulations with the chevrons, that are well-developed in ornithomimosaurs (Kobayashi & Lü, 2003; Makovicky *et al.*, 2004). The centra of *Scipionyx* are bulky in appearance, with the 1st centrum only 4/3 longer than its width. From Ca1, the centra gradually in-

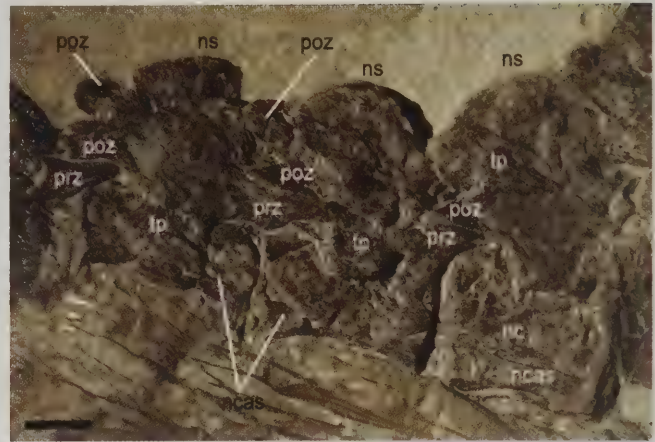


Fig. 70 - Close-up of the proximal caudal vertebrae of *Scipionyx samniticus*. The floor of the neural canal and the neurocentral articular surfaces of the box-like centra are exposed. Left zygapophyses labelled in black, right zygapophyses in white. Scale bar = 1 mm. See Appendix 1 or cover flaps for abbreviations.

Fig. 70 - Particolare delle vertebre caudali prossimali di *Scipionyx samniticus*. I centri, di forma squadrata, espongono il pavimento del canale neurale e le superfici articolari neurocentrali. Zigapofisi sinistre in nero, zigapofisi destre in bianco. Scala metrica = 1 mm. Vedi Appendice 1 o risvolti di copertina per le abbreviazioni.

crease in length proximodistally, as occurs in *Juravenator* (Göhlich *et al.*, 2006: tab. 1). The last undisturbed centrum of *Scipionyx* (Ca7) is about twice as long as tall.

Large pneumatopores are absent, but a single, small foramen is present at about 1/3 of the proximodistal length from the proximal margin and at about 1/3 of the dorsoventral height from the dorsal margins on the lateral surface of the centra of Ca4-Ca6 (Figs. 68, 71). Successive centra seem to lack this foramen, whereas in the preceding ones they cannot be observed because the centra are exposed mainly in dorsal view. The pneumatic or neurovascular nature of the foramina cannot be ascertained. The absence of large pneumatopores and the presence of small foram-



Fig. 71 - Pneumaticity of the caudal vertebrae of *Scipionyx samniticus* (arrows point to pneumatopores). Scale bar = 2 mm.

Fig. 71 - Pneumaticità nelle vertebre caudali di *Scipionyx samniticus* (le frecce indicano pneumatopori). Scala metrica = 2 mm. Vedi Appendice 1 o risvolti di copertina per le abbreviazioni.

ina were found on the middle lateral surfaces of the first 9 caudal centra in *Tyrannosaurus* (Brochu, 2003). Among coelurosaurs, no evidence of pneumaticity has been found in compsognathids, *Ornitholestes*, *Coelurus* (Carpenter *et al.*, 2005b), ornithomimosaur (Makovicky *et al.*, 2004) or *Falcarius* (Kirkland *et al.*, 2005), whereas single pleurocoels have been reported close to the base of the neural arch in the proximal caudals of some derived coelurosaurs such as the Oviraptorosauria (Osmólska *et al.*, 2004). The alleged compsognathid *Orkoraptor* has caudal vertebrae with a single pair of small pleurocoels on each side (Novas *et al.*, 2008a); however, the phylogenetic position of this fragmentary taxon is not yet clear, it belonging probably to a group of non-coelurosaurian tetanurans (see Comments in Phylogenetic Analysis).

Haemal arches - In *Scipionyx*, two complete haemal arches (=chevron bones) are exposed (Figs. 66, 67A). They lie in lateral view in an intercentral position, between Ca4-Ca5 and Ca5-Ca6. A third one, preserving only its proximal portion, is located between Ca6 and Ca7. In theropods, the haemal arches are usually present from the proximalmost intercentral positions, with a certain degree of individual variability (e.g., Weishampel *et al.*, 2004). For example, in *Compsognathus*, chevrons are present from the first intercentral position (i.e., between Ca1 and Ca2) (Peyer, 2006), whereas in *Huaxiagnathus* they are reported to appear first between Ca3 and Ca4 (Hwang *et al.*, 2004). In *Scipionyx*, the presence/absence of haemal arches in the first three intercentral positions cannot be ascertained because of the presence of a large mass of soft tissue, including muscular remains, which covers the ventralmost portion of the caudal skeleton. The thin bone portion aligned to the ventral margin of the centrum of Ca4 may be part of the shaft of a haemal arch, whereas the outline of an element matching in size and orientation the other haemal arches can be seen with CT scanning at the Ca2-Ca3 intercentral position.

The chevrons of *Scipionyx* are generally slender and feebly recurved, like those of all neotetanurans (Holtz *et al.*, 2004) except the most derived Maniraptora. Proximally, they bear cranial and caudal articular facets that, when articulated, extend beneath the ventral surfaces of the adjacent caudal centra (Figs. 68, 72). In the two fully preserved elements, the cranial articular facet appears weakly convex and slightly more extended than the caudal one, which is markedly concave. The portion of bone between the two facets forms an angle greater than 100° . A pointed, cranial process that is little differentiated from the shaft is also present (Figs. 68, 72): it is comparable in size to that of *Sinocalliopteryx* (Ji *et al.*, 2007a) and *Juravenator* (Göhlich *et al.*, 2006), but markedly smaller than in *Allosaurus* (Madsen, 1976) and *Majungasaurus* (O'Connor, 2007), where it approaches the size of the articular facets. Moreover, in these taxa the angle is less than 90° and the orientation of the facets is symmetric with respect to the proximal half of the shaft.

In *Scipionyx*, the marked concavity of the caudal articular facet indicates an intimate connection with the cranial margin of the distal vertebral centrum. This character, together with the asymmetric position of the facets with respect to the shaft, suggests that *in vivo* the proximal portion of the shaft of the proximal haemal arches diverged less than 40° from the long axis of the tail. The divergence



Fig. 72 - Close-up of the 5th haemal arch of *Scipionyx samniticus*. Note the distal flattening and fusion of the two rami. Scale bar = 1 mm. See Appendix 1 or cover flaps for abbreviations.

Fig. 72 - Particolare del 5° arco emale di *Scipionyx samniticus*. Notare l'appiattimento distale e la fusione dei due rami. Scala metrica = 1 mm. Vedi Appendice 1 o risvolti di copertina per le abbreviazioni.

is of about 30° in *Sinocalliopteryx* (Ji *et al.*, 2007a). The curvature of the shaft, uniform for almost 2/3 the length of the haemal arch, disappears distally, where the two counterlateral rami meet and become a single mediolaterally flattened element.

The chevrons of the other compsognathids are more or less similar in general shape. Like in *Scipionyx*, those occupying the intercentral positions 4-5 and 5-6 seem to be slender, rod-like and possibly flattened distally in *Huaxiagnathus* (Hwang *et al.*, 2004: fig. 4C), in the German *Compsognathus* (Ostrom, 1978) and in *Juravenator* (Göhlich *et al.*, 2006: pl. 7, fig. 3). They appear comparatively broader and more recurved in the French *Compsog-*

gnathus (Peyer, 2006), and even broader, gently curved and remarkably spatulate in *Sinosauropteryx* (Currie & Chen, 2001; Ji *et al.*, 2007b). Given the apparent variability of the chevrons from neighbouring intercentral positions in the above-cited complete tails, these differences alone do not deserve much attention.

Ribs

Scipionyx possesses 21, possibly 22, pairs of straight to moderately curved presacral ribs (Figs. 49, 55). Those of the right side are all visible, at least for part of their

length, whereas the left ones are not easily identifiable, emerging only for short tracts, especially in the cervical region. All cervical and cranial dorsal ribs are clearly dichoccephalous; caudal dorsal ribs maintain long capitula, but the tubercula shorten gradually.

Cervical ribs - Nine pairs of cervical ribs are present, from the axis on (Fig. 73). The atlas does not bear ribs, as is the case in all neotheropods (Weishampel *et al.*, 2004). The cervical ribs of *Scipionyx* are more robust proximally and much more elongate distally than previously thought (Dal Sasso & Signore, 1998a); however, they remain thicker than in other compsognathids, such as *Juravena-*

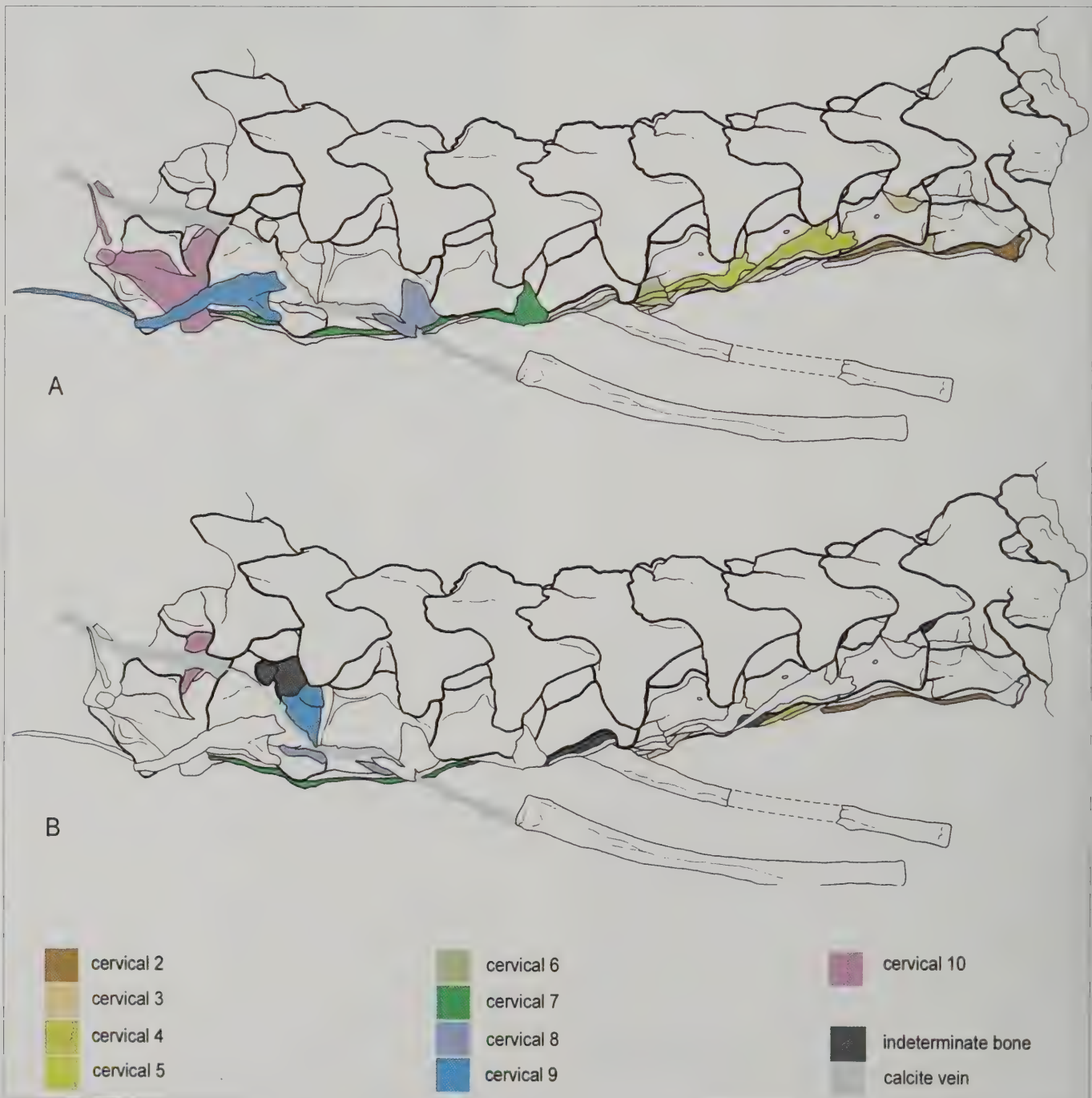


Fig. 73 - Line drawings of the cervical ribs of *Scipionyx samniticus*, illustrated in Fig. 49. A) right ribs; B) left ribs and indeterminate elements.

Fig. 73 - *Scipionyx samniticus*. Disegno al tratto delle costole cervicali illustrate in Fig. 49. A) costole destre; B) costole sinistre ed elementi indeterminati.

tor (Göhlich & Chiappe, 2006: fig. 1b). With the exception of Cr10, all the right cervical ribs have capitula still in place and articulated to their vertebral centra, thus, hiding all parapophyses. On the other hand, all the tubercula except those of Cr3 and Cr4 have lost their contact with the diapophyses.

The right axial cervical rib is characterised by a small head, with adjacent, faintly diverging tuberculum and capitulum. Therefore, as already written, it can be considered dichocapalous, a condition shared by the tetanuran theropods (Holtz *et al.*, 2004). At a first glance, the shafts (stilyform processes *sensu* O'Connor, 2007) of the axial ribs seem to be as long as the axial centrum. However, observing the fossiliferous slab at a high magnification and inclined at 45°, it is apparent that there is continuity between them and the tiny bones ventral to the centrum of C3. Thus, despite their delicate nature, both right and left Cr2 are preserved for their entire length, parallel and paired, and are as long as two vertebral centra (Fig. 74).

The head of Cr3 is the most fragmented of the right side. Its seemingly small size is due to the fact that only the capitulum is still connected to the shaft. The tuberculum is, in fact, detached but still articulated to the diapophysis. The proximal portion, which runs ventral to the centrum of C3 before disappearing under the head of the right Cr4, is thicker than that of Cr2. Observing the order of superimposition of the right and left shafts, and following a process of elimination, the distal end of the right Cr3 can be seen passing under the head of the Cr6 and terminating juxtaposed to the left ceratobranchial I. Thus, from Cr3 the cervical ribs already reach the length of three vertebral centra. As for Cr2, also the distal end of the left Cr3 is well-preserved and lies close to the distal end of the right Cr3, both forming a V and both being juxtaposed to the left ceratobranchial I (Fig. 54).

In the right Cr4, tuberculum and capitulum clearly diverge and the transition between the head and the shaft is more marked, not only by an abrupt decrease in size in transverse section, but also because the shaft seems to change direction, paralleling the concavity of the ventral margin of the centrum.

An abrupt directional change not related to fracturing is present also in the right Cr5, between head and shaft. In our opinion, this pattern is not completely interpretable as an artefact of preservation (see Skeletal Taphonomy) but

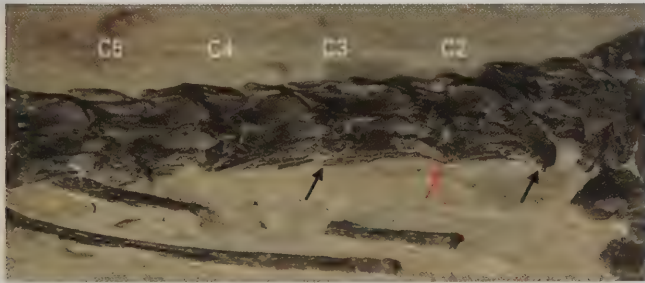


Fig. 74 - Photograph taken in grazing (ventrolateral) view of the neck of *Scipionyx samniticus*, showing origin and end of the 2nd cervical ribs (black arrows), and their continuity under the 2nd and 3rd vertebral centra (red arrow). See Appendix 1 or cover flaps for abbreviations.

Fig. 74 - Vista radente (ventrolaterale) del collo di *Scipionyx samniticus*, che mostra origine e terminazione delle seconde costole cervicali (freccie nere), e la loro continuità sotto il 2° e 3° centro vertebrale (freccia rossa). Vedi Appendice 1 o risvolti di copertina per le abbreviazioni.

reflects, in part, the natural arrangement. Curvature of the neck of the rib is, in fact, preserved also in the right Cr7 and, symmetrically, in both right and left Cr8, the shafts of which, unlike the preceding ones, are not close to the centra of their respective vertebrae. Like Cr3, we identified the end of the left Cr5 by looking at the specimen inclined at 45°. It lies at the level of the caudal margin of the centrum of C7, indicating that Cr5 is as long as three centra as well.

The right Cr6 lacks the tuberculum and part of the neck; it disappears in a caudal direction under the centrum of its corresponding vertebra. Two short segments of uncertain attribution are present between the right Cr6 and the ventral surface of the centrum.

The pair of Cr7 represents the longest cervical ribs. They lie ventral to cervical centra 7, 8 and 9, which are the most elongate craniocaudally. They are also the most clearly exposed ribs, as their mid portion is not hidden by the successive centrum. They preserve a natural dorsal outline with a marked neck convexity, a faint concavity in the mid portion of the shaft, and a distal portion which is almost straight.

The right Cr7 and Cr8 are the cervical ribs which possess the dorsoventrally most expanded heads; they have a markedly elongate tuberculum projecting towards an almost horizontal diapophysis, and an apparently shorter capitulum. The two processes are connected via a bony lamina, the capitotubercular web (*sensu* O'Connor, 2007). The concavity of the tuberculum of the right Cr8 is the best preserved of the cervical series.

The right Cr9 is fractured but well-exposed all along its length; it is shorter than the preceding ones, as it does not reach the length of three vertebral centra, which, in addition, are slightly shorter here than the preceding ones. The neck of the rib displays the above mentioned natural caudodorsal curvature; however, in the mid portion the dorsal concavity is accentuated by the ventral displacement of the centrum of C10, which has caused the fracture of the distal portion of the shaft.

The heads of the left Cr9 and Cr10 emerge considerably in the space between the neural arches and the centra of C9 and C10. The almost erect tubercula are buttressed ventrally by the capitotubercular web (Fig. 75); also, part of the shaft of the left Cr9 can be seen directed caudally. The right Cr10 lacks the shaft but preserves a markedly enlarged head, which is comparable in size to the first dorsal ribs but maintains the shape of the cervical ones. In fact, differently to the dorsal ribs (see below), the tuberculum projects dorsally, where it contacted the diapophysis (they became separated by a calcite vein – see Skeletal Taphonomy), whereas the capitulum is almost aligned with the major axis of the shaft. Thus, the right Cr10 presents a transitional morphology and, similar to its vertebra, can be considered a cervicodorsal rib. Unfortunately, both shafts of Cr10 are missing, so we cannot compare their length with that of the first dorsal rib.

The cervical ribs of *Scipionyx* resemble those of the other compsognathids in being elongate and very thin. Like in *Scipionyx*, the cervical ribs of *Compsognathus* are reported to be very delicate and slightly curved, at least slightly longer than the cervical vertebrae in the French specimen (Peyer, 2006: figs. 2B, 6), and more than double the length of the cervical centra in the German specimen (Ostrom, 1978). The cervical ribs of *Sinosauropteryx* are

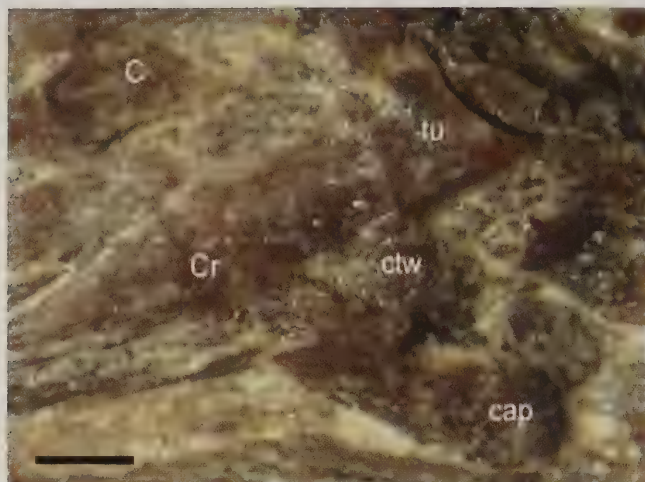


Fig. 75 - Close-up of the head of the 9th right cervical rib of *Scipionyx samniticus*. Scale bar = 0.5 mm. See Appendix 1 or cover flaps for abbreviations.

Fig. 75 - *Scipionyx samniticus*, particolare della testa della 9^a costola cervicale destra. Scala metrica = 0,5 mm. Vedi Appendice 1 o risvolti di copertina per le abbreviazioni.

reported to be very thin and not as long as those reported for *Compsognathus* (Currie & Chen, 2001), given that they are slightly longer than one cervical centrum (Ji *et al.*, 2007b); based on figures, however, they seem to be as long as two centra, or even more in some cases, just like in *Scipionyx* and *Compsognathus*. Slender cervical ribs, longer than the centra to which they attach, are reported also in *Huaxiagnathus* (Hwang *et al.*, 2004) and *Sinocaliopteryx*. In the latter, they are thread-like and extremely long, extending at least along three cervical centra (Ji *et al.*, 2007a: fig. 4a). The cervical ribs are rather short in Maniraptoriformes, whereas longer cervical ribs can be found among non-coelurosaurian theropods: in *Allosaurus*, they overlap at least one-half of the following centrum (Madsen, 1976), and in Coelophysoidea and Neoceratosauria, they surpass caudally at least three vertebrae (up to six in some species) beyond their origin (Tykoski & Rowe, 2004).

Dorsal ribs - The dorsal ribs of *Scipionyx* consist of 12, possibly 13, pairs of gently curved, craniocaudally compressed rods with tubercula shorter than capitula and median longitudinal grooves (costal grooves) emphasised by diagenetic compression (Fig. 76A). There are neither uncinat processes, nor ossified ventral elements, as the so called “abdominal ribs” figured by Dal Sasso & Signore (1998a: fig. 2) are actually lateral gastralia.

It is not easy to distinguish between the right and left ribs, especially at their distal ends, because diagenetic compression has left them often on the same plane, with the latter sometimes pushed onto the former. However, following the right ribs from the heads, and observing the differences in height of the shaft fragments, it is possible to outline each right rib and to estimate which fragments belong to the left side (Fig. 76B). It is then apparent that almost every left rib terminates cranially to the corresponding right rib. Some supernumerary elements have been also identified in the chest of *Scipionyx*: they represent allochthonous bones (see Gastric Contents).

Right dorsal ribs 1 to 5 lie almost undisturbed and almost parallel to each other along their whole length; Dr6 and Dr7 are the most fractured, whereas right Dr8 and Dr12 seem to be complete and still showing their curvature. Dr 9-11 are uplifted and slightly rotated clockwise, but still entire. As mentioned, a small fragment paralleling the shaft of the right Dr12 and preserved against the centra of D13 and S1 is tentatively interpreted as belonging to a Dr13 (Fig. 76A). Currie & Chen (2001) reported that two specimens of *Sinosauropteryx* have 13 dorsal vertebrae and 13 pairs of dorsal ribs; according to Peyer (2006), a rib was certainly present on the last dorsal vertebra of the French *Compsognathus*, although it was not preserved in the fossil specimen. In the Ornithomimosauria and in the Dromaeosauridae, a small but single-headed rib articulates with the last dorsal vertebra (Makovicky *et al.*, 2004; Norell & Makovicky, 2004). A boomerang-shaped bone was tentatively identified by Brochu (2003) as a vestigial rib of the last dorsal vertebra in the giant coelurosaur *Tyrannosaurus*, whereas in the neoceratosaur *Majungasaurus* (O'Connor, 2007), the Dr12 is already vestigial and D13 lacks one rib altogether.

Following the curvature of the shafts, the shape of the trunk of *Scipionyx* can be reconstructed: the cranial dorsal ribs have an almost straight median tract, indicating that the thoracic region was relatively flat laterally; the caudal dorsal ribs are more evenly curved all along their shafts and, thus, delimited a more rounded abdominal region (see Skeletal Reconstruction And...).

Similar to the last cervical rib, the first dorsal rib can be considered transitional. The proximal portion is markedly more expanded than the shaft, as in Cr10; the shaft is also considerably shorter than those of all the other dorsal ribs of the thoracic region and is comparable in length to that of Cr9. Moreover, this rib can be considered to be the first dorsal rib because its tuberculum and capitulum are almost the same size as those of the right Dr2 and, above all, because the tuberculum is almost aligned with the long axis of the shaft whereas the capitulum projects ventrally towards the parapophysis, contrary to what is observed in the right Cr10 but like the situation in the cranial dorsals. This morphology is slightly emphasised by the fact that the capitulum of Dr1 was separated from the head during diagenesis, because of the formation of a calcite vein.

The heads and necks of Dr2-Dr4 are particularly robust, with tubercula that are deeper than capitula, and broad and thin capitolotubercular webs (Fig. 77). The shafts lack the peculiar craniocaudally expanded proximal portion visible in the Ornithomimosauria (Makovicky *et al.*, 2004), and gradually taper all along their length. The shafts of the left and right Dr2 are still relatively slender and short with respect to the successive ones. The shafts of Dr3-Dr7 are long and more or less constant in length, Dr6 and Dr7 being the longest, as in *Compsognathus* (Peyer, 2006). According to Hwang *et al.* (2004), in *Huaxiagnathus* the longest pairs of ribs are attached to the 4th to 8th dorsal vertebrae. In *Scipionyx*, the shafts decrease gradually in length from Dr8 to Dr12. The tubercula shorten between Dr5 and Dr7; they are poorly visible because the shaft of the preceding rib covers exactly the head and the neck of the successive one. This shortening is so considerable that it becomes difficult to locate the tubercula from Dr8 on because the curvature of the shaft is almost uniform up to

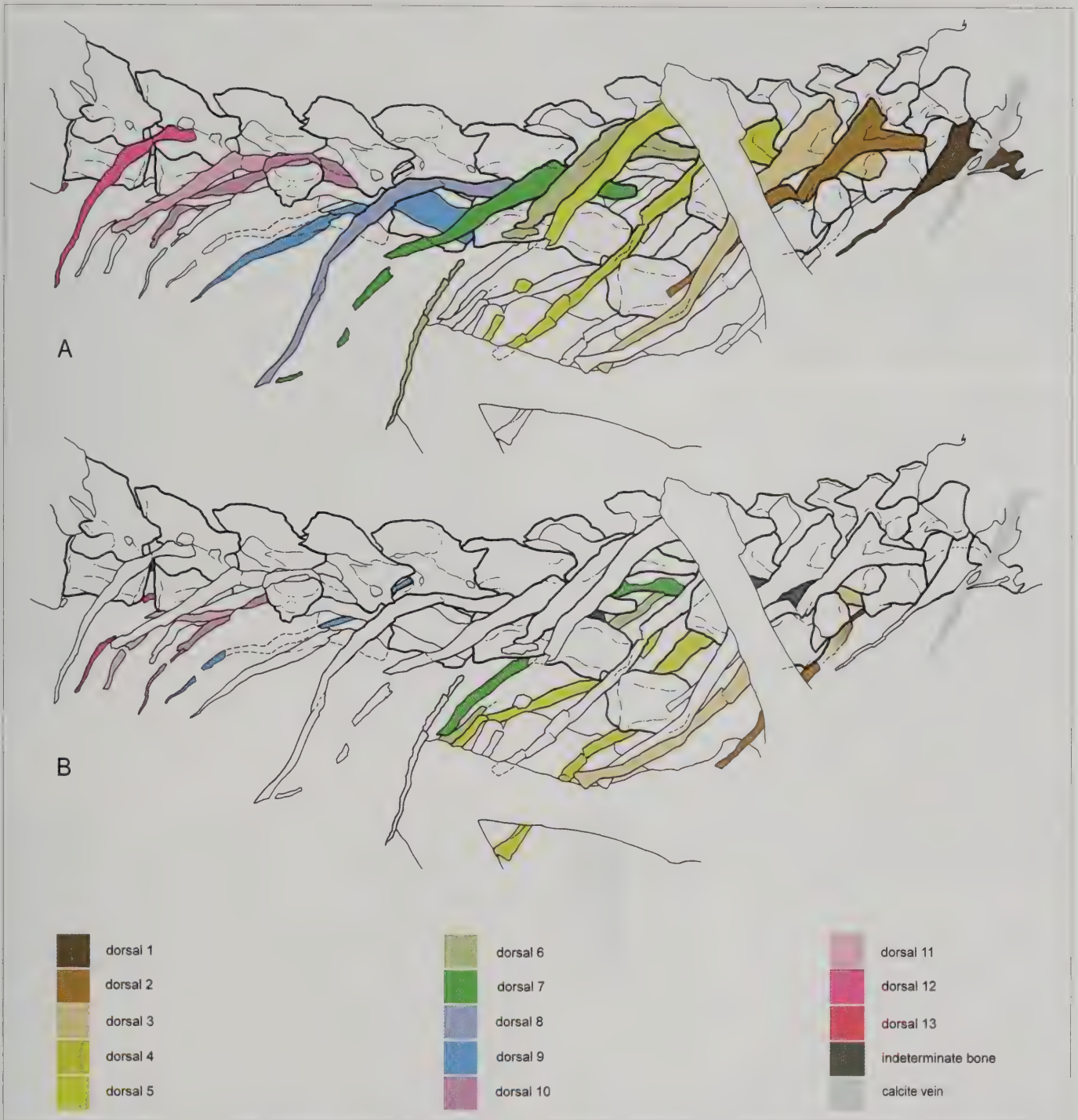


Fig. 76 - Line drawings of the dorsal ribs of *Scipionyx samniticus*, illustrated in Fig. 55. A) right ribs; B) left ribs and indeterminate elements.

Fig. 76 - *Scipionyx samniticus*. Disegno al tratto delle costole dorsali illustrate in Fig. 55. A) costole destre; B) costole sinistre ed elementi indeterminati.

the capitulum (Fig. 76A). In contrast, the capitula remain almost the same length in all dorsal ribs.

Dr3 and Dr4 are the most robust elements of the series. The distal end of the ones of the left side are well-exposed and intact. Rather than tapering to a point, these ribs terminate in an expanded, cup-like surface (Figs. 76B, 78) that articulated with the sternal complex, which is not preserved in this specimen of *Scipionyx* (see also Ontogenetic Assessment), through a system of sternal ribs and/or costal cartilages (see Pectoral Girdle; Godfrey & Currie, 2004; and references therein). Similar cup-like

depressions, interpreted as connections with sternal elements, are reported also by Currie & Chen (2001) in the first two pairs of dorsal ribs of *Sinosauropteryx*. One very similar expansion is likely preserved at the distal end of the left Dr3 in *Juravenator* (Dal Sasso & Maganuco, pers. obs., 2006 on unpublished photographs by Göhlich & Chiappe), and two expanded articular surfaces seem to be present at the distal end of the first pair of elongate dorsal ribs (?Dr3) in *Sinocalliopteryx* (Ji *et al.*, 2007a: fig. 1). In *Majungasaurus* (O'Connor, 2007), a similar morphology is present in Dr2 and Dr3, which terminate with blunt,

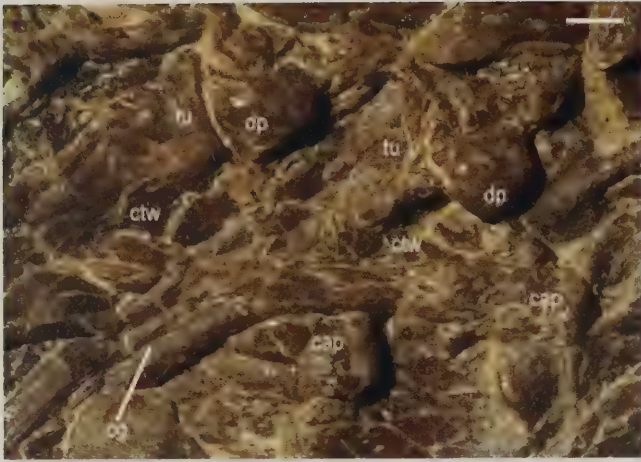


Fig. 77 - Close-up of the heads of the 2nd and 3rd right dorsal ribs of *Scipionyx samniticus*. Scale bar = 1 mm. See Appendix 1 or cover flaps for abbreviations.

Fig. 77 - Particolare delle teste della 2^a e 3^a costola dorsale destra di *Scipionyx samniticus*. Scala metrica = 1 mm. Vedi Appendice 1 o risvolti di copertina per le abbreviazioni.

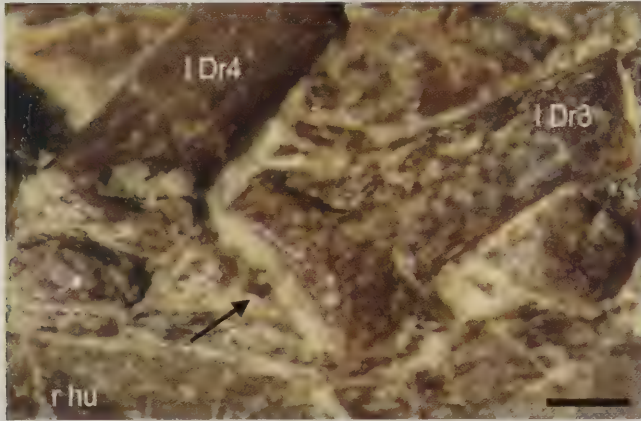


Fig. 78 - Close-up of the cup-like distal end (arrow) of the 3rd left dorsal rib of *Scipionyx samniticus*. Scale bar = 0.5 mm. See Appendix 1 or cover flaps for abbreviations.

Fig. 78 - *Scipionyx samniticus*. Particolare della terminazione distale a coppa (freccia) della 3^a costola dorsale sinistra. Scala metrica = 0,5 mm. Vedi Appendice 1 o risvolti di copertina per le abbreviazioni.

squared-off ends. Squared-off distal ends, possibly for articulation with the cartilaginous sternum or sternal ribs, are also reported by Kobayashi & Lü (2003) in Dr2-Dr8 of *Sinornithomimus*.

Sacral ribs - Two, or possibly 3, disarticulated bones in the sacral region of *Scipionyx* can be identified as sacral ribs (Figs. 63-64). The first element is enclosed between the caudal margin of the ilium and the first caudal vertebra. Although fossilised caudally to Sr5 (see below), we tentatively consider it to be the Sr4, based on the strong resemblance both in shape and in relative size to the one in *Allosaurus* (Madsen, 1976). If this hypothesis is right, it represents the right Sr4 exposed in lateral view and rotated 180°, as shown by the sutural scar for the ilium visible on its more robust end (Fig. 79). A second element, which is certainly a sacral rib, covers the cranial third of the neural spine of S5. Again, based on the strong resemblance with the shape of the 5th sacral rib of *Allosaurus*

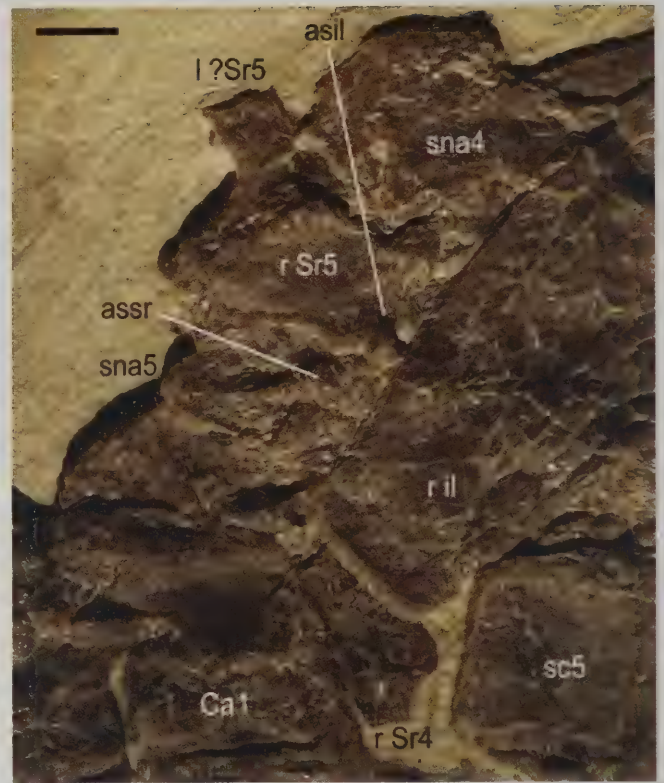


Fig. 79 - Close-up of the disarticulated sacral ribs of *Scipionyx samniticus*. Scale bar = 2 mm. See Appendix 1 or cover flaps for abbreviations.

Fig. 79 - Le costole sacrali disarticolate di *Scipionyx samniticus*. Scala metrica = 2 mm. Vedi Appendice 1 o risvolti di copertina per le abbreviazioni.

(Madsen, 1976: pl. 27F), we interpret the exposed surface as the lateral side of the right Sr5. Larger than Sr4, Sr5 has a rhomboidal shape and bears a caudal ridge that is expanded ventrally to form a robust, craniocaudally enlarged base for contact with the ilium (Fig. 79). This element was misinterpreted as the neural spine of S5 by Dal Sasso & Signore (1998a). The difference in size between Sr4 and Sr5 (the latter is larger than the former) can be explained by the fact that the iliac blades, when seen in dorsal/ventral views, probably diverged at both cranial and caudal ends, increasing the distance between the sacral vertebral centra and the blades themselves.

A third possible sacral rib lies just underneath Sr5, emerging a little dorsal to it: identified originally as a sacral rib by Dal Sasso & Signore (1998a), it seems to be the mirror image of Sr5 and may indeed represent the left Sr5. However, as it is mostly hidden and does not present unequivocal features, we prefer to regard it as an indeterminate element.

Gastralia

Exceptionally preserved *in situ*, there are at least 18 pairs of delicate, rod-like medial gastralial elements (Figs. 80-81). The medial ends lie still aligned to form the ventral margin of the thoracoabdominal region, in ideal continuation with the pubic foot. Their imbricate arrangement (*sensu* Claessens, 2004) is much better maintained in the rows immediately caudal to the left wrist, where a right medial element still lies almost in contact with two



Fig. 80 - Gastralium of *Scipionyx samniticus*. Scale bar = 5 mm.

Fig. 80 - Gastralium di *Scipionyx samniticus*. Scala metrica = 5 mm.

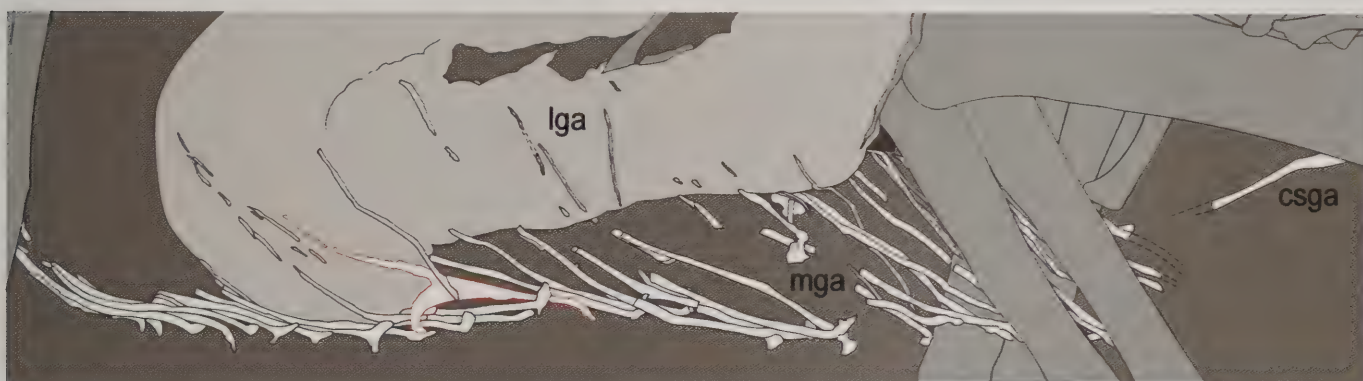


Fig. 81 - Line drawing of the bones illustrated in Fig. 80. The red outline indicates a possibly aberrant element. See Appendix 1 or cover flaps for abbreviations.

Fig. 81 - Disegno al tratto delle ossa illustrate in Fig. 80. Il contorno rosso indica un probabile elemento aberrante. Vedi Appendice 1 o risvolti di copertina per le abbreviazioni.

medial elements from the left side of the body, one at the medial end and the other farther down the shaft, in a zigzag fashion. The successive elements, although still in place, are not preserved in articulation. Generally, the left elements expose their dorsal surface, whereas the right ones are visible in ventral view. Both spacing and length of the medial gastralium decrease considerably towards the pubis. At least 5 slightly longer lateral gastralium are preserved in association with some of the mid medial elements, to which they articulate in parallel, overlapping the intestine of *Scipionyx* in a dorsocaudal direction.

The cranialmost element, thicker than the mid gastralium but much more slender than the dorsal ribs, is incomplete and partly hidden by the right humerus and, maybe (see below), by the right radius. The most expanded portion, emerging from a plane under the humerus, terminates at a distance equal to 1/3 the length of the whole preserved portion. Here, the shaft curves and forms an obtuse angle of about 160° before tapering abruptly, becoming as thin as the medial portion of the successive gastralium. This thin portion seems to continue in a caudal direction, preserved as an imprint in the matrix. Following this imprint, another thin bone fragment can be seen close to the right radius, immediately covered by the successive gastralium and, possibly, by the radius itself (Fig. 81). The whole element was, therefore, at least twice as long as the preserved portion. Based on shape and size, we interpret this element as one arm of the unpaired cranial chevron-shaped gastralium (*sensu* Claessens, 2004). The first regular row of gastralium is composed of only two straight medial elements in *Sinocal-*

liopteryx (Ji *et al.*, 2007a) and *Juravenator* (Göhlich *et al.*, 2006). In the latter, the two elements clearly form a cranial chevron-shaped gastralium, as they are fused in a single element that is twice as thick as the successive ones.

In *Scipionyx*, caudal to the chevron-shaped gastralium, 3 rows of medial gastralium run caudodorsally. As they are sandwiched between the forearms, they cannot be described in detail. The medial ends of the successive 6 rows are hooked and considerably expanded (Fig. 82). According to Claessens (2004), in small theropods the wing-like expansion of the medioventral articular facet is not as pronounced as in larger theropods, and may be absent. In *Scipionyx*, however, just caudal to the point of abrupt curvature, there is a point of maximum expansion which corresponds to the wing-like expansion of the medioventral facet (mvf). A thin continuation, directed medially and terminating in a pointed end, bears the mediodorsal facet (mdf). In these mid gastralium, the largest transverse diameter is at mid-length; from this point on, in lateral direction, the medial gastralium flatten and taper, forming a long sutural surface for the contact with the lateral gastralium (Fig. 83).

The medial portion of the lateral gastralium is as thin and flat as the complementary lateral portion of the medial ones. Beyond the sutural surface, which is oriented medio-caudally, their shafts become rounded in cross section and their diameters become considerably smaller, measuring almost half the diameter of the medial elements to which they articulate. On account of the small size of the individual, the lateral gastralium of *Scipionyx* have a hair-like appearance (Figs. 80-81). The lateral gastralium are very

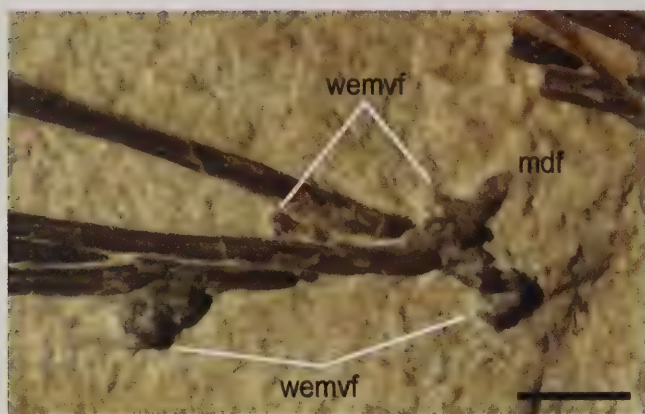


Fig. 82 - Cranial medial gastralia of *Scipionyx samniticus*. Close-up of the medial ends. Scale bar = 1 mm. See Appendix 1 or cover flaps for abbreviations.

Fig. 82 - Gastralia craniali mediiali di *Scipionyx samniticus*. Particolare delle estremità mediiali. Scala metrica = 1 mm. Vedi Appendice 1 o risvolti di copertina per le abbreviazioni.

fragmented and lean against the intestine for about 2/3 of their length. The distalmost fragments reach the dorsal margin of the descending loop of the duodenum. Measured at this level, the lateral gastralia are slightly longer than (about 8/7) the medial ones.

The caudal medial gastralia consist of some 8 rows of shorter rods, not preserved in articulation. Cranial and ventral to the ascending loop of the duodenum, they have an unusual hammer-like conformation: 6-8 bifid medial ends can be seen (Fig. 84), referable to at least four rows of gastralia. These bifid ends possibly derive from a greater separation between the mvf and the mdf. In particular, the end directed towards the intestine would correspond to the mvf of the preceding, enlarged and more elongated gastralium;

the shorter and globular opposite end would correspond to the mdf. The shaft originates at about mid-length of the portion which bears the facets. This conformation possibly increased the length of the sliding surface of the mvf in which the mdf of the successive element was accommodated. As hypothesised by Claessens (2004), inward sliding of the mediadorsal joints on gastralial retraction, combined with outward sliding of the joints upon gastralial protraction, would have accommodated some of the lengthening and shortening of the whole gastralial system during protraction and retraction. According to the model proposed herein (Fig. 85), the range of movement (protraction/retraction) of the gastralia on a plane, described by Claessens (2004) in other theropods, would result similar in *Scipionyx*.

The thin fragments of at least 3 lateral gastralia, in directional continuity with the same number of medial elements, are preserved on the ascending loop of the duodenum and appear as long as the most complete preceding lateral gastralia. In this area too, the lateral gastralia are shorter than their corresponding medial gastralia.

The caudalmost medial gastralia, which are composed of 4 rows, are even smaller and overlap each other. They do not seem to be bifid; however, the better exposed elements appear to maintain the hooked curvature at the medial end which characterises the whole series. In any case, unlike *Shenzhousaurus* (Ji *et al.*, 2003), the last medial gastralia of *Scipionyx* do not form any large caudal chevron-shaped gastralium (*sensu* Claessens, 2004). At this level, the lateral gastralia seem to be absent, or alternatively, they might be so short and perfectly aligned to the medial ones as to seem absent. Makovicky *et al.* (2004) reported that in ornithomimosaurs the last gastralia are composed of the medial elements only, which wrap around the cranial expansion of the pubic foot (absent in *Scipionyx*). In *Sphenodon* and in extant crocodylians, the gastralia are attached to the pubis and



Fig. 83 - Cranial gastralia of *Scipionyx samniticus*. Close-up of the sutural surfaces between medial and lateral elements. Scale bar = 1 mm. See Appendix 1 or cover flaps for abbreviations.

Fig. 83 - Gastralia craniali di *Scipionyx samniticus*. Particolare delle superfici suturali tra elementi mediiali e laterali. Scala metrica = 1 mm. Vedi Appendice 1 o risvolti di copertina per le abbreviazioni.

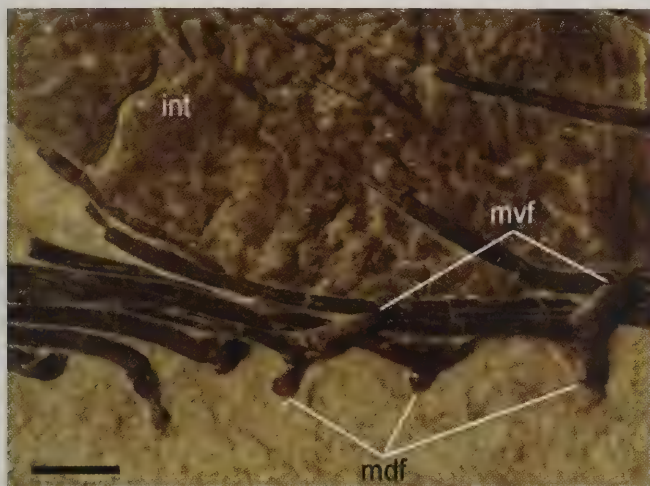


Fig. 84 - Caudal medial gastralia of *Scipionyx samniticus*. Close-up of the medial ends and part of the shafts. Scale bar = 1 mm. See Appendix 1 or cover flaps for abbreviations.

Fig. 84 - Gastralia caudali mediali di *Scipionyx samniticus*. Particolare delle estremità mediali e di parte delle aste. Scala metrica = 1 mm. Vedi Appendice 1 o risvolti di copertina per le abbreviazioni.

sternum through midventral ligaments (Claessens, 2004). In theropods, the attachment of the gastralia to the pubic bones and sternum was probably similar, and they were likely embedded in the superficial layers of the *M. rectus abdominis* in a similar way (Claessens, 2004). Dal Sasso

& Signore (1998a) reported that in *Scipionyx* the gastralian basket seems to constitute effective support for the intestine, whereas the pubic bones are alien to this function. If such supporting function was real, it would have been indirect. In fact, the gastralia are dermal ossifications that cannot attach directly to the intestine. The latter is loose but suspended by the mesentery in the peritoneal cavity, which in turn is surrounded by the body wall consisting of different layers of connective tissue and muscles in which the gastralia are embedded; the whole is surrounded by the dermis. Connective tissue, muscles and dermis constitute the body wall which supports the intestines in the abdominal cavity. Therefore, the intimate connection between the gastralia and the intestine, as we see it in the *Scipionyx* fossil, took place *post mortem*, after decomposition of some tissue.

A triangular bony lamina delimited by two gastralian shafts is related to the duodenum in a similar manner (Fig. 86). The dorsal shaft is superimposed onto the duodenum, whereas the more robust ventral one makes a U-turn just opposite to the duodenum itself and then continues in a cranial direction to contact the bifid medial end of a successive gastralian. The function – if any – of such a structure is unclear, but the fact that the two shafts are fused to the lamina and seem to be the result of the splitting of the shaft of a single medial gastralian suggests that it represents an aberrant structure. To our knowledge, no similar structure has been described to date in the literature, at least in theropod dinosaurs, although different kinds of aberrant fusion and alteration of the rows have been docu-

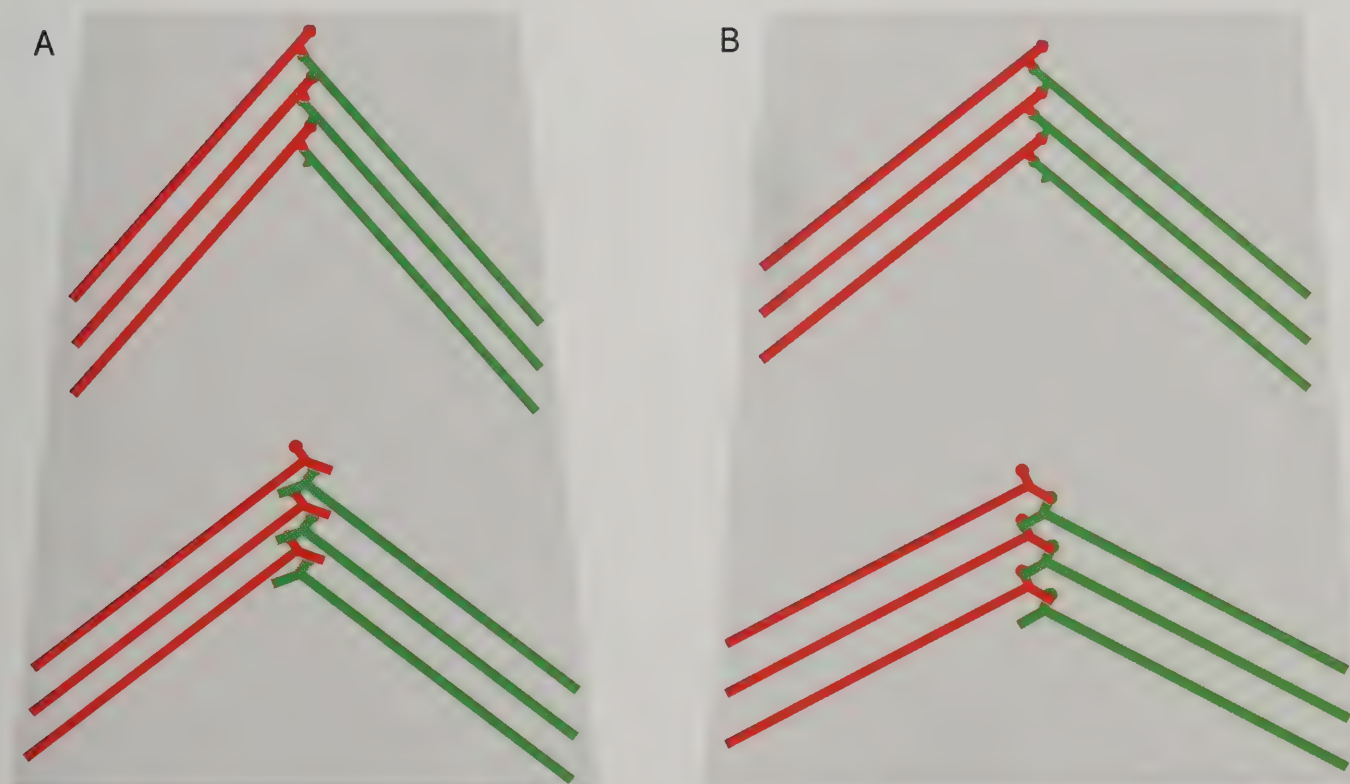


Fig. 85 - Schematic modelling of the retraction and protraction movements of the mid-cranial gastralia (top) and mid-caudal gastralia (bottom) of *Scipionyx samniticus* as seen in dorsal view (left elements in red, right elements in green), showing the degree of widening of the lateral abdominal wall (grey area) upon a rotation (A to B) of about 10 degrees. The inward and outward sliding of the joints during protraction and retraction is appreciable in the mid-caudal gastralia.

Fig. 85 - *Scipionyx samniticus*. Modello di retrazione e protrazione dei gastralia mediali (in alto, gastralia cranio-mediali; in basso, gastralia medio-caudali) in norma dorsale, che mostra il grado di espansione della parete addominale laterale (area grigia) in seguito ad una rotazione di 10 gradi circa (da A a B). In rosso gli elementi del lato sinistro, in verde quelli del lato destro. Lo scorrimento delle giunture verso l'interno e verso l'esterno, durante la protrazione e la retrazione, è più apprezzabile nei gastralia medio-caudali.

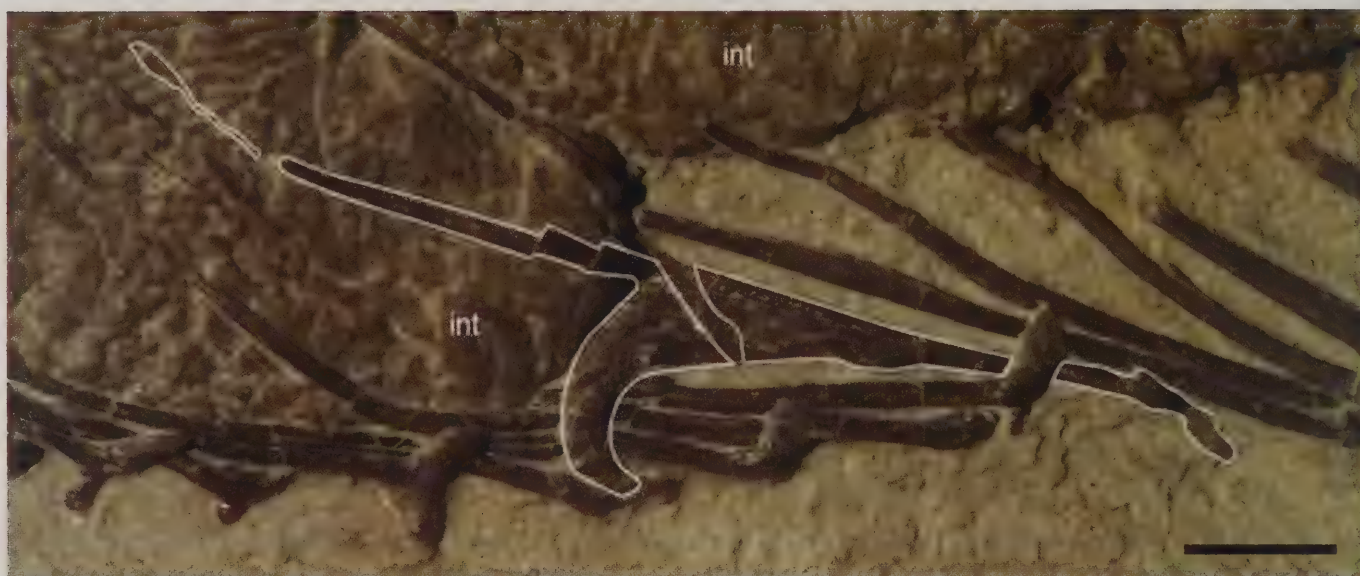


Fig. 86 - Close-up of a possibly aberrant gastralial structure of *Scipionyx samniticus* (white outline). Scale bar = 1 mm. See Appendix 1 or cover flaps for abbreviations.

Fig. 86 - Una probabile struttura gastrale aberrante di *Scipionyx samniticus* (contorno bianco). Scala metrica = 1 mm. Vedi Appendice 1 o risvolti di copertina per le abbreviazioni.

mented (e.g., the bifid element observed in a velociraptorine deinonychosaur by Norell & Makovicky [1997]).

According to Claessens (2004), the variation in the number of rows between different theropod groups seems to be related to size, with smaller theropods generally having the fewest rows of gastralial, and larger theropods appearing to have the most. *Scipionyx*, with its 18 pairs of gastralial, seems to contradict this statement and possess one of the highest counts among the small theropods. A similar, but slightly lower, count is found in *Compsognathus*, which has about 30-34 elements arranged in 15-17 rows (Peyer, 2006: fig. 2), and in *Sinosauropteryx* (Ji *et al.*, 2007b), in which about 15 rows of gastralial are present. Only 12 rows are present in the complete basket of *Sinocalliopteryx* (Ji *et al.*, 2007a), the largest of the compsognathids. At least 14 rows are present in the ornithomimosaur *Sinornithomimus* (Kobayashi & Lü, 2003). The highest count in small to medium sized theropods is found in another ornithomimosaur, *Ornithomimus*: a specimen described by Makovicky (1997) possesses 19 rows of gastralial. The same number is reported in a subadult specimen of *Albertosaurus* and is possibly exceeded by some large theropods (Claessens, 2004), even if in a large specimen of *Tyrannosaurus* only 14 rows are described with certainty (Brochu, 2003). 12-15 rows are present in deinonychosaur (Russell & Dong,

1993; Norell & Makovicky, 1997), whereas 12-13 are preserved in *Archaeopteryx* (Elzanowski, 2002).

Claessens (2004) observed that in large theropods (e.g., allosaurids or tyrannosaurids), the lateral gastralial are much smaller than the medial gastralial, both in length and diameter, whereas in prosauropods and small theropods (e.g., coelophysids, troodontids, oviraptorids and dromaeosaurids), the lateral gastralial are 1.5-2.5 times as long as their medial counterparts. To this list of small theropods having lateral elements that are considerably longer than the medial ones, further taxa can be added, such as troodontids (Russell & Dong, 1993; Currie & Dong, 2001; Ji *et al.*, 2005) and compsognathids (Holtz *et al.*, 2004). In some compsognathids, such as *Scipionyx* and *Compsognathus* (Peyer, 2006: fig. 3a), the lateral gastralial are indeed longer than the medial ones. In contrast, in *Huaxiagnathus* (Hwang *et al.*, 2004), *Sinosauropteryx* (Currie & Chen, 2001; Ji *et al.*, 2007b) and *Sinocalliopteryx* (Ji *et al.*, 2007a), the medial gastralial segments are distinctly longer than the lateral segments. This occurs also in most ornithomimosaur (Makovicky *et al.*, 2004; Kobayashi & Barsbold, 2005), even though it must be noted that medial and lateral elements are approximately equal in length in the most complete row of the basal ornithomimosaur *Shenzhousaurus* (Ji *et al.*, 2003).

APPENDICULAR SKELETON

Pectoral girdle

The pectoral girdle of *Scipionyx* is preserved in relative anatomical connection, with its elements forming a flattened, but still continuous, arc from the left to the right side (Figs. 87-88). The preservation of the furcula is remarkable. The furcula is an unpaired median bone derived from the midline fusion of the paired clavicles (e.g., Nesbitt *et al.*, 2009). Unique to theropods, it is crucial for understanding the link between dinosaurs and birds.

Scipionyx is not only one of the few dinosaur skeletons that preserve a furcula, but also one of the even rarer specimens in which the bone is positioned almost like it was *in vivo*. Moreover, the simultaneous preservation of the gastralial in a definitely more caudal position and the presence of a clear hypocleideum in the furcula permit to state that the two elements, often misinterpreted in past literature, actually do not have any significant resemblance.

Scipionyx lacks sternal plates. The formerly supposed sternum ("st" in Dal Sasso & Signore, 1998a:

fig. 2) is actually the proximal portion of the left humerus with its deltopectoral crest. Sternal plates are not expected to be calcified in a young animal (Gishlick, pers. comm., 2000). Moreover, the only ossified (and thus fossilised) theropod sternum so far known outside the Maniraptoriformes (e.g., Pérez-Moreno *et al.*, 1994; Godfrey & Currie, 2004) is doubtful: reported by Lambe (1917) to be present in *Albertosaurus libratus*, this bone was later re-identified by Claessens (2004) as the apex of two additional fused cranial chevron-shaped gastralia rows. Therefore, a cartilaginous sternum would be expected also in an adult individual of *Scipionyx* (see Ontogenetic Assessment). As mentioned, indirect evidence of the sternum is given by the presence of expanded ends in Dr3 and Dr4 (Figs. 76B, 78), which would have contacted the sternum directly or via cartilaginous sternal ribs, as is the case in other non-maniraptoran theropods.

The scapula of *Scipionyx*, with its dorsalmost margin incomplete, is only slightly shorter than the humerus. With a preserved scapula/humerus ratio of 0.90, it compares well with both specimens of *Compsognathus* (Ostrom, 1978; Peyer, 2006) and with *Huaxiagnathus* (Hwang *et al.*, 2004), in which the maximal length of the scapula approaches that of the humerus. The humeri are comparatively very short in *Sinosauropteryx* (Currie & Chen, 2001) and *Juravenator* (Göhlich & Chiappe, 2006), in which the scapula/humerus ratio is about 1.50 to 1.60. *Sinocalliopteryx* (Ji *et al.*, 2007a) presents an intermediate condition (about 1.30). Despite these differences, all the compsognathids fall within the usual range of scapula/humerus ratio seen in most coelurosaurs, in which the humerus is often as long as, or longer, than the scapula (Holtz *et al.*, 2004). The most significant exceptions, remote from the condition seen in *Scipionyx*, are in fact some advanced coelurosaurs, such as the dromaeosaurids (0.63-Xu *et al.*, 1999; 0.83-Burnham *et al.*, 2000; 0.68-Hwang *et al.*, 2002).

Scapula - The scapula of *Scipionyx* is typical of a theropod in being strap-like: the slender scapular blade, 6-7 times longer than it is deep, has parallel cranial and caudal edges for most of the length up to the beginning of the acromion. The blade of the right scapula opens up into a forked dorsal end on account of the detachment of a fragment from the cranial margin. Of the left scapula, only the acromion emerges, between the coracoids and the furcula. Therefore, the following description refers to the right scapula.

Dorsally, the scapular blade terminates in a pointed, irregular margin which originated after *post mortem* damage; it cannot be known, therefore, if originally there was any terminal expansion or what the precise length of the blade was. However, based on the preserved margins, we can exclude that the possible dorsal expansion was as wide as that in *Nqwebasaurus* (de Klerk *et al.*, 2000) and *Juravenator*, in which the expansion is more than twice the width of the neck of the blade. The dorsal third of the blade of *Scipionyx* is slightly recurved. Ventrally, the blade widens gradually towards the glenoid cavity, rather than having a constriction (neck). This seems to be directed caudally, as in almost all other theropods (compsognathids included),

and differently to deinonychosaurs and birds, in which it faces more laterally than caudally (e.g., Rauhut, 2003). The glenoid cavity is not well-exposed, on account of a partial superimposition of the proximalmost portion of the humerus. However, the scapula of *Scipionyx* had to form the cranial and dorsocranial margins of the cavity, giving a contribution greater than that of the coracoid. On the cranial edge, towards the coracoid contact, there is a pronounced acromion, developed on the same plane as the blade (i.e., not laterally everted, as in advanced Maniraptora). The right acromion is very pronounced, but less abruptly enlarged than appears in the pictures at a first glance (Fig. 87). In fact, a thin patch of soft tissue (muscle and ?connective tissue) has overlapped the cranial lateral margin of the scapular blade, but not enough to completely hide the outline of the bone underneath (see hatched line in Fig. 88). Under a similar circumstance (another patch of soft tissue: Fig. 89), the acromion of the left scapula appears even more squared in shape and more pronounced. The reconstructed outline of the acromion of *Scipionyx* indicates that it is prominent but smoothly merged into the cranial scapular blade, as in *Compsognathus* (Peyer, 2006) and in other compsognathids.

Like in the cranial portion of the coracoid, the surface of the acromion of *Scipionyx* has a radially rugose texture and reinforced margins. Unlike in *Compsognathus* (Peyer, 2006), the strongly convex cranial outline of the two elements, still visible despite the superimposition of the soft tissues, indicates the presence of a scapulocoracoid notch (Fig. 89). The scapulocoracoid suture, the caudal two-thirds of which are still clear, is sigmoidal in shape and crosses the glenoid cavity caudally. Matching the rib cage's cross-section (see Dorsal Ribs), the lateral surface of the scapula of *Scipionyx* seems flat rather than laterally everted towards the coracoid contact as in *Velociraptor* and other deinonychosaurs (Norell & Makovicky, 2004).

Although generally similar, the scapulae of the compsognathids differ from each other in some aspects. The scapular blade of *Compsognathus* (Peyer, 2006) is not as slender and straight as that of *Scipionyx*, and is slightly more recurved. *Juravenator* differs from *Scipionyx* in having a marked, diagnostic narrowest portion, located at the neck of the scapula, close to the acromion (Göhlich & Chiappe, 2006). In *Sinosauropteryx* (Currie & Chen, 2001), the scapular blade appears more elongate than in *Scipionyx* (length almost equal to ten times the width), with the acromion less pronounced. In *Sinocalliopteryx* (Ji *et al.*, 2007a) and *Huaxiagnathus* (Hwang *et al.*, 2004) the elongation is similar to that seen in *Sinosauropteryx* (i.e., greater than in *Scipionyx*), but the acromion is more prominent than that of *Scipionyx*, and triangular. The basal tyrannosauroids *Tanycolagreus* (Carpenter *et al.*, 2005a), *Dilong* (Xu *et al.*, 2004) and *Guanlong* (Xu *et al.*, 2006) have an even more prominent triangular acromion. The former taxon also presents a scapulocoracoid notch, an even more elongated blade and a narrow scapular neck. The basal ornithomimosaur *Sinornithomimus* (Kobayashi & Lü, 2003) has a more slender scapula (length almost eleven times the width), bearing an acromion similar in shape but less developed than that of *Scipionyx*.



Fig. 87 - Pectoral girdle and forelimbs of *Scipionyx samniticus*. Scale bar = 5 mm.

Fig. 87 - Cinto pettorale e arti anteriori di *Scipionyx samniticus*. Scala metrica = 5 mm.

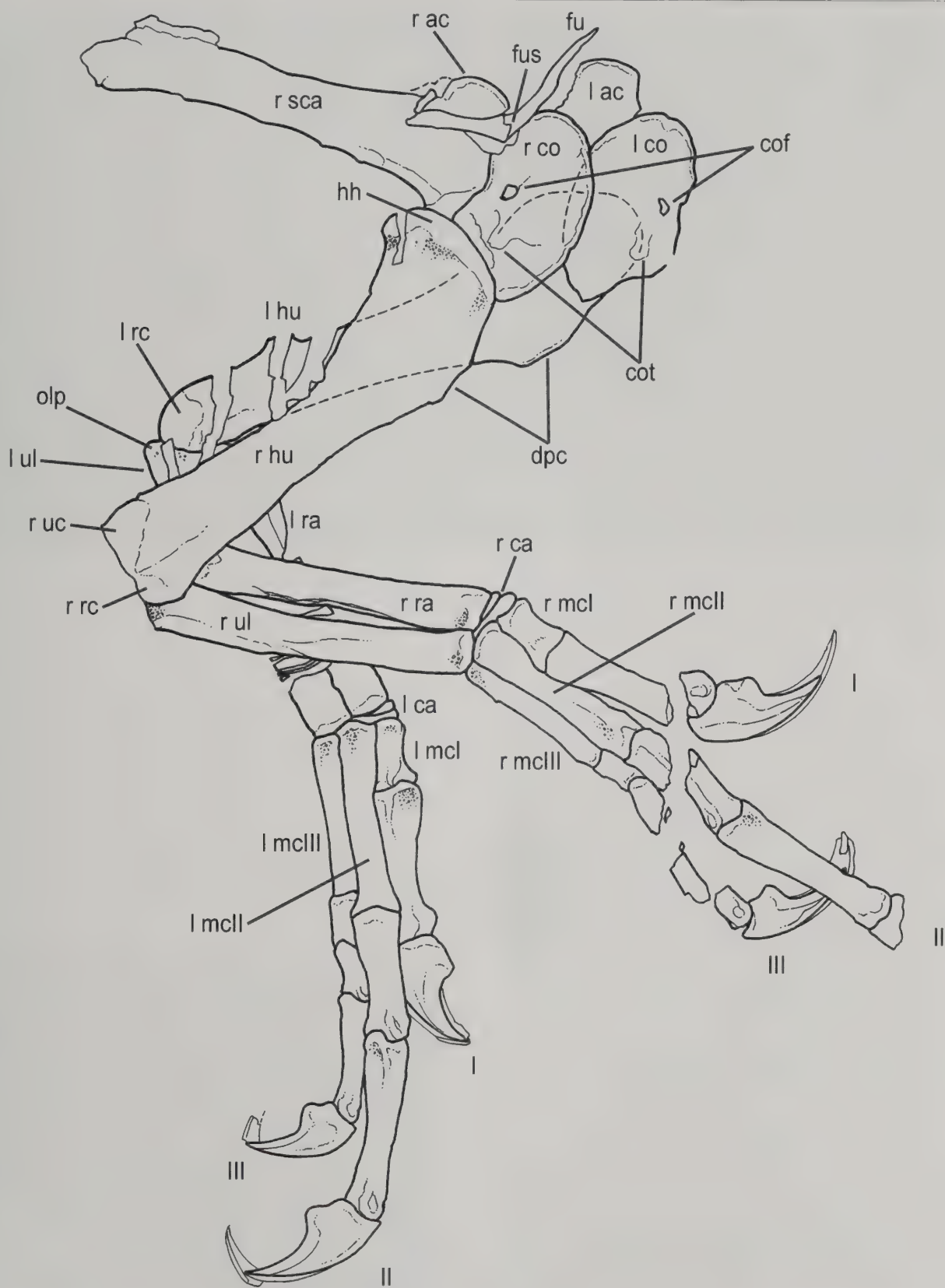


Fig. 88 - Line drawing of the bones illustrated in Fig. 87. See Appendix 1 or cover flaps for abbreviations.

Fig. 88 - Disegno al tratto delle ossa illustrate in Fig. 87. Vedi Appendice 1 o risvolti di copertina per le abbreviazioni.



Fig. 89 - Close-up of the furcula of *Scipionyx samniticus*. Scale bar = 1 mm. See Appendix 1 or cover flaps for abbreviations.

Fig. 89 - Particolare della furcula di *Scipionyx samniticus*. Scala metrica = 1 mm. Vedi Appendice 1 o risvolti di copertina per le abbreviazioni.

Coracoid - Both coracoids are well-exposed in ventral view, one opposite the other as in a mirror, with the right one slightly overlapping the left one. Based on the length of the furcula, which articulated with the acromion of each scapula, the two coracoids had to be almost adjacent and very close to the medial sagittal plane in the undisturbed, articulated skeleton. The right coracoid is better preserved than the left one, which is crossed by two parallel branches of the large calcite vein that runs from the right ceratobranchial I to the right manus, passing also through the caudal cervical region. The coracoid is fan-shaped, semicircular, higher than long, and narrower at the caudal edge, as in *Compsognathus* (Ostrom, 1978; Peyer, 2006), *Huaxiagnathus* (Hwang *et al.*, 2004) and *Sinosauropteryx* (Currie & Chen, 2001). A raised border marks the margins of both coracoids.

Left and right coracoid foramina are clearly visible. The coracoid foramen, suboval in outline, opens at mid-length of the craniocaudal axis and at about 1/3 width from the scapulocoracoid suture. Several scars that represent muscle attachment sites are visible on the surface of both coracoids. The protuberances often interpreted as biceps tubercles in other theropods (but see Carpenter *et al.*, 2005, for a different interpretation) emerge caudally to the coracoid foramen in both coracoids, in the form of digitiform reliefs, with the caudal margin more prominent and rounded (Fig. 90). The caudoventral process extends further caudally to the level of the glenoid cavity, as is the case in tetanurans (Rauhut, 2003). Both extension and outline of this caudoventral process, as well as of the glenoid cavity, are more clearly visible in the left coracoid, the caudal portion of the right one being partly covered by the proximalmost portion of the right humerus. The caudoventral process appears triangular as in *Compsognathus* (Peyer, 2006), but less pointed and developed.

The caudoventral process of the latter is not as pointed and developed as that of *Sinosauropteryx*, which, in turn, is comparatively less pointed and developed than that of the basal tyrannosauroids (Xu *et al.*, 2004, 2006).

The coracoid contributes to the glenoid with its cranioventral margin; this is slightly less than that of the scapula, which forms the cranial and craniodorsal margins (see above). The glenoid portion of the coracoid is non-everted, without any neck marking a definite separation from the perimeter of the bone. Compared to all other elements



Fig. 90 - Close-up of the right coracoid of *Scipionyx samniticus*. Scale bar = 1 mm. See Appendix 1 or cover flaps for abbreviations.

Fig. 90 - Particolare del coracoido destro di *Scipionyx samniticus*. Scala metrica = 1 mm. Vedi Appendice 1 o risvolti di copertina per le abbreviazioni.

of the forelimb, the coracoid of *Scipionyx* is smaller than that of *Compsognathus* and *Sinosauroptryx*; for example, in *Scipionyx* it measures less than half the length of the humerus, whereas in *Compsognathus* it is more than half the length of the humerus.

Furcula - A delicate, boomerang-shaped bone can be seen leaning against the right scapula and coracoid, at the level of the scapulocoracoid suture. By its size and shape, it can be identified without doubt as the furcula seen in cranial view (Fig. 89). The right ramus is superimposed onto the lateral portion of the scapula, and lacks most of its distal extremity, of which only a thin fragment can be seen bent back in a cranial direction. The left ramus is complete and directed towards the left acromion; it is crossed cranially by the already mentioned calcite vein.

In addition to the avian theropods, furculae have been documented in nearly all but the most basal theropods (such as *Eoraptor* and *Herrerasaurus*), including coelophysoids (Tykoski *et al.*, 2002; Carrano *et al.*, 2005; Rinehart *et al.*, 2007), spinosaurids (Lipkin *et al.*, 2007), allosauroids (Chure & Madsen, 1996; Coria & Currie, 2006; Sereno *et al.*, 2008), compsognathids (Hwang *et al.*, 2004; Peyer, 2006; Ji *et al.*, 2007a), tyrannosaurids (Makovicky & Currie, 1998; Larson & Rigby, 2005; Lipkin *et al.*, 2007), therizinosauroids (Xu *et al.*, 1999a; Zhang *et al.*, 2001; Kirkland *et al.*, 2005), oviraptorosaurs (Barsbold, 1983; Barsbold *et al.*, 1990; Ji *et al.*, 1998; Clark *et al.*, 1999, 2001; Lü, 2002; Osmólska *et al.*, 2004), troodontids (Xu & Norell, 2004) and dromaeosaurids (Norell *et al.*, 1997; Xu *et al.*, 1999b; Burnham *et al.*, 2000; Hwang *et al.*, 2002; Makovicky *et al.*, 2005). The paired elements labelled "cl" by Göhlich *et al.* (2006: fig. 1) in the compsognathid *Juravenator*, in our opinion represent a broken furcula. However, taking as reference the data collected by Claessens (2004: Appendix 1), this specimen of *Scipionyx* is one of the few theropod fossils with a simultaneous preservation of gastralia and furcula: this has permitted clear distinction between these often questioned elements. If our identification of the cranial-most gastralial element as a chevron-shaped gastralium is correct, there are only three other specimens having a furcula preserved together with that element: *Allosaurus* DINO 11541, *Albertosaurus* RTMP 91.36.500 and *Daspletosaurus* NMC 11315. Following Larson & Rigby (2005), an unambiguous furcula is presumably preserved among the gastralia of *Tyrannosaurus* FMNH PR2081, but see Brochu (2003) and Nesbitt *et al.* (2009) for a different interpretation.

In *Scipionyx*, the furcula can be easily distinguished from gastralia by the following morphological characteristics: the furcula is larger, having a diameter that is at least twice that of the largest gastralium (i.e., the chevron-shaped gastralium); the rami of the furcula taper more abruptly than those of the chevron-shaped gastralium, whereas the other gastralia have either an almost constant diameter or taper very gradually; the rami of the furcula exhibit a sigmoidal curvature, whereas gastralia are straighter; the furcula has a distinct pointed projection, called the hypocleideum, which is absent in gastralia; the preserved (left) extremity of the furcula of *Scipionyx* bears a flat epicleideal facet (the epicleideum) for articulation with the scapular acromion, which in three-dimensionally

preserved furculae is spatulate and sulcated by scars; gastralia do not have epicleideal facets, even if the lateral and the medial gastralia contact via a flat surface.

As just mentioned above, in *Scipionyx* the furcula is larger and stouter than the cranial chevron-shaped gastralium. According to Claessens (2004), in larger theropods such as allosaurids and tyrannosaurids, the furcula is only about 1/3 the size of a cranial chevron-shaped gastralium.

Besides the characters described above, the furcula of *Scipionyx* has also the following features: based on Nesbitt *et al.* (2009), the general shape of the furcula is more U-shaped than V-shaped, because, towards the symphysis, the dorsal margins of its two rami are slightly concave, rather than straight (Fig. 89); the epicleideal facets are slightly flexed laterally, seem to be not much expanded and taper to a point; the two rami, at least in proximity to the symphysis, seem compressed craniocaudally in cross-section, a character usually found in the Maniraptoriformes; the hypocleideum of *Scipionyx* projects ventrally and seems to belong entirely to the right ramus because of the presence alongside it of a suture with the counter-lateral element. The apex of the hypocleideum is covered by a thin edge of connective tissue. *Contra* Nesbitt *et al.* (2009), who estimated an interclavicular angle (i.e., the angle between the rami of the furcula) of 140° for *Scipionyx*, we obtain an angle not greater than 125° with the same method of measurement. In *Huaxiagnathus* (Hwang *et al.*, 2004), the compsognathid fossil in which the furcula is most clearly preserved, the bone resembles that of *Scipionyx* in being U-shaped and in having an interclavicular angle of 130°, but differs in that it lacks a distinct hypocleideum. In coelophysoids, the furcula is variably U- or V-shaped and has an angle of 115-140°; *Suchomimus* (Lipkin *et al.*, 2007) has a 111° V-shaped furcula; the furcula is V-shaped also in allosauroids and ranges from 120° to 135° (Nesbitt *et al.*, 2009); in tyrannosaurids, the furcula is U-shaped with laterally flexed epicleideal facets and a clavicular angle ranging from 71 to 113° (Nesbitt *et al.*, 2009); in therizinosaurids, the U-shaped furcula ranges from 135° to 160° (Nesbitt *et al.*, 2009); in the Maniraptora, the furcula is generally U-shaped and bears an angle of approximately 80-90°, but can reach 60° in most advanced non-Ornithurae forms (Nesbitt *et al.*, 2009) and 103° in *Velociraptor*, which also presents a short hypocleideum (Norell & Makovicky, 2004). An incipient hypocleideum is preserved in troodontids (Xu & Norell, 2004).

Forelimb

Both forelimbs are articulated and almost complete in *Scipionyx*. The elements of the right arm are visible in their entirety, with the proximal and median segments exposed, respectively, in laterocaudal and in lateral view; the manus is visible in dorsomedial view. Of the left side, only the manus is fully exposed, in palmar view (Figs. 87-88). *Scipionyx* displays also the very rare and superb fossilisation of the horny talons present on the tip of each digit. Only the distal portion of the second right ungual phalanx is lost, as a result of a crack in the supporting slab of Plattenkalk that presumably formed during collection. The phalangeal count is 2-3-4. The unguals have a relatively low curvature and bear sharp horny talons.

As stated by Dal Sasso & Signore (1998a), *Scipionyx* is characterised by elongate raptorial forelimbs, measuring about 48% of the presacral length (skull included). They are comparatively longer than in most other non-avian coelurosaurs except dromaeosaurids, which have by far the longest forelimbs among non-avian theropods (humerus and manus longer than in *Scipionyx*). The relative length of the forelimb is mostly due to elongation of the manus. In *Scipionyx*, the manus measures 42% of the whole forelimb length; therefore, it approaches the range (43-50%) found in other compsognathids (Currie & Chen, 2001; Hwang *et al.*, 2004; Peyer, 2006; Ji *et al.*, 2007a; 2007b) and matches the ratio of several deinonychosaurs and basal birds in which the manus constitutes about 40-45% of the forelimb length, irrespective of age (e.g., Xu *et al.*, 1999; Burnham *et al.*, 2000; Elzanowski, 2002; Russell & Dong, 1993; Norell & Makovicky, 2004; Xu & Norell, 2004). The manus is 34% of the whole forelimb length in the basal ornithomimosaur *Sinornithomimus* (Kobayashi & Lü, 2003), 30% in the basal oviraptorosaur *Caudipteryx* (Zhou *et al.*, 2000), whereas, just like in *Scipionyx*, it is 42% in the basal Alvarezsaur *Nqwebasaurus* (de Klerk *et al.*, 2000).

The epipodials of *Scipionyx* are about half the length of the long manus. In other words, the manus is about 80% of the combined length of humerus and forearm. According to Padian (2004), a value between 66% and 75% is typical of Coelurosauria, but there are many examples of higher ratios, especially among compsognathid coelurosaurs. In *Sinosauropteryx* (Currie & Chen, 2001; Ji *et al.*, 2007b), the manus is 84-91% of the combined length of humerus and radius. In *Sinocalliopteryx* (Ji *et al.*, 2007a) and *Huaxiagnathus* (Hwang *et al.*, 2004), the manus is as long as the humerus plus the radius, whereas in German and French *Compsognathus* the ratios are 74% and 85%, respectively (Peyer, 2006). Similar values are measured also in basal tyrannosauroids (e.g., 91%-Carpenter *et al.*, 2005a; 80% based on the ulna, which includes the olecranon-Xu *et al.*, 2006), in *Nqwebasaurus* (73%-de Klerk *et al.*, 2000) and in basal troodontids (e.g., 83%-Russell & Dong, 1993; Xu & Norell, 2004). Underestimated but still comparable values, based on the ulna (including the olecranon process) are available for dromaeosaurids (e.g., 62%-Xu *et al.*, 1999; 66%-Burnham *et al.*, 2000) and basal birds (64%-Elzanowski, 2002). A shorter manus is, instead, present in the basal ornithomimosaur *Sinornithomimus* (51%-Kobayashi & Lü, 2003) and the basal oviraptorosaur *Caudipteryx* (43%-Zhou *et al.*, 2000).

Humerus - The right humerus is exposed in caudolateral view (Figs. 87-88). In this aspect, the epiphyses and their articular surfaces are clearly visible. The outline of the proximal epiphysis is an evenly convex curvature which delineates the humeral head and continues caudally in the internal tuberosity. This tuberosity is placed distally about 13% of the way down the length of the shaft. The cartilaginous area capping the humeral head is clearly visible under UV light (see Appendicular Articular Cartilages). The margin of the head appears well-marked by a raised, robust border.

The deltopectoral crest of the right humerus is directed craniomedially, dipping into the matrix, so it is difficult to evaluate its morphology. However, following the outline of the left humerus, exposed in medial view, the delto-

pectoral crest of *Scipionyx* appears moderately developed. It extends up to about one-third of the length of the humerus, and expands the width of the proximal end of the humerus up to twice its minimum shaft diameter. In our opinion, the deltopectoral crest of the humerus of *Scipionyx* resembles that of the other compsognathids, and the differences mentioned by Peyer (2006) are mostly due to different degrees of exposures of the humeri. A possible exception is *Sinosauropteryx*, which has a relatively short and massive humerus, with a powerful deltopectoral crest, extending for more than half the length of the bone (Currie & Chen, 2001; Ji *et al.*, 2007b). In the tyrannosauroids, on the other hand, the proximal half of the humerus is narrow, with a proximal end that is only slightly differentiated (e.g., Xu *et al.*, 2004; Carpenter *et al.*, 2005a). It is slender and gracile, with a weak deltopectoral crest and a strong spherical head, in the basal ornithomimosaur *Sinornithomimus* (Kobayashi & Lü, 2003). It is robust, with a strong deltopectoral crest, in the basal Alvarezsaur *Nqwebasaurus* (de Klerk *et al.*, 2000).

Under grazing light, an apparent bump crossing the diaphysis of the right humerus of *Scipionyx*, and a couple of other bumps under the coracoids as well, which cause alteration of the relief of the bones, can be seen. Those bumps mark, respectively, the position of the diaphysis and the proximal epiphysis of the left humerus (Figs. 88, 91), a position that is confirmed by CT scan imaging (Fig. 92). The bump corresponding to the diaphysis of the left humerus tapers distally towards the epiphysis. The left distal epiphysis, which emerges between the 4th and 5th dorsal ribs, is not expanded and shows only the radial condyle. This indicates that the left humerus lies in medial view. On the other hand, the distal epiphysis of the right humerus gradually expands from the diaphysis to form



Fig. 91 - Oblique view under grazing light of the humeri of *Scipionyx samniticus*, showing the elongate bump caused by the diaphysis of the left humerus undercrossing the right one. See Appendix 1 or cover flaps for abbreviations.

Fig. 91 - Vista obliqua e in luce radente degli omeri di *Scipionyx samniticus*, che mostra la gobba allungata causata dalla diafisi dell'omero sinistro nel punto in cui passa sotto il destro. Vedi Appendice 1 o risvolti di copertina per le abbreviazioni.

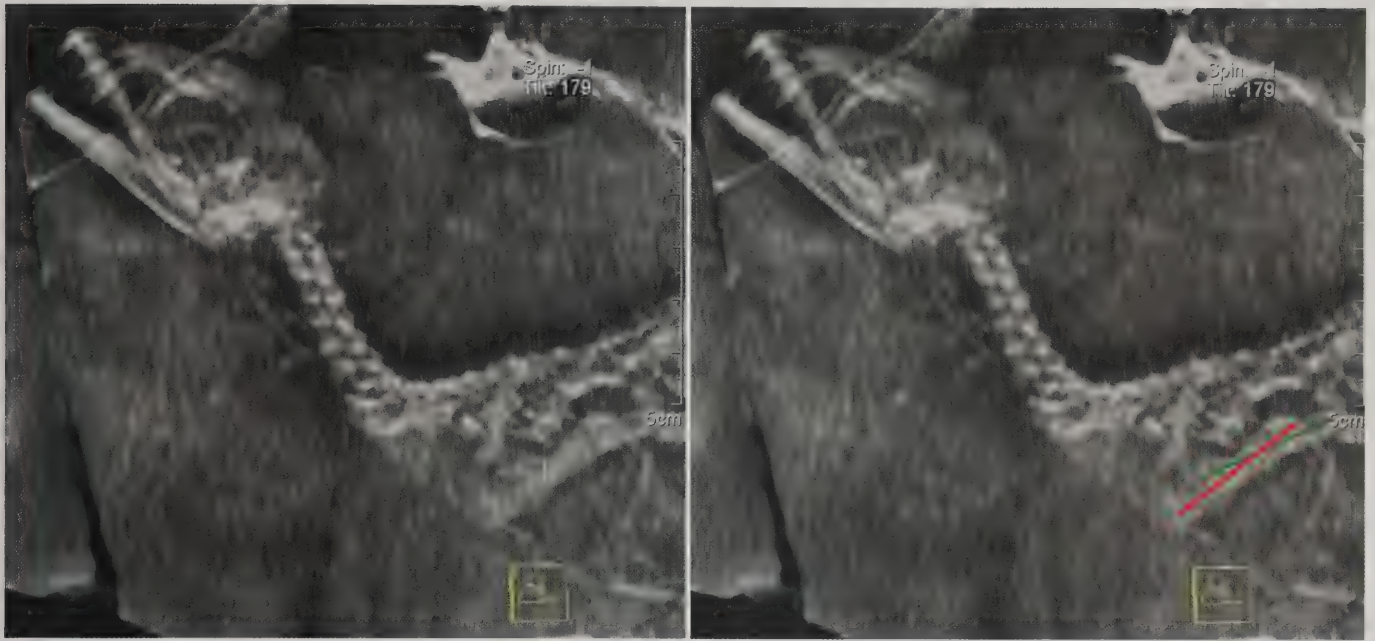


Fig. 92 - Computed tomography image of *Scipionyx samniticus*, showing the left side of the specimen, confirms the position of the left humerus (red line) with respect to the right one (green line), as inferred from observations under grazing light.

Fig. 92 - Tomografia computerizzata di *Scipionyx samniticus* che mostra il lato sinistro dell'esemplare e conferma la posizione dell'omero sinistro (linea rossa) rispetto al destro (linea verde), come si deduce dalle osservazioni in luce radente.

the distal condyles. Of these, the ulnar condyle appears slightly more developed (Figs. 87-88). The entepicondyle lies on the craniomedial side that faces towards the slab and, so, is not visible.

The humerus of *Scipionyx*, especially in its distal half, is rather straight if compared to the typically tetanurine sigmoid shape. As expected, its curvature resembles much more that of the other compsognathids (Currie & Chen, 2001; Hwang *et al.*, 2004; Göhlich & Chiappe, 2006; Peyer, 2006) and, more in general, of the other non-maniraptoran coelurosaurs (e.g., Kirkland *et al.*, 1998; Kobayashi & Lü, 2003; Carpenter *et al.*, 2005a, 2005b) except *Coelurus* (Carpenter *et al.*, 2005b).

Radius - The right radius is clearly exposed in dorsal view (Figs. 88, 93); only a small portion of the proximal epiphysis is not visible. It is a straight, slender bone, cylindrical in shape and with a constant transverse diameter, as is the case in other compsognathids (e.g., Göhlich & Chiappe, 2006), *Coelurus* (Carpenter *et al.*, 2005b) and *Ornitholestes* (Carpenter *et al.*, 2005b). Although the shape of the radius in the Compsognathidae is not diagnostic, the radius of *Scipionyx* clearly appears different from that of some basal tyrannosauroids, which is flattened and expanded distally (Xu *et al.*, 2004, 2006), or bowed (Carpenter *et al.*, 2005a). The bony wall of the diaphysis is partially collapsed, revealing its thinness and the presence of a hollow interior.

The left radius is exposed in ventral view; its distal epiphysis and two short tracts of the diaphysis are visible, the shortest in the *spatium interosseum* of the right forearm, and the other one close to the right elbow. Here, the diaphysis is split into two longitudinal sections, whose displacement clearly reveals the mentioned hollow interior. A small triangular splinter of the proximal epiphysis of the left radius emerges between the diaphyses of the two humeri. Based on the combined observation of the

distal epiphyses of the right and left radii, the articular surface for the carpals appears more expanded dorsally than ventrally (Figs. 88, 93).

The radius of *Scipionyx* is about 60% the length of the humerus. It is 57-61% in *Sinosauroptryx* (Currie & Chen, 2001), 62% in *Huaxiagnathus* (Hwang *et al.*, 2004), 64% in the German *Compsognathus* (Ostrom, 1978), 71% in

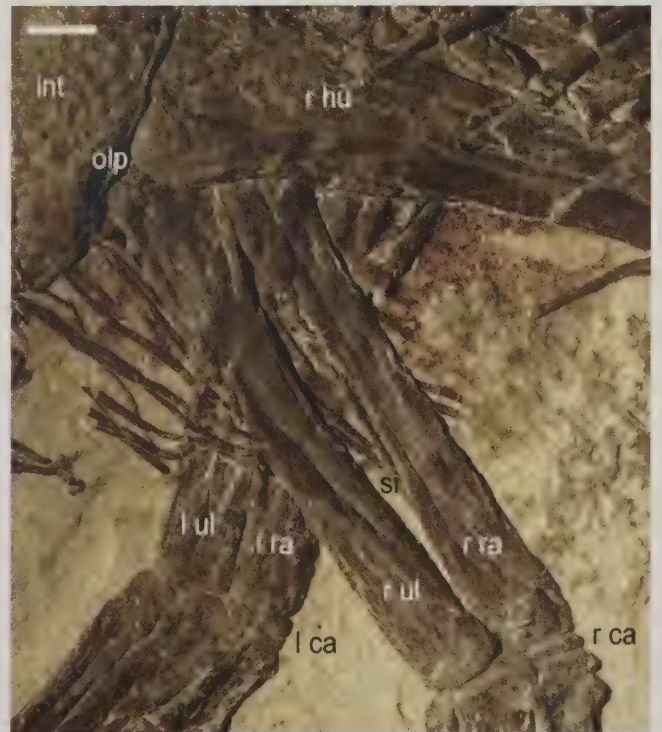


Fig. 93 - Radii, ulnae and carpi of *Scipionyx samniticus*. Scale bar = 2 mm. See Appendix 1 or cover flaps for abbreviations.

Fig. 93 - Radii, ulnae e carpi di *Scipionyx samniticus*. Scala metrica = 2 mm. Vedi Appendice 1 o risvolti di copertina per le abbreviazioni.

Juravenator (Göhlich & Chiappe, 2006) and 79% in the French *Compsognathus*. Similar ratios are found in many other coelurosaurs, such as the basal tyrannosauroids *Guanlong* (68%-Xu *et al.*, 2006), *Coelurus* (68%-Carpenter *et al.*, 2005b) and *Tanycolagrus* (72%-Carpenter *et al.*, 2005a), the basal ornithomimosaur *Sinornithomimus* (75%-Kobayashi & Lü, 2003), *Ornitholestes* (68%-Carpenter *et al.*, 2005b), *Nqwebasaurus* (76%-de Klerk *et al.*, 2000), *Microraptor* (78%-Hwang *et al.*, 2002) and *Sinornithoides* (71%-Russell & Dong, 1993). More elongate radii are found in other Maniraptora, such as *Mei* (93%-Xu & Norell, 2004).

Ulna - Like the radius, the ulna of *Scipionyx* is a slender, cylindrical element (Figs. 88, 93). Its proximal epiphysis is more robust, whereas the distal epiphysis, as far as can be seen in the available views, appears not at all expanded. The right ulna, through a faint concave medial arch, produces an apparent *spatium interosseum*. Parts of the proximal articular surface and of the olecranon are hidden under the right humerus and the cranialmost intestinal loop. As in the right radius, the diaphysis is fractured and hollow.

The diaphysis, the whole distal epiphysis and the proximal portion of the proximal epiphysis of the left ulna, lying in ventral view, are partly visible. In fact, the left ulna, after passing under the right ulna, radius and humerus, emerges in the thoracic region, caudally to the end of the 4th dorsal rib, still in articulation with the humeral condyle. Here, it shows a moderately pronounced olecranon process.

If we follow Peyer (2006) in considering the difference in height between the radius and the ulna as the height of the olecranon, the olecranon of *Scipionyx* is as well-developed as in the German *Compsognathus* (Ostrom, 1978). In *Sinosauropteryx* (Currie & Chen, 2001), it is more developed. On the other hand, *Huaxiagnathus* (Hwang *et al.*, 2004), *Sinocalliopteryx* (Ji *et al.*, 2007a) and *Juravenator* (Göhlich & Chiappe, 2006) have a small, relatively short olecranon process, as is the case also in the basal tyrannosauroids (Carpenter *et al.*, 2005a; Xu *et al.*, 2006). In the basal ornithomimosaur *Sinornithomimus* (Kobayashi & Lü, 2003), the olecranon is even more reduced and the distal expansion is delicate, too.

The distal epiphysis of the ulna is abruptly and greatly expanded in the French *Compsognathus*, but such a marked difference with *Scipionyx* is partly due to different exposure (cranial view in the former taxon). By the way, according to Peyer (2006) *Compsognathus* differs from *Scipionyx* (Dal Sasso & Signore, 1998a) in having a straighter, not at all bowed, ulnar shaft. In our opinion, this difference is not so relevant and may well be a consequence of the different views in which the bones are exposed. As a matter of fact, in *Scipionyx* itself the left and right ulnae appear straight and slightly bowed, respectively.

The ulna of *Sinosauropteryx* (Currie & Chen, 2001) is even more robust and shorter, with a clearly expanded distal epiphysis. In contrast, in *Coelurus* (Carpenter *et al.*, 2005b) the ulna is more slender than in *Scipionyx*, with a very thin shaft and a distal epiphysis that is gradually expanded in all the views.

In *Scipionyx*, as in *Huaxiagnathus* (Hwang *et al.*, 2004), radius and ulna are subequal in transverse diameter

for almost all their length. Unlike *Scipionyx*, the transverse shaft diameter of the ulna is slightly greater than that of the radius in *Compsognathus* (Peyer, 2006); the difference is even more pronounced in *Sinosauropteryx* (Currie & Chen, 2001), although not to the degree of advanced coelurosaurs such as *Microraptor* (Hwang *et al.*, 2002), in which the bowed ulnar shaft is approximately twice the thickness of the radius.

Finally, with regard to the length of the ulna in relation to the humerus, in *Scipionyx* the former is about 70% the length of the latter. The value is 62% in *Huaxiagnathus* (Hwang *et al.*, 2004), about 77% in the German *Compsognathus* (Ostrom, 1978) and *Sinosauropteryx* (Currie & Chen, 2001), and 90% in the French *Compsognathus*. Among non-compognathid coelurosaurs, the value is 76-77% in the basal tyrannosauroids (Carpenter *et al.*, 2005a; Xu *et al.*, 2006), about 75% in the basal ornithomimosaur *Sinornithomimus* (Kobayashi & Lü, 2003), 76% in the basal alvarezsaur *Nqwebasaurus* (de Klerk *et al.*, 2000), 78% in *Sinornithoides* (Russell & Dong, 1993), 82-90% in dromaeosaurids (Xu *et al.*, 1999; Burnham *et al.*, 2000; Hwang *et al.*, 2002) and about 90% in *Archaeopteryx* (Elzanowski, 2002).

Carpus - As noted by Dal Sasso & Signore (1998a), the carpus of *Scipionyx* is composed of two elements only (Figs. 93-95): a small, simple lenticular-shaped bone is more clearly exposed in the right carpus, preserved in contact with the radius on both arms – we interpret this proximal medial carpal bone as the radiale; another bone with a more complex shape and contacts is located distally to the radiale – and interpreted herein as a distal carpal.

In the right wrist, where it is exposed in dorsal view, the distal carpal is a flattened and sigmoid element, deepest proximodistally in its medial half; in the left wrist, it appears in ventral view and is deeper in its lateral half. This pattern reflects the intimate articular contact with the neighbouring bones, which leaves no space for additional cartilaginous elements: proximally, the distal carpal contacts the radiale for half of its articular surface, then it reaches the radius and with its lateralmost extremity the ulna; distally, it caps the proximal end of metacarpal I plus the medial half of the proximal end of metacarpal II – the proximal end of mcII is moderately convex with a slight central elevation in ventral view, which appears to subdivide its articular surface in two halves. Looking at the differences in thickness and shape of the two distal carpals preserved in two opposite views in the right and left wrists of *Scipionyx*, it is apparent that the volume of this bone is complementary to that of the radiale and the proximal articular facet of the first metacarpal (mcI). We interpret this carpal element as the first distal carpal (dc1), which, as in other theropods, overlaps the proximal articular facet of metacarpal I and part of the proximal articular facet of metacarpal II.

There is no other carpal bone in the two wrists of *Scipionyx*. According to Gauthier (1986), in absence of any other distal element, a single distal carpal indicates the fusion of dc1 and dc2 during the ontogeny. However, a suture is not detectable on the surface of neither the right nor the left distal carpal 1 of *Scipionyx*, even at high magnification (Fig. 95). It is interesting to note that Chure (2001) verified that in *Allosaurus* the morphology of the carpals is consistent throughout the ontogenetic series, and that



Fig. 94 - Metacarpals and manual phalanges of *Scipionyx samniticus*. Scale bar = 5 mm. See Appendix 1 or cover flaps for abbreviations.

Fig. 94 - Metacarpali e falangi delle mani di *Scipionyx samniticus*. Scala metrica = 5 mm. Vedi Appendice 1 o risvolti di copertina per le abbreviazioni.

the line of fusion between dc1 and dc2 is still visible as a groove in all but the two largest specimens examined by him. Therefore, based on the fact that *Scipionyx* is a hatchling (see Ontogenetic Assessment), the fusion between dc1 and dc2 would have occurred very precociously during ontogeny, probably already during embryogeny. According to this hypothesis, the adult morphology of the carpus would have been acquired very early and maintained unchanged up to adulthood, without any further substantial modification, although it must be taken into consideration that studies on several specimens of *Allosaurus* (Holtz *et al.*, 2004) and *Falcaurus* (Zanno, 2006) demonstrated a certain individual/ontogenetic variability in the degree of carpal fusion that renders the assessment of a carpal formula, and the homology of carpal elements, complicated. The other possible explanation for the absence of any suture is that the distal carpal of *Scipionyx* derives from a single centre of ossification. Without going further into the discussion of the homology of this element, we remind the reader that autoradiographic studies of the development of the carpus in the chicken indicate a single centre of ossification for the avian semilunate carpal (Chure, 2001).

The radiale in *Sinosauropteryx* is more flattened and comparatively smaller than that in *Scipionyx*. In the former, it is positioned below the middle of the distal end of the radius, rather than being shifted apart towards the medial side of the wrist. A further difference is in the distal contact: according to Currie & Chen (2001), in *Sinosauropteryx* it articulates not only with a large distal car-

pal, but also with the first metacarpal. In *Compsognathus* (Peyer, 2006) and *Huaxiagnathus* (Hwang *et al.*, 2004), the radiale spans almost the entire width of the distal radius, being more similar to that of *Scipionyx* in its mediolateral extension. In the tyrannosauroid *Guanlong*, the radiale is instead considerably larger, being mediolaterally more extended than the distal carpal (Xu *et al.*, 2006 – suppl. info: fig. 2f-g).

The “semilunate carpal” of the Maniraptora (e.g., Rauhut, 2003; Chure, 2001; Elzanowski, 2002) has a bulky trochlea and is markedly crescent-shaped. In *Scipionyx*, in contrast, in both the available views the distal carpal appears somewhat flattened, without any bulky proximal trochlear surface, and, thus, results definitely different from the true semilunate carpals (*sensu* Chure, 2001). In our opinion, the similar flattened morphology of the distal portion of the carpus visible in the French specimen of *Compsognathus* may well represent its original, natural morphology, without the need for supposing that it was originally semilunate and underwent considerable flattening during diagenesis, as hypothesised by Peyer (2006).

In the French *Compsognathus*, according to Peyer (2006), the elements distal to the radiale are two separated, but tightly bound together, elements that might be fused to form the dc1+dc2 block. Peyer (2006) also observed, in the German *Compsognathus*, three isolated elements comparable in shape to the three carpals found in the French specimen, *contra* Ostrom (1978), who suggested that there were probably only two elements in the wrist of the German *Compsognathus*. A total of five carpal

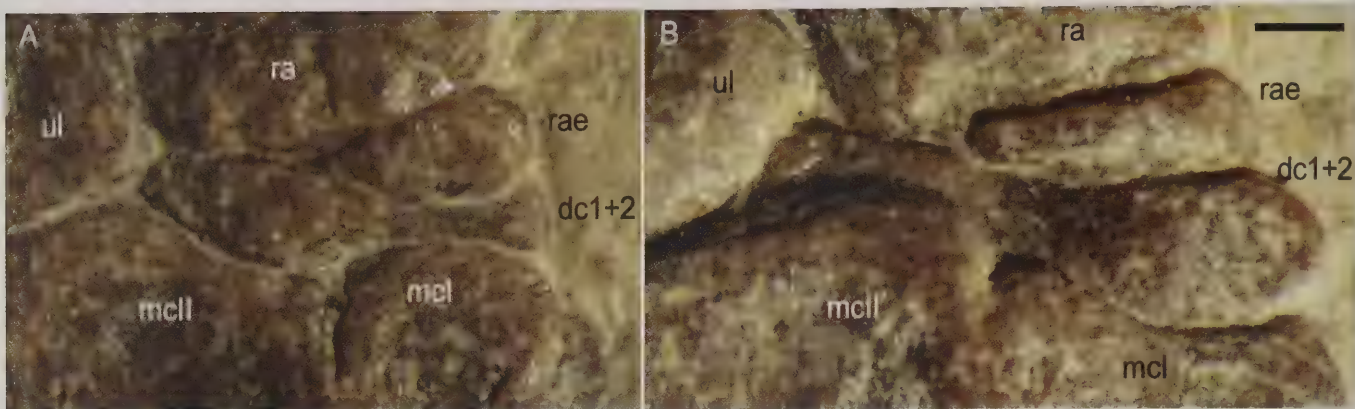


Fig. 95 - Close-ups of the carpal bones of *Scipionyx samniticus*. On the surface of the left (A) and right (B) distal carpal element, no suture is detectable. Scale bar = 0.5 mm. See Appendix 1 or cover flaps for abbreviations.

Fig. 95 - Particolari delle ossa carpali di *Scipionyx samniticus*. Sulla superficie dell'elemento carpale distale sinistro (A) e destro (B) non è individuabile alcuna sutura. Scala metrica = 0,5 mm. Vedi Appendice 1 o risvolti di copertina per le abbreviazioni.

elements has been reported for *Sinosauropteryx* (Currie & Chen, 2001). However, we express some doubt about the association to the same (right) wrist of the two elements tentatively identified by Currie & Chen (2001) as additional carpals, because of their underlying position and uncertain identification: they might simply be the counterlateral left carpals, disarticulated phalanges or other indeterminate bones. Whatever the number of carpals, in *Sinosauropteryx* the distal carpal is broad and low, just like in *Scipionyx*, and extends beyond the first metacarpal to contact metacarpal II; unlike *Scipionyx*, it caps only the lateral half of the first metacarpal, the medial one being occupied by a peculiar proximomedial flange of mcI. A small, disk-like element, identified as the ulnare by Currie & Chen (2001: fig. 8a), can be seen between the ulna and the second metacarpal of *Sinosauropteryx*. In *Scipionyx*, the lateral portion of the distal carpal reaches the same position, so we suggest that the large distal carpal and the ulnare described by Currie & Chen (2001) might, in fact, be the still unfused dc1 and dc2. This might be the case also for the holotype of *Huaxiagnathus* (Hwang *et al.*, 2004), where a purported “semilunate carpal” – which we think is much too small to be this bone in actual fact – contacts laterally a very small “ulnare”, positioned between radius and ulna and close to the middle of the articular surface of mcII.

Among compsognathids, two stacked, plate-like carpals are described only in *Huaxiagnathus* and *Scipionyx*. The exposure of the left and right wrists in the holotype of *Huaxiagnathus* (Hwang *et al.*, 2004: fig. 8) is the same as that of *Scipionyx* and allows direct comparisons. Notably, the shape and size of the radiale and the dc1+dc2 (“semilunate carpal” in Hwang *et al.*, 2004) are similar in both genera: in dorsal view, the radiale is thin and mediolaterally expanded, whereas in ventral (palmar) view, it is shorter and bulkier proximodistally; the distal carpal has a complementary shape in both views. In *Huaxiagnathus*, the presence of an additional small, ossified carpal between the ulna and mcIII, identified as a dc3 by Hwang *et al.* (2004), would be the only noticeable difference with *Scipionyx*. A total of four elements is, in fact, reported in the former as well as in *Sinocalliopteryx* (Ji *et al.*, 2007a): given their comparable position, they are probably homologous to each other.

The tyrannosauroid *Tanycolagreus* (Carpenter *et al.*, 2005a) exhibits a carpal formula identical to that of *Scipionyx*, with a proximal carpal and, functionally, a single distal carpal derived from the fusion of the distal carpals. The proximal carpal, described as “semilunate” but termed “radiale” by Carpenter *et al.* (2005a), is a little more expanded proximodistally and considerably larger than the radiale of *Scipionyx*, its transverse diameter being greater than that of the distal portion of the radius (Carpenter *et al.*, 2005a: fig. 2.11 I). The distal carpal is as flattened and elongate as the one of *Scipionyx*, but it is larger, overlapping mcI, mcII and, although only barely, mcIII too. *Tanycolagreus* and *Huaxiagnathus* are, therefore, the theropod taxa most similar to *Scipionyx* with regard to carpal morphology. A certain resemblance can be seen also with the distal carpal of *Coelurus*, described by Rauhut (2003) as “somewhat rectangular or flattened rather than truly semilunate in ventral (palmar) view”.

In the adult specimen of the tyrannosauroid *Guanlong* (Xu *et al.*, 2006), the distal carpal is much deeper than in *Scipionyx*, possessing a transverse trochlea proximally and a semilunate shape in ventral view. Its position (contacting mcI and half of mcII) is similar to the condition seen in *Allosaurus*, *Scipionyx* and oviraptorosaurs, whereas in therizinosauroids, troodontids, dromaeosaurids and basal birds it articulates primarily with mcII. The basal ornithomimosaurids are considerably different from *Scipionyx*: no stacked elements are present, and the carpals are represented by three or more disk-like elements, one being a well-developed ulnare, all aligned on the same plane (Kobayashi & Lü, 2003). In *Nqwebasaurus* (de Klerk *et al.*, 2000), two carpals are preserved, tentatively identified as dc1 and dc2. *Sinornithoides* (Russell & Dong, 1993) is described in having a carpus composed of two elements: a radiale and a semilunate. This count is reminiscent of *Scipionyx*, but in the former the radiale contacts laterally also the ulna and, in all likelihood, the semilunate is larger and crescent-shaped as in other deinonychosaurs and, more in general, in most of the Maniraptora. As a matter of fact, in the closely related *Mei* the manus is fossilised folded in avian fashion (Xu & Norell, 2004), a position probably not feasible for *Scipionyx*.

Metacarpus - The metacarpus of *Scipionyx* is composed of three elements and, on the whole, it appears moderately slender (length/width ratio of mcI-III = 2) and not as narrow and elongate as in *Ornitholestes* and most of the Maniraptora (e.g., Rauhut, 2003). The metacarpus is compact, with mcII and mcIII closely appressed in lateral contact (Figs. 88, 94). On the other hand, contrary to *Sinosauropteryx* (Currie & Chen, 2001), the lateral margin of mcI in *Scipionyx*, well-visible in the right element, is concave. As a consequence, the contact between mcI and mcII would have been partly limited, although not as limited as in *Deinonychus* (Gishlick, pers. comm., 2000). The right metacarpus, exposed in a view that is mainly dorsal but permits to see the medial side, shows a few marked extensor pits. The left metacarpus is exposed in medioventral (mediopalmar) view, allowing observation of the condyles.

In *Scipionyx*, mcI is 40% of the length of mcII and twice as long proximodistally than wide transversely, resulting narrower than the bulky, squared mcI of *Sinosauropteryx* (Currie & Chen, 2001). McI is 40-50% of the length of mcII also in *Sinosauropteryx* (Currie & Chen, 2001), *Juravenator* (Göhlich & Chiappe, 2006), *Sinocalliopteryx* (Ji *et al.*, 2007a), *Huaxiagnathus* (Hwang *et al.*, 2004), basal tyrannosauroids (Xu *et al.*, 2004: fig. 2; Carpenter *et al.*, 2005a; Xu *et al.*, 2006, suppl. info: fig. 2f) and basal ornithomimosaur (Makovicky *et al.*, 2004), whereas it is as long as mcII, or slightly shorter, in derived forms. It is a bit shorter in *Compsognathus* (Gishlick & Gauthier, 2007; Peyer, 2006) and tends to become even shorter in some Maniraptora (Norell & Makovicky, 1999; Russell & Dong, 1993; Osmólska *et al.*, 2004; Padian, 2004). On the other hand, mcI is more elongate (63% of the length of mcII) than that in *Scipionyx* in the basal alvarezsaur *Nqwebasaurus* (de Klerk *et al.*, 2000), in which mcII is notably more gracile at its mid-shaft than mcI (58%). In *Scipionyx*, the proximal end of mcI, which is regular in outline and lacks any trace of the proximomedial flange visible in *Sinosauropteryx* (Currie & Chen, 2001), is not perfectly aligned with the ones of mcII and mcIII; in fact, it is slightly more distally positioned, as is the case in many Tetanurae (Gishlick, pers. comm., 2000). On the right mcI, a faint extensor pit can be seen; the distal condyles are asymmetric, with the medial wider and located more proximally than the lateral one. This asymmetry matches the asymmetry of the proximal facet of the phalanx I-1 and, in life, made the pollex divergent from the other digits (see below), albeit not as much as in *Tugulusaurus* (Rauhut & Xu, 2005), in which the medial side is entirely situated more proximally than the lateral one, and in advanced Maniraptora, in which the asymmetry is more marked. Rauhut (2003) and Langer (2004) reported that this condition is widespread in saurischian dinosaurs.

McII is the longest bone in the manus of *Scipionyx*, and its shaft is subequal in width to that of mcI. Very similar length and proportions can be seen in *Huaxiagnathus* (Hwang *et al.*, 2004) and *Juravenator* (Göhlich & Chiappe, 2006). Its cylindrical structure, without any marked medial expansion in the proximal epiphysis, is characteristic of the majority of coelurosaurs (e.g., Rauhut, 2003; Holtz *et al.*, 2004). As mentioned in the description of the carpus, the proximal margin has a central

elevation in ventral (palmar) view: this indicates that the articular surface is subdivided in two equally expanded facets, one for the contact with the ulna and the other for the contact with the distal carpal (Fig. 95A). On the distal epiphysis of the right mcII is an extensor pit that is slightly more developed than the faint ones visible on mcI and mcIII. Also, the medial collateral ligament fossa is well-exposed (Fig. 96). According to Rauhut (2003), the extensor pits are shallow or absent in the metacarpals of most coelurosaurs.

In *Scipionyx*, mcIII is slightly thicker than half mcII, and it is slightly shorter than the latter, as in the other compsognathids (Ostrom, 1978; Currie & Chen, 2001; Hwang *et al.*, 2004; Göhlich & Chiappe, 2006; Peyer, 2006). Contrary to mcI and mcII, which have expanded ends (especially the distal ones), mcIII straight, slender and unexpanded distally. In the Italian compsognathid, however, it is not as slender as in *Compsognathus* (Peyer, 2006; Gishlick & Gauthier, 2007), in which it resembles the derived maniraptorans in its degree of slenderness and in having the bone bowed laterally rather than being straight. In *Sinocalliopteryx* (Ji *et al.*, 2007a), as well as in the basal tyrannosauroid *Tanycolagreus* (Carpenter *et al.*, 2005a), mcIII is even more slender and also considerably shorter than in *Scipionyx*.



Fig. 96 - Close-up of the distal epiphysis of the 2nd right metacarpal (dorsal view) of *Scipionyx samniticus*. Scale bar = 0.5 mm. See Appendix 1 or cover flaps for abbreviations.

Fig. 96 - *Scipionyx samniticus*, particolare dell'epifisi distale del 2^o metacarpale destro (norma dorsale). Scala metrica = 0,5 mm. Vedi Appendice 1 o risvolti di copertina per le abbreviazioni.

The fact that the proximal epiphysis of mcIII lies on that of mcII in the left manus – exposed in ventral (palmar) view – and under the one of mcII in the right manus – exposed in dorsal view – is not random. Rather, it reflects a natural anatomical condition that is diagnostic for the Tetanurae (Holtz *et al.*, 2004). Finally, mcIV is definitely absent in *Scipionyx*, contrary to *Guanlong* and *Ornitholestes* (Xu *et al.*, 2006), which are the only known coelurosaurs to preserve a reduced metacarpal IV.

Manual phalanges - The hands of *Scipionyx* have three digits each: digit I is the shortest, digit II is the longest and digit III is the most gracile. The proximal phalanges are exposed in the same view as their metacarpals, whereas the distal phalanges and, in particular, all the ungual phalanges are rotated to expose the medial side, with the exception of the left ungual I, which lies in lateral view. The phalanges I-1, II-1, III-2 and III-3 of the right manus are traversed by the same calcite vein that crosses the neck and the left scapulocoracoid. This secondary mineralisation (see Diagenetic Formations Possibly Related To Soft Tissues) has fractured and separated the bones with a 1 mm-wide gap.

The non-ungual phalanx of the first digit has a condylar asymmetry analogous to that of mcI and a slightly twisted shaft (Figs. 88, 94). For these reasons, the first digit of *Scipionyx* diverged from the other two, like in many other theropods; this increased the spread of the fingers and permitted these dinosaurs to grasp larger objects during flexion. On the contrary, the non-ungual phalanges of digits II and III have straight, definitely non-twisted, shafts and aligned condyles that are equally developed in a distal direction. From the combined observation of the non-ungual phalanges of both manus, it can be inferred that each phalanx bears ginglymoid condyles; moreover, the distal condylar portion has lateral and medial collateral ligament fossae, which are well-delimited, deep and opened proximally.

Remarkably, the shaft diameter of manual phalanx I-1 is subequal to the shaft diameter of the radius (Figs. 88, 94). In *Compsognathus* (Peyer, 2006), *Juravenator* (Göhlich & Chiappe, 2006), *Huaxiagnathus* (Hwang *et al.*, 2004) and *Sinocalliopteryx* (Ji *et al.*, 2007a: fig. 3b), the proximal shaft diameter of manual phalanx I-1 is even greater than the minimum shaft diameter of the radius, and the authors above regard this character as diagnostic of the Compsognathidae. In *Sinosauropteryx* (Currie & Chen, 2001), this condition is even more emphasised: the first phalanx of digit I and the ungual phalanx that it supports are massive, each being as long as the radius and thicker than the shafts and the distal ends of either the radius or the ulna. In *Sinosauropteryx*, *Huaxiagnathus* and *Sinocalliopteryx* (Ji *et al.*, 2007a), phalanx I-1 (except unguals) is the longest, whereas in *Scipionyx*, *Compsognathus* (Peyer, 2006) and the basal tyrannosauroid *Tanycolagreus* (Carpenter *et al.*, 2005a), the longest phalanx is II-2. Unlike *Sinosauropteryx* (Currie & Chen, 2001), phalanx I-1 of *Scipionyx* is shorter than mcII, and the first digit is not larger than the forearm bones; rather, it equals the epipodials in length and thickness. In *Scipionyx*, all the penultimate phalanges are elongate: phalanx III-3 is longer than the sum of III-1 and III-2, which are both very short; phalanx II-2 surpasses II-1; similarly, the length of I-1, which is

not preceded by other phalanges, is more than twice that of mcI. These proportions are similar to those found in the vast majority of coelurosaurs (Rauhut, 2003).

Peyer (2006) described two possible phalanges, III-1 and III-2, of the left manus of *Compsognathus*. These phalanges, especially the latter, are very short, measuring only 25% and 10% of the length of mcIII, respectively; in other compsognathids, the respective ratios for these phalanges are 32% and 41% in *Scipionyx*, 30% and 38% in *Sinosauropteryx*, and 40% and 50% in *Juravenator* (Göhlich & Chiappe, 2006). The odd ratio of the alleged phalanx III-2 of *Compsognathus* arouses doubts on the completeness of that element. By the way, Gishlick & Gauthier (2007) suggested that the third digit was reduced, perhaps even non-functional, based on the overall morphology and slenderness of metacarpal III and the possibly preserved phalanges, highlighting the fact that there is no evidence on either specimen of *Compsognathus* of a claw-bearing ungual phalanx. In any case, following the reconstruction by Peyer (2006: fig. 9), digit III would be shorter than digit I. A digit III shorter than digit I is present also in *Sinosauropteryx* (Currie & Chen, 2001), *Huaxiagnathus* (Hwang *et al.*, 2004) and *Sinocalliopteryx* (Ji *et al.*, 2007a), whereas in *Juravenator*, according to Göhlich & Chiappe (2006, suppl. info, table I), digits I and III are subequal in length, with the latter digit slightly shorter than (95% of its length) the former.

Based on these comparisons, *Scipionyx* differs from all known compsognathids in having a digit III that is considerably longer (123%) than digit I. Among non-maniraptoran coelurosaurs, a digit III longer (110%) than digit I is present in the adult individual IVPP V 14531 of the basal tyrannosauroid *Guanlong* (Xu *et al.*, 2006: fig. 2b). Based on the proportions of digits I and III, the manus of *Scipionyx* can be compared – although not from a morphological point of view – to that of some oviraptorosaurs such as *Citipati*, *Conchoraptor* and *Oviraptor* (e.g., Clark *et al.*, 2001; Osmólska *et al.*, 2004). Manual digit I is reported to be shorter than digit III also in the troodontid *Jinfengopteryx* (Ji *et al.*, 2005): we regard this feature as unclear, because it is difficult to confirm and quantify that statement based on the published figures, and there are some inconsistencies in the table of measurements in Ji *et al.* (2005). Digits I and III are subequal in several Maniraptora (e.g., Ostrom, 1969; Xu *et al.*, 1999: fig. 2; de Klerk *et al.*, 2000: fig. 2; Xu *et al.*, 2002b; Russell & Dong, 1993), whereas digit III is longer than digit I (115%) in *Velociraptor* (Norell & Makovicky, 1999). Finally, the digits of *Archaeopteryx* (Elzanowski, 2002) resemble those of *Scipionyx* in their relative proportions, digit II being the longest, digit I the shortest and digit III intermediate in length. However, based on other sources (e.g., Wellnhofer, 1985: fig. 1; Elzanowski, 2002: fig. 2.1; Paul, 2002: fig. 4.3; Padian, 2004: fig. 11.1), the difference in length between digits I and III is negligible as they appear almost subequal. Outside the Tetanurae, a digit III longer (121%) than digit I is reported also in *Dilophosaurus* (Welles, 1984).

In *Scipionyx*, the curvature of the bony claws (ungual phalanges) is emphasised by the horny sheaths, which are rarely preserved in fossils. The dorsal margin of the ungual phalanges is uniformly convex up to the articular margin, without the dorsal lip found in oviraptorosaurs, deinoychosaurus and birds (Currie & Russell, 1988).

The base of the bony claws (i.e., their articular surface) is quite tall, similar to what is seen in *Juravenator* (Göhlich & Chiappe, pers. comm., 2006). However, the transition from the proximal articular surface to the main body of the ungual is not as markedly distinct in *Scipionyx* as in several other theropods (e.g., via a small, shallow transverse groove [Rauhut & Xu, 2005]), especially ventrally. There, close to the articular margin, a quite developed flexor tubercle, that is however shorter than half the height of the articular surface, gradually rises up (Figs. 88, 94). Thus, *Scipionyx* is similar to the other compsognathids except *Compsognathus* in having flexor tubercles taller than 1/3 of the height of the ungual articular facets. Even larger flexor tubercles, i.e., that are more than half the height of the articular facets, are instead present in deinonychosaurs and birds (Rauhut, 2003).

There is some variation in the morphology of the flexor tubercles in *Scipionyx*. In ungual I, seen in lateral and medial views, the ventral (palmar) margin runs straight from the flexor tubercle to the articulation. In unguals 2 and 3, this margin is concave and, consequently, the tubercles appear more distinct from the main body of the bones. A similar variation seems to be present in the holotype of *Huaxiagnathus* (Hwang *et al.*, 2004: fig. 7B), which, on the other hand, has unguals that are more curved and more gradually tapering. In contrast, the first ungual in *Nedcolbertia* is more robust, with a more prominent flexor tubercle (Kirkland *et al.*, 1998).

In *Scipionyx*, the ungual phalanx of digit I, which is the only ungual preserved in medial and in lateral views, has slightly asymmetric vascular grooves (Fig. 88): on the medial side (right phalanx), the sulcus bifurcates immediately from its apical portion towards a proximal direction, delimiting a thin ventral lip; on the lateral side (left phalanx), the sulcus bifurcates where it approaches the half length of the phalanx, and delimits a deeper ventral lip. Vascular grooves bifurcating in the distal half of the bone are present on the medial sides of the ungual phalanges of the second and third digit.

Concerning the relative size, in *Scipionyx* manual unguals I and II are subequal in size, whereas ungual III is slightly smaller. In the compsognathids *Sinocallopteryx* (Ji *et al.*, 2007a) and *Huaxiagnathus* (Hwang *et al.*, 2004), as well as in the basal tyrannosauroids *Dilong* (Xu *et al.*, 2004: fig. 2i) and *Guanlong* (Xu *et al.*, 2006, suppl. info: fig. 2d) and in *Sinornithosaurus* (Xu *et al.*, 1999), the trend is the same, but ungual III is considerably smaller. Therefore, *contra* Hwang *et al.* (2004), the large second ungual is not a diagnostic character of *Huaxiagnathus*. By combining information from the French and German specimens, Peyer (2006) reconstructed the ungual phalanx II of *Compsognathus* as the largest, and the ungual phalanx III as the smallest, as is the case in *Velociraptor* (Norell & Makovicky, 1999) and *Archaeopteryx* (Elzanowski, 2002). In *Juravenator* (Göhlich & Chiappe, 2006), the three ungual phalanges share an autapomorphic shape in being high proximally and abruptly tapering at the midpoint, and differ from each other only in size, ungual I being the largest, and ungual III being the smallest. Similar but more emphasised proportions can be seen in the basal tyrannosauroid *Tanycolagreus* (Carpenter *et al.*, 2005a). In the majority of theropods, ungual I is considerably larger than ungual II, which is almost equal to ungual III (Senter, 2007). This is especially true for *Torvosaurus* and

the spinosauroids, where ungual I is 2/3 the length of the radius, and also for *Nqwebasaurus* (de Klerk *et al.*, 2000), where ungual I measures 3/2 the length of ungual III. Remarkably, a similar but even more emphasised condition is present in the compsognathid *Sinosauropteryx* (Rauhut, 2003). Therefore, *Sinosauropteryx* markedly differs from *Scipionyx*: in the latter, the ungual I is 2/5 the length of the radius; in the former, ungual I slightly surpasses the length of the radius.

Apart from their size, the unguals of *Scipionyx* resemble those of *Compsognathus* and *Juravenator* in their moderate degree of curvature and in the proportions of the flexor tubercles. The ungual phalanges are gently curved also in *Nqwebasaurus* (de Klerk *et al.*, 2000), but they are definitely more elongate than in *Scipionyx*. In ornithomimosaurs (Makovicky *et al.*, 2004), the flexor tubercle is even less pronounced and the curvature is even less emphasised, especially proximally. In contrast, the unguals of many other maniraptoriforms are often more curved than in *Scipionyx* and bear stronger flexor tubercles.

Pelvic girdle

The pelvic girdle of *Scipionyx* is incomplete. Part of the dorsal blade of the left ilium, as well as the proximal portion of the ischia, broke away and were irremediably lost during collection of the specimen, when one of the three main cracks of the slab occurred (Figs. 9-10). However, most of the pelvic girdle is preserved and the bones, although unfused, partly maintained the orientation they had *in vivo*. *Scipionyx* possesses an orthopubic pelvis with a dolichoiliac ilium and an estimated length of the ischium 3/4 the length of the pubis (Figs. 97-98).

In all compsognathids the shaft of the pubis is straight in lateral view, but forms different angles with the ilium and the long axis of the body. It is propubic (i.e., it points cranioventrally) in *Compsognathus* (Ostrom, 1978; Peyer, 2006) and *Mirischia* (Martill *et al.*, 2000; Naish *et al.*, 2004), whereas it is almost orthopubic (i.e., almost vertical) in *Sinosauropteryx* (Currie & Chen, 2001), *Sinocallopteryx* (Ji *et al.*, 2007a), *Huaxiagnathus* (Hwang *et al.*, 2004) as well as in the basal tyrannosauroid *Guanlong* (Xu *et al.*, 2006: fig. 2e). In *Ornitholestes* (Carpenter *et al.*, 2005b), the pelvis is almost orthopubic because of a combination of structures: the pubic peduncle points slightly cranially, but the pubic shaft is recurved. Although the shape of the single girdle elements is different, the basal therizinosauroid *Falcarius* (Kirkland *et al.*, 2005) and most oviraptorosaurs (Osmólska *et al.*, 2004) have also an orthopubic pelvis. On the other hand, the pelvis is often opisthopubic (i.e., with a retroverted, caudoventrally pointing pubis) in deinonychosaurs (e.g., Xu *et al.*, 1999; Burnham *et al.*, 2000; Hwang *et al.*, 2002).

Ilium - Except for a thin fragment of the mediodorsal edge of the blade, the left ilium is completely obscured by the sacral bones and by the right counterlateral element. The latter is fairly complete, just partly eroded along the cranial margin and lacking a dorsolateral portion of the preacetabular ala (Figs. 97-98).

The ilium of *Scipionyx* appears craniocaudally short in comparison with total body length or femur length, but comparable proportions (ilium shorter than femur) can be



Fig. 97 - Pelvic girdle and hindlimbs of *Scipionyx sammiticus*. Scale bar = 5 mm.

Fig. 97 - Cinto pelvico e arti posteriori di *Scipionyx sammiticus*. Scala metrica = 5 mm.

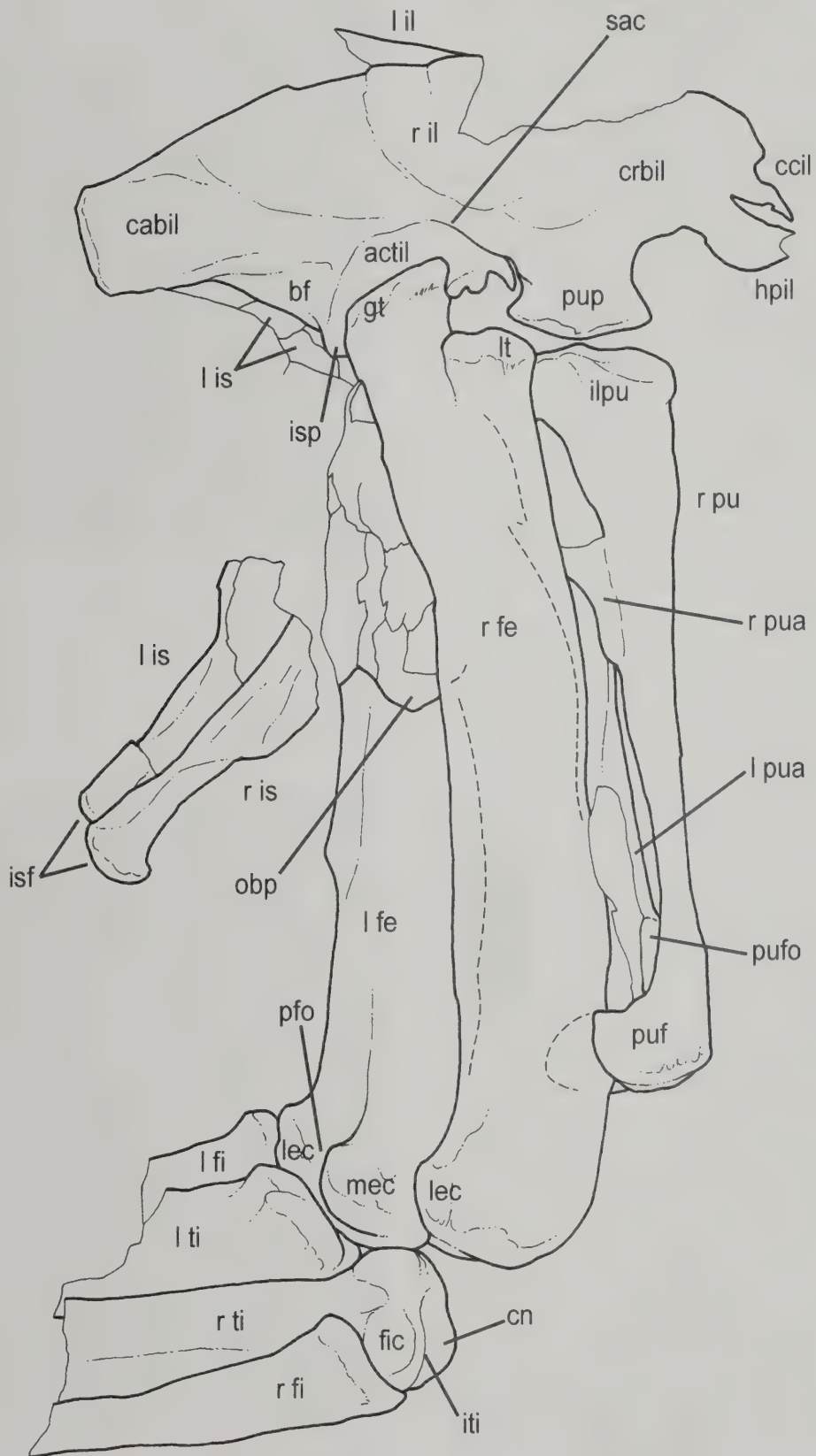


Fig. 98 - Line drawing of the bones illustrated in Fig. 97. See Appendix 1 or cover flaps for abbreviations.

Fig. 98 - Disegno al tratto delle ossa illustrate in Fig. 97. Vedi Appendice 1 o risvolti di copertina per le abbreviazioni.

seen also in other compsognathids, including *Sinosauropteryx* (Currie & Chen, 2001), *Compsognathus* (Peyer, 2006) and the large *Sinocalliopteryx* (Ji *et al.*, 2007a: fig.1), and in a number of coelurosaurs (e.g., Xu *et al.*, 1999; Burnham *et al.*, 2000; Hwang *et al.*, 2002; Xu *et al.*, 2004). The preacetabular portion is as long and high as the postacetabular portion is, as is the case in many other theropods, including most coelurosaurs (e.g., Rauhut, 2003) and all other compsognathids except *Huaxiagnathus* (Hwang *et al.*, 2004), which, similar to the tyrannosauroids (Brochu, 2003; Xu *et al.*, 2004; Xu *et al.*, 2006), has a slightly longer postacetabular ala.

The dorsal margin of the ilium of *Scipionyx* is uniformly convex, as in *Mirischia* (Naish *et al.*, 2004), whereas it is straight in *Sinosauropteryx* (Currie & Chen, 2001). The preacetabular ala of *Scipionyx* is dorsoventrally expanded, forming a hooked process directed cranioventrally. According to Rauhut (2003), the ilium has a dorsoventral expansion of the preacetabular ala that is more-or-less hooked in many neotheropods, with the exception of the forms more closely related to birds. This expansion is indeed well-marked in ornithomimosaur (Makovicky *et al.*, 2004) and in tyrannosauroids (Holtz, 2004) except *Dilong* (Xu *et al.*, 2004), whereas in *Ornitholestes* (Carpenter *et al.*, 2005b) and in some compsognathids, it is either only faintly developed or absent. In *Compsognathus*, the cranial process of the ilium is not expanded dorsoventrally, and its ventral edge, although not well-preserved, is straight (Peyer, 2006). In *Sinosauropteryx* (Currie & Chen, 2001) and *Huaxiagnathus* (Hwang *et al.*, 2004), the ventral margin of the preacetabular ala curves gently cranioventrally and, like in *Compsognathus*, does not have a distinct hooked process. In *Mirischia*, the dorsoventral expansion is well-developed but not hooked, terminating “in a square-ended process that is directed cranio-ventrally” (Naish *et al.*, 2004). Thus, the only compsognathid showing a condition very similar to that of *Scipionyx* is *Sinocalliopteryx* (Ji *et al.*, 2007a).

In *Scipionyx*, the preacetabular ala bears along its craniodorsal margin a small, but well-incised semicircular notch that, if compared to the eroded, irregularly indented margin of the neighbouring areas, does not seem an artefact of preservation (Fig. 99). As a matter of fact, a notch or concavity is found in exactly the same position in the ilia of some other basal coelurosaurs, especially tyrannosauroids such as *Dilong* (Xu *et al.*, 2004), *Guanlong* (Xu *et al.*, 2006) and *Stokesosaurus* (Rauhut, 2003), and the derived forms. This craniodorsal concavity, together with a preacetabular hooked ventral projection (see above), is often considered a synapomorphy of the clade Tyrannosauroidea (Holtz, 2004). A notch is present also in *Ornitholestes* (Carpenter *et al.*, 2005b: fig. 3.10A), where it faces cranially rather than craniodorsally.

Unlike *Sinosauropteryx* (Currie & Chen, 2001), *Scipionyx* has a supracetabular crest, albeit a weak one. Cranially, it parallels the concave outline of the acetabulum, whereas caudally it becomes straight and joins the ventral margin of the postacetabular blade. The right ilium has also two subparallel ridges, oriented vertically on the surface of the iliac blade dorsal and caudal to the acetabulum. Nevertheless, these ridges are not true iliac structures – none of them, for example, is homologous to the “prominent medial vertical crest” typical of the tyrannosauroids (see Xu *et al.*, 2006) – but rather are due to the presence

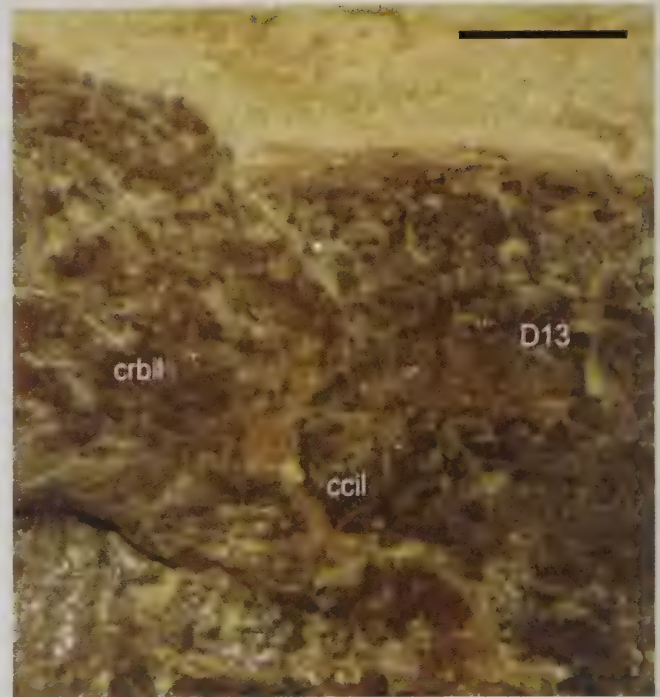


Fig. 99 - Close-up of the craniodorsal margin of the preacetabular ala of the right ilium of *Scipionyx samniticus*, where a small concavity is found. Scale bar = 1 mm. See Appendix 1 or cover flaps for abbreviations.

Fig. 99 - *Scipionyx samniticus*. Particolare del margine craniodorsale dell'ala preacetabolare dell'ileo destro, dove si trova una piccola concavità. Scala metrica = 1 mm. Vedi Appendice 1 o risvolti di copertina per le abbreviazioni.

of a sacral vertebral centrum underneath, which during diagenetic crushing was sandwiched between the left and right ilia (see Sacral Vertebrae).

The right ischial peduncle of *Scipionyx* is partly covered cranially by the right femur, whereas the left one is indistinctly visible. As far as can be seen, the squared end of the ischial peduncle extends ventrally as much as the pubic peduncle, as seems to be the case in *Compsognathus* (Peyer, 2006: fig. 7) and *Ornitholestes* (Carpenter *et al.*, 2005b). In *Juravenator* (Göhlich & Chiappe, 2006), the ischial peduncle is more expanded ventrally, whereas in *Sinosauropteryx* the pubic peduncle is only slightly longer than the ischial one (Currie & Chen, 2001), as is the case also in the basal tyrannosauroid *Guanlong* (Xu *et al.*, 2006) and in the basal ornithomimosaur *Sinornithomimus* (Kobayashi & Lü., 2004).

In *Scipionyx*, *Compsognathus*, *Huaxiagnathus* (Hwang *et al.*, 2004) and *Sinosauropteryx* (Currie & Chen, 2001), as well as in most tetanuran theropods (Rauhut, 2003; Holtz *et al.*, 2004), the pubic peduncle is very large in lateral aspect, and craniocaudally expanded, whereas the ischial peduncle is fairly small. In contrast, *Juravenator* (Göhlich & Chiappe, 2006) has a well-developed ischial peduncle.

In *Scipionyx*, the cranial and the caudal margins of the pubic peduncle are distinctly concave, and the ventral margin has a low central peak, so the whole process appears fan-like in lateral view. In *Mirischia*, *Juravenator* (Göhlich *et al.*, 2006: pl. 7, fig. 2), the basal tyrannosauroids *Stokesosaurus* (Rauhut, 2003) and *Guanlong* (Xu *et al.*, 2006), and *Ornitholestes* the pubic peduncle is expanded cranially, so that its cranial margin is con-

cave as well. Because of the mentioned low central peak, the articular surface of the pubic peduncle in *Scipionyx* is gently convex, like in *Mirischia* (Naish *et al.*, 2004).

Caudal to the ischial peduncle, the medial wall of the *brevis fossa* (i.e., the “medial blade” *sensu* Currie & Zhao, 1993a) appears in lateral view as a robust triangular ala, strengthened by ridged buttresses. The lateral wall of the *brevis fossa* consists of a marked lateral ridge that caudally joins the ventral margin of the postacetabular ala. The postacetabular ala terminates in a caudal truncation. The ilium is caudally squared (i.e., “truncated”) in many theropods, with the exception of *Ornitholestes* and the Maniraptor (Rauhut, 2003), in which it tapers, and *Huaxiagnathus* (Hwang *et al.*, 2004), in which it is gently rounded.

Pubis - The right and left pubes run coupled perpendicularly to the long axis of the ilium and parallel to the right femur, very close to its cranial margin (Figs. 97-98). Except for the ischial process, hidden by the right femur, the right pubis is well-exposed in lateral view. The fact that the dorsal extremity of its apron is exposed, partially covered by the intestine, suggests that this thin bony lamina bent caudally during sliding of the right pubis onto, and cranially towards, the left one. In contrast, the apron of the left pubis bent cranially, and now emerges obliquely from the plane of the fossiliferous slab as a tall, thin crest running along nearly half the length of the entire pubis. A photograph taken with a grazing view (Fig. 100) reveals that the top of the crest divides the cranial face and the caudal face of the apron itself. Part of the medial side of the left pubis emerges to the left of the caudal

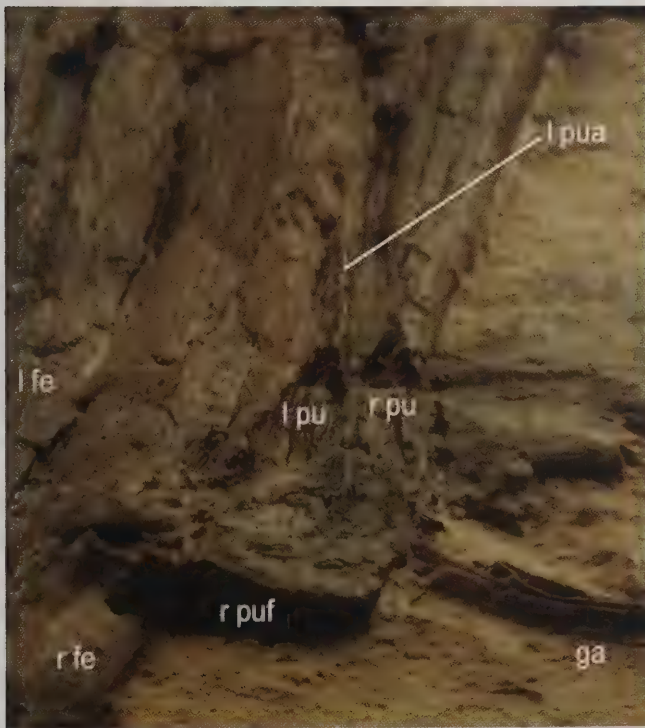


Fig. 100 - Grazing view of the pubic bones of *Scipionyx samniticus*. The top of the crest, indicated by the white line, divides the cranial face from the caudal face of the left pubic apron. See Appendix 1 or cover flaps for abbreviations.

Fig. 100 - Vista radente delle ossa pubiche di *Scipionyx samniticus*. La sommità della cresta indicata dal connettore divide la faccia craniale del grembiule pubico sinistro da quella caudale. Vedi Appendice 1 o risvolti di copertina per le abbreviazioni.

face: it is marked by a deep groove, by a further change of plane and by a more rugose texture, and overlaps the shaft of the right femur for a short tract. The left apron does not extend ventrally up to the distal end of the pubis. The ventral interruption of the left apron indicates the presence of an elongate, oval opening (pubic foramen) that was located ventral to the conjoined aprons of the pubes and dorsal to their distal ends. Such an opening is present in the Ceratosauria and the vast majority of the Tetanurae (Rauhut, 2003), including compsognathids (e.g., Naish *et al.*, 2004) but not *Ornitholestes* (Carpenter *et al.*, 2005b). According to Martill *et al.* (2000), this opening may have accommodated a ventral pneumatic duct leading to a post-pubic air sac.

The pubis of *Scipionyx* measures about 2/3 of the length of the femur, like in the basal troodontid *Sinornithoides* (Russell & Dong, 1993). The length of the pubis is approximately that of the femur in *Compsognathus* (Ostrom, 1978; Peyer, 2006), *Coelurus*, *Ornitholestes* (Carpenter *et al.*, 2005b) and *Sinornithomimus* (Kobayashi & Lü, 2004); is 3/4 and 4/5 the length of the femur respectively in the specimens NIGP 127586 (Currie & Chen, 2001: fig. 1a) and NIGP 127587 (Currie & Chen, 2001: fig. 1b) of *Sinosauropteryx*; and is 3/4 the length in *Sinocalliopteryx* (fig. 3c) and *Dilong* (Xu *et al.*, 2004: suppl. info).

Proximally, the pubis contacts the ilium through an expanded, well-rimmed iliac process, which shows a faintly concave articular margin complementary to the fan-like pubic peduncle of the ilium. Proximocaudally, the pubis of *Scipionyx* tapers to form an ischial process that, although covered by the right femur, can be seen with a CT scan (Fig. 101). The ischial process seems quite short and rectangular in outline, and incised ventrally by an obturator notch that is very similar in size to that of *Compsognathus* (Peyer, 2006).

As mentioned above, the pelvis of *Scipionyx* is orthopubic: the pubes form a right angle with the long axis of the body. The pubic shaft is definitely slender, straight in lateral view and, based on the observable relief, is also rod-shaped in cross-section. It terminates in a distinct foot with a finely pitted surface. The right pubic foot, previously thought to be hidden by the right femur (Dal Sasso & Signore, 1998a: fig. 2), is, in fact, entirely exposed but difficult to see except under proper light orientation (Fig. 102) because it is tightly appressed onto the lateral wall of the femur. As first suggested by Audatore (pers. comm., 2008) during preparation of his drawings for this monograph, the low bump seen at the same level under the right femur represents the underlying left pubic foot (Figs. 98, 102), a fact confirmed by CT scan. The pubic foot has the shape of a wooden golf-club and lacks the cranial process; caudally it projects to form a process four times longer craniocaudally than the minimum craniocaudal diameter of the pubic shaft. In the compsognathids *Compsognathus* (Peyer, 2006), *Huaxiagnathus* (Hwang *et al.*, 2004), *Sinocalliopteryx* (Ji *et al.*, 2007a), *Mirischia* (Naish *et al.*, 2004) and *Aristosuchus* (Naish *et al.*, 2001), the pubic foot also projects only caudally, but it is definitely longer (i.e., half or more than half as long as the pubic shaft) and more pointed than in *Scipionyx*, in which the limited development of this bone is probably due to its earlier ontogenetic stage (see Ontogenetic Assessment). *Sinosauropteryx* represents an exception among compsognathids (Currie & Chen, 2001): in this

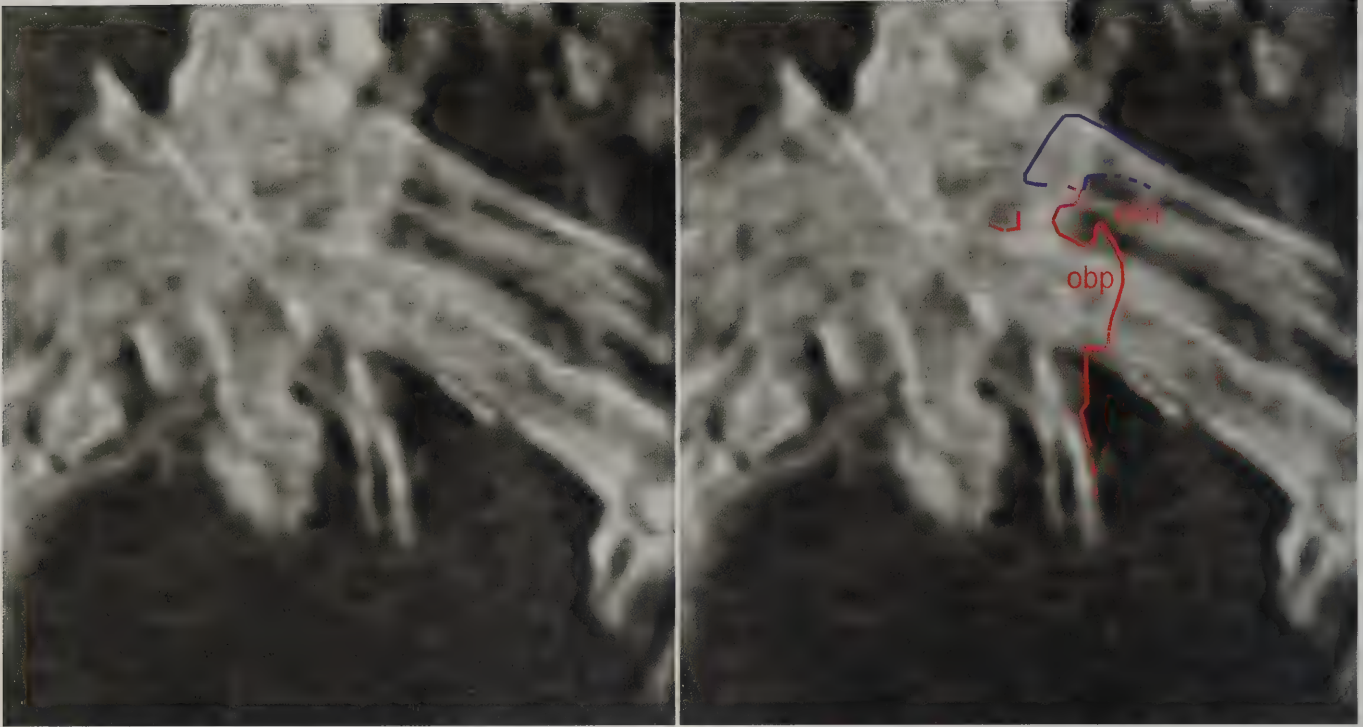


Fig. 101 - Computed tomography of the pelvic region of *Scipionyx samniticus*. A parasagittal slice between the two femora, virtually cutting the right ischium (red) and the right pubis (blue), reveals that the exposed portion of the obturator process continues into an axe-shaped lamina. See Appendix 1 or cover flaps for abbreviations.

Fig. 101 - Tomografia computerizzata della regione pelvica di *Scipionyx samniticus*. Una fetta parasagittale tra i due femori, che taglia virtualmente l'ischio destro (rosso) e il pube destro (blu), rivela che la porzione esposta del processo otturatore continua in una lamina a forma di scure. Vedi Appendice 1 o risvolti di copertina per le abbreviazioni.

taxon, the pubic foot expands caudally from the shaft of the pubis but bears also a moderate cranial expansion, as seen in basal tyrannosauroids *Dilong* (Xu *et al.*, 2004), *Tanycolagreus* (Carpenter *et al.*, 2005a) and *Coelurus* (Carpenter *et al.*, 2005b), in which the pubic foot is in any case definitely larger (more than half the pubic length). The cranial expansion is larger in *Guanlong* (Xu *et al.*, 2006), advanced tyrannosauroids and ornithomimosaur (e.g., Kobayashi & Lü, 2004). In *Nqwebasaurus*, the pubis expands equally cranially and caudally into a small, mediolaterally narrow pubic foot with a very indistinct outline (de Klerk *et al.*, 2000), whereas in oviraptorosaurs

and therizinosauroids it has a well-developed cranial process and a caudal process of variable length (Osmólska *et al.*, 2004). In deinonychosaurs and birds, the caudal projection of the pubic foot is again reduced to a round knob or is completely absent (e.g., Xu *et al.*, 1999; Burnham *et al.*, 2000; Elzanowski, 2002; Russell & Dong, 1993; Makovicky & Norell, 2004).

The minimum diameter of the pubic shaft equals the minimum diameter of the ischium, as is the case in *Sinornithomimus* (Kobayashi & Lü, 2004). The shaft of the ischium is more slender than the pubic shaft in *Huaxiagnathus* (Hwang *et al.*, 2004: fig. 9), *Compsognathus*

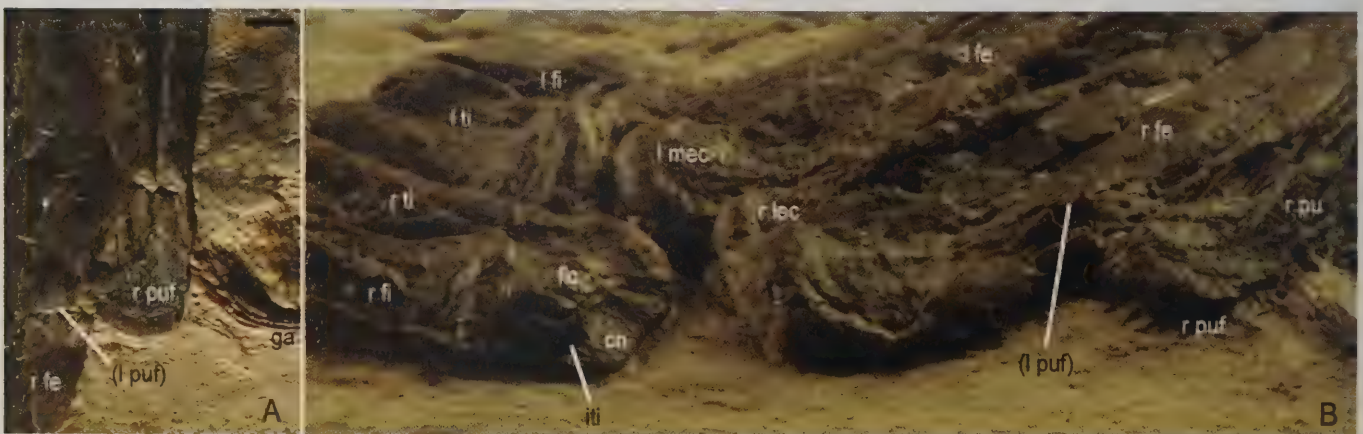


Fig. 102 - Photographs taken in perpendicular (A) and grazing (B) view of the right pubic foot and knee joints of *Scipionyx samniticus*. Scale bar = 2 mm. See Appendix 1 or cover flaps for abbreviations.

Fig. 102 - *Scipionyx samniticus*. A) piede pubico destro; B) vista radente dello stesso e delle articolazioni delle ginocchia. Scala metrica = 2 mm. Vedi Appendice 1 o risvolti di copertina per le abbreviazioni.

(Peyer, 2006: fig. 7), *Sinosauropteryx* (Currie & Chen, 2001: fig. 10) and, probably, *Sinocalliopteryx* (Ji *et al.*, 2007a: fig. 3c), and is even more slender in *Ornitholestes* (Carpenter *et al.*, 2005b), where it is about half the diameter of the pubic shaft. On the other hand, the ischial shaft is more robust than the pubic shaft in the basal tyrannosauroid *Guanlong* (Xu *et al.*, 2006), and is even more robust in deinonychosaurs and birds (e.g., Russell & Dong, 1993; Norell & Makovicky, 2004; Padian, 2004), where the diameter of the ischial shaft is up to twice the diameter of the pubic shaft.

Ischium - The distal halves of both ischia are exposed, parallel to one another and projecting caudoventrally at an angle of about 54° with the pubic shafts (Figs. 97-98). The shaft of the right ischium, interrupted by a vertical fracture that occurred in the fossiliferous slab, continues cranially to the fracture overlapping onto the medial surface of the left femur. Here, as in the mid-distal portion of the ischial shaft, the surface of the ischium can be easily distinguished from the surface of the femur because of the smoother texture of the preserved periosteum (see Periosteal Remains). In this area, the ischium abruptly widens to form an obturator process that served as an attachment for the ischial head of the *M. puboischiofemoralis externus* (Hutchinson, 2001). In *Scipionyx*, the distal portion of the obturator process, which is not covered by the right femur and is more clearly visible under UV light (Fig. 103), appears squared and forms a right angle with the shaft of the ischium rather

than a ventrodistal notch. The ventrodistal notch is absent also in *Sinocalliopteryx* (Ji *et al.*, 2007a), *Huaxiagnathus* (Hwang *et al.*, 2004), *Compsognathus* (Peyer, 2006), *Dilong* (Xu *et al.*, 2004: fig. 2), *Ornitholestes* (Carpenter *et al.*, 2005b: fig. 3.10A), the oviraptorosaurs (Osmólska *et al.*, 2004), the therizinosauroids (Kirkland *et al.*, 2005) and the dromaeosaurids (Xu *et al.*, 1999; Burnham *et al.*, 2000; Hwang *et al.*, 2002). Unlike *Scipionyx*, however, in all these taxa the obturator process gradually rises from the shaft of the ischium and forms a pointed triangular process. This triangular morphology, resulting from the absence of the notch at the distal base of the obturator process, has been considered by Rauhut (2003) to be a reversal of a derived character within theropods. The scenario is complicated by *Sinosauropteryx*, in which a triangular morphology and the notch are present (Currie & Chen, 2001), and by *Mirischia* (Naish *et al.*, 2004), in which a triangular morphology and the notch are present in the right ischium but not in the left one.

The obturator process of *Scipionyx*, as can be seen from CT scans, is not triangular, even proximally: apart from the squared distal base, its proximal outline is definitely axe-shaped (Fig. 101). An obturator notch opens proximally, separating the cranial margin of the obturator process and the ischial process. A similar obturator notch is found in *Compsognathus* and in most coelurosaurs. Unlike *Scipionyx* and other tyrannosauroids (and more generally the Coelurosauria), but like more basal tetanurans, in *Guanlong* (Xu *et al.*, 2006) the notch is replaced by a relatively large foramen. The compsognathid *Mirischia asymmetrica*, as its name celebrates, has a pelvic foramen on the left ischium and a notch on the right element.

Distally, the ischia of *Scipionyx* are expanded into two small, cranially hooked ischial feet, the craniocaudal diameter of which is twice the minimum craniocaudal diameter of the ischial shafts. The ischial foot of the Italian compsognathid is very similar to that of *Compsognathus* (Peyer, 2006), *Sinosauropteryx* NIGP 127587 (Currie & Chen, 2001: fig. 10), *Huaxiagnathus* (Hwang *et al.*, 2004), *Sinocalliopteryx* (Ji *et al.*, 2007a), *Ornitholestes* (Carpenter *et al.*, 2005b) and, possibly, *Dilong* IVPP V 11579 (Xu *et al.*, 2004: fig. 2j), albeit slightly more expanded in some of these taxa (e.g., *Compsognathus*). The ischial foot is also similar but variably expanded in ornithomimosaur (Rauhut, 2003), whereas, unlike *Scipionyx*, the ischium tapers distally to a point in the compsognathid *Mirischia* (Naish *et al.*, 2004) and in many Maniraptora and tyrannosaurids (Hutchinson, 2001; Rauhut, 2003).

The ischial feet of *Scipionyx* have a finely pitted texture and raised borders. A flat facet (Fig. 104) is exposed on the medial side of the left one; in life, this facet probably formed a symphysis with the opposite (right) facet, but it is not possible to assess if they remained unfused during ontogeny or later co-ossified, possibly in relation to gender. Some soft tissue remains are preserved on the caudal tip of the left ischial foot of *Scipionyx*, as well as cranially and caudally to both shafts (see Pelvic And Hindlimb Muscles).

Except for the well-exposed distal end, the left ischium is less complete than the right one. Its caudal margin, marked distally by a small fracture, can be followed up to the large crack in the slab, where it becomes vertical. The medial wall of the bone is lost, unveiling its internal aspect, just right to this vertical caudal margin. A possible



Fig. 103 - The pelvis of *Scipionyx samniticus* under ultraviolet-induced fluorescence. See Appendix 1 or cover flaps for the abbreviation.

Fig. 103 - Il cinto pelvico di *Scipionyx samniticus* visto in fluorescenza indotta da luce ultravioletta. Vedi Appendice 1 o risvolti di copertina per l'abbreviazione.



Fig. 104 - Close-up of the ischial feet of *Scipionyx samniticus*. Scale bar = 1 mm. See Appendix 1 or cover flaps for abbreviations.

Fig. 104 - Particolare dei piedi ischiatici di *Scipionyx samniticus*. Scala metrica = 1 mm. Vedi Appendice 1 o risvolti di copertina per le abbreviazioni.

proximal portion of the left ischium can be seen between the 5th sacral centrum and the medial wall of the *breviss fossa* (Fig. 105). It consists of a knob-like caudal bump, possibly representing the contact with the ilium, and a free cranial margin, that we tentatively regard as the proximo-medial contribution to the acetabulum. We consider this proximal portion as being the left ischium, also because it is in ideal continuity with the vertical caudal margin of this bone and lies on a similar sagittal plane. In fact, it is covered either by the centrum of S5 or by the intestine.

Measured from the iliac suture to the distal end, the ischium of *Scipionyx* is estimated to be about 75% the

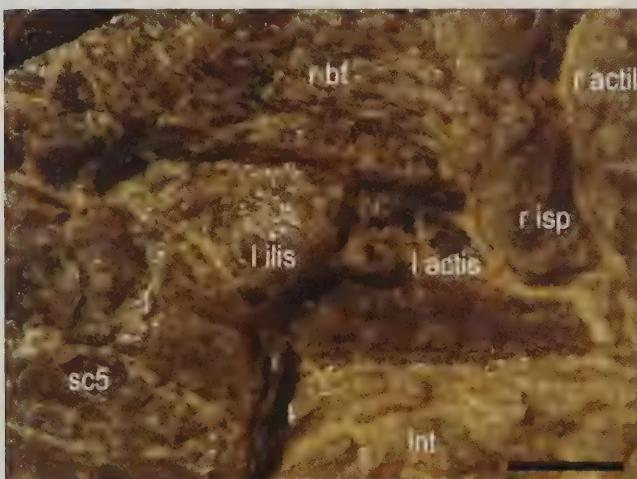


Fig. 105 - Close-up of a bone here interpreted as the only exposed proximal portion of the left ischium of *Scipionyx samniticus*. Scale bar = 1 mm. See Appendix 1 or cover flaps for abbreviations.

Fig. 105 - *Scipionyx samniticus*. Particolare di un osso qui interpretato come l'unica parte esposta della porzione prossimale dell'ischio sinistro. Scala metrica = 1 mm. Vedi Appendice 1 o risvolti di copertina per le abbreviazioni.

length of the pubis, as is the case in *Ornitholestes* (Carpenter *et al.*, 2005b), *Falcaris* (Kirkland *et al.*, 2005: fig. 1g) and *Sinornithomimus* (Kobayashi & Lü, 2004). The ischium is slightly longer in *Guanlong* (80%-Xu *et al.*, 2006: fig. 2e), slightly shorter in *Sinocalliopteryx* (70%-Ji *et al.*, 2007a), *Sinosauropteryx* (66-70%-Currie & Chen, 2001), *Huaxiagnathus* (66%-Hwang *et al.*, 2004), *Compsognathus* (64%-Peyer, 2006), most ornithomimosaur (around 60%-Makovicky *et al.*, 2004) and *Caudipteryx* (60%-Zhou *et al.*, 2000: tab. 1), and much shorter in deinonychosaurs (more or less about 50% the length of the pubis [Norell & Makovicky, 1997; Xu *et al.*, 1999; Burnham *et al.*, 2000; Hwang *et al.*, 2002; Russell & Dong, 1993]).

Hindlimb

The crack crossing the pelvic girdle of *Scipionyx* continues all along the caudal margin of the left femur and, in the end, transversely cuts the bones of the crus (tibiae and fibulae) not distant from the knee joint. In all likelihood, that crack is responsible for the irremediable loss of the distal portions of the hindlimb when the calcareous slab was collected. Thus, the length of the tibia and fibula can be estimated only (see Skeletal Reconstruction And...). Whatever the length of the crus, the hindlimbs would have been well-developed, as indicated by the femur/humerus ratio (143%). Like in the bones of the forelimbs, the thin walls of the femora are partly collapsed in some areas, revealing spacious, hollow internal cavities. In *Scipionyx*, the craniocaudal length of the proximal end of the fibula is about 85% the craniocaudal length of the proximal end of the tibia and, thus, falls within the range of values (equal or greater to 75%) for Coelurosauria (Holtz *et al.*, 2004).

Femur - The thigh bone is the largest preserved element of the skeleton of *Scipionyx* (Figs. 97-98). It is almost straight, being slightly bowed cranially, like in other compsognathids (Currie & Chen, 2001; Hwang *et al.*, 2004; Naish *et al.*, 2004; Peyer, 2006; Ji *et al.*, 2007a) and *Ornitholestes* (Carpenter *et al.*, 2005b), but unlike *Coelurus* (Carpenter *et al.*, 2005b) and the dromaeosaurids (e.g., Burnham *et al.*, 2000), in which the shaft is strongly bowed cranially and medially. In the right femur, the greater trochanter clearly emerges just below the supracetabular margin of the ilium, but the lateral aspect of the bone allows us to follow only its dorsal outline. The lateral aspect precludes also any information on the femoral head. The lesser (=cranial) trochanter is placed proximally at a lower level, but it is well-developed dorsoventrally and craniocaudally into a squared end and seems to be separated from the femoral shaft by a narrow cleft. The lesser trochanter can be defined as "alariform" ("wing-like" in Gauthier, 1986) because, in dorsal view, its end has a lenticular shape, is mediolaterally flattened and is craniocaudally elongate. A similarly developed, plate-like lesser trochanter, separated from the greater trochanter by a narrow cleft, is present in *Compsognathus* (Peyer, 2006), *Juravenator* (Göhlich & Chiappe, 2006), *Huaxiagnathus* (Hwang *et al.*, 2004), *Sinosauropteryx* (Currie & Chen, 2001) and in a number of basal tetanurans and basal coelurosaurs (Rauhut, 2003). It markedly differs from the condition seen in most Maniraptora, in which

it is fused to the very well-developed greater trochanter, forming a high crest. No accessory trochanter, homologous to that of the ornithomimosaurids, present more or less in the vicinity of the cranial base of the cranial (lesser) trochanter (e.g., Kobayashi & Barsbold, 2005), is visible in *Scipionyx*. In contrast, a trace of this accessory trochanter is visible in the compsognathids *Mirischia* (Naish *et al.*, 2004) and *Aristosuchus* (Naish *et al.*, 2001), which exhibit a peculiar bifid, craniodorsally directed trochanter: this trochanter was regarded by Hutchinson (2001b) as a fused accessory and lesser trochanter, and according to him it probably represents a primitive feature for coelurosaurids and not a shared derived similarity between these two compsognathids. An accessory trochanter distal to the lesser trochanter is reported also in the tyrannosauroid *Guanlong* and in some oviraptorosaurs and dromaeosaurids (Xu *et al.*, 2006). In *Scipionyx*, the caudolateral trochanter seems to be absent, as in *Compsognathus* (Peyer, 2006). Because of their caudomedial orientation, the fourth trochanters, if well-developed, should be visible in the right and left femora. No trace of this fourth trochanter can be seen on the right femur of *Scipionyx*, whereas the left femur is covered by the ischial shaft in that area. Therefore, we cannot establish whether the fourth trochanter was feebly developed or totally absent. The fourth trochanter is absent in *Compsognathus* (Peyer, 2006), coded as absent or greatly reduced in *Juravenator* (Göhlich & Chiappe, 2006), present as a low ridge (i.e., greatly reduced) in *Coelurus* (Carpenter *et al.*, 2005b), *Mirischia* (Naish *et al.*, 2004) and *Aristosuchus* (Naish *et al.*, 2001), and strongly reduced to a weakly developed crest or a slight depression, or even entirely absent, in *Ornitholestes* (Carpenter *et al.*, 2005b), *Tanycolagreus* (Carpenter *et al.*, 2005a) and most of the Maniraptoriformes (Rauhut, 2003). The fourth trochanter is reported

to be present, but was not described, in *Sinosauropteryx* (Currie & Chen, 2001), and is prominent in *Dilong* and *Guanlong* (Xu *et al.*, 2006).

Distally, the femoral epicondyles of *Scipionyx* slightly protrude in respect to the caudal margin of the diaphysis. Comparing the left medial epicondyle with the left and right lateral epicondyles, the latter appear larger than the former, the ratio of the cranio-caudal extension of the lateral to medial one being 4/3. The marked separation between medial and lateral epicondyles, well-visible in the distal epiphysis of the left femur (which is exposed in medio-caudal view), suggests that the popliteal fossa is open distally (Figs. 106-107).

Tibia - Of the tibiae of *Scipionyx*, only the proximal epiphyses and probably less than half of the diaphyses are preserved, exposed mostly in lateral (right) and medial (left) views (Figs. 97-98). The right tibia is also partly rotated, showing a small portion of its caudal wall. The cnemial crest of *Scipionyx* is weakly developed, as in most small-bodied tetanuran theropods, including compsognathids (Currie & Chen, 2001; Hwang *et al.*, 2004; Göhlich & Chiappe, 2006; Peyer, 2006; Ji *et al.*, 2007a). The fibular condyle is well-distinct and well-developed: cranially, as is the case in tetanurans, including many coelurosaurids (Rauhut, 2003), it is separated from the cnemial crest by a narrow and deep notch, the *incisura tibialis* (Figs. 102B, 106); caudally, as in most theropods (Rauhut, 2003), it is separated from the internal condyle and the main body of the tibia by a deep caudal cleft (Figs. 106-107). The latter is visible in the form of a well-excavated sulcus also in the left tibia.



Fig. 106 - Close-up of the crura of *Scipionyx samniticus*. The arrow points to the caudal cleft separating the fibular condyle from the internal condyle and the main body of the tibia. Scale bar = 2 mm. See Appendix 1 or cover flaps for abbreviations.

Fig. 106 - Particolare delle crura (gambe) di *Scipionyx samniticus*. La freccia indica la fenditura caudale che separa il condilo fibulare dal condilo interno e dal corpo principale della tibia. Scala metrica = 2 mm. Vedi Appendice 1 o risvolti di copertina per le abbreviazioni.

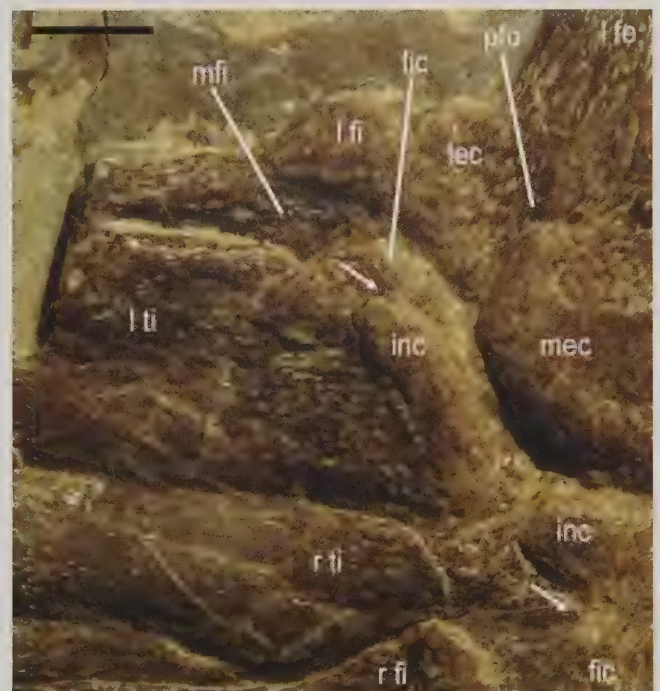


Fig. 107 - Close-up of the proximal epiphyses of the left tibia and fibula of *Scipionyx samniticus*. The arrow points to the caudal cleft shown also in Fig. 106. Scale bar = 2 mm. See Appendix 1 or cover flaps for abbreviations.

Fig. 107 - Particolare delle epifisi prossimali di tibia e fibula sinistre di *Scipionyx samniticus*. La freccia indica la fenditura caudale mostrata anche in Fig. 106. Scala metrica = 2 mm. Vedi Appendice 1 o risvolti di copertina per le abbreviazioni.

Fibula - Like the tibiae, the fibulae of *Scipionyx* preserve only their proximal epiphyses and a short tract of their diaphyses (Figs. 97-98). This is particularly true for the left fibula, which is preserved for a distance less than half that of the right one. The fibula is slender and medio-laterally compressed, the lateral surface is convex, and the dorsal margin is equally convex and seems to be able to accommodate an extensive contact with the fibular condyle of the tibia. Among compsognathids, a comparable concavity is present in *Compsognathus* (Peyer, 2006), whereas it seems particularly shallow in *Sinosauropteryx*

(Currie & Chen, 2001). However, possible diagenetic deformation of the curvature of the fibular condyle leads us to consider this condition in *Scipionyx* with caution. On the left fibula, a fossa can be seen on the medial surface near its proximal end (Fig. 107): therefore, as in many theropods (Rauhut, 2003), except, for instance, *Coelurus* (Carpenter *et al.*, 2005b), the concave dorsal margin seen on the right element would continue in this medial fossa. The marked, gradual distal tapering of the preserved right fibula suggests that the missing diaphyseal portion of this bone was very slender, as is often the case in coelurosaurs.

Table 1 - Selected numbers and measurements (in mm) of the skeleton of the holotype of *Scipionyx samniticus*. Symbols: ~ approximate measurement; - measurement not possible; ? incomplete or partially covered element. Where not specified, height or width or diameter are taken perpendicular to the length. Diameter refers to both craniocaudal and mediolateral measurements, or to any intermediate plane, according to the exposed view of each element.

General	Right	Left
Preserved body length (premaxilla to Ca9)	237.0	
Estimated body length (whole tail included)	~461.0	
Presacral length (skull included)	164.7	
Presacral length	113.0	
Cervical length	44.0	
Dorsal length	69.0	
Estimated sacral length	23.0	
Preserved caudal length	50.5	
Gleno acetabular length (at acetabular cranial margin)	63.0	-
Forelimb length (humerus to end of phalanx II-3)	78.7	-
Manual digit I length	16.2	14.8
Manual digit II length	?18.6	25.0
Manual digit III length	~17.1	18.3

Skull	Right	Left
Skull length (premaxilla to quadrate)	48.9	
Maximum skull length	51.7	
Skull height (frontal to jugal)	28.5	
Reconstructed skull height above orbit	~22.5	
Antorbital length (premaxilla to lacrimal)	22.8	-
Supratemporal fenestra length	6.7	-

Supratemporal fenestra height	4.0	-
Infratemporal fenestra length	6.3	-
Infratemporal fenestra height	12.8	-
Orbit length	17.1	-
Orbit height	18.2	-
Antorbital fenestra length	7.9	-
Antorbital fenestra height	8.6	-
Maxillary fenestra length	1.7	-
Maxillary fenestra height	4.3	-
Promaxillary fenestra length	0.7	-
Promaxillary fenestra height	1.5	-
<i>Apertura nasi ossea</i> length	6.3	-
<i>Apertura nasi ossea</i> height	2.8	-
Frontal length	22.8	-
Frontal maximum width	13.0	-
Nasal length	18.9	-
Prefrontal length	10.0	-
Lacrimal length of horizontal ramus	8.7	-
Lacrimal height of vertical ramus	11.8	-
Maxilla length	23.2	-
Maxilla height	10.6	-
Pterygoid length	?31.8	-
Number of scleral plates	16-18	

Mandible	Right	Left
Hemimandible length	-	47.3

Estimated hemimandible length at glenoid	-	~44.4
Reconstructed hemimandible maximum height (above surangular)	~7.9	-
Dentary length	29.3	-
Dentary height at mid-length	4.2	-
Ceratobranchial I length	18.7	?18.0
Ceratobranchial I minimum mid-shaft diameter	0.7	~0.8

Teeth	Right	Left
Upper tooth row length	18.4	-
Lower tooth row length	19.5	-
Premaxillary tooth row length	4.4	-
Maxillary tooth row length	13.0	?12.7
Number of upper teeth (pm+m)	12 (5+7)	
Number of lower teeth	10	
Largest pm tooth (pm2) crown height	3.0	-
Largest pm tooth (pm2) fore-aft basal length	1.3	-
Largest m tooth (m4) crown height	4.0	?3.8
Largest m tooth (m4) fore-aft basal length	1.5	-
Largest dentary tooth (d3) crown height	2.3	-
Largest dentary tooth (d3) fore-aft basal length	1.3	-
Serrations per mm in maxillary teeth (distal carina)	11-12	
Serrations per mm in dentary teeth (distal carina)	13	

Axial skeleton		
Cervical vertebrae length= exposed length at centrum height= height of neural arch (top of spine to base of arch)	Length	Height
C1	-	5.6
C2	4.8	7.4
C3	4.3	5.3
C4	4.5	5.8
C5	4.7	6.2

C6	~4.7	6.7
C7	4.9	6.1
C8	5.4	6.0
C9	~5.0	6.0
C10	4.9	7.0
Dorsal vertebrae length= exposed length at centrum height= height of neural arch (top of spine to base of arch)	Length	Height
D1	5.1	6.4
D2	4.9	?5.4
D3	-	6.0
D4	?4.6	5.3
D5	?3.7	?3.8
D6	?6.3	6.9
D7	?5.7	?5.0
D8	~5.9	?4.5
D9	6.0	~7.4
D10	6.5	~6.8
D11	-	?4.9
D12	6.3	5.8
D13	6.3	6.7
Sacral vertebrae length= exposed length at centrum height= height of neural arch (top of spine to base of arch)	Length	Height
S1	7.4	8.1
S2	-	-
S3	-	-
S4	-	?6.2
S5	5.1	?4.8
Caudal vertebrae length= exposed length at centrum height= height of neural arch (top of spine to base of arch)	Length	Height
Ca1	5.4	4.9
Ca2	5.4	5.4
Ca3	5.6	4.7
Ca4	5.7	4.2
Ca5	7.4	5.3
Ca6	6.6	4.8

Ca7	6.8	4.5
Ca8	77.1	4.1
Ca9	-	73.1
	Length	Min. diameter
Chevron 4	8.1	0.7
Chevron 5	6.7	0.7
Cervical ribs linear length	Right	Left
Cr2	9.2	9.1
Cr3	14.3	78.5
Cr4	79.2	73.0
Cr5	76.0	-
Cr6	76.0	-
Cr7	15.9	712.2
Cr8	73.2	75.5
Cr9	12.8	72.1
Cr10	78.9	71.6
Dorsal ribs linear length	Right	Left
Dr1	15.6	71.5
Dr2	22.1	710.7
Dr3	26.1	~25.4
Dr4	~27.1	722.3
Dr5	721.4	717.8
Dr6	30.6	719.7
Dr7	30.0	721.1
Dr8	~24.3	-
Dr9	21.5	~27.0
Dr10	715.9	712.9
Dr11	715.4	711.4
Dr12	15.3	79.3
Dr13	70.7	-
Sacral ribs length	Right	Left
Sr1	-	-
Sr2	-	-
Sr3	-	-

Sr4	~4.6	-
Sr5	~6.4	-
Gastralia	Right	Left
Chevron-shaped gastralium linear length	78.50	
Chevron-shaped gastralium maximum shaft diameter	0.48	
Cranial medial gastralium linear length (best exposed element)	9.50	-
Cranial medial gastralium maximum shaft diameter (best exposed element)	0.32	-
Cranial lateral gastralium linear length (same row)	10.30	-
Mid-medial gastralium linear length (best exposed element)	9.20	-
Mid-medial gastralium maximum shaft diameter (best exposed element)	0.19	-
Mid-lateral gastralium linear length (same row)	76.30	-
Caudal medial gastralium linear length (best exposed element)	7.80	-
Caudal medial gastralium maximum shaft diameter (best exposed element)	0.26	-
Caudal lateral gastralium linear length (same row)	-	-

Pectoral girdle and forelimbs	Right	Left
Scapula length	23.8	-
Scapula maximum dorsal width	4.3	-
Scapula minimum midshaft width	3.0	-
Scapula maximum ventral width	~8.4	-
Coracoid width	10.8	11.4
Coracoid height	6.8	6.8
Furcula width	~12.0	
Furcula angle between two rami	~125°	
Humerus length	26.3	725.4
Humerus proximal diameter	6.8	-
Humerus minimum mid-shaft diameter	3.4	-
Humerus distal diameter	6.0	73.5

Radius length	?16.1	17.5
Radius minimum mid-shaft diameter	1.9	-
Ulna length	?17.8	19.3
Ulna minimum mid-shaft diameter	1.8	-
Proximal carpal diameter	1.7	?1.4
Distal carpal diameter	3.0	2.4
Metacarpus width (mCI-III)	5.2	4.9
Metacarpal I length	4.0	4.0
Metacarpal I minimum mid-shaft diameter	1.7	?1.5
Metacarpal II length	10.6	10.6
Metacarpal II minimum mid-shaft diameter	?1.6	?1.6
Metacarpal III length	8.7	8.6
Metacarpal III minimum mid-shaft diameter	?1.5	?1.1
Manual phalanx I-1 proximal diameter	2.5	2.5
Manual phalanx I-1 length	~9.5	9.1
Manual phalanx I-2 (ungual) maximum length	8.2	?6.6
Manual phalanx II-1 length	~6.7	7.3
Manual phalanx II-2 length	10.2	10.4
Manual phalanx II-3 (ungual) maximum length	?1.7	8.1
Manual phalanx III-1 length	2.9	3.1
Manual phalanx III-2 length	?2.6	3.1
Manual phalanx III-3 length	6.7	7.4
Manual phalanx III-4 (ungual) maximum length	?4.9	6.1

Pelvic girdle and hind limbs	Right	Left
Ilium length	~26.7	-
Ilium preacetabular length	11.0	-
Ilium postacetabular length	~9.4	-
Ilium height at pubic process	~11.5	-
Ilium height at supracetabular margin	5.9	-
Pubis length	27.3	-
Pubis minimum shaft diameter	1.1	-
Pubic foot length	4.6	-
Ischium length	~20.4	-
Ischium minimum shaft diameter	1.6	?1.4
Ischial foot length	3.1	-
Femur length	37.3	-
Femur proximal diameter	7.1	-
Femur minimum mid-shaft diameter	~4.8	-
Femur distal diameter	6.4	?7.0
Tibia preserved length	14.7	8.5
Tibia proximal diameter	5.5	4.7
Tibia minimum preserved shaft diameter	4.6	-
Fibula preserved length	14.5	4.7
Fibula proximal diameter	4.1	-
Fibula minimum preserved shaft diameter	1.8	-

Table 2 - Anatomical proportions of the holotype of *Scipionyx samniticus* (selected ratios).

Skull / Presacral	0.48
Skull / Femur	1.39
Humerus / Femur	0.71
Forelimb / Presacral (skull included)	0.48
Orbit / Skull	0.33
Humerus / Scapula	1.11

Radius / Humerus	0.67
Manus / Forelimb	0.42
Length/width of McI-III	2.00
Length digit III / digit I	1.23
Pubis / Femur	0.73
Pubis / Ischium	~1.34

ONTOGENETIC ASSESSMENT

Introduction - Although several individuals of embryonic, hatchling and juvenile dinosaurs have been found and described especially in recent years (e.g., Coombs, 1982; Horner & Currie, 1994; Norell *et al.*, 1994; Mateus *et al.*, 1998; Carpenter, 1999; Norell *et al.*, 2001; Xu *et al.*, 2001; Varricchio *et al.*, 2002; Rauhut & Fechner, 2005; Reisz *et al.*, 2005; Goodwin *et al.*, 2006; Schwarz *et al.*, 2007a; Balanoff *et al.*, 2008; Kundrát *et al.*, 2008; Bever & Norell, 2009), the fossil record of theropods representing early stages of skeletal ontogeny with well-preserved cranial material, remains extremely poor (e.g., Rauhut & Fechner, 2005; Bever & Norell, 2009). *Scipionyx* is one of these few theropods and is probably the best preserved one. It was identified as a juvenile individual by Dal Sasso & Signore (1998a, 1998b) and as probably a hatchling by Holtz *et al.* (2004), who pointed out the difficulty in determining whether the generally plesiomorphic condition of this dinosaur is due to a primitive position of the taxon in the coelurosaur tree or to the early ontogenetic stage of the type specimen. Therefore, recognition of the ontogenetic stage of *Scipionyx samniticus* is important for two aspects: it is critical for proper anatomical comparison and subsequent interpretation of character states in this species (see Phylogenetic Analysis); and it may improve our understanding of skeletal development and its phylogenetic patterns within Theropoda and, in the final analysis, of the evolutionary history of this group.

In assessing the ontogenetic stage of *Scipionyx*, it must be taken into account that ontogeny of a genus or of a “family-level” taxon does not exist (Steyer, 2003). Developmental events can occur at different times along the ontogenetic trajectories of different lineages, even in strictly related taxa. Therefore, a growth series within a unique species, with intraspecific variations, is needed to study its development.

Unfortunately, *Scipionyx samniticus* is known only from a single specimen, and virtually no growth series are known among its closest relatives, the Compsognathidae. *Juravenator*, *Huaxiagnathus* and *Sinocalliopteryx* are also known from single specimens. The only species represented by more than one specimen are *Compsognathus* and *Sinosauropteryx*. According to Peyer (2006), who based her interpretation not merely on whole body size, both specimens of *Compsognathus longipes* are juveniles, with the German specimen – the holotype described by Ostrom (1978) – being more immature than the French specimen. Concerning *Sinosauropteryx*, few specimens have been described to date: Currie & Chen (2001) considered the small holotype NIGP 127586 a juvenile, and specimen NIGP 127587 a young adult – more precisely, an animal of reproductive age and probably approaching mature size, but still young, when it died; the specimen described more recently by Ji *et al.* (2007b) is intermediate in size, but its poor preservation renders it difficult to compare it with the other specimens and to recognise whether it is also intermediate ontogenetically. Göhlich & Chiappe (2006) considered *Juravenator* a juvenile, based on features such as bone texture and the degree of fusion of the neural arches. Hwang *et al.* (2004) briefly commented on the ontogenetic assessment of *Huaxiagnathus*, suggesting that it is juve-

nile (but see Incomplete Ossification Of The Vertebral Column), whereas *Sinocalliopteryx* (Ji *et al.*, 2007a), which is the largest compsognathid known, seems to be a mature animal.

Therefore, as mentioned above, a developmental sequence for any compsognathid species is still not known, and it is not our intention to reconstruct one for the whole Compsognathidae taxon based on these composite data, as we consider this practice inadequate and unorthodox. However, some allometric trends may be tentatively identified and discussed for *Scipionyx*, based on comparisons with other compsognathids (considered in their aforementioned ontogenetic stages) and theropods, and sometimes extending the comparison to other extinct and extant archosaurs and, more generally, vertebrates, with the aim of assessing the ontogenetic stage of *Scipionyx*.

Dal Sasso & Signore (1998a) interpreted *Scipionyx* as a juvenile, based on the following set of characters: general body proportions; high skull/presacral length ratio; short antorbital region; large, circular orbit; many unfused skeletal elements (scapulocoracoids, sternal plates, sacral vertebrae); several neural arches separated from their centra; symmetry of tooth development as an indication that the first replacement had not yet occurred; and low denticle count. All these characters that potentially give some indication of the ontogenetic stage of the holotype of *Scipionyx samniticus*, plus some new ones, are discussed in detail in the following paragraphs.

Gut contents - The first, unequivocal datum useful for assessing the ontogenetic stage of *Scipionyx* is the presence of gut contents (see Gut Contents And Feeding Chronology): this clearly indicates that the individual is not embryonic.

Scarred bone surfaces - Incomplete ossification of the periosteum is particularly evident in the long bones of sauropod embryos from the Morrison Formation, USA (Britt & Naylor, 1994) and Auca Mahuevo, Patagonia (Salgado *et al.*, 2005), and in the embryonic theropods from Lourinhã, Portugal (Mateus, pers. comm., 2005). In these embryos, the periosteum exhibits the porous appearance typical of embryonic and hatchling archosaurs (Bennett, 1993; Sanz *et al.*, 1997; Horner, 2000; de Ricqlès *et al.*, 2000). Such a porous appearance, with furrows and pits producing a “scarred” effect, tends to disappear gradually during growth, as can be inferred from fossil specimens and clearly seen in extant birds (Chiappe, pers. comm., 2006). The scarred effect is marked on the long bones of the juvenile theropods, such as *Sinornithoides* (Currie & Dong, 2001) and *Juravenator* (Göhlich & Chiappe, 2006), in immature extant crocodylians (Dal Sasso & Maganuco, pers. obs., 2010, on a *Crocodylus niloticus* hatchling; Fig. 108A) and birds, and in the young adult *Sinosauropteryx* (Currie & Chen, 2001). A striated bony texture characterises also the maxilla from Guimarães (Portugal) referred to an early post-hatching individual by Rauhut & Fechner (2005). The extensive “scarred” texture of the bone surfaces of *Scipionyx* (e.g., on the external surface of the lower jaw, scapular blade and femoral shaft; Fig. 108B-D) closely resembles that of embryos and hatchlings, rather than that of late juvenile or young adult individuals. Al-

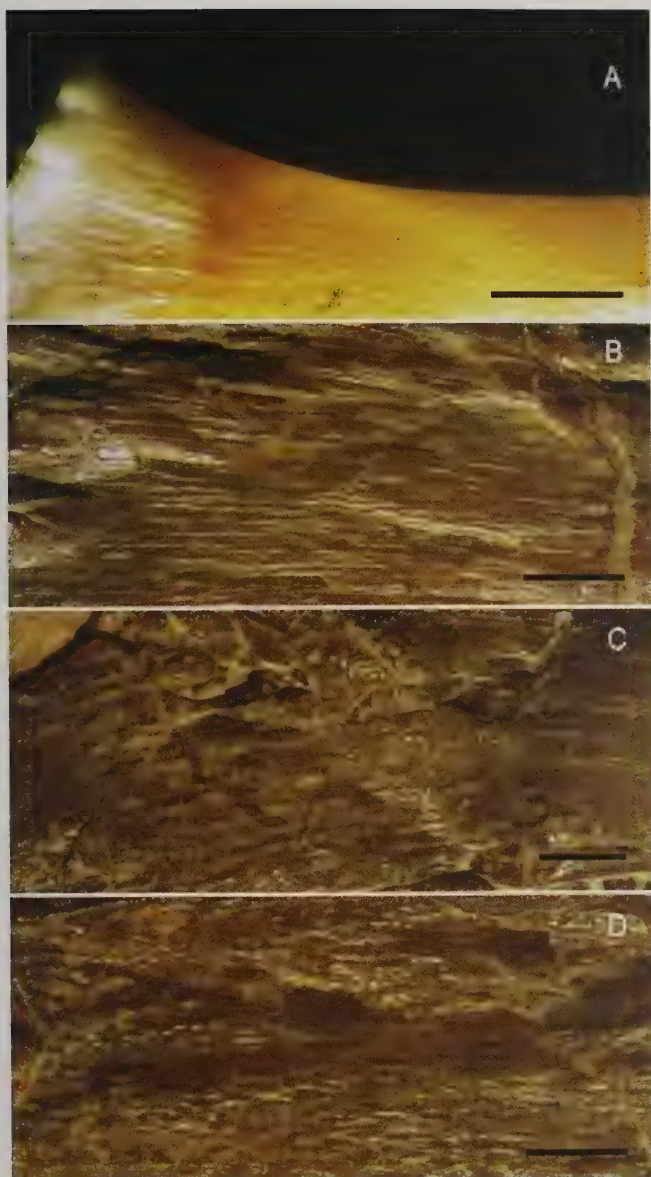


Fig. 108 - The bone surface of a *Crocodylus niloticus* hatchling (A, femur) is comparable in texture with that of *Scipionyx samniticus* (B, dentary; C, scapula; D, femur). Scale bar = 1 mm.

Fig. 108 - Tessitura ossea fittamente solcata sul femore di un *Crocodylus niloticus* neonato (A), messa a confronto con la tessitura, del tutto analoga, presente sulle ossa di *Scipionyx samniticus* (B, dentale; C, scapola; D, femore). Scala metrica = 1 mm.

so, this scarred aspect does not look in any way like that seen as a consequence of exaggerated bone reabsorption in older, stressed crocodiles (Huchzermeyer, 2003: fig. 6.10) or like the well-developed pits and grooves forming articular rugosities in the articular surfaces of mature specimens of the sauropod *Camarasaurus* (Schwarz *et al.*, 2007b). Thus, the intensively scarred bone surface clearly indicates that *Scipionyx* is not a mature animal, and that it is more likely a hatchling.

Large skull - The skull of *Scipionyx* is very large with respect to its body. The skull/presacral length ratio (0.48) is higher than in the vast majority of the well-known adult theropods (e.g., Weishampel *et al.*, 2004) but comparable to that of the tyrannosaurids, some compsognathids (see below) and some dromaeosaurids (e.g., Ostrom, 1969; Burnham *et al.*, 2000). The carcharodontosaurids, the re-

cently found long-snouted tyrannosauroids (e.g., Li *et al.*, 2009) and the gondwanan dromaeosaurids (e.g., Novas *et al.*, 2008b) are too incomplete in the postcranium to permit any comparison. A negative growth allometry of the skull respect to the postcranium is common in most extant and extinct vertebrates: compared with the rest of the body, the juvenile skull is relatively larger than the adult one. A similar estimation can be obtained by comparing the length of the skull to that of the femur. In the holotype of *Compsognathus*, the skull length is 72 mm, representing some 40% of the length of the presacral vertebral column. In the French *Compsognathus*, the skull is long and slender and has a reconstructed maximal length of 100 mm, i.e., about 30% of the length of the presacral vertebral column (as in Peyer [2004]; *contra* Peyer [2006], who reported that the skull is 22% of the length of the presacral vertebral column but, according to figures and measurements, it is in reality 22% of the whole presacral length, skull included). The skull/presacral length ratio in *Sinosauropteryx* ranges from 0.5 in the smallest individual to 0.35 in the other two, although in the third, poorly preserved specimen (Ji *et al.*, 2007b), this ratio cannot be measured with precision based on the published photographs. The remaining well-known compsognathids are represented by a single specimen each, all of them having a large skull, with a ratio possibly greater than 0.5 in *Juravenator*, approaching 0.5 in *Huaxiagnathus* and greater than 0.4 in *Sinocalliopteryx*.

Summing up, the Compsognathidae have a proportionally large skull in early/late juveniles or adults. So, based on the available data, it is not clear whether the comparatively large size of the skull of *Scipionyx* can be interpreted as a juvenile trait or a representative feature which would have been maintained, with little or no modification, during ontogeny, as seems to occur in some compsognathid species such as – at least – *Sinocalliopteryx gigas*.

Therefore, juvenile features must be ascribed to the skull based on the shape and the proportions of its various elements/portions, rather than on overall skull size with respect to the rest of the body. A similar conclusion can be drawn for the hyoids, which seem to be oversized in *Scipionyx* at first glance (Holtz, pers. comm., 1998). The skull/hyoid length ratio is 2.6 in *Scipionyx*, about 3.6 in *Huaxiagnathus* and 3.7 in *Sinosauropteryx* (Ji *et al.*, 2007b). A close value (i.e., 2.5) is found in the French *Compsognathus* (Peyer, 2006), which has a head that is comparatively smaller than that of *Scipionyx*. Large hyoids are present also in *Proceratosaurus*, in which the ratio is 2.2 (Rauhut *et al.*, 2009). A ratio of 4.2 can be estimated for *Bambiraptor* (Burnham *et al.*, 2000). Based on those data it appears that, as expected, the size of the hyoids parallels that of the head.

Orbital foramina rounded and proportionally very large and antorbital region short and deep - In juvenile dinosaurs, as in the vast majority of extant and extinct vertebrates, the snout is relatively short and deep (e.g., Norell *et al.*, 1994), and the orbits are proportionally large with respect to the length of the skull (e.g., Coombs, 1982; Carpenter, 1994; Horner & Currie, 1994; Weishampel *et al.*, 2004; Rauhut & Fechner, 2005; Reisz *et al.*, 2005; Tykoski, 2005; Goodwin *et al.*, 2006; Kundrát *et al.*, 2008). These characters are size- and age-related, and are subjected to strong allometry in relation to other portions of the skull

during growth (e.g., Currie & Dong, 2001). In particular, the orbits are subjected to negative allometry, as they tend to become relatively smaller. They reach their maximum relative size in embryos, as exemplified by the titanosaur embryos preserving the skull (Salgado *et al.*, 2005), in which the orbits are at least 50% of the skull length.

The orbits are relatively large and rounded in shape in species represented by immature individuals, such as *Compsognathus longipes* and *Juravenator starki*, but also in many adult theropods which attained small-to-medium body size in adulthood, independently of their phylogenetic affinities (e.g., Currie, 2003; Weishampel *et al.*, 2004). This can be seen in the juvenile holotype and in the young adult individual of *Sinosauropteryx prima* described by Currie & Chen (2001): although both suffered *post mortem* dorsoventral crushing, it is interesting to note that although the largest specimen has a larger skull, the orbits were reconstructed with approximately the same shape and absolute size. The orbits are subjected to a stronger negative allometry in the adults of species that attained a large body size (e.g., tyrannosaurids), in which they also become keyhole shaped.

In small- to medium-sized coelurosaurs, the antorbital portion of the skull tends to increase in length much more than the orbital and postorbital portions, showing a strong positive allometry. As a consequence, both orbits and frontals appear larger in juveniles. The orbits of *Scipionyx* are intermediate in size between those of the embryos and other juveniles. In *Scipionyx*, the orbit is twice as long as the antorbital fenestra (Fig. 26), just like in the juvenile specimens IVPP-V11797-10 and IVPP-V11797-11 of *Sinornithomimus* (Kobayashi & Lü, 2003) and in the perinate *Byronosaurus* IGM (= MGI) 100/972 (Bever & Norell, 2009), in which the snout looks even shorter than in *Scipionyx*. In a therizinosauroid embryo (Kundrát *et al.*, 2008), the length of the orbit is at least three times that of the antorbital fenestra, which is higher than it is long (longer than high in adult *Erlikosaurus*). In juvenile individuals, such as the dromaeosaur *Bambiraptor* (specimen FIP 001 [Burnham *et al.*, 2000]) and the compsognathids *Huaxiagnathus*, *Juravenator*, *Sinosauropteryx* and *Compsognathus*, the antorbital fenestra approaches in length that of the orbit, whereas it is equal or even longer in the putative mature holotype of *Sinocalliopteryx*. In the Guimarota hatchling referred to *Allosaurus* (specimen IPFUB Gui Th 4 [Rauhut & Fechner, 2005]), only the maxilla is preserved and, similar to *Scipionyx*, it is short and high, with an almost vertical rostral margin of the antorbital fenestra and a low maxillary body. Certainly, *Scipionyx* and most of the other theropods, including non-coelurosaurs tetanurans (e.g., Rauhut & Fechner, 2005) and non-tetanuran taxa (e.g., Tykoski, 2005), show the opposite condition to that of the tyrannosaurid coelurosaurs, in which the snout is already elongate in juveniles, and there is little ontogenetic change in the relative length of the antorbital fenestra during growth (Currie, 2003). Thus, based on these data, the relative size of the orbit in relation to the antorbital fenestra indicates that the *Scipionyx* specimen is a hatchling or an early juvenile.

Position of the maxillary fenestra - In lateral view, the maxillary fenestra of *Scipionyx* is located more dorsally and more rostrally than in the other compsognathids, and its rostral margin coincides with that of the antorbital fossa (Fig. 26). As a consequence, the maxillary fenestra

seems to be bordered by the maxillary medial wall of the antorbital fossa only caudally and ventrally. In the other compsognathids, the maxillary fenestra opens within the maxillary medial wall of the antorbital fossa, so that part of this wall is visible rostrally to the rostral margin of the maxillary fenestra in lateral view, separating the latter from the rostral margin of the antorbital fossa. The condition in *Scipionyx* might be related to the immaturity of the specimen and/or to the consequent shortness of its snout.

An opposite trend can be seen in the ontogenetic series of *Tyrannosaurus* (Carr & Williamson, 2004: fig. 6) and in other tyrannosaurids (e.g., Currie & Dong, 2001): the maxillary fenestra, which appears within the maxillary medial wall in juveniles, migrates towards the rostral margin of the antorbital fossa in adults, in parallel with the growth of the snout, which becomes bulkier.

Rostral ramus of the maxilla - In *Scipionyx*, the rostral ramus of the maxilla is little developed and is shorter than high (Fig. 29). In *Juravenator* and in the holotype of *Sinosauropteryx*, it is slightly longer than high. In *Huaxiagnathus* and *Sinocalliopteryx*, it is almost twice as long as high, and in the French *Compsognathus* (Peyer, 2006) it is intermediate in size. Although no ontogenetic series is known for compsognathids, this portion of the maxilla undergoes, in all likelihood, great elongation during ontogeny (see also Maxilla).

Unfused interdental plates - Contrary to Dal Sasso & Signore (1998a), unfused interdental plates (Fig. 30) are not necessarily indicative of the juvenile stage of *Scipionyx*. As a matter of fact, they are unfused also in many other compsognathids (see Maxilla) and do not fuse even in the late adult of tyrannosaurid coelurosaurs (e.g., Currie *et al.*, 2003).

Nasals shorter than frontals - The nasals in *Compsognathus* (Peyer, 2006) and *Juravenator* (Göhlich & Chiappe, 2006) are proportionally much longer than in *Scipionyx* and make up almost half of the length of the skull. They are even longer in *Sinocalliopteryx*. In adult theropods, the nasals are shorter than the frontals only in oviraptorosaurs (Rauhut, 2003). In the perinatal skull of *Byronosaurus* (Bever & Norell, 2009), the nasal is comparable in length to the frontal. Unfortunately, the frontal is not preserved in more mature individuals (Norell *et al.*, 2000). The nasal/frontal length ratio is approximately 1/3 in the therizinosauroid embryo and 1/1 in the adult *Erlikosaurus* (Kundrát *et al.*, 2008). The presence of shorter-than-frontal nasals in *Scipionyx* (Figs. 24, 25A) supports its immaturity and suggests that, together with the maxilla, the nasals undergo positive allometric growth associated with a rostral elongation of the snout region during postnatal ontogeny. A similar pattern of positive allometric growth of the nasals has been reported in the growth series of the skull of the prosauropod dinosaur *Massospondylus* (Reisz *et al.*, 2005).

Position of the caudal margin of the apertura nasi ossea - In *Scipionyx*, the caudalmost portion of the naris terminates slightly caudally to the rostralmost border of the antorbital fossa (Fig. 26; see Apertura Nasi Ossea). *Scipionyx* is the only compsognathid with such a partial, virtual overlapping, although a similar condition occurs

in *Huaxiagnathus*, where the caudal margin of the naris seems to reach the level of the rostral margin of the fossa. According to Chiappe (pers. comm., 2006), the condition in *Scipionyx* might be related to the immaturity of the specimen and to the shortness of its snout, in particular of the rostral ramus of the maxilla and of the nasals. This, however, cannot be definitely demonstrated, as the same overlapping occurs in the basal tyrannosauroids *Proceratosaurus* (Woodward, 1910) and *Guanlong* (Xu *et al.*, 2006), and in other more derived coelurosaurids such as *Incisivosaurus* (Xu *et al.*, 2002a), *Sinovenator* (Xu *et al.*, 2002b) and *Archaeopteryx* (Elzanowski, 2002); moreover, the two margins are very close in *Dilong*, *Ornitholestes* (Osborn, 1916: fig. 1; Rauhut, 2003: fig. 5H) and, potentially, in the already mentioned *Huaxiagnathus*.

Shape of the lacrimal - In *Scipionyx*, the horizontal ramus of the lacrimal is shorter than the vertical ramus (Fig. 25A). In *Juravenator*, which is a juvenile specimen, both rami are subequal in length. In the French *Compsognathus*, a late juvenile, and in *Sinocalliopteryx*, an individual close to maturity, the horizontal ramus is longer than the vertical ramus. The condition in *Scipionyx* likely reflects its earlier ontogenetic stage.

Large prefrontals, with descending lateral process well-exposed in lateral view - In *Scipionyx*, the prefrontal is large and robust, is rostrocaudally longer than the horizontal ramus of the lacrimal, and has a descending lateral process that is well-exposed in lateral view (Fig. 25A). Brochu (2003) proposed that in tyrannosaurids the prefrontals are ontogenetically ephemeral structures that gradually merge with the lacrimals. In perinates *Byronosaurus*, there is no evidence of separate prefrontal ossification, as described for in other troodontids (Bever & Norell, 2009). The prefrontal is absent in *Archaeopteryx*, too, and in all other birds (e.g., Elzanowski, 2002). In contrast, the prefrontal is present and visible in lateral view in a large number of coelurosaurids, including compsognathids, basal tyrannosauroids, therizinosauroids (where it is comparatively larger in the embryos [Kundrát *et al.*, 2008]), alvarezsaurids and ornithomimosaurids, being particularly large in some ornithomimosaur species (for further comparisons, see Prefrontal). Thus, among coelurosaurids, *Scipionyx* is unusual particularly in the ventral prolongation of the bone and in its comparatively large size, although it is not as large as in the ornithomimosaurids. Based on the present data, it is impossible to establish to what extent the comparatively large size and exposition of this bone in *Scipionyx* is related to its early ontogenetic stage (i.e., earlier than that of any other compsognathid), or if this is a characteristic of the taxon that would have persisted in adults, or partly both.

Sublacrimal expansion of the jugal - The horizontal body of the jugal of *Scipionyx* lacks any sublacrimal expansion (Fig. 25A). The same occurs in other juveniles, such as *Compsognathus* (Peyer, 2006) and *Juravenator* (Göhlich & Chiappe, 2006). On the other hand, the possibly early adult *Huaxiagnathus* (Hwang *et al.*, 2004: 2a) shows a feeble expansion, whereas the mature *Sinocalliopteryx* has a distinct expansion (Ji *et al.*, 2007a: Fig. 2b). The condition in the immature individuals might reflect their earlier ontogenetic stage.

Frontoparietal fontanelle open - The skull roof of *Scipionyx* unequivocally has a frontoparietal fontanelle (see Frontal), which is well-open (Figs. 23-34). As reported by Balanoff & Rowe (2007), the frontoparietal fontanelle is a diamond-shaped space between the paired frontals and parietals, the size of which is an indicator of age (i.e., the larger the opening, the younger the specimen). In extant crocodylians, there are no signs of a frontoparietal fontanelle after hatching (Kundrát *et al.*, 2008; Brochu, pers. comm., 2009). The same occurs in the Triassic sauropodomorph *Mussaurus*, in which there are no signs of a frontoparietal fontanelle in either post-hatching or subadult specimens (Pol & Powell, 2007). According to Salgado *et al.* (2005), there is a frontoparietal fontanelle in titanosaur embryos from the Upper Cretaceous of Patagonia. The existence of a frontoparietal fontanelle has been proposed in *Diplodocus*, *Camarasaurus*, *Dicraeosaurus* and *Amargasaurus* (Salgado *et al.*, 2005; and reference therein). In the last two genera, the fenestra remains open in adults, whereas in the remaining taxa it is apparently present only in immature individuals.

Unfortunately, few data are available for Mesozoic theropods. A frontoparietal fontanelle has been identified in the perinates referred to the troodontid *Byronosaurus* (Bever & Norell 2009). In contrast, no signs of an opening were recognised on the caudomedial edge of the frontal in a therizinosauroid embryo (Kundrát *et al.*, 2008). No signs of the frontoparietal fontanelle have been reported either in the other immature theropods, including compsognathids, in all likelihood because none of these specimens is of a hatchling and at the age of death, the fontanelle, even if present when hatching, was probably already closed.

More data are available for extant avian theropods. In the zebra finch, *Taeniopygia castanotis*, which leaves the nest 21 days after hatching, the frontoparietal fontanelle greatly decreases in size between days 24-27 and finally disappears after 36 days (Serventy *et al.*, 1966). The same trend can be seen in the Indian weaver bird, *Ploceus philippinus*, which leaves the nest 17-18 days after hatching, and has the complete closure of the fontanelle around day 40 (Biur & Thapliyal, 1972). In the ratites *Struthio* and *Rhea*, the fontanelle does not close until well-after hatching, and is still well-visible for 10 days (Balanoff, pers. comm., 2009).

Based on these composite data, we can suppose that the frontoparietal fontanelle remained open in hatchling coelurosaurids, disappearing a few weeks later, just like in some extant forms. If this postnatal trajectory is confirmed within coelurosaurids or more inclusive nodes, then the presence of a comparatively large frontoparietal fontanelle in *Scipionyx* indicates that it could have had no more than two weeks when it died.

Elements of the braincase in loose contact - The visible elements of the braincase of *Scipionyx* have loose contacts (Fig. 25C). Among the examples of uncontroversial ontogeny-related characters present in most dinosaurs is co-ossification and fusion of braincase elements (e.g., Tykoski, 2005). The condition of *Scipionyx* is the one expected in a juvenile individual; nevertheless, this does not help to clarify its degree of maturity because the fusion of these elements occurs at different times along the ontoge-

netic development of different theropod taxa, and often close to maturity; moreover, some interorbital braincase elements do not ossify at all by adulthood in some lineages (e.g., Carrano *et al.*, 2002).

Vomers unfused to each other all along their length - Madsen (1976) reported that “evidently the vomers are not paired in *Allosaurus fragilis*, but, if they are, fusion must occur embryonically because even the smallest, apparently juvenile, examples show no separation”. The vomers are indeed fused for nearly all their length in many adult theropods (e.g., Clark *et al.*, 2002; Currie, 2003; Holtz *et al.*, 2004). The condition in *Scipionyx* in all likelihood reflects its early ontogenetic stage (Figs. 25C-D, 37). It must be taken into account, however, that there are some exceptions among adult individuals of coelurosaurs, such as *Incisivosaurus*, in which the vomers are unfused along most of their length and are fused only dorsally at the rostral end of the element (Balanoff *et al.*, 2009), and *Velociraptor*, which is reported to be unique among theropods in having the vomers distinctly separated along their entire length (Barsbold & Osmolska, 1999).

Craniocaudal length of the dentary - In *Compsognathus* (Ostrom, 1978; Peyer, 2006), *Huaxiagnathus* (Hwang *et al.*, 2004), *Sinosauroptryx* (Currie & Chen, 2001) and *Juravenator* (Göhlich & Chiappe, 2006), the dentary is proportionally longer than in *Scipionyx*. This suggests that during ontogeny this bone undergoes greater elongation than the rest of the lower jaw. As for the snout, its relative shortness is another indication of the immaturity of the specimen.

Angular moved dorsally - As mentioned in the description of this bone, during diagenesis the right angular lost its contact with the dentary and has moved dorsally, partially overlapping the surangular (Fig. 25B). It is not possible to establish whether the weak sutural contact between the angular and the dentary is primarily linked to the ontogenetic stage of *Scipionyx* or to the presence of an intramandibular joint between the dentary and the postdentary bones, as is the case in most basal tetanurans (Holtz *et al.*, 2004).

Symmetrical tooth crown height in counterlateral tooth rows - The symmetrical development of the tooth series in the left and right tooth rows of *Scipionyx* (Figs. 24, 44-46) is consistent with tooth replacement having not yet started. As a matter of fact, there are no alveoli with erupting replacement teeth, with the possible exception of the right m3, which is slightly smaller than the left m3. Empty alveoli were clearly identified, for example, by Ostrom (1978) in the juvenile holotype of *Compsognathus*.

In archosaurs, tooth formation starts in embryos, and the first wave of teeth erupts before hatching. This has been observed, for example, in extant crocodylians (Martin, pers. comm., 2009), fossil theropods from Lourinhã, Portugal (Dal Sasso & Maganuci, pers. obs., 2005) and fossil titanosaurs from Patagonia (Salgado *et al.*, 2005). First replacement occurs in just weeks in hatchling crocodylians, and probably the same occurred in hatchling dinosaurs (Erickson, pers. comm., 2009). In *Alligator mississippiensis*, several generations of teeth are already

replaced during embryonal development and, after hatching, the first teeth of the functional group are expected to be shed after 3-4 weeks (Westergaard & Ferguson, 1990; Huchzermeyer, pers. comm., 2010). In archosaurs, tooth replacement rate seems to be faster in juveniles than in adults (Erickson, 1996a; D’Emic, pers. comm., 2009), possibly as a direct consequence of the very fast growth rate of the tooth-bearing bones at this developmental stage (Martin, pers. comm., 2009).

Concerning the tooth growth rate, some information can be inferred by the incremental lines of von Ebner: these are microstructural features that demarcate the daily apposition of dentin, such that the total number of incremental lines in a tooth serves as a measure of its age (Erickson, 1996a, 1996b; D’Emic, 2009). Given the uniqueness and the aesthetic value of the Italian compsognathid, we refused to thin-section a tooth of *Scipionyx* in order to count the incremental lines of von Ebner. However, because the incremental lines do not vary much in thickness in archosaur taxa (Erickson, 1996b), being around 10-20 μm each in most teeth, tooth-formation times are expected to be in the order of weeks in teeth such as those of *Scipionyx* (D’Emic, pers. comm., 2009).

Summing up, the fact that tooth replacement had not yet started, and the dimension of *Scipionyx*’s teeth both suggest that this individual was not more than a few weeks old at death.

Low number of lateral teeth - The dental formula in *Scipionyx* is 5pm+7m/10d teeth, whereas most non-avian theropods bear at least 11-12 teeth in the maxilla (Tykoski, 2005). The low number of lateral teeth in *Scipionyx* might either reflect a low number of teeth in this species or is related to ontogeny, as a consequence of the rostrocaudal shortness of the lateral tooth-bearing bones (the dentary and the maxilla). As these bones have been recognised among the elements which generally undergo greater elongation during ontogeny, the formation of new tooth positions would be expected during growth if the teeth maintain the same size relative to the dorsoventral depth of the bone. Concerning the maxilla, the formation of new tooth positions seems to occur in *Compsognathus longipes*: there are 17-18 maxillary teeth in the more mature French specimen, and 15-16 in the more immature German specimen, suggesting that this intraspecific variation might be related to ontogeny (Peyer, 2006). Rauhut & Fechner (2005) noted an increase in the number of maxillary teeth, from 13 to 16 (more rarely 15), in *Allosaurus fragilis* during postnatal ontogeny. Bever & Norell (2009) offered three possible interpretations of the small number (13-15) of maxillary teeth for a troodontid in the Mongolian perinates: it represents the retention of the plesiomorphic paravian condition (based on comparison with dromaeosaurs); it represents a secondarily derived condition within troodontids (this implies that the perinates belong to a new species of *Byronosaurus*); or *Byronosaurus* exhibits a significant postnatal increase in the number of maxillary teeth, without a significant relative increase in the length of the maxillary tooth row.

The number of maxillary teeth may increase through ontogeny also in basal sauropodomorphs (Galton, 1990) and ornithischians (Varricchio, 1997), whereas an opposite trend occurs in tyrannosaurids, in which the teeth undergo great changes during ontogeny: an increase in

tooth width is accompanied by a loss of 3-5 tooth positions (Carr, 1999). Based on Varricchio (1997) and Carr (1999), Rauhut & Fechner (2005) considered the increase in the number of maxillary teeth to be the plesiomorphic postnatal trajectory within Tetanurae, with coelurosaurs exhibiting a derived trajectory in which the number of maxillary teeth during postnatal growth either remained stable or decreased. *Compsognathus* and *Byronosaurus*, however, seem to indicate that the scenario is more complex within Coelurosauria.

Concerning the fact that most non-avian theropods bear at least 11-12 teeth in the maxilla, 12 maxillary teeth are indeed reported in the NIGP 127587 specimen of *Sinosauropteryx* (Currie & Chen, 2001). Only 6 maxillary teeth have been reported in *Sinocalliopteryx*, although at least 12 tooth positions seem to be present based on the right maxilla in medial view (Ji *et al.*, 2007a: fig. 2a). If this interpretation is correct, in that specimen there is an alternation of empty and occupied alveoli, reflecting the pattern visible in the lower jaw, which bears short and tall crowns. Ostrom (1978) interpreted the similar alternation of empty and occupied alveoli in *Compsognathus* as a direct evidence of the alternate pattern of the replacement of the teeth. A low number of maxillary teeth is reported for the remnant compsognathids: 8 maxillary teeth in *Juravenator* (Göhlich & Chiappe, 2006) and at least 8 maxillary teeth in *Huaxiagnathus*, although the tooth count in its maxilla is not clear (Hwang *et al.*, 2004). Comparatively few maxillary teeth are known also in other, not strictly related, small theropods, such as *Incisivosaurus* (9-Balanoff *et al.*, 2009), *Bambiraptor* (9-Burnham *et al.*, 2000), *Archaeopteryx* (8/9-Elzanowski, 2002) and *Noasaurus* and *Masiakasaurus* (10 or fewer-Tykoski & Rowe, 2004; Tykoski, 2005).

Summing up, based on all these data, we conclude that the maxillary tooth count may be affected not only by the ontogenetic stage of the individual but also by the overall body size attained by the species. This difficulty in the interpretation of the data and in the recognition of postnatal trajectories reflects both the scarcity of ontogenetic data and the complexity of theropod evolution.

Teeth with few denticles - In *Scipionyx*, denticles are present on the distal carinae of lateral teeth for 3/5 to 4/5 of the crown height in crowns not exceeding 3 mm in height; the denticle count is approximately 13 denticles per mm (Figs. 45-48). In the perinate theropods referred to *Byronosaurus* (Bever & Norell 2009), no serrations are present, as in the adult individuals of that taxon and of other troodontids. A comparison can be made with the ML565 specimen - a right maxilla of a theropod embryo from Lourinhã (Mateus *et al.*, 1998) - in which the best exposed maxillary crown measures no more than 1 mm in height, the basal half of the distal carina bears 4-5 well-developed denticles and the denticles gradually tend to disappear in the apical half (Mateus, pers. comm., 2004; Dal Sasso & Maganuco, pers. obs., 2004). In some theropods, the size of the denticles decreases at both apical and basal ends of the carinae, but even when this occurs, the denticles do not completely disappear in the apical half of the carina (e.g., Maganuco *et al.*, 2005; and references therein). Denticles that are well-developed only in the basal half of the carina might reflect the ontogenetic stage of the embryos from Lourinhã. The condition in *Scipionyx*

might be intermediate between that of these embryos and that observed in non-neonate juveniles and adult individuals of other species. More data are required in order to support or challenge this preliminary hypothesis.

Denticle size and density - Within a single theropod species, the absolute size of the denticles is related to tooth size, which in turn is related to skull size and body size, without any particular variation during ontogeny. In other terms, the teeth of the small juvenile individuals look like a scaled-down version of the teeth of the large adults of the same species. As a consequence, within a species the density per mm is higher in smaller individuals because they have smaller teeth. In all likelihood, therefore, the very high density of denticles in *Scipionyx* is related mostly to the absolute small size of the specimen, and does not help in the assessment of its ontogenetic stage. Among compsognathids, in fact, *Sinosauropteryx* has 11-14 denticles per mm, *Compsognathus* has no more than 12 denticles per serrated margin in crowns up to 4 mm high - although it must be taken into consideration that they are present only in the upper third of the distal carina where they are about 9 per mm - *Huaxiagnathus* has 7 denticles per mm and *Sinocalliopteryx*, which is the largest known genus, has about 4 denticles per mm.

Incomplete ossification of the vertebral column - In the postcranial skeleton, evidence that an archosaur was neither fully mature nor fully grown at death is provided by the incomplete ossification of the vertebral column (e.g., Currie & Zhao, 1993a; Brochu, 1996; Xu *et al.*, 2001; O'Connor, 2007; Schwarz *et al.*, 2007a). The pattern of closure of the neurocentral suture within Archosauria is not uniform. Kobayashi & Lü (2003) pointed out that in the holotype of *Sinornithomimus*, which is considered a juvenile individual, the neurocentral sutures are fused in all of the cervical vertebrae and in the first three dorsal vertebrae, whereas the rest are unfused. In the subadult *Majungasaurus* specimen described by O'Connor (2007), the postaxial cervical neural arches are fused to their respective centra, the first two dorsals are partially fused, the remainder of the dorsal vertebrae are unfused, the preserved sacra are fused, the other sacral components are not fused, as are neither some proximal caudals. Not completely fused neurocentral sutures are found also in the dorsal and caudal vertebrae of the holotype of *Garudimimus brevipes* (Kobayashi & Barsbold, 2005), whereas complete obliteration of the neurocentral suture can be seen in the allegedly super-precocial therizinosauroid embryo (Kundrát *et al.*, 2008). These examples - but many others are reported in the literature - suggest that in non-avian theropods the closure of the neurocentral sutures proceeds from the cervical vertebrae in a caudal direction, with the sacrum preceding most of the dorsals, as in extant chelonians, squamates (Rieppel, 1992a; 1992b; 1993) and birds (e.g., Norell *et al.*, 1994; Balanoff & Rowe, 2007). In contrast, in extant crocodylians closure of the neurocentral sutures follows a distinct caudal-to-cranial sequence (Brochu, 1996), with most of the caudal vertebrae showing fully closed sutures in hatchlings, even if the ossification sequence is craniocaudal as in the other extant diapsids. A caudocranial direction in the closure of the neurocentral sutures seems to be present also in sauropodomorph dinosaurs (Schwarz *et al.*, 2007a; and

references therein; see also *Respiratory Physiology*, this volume).

Whatever the direction of the sequence of closure of the neurocentral sutures, the process in *Scipionyx* was not yet started, as is the case in one oviraptorid embryo apparently close to hatching (Norell *et al.*, 1994; Norell *et al.*, 2001) and in one *Troodon* embryo (Varricchio *et al.*, 2002). In *Scipionyx*, many vertebrae of which are disarticulated and expose their neurocentral articular surfaces (i.e., C2-3, C5, C7-10; D1, D4-11; S1, S4-5; Ca1-3 and Ca5-6; Fig. 109), all neural arches are unfused to their

centra (Figs. 50, 56, 64, 67). In the few cases in which the arches are adjacent to their centra, the neurocentral sutures are well-marked. The neural arches preserved closest to their respective centra are those of the cervicals, and this condition is somewhat reminiscent of the sequence of closure of the neurocentral suture seen in other theropods. Over the length of the sacrum, all the visible axial elements are disarticulated (neural arches, neural spines, ?transverse processes and sacral ribs), whereas in mature archosaurs these elements coalesce and fuse to the medial walls of the ilia.

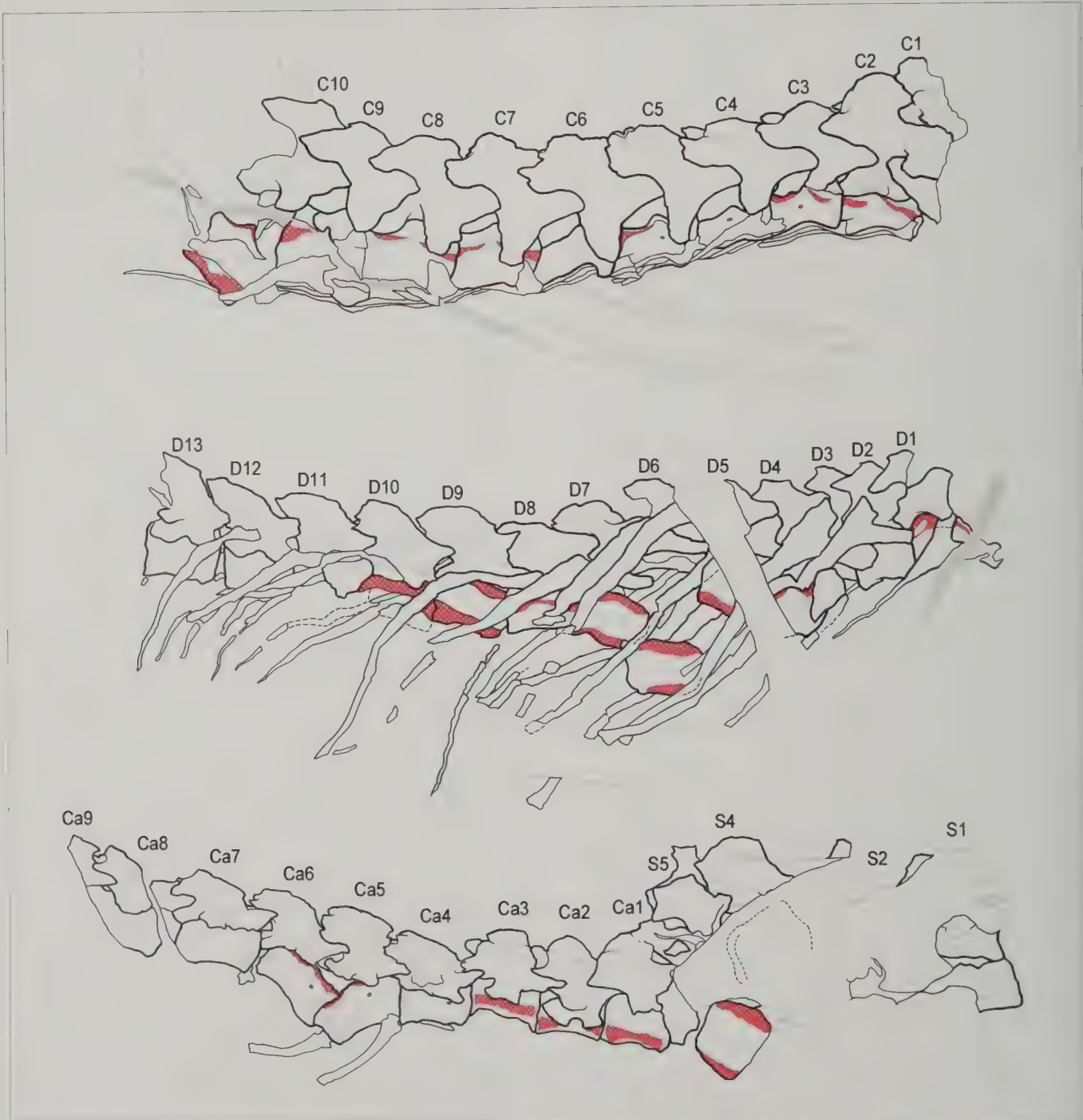


Fig. 109 - Line drawings highlighting the incomplete ossification of the vertebral column of *Scipionyx samniticus*. The red shading identifies the exposed neurocentral articular surfaces. See Appendix 1 or cover flaps for abbreviations.

Fig. 109 - Incompleta ossificazione della colonna vertebrale in *Scipionyx samniticus*. Il reticolo rosso evidenzia le superfici articolari neurocentrali esposte. Vedi Appendice 1 o risvolti di copertina per le abbreviazioni.

Among the other compsognathids, the French *Compsognathus* has sacrales that are tightly co-ossified, except for the last vertebra, i.e. the caudosacral (Peyer, 2006). According to Currie & Chen (2001), some evidence of immaturity can be seen in the axial skeleton of the holotype of *Sinosauropteryx* (specimen NIGP 127586). In this specimen, most of the centra and neural arches are not fused and a large attachment scar is present between the sacral centra for a sacral rib, which was apparently not fused to the sacral vertebrae at the time of death (a scar for an unfused sacral rib has been reported also in a juvenile dromaeosaurid by Norell & Makovicky [1997]). Göhlich & Chiappe (2006) reported the lack of fusion of sacral vertebrae and the presence of open neurocentral sutures in *Juravenator*. Hwang *et al.* (2004) supposed that the holotypic and only known individual of *Huaxiagnathus* may represent a juvenile, based on the unfused neural arches in the proximal caudals and the large size of the skull relative to the rest of the body. However, a large skull seems to be a feature common to most compsognathids (see Large Skull), and, from the published figures (Hwang *et al.*, 2004: fig. 4), the proximal caudals seem to be the only vertebrae in which the neural arches are detached from their centra. As the caudal vertebrae are the last to fuse in theropods, and the specimen also has well-ossified carpals and tarsals, *Huaxiagnathus* may have been a juvenile closer to maturity than previously considered. Lastly, given the above-mentioned pattern of closure of the neurocentral suture in theropods, *Sinornithoides youngi* may be actually an immature individual approaching maturity, as suggested by Currie & Dong (2001), based on the fact that, among other things, the neural arches are indistinguishably fused to the centra in the middle and distal regions of the tail.

Cervical ribs not fused to the corresponding vertebrae - The cervical ribs of *Scipionyx* are not fused to the corresponding vertebrae (Fig. 73). Lack of co-fusion of these elements has been considered as an indicator of immaturity (e.g., Currie & Dong, 2001). Although the cervical ribs are fused to their corresponding vertebrae in some adult coelurosaurs (e.g., Norell *et al.*, 2001), Tykoski (2005) reported that this is not the case in adults of most basal tetanuran taxa; the character is also widely distributed among non tetanurans. In those taxa that exhibit fusion in the adult, not all the cervical ribs fuse to their vertebrae. Moreover, the cervical ribs are fused with the corresponding vertebrae in the therizinosauroid embryo (Kundrát *et al.*, 2008), which was certainly immature. So, it is apparent that this character is not strictly controlled by ontogeny.

Regarding *Scipionyx*, we can conclude that the condition exhibited in the specimen is the one expected in immature individuals; however, although this cannot be used to prove the ontogenetic assessment hypothesised on the basis of the other data, it does not disprove it either.

Unfused girdle elements - In *Scipionyx*, the girdle elements are clearly unfused, with clearly visible lines of separation (Figs. 87-88, 97-98, 103). The coracoids are not fused to the scapulae in *Sinosauropteryx* (Currie & Chen, 2001), *Huaxiagnathus* (Hwang *et al.*, 2004), embryos of therizinosauroids (Kundrát *et al.*, 2008) and in

juvenile coelophysoids (Tykoski & Rowe, 2004); however, scapula and coracoid are clearly fused in adults of the latter group and of many other ones (e.g., Weishampel *et al.*, 2004). The same lack of fusion characterises the ends of the paired pubes in many taxa (e.g., Currie & Dong, 2001). Therefore, unfused girdle elements are often related to immaturity of the individuals. To complicate the scenario, however, it must be taken into account that the production of hormones (relaxin or relaxin-like) in reproductive females of various vertebrates affects the complete closure of some sutural contacts, such as the pubic symphysis, which remains elastic to permit passage of the eggs/foetuses. Similarly, it may have affected the process in dinosaurs, as hypothesised for the pubic symphysis of some adult *Allosaurus* specimens (Madsen, 1976; and reference therein).

Relative size of the girdle elements - Girdles are comparatively small in size in immature theropods such as the juveniles of *Albertosaurus* and the hatchlings of *Lourinhanosaurus* (Mateus, pers. comm., 2004): as for the ilium, this bone appears smaller, and craniocaudally shorter compared to total body length, than what is expected in adults (Mateus, pers. comm., 2004). A comparatively short ilium is observed in *Scipionyx* (Figs. 21-22). A similar condition is visible in *Sinosauropteryx*, in which the ilium is conspicuously shorter than both skull and femur, especially in the smallest specimen, NIGP 127586 (Currie & Chen, 2001), but it must be noted that an ilium that is relatively small and shorter than the femur is found also in other compsognathids, including the large and probably adult holotype of *Sinocalliopteryx* (Ji *et al.*, 2007a).

More precise data are available about the pubic foot. The pubic foot of *Scipionyx* (Figs. 98, 102A), although developed caudally, is comparatively less developed than in other compsognathids considered ontogenetically older (Chiappe, pers. comm., 2006). Size and shape of the pubic foot change through ontogeny in *Ceratosaurus* (Britt *et al.*, 1999, 2000), in some oviraptorosaurs (Osmólska *et al.*, 2004) and in *Nedcolbertia*, whose pubic foot is more elongate craniocaudally in the subadult paratype (CEUM 5072) than in the juvenile holotype (CEUM 5071) (Kirkland *et al.*, 1998). These data support the idea that ontogeny is responsible, at least in part, for the development of the caudal process of the pubic foot. Based on *Compsognathus*, ontogeny may have affected also the development of the ischial foot, as it is more developed in the French specimen, which, according to Peyer (2006), is ontogenetically older than the German specimen.

Degree of ossification of the ilium - The ilium of *Scipionyx* is well-defined in outline and well-ossified. According to Geist & Jones (1996), the extent of ossification of the pelvis at hatching is a reliable indicator of the precocial or altricial nature of a neonate archosaur. These authors, in fact, show that the pelvis of late foetal crocodylians and precocial birds are more ossified than those of altricial birds, which, however, become active in the nest in a matter of days after hatching, showing rapid postnatal ossification of the pelvis. Based on these data, the only information we can infer from the fully ossified ilium of *Scipionyx* is that, if altricial, it was at least a few days old at the time of its death.

Non-ossified sternal plates - *Contra* Dal Sasso & Signore (1998a), *Scipionyx* lacks bony sternal plates (see Humerus): it might have had, though, cartilaginous sternal plates (see Ribs). Sternal plates are large and well-ossified in adult Maniraptoriformes, but seem to be absent in embryos of that clade (Norell *et al.*, 2001). However, there is no evidence of calcified sternal plates in theropods outside the Maniraptoriformes, not even in adult individuals. Therefore, the condition exhibited by *Scipionyx* can be considered ontogenetically uninformative.

Limb proportions - Compsognathid theropods have forelimbs that are comparatively shorter than those in several other coelurosaurs. In *Compsognathus* (Peyer, 2006), the forelimb measures 42% of the hindlimb. The forelimb of *Sinosauropteryx* is shorter and stouter: according to Currie & Chen (2001), it is less than 1/3 of the length of the hindlimb (36% following Hwang *et al.* [2004]). The highest forelimb/hindlimb ratio among compsognathids (i.e., 48%) is found in *Huaxiagnathus* (Hwang *et al.*, 2004). Göhlich & Chiappe (2006) stated that *Juravenator* has the longest forelimb among compsognathids: precise measurements are not available but it must be noted that, although the forearms seem to be long, such a statement is based on the forelimb/hindlimb comparison without taking into consideration that the hindlimbs of *Juravenator* are rather short, possibly the shortest among compsognathids. As mentioned, most other coelurosaurs, including basal tyrannosaurids, have comparatively longer forelimbs. For example, the forelimb/hindlimb ratio is 60% in *Guanlong* (Xu *et al.*, 2006), 52% in *Sinornithomimus* (Kobayashi & Lü, 2003), 75–80% in almost all Laurasian dromaeosaurids (e.g., Xu *et al.*, 1999; Burnham *et al.*, 2000) except *Tianyuraptor* (53%—Zheng *et al.*, 2009), and even higher, i.e., 86–102%, in the Aves (e.g., Elzanowski, 2002). Some other coelurosaurs that are not strictly related to each other have forelimbs as long as, or comparatively shorter than, those of the compsognathids. Among these are tyrannosaurids, alvarezsaurids including *Nqwebasaurus* (43%—de Klerk *et al.*, 2000), the basal oviraptorosaur *Caudipteryx* (40%—Zhou *et al.*, 2000), troodontids (47%—Xu & Norell, 2004; 38%—Russell & Dong, 1993), some secondarily flightless avians (Gauthier, 1986) and, probably, the Gondwanan dromaeosaurids (e.g., Novas *et al.*, 2008b).

In *Scipionyx*, measurements of the hindlimb are not available because the specimen lacks the distal half of the legs. With a forelimb/presacral ratio of 48%, it does not differ considerably from *Compsognathus* (46%), although the proportions are slightly different, *Scipionyx* having comparatively longer skull and manus. The forelimb/presacral ratio is only 39% of the length of the presacral vertebral column in the NIGP 127586 specimen of *Sinosauropteryx*, roughly 10% less than in *Scipionyx*, emphasising the shortness of the forelimb of the former taxon.

Another, more consistent way to assess the proportions of the Italian compsognathid by comparing forelimb and hindlimb based on the preserved parts, is to look at the femur/humerus ratio. This ratio is 1.42 in *Scipionyx*, about 1.75 in *Sinocalliopteryx*, 1.80 in the German *Compsognathus* and in *Huaxiagnathus* (Hwang *et al.*, 2004), about 2.00 in *Juravenator*, 2.10 in the French *Compsognathus* (Peyer, 2006) and 2.50 in *Sinosauropteryx*. In other coelurosaurs, the ratio is 1.66 in *Guanlong* (Xu *et al.*, 2006),

1.76 in *Coelurus* (Carpenter *et al.*, 2005b), 1.80 in *Tanycolagreus* (Carpenter *et al.*, 2005a), 1.88 in *Dilong* (Xu *et al.*, 2004), 1.60 in *Ornitholestes* (Carpenter *et al.*, 2005b), 1.52 in *Sinornithomimus* (Kobayashi & Lü, 2003), 1.69 in *Sinornithoides* (Russell & Dong, 1993), 1.93 in *Mei* (Xu & Norell, 2004) and about 2.00 in *Caudipteryx* (Zhou *et al.*, 2000) and *Nqwebasaurus* (de Klerk *et al.*, 2000); on the other hand, it is 1.13 in *Bambiraptor* (Burnham *et al.*, 2000), 1.10 in *Sinornithosaurus* (Xu *et al.*, 1999) and 1.18 in *Microraptor* (Hwang *et al.*, 2002). Thus, in *Scipionyx* the humerus is comparatively longer with respect to the femur than in any other non-avian coelurosaur except the dromaeosaurids, which have by far the longest forelimbs among non-avian theropods. The ratio in *Scipionyx*, however, is not much greater than that in some other compsognathids such as *Sinocalliopteryx*; therefore, the difference might be related to the ontogenetic stage of the individual, and there possibly would have been positive allometric growth of the hindlimb with respect to the forelimb. In *Compsognathus*, the difference between the German and the French specimens is comparable to that between *Scipionyx* and *Sinocalliopteryx*. On the other hand, both specimens of *Sinosauropteryx* described by Currie & Chen (2001) show a similar ratio.

In conclusion, limb proportions and, in particular, elongation of the humerus respect to the femur, distinguish *Scipionyx samniticus* from all other basal coelurosaurs but are not useful in assessment of ontogenetic stage, pending the discovery of other individuals of this species representing different ontogenetic stages.

Carpal count and ossification - *Scipionyx* possesses only 2, but well-ossified, carpal bones, which are tightly and precisely articulated with the epipodial and the metapodial elements, so much so that there is no space left for cartilaginous elements (Fig. 95). Based on this evidence, such a definitive-looking arrangement would have been acquired very precociously during ontogeny, or even during embryogeny. Although early ossification of the carpals in a bipedal predator may reflect a precocial functional utility, the condition exhibited by *Scipionyx* is ontogenetically uninformative. This issue is more extensively discussed in the osteological description (see Carpus).

Elongation of the manus - The metacarpals of *Scipionyx* are very long with respect to the epipodials (Fig. 94). Although at first glance the long manus of *Scipionyx* appears as one of the most striking features of its skeleton – raising the doubt that the proportions might be related to ontogeny (Gishlick, pers. comm., 2000; Mateus, pers. comm., 2004) – its manus is not comparatively larger than in most other compsognathids (see Forelimb). Thus, the ratio between the manus and the rest of the forelimb results ontogenetically uninformative, pending adult material of this species.

Development of the fourth trochanter - The absence of well-developed processes such as the fourth trochanter may be indicative of the early ontogenetic stage of an individual. This correlation is clearly seen in the ornithischian dinosaur *Maiasaura*, where bony attachments for muscles form much later in response to muscle-induced mechanical stresses on long bones (e.g., Geist & Jones, 1996). According to its phylogenetic position, however,

it is most parsimonious to hypothesise that the fourth trochanter was absent or greatly reduced in *Scipionyx*, whatever the ontogenetic stage. The fourth trochanter is indeed absent or greatly reduced in many small-bodied coelurosaurs, including compsognathids (see Femur).

Remarks - Summing up, most of the above-listed features of *Scipionyx* are typical of immature animals, or, at least, are representative of the condition expected to be seen in an immature animal. Some of these features, such as the presence of a frontoparietal fontanelle, no tooth replacement and no closure of the neurocentral sutures, suggest that *Scipionyx* was a neonate, less than three weeks old at the time of death.

This hypothesis calls for the re-interpretation of some aspects of the palaeobiology and the soft anatomy of the specimen. Concerning its palaeobiology, the presence of a variety of prey (fish and lizards) in the gut of the neonate might indicate that *Scipionyx* scavenged dead fish and lizards right after hatching or, alternatively, might evidence parental care, whether the animal was precocial or not. A third hypothesis, that cannot be ruled out, is that *Scipionyx* hunted actively for its prey, or at least some of it, but it is difficult to imagine neonates such as the Pietraraja dinosaur being capable of catching fast-moving prey, such as live fish and lizards, without parental assistance (see also Palaeobiological Significance Of The Gut Contents of *Scipionyx*). Interestingly, even in extant crocodiles, which are without doubt precocial animals, parental feeding has been observed a few times in captive specimens (Huchzermeyer, pers. comm., 2010).

Regarding its soft anatomy, the unusual arrangement of the intestine, with an empty space in the abdominal-pelvic area (see Rectum), may actually be indicative of the presence of a yolk sac (Huchzermeyer, pers. comm., 2010). In extant crocodylians, resorption of the yolk sac depends, to some degree, on food intake – the earlier the hatchling starts feeding, the faster the resorption in the 3 weeks, circa, after hatching. In *Crocodylus niloticus* hatchlings, the yolk sac occupies practically the whole abdominal cavity, becoming about half-size by the age of 2 weeks (Huchzermeyer, pers. comm., 2010). In extant birds (chickens, geese and ducks), intensive absorption of

yolk sac ingredients is observed during the first 5 days of life, but residues of the yolk sac can be found up to day 7 in more than 30% of chickens and 10% of geese; in 10% of chickens, yolk sac remains can be seen even up to day 16 (Jamroz *et al.*, 2004). The empty abdominal-pelvic space in *Scipionyx samniticus* is consistent with the space occupied by the yolk sac in a 2-week-old *C. niloticus* that has died of yolk sac retention (Fig. 110). In a normal hatchling of that age, the yolk sac would have been about half that size. Considering a postulated faster growth rate and, therefore, a faster metabolic rate for dinosaur hatchlings, one can infer the age of *Scipionyx* to be 3-7 days old, maximum (Huchzermeyer, pers. comm., 2010). The size of the supposed yolk sac of *Scipionyx* is also comparable to the maximum found in one-week-old extant birds (Jamroz *et al.*, 2004). This would not preclude that the hatchling had had several meals.

Another interesting point is the overall body size of *Scipionyx*: the Italian compsognathid has a skull length of about 5 cm and an estimated body length of about 50 cm. Embryos from Lourinhã, referred to *Lourinhanosaurus*, are estimated to be 40 cm in length (Mateus *et al.*, 1998); the maxilla of a post-hatching *Allosaurus* is 23 mm in length (Rauhut & Fechner, 2005), suggesting that the individual was 40-50 cm in length; the maxilla of an unhatched *Troodon* embryo is only slightly smaller, 18 mm long (Varricchio *et al.*, 2002); the skull of the oviraptorid embryo is about 4 cm long (Norell *et al.*, 1994); the skull of the *Byronosaurus* perinates is estimated to be approximately 5 cm long (Beaver & Norell, 2009); and the skull of the therizinosaur embryo is less than 3 cm long (Kundrát *et al.*, 2008). Therefore, the holotype of *Scipionyx* is within the size-range of the known late-stage embryos and neonates of non-avian theropods. More interestingly, considering that the holotype of *Scipionyx* was probably slightly smaller at hatching, it may well have fitted into eggs as large as those of *Troodon* (12-16 cm × 5-6 cm [Varricchio *et al.*, 2002]) or oviraptorids (18-19 cm × 6.5-7.2 cm [Clark *et al.*, 1999]). As a matter of fact, the 1:1 *in ovo* restoration of *Scipionyx*, based on its actual size, i.e., disregarding that it was probably slightly smaller at hatching, yields an 11×6 cm egg (Fig. 111). Among the above mentioned theropods, it must be noted that the non-

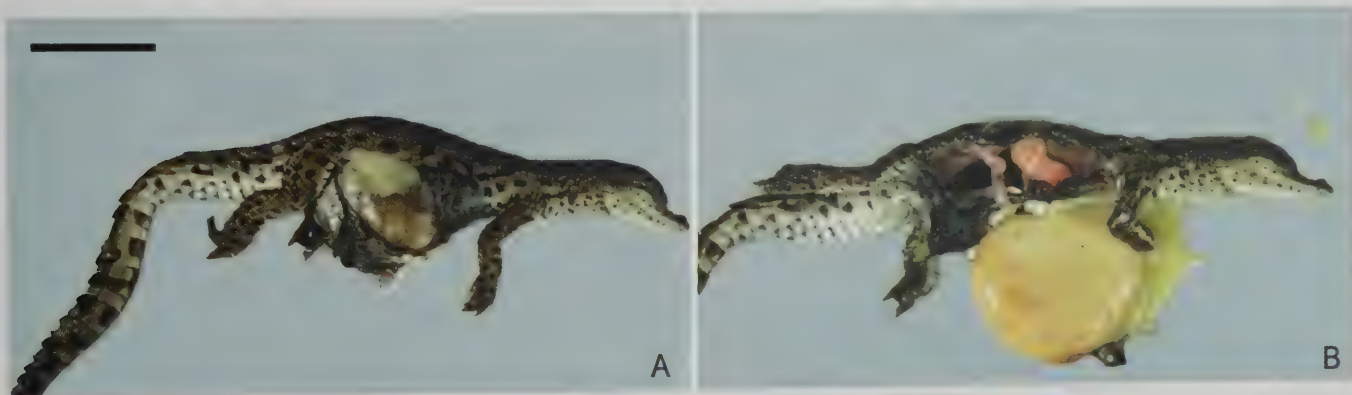


Fig. 110 - A two-week-old *Crocodylus niloticus* died because of yolk sac retention, before (A) and after (B) removal of the yolk sac. The position of the yolk sac in the hatchling crocodile is consistent with the space left by the unusually displaced intestine of *Scipionyx samniticus*. Scale bar = 40 mm.

Fig. 110 - Un *Crocodylus niloticus* di due settimane morto per ritenzione del sacco del tuorlo, prima (A) e dopo (B) la rimozione dello stesso. La sua posizione è compatibile con lo spazio lasciato dall'inusuale dislocazione dell'intestino in *Scipionyx samniticus*. Scala metrica = 40 mm.

coelurosaurian taxa *Lourinhanosaurus* and *Allosaurus* attained an adult body size of more than 4 m and 7-9 m, respectively (Mateus, 1998; Rauhut & Fechner, 2005), whereas the adults of the remnant taxa (or the adults of the most similar taxa in the case of the therizinosaurs), which are coelurosaurs, were considerably smaller (*Troodon*, *Byronosaurus* and the oviraptorosaurs being 2 m or less in total body length and therizinosauroids probably related to the embryo being 2-3 m in length). Thus, taking into account 1) the size of the mentioned coelurosaurian eggs, embryos and respective adults, 2) the estimated age of *Scipionyx* and its estimated size at hatching, and 3) the fact that compsognathids are among the smallest non-avian theropods known and that *Sinocalliopteryx*, the largest known member of this taxon, measures 2.34 m in total body length (Ji *et al.*, 2007a), we may hypothesise that adults of the Italian compsognathid did not exceed this size (Fig. 112).

Although *Sinocalliopteryx gigas* is indeed the largest of the compsognathids, being markedly larger than *Sinosauropteryx* or *Compsognathus*, it must be taken into account that it is one of the few species probably represented by mature individuals. The fragmentary *Aristosuchus pusillus* is estimated to be about 2 m long (Holtz *et al.*, 2004) and *Huaxiagnathus orientalis*, represented by an individual potentially approaching maturity, is estimated to be 1.6 m long by Hwang *et al.* (2004) and about 1.9 m long by Peyer (2006). The probable compsognathid *Mirischia asymmetrica* is also estimated to be about 1.9 m long. Although immature, the French specimen of *Compsognathus*, which is approximately as large as the largest specimen of *Sinosauropteryx*, is estimated to be about 1.4 m long, and would have grown further before reaching sexual maturity. Based on these observations, we think that all compsognathids could have been able to lay eggs matching the size of *Scipionyx* at hatching. Comparison with extant non-flying birds suggests that in the ecologically equivalent non-avian theropods, a small adult body size would not have precluded a relatively large egg size.



Fig. 111 - Life-size *in ovo* restoration of *Scipionyx samniticus*, based on its size at the time of death.

Fig. 111 - Ricostruzione *in ovo* di *Scipionyx samniticus* in grandezza naturale, basata sulla taglia che aveva al momento della morte.

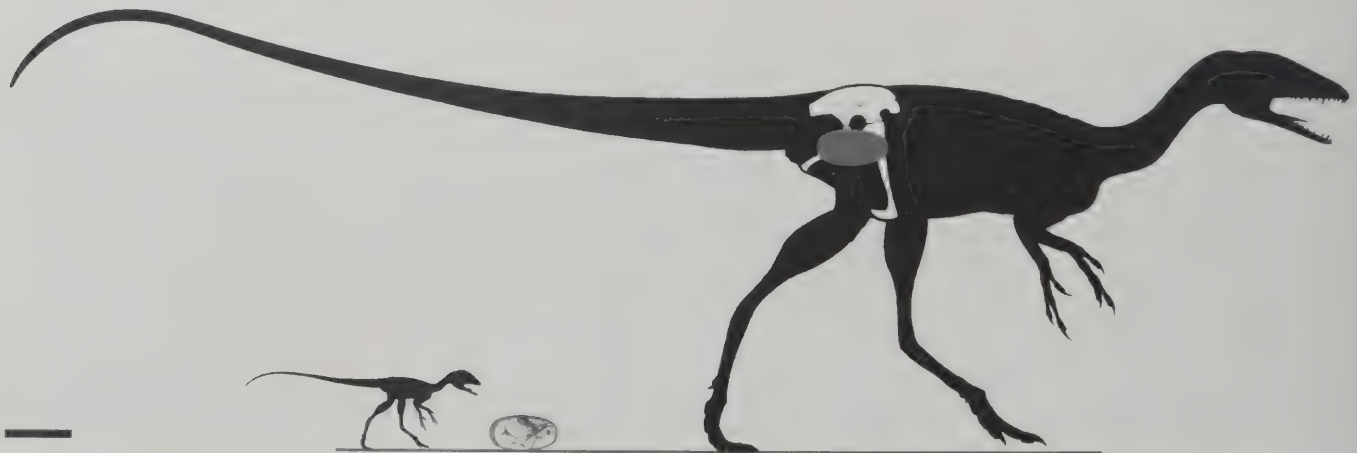


Fig. 112 - Body size of the hatchling *Scipionyx samniticus* (standing and *in ovo*) compared to the estimated body size of an adult individual. Scale bar = 10 cm.

Fig. 112 - Dimensioni corporee (in piedi e *in ovo*) di *Scipionyx samniticus* neonato, confrontate con la taglia stimata di un individuo adulto. Scala metrica = 10 cm.

PHYLOGENETIC ANALYSIS

The present phylogeny is based on the phylogenetic data matrix of Senter (2007), which still represents one of the most comprehensive phylogenetic analyses of the theropod clade Coelurosauria published to date: 83 coelurosaurian ingroup taxa vs 40 in one of the latest data matrices (Choiniere *et al.*, 2010, and references therein). The analysis was performed in order to test the phylogenetic position of *Scipionyx samniticus* within the Coelurosauria, and to see how the resulting topology would differ from that of Senter (2007), after: 1) inclusion of new taxa from recent studies and highly incomplete taxa; 2) some changes concerning character coding in the matrix; 3) inclusion/exclusion of characters possibly related to ontogeny, in order to minimise the risk derived by inaccurate identification of the ontogenetic stage in fossil forms.

Modification of the data matrix

Terminal taxa - Besides *Scipionyx samniticus*, 9 more coelurosaur – or alleged coelurosaur – taxa were added, thereby increasing the information content (95 taxa \times 360 characters = 34,200 data points) of the Senter (2007) matrix (85 taxa \times 360 characters = 30,600 data points). The new taxa in the matrix are *Aniksosaurus darwinii*, *Guanlong wucuii*, *Juravenator starki*, *Mirischia asymmetrica*, *Nedcolbertia justinhoffmani*, *Nqwebasaurus thwazi*, *Orkoraptor burkei*, *Santanaraptor placidus* and *Sinocalliopteryx gigas*. Although described in preceding years, *Mirischia asymmetrica* (Naish *et al.*, 2004), *Nedcolbertia justinhoffmani* (Kirkland *et al.*, 1998), *Nqwebasaurus thwazi* (de Klerk *et al.*, 2000) and *Santanaraptor placidus* (Kellner, 1999) were not in the Senter (2007) matrix. Senter (2007) did not comment on the exclusion of these taxa. Although all except *Nqwebasaurus* are represented by highly incomplete specimens, we decided to include them in the analysis. As recently reported by Butler & Upchurch (2007; and references therein), it has been demonstrated that even highly incomplete taxa have the potential to provide significant phylogenetic information, and taxa should only be excluded from a phylogenetic analysis *a priori* when their deletion will have no effect on the inferred interrelationships of the remaining taxa.

Concerning the other newly added taxa, *Orkoraptor burkei* appeared in the literature in 2008, whereas the remaining 4 taxa were not included by Senter (2007) presumably because the papers, published around 2006–2007 were in preparation at the same time as his own paper.

The character states of *Aniksosaurus darwinii* were scored according to Martinez & Novas (2006); those of *Guanlong wucuii* according to Xu *et al.* (2006); those of *Juravenator starki* according to Göhlich & Chiappe (2006), Göhlich *et al.* (2006) and unpublished photographs provided by Göhlich & Chiappe in 2006; those of *Mirischia asymmetrica* according to Naish *et al.* (2004) and photographs by Göhlich & Chiappe; those of *Nedcolbertia justinhoffmani* according to Kirkland *et al.* (1998); those of *Nqwebasaurus thwazi* according to de Klerk *et al.* (2000), and personal communications

and photographs by de Klerk (2004); those of *Orkoraptor burkei* according to Novas *et al.* (2008a); those of *Santanaraptor placidus* according to Kellner (1999); and those of *Sinocalliopteryx gigas* according to Ji *et al.* (2007a). Following Norell *et al.* (2009), the taxon name *Saurornithoides junior* has been replaced by *Zanabazar junior*, this taxon being distinct at generic level from *Saurornithoides mongoliensis*.

Characters - Several changes were made to the Senter (2007) matrix concerning wording, coding of character states for some taxa, addition/deletion of some character states and total replacement of characters considered unclear. Few of these changes are due to disagreement with Senter's codings or to changes in the wording for some characters, but most are due to: recognition of new character states for other characters, availability of illustrations and description of a new specimen of *Sinosauropteryx* (Ji *et al.*, 2007b), recent redescription of *Compsognathus* (Peyer 2006), personal observation on that specimen (MNHN CNJ 79) and personal communications by Peyer (2005), as well as availability of photographs of *Coelurus* and *Huaxiagnathus* (courtesy of Göhlich and Chiappe). All these changes are listed in Appendices 2–4 to make them easier to find for the sake of evaluating or challenging them.

Other changes are due to the assessment of the maturity-dependent characters (see Appendix 5), as some of them proved not to be of taxonomic significance but, rather, linked to maturity (i.e., to ontogenetic changes) of the specimens. Whatever its precise ontogenetic stage (see Ontogenetic Assessment), *Scipionyx* is not represented by mature individuals or individuals of relatively late ontogenetic stage, as is the case in some other theropod taxa. As pointed out by Tykoski (2005), treating such taxa as if they were represented by adult specimens could result in undeveloped (or under-developed) morphologies being assessed for maturity-dependent characters that are expressed only in later stages of life. Coding as unambiguously “absent” a character that is usually expressed only late in ontogeny, ignoring that this is the result of immaturity and not phylogeny, may eventually alter the results of the cladistic phylogenetic analysis. Similarly, it must be recalled that allometric trends and heterochronic processes characterise the skeletal ontogeny of all tetrapods, theropods included (Nicholls & Russell, 1981; Long & McNamara, 1997; Rauhut & Fechner, 2005), resulting in proportional differences between very young and fully mature individuals and having a potentially negative impact on coding of characters that compare an element's size relative to another skeletal component (i.e., ratio-characters). Therefore, potentially late-appearing, maturity-dependent characters and ratio-characters must be carefully assessed for the taxon (see Appendix 5) and, where necessary, scored as missing data in the absence of adult specimens, which may or may not possess these characters or show definitive skeletal proportions. Similarly, ratio-characters must be carefully assessed also because of allometric differences that are sometimes more related to the absolute size attained by the taxon than to its phylogenetic affinities (Nicholls & Russell, 1981).

Multistate characters were considered as unordered, unless they corresponded in all likelihood to a transformation series. Multistate characters considered as ordered are: ch17, ch18, ch38, ch41, ch46, ch66, ch77, ch84, ch110, ch113, ch119, ch123, ch156, ch157, ch164, ch169, ch172, ch175, ch176, ch200, ch217, ch277, ch298, ch299, ch302, ch331, ch335 and ch345. A missing state of a multistate character (due to the preservation of the specimen) is coded as uncertain (e.g., 0/1). Multistate characters have been coded as uncertain also when taxa represented by immature specimens possess a character state which could have been developed into a successive state but not reversed into a preceding one during ontogeny (e.g., Appendix 5, ch169).

The two-stage approach recommended by Butler & Upchurch (2007) was followed first. The application of “safe taxonomic reduction” to a simplified version of our data matrix (simplified to allow the program to run), performed with the program TAXEQ3 (Wilkinson, 2001a) with the aim to identify taxa that can be deleted *a priori* without having an impact on the inferred interrelationships of the remaining taxa, did not identify any taxa that could be safely removed. Redcon 3.0 (Wilkinson, 2001b) resulted as inapplicable because of the high number of terminal taxa present in our analysis. The parsimony analysis was therefore carried out normally.

Results

A data matrix of 360 characters in 95 terminal taxa (Appendix 6) compiled in NDE (Page, 2001) was analysed using the heuristic search of the most parsimonious tree (MPT) of PAUP 4.0b10 (Swofford, 2002). Drawings of the trees (Fig. 113) are based on the trees displayed with Tree View (Page, 1996). The heuristic search was performed using 1,000 random addition-sequence replicates with “maxtrees” set at 10,000. In total agreement with the considerations of Kitching *et al.* (1998), no bootstrap analysis was run.

The analysis generated 10,000 MPTs (L=1418 steps, CI=0.3159, RI=0.7395 and RC=0.2336). The “tree description” option of PAUP was used to obtain the reconstructed states for internal nodes, the character change list and the apomorphy list (see Supplementary Information).

Character transformation was optimised under both accelerated transformation (ACCTRAN) and delayed transformation (DELTRAN) options of PAUP. Character state changes that shift from one node to another under different optimisation regimes are listed as “ambiguous apomorphies” while those that are tied to one node despite differing the optimisation are listed as “unambiguous apomorphies” according to the terminology of Holtz (1994) and Chiappe *et al.* (1996) followed by Yates & Warren (2000) and Maganuco *et al.* (2009). According to those authors, the terms “ambiguous” and “unambiguous” are not meant to imply the presence or absence of homoplasy in the distribution of a given character state. This means that an unambiguous synapomorphy may be reversed deeper into the clade or may appear convergently in another clade. Ambiguity may be caused by missing data or incongruence in the data.

As this section is primarily concerned with the phylogenetic affinities of *Scipionyx samniticus*, we adopted the same formal names and definitions for the clades within the Coelurosauria as already adopted by Senter (2007). The only exception is represented by the taxon Ornithomimosauria. According to the phylogeny of Senter (2007), Ornithomimosauria would be a junior synonym of Arctometatarsalia. However, we prefer to refer to the most used term (i.e., Ornithomimosauria), waiting for further studies which will confirm this conclusion or not. To avoid proliferation of taxon names, formal names and definitions are therefore not provided for the groups not defined in those papers such as *Aniksosaurus* + *Nedcolbertia*, the content and the interrelationships of which have yet to be elucidated and corroborated by further studies. The clade notation used below, “taxon X + taxon Y”, refers to the least inclusive clade in the MPT2/majority-rule consensus tree comprising the two given taxa, and does not imply that these taxa share a direct sister-taxon relationship. Node numbers are indicated in Fig. 113.

Comments - Despite several changes to the data matrix (see above) and the addition of 10 taxa (*Scipionyx* included), most of the results of this analysis agree with those of Senter (2007), which in their turn agreed with those of most other published numeric phylogenetic analyses (Senter, 2007; and references therein). Therefore, the nodes that in Senter (2007) show the same topology are not discussed here, and a simplified version of the cladogram is represented in Fig. 113. As mentioned above, the whole cladogram with node numbers, the reconstructed states for internal nodes, the character change list and the apomorphy list are available to the reader as Supplementary Information. The present discussion refers to this simplified cladogram, emphasising the position of the newly added taxa and the phylogenetic affinities of *Scipionyx samniticus*. The apomorphy list is extensively reported only for nodes internal to the Compsognathidae.

Mirischia asymmetrica, *Aniksosaurus darwinii* and *Nedcolbertia justinhoffmani* are found to occupy a basal position within Coelurosauria. *Mirischia asymmetrica* is here the basal-most of the three species, whereas *Aniksosaurus darwinii* and *Nedcolbertia justinhoffmani* form a monophyletic group. Martinez & Novas (2006) considered *Aniksosaurus* a coelurosaur basal to Maniraptoriformes (including tyrannosauroids) and more derived than *Ornitholestes* and compsognathids, without testing its position in a phylogenetic analysis. We agree with Naish *et al.* (2004, and references therein), who found some compsognathid affinities in *Mirischia asymmetrica* suggesting that it was more closely related to *Compsognathus* than to *Sinosauropteryx*. Their hypothesis, however, was not tested in a phylogenetic analysis. According to the phylogeny of Rauhut (2003), *Mirischia* (at that time “the Santana compsognathid”), *Compsognathus* and *Sinosauropteryx* were indeed united into the clade Compsognathidae. This result is not supported in the present phylogeny, being in all likelihood influenced by the incompleteness of *Mirischia*, *Aniksosaurus* and *Nedcolbertia*, which lack parts of the skeleton that might have supported their inclusion in one of the more derived groups. As a matter of fact, both *Mirischia* and *Nedcolbertia* were deleted *a posteriori* by Butler & Upchurch (2007) because they resulted as

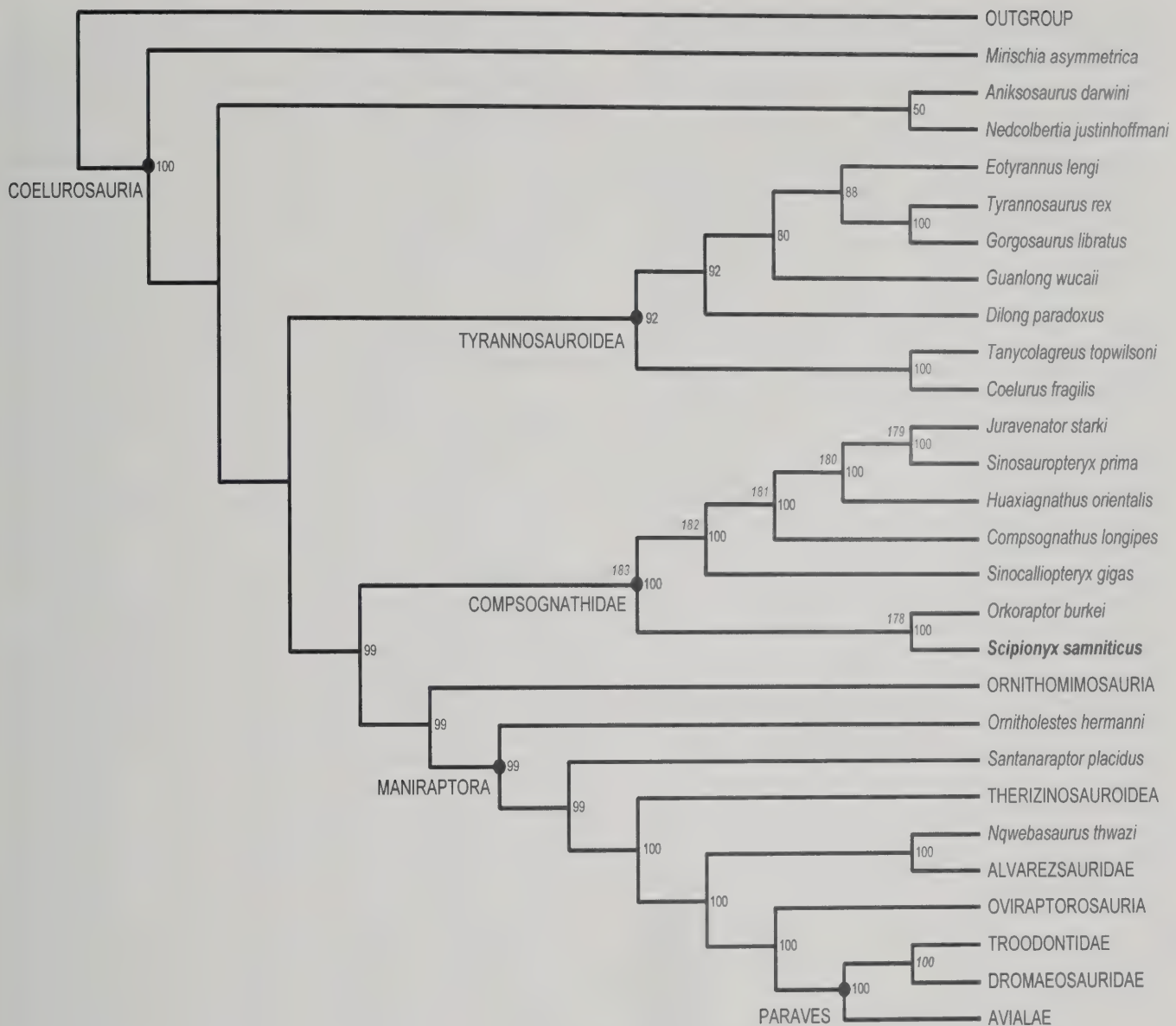


Fig. 113 - 50% majority-rule consensus tree of the most parsimonious trees (MPTs) generated by PauP 4.0.b10 (Swofford, 2002), based on the data matrix given in Appendix 6. Percentages at nodes are indicated to the right of the nodes. The topology of this consensus tree is identical to that of MPT number 2. Numbers in italic grey to the left of the nodes refer to the nodes of MPT number 2 that are discussed in the text.

Fig. 113 - "50% majority-rule consensus tree" degli alberi filogenetici più parsimoniosi (MPTs) generati con PauP 4.0.b10 (Swofford, 2002) sulla base della matrice di dati pubblicata in Appendice 6. Le percentuali dei nodi sono indicate a destra dei nodi stessi. La topologia di questo consensus tree è identica a quella del MPT n. 2. I numeri a sinistra dei nodi (in corsivo grigio) si riferiscono ai nodi del MPT n. 2 discussi nel testo.

unstable taxa. In Holtz *et al.* (2004), *Nedcolbertia* is allied with a clade composed by *Scipionyx* and all the coelurosaurs more derived than the compsognathids. *Guanlong wucaii* is a tyrannosauroid found to be more advanced than *Dilong paradoxus* but basal to the Tyrannosauridae. This is the only result which contrasts with the most recent phylogenies (Xu *et al.*, 2006; Li *et al.*, 2009; Sereno *et al.*, 2009), where *Guanlong wucaii* is basal to *Dilong paradoxus*, the former showing more plesiomorphic features. Some of the features which acted as synapomorphies shared by *Dilong* and the other tyrannosauroids in those phylogenies are indeed not included in Senter (2007). Their exclusion might be responsible for the more advanced position of *Guanlong wucaii* here: this is an-

other clear indication that larger data sets with more taxa are needed to test the phylogenetic hypotheses to the best of our knowledge. *Santanaraptor placidus* is found to be a basal maniraptoran that is more advanced than *Ornitholestes*. In the present phylogeny, *Nqwebasaurus thwazi* is basal to the Alvarezsauridae. No phylogenetic analysis was performed by de Klerk *et al.* (2000), and *Nqwebasaurus* was deleted *a priori* by Göhlich & Chiappe (2006) and *a posteriori* by Butler & Upchurch (2007), being considered an unstable taxon. In the phylogeny of Holtz *et al.* (2004), *Nqwebasaurus* resulted to be a basal coelurosaur more advanced than compsognathids, whereas Sereno (2001) suggested that this taxon is part of a clade including alvarezsaurids and ornithomimosaurids.

The affinities of the Compsognathidae and the apomorphies characterising both nodes internal to that taxon and terminal taxa are listed below.

Node 183

Compsognathidae

Included taxa: *Scipionyx* + *Juravenator*

Unambiguous synapomorphies: 73 (0 → 2), external mandibular fenestra absent; 109 (0 → 2), interspinal ligament attachments in form of beak-like processes below apex of neural spine; 206 (0 → 1), neural spines on caudal dorsal vertebrae in lateral view craniocaudally expanded distally, fan-shaped; 207 (0 → 1), shaft diameter of phalanx I-1 equal/greater than shaft diameter of radius; 299 (0 → 1), manual unguis II and III weakly curved.

Ambiguous synapomorphies under DELTRAN: 46 (1 → 0), dorsal surface of parietals flat, lateral ridge borders supratemporal fenestra; 101 (0 → 1), cervical and cranial trunk vertebrae strongly opistocoelous; 163 (0 → 1), ridge bordering cuppedicus fossa terminates rostrally to acetabulum or curves ventrally onto cranial end of pubic peduncle; 185 (1 → 0), accessory trochanteric crest distal to lesser trochanter absent; 237 (0 → 1), body of premaxilla dorsoventrally shallow; 263 (0 → 1), cervical prezygapophyses flexed; 284 (0 → 1), manual phalanx I-1 shorter than metacarpal II.

Ambiguous synapomorphies under ACCTAN: 9 (0 → 2), basisphenoid recess between basisphenoid and basioccipital absent; 32 (1 → 0), postorbital process of the jugal well-developed, taller than half orbit; 43 (0 → 1), rostral emargination of supratemporal fossa on frontal strongly sinusoidal and reaching onto postorbital process; 53 (0 → 1), quadrate hollow, with depression on caudal surface; 101 (0 → 1), cervical and cranial trunk vertebrae strongly opistocoelous; 119 (0 → 1), neural spines on distal caudals absent; 120 (0 → 2), prezygapophyses of distal caudal vertebrae strongly reduced as in *Archaeopteryx lithographica*; 272 (0 → 1), wide distal expansion of scapula present.

Remarks - The taxon Compsognathidae was erected by Cope in 1871. It is defined as *Compsognathus longipes* and all taxa sharing a more recent common ancestor with it than with *Passer domesticus*. According to Holtz (2000), it has proven difficult to find convincing derived characters that unite compsognathids, setting them apart from all other theropods, because the former ones retain the basic, relatively unspecialised coelurosaurian body plan. For this reason, the Compsognathidae have long been known only from *Compsognathus*. Several new alleged compsognathids have been discovered in recent years. The Compsognathidae were recognised as the basalmost clade of coelurosaurs by Holtz *et al.* (2004), including *Compsognathus* and *Sinosauropteryx*. In the phylogeny of Rauhut (2003), the Compsognathidae, including *Compsognathus*, *Sinosauropteryx* and *Mirischia*, resulted as monophyletic and placed within Coeluridae near the base of Coelurosauria. After *a priori* deletion of 7 “highly incomplete” or “less relevant” taxa, *Scipionyx* included, Göhlich & Chiappe (2006) found a monophyletic Compsognathidae placed at the base of Coelurosauria (tyrannosaurids excluded) and composed of *Juravenator*, *Sinosauropteryx*, *Huaxiagnathus* and *Compsognathus*. The 4 taxa formed an unresolved polytomy. Butler & Upchurch (2007) criticised the analysis

of Göhlich & Chiappe (2006), pointing out that the result was strongly influenced by the *a priori* deletion. They showed that in the total evidence strict component consensus (i.e., without any deletion), the 4 mentioned taxa plus *Scipionyx* resulted in an unresolved position at the base of Maniraptora, in a more derived position than ornithomimosauria. After *a posteriori* deletion of 3 unstable taxa, they obtain a strict reduced consensus tree in which Compsognathidae was a monophyletic taxon at the base of Maniraptora and more advanced than Ornithomimosauria, composed only of *Compsognathus* and *Coelurus*. *Huaxiagnathus* and *Sinosauropteryx* resulted to be more derived than Compsognathidae, whereas *Scipionyx* and *Juravenator* resulted to be more basal.

Peyer (2006) considered Compsognathidae as consisting of 7 taxa: *Compsognathus longipes* Wagner, 1861; *Sinosauropteryx prima* Ji & Ji, 1996; *Huaxiagnathus orientalis* Hwang *et al.*, 2004; *Mirischia asymmetrica* Naish *et al.*, 2004; *Aristosuchus pusillus* Owen, 1876; *Juravenator starki* Göhlich & Chiappe, 2006; *Scipionyx samniticus* Dal Sasso & Signore, 1998. Although her hypothesis needs to be supported by a published phylogenetic analysis, Peyer (2006) carefully recognised numerous anatomical key features of the taxon and proposed the following revised diagnosis: “absence of an external mandibular fenestra, anteroposteriorly expanded; dorsally fan-shaped mid-to-posterior dorsal neural spines; hook-shaped ligament attachments on dorsal neural spines; short, wide and only slightly inclined dorsal transverse processes; absence of pleurocoels in dorsal vertebrae; Mcl very stout, approximately as broad as long; and proximal width of PhI-1 more than minimal shaft diameter of radius”. In the present analysis, 4 of these characters resulted in unambiguous synapomorphies of the taxon (see above), and we agree with Peyer (2006) that the remnant mix of characters is also useful to diagnose the compsognathids and indicate membership of this group, although some of these characters are widely distributed within Theropoda. Among these characters, as suggested by Currie & Chen (2001), are: presence of a proportionally large skull; unserrated rostralmost but serrated lateral teeth; slender, hair-like cervical ribs; and pubic foot with a limited cranial extension (Martill *et al.*, 2000; Naish *et al.*, 2001) but caudally elongate, prominent ischial obturator process. Other characters recalling the Compsognathidae and a more generalised coelurosaurian bauplan (Ostrom, 1978; Gauthier, 1986; Holtz *et al.*, 2004) are: acute, needle-shaped quadrate process of the quadratojugal; stout, L-shaped lacrimal; large prefrontal; pronounced scapular acromion; fan-like coracoid and caudally facing glenoid; manual claws with low curvature; and feeble development of the fourth trochanter in the femur.

In the original analysis of Senter (2007), only 3 of the taxa forming the Compsognathidae in the present analysis were included: *Sinosauropteryx*, *Huaxiagnathus* and *Compsognathus*. They formed a monophyletic Compsognathidae, more derived than Tyrannosauriidae and less derived than Maniraptoriformes. Here, 4 of the newly added taxa, *Scipionyx* included, fall within a monophyletic Compsognathidae (but see comments about *Orkoraptor*, below), which results as composed of 7 taxa. Finally, according to Naish *et al.* (2004), Holtz *et al.* (2004) and Peyer (2006), the fragmentary

taxon *Aristosuchus pusillus*, although not included in the present phylogeny or in the ones mentioned above, is also supposed to be a compsoognathid because of the strongly similar form of the pubis, with its foot enlarged caudally.

Node 178

Included taxa: *Scipionyx* + *Orkoraptor*

Unambiguous synapomorphies: 359 (0 → 1), cranial caudal vertebrae with pneumatopores.

Ambiguous synapomorphies under DELTRAN: none.

Ambiguous synapomorphies under ACCTTRAN: 21 (0 → 1), internarial bar flat; 49 (0 → 1), descending process of squamosal does not contact quadratojugal; 52 (0 → 1), quadrate strongly inclined anteroventrally so that distal end lies far forward of proximal end; 82 (0 → 1), second premaxillary tooth markedly larger than third and fourth premaxillary teeth; 85 (0 → 2), small number of dentary teeth (≤ 11); 93 (0 → 1), axial epiphyses large and caudally directed, extend beyond postzygapophyses; 117 (0 → 1), box-like centra in caudals I-V; 132 (0 → 1), hypocleideum on furcula present; 139 (0 → 1), humerus longer than scapula; 184 (0 → 1), fourth trochanter on femur absent; 231 (0 → 1), dentary teeth increase in size rostrally; 244 (0 → 1), nasals shorter than frontals; 298 (0 → 1), manual ungual I weakly curved.

Remarks - *Orkoraptor* was described by Novas *et al.* (2008a) on the basis of a fragmentary skeleton from the early Maastrichtian of Patagonia. According to their majority-rule consensus tree, *Orkoraptor* resulted to be a basal member of a monophyletic Compsognathidae. Novas *et al.* (2008a), however, pointed out that such result is unexpected and needs to be taken with caution, as *Orkoraptor* is considerably larger than the characteristically small-sized compsoognathids, it does not fit with the Early Cretaceous biochron of the Compsognathidae, and it lacks compsoognathid synapomorphies other than the unserrated mesial margin of each tooth and the lack of a caudoventral process on the quadratojugal. Novas *et al.* (2008a) also considered the rostradorsally inclined rostral process of the postorbital as a condition documented in coelurosaurians more derived than tyrannosauroids. According to Benson *et al.* (2010), the postorbital of *Orkoraptor* is almost identical to that of the allosauroid *Aerosteon*, and in both taxa a pneumatopore is apparent on the dorsolateral surface of the atlantal neural arch, and the proximal caudal vertebrae are intensely pneumatized. Based on those characters, *Orkoraptor* resulted to be a neovenatorid allosauroid in the phylogeny of Benson *et al.* (2010), which differs from the present phylogeny and from the phylogeny of Novas *et al.* (2008a) in being focussed on non-coelurosaurian taxa. In the present phylogeny, which is based on Senter (2007) and neither includes non-coelurosaurian taxa (with the exception of the outgroups) nor some of the characters used by Benson *et al.* (2010), *Orkoraptor* resulted to be a basal member of the Compsognathidae and the sister taxon of *Scipionyx*. It must be noted, however, that none of the present compsoognathid synapomorphies and none of the synapomorphies shared with *Scipionyx* under ACCTTRAN are coded for *Orkoraptor*. Its position is therefore a consequence of the presence of pneumatopores in the cranial caudal vertebrae. Thus, despite our result, we do not refer *Orkoraptor* to the Compsognathidae because of the fragmentary

nature of the specimen, and the fact that this coelurosaurian phylogeny based on Senter (2007) is not adequate either in characters or in number of non-coelurosaurian taxa to test other possible affinities. Although the non-coelurosaurian phylogenies (e.g., Benson *et al.*, 2010) do not include an adequate number of coelurosaurian taxa to definitely solve the question, we regard *Orkoraptor* as a tetanuran theropod of possible neovenatorid affinities. A certain degree of caution is needed, pending more complete material and more comprehensive phylogenetic analyses of Theropoda.

Orkoraptor

Unambiguous autapomorphies: none.

Ambiguous autapomorphies under DELTRAN: none.

Ambiguous autapomorphies under ACCTTRAN: none.

Scipionyx

Unambiguous autapomorphies: none.

Ambiguous autapomorphies under DELTRAN: 8 (0 → 1), subotic recess (pneumatic fossa ventral to *fenestra ovalis*) present; 21 (0 → 1), internarial bar flat; 43 (0 → 1), rostral emargination of supratemporal fossa on frontal strongly sinusoidal and reaching onto postorbital process; 49 (0 → 1), descending process of squamosal does not contact quadratojugal; 52 (0 → 1), quadrate strongly inclined anteroventrally so that distal end lies far forward of proximal end; 82 (0 → 1), second premaxillary tooth markedly larger than third and fourth premaxillary teeth; 117 (0 → 1), box-like centra in caudals I-V; 132 (0 → 1), hypocleideum on furcula present; 184 (0 → 1), fourth trochanter on femur absent; 213 (0 → 1), quadrate cotyle of squamosal open laterally exposing quadrate head; 231 (0 → 1), dentary teeth increase in size rostrally; 233 (0 → 1), height of skull (minus mandible) at middle of naris less than half the height of skull at middle of orbit; 235 (0 → 1), cranial concavity of the preacetabular blade of the ilium in lateral view present and slightly developed; 298 (0 → 1), manual ungual I weakly curved.

Ambiguous autapomorphies under ACCTTRAN: none.

Remarks - On account of the large amount of anatomical details not available to previous authors, it is partly out of place to compare the present phylogenetic position of *Scipionyx* with those found in the few previous analyses that included the Italian theropod (e.g., Holtz *et al.*, 2004; Butler & Upchurch, 2007). *Scipionyx* was previously considered to be a basal member of the Maniraptoriformes (Dal Sasso & Signore, 1998a; 1998b) of uncertain affinity (Dal Sasso, 2001; 2003), then it was ascribed to the Coelurosauria *incertae sedis* (Dal Sasso, 2004; Holtz *et al.*, 2004). Peyer (2006) was the first to refer *Scipionyx* to the Compsognathidae, based on the absence of an external mandibular fenestra, the dorsal vertebrae dorsally fan-shaped with a “hook-like” ligament attachment, a very short McI, and the proximal width of PhI-1 more than the shaft diameter of the radius. Her assignment of *Scipionyx* to the Compsognathidae, however, was not based on a published phylogenetic analysis.

In the present phylogeny, *Scipionyx samniticus* clearly results to be a compsoognathid. Even though we did not include in the matrix the characters we found to be strictly ontogeny-related (Appendix 5), it remains difficult to determine to what extent its basal position within Compsognathidae is due to its generally plesio-

morphic condition in respect to the other compsognathids, or to the early ontogenetic stage of the only known individual.

Node 182

Included taxa: *Sinocalliopteryx* + *Juravenator*

Unambiguous synapomorphies: 28 (0 → 1), accessory antorbital fenestra situated caudal to rostral border of fossa; 41 (0 → 1), prefrontal greatly reduced in exposure; 286 (0 → 1), metacarpals II and III are appressed for their entire lengths; 304 (0 → 1), shaft of ischium slenderer than the pubic shaft.

Ambiguous synapomorphies under DELTRAN: 120 (0 → 2), prezygapophyses of distal caudal vertebrae strongly reduced as in *Archaeopteryx lithographica*; 272 (0 → 1), wide distal expansion of scapula present.

Ambiguous synapomorphies under ACCTTRAN: 127 (1 → 0), lateral gastral segment shorter than medial one in each arch; 157 (1 → 2), supraacetabular crest on ilium as a separate process from antitrochanter absent; 213 (1 → 0), quadrate head covered by squamosal in lateral view; 257 (0 → 1), premaxillary teeth much smaller than the maxillary teeth.

Sinocalliopteryx

Unambiguous autapomorphies: 39 (0 → 1), enlarged foramen or foramina opening laterally at the angle of the lacrimal, present; 142 (1 → 0), olecranon process weakly developed; 166 (0 → 1), shaft of ischium, ventrodistal end curved cranially; 243 (1 → 0), suborbital process of jugal short and dorsoventrally stout; 274 (1 → 0), humeral length is half femoral length or less; 282 (1 → 0), medial side of metacarpal II: expanded proximally; 283 (0 → 1), metacarpal III < 0.8x length of metacarpal II; 288 (1 → 0), length of manual phalanx II-2 < 1.2x length of phalanx II-1; 346 (1 → 0), premaxillary teeth serrated; 347 (1 → 0), sublacrimal process of jugal dorsoventrally expanded (taller than suborbital bar of jugal).

Ambiguous autapomorphies under DELTRAN: 9 (0 → 2), basisphenoid recess between basisphenoid and basioccipital absent; 127 (1 → 0), lateral gastral segment shorter than medial one in each arch; 235 (0 → 1), cranial concavity of the preacetabular blade of the ilium in lateral view present and slightly developed; 257 (0 → 1), premaxillary teeth much smaller than the maxillary teeth.

Ambiguous autapomorphies under ACCTTRAN: none.

Node 181

Included taxa: *Compsognathus* + *Juravenator*

Unambiguous synapomorphies: 154 (1 → 0), ventral edge of cranial ala of ilium straight or gently curved; 349 (1 → 0), distal chevrons straight or L-shaped in lateral view.

Ambiguous synapomorphies under DELTRAN: 32 (0 → 1), postorbital process of the jugal reduced/absent; 93 (1 → 0), axial epiphyses absent or poorly developed, not extending past caudal rim of postzygopophyses.

Ambiguous synapomorphies under ACCTTRAN: 32 (0 → 1), postorbital process of the jugal reduced/absent; 171 (0 → 1), ischium 70% or less of pubis length; 235 (1 → 0), cranial concavity of the preacetabular blade of the ilium in lateral view absent; 302 (1 → 0), manual phalanx III-3 markedly shorter than combined lengths of phalanges III-1 and III-2.

Compsognathus

Unambiguous autapomorphies: 33 (0 → 1), jugal quadratojugal process beneath lower temporal fenestra rod-like; 148 (1 → 0), distal carpals 1+2 well-developed, covering all of proximal ends of metacarpals I and II; 169 (2 → 3), caudal process of the pubic foot present and longer than 1/3 of the proximodistal length of the pubis; 175 (1 → 0), pubis propubic; 298 (0 → 1), manual ungual I weakly curved; 348 (0 → 1), flexor tubercles of manual unguals < 1/3x height of articular facet.

Ambiguous autapomorphies under DELTRAN: 171 (0 → 1), ischium 70% or less of pubis length; 233 (0 → 1), height of skull (minus mandible) at middle of naris less than half the height of skull at middle of orbit.

Ambiguous autapomorphies under ACCTTRAN: 127 (0 → 1), distal gastral segment longer than proximal segment.

Node 180

Included taxa: *Huaxiagnathus* + *Juravenator*

Unambiguous synapomorphies: 29 (1 → 0), tertiary antorbital fenestra (promaxillary fenestra) absent; 71 (0 → 1), dentary with subparallel dorsal and ventral edges; 275 (1 → 0), length of humeral shaft between deltopectoral crest and distal condyles < 4.5x shaft diameter.

Ambiguous synapomorphies under DELTRAN: 127 (1 → 0), lateral gastral segment shorter than medial one in each arch; 157 (1 → 2), supraacetabular crest on ilium as a separate process from antitrochanter, absent.

Ambiguous synapomorphies under ACCTTRAN: 101 (1 → 0), cervical and cranial trunk vertebrae amphiplatyan to platycoelous; 233 (1 → 0), height of skull (minus mandible) at middle of naris, more than half the height of skull at middle of orbit; 240 (0 → 4), maxillary fenestra small and round, not dorsally displaced; 327 (0 → 1), diameter of non-ungual phalanges of manual digit III < 0.5x diameter of non-ungual phalanges of digit II.

Huaxiagnathus

Unambiguous autapomorphies: 272 (1 → 0), wide distal expansion of scapula absent; 283 (0 → 1), metacarpal III < 0.8x length of metacarpal II.

Ambiguous autapomorphies under DELTRAN: 240 (0 → 4), maxillary fenestra small and round, not dorsally displaced; 257 (0 → 1), premaxillary teeth much smaller than the maxillary teeth; 327 (0 → 1), diameter of non-ungual phalanges of manual digit III < 0.5x diameter of non-ungual phalanges of digit II.

Ambiguous autapomorphies under ACCTTRAN: 171 (1 → 0), ischium more than 70% of pubis length.

Node 179

Included taxa: *Sinosauropteryx* + *Juravenator*

Unambiguous synapomorphies: 267 (0 → 1), cranialmost haemal arches < 1.5x as long as associated centra; 274 (1 → 0), humeral length is half femoral length or less; 277 (1 → 0), length of radius < 1/3x femoral length; 284 (1 → 0), manual phalanx I-1 longer than metacarpal II.

Ambiguous synapomorphies under DELTRAN: 302 (1 → 0), manual phalanx III-3 markedly shorter than combined lengths of phalanges III-1 and III-2.

Ambiguous synapomorphies under ACCTTRAN: 257 (1 → 0), premaxillary teeth subequal in size to the maxillary teeth; 286 (1 → 0), metacarpals II and III are not appressed for their entire lengths.

Sinosauropteryx

Unambiguous autapomorphies: 41 (1 → 0), prefrontal large, dorsal exposure similar to that of lacrimal; 115 (0 → 1), caudal vertebrae without transition point; 118 (0 → 1), neural spines of caudal vertebrae separated into cranial and caudal alae throughout much of caudal sequence; 152 (0 → 1), digit I bearing large ungual and unguals of other digits distinctly smaller; 226 (0 → 1), distal humeral condyles on cranial surface; 345 (0 → 1), with fingers extended, tip of ungual I extends past flexor tubercle of ungual II but does not extend past tip of ungual II.

Ambiguous autapomorphies under DELTRAN: 53 (0 → 1), quadrate hollow, with depression on caudal surface; 101 (1 → 0), cervical and cranial trunk vertebrae amphiplatyan to platycoelous; 119 (0 → 1), neural spines on distal caudals absent; 171 (0 → 1), ischium 70% or less of pubic length; 286 (1 → 0), metacarpals II and III are not appressed for their entire lengths; 327 (0 → 1), diameter of non-ungual phalanges of manual digit III < 0.5 × diameter of non-ungual phalanges of digit II.

Ambiguous autapomorphies under ACCTAN: 240 (4 → 0), maxillary fenestra large and round.

Remarks - According to Currie & Chen (2001), relatively short forelimb, a prominent ulnar olecranon process and a powerful manual phalanx I-1 are characters indicating a monophyletic Compsognathidae. These characters likely represent specializations of *Sinosauropteryx*, the taxon they described.

Juravenator

Unambiguous autapomorphies: 23 (1 → 0), caudal margin of naris farther rostral than the rostral border of the antorbital fossa; 39 (0 → 1), enlarged foramen or foramina opening laterally at the angle of the lacrimal, present; 84 (1 → 0), maxillary and dentary teeth serrated; 85 (0 → 2), small number of dentary teeth; 120 (2 → 1), prezygapophyses of distal caudal vertebrae with extremely long extensions of the prezygapophyses (up to 10 vertebral segments long in some taxa); 142 (1 → 0), olecranon process weakly developed; 175 (1 → 0), pubis propubic; 239 (1 → 0), rostral portion of the maxillary antorbital fossa: small, from 10% to less than 40% of the rostrocaudal length of the antorbital cavity; 298 (0 → 1); 321 (0 → 1), total length of pedal phalanx II-2 (not counting posteroventral lip, if any) < 2x length of distal condylar eminence; 346 (1 → 0), premaxillary teeth unserrated; 349 (0 → 1), distal chevrons straight upside-down T-shaped.

Ambiguous autapomorphies under DELTRAN: 161 (1 → 0), *brevis fossa* shelf-like; 233 (0 → 1), height of skull (minus mandible) at middle of naris less than half the height of skull at middle of orbit; 240 (0 → 4), maxillary fenestra small and round, not dorsally displaced.

Ambiguous autapomorphies under ACCTAN: 233 (0 → 1), height of skull (minus mandible) at middle of naris less than half the height of skull at middle of orbit; 327 (1 → 0), diameter of non-ungual phalanges of manual digit III > 0.5 × diameter of non-ungual phalanges of digit II.

SKELETAL TAPHONOMY

In this section we analyse the taphonomy of the specimen, focussing on the skeletal parts. We will dedicate a specific chapter of the monograph (see Part II) to the taphonomy of the soft tissues, together with some notes on the diagenesis of local calcite areas of the embedding sediment that in our opinion were partly affected by the proximity to the soft tissues, during the decay of the carcass.

As mentioned in the description, the position of fossilisation of *Scipionyx* cannot be taken as informative about the cause of death. For one part, the lack of the distal portions of the hindlimbs and of the tail does not depend either on traumatic *pre mortem* events (e.g., predation) or on *post mortem* scavenging, nor on taphonomical dispersal conditions, because the rest of the skeleton is complete, articulated and even associated to soft tissues of its own body. On the other hand, the mouth of *Scipionyx* is likely open because of bone dislocation and crushing during diagenesis, rather than to jaw-muscle contraction or to supposed suffocation, as the bones forming the mandibular hinge are apparently disarticulated and deformed. So, whether the animal died in the water or was instead carried out to sea after death, cannot be ascertained. As the head is upturned with respect to the neck, but not in an "opisthotonic" condition (*sensu* Ostrom, 1978), the carcass of *Scipionyx* could have been exposed to sunlight for a short period at the most. Its dehydration was likely caused by other factors, such as osmosis (see Soft Tissue Taphonomy), and probably occurred after burial, when the animal was already trapped by the weight of the sediments.

During the taphonomical processes, most of the cranial bones of the left side, the left dorsal ribs and the left ele-

ments of the pectoral girdle slid in the same direction under the counterlateral elements of the right side (Fig. 114). This might indicate that the forces of diagenetic compression did not act completely vertically but had also an oblique component. However, caudally to the caudal dorsal vertebrae, all pelvic bones show a sliding direction that is opposite to that of the paired presacral bones. It is very unlikely that such a bi-directional dislocation, which occurred in body regions distant from each other by only 1-10 centimetres, was the result of two different diagenetic compression forces that acted one opposite to the other. Thus, we think that this sliding pattern reflects the lying down (depositional) position of the specimen. The carcass might have reached the sea floor and sunk in the substrate on one side, but in an arched, inverted U-shaped passive pose, with the mid-abdomen as the highest portion of the body, or vice versa. This hypothesis is consistent with the position of the centre of buoyancy of a bipedal vertebrate with a laterally compressed body, irrespective of whether the carcass of *Scipionyx* sank to the seafloor by gravity after floating or was dragged there by a current. Subsequently, sediment compaction would have favoured the sliding of the paired, relatively non-mobile bones in opposite directions.

It is interesting to note that in *Scipionyx* the compression of the skull caused the palatine-pterygoid complex to move towards the centre of the orbital and antorbital cavities, just like in *Juravenator* (Göhlich & Chiappe, 2006: fig. 2a) and *Compsognathus* (Peyer, 2006: fig. 4A). The rostral end of the left dentary bent medially, forming a U-shaped turn that is still in contact with the end of the right dentary (Fig. 42). This indicates that the preserved medial bending of the den-

taries is natural, and that the two bones formed a U-shaped symphysis. In fact, as we pointed out in the description (see Dentary), it is unlikely that the symphysis of the young *Scipionyx* was so firmly sutured to favour distortion of the right dentary rather than separation of the two rami during diagenesis, taking also into account that *Scipionyx* is a hatchling and the symphyseal contact is often relatively weak even in sub-adult and adult theropods (e.g., Britt, 1991).

Regarding the ceratobranchials I, these bones are still coupled albeit fossilised distant from the lower jaw. This suggests that they moved when they were still united by the hyoid cartilages.

The neck of *Scipionyx* is strongly bent backwards, with the postzygapophyses slid onto the prezygapophyses up to the maximum limit of craniocaudal sliding permitted by their articular surfaces. The *post mortem* conditions certainly favoured this bending and the related extreme interlocking of the neural arches, but the neck is still articulated and in a position that could have been achieved in life, and it is not comparable with the unnatural *post mortem* bending visible in some fossil specimens (e.g., both specimens of *Compsognathus*). The bending is present all along the postaxial cervical series of *Scipionyx*, but the neck appears more recurved at the base because the cranial cervicals are fossilised in a lateral-laterodorsal view, limiting the observer's perception of the bending and giving a more rigid appearance to the neck with respect to, for example, that of *Sinocalliopteryx*.

In life, the distal extremities of the cervical ribs were probably not so tightly appressed to the centra. However,

soft tissue dehydration occurring after death caused the ribs to adhere to the vertebrae, and the favourable neck posture and the structural flexibility of the ribs limited their fracture.

As reported in the description, the neural arches are well-articulated all along the vertebral column, with the zygapophyses interlocking: their conformation has kept them linked together. However, most of the centra (i.e., C5, C7-10, D1, D3-11, S4-S5 and Ca1-5) – which are not yet fused to their arches, not held by the apophyses and definitely more inclined to move and roll because of their shape – have detached from the arches in various ways. It is interesting to note that, in the caudal series, the centra have detached from the arch in a manner very similar to the holotype of *Huaxiagnathus* (Hwang *et al.*, 2004: fig. 4C). The D7 neural arch of *Scipionyx* shows a strange plastic deformation: instead of it being straight, the dorsal margin of this bone shows a S-shaped bending at the level of the diapophysis, despite it being reinforced by a ridge.

In both manus, the position of fossilisation of the first digits compared to the others gives an interesting insight into the functional anatomy of the Italian compsognathid (see Pectoral Girdle And Forelimb in Skeletal Reconstruction And...).

Summing up, the cause of death of *Scipionyx* cannot be hypothesised with this set of data. The mode of preservation of the skeleton indicates that the carcass, rather than undergoing violent crushing, was subjected to slow, plastic diagenetic deformation after rapid and complete burial in a soft substrate.



Fig. 114 - Interpretive drawing of the passive pose of the carcass of *Scipionyx samniticus* on reaching the sea floor (A), based on the relative position of the left (red) and right (green) paired bones in the fossil skeleton as seen from below (B).

Fig. 114 - Ricostruzione ipotetica della posa passiva della carcassa di *Scipionyx samniticus* al momento della deposizione sul fondale marino (A), basata sulla posizione relativa, nel fossile visto dal basso (B), delle ossa pari del lato sinistro (rosse) e destro (verdi).

PART II - SOFT TISSUE ANATOMY

Introduction

The notoriety, even at the popular level, of *Scipionyx* is primarily due to the preservation of soft tissues and anatomical detail, including exquisitely fossilised internal organs, never seen before in any other dinosaur. Its level of preservation was already considered exceptional at the macroscopic level, so much so that *Scipionyx* represents an essential reference point for reconstructing the internal anatomy of dinosaurs as a whole (e.g., Leahy, 2000; Paul, 2002; Chinsamy & Hillenius, 2004).

The employment of more sophisticated investigative methods, including examination under UV light and SEM, has revealed that the soft tissues of this 110-million-year-old fossil are not simply imprints but mineralised in three dimensions and are exceptionally preserved even at a cellular, and, in some instances, a subcellular, level. Moreover, SEM element microanalysis has revealed the presence of remains preserved as thin organic films of endogenous chemical compounds derived from the decay of the dinosaur's carcass. Here, we describe the astounding level of preservation not only of previously seen organic remains but also of those that have been newly detected, most of which are unique to the

fossil record. However, despite the high degree of preservation of *Scipionyx* there are no traces of scales, feathers or other integumentary structures. This unique kind of fossilisation, whereby internal organs are preserved but the integument is not, depends upon the particular physico-chemical conditions of the aquatic environment in which the dinosaur became fossilised; this will be examined later. Evidence of the high preservational potential of the Pietraraja outcrop dates back two centuries to when the fossil locality was first described. Costa (1853-1864), for example, reported the exceptional fossilisation of skin and cartilaginous parts of a guitarfish of the genus *Rhinobatus* (Fig. 14D). Among reptiles, at least two specimens of lepidosaurs were found with preserved remnants of soft tissue: the holotype of the squamate *Chometokadmon fitzingeri* is pictured by Costa (1853-1864) as broadly covered with patches of skin, the squamation of which is clearly visible on the skull and neck (Fig. 16); an indeterminate rhynchocephalan recently described by Evans *et al.* (2004) preserves an intestinal tract, linking the remnants of an ingested lizard to a faecal mass ready to be voided. So, without any doubt, the Pietraraja Plattenkalk represents a Konservatt-Lagerstätte (*sensu* Seilacher, 1970).

INTERNAL SOFT TISSUES

As extensively documented herein, all the internal soft parts of *Scipionyx*, except for the oesophagus and the purported liver, are three-dimensionally mineralised tissues, not simply imprints. The most important internal soft tissues, which had not yet been examined in detail at the time, were first described by Dal Sasso & Signore (1998a, 1998b). These include skeletal muscle remains at the base of the neck and in the proximal region of the tail, connective tissue associated to the muscle bundles in the same areas, tracheal rings close to the furcula, faint traces of what might have been the liver, and the entire intestine – despite some claims, no heart is preserved in *Scipionyx*, at least not with its original morphology (see Liver And Other Blood-Rich Organs). These relatively large structures emerge in relief and are clearly visible to the naked eye; they are perfectly distinguishable from the skeletal elements, also on account of their distinctive ochre colour, intermediate between the brown bones and the grey-yellowish matrix (Fig. 115). Other organic remains are preserved as thin films, which can be seen under UV light as fluorescent areas of different colours (Fig. 116). With the exception of a peculiar dark blue-purple colour marking the hepatic and other blood-rich remnants, the soft tissues exhibit a brilliant golden-yellow hue. In addition to the soft tissues formerly described by Dal Sasso & Signore (1998a, 1998b) and later by Dal Sasso (2003, 2004), traces of oesophagus, blood vessels, visceral muscles, other small patches of skeletal muscles, cartilages and ligaments have been subsequently found and are discussed herein.

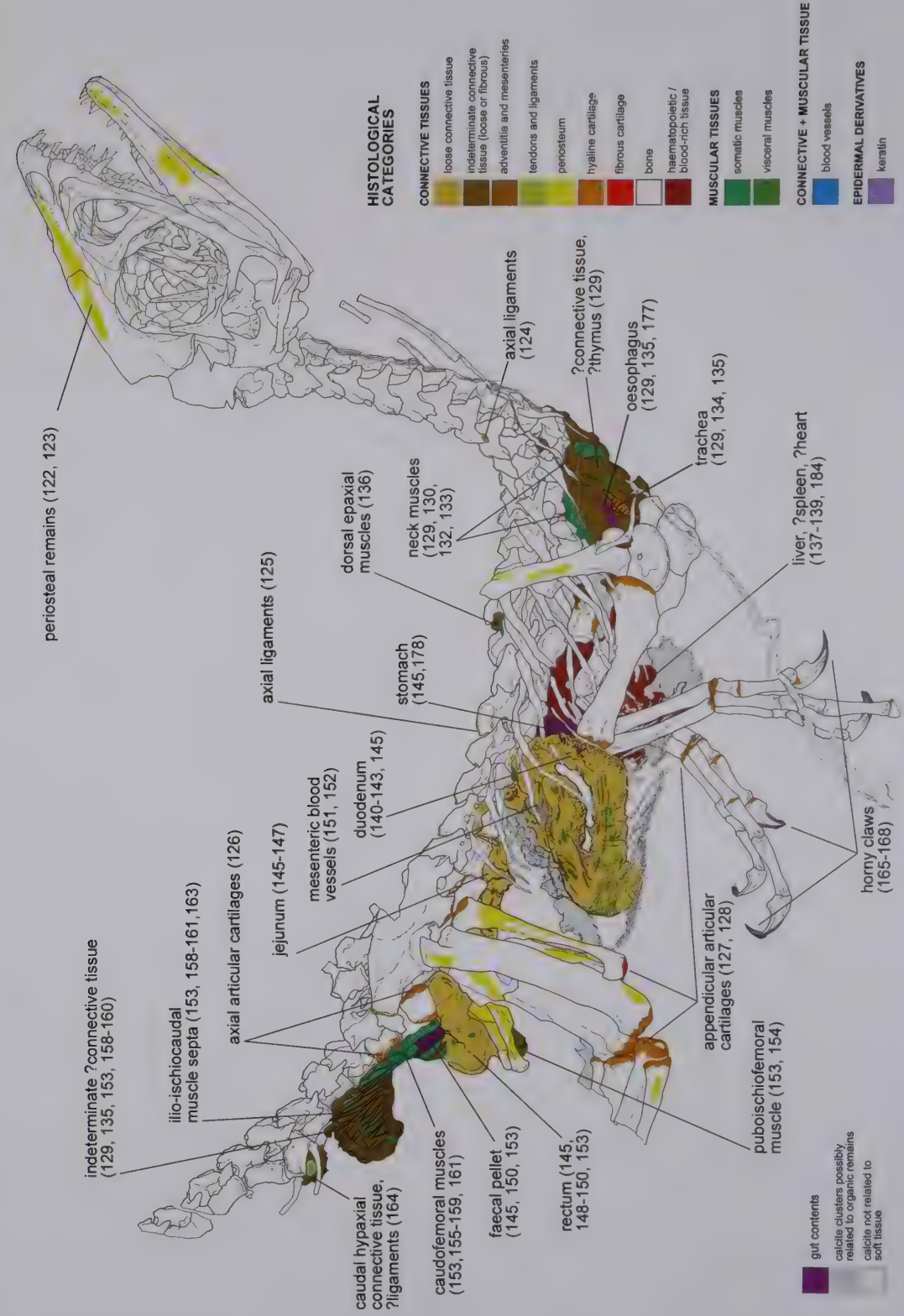
Besides *Scipionyx*, three-dimensional preservation of muscle remains and other non-osseous internal soft tissue has been described only in six, possibly seven, other dinosaur specimens. First were two Brazilian theropods of simi-

lar age (Albian, Romualdo Member of Santana Fm.), fossilised in calcareous concretions (Kellner, 1996a, 1996b). One of the specimens, later named *Mirischia* (Naish *et al.*, 2004), preserves a short tract of intestine in association with the pelvic bones (Martill *et al.*, 2000); the other, later named *Santanaraptor* (Kellner, 1999), preserves remains of skin and muscle fibres. In describing the latter, Kellner (1996b) stated that “since epidermis and muscle fibres are preserved in three dimensions, this might be the best fossilised soft tissue of a dinosaur known so far”. However, the comparison of analogous soft-tissue structures shows that *Scipionyx* is better preserved: for instance, *Scipionyx*'s blood vessels, which are either encased within bones or embedded in phosphatised soft tissue, are not simply channels or rod-like structures that have been secondarily filled in – they have retained their walls as a distinct texture (see below).

Mineralised dinosaurian soft tissue was also unearthed in the Lower Cretaceous deposits of Las Hoyas, Spain: a single specimen of the ornithomimosaur *Pelecanimimus* has fossilised in a lacustrine lithographic limestone, and has preserved skin and muscle with some three-dimensional detail, replicated in an iron carbonate (Briggs *et al.*, 1997).

In 2000, the discovery of a fossil dinosaurian heart was announced (Fisher *et al.*, 2000). The putative heart, including purported remnants of the aorta, was preserved as a nodule of iron minerals inside the thorax of an ornithischian of the genus *Thescelosaurus* (nicknamed “Willow”) from the Upper Cretaceous of South Dakota, USA. The authors suggested that the organ had been saponified under anaerobic burial conditions, and then changed into goethite. Computed tomography imagery showed a four-chambered structure, corresponding to the two atria and the two ventricles of the heart of mammals and birds.





Fisher *et al.* (2000) interpreted this structure as indicating an elevated metabolic rate for *Thescelosaurus*. However, modern crocodylians and birds both have four-chambered hearts, so dinosaurs probably had one as well, but the different metabolism of the two living clades of archosaurs indicates that the heart structure is not necessarily tied to metabolic rate (Chinsamy & Hillenius, 2004). What's more, the interpretation of the ferrous nodule as a fossil heart is not universally accepted: according to Rowe *et al.* (2001), the heart is actually a concretion. As they note, the anatomy given for the object is incorrect (for example, the "aorta" narrows coming into the "heart" and lacks arteries coming from it), and the concretion partially engulfs one of the ribs and has an internal structure of concentric layers in some places; another concretion is preserved behind the right leg.

Murphy *et al.* (2007) reported three-dimensional muscle remains in the ventral portion of the neck, in the right shoulder and in the tail of a hadrosaurid of the genus *Brachylophosaurus*, coming from the Upper Cretaceous of Montana, USA. The specimen, nicknamed "Leonardo", preserves integumental remains over 90% of its body, as well as some gastric contents.

Manning (2008) described preliminarily the finding of another partially intact hadrosaurid mummy, provisionally nicknamed "Dakota", unearthed in 1999 in the Upper Cretaceous of North Dakota, USA. The fossilised remains, which include skin, muscle, tendons and ligaments, represent the first-ever find of a dinosaur where the skin "envelope" had not collapsed onto the skeleton, allowing to calculate muscle volume and mass.

A seventh possible finding of dinosaurian soft tissue was reported by Chin *et al.* (2003), who identified undigested muscle and connective tissue of a possible pachycephalosaurid dinosaur within a tyrannosaurid coprolite from the Late Cretaceous of Alberta, Canada.

Lastly, Carrano & Sampson (2008) mentioned the presence of muscle impressions and other soft tissue remains in the abelisaurid theropod *Aucasaurus* from the Upper Cretaceous of Argentina.

In any case, none of the specimens above provides as much information on the anatomy of internal organs as does *Scipionyx samniticus*: even before the present monograph, the little Italian theropod has been a reference specimen for the reconstruction of the position of the thoracic and abdominal organs, for supporters (e.g., Leahy, 2000; Paul, 2001, 2002) and opposers (e.g., Ruben *et al.*, 1999, 2003; Chinsamy & Hillenius, 2004) of the avian origin of dinosaurs, alike. We relegate to a specific chapter our opinion on this matter, as we intend first to describe, with the utmost accuracy, what in actual fact can be seen in the specimen. Detailed examination of the holotype of *Scipionyx samniticus* allows to identify a variety of soft tissues, some of which are still associated into whole, or parts of, organs. For this reason, and for ease of description, we have subdivided this chapter into sections dedicated to the best preserved anatomical parts, topographically ordered in a craniocaudal direction, and beginning with the innermost tissues, i.e., the ones most intimately related to the skeletal elements. The histological attribution to individual tissue categories and/or to a pool of tissues composing each organ has been dealt with in the discussion part of each chapter and in the synoptic table of the soft tissues (Fig. 117).

Soft tissue within the bones

The presence of soft tissue remains within the bones was investigated through SEM analysis of a microsample taken from the dorsal margin of the shaft of the right third dorsal rib. The sample contains blood vessels and shows a cellular morphology, with a level of preservation that, presumably, is present in the whole skeleton.

The most informative image shows a portion of the compact bone layer of the rib in oblique section with a blood vessel going through it (Fig. 118A). The lamellae are 1.5-2.0 μm thick and show a fine-grained texture; here and there, the interlamellar lines accommodate lenticular spaces which, by comparative anatomy (e.g., Kardong, 1997), represent the lacunae of the osteocytes. On closer examination (Fig. 118B), the lacunae preserve subcellular details such as a finely zig-zag shaped margin, made by alternating bony papillae and thin intrusions into the lamellae, which represent the canaliculi, i.e., the ultrastructural lacunae left by the net of the filipodia. The fine interconnections among the densely branched canaliculi is likely responsible for the fine-grained texture of the lamellae. This is confirmed by comparison with published pictures of dinosaur osteocytes (Schweitzer *et al.*, 2008: fig. 2), in which lenticular cells are interconnected by peculiar branched filipodia.

Pointed bony structures, protruding from the cutting plane but well-rooted in the compact bone by branched pillars, may represent transitional connections with the spongy part of the rib or, simply, strengthening structures (Fig. 118A-B). The blood vessel cut by the sampling has an oval cross-section, measuring 3.0-5.5 μm in diameter, and preserves its wall in the form of a constantly thick (0.5 μm), differently textured, lighter coating (Fig. 118C). The lumen, virtually undeformed by diagenesis, appears paved by a smooth, wavy layer (possibly, the endothelial cells).

Soft tissue and cellular remains within cortical and medullary dinosaur bone were recently investigated by Schweitzer *et al.* (2007, 2008), who, after proper demineralisation, found remarkable preservation of flexible and fibrous bone matrix, hollow blood vessels, intravascular material and osteocytes: this demonstrated that, exceptionally, a fossil bone is capable of encasing and preserving soft tissue for millions of years.

With respect to these unique results, we will comment at least on the most comparable elements, i.e., the blood vessels. In *Scipionyx*, although these structures have been preserved in the form of a mineralised tissue, they are present not only within the undoubtedly protective bone but also in the soft tissue of the intestines (see below). In both locations, the vessels are hollow, even though no demineralisation or any other chemical cleaning technique has been applied. Anticipating criticism on the part of the reader, we would like to point out that the structures we regard as being the walls of blood vessels do not represent a mineral precipitate or a human artefact. In the first case, one would expect nearby hollow structures to be similarly lined with precipitate deriving from interstitial mineral water; however, it is evident from the SEM images that this is not the case, at least in this portion of the examined bone (Fig. 119). With regard to a human artefact, two facts rule out any chance of recent organic contamination: first, we know that the person who discovered and first prepared

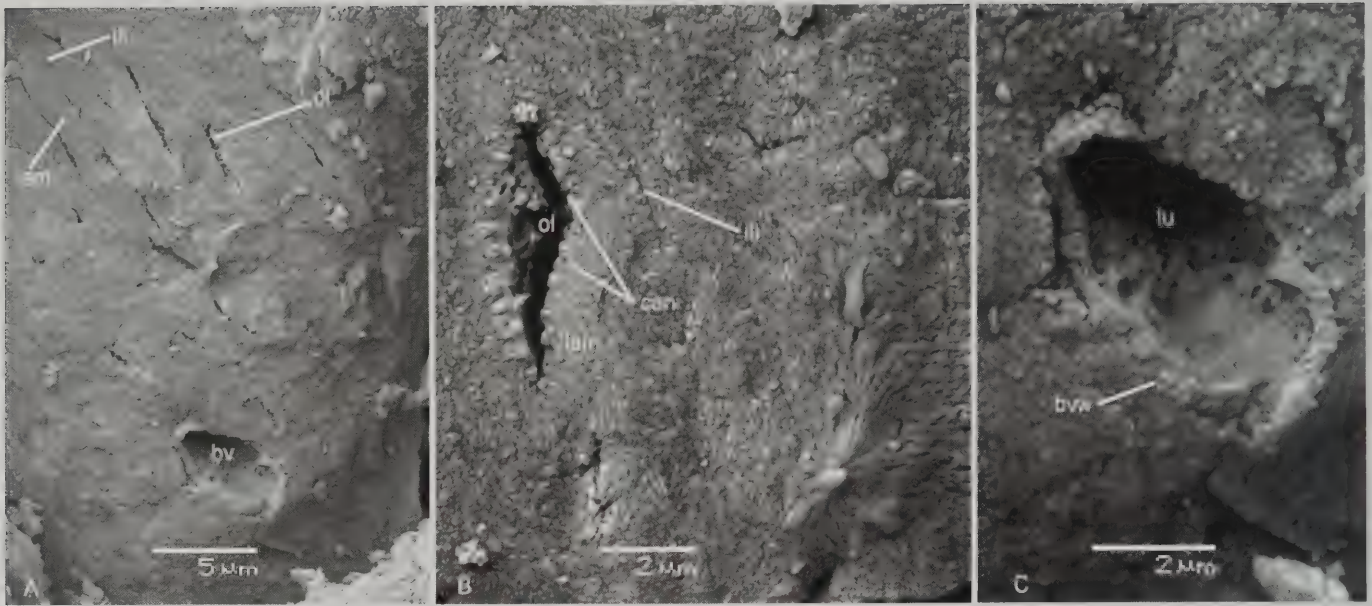


Fig. 118 - Soft tissue preservation at the cellular level within the bones of *Scipionyx samniticus*. A) SEM image of a dorsal rib, showing a portion of the compact bone layer in transverse section. Besides the lacunae of the osteocytes (B), a blood vessel is exposed and shows preservation of its wall (C). See Appendix 1 or cover flaps for abbreviations.

Fig. 118 - Conservazione dei tessuti molli a livello cellulare, all'interno delle ossa di *Scipionyx samniticus*. A) immagine SEM di una costola dorsale, che mostra una porzione di tessuto osseo compatto in sezione trasversa. Oltre alle lacune degli osteociti (B), è esposto un vaso sanguigno con la sua parete ben conservata (C). Vedi Appendice 1 o risvolti di copertina per le abbreviazioni.

the fossil used an industrial chemical product (polyester resin), but only for assembling three fractures of the original slab – one crossing the skull, one crossing the pelvis, one crossing the tibiae (G. Todesco, pers. comm., 2003) – and applied as a paste to the fossil's surface, so without a permeating capability (Fig. 9); second, after Todesco's work, the specimen was restored and further prepared by a collaborator of the Museo di Storia Naturale di Milano (S. Rampinelli) along with one of the authors of this study

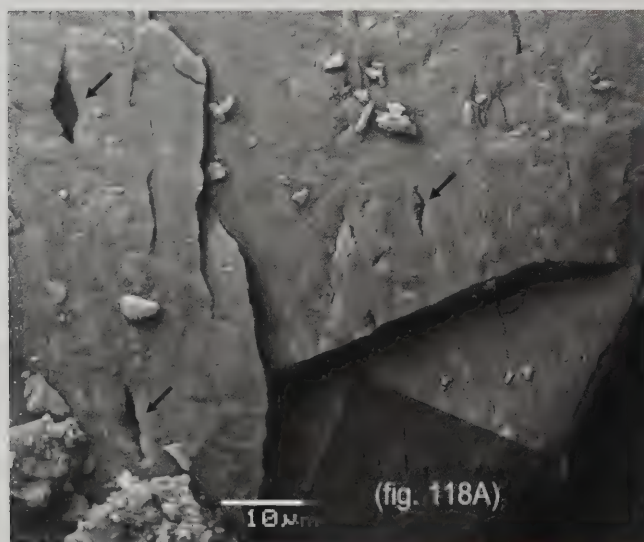


Fig. 119 - SEM image documenting that, in the vicinity of the blood vessel shown in Fig. 118A (shaded area), even the largest bone vacuities (arrows) are not lined with any mineral precipitate or recent organic contaminant.

Fig. 119 - Questa immagine SEM documenta che, vicino al vaso sanguigno mostrato in Fig. 118A (area ombreggiata), anche le cavità ossee più grandi (freccie) non sono tappezzate da alcun precipitato minerale, né da inquinanti organici recenti.

(CDS), who lightly impregnated the fossil with 5% Paraloid-B72 in acetone to protect the exposed surface of the fossil. For this reason, the samples of *Scipionyx* that we describe here were analysed along with a set of control samples taken from fragments of a fossil fish found in a similar layer of the upper Plattenkalk at Pietraraja, that had been previously impregnated with the same preservative (5% Paraloid-B72). SEM element microanalysis revealed immediately the presence of the preservative on the portions of control samples impregnated with Paraloid-B27, as a medium-high carbon (C) peak (Fig. 120). This peak was absent in all the microanalyses we conducted on the samples taken from the rib of *Scipionyx*, even when we aimed the microprobe at the cross-sectioned wall of the blood vessel (Fig. 121A) or the surrounding bone (Fig. 121B). The C peak is also absent or low in most SEM-analysed soft tissues of *Scipionyx* (see below), indicating that the preservative we used did not contaminate the specimen in depth, but it is limited to the exposed surfaces. This confirmed the validity of our choice of always analysing the reverse side of the samples.

Summing up, our SEM element microanalysis revealed that the blood vessel in the rib of *Scipionyx* is composed mostly of calcium phosphates, with proportions strictly similar to all other phosphatised tissues, which clearly belong to the dinosaur and, thus, cannot be alien to its body (see peaks of all soft tissues, in the following chapters). The same elemental ratios occurred when analysing other blood vessels preserved in the specimen (see Intestine). Therefore, these vessels, their hollow lumina and their finely ridged walls, which are of uniform thickness but tapering at branching points, cannot be artefacts derived from contamination with preservatives, such as polyvinyl acetate, nor any other organic, equally carbon-rich exogenous intrusion, such as fungal invasions or extracellular polymeric substances secreted by microbes.

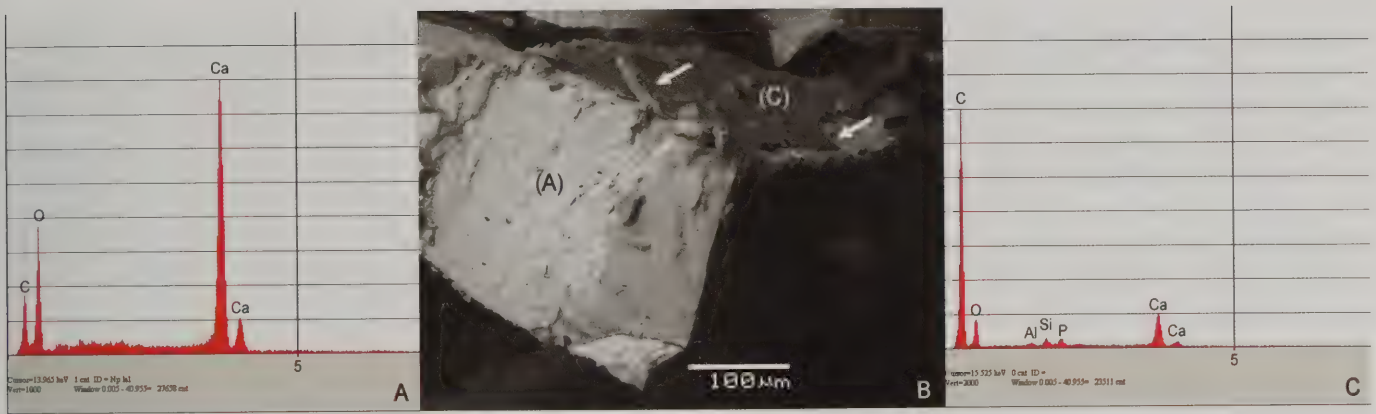


Fig. 120 - SEM element microanalysis of a control sample (bone of a fish from the Pietraraja Plattenkalk) impregnated with the same preservative (5% Paraloid B72) used on *Scipionyx samniticus*, and then cross-sectioned. Note the carbon peak (C) and the amorphous cuticle (B, arrows) produced by the preservative, which are both much lower/absent in the internal portions of the sample (A).
 Fig. 120 - Microanalisi degli elementi al SEM di un campione di controllo (tessuto osseo di un pesce del Plattenkalk di Pietraraja) impregnato con lo stesso consolidante (Paraloid B72 al 5%) usato su *Scipionyx samniticus*, e poi sezionato. Si noti il picco del carbonio (C) e la cuticola amorfa (B, frecce) originati dal consolidante, che sono molto inferiori/assenti nelle porzioni interne del campione (A).

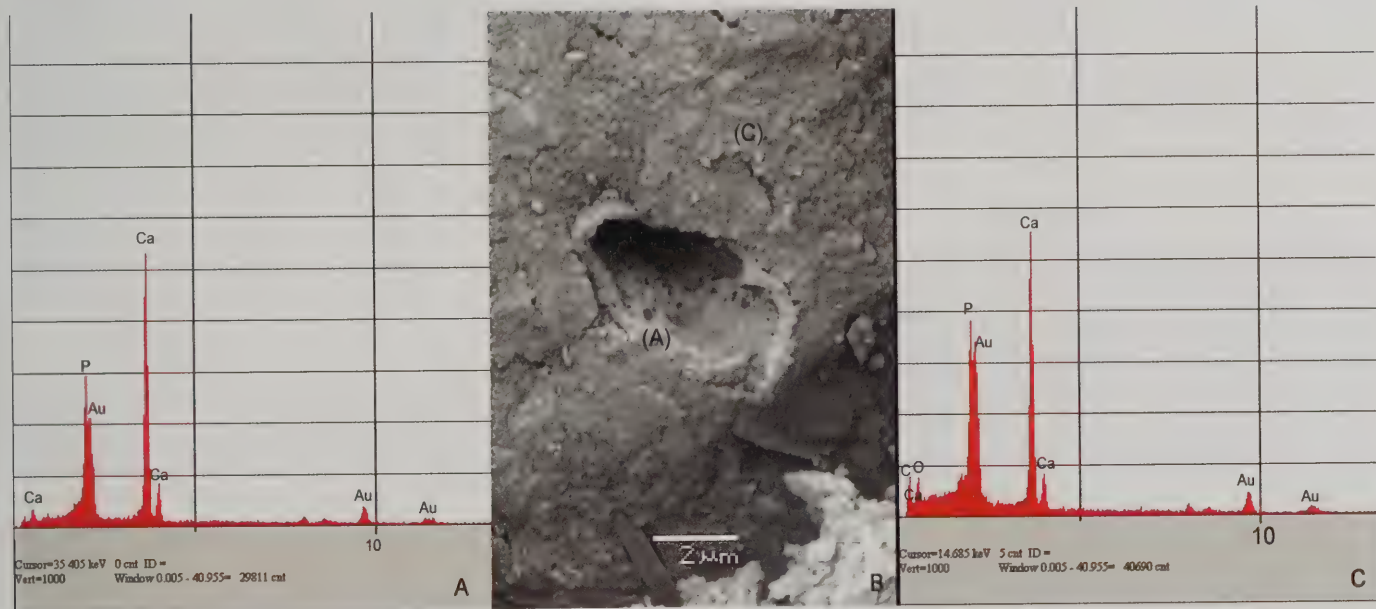


Fig. 121 - SEM element microanalysis of the wall of a blood vessel (A) encased in the sampled rib of *Scipionyx samniticus* (B), compared with element microanalysis of the surrounding bone tissue (C). Both are composed of calcium phosphate and are devoid of any recent carbon-rich, natural or synthetic contaminant.
 Fig. 121 - Microanalisi degli elementi al SEM della parete del vaso sanguigno (A) incorporato nella costola campionata di *Scipionyx samniticus* (B), a confronto con la microanalisi del tessuto osseo circostante (C). Entrambi sono composti da fosfato di calcio e sono privi di qualsiasi contaminante organico, sia naturale che sintetico.

Periosteal remains

Some bone surfaces are covered with a yellowish patina that gives them an opaque aspect when observed with the naked eye or under the light microscope. As experimented during the mechanical preparation of the specimen (Dal Sasso, pers. obs, 1994-1997), this patina is almost as hard as the underlying bone, so is not consistent with the kind and the amount of preservative we applied (see above). More importantly, we are sure that the patina was present prior to any human activity, because we found it even on the portions — such as the cranial sides of the ischia — brought to light subsequently by one of us (Dal Sasso, pers. obs., 2004). Indeed, the patina is more extensively preserved in these newly exposed ar-

eas, suggesting that it was likely widespread in the original fossil. Under Wood's lamp, the areas covered with this patina gain an opaque brown colour that is lighter than the dark brown of adjacent bone surfaces.

In our opinion, this patina represents residual patches of the periosteum, a thin sheath of dense fibrous connective tissue that, *in vivo*, coats the cortical layer of all bones. As shown in the synoptic table of the soft tissues preserved in *Scipionyx* (Fig. 117) and from some exemplifying photos (Figs. 122-123), the most extended periosteal patches are preserved on the right nasal, right frontal and left splenial of the skull, and on the right scapular blade, right pubic shaft, left pubic apron, right proximal and distal femoral shafts, right fibula and, more extensively, on both ischial shafts, in the appendicular skeleton.

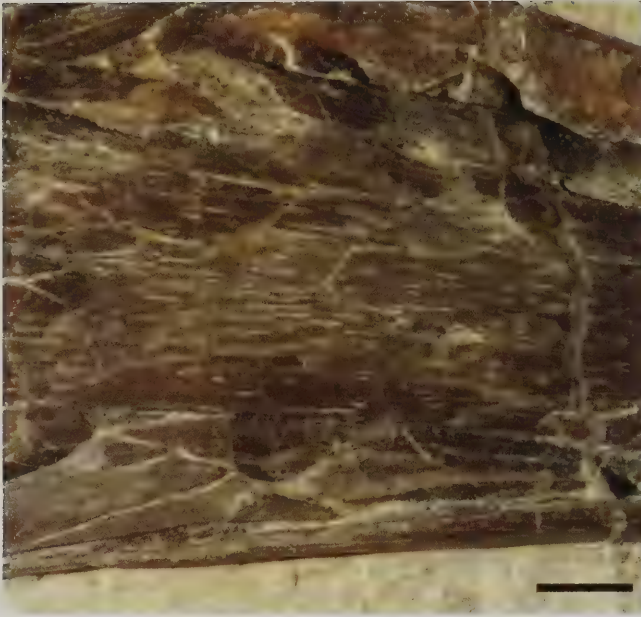


Fig. 122 - Close-up of the right dentary of *Scipionyx samniticus*, showing periosteal remains in the form of a yellowish opaque patina. Scale bar = 1 mm.

Fig. 122 - Particolare del dentale destro di *Scipionyx samniticus*, con residui di periosteo sotto forma di una opaca patina giallastra. Scala metrica = 1 mm.

Axial ligaments

Thin strips of an ochre-yellow material having a consistency intermediate between the matrix and the bone can be found in few, quite limited, points along the vertebral column. Although no particular microstructure can be distinguished under the light microscope, the arrangement of these strips, which are located on the apophyses of some neural arches, suggests that they may represent remnants of intervertebral connecting structures. The most cranial structure is located on the lateral wall of the prezygapophysis of the 9th cervical vertebra, close to the prezygapophyseal articular surface (Fig. 124). This position corresponds to the zygapophyseal articular capsule, which is present, just in the formerly described point, in extant

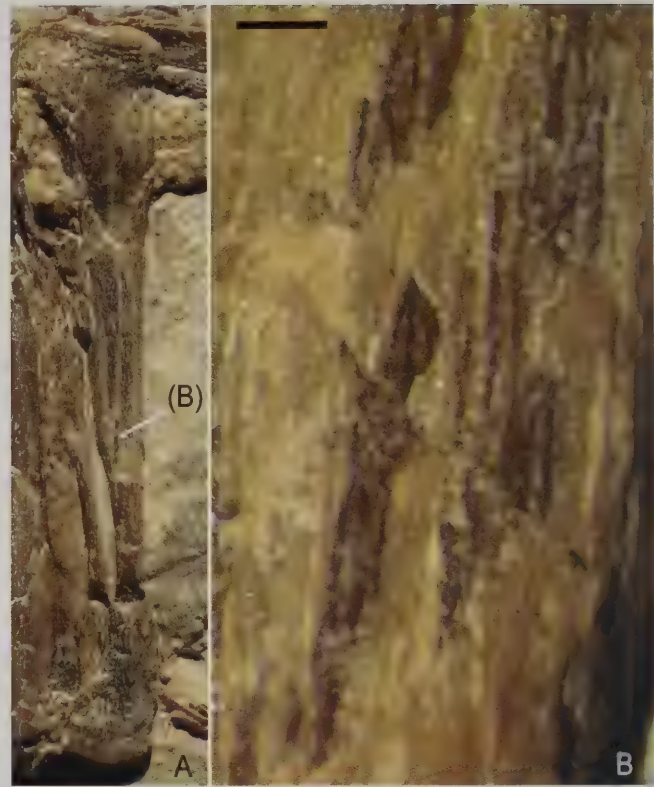


Fig. 123 - Patches of periosteum are well-preserved on the right pubic bone of *Scipionyx samniticus* (A), in particular on its shaft (B). Scale bar = 0.5 mm.

Fig. 123 - Lembi di periosteo sono ben conservati sull'osso pubico destro di *Scipionyx samniticus* (A), in particolare sulla sua diafisi (B). Scala metrica = 0,5 mm.

crocodilians (Frey, 1988) and birds (Baumel & Raikov, 1993), and indirectly found in sauropod dinosaurs as well (Schwarz *et al.*, 2007c). *In vivo*, the zygapophyseal articular capsule is composed of fibrous connective tissue enclosing a synovial joint between the prezygapophysis of a vertebra and the postzygapophysis of the preceding vertebra.

Other structures that probably acted as intervertebral connections run along the dorsal margin of the neural

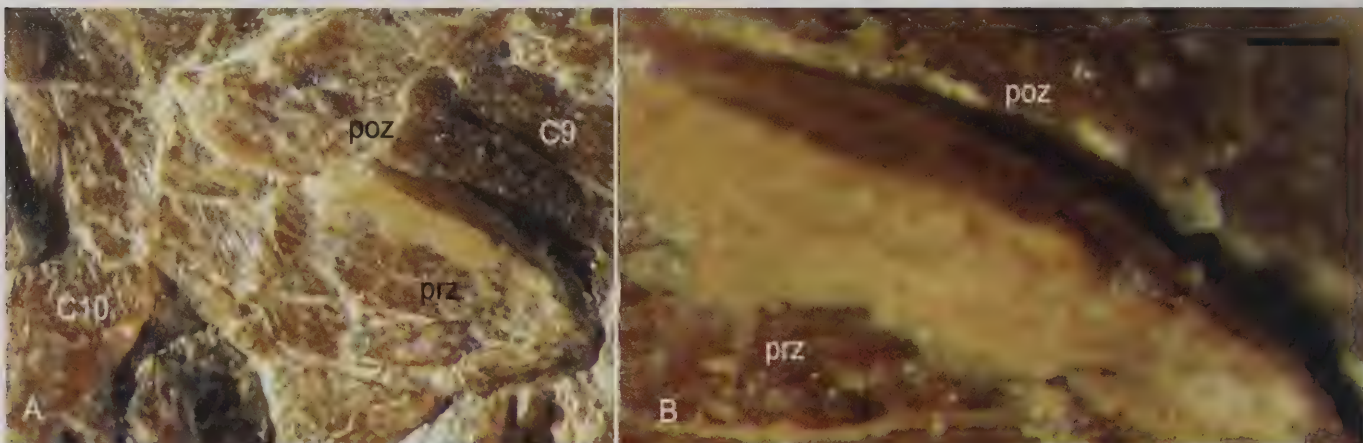


Fig. 124 - Articulated 9th and 10th cervical neural arches of *Scipionyx samniticus* (A), and close-up of the remnants of the right zygapophyseal articular capsule (B). Scale bar = 0.2 mm. See Appendix 1 or cover flaps for abbreviations.

Fig. 124 - Archi neurali articolati della 9^a e 10^a vertebra cervicale di *Scipionyx samniticus* (A), e particolare dei resti della capsula articolare della zigapofisi destra (B). Scala metrica = 0,2 mm. Vedi Appendice 1 o risvolti di copertina per le abbreviazioni.

spines of the dorsal vertebrae 9, 11, 12 and 13, as well as from the apex of the spines to the beak-like ligament attachments described in the Osteology section (see Dorsal Vertebrae). Given the link to the latter, we regard these structures as remnants of the interspinal ligaments, whereas the most dorsally placed, apical fragments would derive from the supraspinal ligaments. Only very thin stripes adjacent to the bones are preserved of these ligaments; these are scarcely perceptible under visible light but well-contrasted under ultraviolet light (Fig. 125).

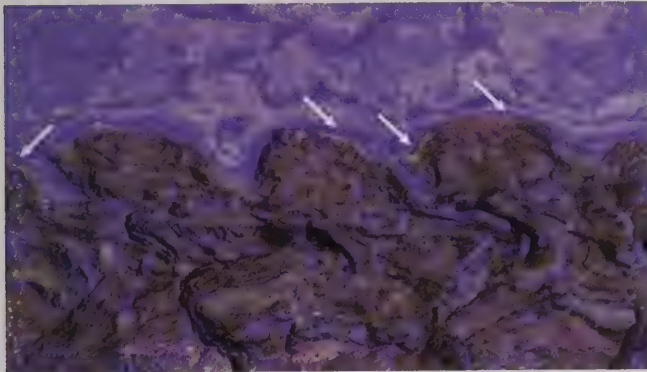


Fig. 125 - Ultraviolet-induced fluorescence photograph of the caudal dorsal neural spines of *Scipionyx samniticus*, showing possible fragments of the supraspinal ligaments (arrows).

Fig. 125 - *Scipionyx samniticus*. Fotografia in fluorescenza indotta da luce ultravioletta delle spine neurali dorsali caudali, che mostra i probabili frammenti dei legamenti soprasspinali (frece).

Axial articular cartilages

The Wood's lamp highlights a frankly light and bright colouring on some vertebrae of *Scipionyx*, indicating the possible presence of organic remnants in correspondence to the neurocentral articular surfaces. More precisely, the fluorescence runs along the articular surfaces of the dorsal centra 6 and 10, sacral centra 1 and 5, and caudal centra 1 and 2 (e.g., Fig. 126). Given their precise localisation, we regard these organic films as remnants of the neurocentral cartilages, which in a very immature specimen, such as

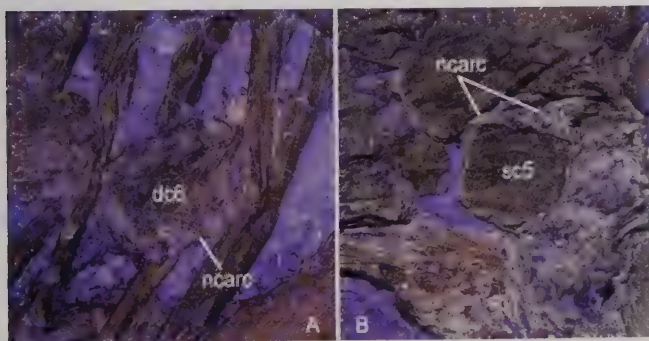


Fig. 126 - Remains of the neurocentral articular cartilages on the 6th dorsal (A) and 5th sacral (B) vertebrae of *Scipionyx samniticus* fluoresce under ultraviolet light. See Appendix 1 or cover flaps for abbreviations.

Fig. 126 - In luce ultravioletta, sulla 6^a vertebra dorsale (A) e sulla 5^a vertebra sacrale (B) di *Scipionyx samniticus* assumono fluorescenza i resti delle cartilagini articolari neurocentrali. Vedi Appendice 1 o risvolti di copertina per le abbreviazioni.

Scipionyx, are expected still to be abundantly present. In fact, we remark that the neurocentral vertebral joints are synchondroses, i.e., a type of cartilaginous joint that is temporary, existing only during the growing phase – they become progressively thinner during skeletal maturation and, ultimately, become obliterated by bone union. Histologically, synchondroses consist of hyaline cartilage.

Appendicular articular cartilages

UV light analysis also reveals that most of the limb and girdle joints of *Scipionyx* is marked by a golden-white film of organic remnants delimiting, with precision and continuity, the articular ends of the bones. This film corresponds to the position of the hyaline and fibrous symphyseal articular cartilages (Figs. 127-128). Articular fibrocartilaginous caps – present on the epiphyses of the long bones of all extant archosaurs – rarely fossilise (e.g., Geist & Jones, 1996; Reisz *et al.*, 2005; Schwarz *et al.*, 2007b), so the remarkable level of preservation of *Scipionyx* reveals that, in the forelimbs, these caps are more extended in the shoulder, elbow and wrist joints, but also clearly visible even where sandwiched in-between smaller distal elements, like between metacarpals and phalanges, and between proximal and distal phalanges. In the pelvic girdle, the proximal articular

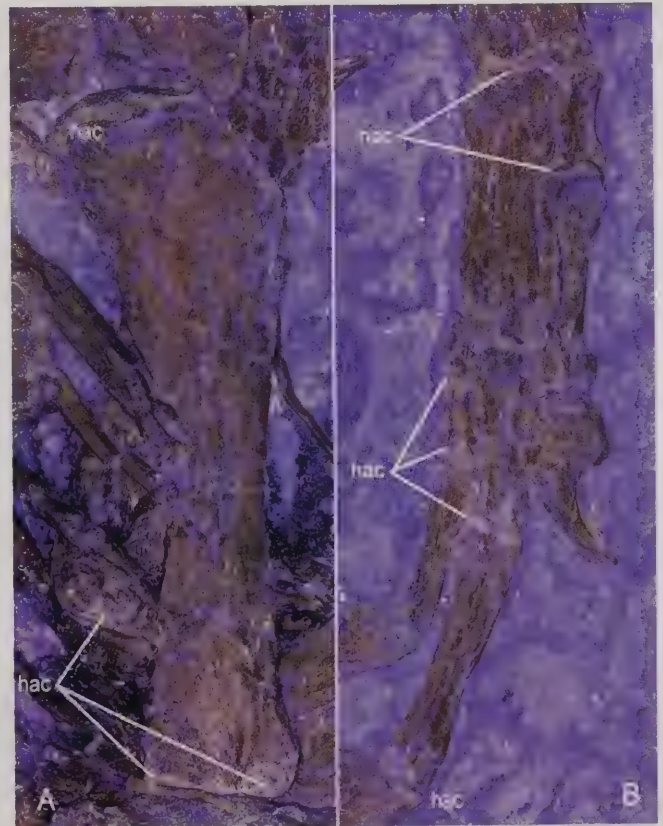


Fig. 127 - Close-ups of the remains of the articular cartilages of the right humerus (A) and left manus (B) of *Scipionyx samniticus* under ultraviolet-induced fluorescence. See Appendix 1 or cover flaps for abbreviations.

Fig. 127 - *Scipionyx samniticus*. Particolare dei resti delle cartilagini articolari dell'omero destro (A) e della mano sinistra (B), fotografati in luce ultravioletta. Vedi Appendice 1 o risvolti di copertina per le abbreviazioni.

surfaces of the tibiae and the fibulae are evidently coated by cartilage, as are the distal condyles of the femora, the extremity of the pubic peduncle of the right ilium, and, in front of it, the iliac process of the right pubis. The ventral extremities of the pubic feet are also covered by cartilage which, under UV light, appears indistinguishable in the fossil from the other areas of cartilage, even if the cartilage of ileo-pubic and interpubic joints should be of a fibrous nature, i.e., the type of tissue that, in vertebrates, connects the symphyses, making them capable of supporting both compressive and tractional stresses. In order to avoid invasive analyses (e.g., drilling, thin sectioning), which would have damaged this unique specimen, no details of the growth zone overlain by the articular caps have been studied in *Scipionyx*.

A film that fluoresces like cartilage under UV light is seen as well on the thin caudal surface of the iliac blade (Fig. 128). However, its position and well-delimited extension are consistent with the posterior sacroiliac ligament attachment, which *in vivo* would have been composed of fibrous connective tissue.

Muscles, connective tissue and other soft tissues in the neck

As already noted, tissue remains are preserved in several anatomical regions of the hatchling Italian theropod. The most cranial area (and also one of the most extended) in which these tissues can be clearly seen is at the base of the neck, where they are observable even with the naked eye under visible light on account of their yellowish colour. Here, the remains occupy a flat, triangular area, 19.3 mm long and 12.6 mm wide, positioned ventral to the last cervical vertebra and the first four dorsals, and delimited caudally by the scapular girdle elements (Fig. 129).

In the former description of *Scipionyx*, the tissue in this area was improperly referred to the pectoral musculature (pem in Dal Sasso & Signore, 1998a: fig. 2). However, most of the original structural arrangement of the soft tissues is lost here, so much so that the background mass, which has a consistency intermediate between fossilised bone and sediment, appears as an amorphous matrix. At first sight, this area was thought to possibly include part of the dinosaur's skin; in actual fact, patches of somatic musculature (Fig. 130), as well as frayed collagen bundles (Fig. 131), are discernible within its mass under the light microscope at a magnification of more than 50X, and, remarkably, a tract of trachea protrudes from it as well (see below). In extant archosaurs there is not a large amount of connective tissue in this region, and there should be no fat in a young hatchling, so this amorphous mass likely derives from another kind of tissue, which suffered much more decay. The most prevalent tissue/organ in the ventral region of the base of the neck in a neonate archosaur would be the thymus gland. In neonate crocodiles and most neonate birds, the thymus stretches from the cranial part of the lungs along the ventrolateral region of the whole neck (Huchzermeyer, pers. comm., 2010). Nevertheless, in the absence of morphological evidence of fossilised lymphoid tissue in *Scipionyx*, the conclusion that this mass represents the remains of the dinosaur's thymus gland is a speculation based on anatomical position.



Fig. 128 - The remains of the articular cartilages of the pelvic and hind-limb bones of *Scipionyx samniticus* under ultraviolet-induced fluorescence. See Appendix 1 or cover flaps for abbreviations.

Fig. 128 - *Scipionyx samniticus*. I resti delle cartilagini articolari delle ossa del cinto pelvico e degli arti posteriori, fotografati in luce ultravioletta. Vedi Appendice 1 o risvolti di copertina per le abbreviazioni.

The most evident patch of musculature in the neck of *Scipionyx* runs along the ventral side of the centra of the dorsal vertebrae 2, 3 and 4. Worth of mention is the fact that at least two series of dark parallel bands, regularly spaced by lighter intervals, perpendicular to the craniocaudal orientation of the bundle, are visible in the remnants of this muscle, just below the ventral margin of the 3rd dorsal centrum, at 60X magnification under the light microscope. This banding does not match any

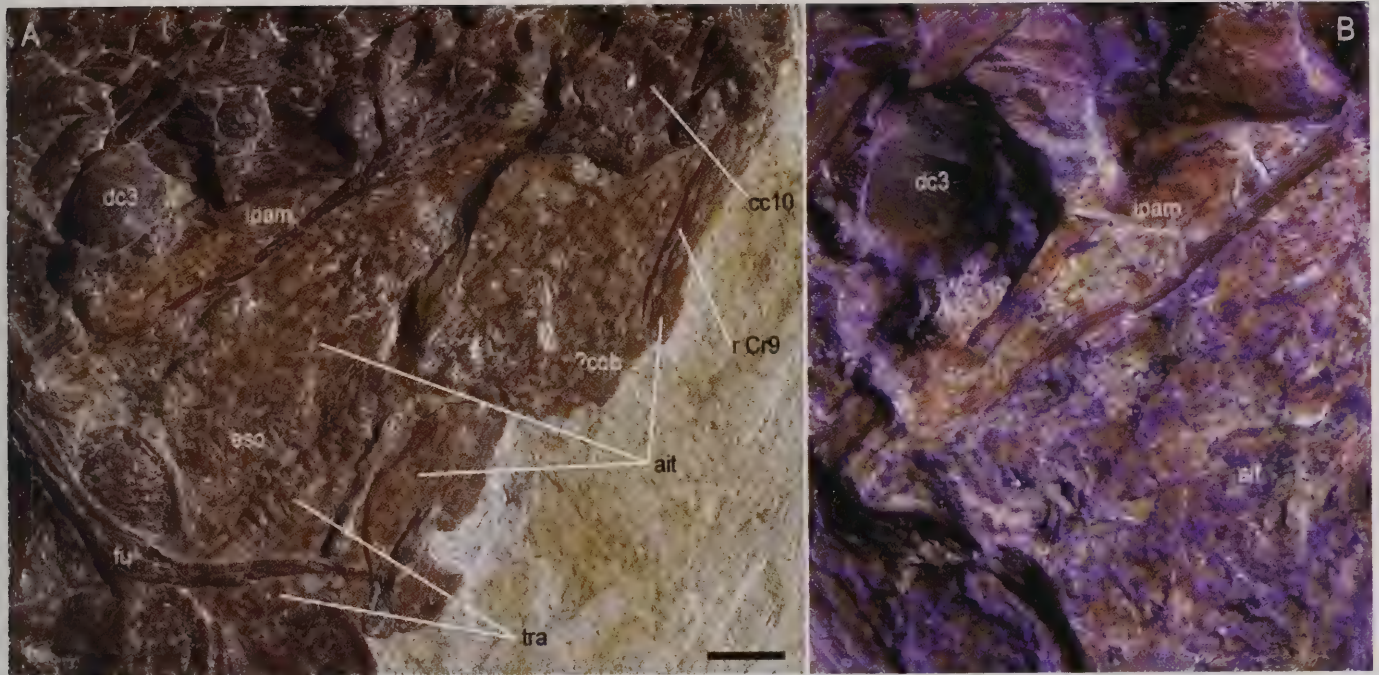


Fig. 129 - Soft tissues preserved at the base of the neck of *Scipionyx samniticus*. A) overall view in visible light. Regarding the dislocated centrum of the 10th cervical vertebra, see Trachea in Respiratory Physiology. B) UV close-up of a brightly fluorescing strip of tissue marking the position of the best preserved hypaxial muscle remains. Scale bar = 2 mm. See Appendix 1 or cover flaps for abbreviations.

Fig. 129 - Tessuti molli conservati alla base del collo di *Scipionyx samniticus*. A) vista generale in luce visibile (in merito al centro dislocato della 10^a vertebra cervicale, vedi Trachea in Respiratory Physiology); B) particolare in luce UV di una striscia di tessuto a fluorescenza brillante, che marca la posizione dei resti di muscolatura ipoassiale meglio conservati. Scala metrica = 2 mm. Vedi Appendice 1 o risvolti di copertina per le abbreviazioni.



Fig. 130 - Close-up of the muscle remains of *Scipionyx samniticus* shown in Fig. 129. The arrow points to the chromatic bands shown also in Fig. 133. Scale bar = 1 mm. See Appendix 1 or cover flaps for abbreviations.

Fig. 130 - *Scipionyx samniticus*. Particolare dei resti muscolari mostrati in Fig. 129. La freccia indica le bande cromatiche illustrate anche in Fig. 133. Scala metrica = 1 mm. Vedi Appendice 1 o risvolti di copertina per le abbreviazioni.

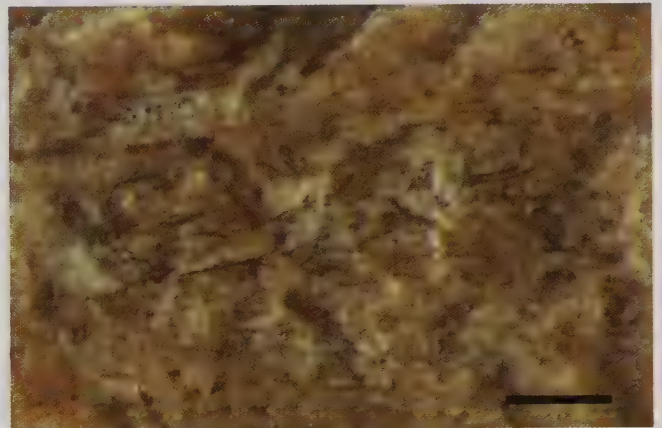


Fig. 131 - Possible frayed collagen bundles embedded in the amorphous indeterminate tissue at the base of the neck of *Scipionyx samniticus*. Scale bar = 1 mm.

Fig. 131 - Probabili fasci sfilacciati di collagene, immersi nel tessuto amorfo indeterminato alla base del collo di *Scipionyx samniticus*. Scale bar = 1 mm.

relief, but is fairly chromatic in nature, with a frequency of 24-28 dark and light bands per mm. Such an order of magnitude is not at all consistent with the nanometric banded structure of collagen (e.g., Kadler *et al.*, 1996; Lingham-Soliar & Wesley-Smith, 2008; Smith, 1968), and it also rules out any possible artefact of preparation. More importantly, the appearance of clear banding leads one to think of highly ordered and repeated, micrometric biological structures, which, if aligned with

one another, would produce an overall striated effect visible even under a light microscope. This phenomenon does not occur in collagen, but is typical of somatic skeletal musculature (e.g., Kardong, 1997). However, the striated pattern of skeletal muscles is usually visible only with polarised light under the light microscope (Mascarello, pers. comm., 2009) and has a micrometric order of magnitude, inconsistent with the one we describe above.

In order to investigate these structures more deeply, we took a microsample nearby. Morphological and chemical elemental analysis of this sample under SEM confirmed unequivocally the presence of phosphatised muscular tissue with still intact bundles of myofibres (Fig. 132A-C). The myofibres are preserved in three dimensions, are still appressed to one another, are parallel and straight, and have margins that are clearly delimited by narrow spaces left by the dissolution of the muscle cell membrane (sarcolemma) and of the connective tissue surrounding it (endomysium). Remarkably, the myofibres have an internal, continuous and regular transverse banding pattern with a periodicity (2.9 μm) consistent with the mean sarcomeric size of extant vertebrates (Panchangam *et al.*, 2008; Botte & Pelagalli, 1982; Cavitt *et al.*, 2004; Cross *et al.*, 1981; Muhl *et al.*, 1976; Wheeler & Koochmarai, 1994). These structures definitely differ from those produced by collagen fibres, which are typically arranged in cross-striated fibrils (D-banding) with a specific axial periodicity of 67 nm (Kadler *et al.*, 1996; Lingham-Soliar & Wesley-Smith, 2008; Smith, 1968). The SEM images of other samples (Fig. 132D) show that most of the surrounding musculature has lost some detail during fossilisation: the individual fibres can be resolved but the sarcomere-related banding is faint or lost. Nevertheless, their arrangement in multiple layers of packed, straight elements with constant transverse diameter, as well as their order of magnitude, are consistent with the morphology of fossilised vertebrate myofibres (e.g., Chin *et al.*, 2003; Kellner, 1996a; Wilby & Briggs, 1997). As better explained below (see Soft Tissue Taphonomy), an intermediate microfabric (*sensu* Wilby & Briggs, 1997) might have been produced in this area during early diagenetic stages, with muscle

fibres being replaced by apatite crystals in the form of coarse to large agglomerations.

The biological structure responsible for the banded pattern visible with non-polarised light under the optical microscope (Fig. 133) remains unknown, as we have not yet found anything comparable to that order of magnitude, at least in the palaeontological literature devoted to soft-tissue preservation.

Even though we did not have the possibility of taking samples for SEM analysis in other areas of the soft tissues at the base of the neck of *Scipionyx*, we reasonably refer the brown-reddish fibrous structures surfacing close to the distal half of the 9th right cervical rib (Fig. 131) as collagen fibres rather than muscle remains. This attribution relies on the observation that *Scipionyx*'s myofibres invariably show a clearly different aspect under the optical and scanning-electron microscopes, i.e., a packed, cord-like arrangement, with diameters that remain constant even for relatively long distances (see images of other muscle remnants of the specimen in the following chapters). On the contrary, despite displaying a filamentous aspect and a craniocaudal co-orientation, the fibrous structures close to the 9th right cervical rib follow a curved, sinuous path, and have intersections or V-shaped bifurcations as well; most importantly, they show a quite variable, non constant diameter (8-40 μm), not only along a single filament, but also from fibre to fibre. Given the micrometric order of size, which is not consistent with the nanometric order of the single fibril, Mascarello (pers. comm., 2009) hypothesised that each individual filament may correspond to collagen bundles and the bifurcations may match inhomogenous partitions of fibrils (i.e., frayed collagen bundles).

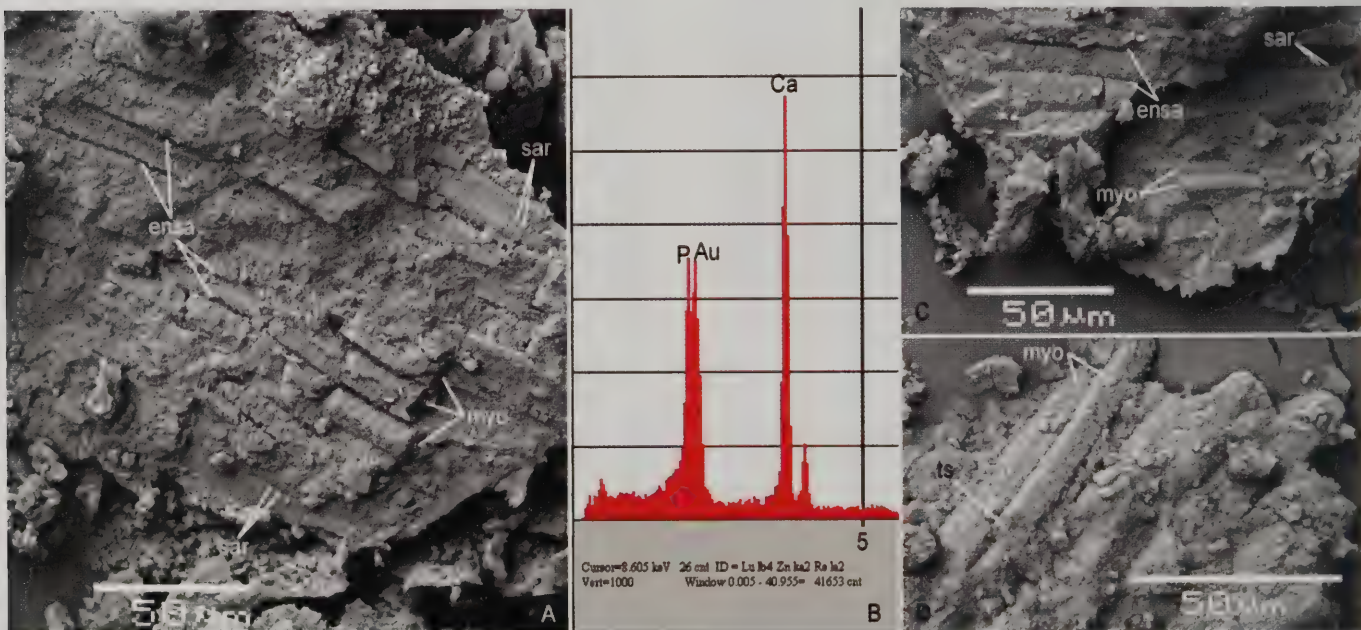


Fig. 132 - Soft tissue preservation at the cellular level in the neck muscles of *Scipionyx samniticus*. A) SEM image of a bundle of myofibres showing sarcomere-related banding; B) SEM element microanalysis of the same sample, indicating that the myofibres are lithified in calcium phosphate. In other bundles of myofibres, the sarcomere-related banding is faint (C) or lost (D). See Appendix 1 or cover flaps for abbreviations.

Fig. 132 - Conservazione dei tessuti molli a livello cellulare nei muscoli del collo di *Scipionyx samniticus*. A) immagine SEM di un fascio di miofibre che mostrano bande riferibili a sarcomeri; B) la microanalisi degli elementi al SEM sullo stesso campione indica che le miofibre sono litificate in fosfato di calcio. In altri fasci di miofibre le bande dei sarcomeri sono meno marcate (C) o sono andate perse (D). Vedi Appendice 1 o risvolti di copertina per le abbreviazioni.

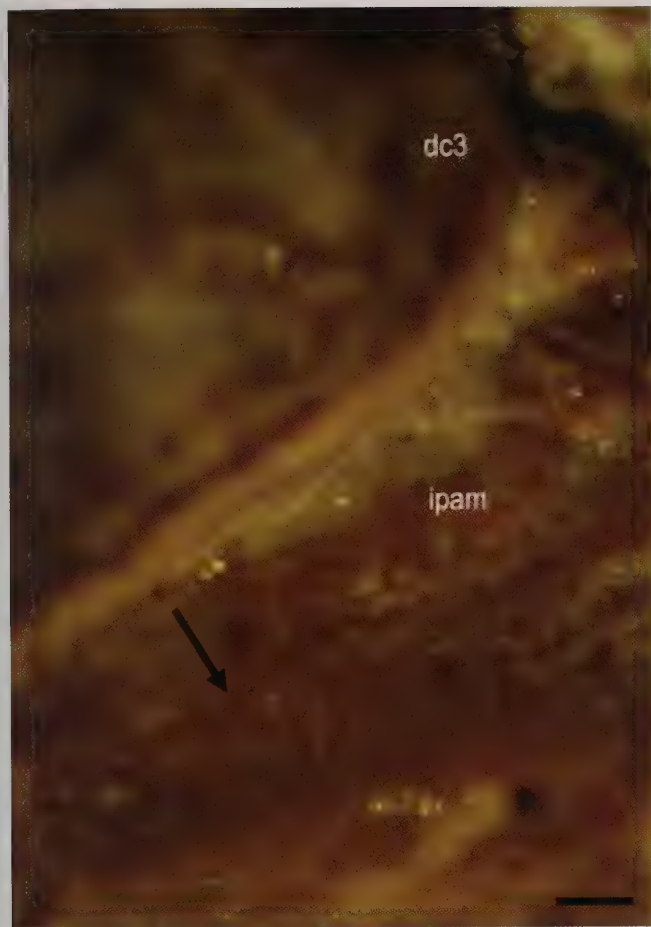


Fig. 133 - Close-up of Fig. 130, showing parallel, regularly-spaced chromatic bands (arrow), visible under the optic microscope and non-polarised light in the soft tissue remains at the base of the neck of *Scipionyx samniticus*. This banded pattern is maybe related to a supra-cellular level of organisation of the muscular tissue. Scale bar = 100 μ m. See Appendix 1 or cover flaps for abbreviations.

Fig. 133 - *Scipionyx samniticus*. Particolare di Fig. 130 che mostra bande cromatiche parallele, spaziate in modo regolare (freccia), visibili al microscopio ottico e in luce non polarizzata nei resti dei tessuti molli alla base del collo. Questa struttura a bande dipende forse da un livello di organizzazione supracellulare del tessuto muscolare. Scala metrica = 100 μ m. Vedi Appendice 1 o risvolti di copertina per le abbreviazioni.

About 1 mm from these filaments, towards the ventral edge of the amorphous soft-tissue mass, another series of parallel and regular chromatic bands can be seen. Here, the banding seems to have a smaller size and/or a higher periodicity (around 40 per mm), but its aspect is quite analogous to that described above. Again, we suggest that these bands support the presence of muscular remains, but we are unable to explain the physical nature of this optical effect.

The patches of musculature preserved at the base of the neck of *Scipionyx* are too fragmentary to infer their arrangement, their origin or their insertion sites. Nevertheless, we can reasonably suppose that they pertain to the hypobranchial and hypaxial complexes. The latter includes, for example, the intrinsic and extrinsic tracheal muscles, as well as the *M. sternohyoideus* and the *M. sternotrachealis* (Berger, 1960; George & Berger, 1966). The *M. sternotrachealis* is particularly well-developed in extant long-necked avian theropods (Botte & Pelagalli, 1982).

Evident rows of parallel striations, with a periodicity of at least 14-16 per mm, can be seen at the centre of the amorphous mass at the base of the neck and in the corner formed by the right scapular acromion and the furcula (Fig. 134A). At a first glance, based on their macroscopic aspect and size, the striations seem to represent fascicula of myofibres, but after careful examination under the optic microscope, these striations are seen to disappear almost completely when the light is oriented parallel to them (Fig. 134B). Therefore, they consist of fine scratches (carvings) made on the soft tissue remains. The complete lack of pigmentation confirms that these striations are not organic traces, but artefacts of preparation; namely, they are very fine, light scratches caused by the tiniest metal pins that were used to manually remove the sediment from the fossil (Rampinelli, pers. comm., 2009).

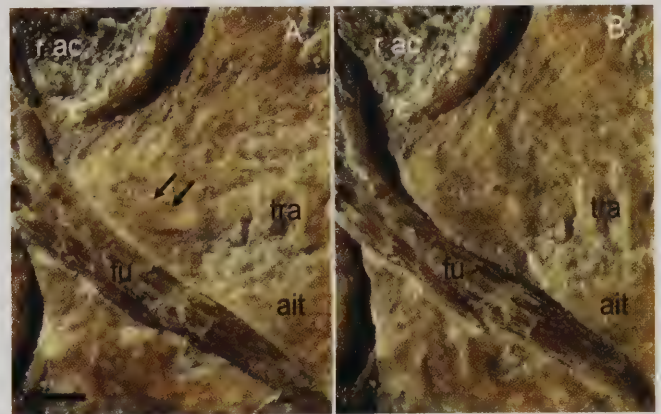


Fig. 134 - Soft tissue remains at the base of the neck of *Scipionyx samniticus*. Parallel striations (A, arrows) that disappear when the light is oriented parallel to them (B) do not indicate muscle bundle orientation, but are artefacts of preparation (fine scratches). Scale bar = 1 mm. See Appendix 1 or cover flaps for abbreviations.

Fig. 134 - Resti di tessuti molli alla base del collo di *Scipionyx samniticus*. Strie parallele (A, frecce) che scompaiono quando la luce viene orientata parallelamente ad esse (B) non indicano la disposizione di fasci muscolari ma sono artefatti di preparazione (incisioni sottili). Scala metrica = 1 mm. Vedi Appendice 1 o risvolti di copertina per le abbreviazioni.

Trachea

Within the triangular-shaped area of neck muscle and connective remains, are 8-10 light-coloured, almost diaphanous rings, partly embedded in the putative connective tissue (Fig. 135). These structures form an about 7 mm-long row, aligned in a craniocaudal direction: caudally to the furcula, they rest underneath the right coracoid; cranially to the furcula, they fade into the mass of neck tissue. Therefore, these rings lie exactly where the trachea is expected to be, i.e., in the prethoracic region, aligned with the plane of symmetry of the bones of the pectoral girdle.

The individual rings are found in place, one in front of the other, and regularly separated by gaps which measure about half the craniocaudal length of each ring. This structure is commonly found in extant vertebrates: it reinforces the ventral and lateral sides of the trachea, and protects and maintains the airway pat-

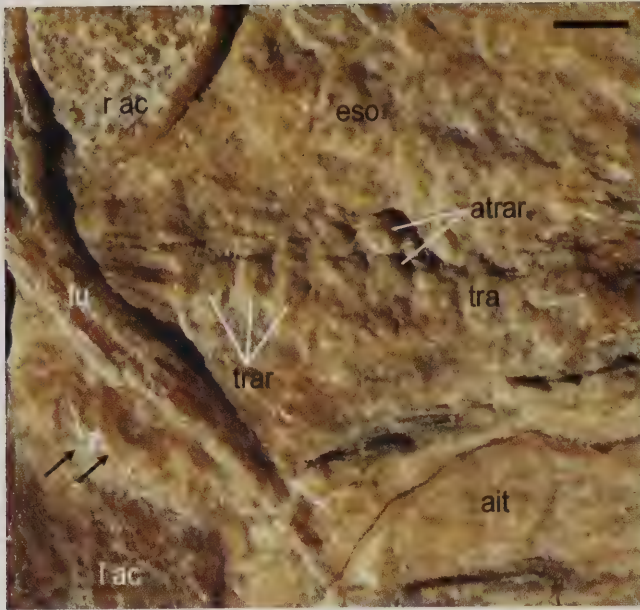


Fig. 135 - The visible tract of the trachea of *Scipionyx samniticus*. Arrows point to the two tracheal rings exposed in cranial view. Scale bar = 1 mm. See Appendix 1 or cover flaps for abbreviations.

Fig. 135 - Il tratto visibile della trachea di *Scipionyx samniticus*. Le frecce indicano i due anelli tracheali esposti in norma craniale. Scala metrica = 1 mm. Vedi Appendice 1 o risvolti di copertina per le abbreviazioni.

ent while giving the tracheal tube maximum flexibility (e.g., Romer & Parsons, 1977). In *Scipionyx* the size of each ring is around 0.33 mm and the gaps are about 0.17 mm, so 2 rings and 2 gaps are about 1mm long. It is difficult to measure the height of the rings, as most of them are incomplete. Two elements (5th and 6th), occupying a central position within the row cranial to the furcula, are exposed laterodorsally and form an incomplete ring opened dorsally and having dorsally rounded apexes (in this view, both right and left apexes are visible). The lateral walls seem slightly compressed, so these two rings have a U-shape. The height of these rings is a little less than 1mm.

The potentially best preserved ones are the two tracheal rings caudal to the furcula: they are still coated with a thin patch of ?connective tissue. The ring lying closer to the furcula, well-exposed in cranial view, is C-shaped, confirming that the cranialmost tracheal rings are a bit crushed and dorsally opened. Observed *in vivo*, this morphology is consistent with that of the young individuals of many extant terrestrial vertebrates and the adults of some, in which the dorsal arches of the tracheal rings, made of hyaline cartilage, are not chondrified (e.g., Romer & Parsons, 1977). In *Homo sapiens*, for instance, each tracheal element forms an incomplete ring occupying the ventral 2/3 of the circumference of the trachea; they are incomplete behind, where the tube is completed by fibrous tissue and smooth muscle fibres (e.g., Saladin, 2010). Incomplete chondrification (and consequently, fossil preservation) may well explain the relatively small size of the tracheal rings in *Scipionyx*. Compared with crocodiles and birds, one would expect an animal with the size of *Scipionyx* to have complete tracheal rings with a larger diameter. For example, a 29 cm-long Nile crocodile hatchling, studied for the pur-

pose of this monograph, had a tracheal diameter at mid-length of the trachea of 1.4 mm (Huchzermeyer, pers. comm., 2010): this means that an individual the size of *Scipionyx* would have had a tracheal diameter of about 2 mm. Nonetheless, the size of the preserved (chondrified) portion of the rings in *Scipionyx* does not correspond to the actual tracheal diameter: the C-shaped rings need almost another 1 mm to be completed, thus reaching an overall diameter of 2 mm. We do not believe that the rings were subjected to shrinkage during their fossilisation, nor to belong to one of the (much smaller) animals preyed upon by *Scipionyx* (see Gut Contents And Feeding Chronology).

Oesophagus and stomach

The oesophagus and stomach of *Scipionyx* are not preserved; however, we have some indirect evidence of their position. A faint trace of the oesophagus can be seen just dorsal to the trachea (Fig. 135). About 5 mm-long, this trace is marked by tiny fragments of bones and scales which parallel the trachea in a craniocaudal direction, at the level of the acromion of the right scapula. This arrangement is consistent with the position of the oesophageal tube, as seen in extant vertebrates (e.g., Romer & Parsons, 1977). The intimate embedding of the remains within the decayed tissue of the neck rules out the possibility of them being the bodies of organisms that were deposited of their own accord above or below the dinosaur's carcass. The nature of these remains, which, consequently, are swallowed, partially crushed prey, is discussed in a dedicated section (Gut Contents And Feeding Chronology).

Food remains pertaining to the stomach can also be discerned, found in the form of a cluster of tiny allogeneous bones (for a detailed description, see Stomach Contents). Their position indicates that the organ, or better, the portion of it that had contained them, was situated in the thorax of *Scipionyx* at the level of the 9th dorsal vertebra, close to the cranialmost tract of the intestine (Fig. 117). Unlike what is observed for the oesophagus, the stomach contents are not intimately embedded in the surrounding soft tissue. Nevertheless, the little mass of bones is certainly encased in the thoracic cavity, being positioned in an intermediate plane between the 6th and 7th left and right dorsal ribs, at the same depth as the adjacent vertebral centrum of D9. Most importantly, the swallowed bones are partially overlapped by the cranial portion of the duodenum: this indicates that they are positioned in the left side of the thorax, i.e., just where in extant archosaurs the stomach is situated (Huchzermeyer, 2003; McLelland, 1990).

Contrary to what is seen in the intestine, the stomach is not preserved even as a mould. There is reasonable ground to suppose that the dissolution of this organ, which *in vivo* is endowed with a thick muscular wall, was caused by its own physiology. The vertebrate stomach is typically a site of chemical digestive secretions, collectively called gastric juice, the presence of which has been proven indirectly also in theropod dinosaurs (e.g., Varricchio, 2001). Gastric juice includes some enzymes and mucus, but is primarily composed of

hydrochloric acid released from glands in the mucosal wall of the stomach (Kardong, 1997); in crocodiles, for instance, the acid is capable of dropping the gastric pH to as low as 1.2 (Huchzermeyer, 2003). Probably, the acidic environment, controlled by physiological processes, persisted for a while even after *Scipionyx* died, simply because the stomach is made to be an efficient liquid-storage bag. Under these conditions, a strongly acidic pH would have sped up the decay of the stomach compared with the rest of the carcass. This hypothesis is endorsed by the experimental observation that an acidic environment not only inhibits bacterial action, but also enhances the decomposition of biological tissues (Lyman, 1994). In other terms, the physiological pH present in the stomach at death prevented the precipitation of phosphates and carbonates for long enough to let the organ decompose (see also Soft Tissue Taphonomy).

On the other hand, the intestine of *Scipionyx* took more time to decay and was partially fossilised because its lumen was characterised by a neutral pH. In fact, it is well known (e.g., Kardong, 1997) that the pyloric glands, opening into the terminal tract of the stomach, produce secretions that help neutralise the acid chyme as it moves into the intestine. Notably, also the sphenodontid reptile from Pietraraja recently described by Evans *et al.* (2004) preserves some intestinal portions but not the stomach.

Nothing can be said about the shape and size of the stomach in *Scipionyx*. From gut contents reported in the tyrannosaurid *Daspletosaurus*, it was supposed that the theropod stomach was similar to the two-part stomach of birds (Varricchio, 2001). Based upon swallowed, acid-etched juvenile hadrosaur bones and other gut contents, and also upon tooth-marked bones, Varricchio (2001) inferred that *Daspletosaurus* and most theropods ingested and digested prey in a manner similar to that of extant archosaurs (crocodilians and birds), employing a two-part stomach with an enzyme-producing proventriculus followed by a thick-walled muscular gizzard. However, if one neglects the presence of a tiny pyloric chamber, the crocodilian stomach has only one chamber, lined entirely by secretory glands in the mucosa, which in any case extend into the pyloric chamber as well (Huchzermeyer, pers. comm., 2010). Therefore, there is not the functional distinction in crocodilians seen in the stomach of birds, in which the secretory glands are limited to the proventriculus (which, with the exception of the ostrich [Huchzermeyer, 2000], is small), whereas the gizzard is lined by koilin excreted by shallow glands and serves as storage (e.g., in raptors) or as a grinding organ (e.g., in the domestic fowl and in the ostrich). The fact that pieces of undigested bone are found in the intestine of *Scipionyx* (see Intestinal Contents) would suggest that it had a bird-like, two-chambered stomach, rather than a crocodilian stomach (in which bones are usually dissolved entirely). However, digestive physiology varies considerably even in the same individual, depending on a number of factors that do not leave any fossil trace (see Digestive Physiology).

Summing up, in absence of a fossil stomach, in our opinion it can be only postulated that *Daspletosaurus* or *Scipionyx*, or any other non-avian theropod, must have had a two-chambered stomach.

Dorsal epaxial muscles

In between the neural spines of the dorsal vertebrae 6 and 7 is a small patch of yellowish soft tissue (Fig. 136A) that markedly fluoresces a gold colour under UV light (Fig. 136B), similar to the musculature preserved at the base of the tail (see below). A cranial portion, next to the distal apex of the right transverse process of the 6th dorsal vertebra, and a caudal portion, in a more medial position, overlaying the right postzygapophysis of the 6th and part of the right prezygapophysis of the 7th dorsal vertebra, are discernible. Given their position, these soft-tissue remains likely represent part of the epaxial musculature and epaxial connective tissue, in particular a residual patch of the *M. transversospinalis* group or of the *M. longissimus dorsi*.

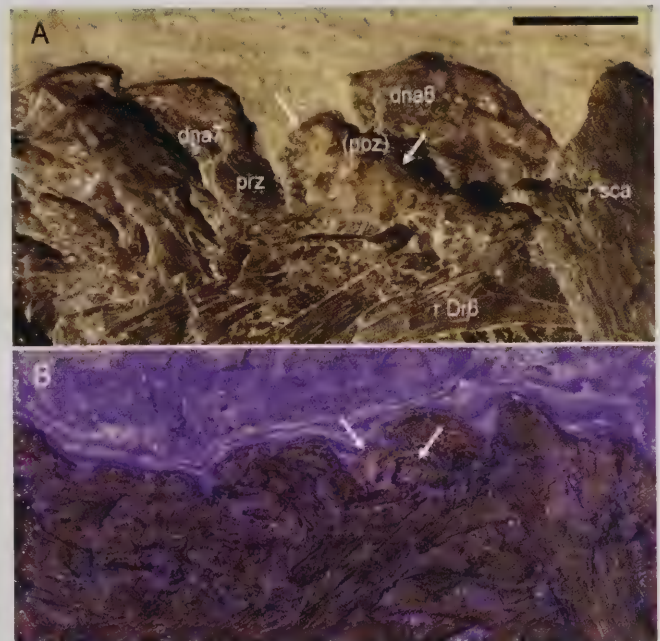


Fig. 136 - Close-up under visible light (A) and ultraviolet-induced fluorescence (B) of a residual patch of the epaxial musculature and epaxial connective tissue (arrows) in the dorsal tract of the vertebral column of *Scipionyx samniticus*. Scale bar = 2 mm. See Appendix 1 or cover flaps for abbreviations.

Fig. 136 - *Scipionyx samniticus*. Particolare in luce visibile (A) e ultravioletta (B) di un lembo residuale della muscolatura epiassiale e del connettivo epiassiale (freccie) nel tratto dorsale della colonna vertebrale. Scala metrica = 2 mm. Vedi Appendice 1 o risvolti di copertina per le abbreviazioni.

Liver and other blood-rich organs

In the thoracic portion of the visceral cavity, just cranial to the intestine and between the forelimbs of *Scipionyx*, a halo made by a reddish matter is seen to impregnate the sediment, as well as the left arm elements, the cranial gastralia and some dorsal ribs (Figs. 137A, 138A-C). Basing their hypothesis on colour and anatomical position, Dal Sasso & Signore (1998a) postulated in the former description of *Scipionyx* that this reddish macula was composed of iron-rich minerals derived from the decay of the liver, which in vertebrates is the single largest visceral organ (e.g., Schaffner, 1998) and the major organ accumulating



Fig. 137 - A) the reddish halo deriving from the decay of the liver (and of other blood-rich organs) of *Scipionyx samniticus*, seen under visible light; B) ultraviolet-induced fluorescence reveals that this material impregnates a larger area of the thorax. The distinct blue-indigo fluorescence corresponds to the primary light emission peak of biliverdin and, therefore, might be consistent with the presence of bile pigment residues. Scale bar = 5 mm.

Fig. 137 - *Scipionyx samniticus*. A) l'alone rossastro derivante dalla decomposizione del fegato (e di altri organi ricchi di sangue), fotografato in luce visibile; B) una foto in luce ultravioletta mostra che questo materiale ha impregnato un'area più ampia del torace. La ben distinta fluorescenza in blu-indaco corrisponde al picco di emissione primaria della biliverdina e dunque è compatibile con la presenza di pigmenti residui di bile. Scala metrica = 5 mm.

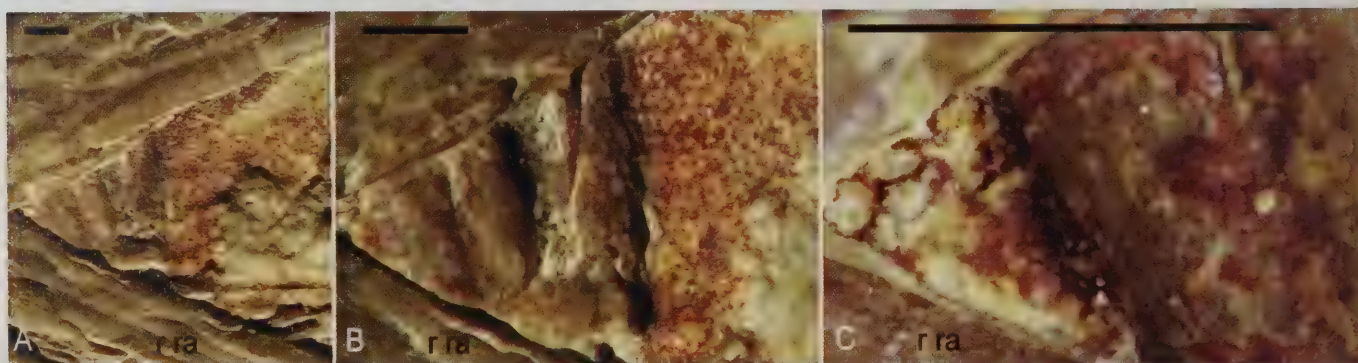


Fig. 138 - Close-ups taken under the optical microscope, with magnification increasing from A to B to C, of the reddish material encrusting bone and sediment in the ventral portion of the thorax of *Scipionyx samniticus*. Scale bars = 1 mm. See Appendix 1 or cover flaps for abbreviation.

Fig. 138 - Particolare al microscopio ottico, con ingrandimento crescente da A a B a C, del materiale rossastro che incrosta le ossa e il sedimento nella porzione ventrale del torace di *Scipionyx samniticus*. Scale metriche = 1 mm. Vedi Appendice 1 o risvolti di copertina per l'abbreviazione.

blood (e.g., Kardong, 1997). Under UV light (Fig. 137B), the reddish halo becomes subcircular in outline and is seen to impregnate a larger area of the rib cage, with a diameter of about 17 mm. More remarkably, it produces a distinct blue-indigo fluorescence under UV light, which corresponds to the primary light emission peak of biliverdin and is, therefore, consistent with the presence of bile pigment residues (Ruben *et al.*, 1999).

In the absence of direct chemical evidence, the characterisation of the supposed iron-rich mineral remained non-compelling until we conducted SEM element microanalysis. We examined six microsamples of the red matter encrusting the bone and the matrix (see Appendix 7), and all of them showed the same composition, unique to that area: hydrated iron oxide (limonite). The iron peak is as high as that of the gold coating (Fig. 139), and there

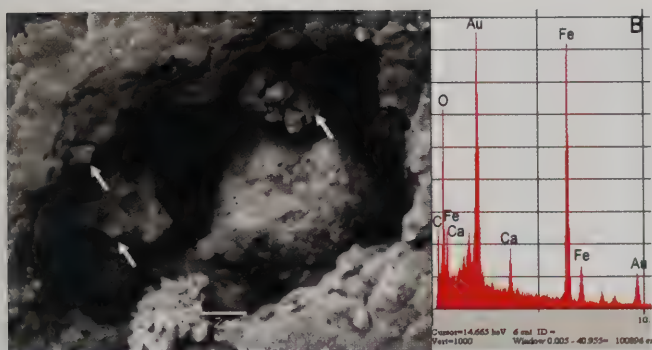


Fig. 139 - *Scipionyx samniticus*. SEM imaging (A) and element microanalysis (B) of the reddish material shown in Fig. 138 indicate that it is composed of microcrystals of hydrated iron oxide (arrows). Note that the iron peak is as high as the one of the gold coating, and that there are only traces of carbonates and phosphates, which are the prevailing components of the sediment (Fig. 13A) and of the fossil (e.g., Figs. 121C, 132B). See Appendix 1 or cover flaps for abbreviations.

Fig. 139 - *Scipionyx samniticus*. Le immagini al SEM (A) e la microanalisi degli elementi (B) del materiale rossastro mostrato in Fig. 138 indicano che questo è composto da microcristalli di idrossido di ferro (freccie). Si noti che il picco del ferro è alto quanto quello dell'oro derivante dalla doratura del campione, e che vi sono solo tracce di carbonati e fosfati, che sono i componenti prevalenti del sedimento (Fig. 13A) e del fossile (es., Figs. 121C, 132B). Vedi Appendice 1 o risvolti di copertina per le abbreviazioni.

are only traces of carbonates and phosphates, which are the prevailing compounds in the matrix (Fig. 13A) and the fossil (e.g., Figs. 121C, 132B), respectively. Therefore, this iron cannot be allogenous – for instance deriving from the pyrite formed from sulphate reduction in the centre of a carcass and drawing iron from the sediment as well as from the carcass itself – because in this case one would find the presence of its drainage into the surrounding environment. Rather, because of its single localisation and large amount, this iron represents an endogenous element derived from *post mortem* degradation of the dinosaur's haemoglobin.

This haematic nature, and its association to possible bile remains, strengthens the idea that the reddish halo is a product of liver decay. Such an interpretation is also consistent with the anatomical position of the liver in extant archosaurs: in the Nile crocodile, the liver is made from two lobes embracing the heart situated between the 4th and 8th thoracic rib (Huchzermeyer, 2003); in birds, the liver lobes embrace cranially the caudal half of the heart, and the two organs are ventrally protected by the large sternum (McLelland, 1990: figs. 120-121). Given the proximity of the two organs, it can be hypothesised that the stain may derive also from the decay of *Scipionyx*'s heart, although no trace of it, in the form of muscular tissue, is present in the specimen. According to Huchzermeyer (pers. comm., 2010), a third contribution to the large reddish halo might have been made by the spleen, another blood-storing organ that in extant archosaurs, similar to the heart, is positioned in-between the two liver lobes, but limited to their caudal halves.

Intestine

The intestine is the largest, most complete and most visible internal organ of *Scipionyx*: its three-dimensional loops are lumpy and shiny, reminiscent of the aspect one would see after dissecting a modern animal (Fig. 140). Whereas the cranial portion is tangled around itself, the caudal portion runs ventral and parallel to the caudal dorsal vertebrae, suggesting that it was attached to the roof of the abdominal cavity by a mesentery, and then passes through the pelvic cavity between the pubic and ischial shafts, ending at the base of the tail (Figs. 115-117). The surface of the digestive tube appears to be more irregular in the cranialmost portion, because of the presence of not completely liquefied ingested food, the nature of which is described in a dedicated section (see Intestinal Contents).



Fig. 140 - A grazing view of the intestine of *Scipionyx samniticus* highlights the preservation of the organ in three dimensions.
Fig. 140 - Una vista radente dell'intestino di *Scipionyx samniticus* evidenzia la conservazione tridimensionale dell'organo.

A relevant feature is the intestine's position: this organ is placed much further cranially in the abdominal cavity than was previously thought for dinosaurs (e.g., Paul, 1988; Wellnhofer, 1985), so, consequently, the intestine was not supported by the pubic bones. Because soft tissues by their very nature are quite mobile, it is always difficult to be certain that they have retained their original position in fossils. However, *Scipionyx* was very slowly and plastically deformed during a long-term diagenetic process. Besides that, the gastralgia provide convincing proof that at least some portion of the intestine is positioned as it

was *in vivo*. In the Pietraraja theropod, these tiny, fragile abdominal ossifications, that are usually dispersed in the sediment, are all very well aligned. Some gastralgia follow the curvature of a ventral loop of the intestine, indicating that this loop has not moved with respect to the skeletal elements. The shapes of the gastralgia and of the intestinal loop are complementary, to a point that the former seem to embrace the latter, contributing to its support (Fig. 141). If real, this support must be regarded as indirect, because the gastralgia cannot have been anatomically connected to the intestine: the gastralgia are part of the body wall, strengthening it and, as such, support the intestinal mass not individually but as a whole (see Gastralgia).

A close-up of the duodenal loop (Fig. 141) shows that the intestine is mostly (but not simply) an endocast, as its well-exposed, sometimes anastomosed, circular folds (*plicae circulares*) are typical of the mucosal layer, which *in vivo* represents the innermost tissue of vertebrate gut (e.g., Kardong, 1997). Actually, remnants of longitudinal fibres arranged perpendicular to the circular folds are seen here and there (e.g., Fig. 142), so some patches of *muscularis externa* and/or *adventitia* (i.e., the sheaths of smooth musculature and fibrous connective tissue that in vertebrate gut wrap around the mucosa) have been likely preserved. As a matter of fact, our recent SEM microsamples document the preservation of some phosphatised tissue layers, including a multi-layered epithelium in the duodenum (Fig. 143), and capillary-sized, branched blood vessels in the rectum (Fig. 144). This evidence clarifies once and for all that the supposition that the intestine of *Scipionyx* was a cololite (e.g., Holtz *et al.*, 2004) was simplistic and due to indirect knowledge of the specimen, the preservation of which is without doubt more complex than one could expect (see also Soft Tissue Taphonomy).

Because the intestine of *Scipionyx* folds over upon itself several times, at first sight it seems impossible to discriminate its regions. However, based on their relative position, shape, length, relative diameter, texture, demolition status of the contents, remnants of mesenteric con-

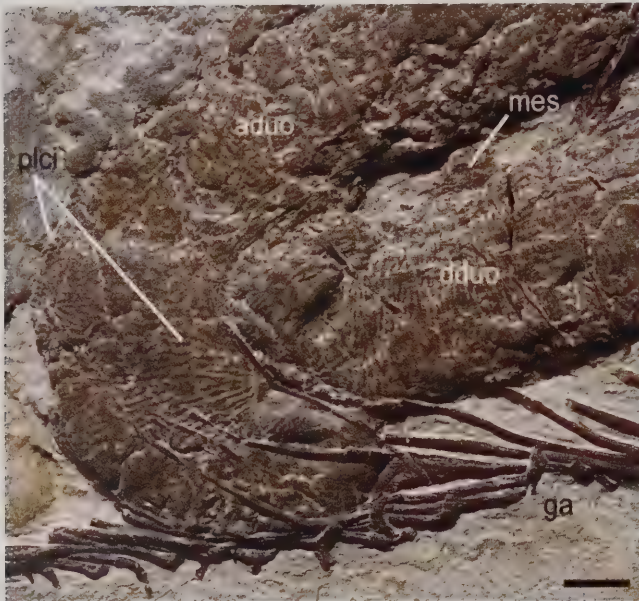


Fig. 141 - Close-up of the duodenal loop of *Scipionyx sammiticus*, showing the *plicae circulares* (circular folds) of the mucosa. Scale bar = 2 mm. See Appendix 1 or cover flaps for abbreviations.

Fig. 141 - Particolare dell'ansa duodenale di *Scipionyx sammiticus*, in cui sono visibili le *plicae circulares* (pieghe circolari) della mucosa. Scala metrica = 2 mm. Vedi Appendice 1 o risvolti di copertina per le abbreviazioni.

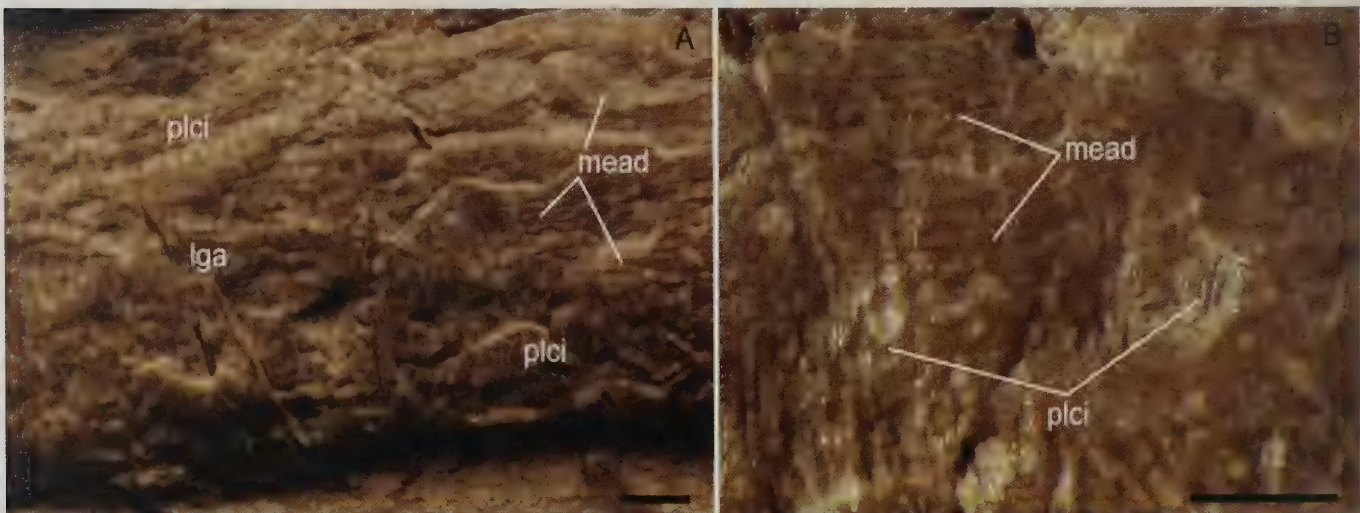


Fig. 142 - Close-ups, with magnification increasing from A to B, of a tract of the descending loop of the duodenum of *Scipionyx sammiticus*, with remnant longitudinal fibres of the *muscularis externa* and/or *adventitia* layer arranged perpendicular to the inner layer of *plicae circulares*. Scale bars = 1 mm. See Appendix 1 or cover flaps for abbreviations.

Fig. 142 - *Scipionyx sammiticus*. Particolari, con ingrandimento crescente da A a B, di un tratto dell'ansa discendente del duodeno con residui delle fibre longitudinali della *muscularis externa* e/o della tonaca avventizia, disposte perpendicolarmente allo strato interno delle pieghe circolari. Scala metrica = 1 mm. Vedi Appendice 1 o risvolti di copertina per le abbreviazioni.

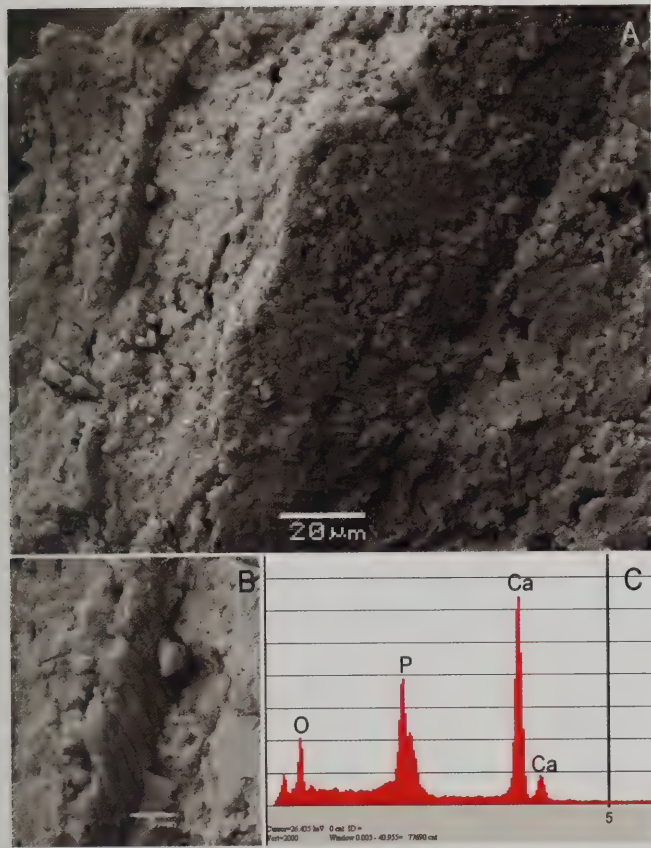


Fig. 143 - Soft tissue preservation at the cellular level in the intestine of *Scipionyx samniticus*. A) SEM image of a multi-layered visceral epithelium found in a microsample of the duodenal loop; B) close-up of one of the cell layers shown in A; C) SEM element microanalysis of the same tissue. See Appendix 1 or cover flaps for abbreviations.

Fig. 143 - Conservazione dei tessuti molli a livello cellulare nell'intestino di *Scipionyx samniticus*. A) immagine SEM di un epitelio viscerale pluristratificato trovato in un microcampione dell'ansa duodenale; B) particolare di uno degli strati di cellule mostrati in A; C) microanalisi degli elementi al SEM sullo stesso epitelio. Vedi Appendice 1 o risvolti di copertina per le abbreviazioni.

nections and/or ligaments and comparative anatomy with extant archosaurs, and with the help of computed tomography in-sequence slicing, we propose below our most likely morpho-functional subdivisions (Fig. 145).

Duodenum - The duodenum constitutes a widely exposed region of the intestine of *Scipionyx*. We are confident in attributing its ventralmost protruding portion to the duodenal loop, as it shares at least four characters with extant archosaurs (Botte & Pelagalli, 1982; Huchzermeyer, 2003; McLelland, 1990; Ziswiler & Farner, 1972): U-shaped loop made by two appressed tubes; cranio-caudal direction and asymmetrical position on the right side of the abdomen; cranio-dorsal proximity to liver and stomach; and higher density of folds in the mucosa layer. The proximity to the liver and stomach is an anatomical constraint of most extant vertebrates due to two links, the gastroduodenal ligament and the hepatoduodenal ligament. Similarly, the descending loop and the ascending loop are held together all along their length by a mesenteric connection, which usually encloses also the ventral portion of the pancreas. The position of the duodenum in *Scipionyx* matches these conditions, to a point that we can reasonably think that mesenteries and ligaments survived the decay of the carcass long enough to hold the intestinal loops in place until they became fossilised.

The duodenum of *Scipionyx* has an average diameter of 5.2 mm. Its fossilisation in the form of an internal mould is exquisite also at a microstructural level, to a point that in the U-turn between the descending loop and the ascending loop, the folds of the mucosa, that measure a few tenths of a millimeter, are clearly visible to the naked eye (Fig. 141). Similarly to crocodylians (Dal Sasso & Maganuco, pers. obs., 2009) and birds (McLelland, 1990), the U-turn is the most ventrally situated part of the intestine in the abdomen of *Scipionyx*. The tract embraced by the gastralia looks like a caecum but, most likely, it is the point

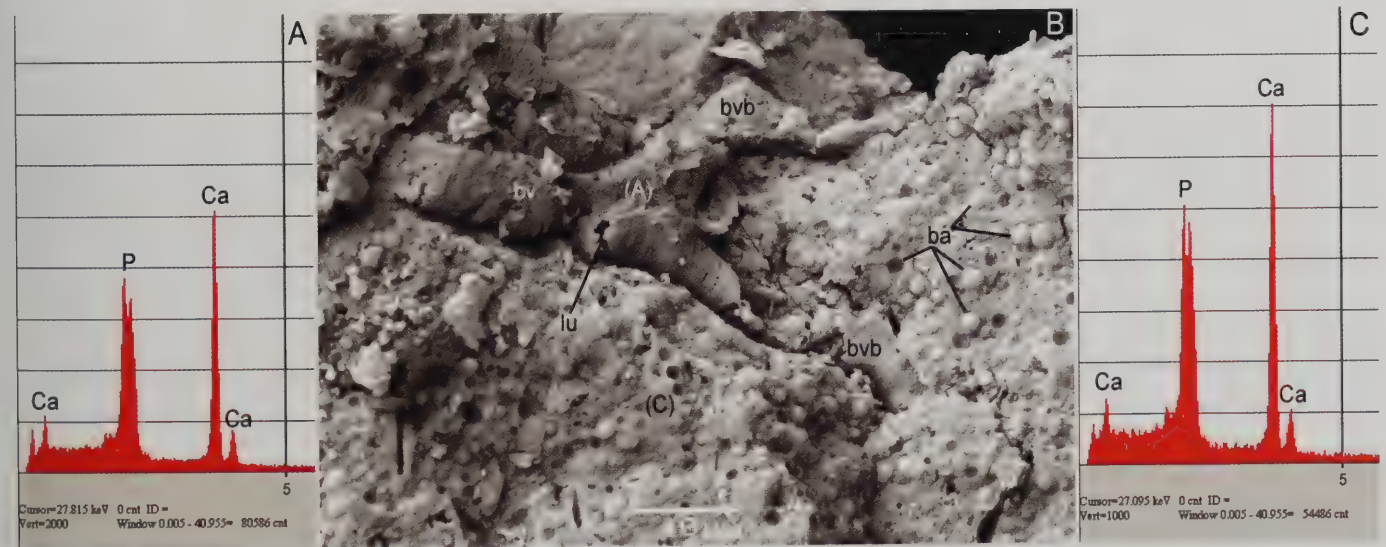


Fig. 144 - Soft tissue preservation at the cellular level in the intestine of *Scipionyx samniticus*: SEM element microanalysis (A) and SEM imaging (B) of a phosphatised capillary-sized blood vessel in a microsample of the rectum. The vacuolar aspect of the matrix, which has the same chemical composition (C) as the capillary, is consistent with the tissue having been replaced by pseudomorphed phosphatised bacteria, many of which are preserved as hollow spheres (see also Fig. 170). See Appendix 1 or cover flaps for abbreviations.

Fig. 144 - Conservazione dei tessuti molli a livello cellulare nell'intestino di *Scipionyx samniticus*: microanalisi degli elementi al SEM (A) e immagine SEM (B) di un vaso sanguigno della taglia di un capillare trovato in un microcampione del retto. L'aspetto vacuolare della matrice, che ha la medesima composizione chimica (C), è compatibile con una sostituzione dei tessuti da parte di batteri fosfatizzati pseudomorfi, molti dei quali sono conservati come cavità sferiche (vedi anche Fig. 170). Vedi Appendice 1 o risvolti di copertina per le abbreviazioni.

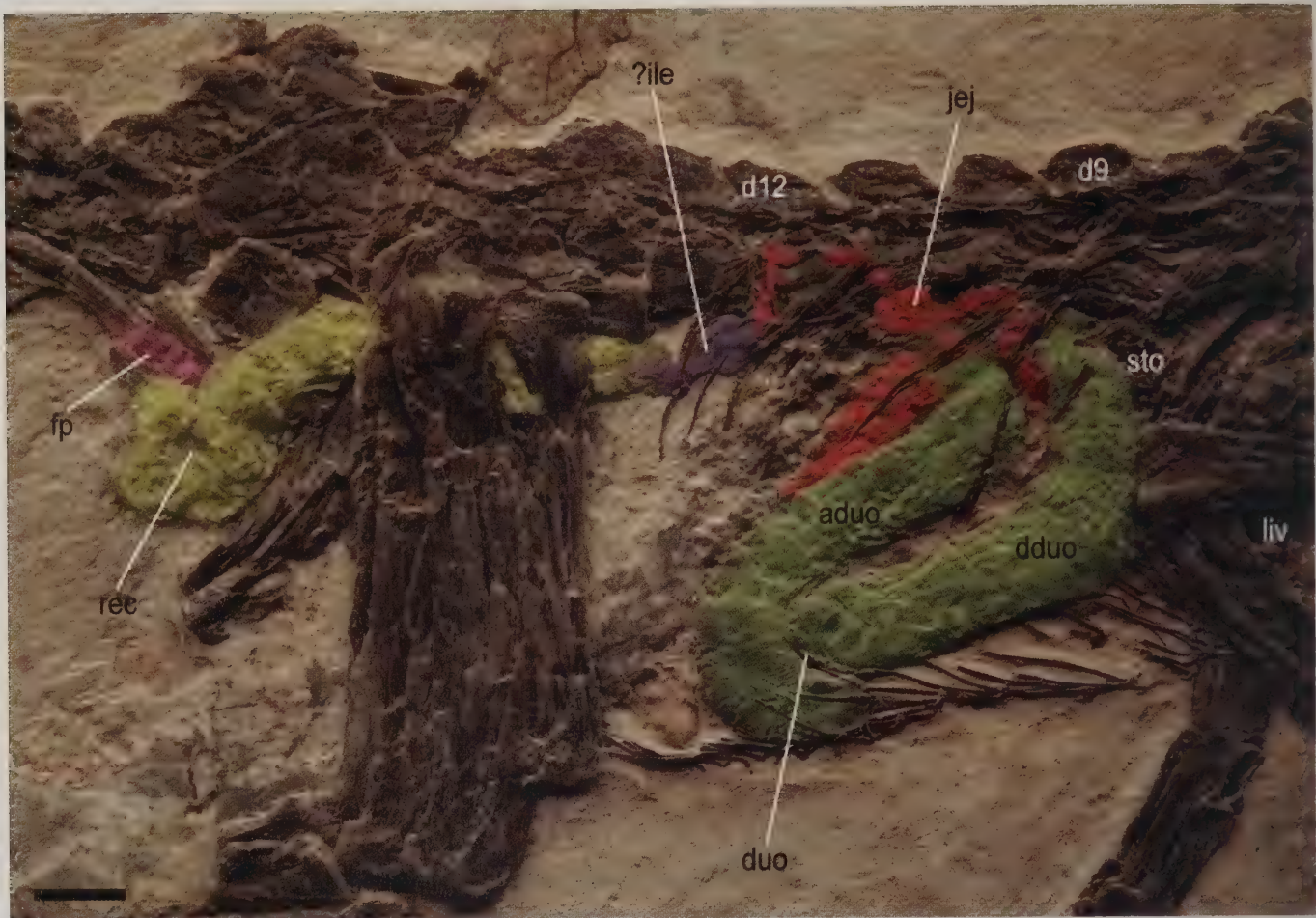


Fig. 145 - The intestine is the most complete internal organ of *Scipionyx samniticus*. In this false-colour image, various parts of the intestine are distinguished according to the morphofunctional subdivisions proposed in the text. Scale bar = 5 mm. See Appendix 1 or cover flaps for abbreviations.

Fig. 145 - L'intestino è l'organo interno più completo di *Scipionyx samniticus*. I cambi di colore virtuale seguono la suddivisione morfofunzionale proposta nel testo. Scala metrica = 5 mm. Vedi Appendice 1 o risvolti di copertina per le abbreviazioni.

where the descending loop surfaces again after a medial invagination. In *Crocodylus*, for instance, the duodenum does not consist of a simple U-shape, but folds over again, forming a double loop (Huchzermeyer, 2003).

The cranialmost side of the descending loop contains two adjacent clusters of ingested organic remains, likely consisting of horny squamae from a small lizard-like reptile, and a single vertebra, possibly referred to a fish, the description of which can be found in the Intestinal Contents section. Here we point out that the abundance of undigested food in this region of the intestine supports the idea that this loop may be not far from the connection to the stomach.

Jejunum - Towards the left side of the abdominal cavity, a portion of intestine that is more deeply embedded in the sediment runs medial to the dorsal edge of the ascending loop of the duodenum, then continues dorsally to the right side, overlapping the centra of the dorsal vertebrae. We refer this portion to the jejunum, as it shares the following characters with most extant archosaurs (Botte & Pelagalli, 1982; McLelland, 1990; Huchzermeyer, 2003): supra-duodenal localisation; lower density of mucosal folds; and relatively uncomplicated arrangement in the form of short, garland-like coils in the dorsal portion of

the abdomen. In addition, the visible tract of the jejunum has a smaller diameter than the duodenum, and a fewer solid inclusions.

It is unclear what point of the digestive tract marks the transition from duodenum to jejunum, but probably it is where the intestine slopes caudoventrally along the left side of the abdomen, under and parallel to the shaft of the right dorsal rib 9. Thus, the jejunum likely originates from a medial invagination that the ascending loop of the duodenum seems to form after reaching back cranially the initial tract of the descending loop. As a matter of fact, in extant avian theropods (Botte & Pelagalli, 1982) the transition point is found right where the ascending loop of the duodenum reaches the caudal wall of the gizzard, first curving dorsally, then U-turning caudally.

So, in *Scipionyx* the first tract of the jejunum should be the one that runs caudoventrally under the 9th right dorsal rib. After making an abrupt, swollen curve, of which only the dorsocaudal margin can be seen, the jejunum disappears under the duodenum, at the level of the 12th dorsal vertebra, and appears again at the level of the 10th dorsal vertebra, between the shafts of the right dorsal ribs 7 and 8, before heading sinuously dorsally and vanishing. Under UV light, residual fluorescence of organic remnants

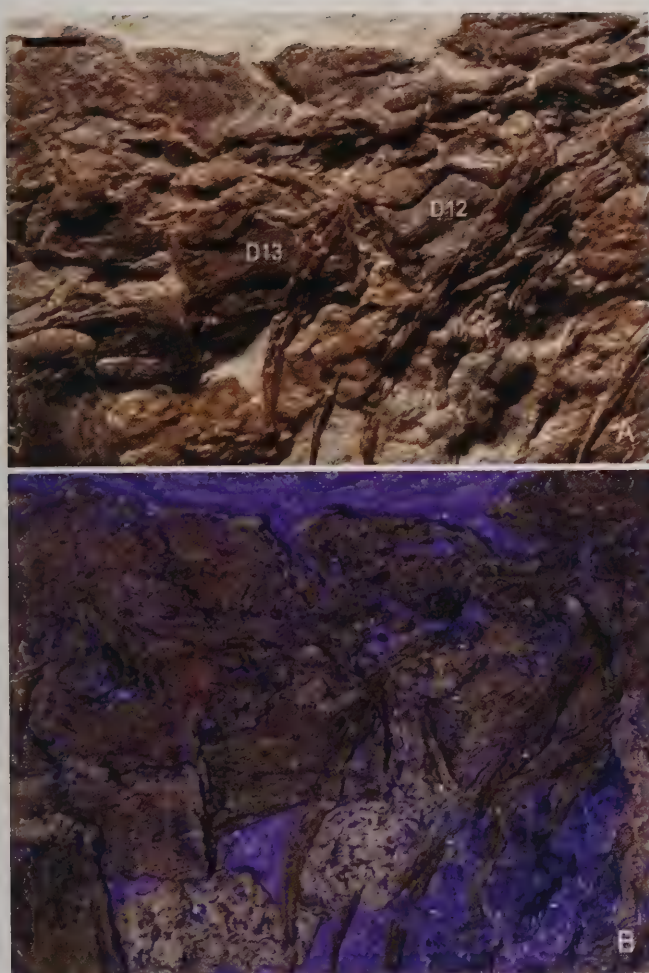


Fig. 146 - Remnants of the jejunum of *Scipionyx samniticus* under visible light (A) and ultraviolet-induced fluorescence (B). The latter reveals that this tract of the intestine follows a garland-like path over the dorsal vertebrae. Scale bar = 2 mm. See Appendix 1 or cover flaps for abbreviations.

Fig. 146 - Residui del digiuno di *Scipionyx samniticus*, fotografati in luce visibile (A) e in fluorescenza indotta da luce ultravioletta (B). Quest'ultima mostra che, con un andamento a festoni, questo tratto dell'intestino si è sovrapposto alle vertebre dorsali. Scala metrica = 2 mm. Vedi Appendice 1 o risvolti di copertina per le abbreviazioni.

impregnating the sediment and superimposed on some vertebrae can be seen, revealing that this tract of the jejunum had a garland-like path (Fig. 146). This arrangement is consistent with *post mortem* persistence of the jejunal mesentery, which prevented the jejunum from moving away from the vertebral column after death but allowed it to overlap onto the centra of the 10th and 11th dorsal vertebrae and the base of the neural arch of the 12th, a position that it certainly did not occupy in life. Portions of this tract of the intestine were probably removed during the early coarse preparation of the fossil when trying to uncover the vertebral column.

The final tract of the jejunum is better preserved and still clearly visible under the light microscope: this portion goes back down ventrally, trapped and protected by the adjacent facing articular faces of the 12th and 13th dorsal vertebral centra. Here, a tiny patch of visceral musculature has been preserved (Fig. 147A). Remnants of longitudinally arranged visceral musculature (?*muscularis externa*) also lie just ventral to the 10th-11th dorsal centra (Fig. 147B).

The jejunum contains a single solid inclusion: a somewhat round cluster of dozens of small cylindrical elements (see Intestinal contents) found next to the cranial face of the 11th dorsal centrum, more or less the same size of the latter. Hollow, elongated structures, which we regard as remnants of the cranial mesenteric artery and vein, or their branches (see below), are seen immediately ventral to this cluster.

Ileum - Just cranial to the pelvic girdle, precisely at the level of the 13th dorsal vertebral centrum, the intestinal tube seems to form a natural, non-artefactitious constriction. This constriction is reminiscent of a possible ileorectal valve (Botte & Pelagalli, 1982; Kardong, 1997) and is the main clue leading to our tentative ascription of this portion of intestine to the ileum. The ileum is generally known as a considerably short tract, connecting the jejunum to the rectum, but in crocodylians, for instance, the ileum is about as long as the jejunum (Huchzermeyer, pers.

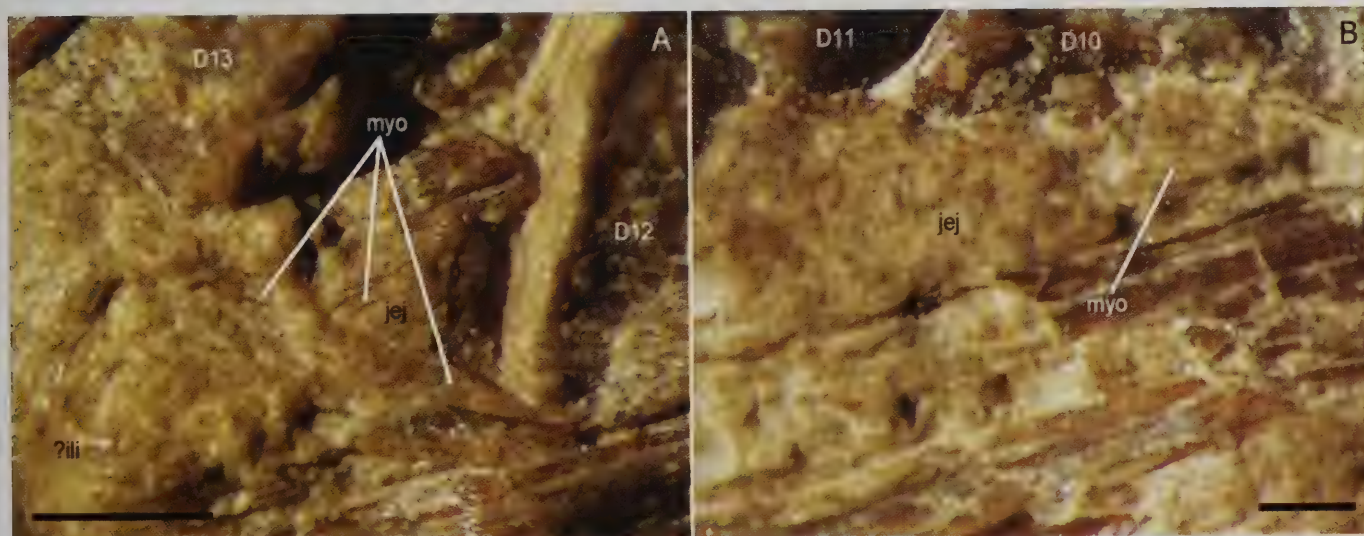


Fig. 147 - Tiny patches of visceral musculature of the jejunum of *Scipionyx samniticus*, preserved in between adjacent dorsal vertebral centra (A), and ventral to the preceding dorsal centra (B). Scale bars = 1 mm. See Appendix 1 or cover flaps for abbreviations.

Fig. 147 - Minuti frammenti di muscolatura viscerale del digiuno di *Scipionyx samniticus*, conservati fra centri vertebrali dorsali adiacenti (A) e ventralmente a centri dorsali che li precedono (B). Scale metriche = 1 mm. Vedi Appendice 1 o risvolti di copertina per le abbreviazioni.

comm., 2010). Therefore, its length in *Scipionyx* remains unknown, and the pelvic bones hiding it prevent us from observing its arrangement. A couple of tiny, somewhat round bone fragments, maybe two vertebrae are embedded in the supposed ileum (see Intestinal Contents).

Rectum - Following the basic bauplan of the digestive system in most vertebrates (e.g., Kardong, 1997), we refer to the large intestine the terminal, enlarged tract of the gut of *Scipionyx* that, after passing through the pubic and the ischial foramina, reaches the base of the tail. According to

some authors (e.g. Ziswiler & Farner, 1972; Botte & Pelagalli, 1982), the large intestine includes the caeca, the colon, the rectum and the cloaca. Actually, in extant archosaurs - crocodiles and birds - the cloaca is not part of the large intestine (the rectocoprodaeal valve is understood as the equivalent of the anus of mammals), and there is no distinction between colon and rectum, so that this part of the digestive tract is referred to as the rectocolon, or usually just as the rectum (Huchzermeyer, pers. comm., 2010). Therefore, the rectum starts where the ileum ends (caeca present or not), often without a clear transition.

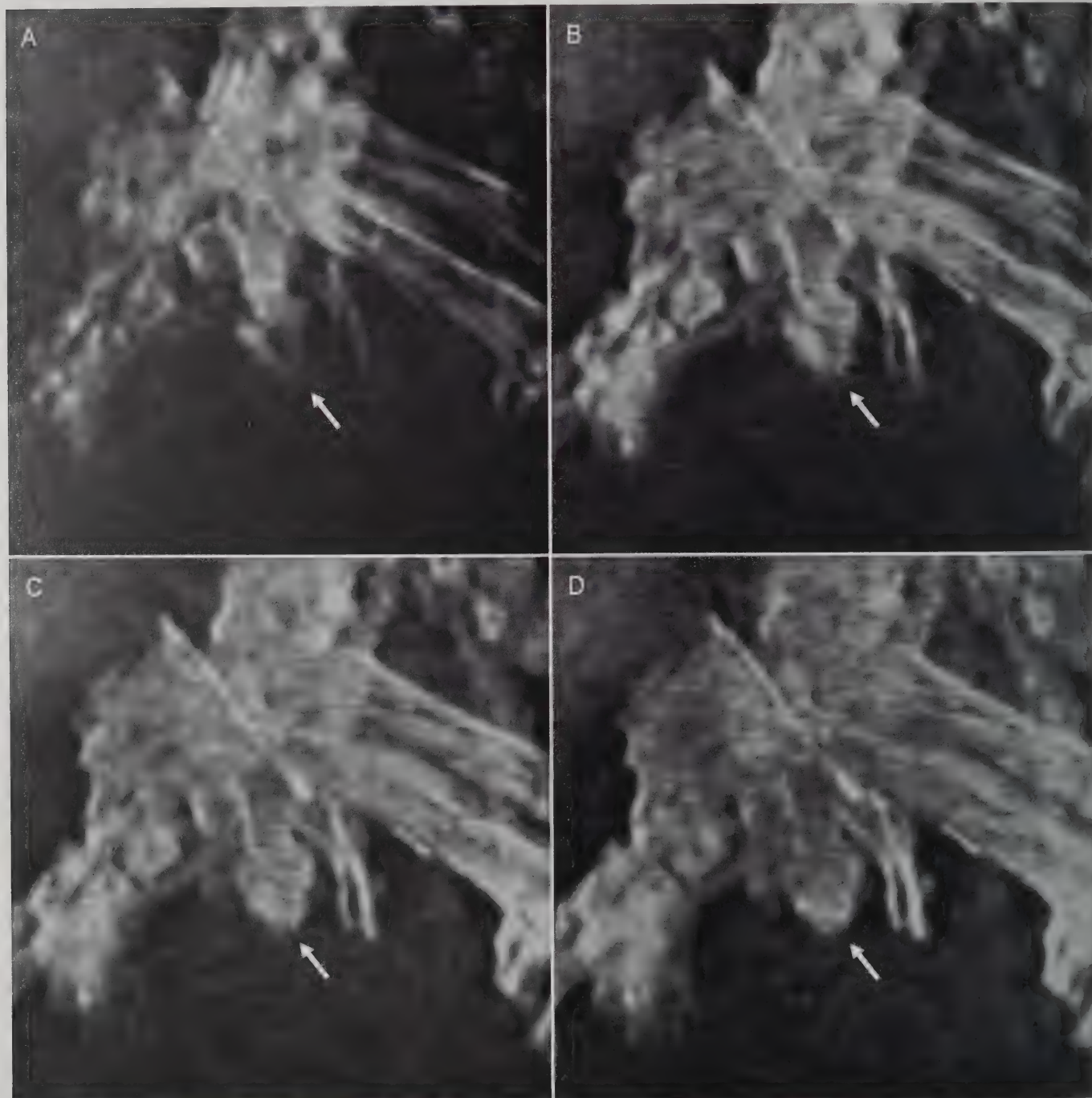


Fig. 148 - Computed tomography of the pelvic region of *Scipionyx samniticus*. The images (A-D) are of a sequence of 4 parallel parasagittal sections moving from the left (A) to the right side (D) of the specimen. Note the U-shaped tract of the rectum, obliquely embedded in the sediment (arrows).

Fig. 148 - Tomografia computerizzata della regione pelvica di *Scipionyx samniticus*. La sequenza di immagini (A-D) mostra 4 fette parasagittali parallele che tagliano l'esemplare dal suo fianco sinistro (A) al suo fianco destro (D). Notare il tratto a U del retto, immerso obliquamente nel sedimento (freccie).

This is the case in *Scipionyx*, too, in which the caeca are absent, like in crocodylians and many carnivorous and piscivorous birds (Huchzermeyer, 2003). In fact, caeca basically are fermentation chambers, specialisations for herbivorous amniota.

With respect to most extant tetrapods, *Scipionyx* shows a quite anomalous caudodorsal displacement of the rectum. Notably, this displacement is remarkably similar to the one that can be observed in Nile crocodile hatchlings before their voluminous yolk sac is resorbed (Fig. 110; Huchzermeyer, pers. comm., 2010). In fact, the yolk sac of reptile and bird hatchlings occupies most of the pelvic cavity, and so during the first days of life, their intestines undergo considerable rearrangement, moving in to fill the space left free as the yolk gets resorbed – a process that takes one to three weeks in extant archosaurs (see Ontogenetic Assessment). Occasionally, a yolk sac can persist longer, a pathological condition called yolk sac retention: this happens when the duct between the yolk sac and the intestine becomes closed due to infection (Huchzermeyer, pers. comm., 2010). The average time of absorption of the yolk sac in extant archosaurian hatchlings, and the ontogenetic assessment of *Scipionyx*, are consistent with an almost full yolk sac having displaced most of the rectum caudally. Consequently, by assuming the displacement of the rectum as entirely due to the presence of a yolk sac, according to Huchzermeyer (pers. comm., 2010) the estimated age of *Scipionyx* at death would be about three days, absolute maximum one week.

Apart from that hypothesis (no vitelline diverticulum is seen opening opposite the branches of the cranial mesenteric artery, nor any fossilised yolk sac-like sac or yolk remnant), it appears that the rectum of *Scipionyx*, once emerged from the ischial foramen, runs ventrocaudally along the ischial shafts to their extremities, and then curves dorsally to reach a straight and short, craniocaudally aligned, terminal tract, that contains an apparent faecal mass. Actually, CT scan imaging shows an underlying tract, intermediate between the one contacting the ischial shafts and the one containing the faecal mass, obliquely embedded into the matrix in the form of a U tube (Fig. 148). In *Scipionyx*, the diameter of the rectum is greater than that of the jejunum and the supposed ileum, but in any case does not attain the diameter of the duodenum, just like in birds (Ziswiler & Farner, 1972). The surface of the rectum is lumpy, but cranial to the faecal mass no visible solid inclusion stands out from the amorphous, grey-yellowish contents.

A mysterious, micrometric structure was found in a SEM sample of the rectum (Fig. 149A). It consists of a very thin, hemispherical sheet, densely punched with circular holes forming a sort of reticulum. Its chemical composition (Fig. 149B), consistent with all other remains of the dinosaur (i.e., calcium phosphate), together with the micrometric diameter of the holes (2–8 μm), excludes any artefact or trace of commonly used human products. Among biological structures, such a reticulum is reminiscent of some sort of absorption or filtering membrane, and its localisation in the rectum would lead to think of the function of liquid re-absorption. This might be more likely inferred by the presence of capillary-sized blood vessels in the same sample (Fig. 144B). On the other hand, the very small size and the very limited extension

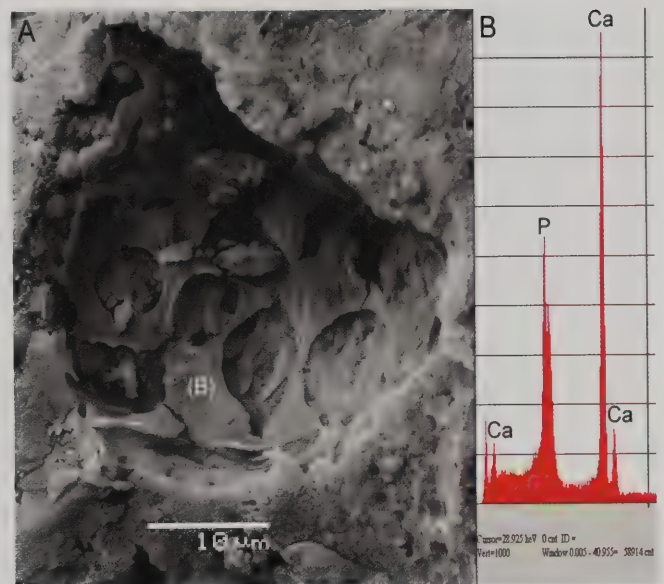


Fig. 149 - SEM imaging (A) and SEM element microanalysis (B) of an enigmatic micrometric structure found in the rectum of *Scipionyx samniticus*. Its chemical composition is consistent with all other nearby fossil remains, thus excluding it is a human artefact. See Appendix 1 or cover flaps for abbreviations.

Fig. 149 - Immagine al SEM (A), e relativa microanalisi degli elementi (B), di una enigmatica struttura micrometrica trovata nel retto di *Scipionyx samniticus*. La sua composizione chimica è analoga a quella di tutti gli altri resti fossili circostanti, per cui si deve escludere che si tratti di un artefatto. Vedi Appendice 1 o risvolti di copertina per le abbreviazioni.

of this membrane with respect to the sample suggests that it might be part of an allogenuous, ingested and, maybe, partially digested object (?plant cuticle, ?animal integument). In the palaeontological literature, we found just one similar SEM image (Zhang *et al.*, 2010: fig. 1c), obtained from an isolated pennaceous feather dated back to the Early Cretaceous of Inner Mongolia, China. Following Zhang *et al.* (2010), the reticulum of our microsample might be degraded (originally keratinous) feather matrix, and the holes within it might represent melanosome moulds. However, some parameters do not fit the melanosome hypothesis: the holes in the sample of *Scipionyx* have a larger order of magnitude (about 5:1) and have a lower density than the mouldic melanosomes illustrated by Zhang *et al.* (2010), and the margins of the isolated hemispherical membrane do not show any anastomosing ridge suggesting the presence of repeated adjacent units. At present, the lack of a truly comparable biological structure in the SEM images we examined does not allow us to give a more reliable interpretation.

Faecal pellet - The rectum of *Scipionyx* terminates just in front of a compact faecal mass, more properly referred to as a faecal pellet, that embeds a cluster of bright scaly remains, aligned in a craniocaudal direction for about 6 mm (see Intestinal Contents). With the aim of bringing to light these remains and determining their nature, some work was done in this area that changed the original appearance of this tract of the intestine (Fig. 150A); actually, the oldest photos of the fossil (Fig. 150B) document that a thin, opaque sheet of ochre-yellowish material covered the scaly remains, embedding them in an internal mould of the gut similarly to the preceding portions.



Fig. 150 - The rectum of *Scipionyx samniticus* shows an abrupt shift from wide loops to a narrow, straight terminal tract (A). Here, the gut moulds itself around a faecal mass containing many scales. This mass was visible even before preparing the specimen in detail (B). Scale bar = 2 mm. See Appendix 1 or cover flaps for abbreviations.

Fig. 150 - Il retto di *Scipionyx samniticus* presenta un punto di brusca transizione, passando da anse voluminose ad un tratto terminale stretto e rettilineo (A). Qui, anche prima che l'esemplare venisse preparato in dettaglio (B), affiora un modello interno delle interiora fatto di resti scagliosi immersi in una massa fecale. Scala metrica = 2 mm. Vedi Appendice 1 o risvolti di copertina per le abbreviazioni.

At least four characteristics lead us to think that this tract of the intestine of *Scipionyx* is actually the terminal tract of the rectum rather than the cloaca hypothesised in previous works (Dal Sasso, 2001, 2003, 2004), or the coprodaeum, which was mistakenly identified in crocodiles by Kuchel & Franklin (2000) as the anatomical continuum of the rectum (Huchzermeyer, pers. comm., 2010): as mentioned above, this tract of the intestine is straight, forming an abrupt restriction and an abrupt angle with the preceding loops; its cranial half emerges from the left side of the body, overlapped by the preceding loops; it is nested in a frankly internal position, close to the vertebral column and flanked all along its ventral side by caudofemoral musculature; and it is the site of storage of a compact faecal mass.

Its straightness, as the Latin name *rectum* indicates, represents the commonest morphological aspect in the digestive system of vertebrates, and, therefore, a good diagnostic character for the end of the large intestine. Even in the fossil *Scipionyx*, a straight arrangement clearly distinguishes the terminal tract of the gut from the preceding ones. With regard to its position on the left side, such a localisation can be observed in the terminal portion of the rectum of some extant archosaurs: in Nile crocodiles, for example, a short rectum emerges caudally from the left side of the body, stretching medially only when it reaches the cloacal chambers (Huchzermeyer, pers. comm., 2010). As for the nearby musculature, the faecal pellet seems to

be trapped in-between two muscle bundles, which actually do not have any relationship with it (see Caudofemoral Muscles). In fact, these bundles are unlikely referred to rectal or cloacal muscles because their myofibres are definitely straight and craniocaudally directed. This feature is not consistent with the circular pattern of sphincters, which are unpaired muscles located ventrally along the plane of symmetry of the body. Attribution to highly specialised, copulation-related muscles (e.g., anal sac constrictors) associated to the cloaca of some reptiles (e.g., Kardong, 1997: fig. 14.43) is unlikely because of the immaturity of our specimen, and is misleadingly suggested by the abrupt caudal termination of the two muscle bundles (such a termination in *Scipionyx* is an artefact of preparation – see Caudofemoral Muscles). In any case, the position of a purported cloacal opening would have been more ventral (peripheral) both in the fossil and *in vivo* (see Reconstructing *Scipionyx*): osteological markers of the position possibly reached by the cloacal opening are the ischial feet, as they are the site of attachment of the ventral base of the tail. The faecal pellet of *Scipionyx* is rather far from the ischial feet, thus it cannot be interpreted as cloacal contents. Moreover, in extant vertebrates that possess a cloaca (including all reptiles and birds), in normal conditions the faeces accumulate in the rectum, whereas the coprodaeum and the more distal cloacal chambers are a transit-way out of the body (e.g., Skoczylas, 1978; Ziswiler & Farner, 1972).

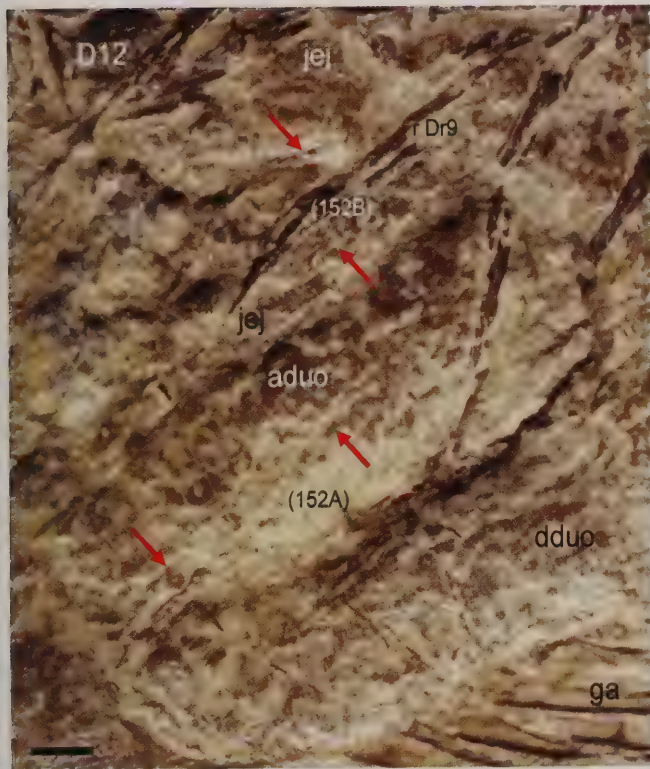


Fig. 151 - This photograph of the abdomen of *Scipionyx samnticus*, taken prior to preparation, documents the untouched blood vessels (arrows) of the cranial mesenteric artery. Scale bar = 2 mm. See Appendix 1 or cover flaps for abbreviations.

Fig. 151 - Questa fotografia dell'addome di *Scipionyx samnticus*, scattata prima della preparazione, documenta l'integrità dei vasi sanguigni dell'arteria mesenterica craniale (freccce). Scala metrica = 2 mm. Vedi Appendice 1 o risvolti di copertina per le abbreviazioni.

In extant crocodiles, the faecal pellet is formed in the very short rectum (Huchzermeyer, pers. comm., 2010). *Scipionyx* seems to fit this pattern. In crocodiles, the rectocoprodaeal valve connects the rectum to the coprodaeum, which together with the urodaeum forms the urine chamber of the cloaca. Crocodiles, as well as ostrich and rhea, excrete urine separately from the faeces. The mixture of urine and faeces in the rectum of flying birds appears to be a later adaptation (Huchzermeyer, pers. comm., 2010). Internal retention and compactness of the faecal pellet of *Scipionyx* suggests that, like extant crocodiles and ratites, theropod dinosaurs did possess a rectocoprodaeal valve, and did not mix urine and faeces. Internal retention and compactness of the faeces might suggest also that *Scipionyx* did not suffer *post mortem* relaxation of the sphincters, just like modern crocodiles. This possibility will remain impossible to ascertain, because no anatomical structures or intestinal products have been preserved caudal to the faecal pellet described here. If fossilised, the cloacal tissue and its contents were likely removed during the earlier preparation, as the deeply excavated matrix caudal to the preserved faecal pellet and cranial to the caudalmost soft-tissue remains attest in the oldest photographs of the specimen (Figs. 18, 150B).

Mesenteric blood vessels

A number of fine, delicate, almost uncoloured and hollow filamentous structures, which were already visible before preparing the specimen, lie superimposed on the surface of the jejunal loops (Fig. 151). They have a wavy arrangement and a prevailing dorsoventral orientation (Fig. 152), with diameters that vary either along a

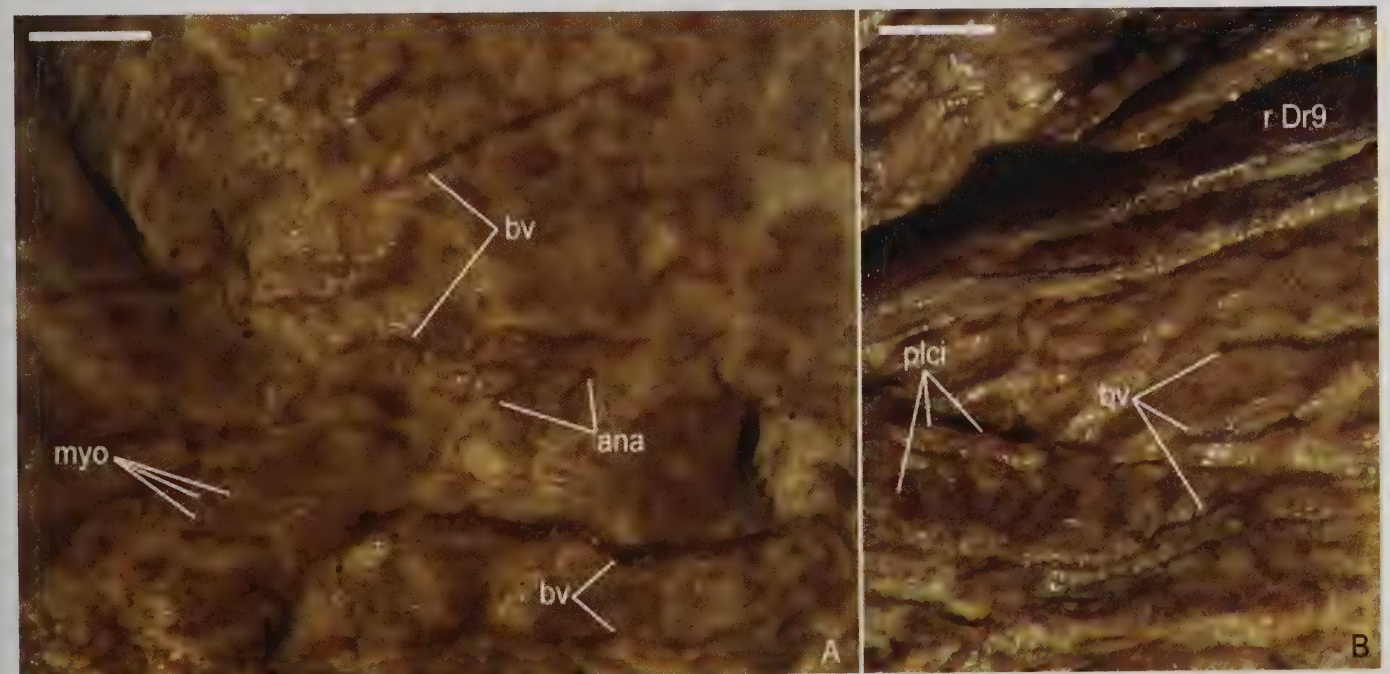


Fig. 152 - Close-ups of two selected portions of the abdominal area of *Scipionyx samnticus* illustrated in Fig. 151 (A, ascending loop of the duodenum; B, jejunum), after preparation, highlighting the wavy arrangement and the hollowness of the fossilised blood vessels. Scale bars = 0.5 mm. See Appendix 1 or cover flaps for abbreviations.

Fig. 152 - *Scipionyx samnticus*. Ingrandimenti di due porzioni dell'area addominale illustrata in Fig. 151 (A, ansa ascendente del duodeno; B, digiuno) e fotografata dopo la preparazione dell'esemplare, che evidenziano le ondulazioni e le cavità dei vasi sanguigni fossilizzati. Scale metriche = 0,5 mm. Vedi Appendice 1 o risvolti di copertina per le abbreviazioni.

single element (0.04-0.1 mm in the largest one) or from one element to another (the thinnest one measures 0.02 mm); their preserved length does not exceed 10 mm. These filamentous structures run obliquely, more-or-less paralleling the first tract of the jejunum, from the ventral edge of the 10th dorsal centrum to the caudoventral loop of the jejunum, where the latter curves underneath the duodenum (i.e., at the level of the caudal margin of the 12th dorsal centrum).

Hollow, filamentous structures are found in *Scipionyx* also at the base of the tail; however, these are longer, greater in diameter, evidently coloured, frequently bifurcated and imbricate caudally, and appear to be more stiffened. Therefore, we maintain that, despite a superficial similarity, the two hollow structures have different origins.

A frankly sinuous arrangement indicates that the hollow structures overlaying the intestine were elastic and flexible. Given these features and the presence of some branching and anastomosing, we regard these delicate, nearly transparent structures as blood vessels, ruling out any possible integumentary derivative, such as hair, bristles or protofeathers. The preservation of structures as delicate as blood vessels must not surprise too much, especially in *Scipionyx*. Janvier (pers. comm., 2009),

for instance, reports that after axial musculature, blood vessels are the most frequently found preserved soft tissue in fossil fishes.

A survey of the surface of the whole intestine confirmed that in *Scipionyx* the preservation of macrovessels (i.e., blood vessels that are visible under the light microscope) is limited to the ascending loop of the duodenum, where they are very rare, and to the jejunum, where they are abundant. The intimate contact between the vessels and the dorsal loops of the jejunum, and the caudal loop of the duodenum as well (Figs. 117, 151), is in favour of the attribution of all preserved blood vessels to the branches of the cranial mesenteric artery and vein. In fact, such a distribution is consistent with the cardiovascular anatomy of extant vertebrates, in which the cranial mesenteric artery, arising from the abdominal aorta, branches into the caudal duodenal pancreatic artery, the middle and right colic, as well as the jejunal and ileocaecocolic arteries (e.g., McLelland, 1990; Pinto e Silva *et al.*, 2008). Notably, in crocodylians the cranial mesenteric artery meets the intestine right at the point at which the jejunum, after running straight along the dorsal aspect of the abdominal cavity, becomes suspended in loose coils by the mesentery (Huchzermeyer, 2003).



Fig. 153 - Bundles of somatic muscles are remarkably preserved in three dimensions (see also Fig. 158) at the base of the tail of *Scipionyx samniticus*. Scale bar = 5 mm. See Appendix 1 or cover flaps for abbreviations.

Fig. 153 - Fasci di muscoli somatici sono conservati in tre dimensioni (vedi anche Fig. 158) alla base della coda di *Scipionyx samniticus*. Scala metrica = 5 mm. Vedi Appendice 1 o risvolti di copertina per le abbreviazioni.

Pelvic and hindlimb muscles

Even more remarkable than that of the intestine is the preservation of somatic muscle bundles at the base of the tail. In less than 20 mm², that area contains the best preserved muscle tissue of *Scipionyx*: in fact, these bundles are still arranged in compact fascicula composed of parallel, strictly appressed cells fossilised in three dimensions (Fig. 153). In addition, the distribution of muscle remains and their association to skeletal elements in this area suggests that, in topographical and functional terms, they represent at least three different pelvic and hindlimb muscles (Figs. 117,153).

Puboischiofemoral muscle - The most cranial remains of the pelvic musculature lie in strict contact with the craniomedial face of the right ischial shaft (Fig. 154A). They consist of a residual patch shaped into a rough drop by mechanical preparation, 5 mm long and 2 mm wide, that at high magnification shows a whitish, amorphous matrix, probably made of muscle-related connective tissue in which several myofibres are embedded (Fig. 154B). Apart from the preservation of well-visible muscle cells, the most interesting feature is their arrangement: the myofibres intimately contacting the shaft of the ischium parallel the bone in a craniodorsal direction; the distalmost ones begin almost parallel, then curve in a cranial direction, giving the bundle a fan-like appearance. There is no muscle scar or any other sign of muscular insertion on the shaft of the ischium, but proximal to the bone all myofibres converge towards the cranial tip of the ischial foot.

Based on observations in a number of fossil taxa, and using the extant phylogenetic bracket, Carrano & Hutchinson (2002) offered well-supported inferences concerning most of the hindlimb musculature in *Tyrannosaurus*

rex. In *Scipionyx*, the bone surface in strict contact with the muscle remains is topographically equivalent to the one that in *Tyrannosaurus* would have given attachment to the *M. adductor femoris I* (Carrano & Hutchinson, 2002). According to these authors, this muscle probably originated from the cranioventral surface of the ischium, then passed laterally and cranioventrally to insert on the caudal surface of the femoral shaft, approximately two-thirds of the way towards its distal end, where an oval, rugose medial attachment site is located. In *Scipionyx*, the cranial and caudal directions of the preserved myofibres, and their fan-like arrangement that matches well the anatomy of the *M. adductor femoris I* seen in extant archosaurs (Hutchinson & Gatesy, 2000: fig 3A - *errata corrigere*: ADD2 and ADD1 labels are inverted), are both consistent with the two bone attachments suggested by Carrano & Hutchinson (2002).

This adductor muscle is reconstructed by Carrano & Hutchinson (2002) with a level I' inference (*sensu* Witmer, 1995, 1997): it is present in Crocodylia and in Neornithes, but the insertion on the cranioventral edge of the ischium is slightly different in the two taxa – in Crocodylia, it is called *M. adductor femoris I*, whereas in Neornithes it is the *M. puboischiofemoralis pars medialis*. As for *Tyrannosaurus*, Carrano & Hutchinson (2002: fig. 3) refer this muscle to the *M. adductor femoris I*, placing its origin near the obturator process and leaving the ischial shaft empty. Given the vicinity of the myofibres to the bone and the lack of tendineous remains, *Scipionyx* supports the supposition (Carrano & Hutchinson, 2002) that this muscle has a fleshy attachment. On the other hand, given the convergent caudal orientation of the fibres, we infer that the *M. adductor femoris I* does not originate on or near the obturator process, but rather from the ischial foot and a cranioproximal adjacent area. This evidence also contradicts Paul (1988), who argued on functional

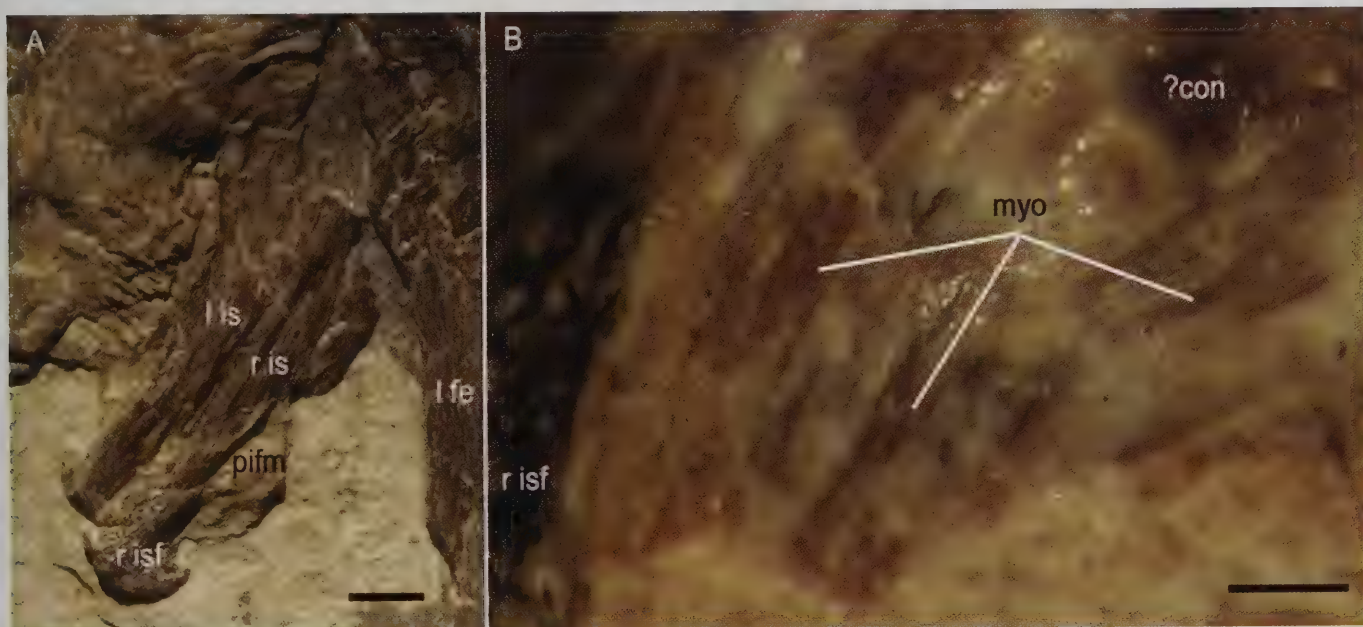


Fig. 154 - *Scipionyx samniticus*. A) remains of the puboischiofemoral musculature preserved on the shafts of the ischia; B) close-up of a patch of muscle adjacent to the right ischial foot. Scale bars = 2 mm (A) and 200 μ m (B). See Appendix 1 or cover flaps for abbreviations.

Fig. 154 - *Scipionyx samniticus*. A) resti della musculatura puboischiofemorale conservata lungo le ossa ischiatiche; B) particolare di un lembo di muscolo adiacente il piede dell'ischio destro. Scale metriche = 2 mm (A) e 200 μ m (B). Vedi Appendice 1 o risvolti di copertina per le abbreviazioni.

grounds that in theropod dinosaurs it was unlikely that any muscle originated from the ischial shaft.

In conclusion, *Scipionyx* shows unequivocally that at least one muscle inserts onto the ischial shaft of theropods: this insertion is distal to the obturator process and, more precisely, on a craniodistal area that, judging from relatively recent descriptions and drawings (Carrano & Hutchinson, 2002: fig. 3), is consistent with the *M. puboischiofemoralis pars medialis* of *Gallus* and the *M. adductor femoris I* of *Tyrannosaurus*. It cannot be excluded that this muscle in *T. rex* or in other theropods would have had a craniodistal insertion that is more extended than the one suggested in the literature.

Caudofemoral muscles - Evidence for the caudofemoral musculature in extinct archosaurs rests on skeletal features associated with the origin and insertion of these muscles (Gatesy, 1990) – except in *Scipionyx*. In fact, three evident muscle bundles can be clearly seen with the naked eye in the Italian compsognathid to parallel the caudal vertebral column and reach cranially towards the femora (Fig. 153). The most cranial ones consist of two short bundles that emerge from the left side of the rectum and run for about 5 mm below the 5th sacral centrum, dorsal and ventral to the faecal pellet. In a caudal direction, the two bundles would seem to terminate abruptly at the same level, but, in fact, the dorsal one continues under the first caudal centrum, whereas the ventral one has an irregular margin clearly produced by mechanical preparation. As outlined above, we exclude that these two bundles belong to rectal or cloacal muscles, as the cranio-caudal direction of the well-preserved myofibres is not consistent with the circular arrangement of the sphincters. Proximity to remains of the terminal tract of the rectum is not evidence of any morphofunctional relationship with it, as is topographically obvious for tail muscles: for instance, in *Alligator* hatchlings (Dal Sasso & Maganuco, pers. obs., 2009) the proximocaudal hypaxial musculature runs both dorsal and ventral to the rectum and also very close to it. A third muscle bundle, with the same direction and a similar diameter (2 mm) but more distally placed, emerges from the left side of the faecal pellet, i.e., from an innermost plane, which underlies also the former bundles. This third bundle is the best preserved in length, running in a caudal direction for 15 mm, below caudal centra 1-3. Actually, its caudal third is overlaid by another muscular and connective tissue mass (see below).

Given the common parallel fibre arrangement and direction and the absence of myosepta, and given the deep, left lateral position of all three bundles with respect to the midline elements (proximal rectum, caudal vertebrae), we refer these muscle remains to the left *M. caudofemoralis*. *M. caudofemoralis longus* (CFL) represents the primary femoral retractor muscle of lepidosaurs and crocodylians (Gatesy, 1990); its smaller counterpart, *M. caudofemoralis brevis* (CFB), is also likely important in hip extension. In extant reptiles, the *M. caudofemoralis* is morphologically unique among the caudal muscles in being not partitioned by conical myosepta, its overall form more closely resembling a limb muscle rather than an axial muscle (Persons & Currie, 2011).

We encounter big problems when considering a possible attribution of the three muscle bundles of *Scipionyx* to the CFB. In fact, such an attribution is incompatible

with the position of the preserved portions of the bundles because even the two most proximal ones lie at some distance from the ilium, caudal to it, and display a fibre orientation parallel to the long axis of the tail. As demonstrated by Carrano & Hutchinson (2002) for *Tyrannosaurus*, the CFB originated within the *brevis fossa* of the ilium, along its ventral edge caudal to the acetabulum, and extended cranioventrally to insert on the caudolateral shaft of the femur.

As in extant crocodylians and lepidosaurs, the CFL in *Tyrannosaurus* and in *Scipionyx* was probably the largest single muscle of the hindlimb. According to Carrano & Hutchinson (2002), this muscle originated from the lateral faces of the proximal caudal vertebral centra, passing cranioventrally to insert on the medial portion of the fourth trochanter. Proximity to caudal centra and cranial orientation of the myofibres in *Scipionyx* are consistent with this arrangement, i.e., with a muscle that would have filled the ventrolateral sulcus created by the transverse processes and the chevrons (Gatesy, 1990).

The three-dimensional fossilisation of the *M. caudofemoralis* is apparent to the naked eye, but it becomes dramatic at high magnification. The preservation is so exquisite that it allows not only to distinguish the individual myofibres under the optical microscope (Fig. 155), but also subcellular details with scanning electron microscopy. Under the optical microscope, the myofibres have an intensely brown-reddish colour, and the intercellular spaces are diaphanous; if brightly illuminated, the crystallised tissue allows some vision through it (Fig. 156). Like the myofibres preserved at the base of the neck, those of the caudofemoral musculature are parallel, straight and stacked in multiple layers, as in most somatic muscles of extant vertebrates. Therefore, although they vary in size from one another in the different portions of the three muscle bundles (10-26 µm), the diameter of each individual myofibre is very constant.



Fig 155 - Close-up taken under the optical microscope of the caudofemoral myofibres, still forming a compact muscle bundle just ventral to the 1st caudal vertebral centrum of *Scipionyx samniticus*. Scale bar = 200 µm.

Fig 155 - *Scipionyx samniticus*. Particolare al microscopio ottico delle miofibre caudofemorali, che sono ancora unite a formare un fascio muscolare compatto, sotto il 1° centro vertebrale caudale. Scala metrica = 200 µm.

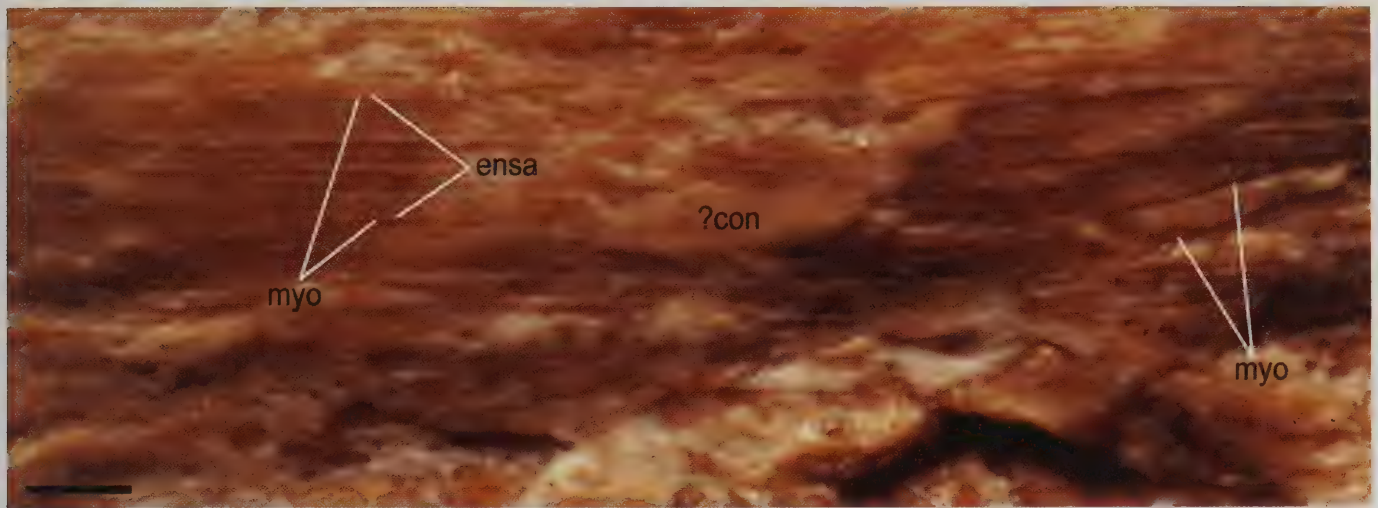


Fig. 156 - The cellular-level preservation in the caudofemoral muscles of *Scipionyx samniticus* can be seen even with a camera equipped with a macro lens. Scale bar = 200 μ m. See Appendix 1 or cover flaps for abbreviations.

Fig. 156 - Nei muscoli caudofemorali di *Scipionyx samniticus* la conservazione dei tessuti molli a livello cellulare è visibile anche con una fotocamera con obiettivo macro. Scala metrica = 200 μ m. Vedi Appendice 1 o risvolti di copertina per le abbreviazioni.

SEM imaging reveals the spectacular preservation of a sarcomere-related banded pattern within every single myofibre (Fig. 157A-C). The myofibres are polygonal in transverse section, with individual margins that are well-delimited by narrow spaces left by the dissolution of the cell membrane (sarcolemma) and its connective tissue sealing (endomysium); the striations of the sarcomeres are continuous, regular, complete and evident, as seen only in muscle tissue from some invertebrates and fishes from the Upper Jurassic of Cerin (France) and Solnhofen (Germany) (Briggs, 2003: fig. 7a). The sarcomere periodicity (2.5 μ m) is consistent with the mean sarcomeric size in extant vertebrates (e.g., Muhl *et al.*, 1976; Cross *et al.*, 1981; Botte & Pelagalli, 1982; Wheeler & Koochmarai, 1994; Cavitt *et al.*, 2004; Panchangam *et al.*, 2008).

At the highest magnification that can be used to see the myofibres of *Scipionyx*, the myofibrils can be seen to have been replaced by characteristic “furry” microspheres and coated by dispersed euhedral apatite crystals (Fig. 157C), just like in some samples from decapod crustaceans published by Wilby & Briggs (1997: figs. 3d, 4d). In the literature, the only other dinosaurian muscle tissue with a similar appearance is found in *Santanaraptor* from the Lower Cretaceous Santana Formation of Brazil (Kellner, 1996a, 1996b); however, different to *Scipionyx*, it has incomplete sarcomere-related bands, described by the authors as “partial striations” (Kellner, 1996a). Moreover, considering that the average diameter of the myofibres in the Brazilian specimen is about four times that of *Scipionyx*'s, preservation at ultrastructural level is definitely better in the Italian compsognathid. Three-dimensional myofibres, preserving polygonal cross-sections, transverse striations and even perimysial or epimysial remains are also described by Chin *et al.* (2003) in the fossilised muscle tissue from an indeterminate vertebrate, possibly a pachycephalosaur, embedded within a possible tyrannosaurid coprolite from the Late Cretaceous of Canada.

All SEM samples from the caudofemoral musculature of *Scipionyx* show the same spectacular level of preservation of the sarcomeres, and their banded pattern can be recognised even in non-conventional views: for exam-

ple, in a relatively peripheral sample from the dorsalmost bundle (Fig. 157E), the ultrastructural aspect of the sarcomeres differs in appearance only because of its oblique, rather than longitudinal, cutting plane. As a matter of fact, our sample looks strikingly similar to obliquely sectioned, three-dimensionally preserved fossil muscles illustrated by Wilby & Briggs (1997: figs. 1d-e).

The exceptionally detailed preservation of the caudofemoral muscle tissue of *Scipionyx*, as well as the SEM element microanalysis of this tissue (Fig. 157D), indicate that, after the hatchling theropod died, its carcass was subjected to very little decay and to rapid mineralisation in the presence of a high concentration of phosphates; diagenetic processes were halted very early on and fossilisation outpaced degradation through a process called authigenic mineralisation (Briggs, 2003), which will be discussed in the section devoted to soft tissue taphonomy.

Ilio-ischiocaudal muscle septa - Several hollow filamentous traces, embedded in connective tissue and seemingly related to muscle remains, lie under the tail of *Scipionyx* (Figs. 153, 158, 159). Despite this, these traces differ definitely in aspect, structure and size from the surrounding muscle fibres, as well as from those of the neck. In fact, these hollow structures are dark coloured and taper to a pointed end both proximally and distally, but in a distal direction they exhibit a bifurcated, V-shaped, often imbricate pattern; they show some flexural stiffness for most of their length, but have wavy distal ends (Figs. 159A-B; 160A-B). Moreover, the ventralmost structures become shorter and thinner: their length ranges from 9 mm (dorsal structures) to 4-5 mm (ventral structures), and their diameter ranges from 0.16 mm to 0.06 mm, respectively.

Several interpretations have been tentatively hypothesised for these enigmatic structures. Dal Sasso & Signore (1998a), observing a seeming connection with the caudofemoral bundles (Fig. 161 – see in particular the proximalmost point in which the filaments overlap onto the ventrolateral CFL bundle; see also below), wrote about large

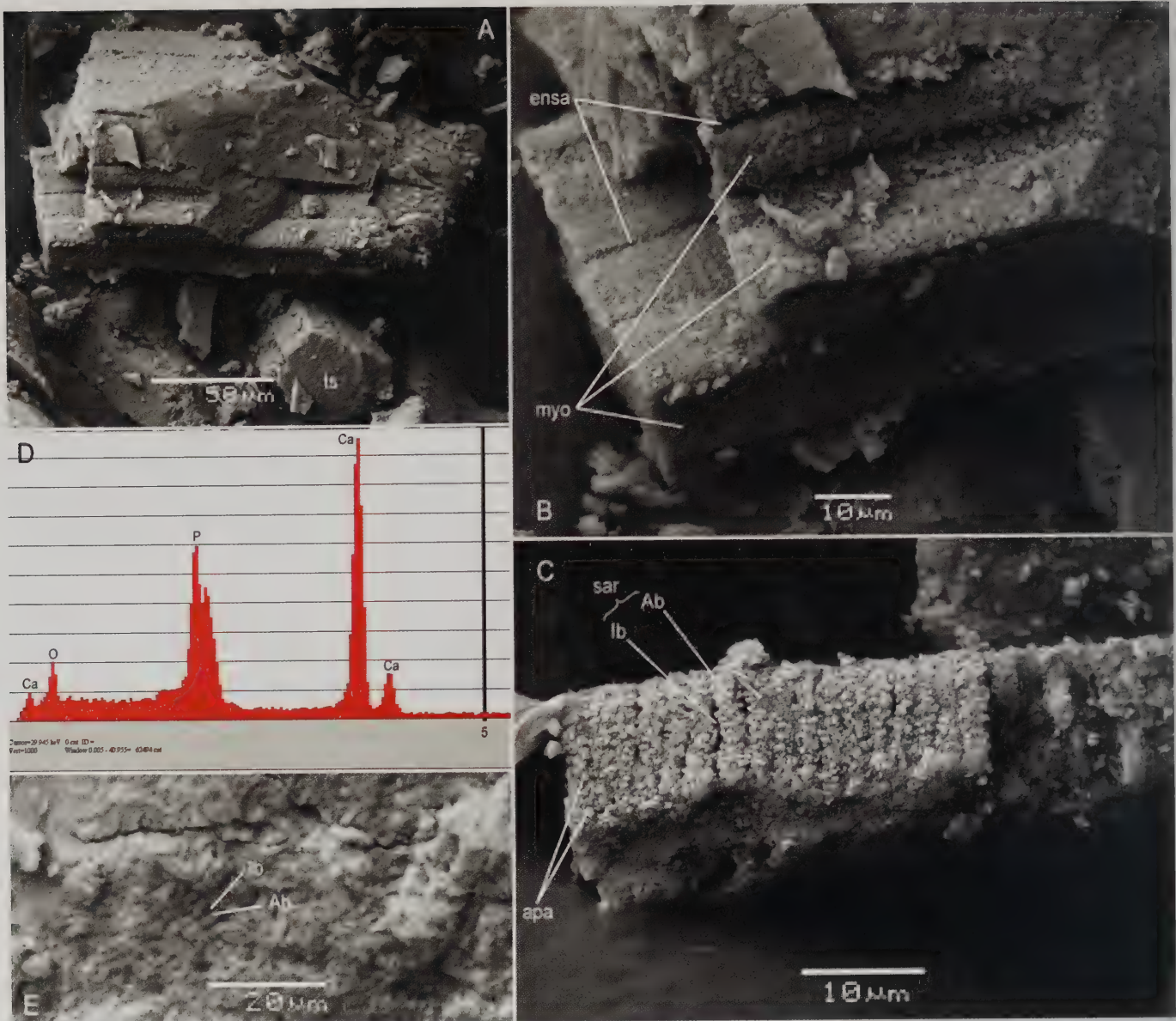


Fig. 157 - SEM imaging of the dorsalmost bundle of the caudofemoral muscle of *Scipionyx samniticus*: A) fragment of a fasciculus of myofibres; B) close-up of A; C) close-up of an isolated myofibre. While sampling the specimen, longitudinal partition occurred along natural intercellular spaces, like *in vivo*, except for one chip-like fracture (A, centre-right). D) SEM element microanalysis of the myofibre shown in C. E) the sarcomere-related banded pattern is observable also when the myofibres are cut obliquely. In taphonomy, such a level of preservation is related to the formation of a substrate microfabric (*sensu* Wilby & Briggs, 1997). See Appendix 1 or cover flaps for abbreviations.

Fig. 157 - Immagine al SEM del fascio più dorsale di muscolo caudofemorale di *Scipionyx samniticus*: A) frammento di un fascicolo di miofibre; B) particolare di A; C) particolare di una miofibra isolata. Nel prelievo del campione, il distacco in senso longitudinale è avvenuto lungo gli spazi intercellulari naturali, come *in vivo*, fatta eccezione per una frattura di aspetto scheggiato (A, centro-destra). D) microanalisi degli elementi al SEM della miofibra mostrata in C. E) il taglio obliquo delle miofibre non nasconde la struttura a bande derivante dalla fossilizzazione dei sarcomeri. In tafonomia, un tale livello di conservazione identifica una "substrate microfabric" (*sensu* Wilby & Briggs, 1997). Vedi Appendice 1 o risvolti di copertina per le abbreviazioni.

muscle fibres (Dal Sasso & Signore, 1998a: fig. 2). Given the different aspect, size and kind of preservation of all other muscle fibres (more properly, myofibres) preserved in the specimen and described in detail herein, today this interpretation must be rejected.

Tendons were another possible anatomical interpretation. A lattice of ossified tendons is found in the hypaxial region of ornithopod dinosaur tails (e.g., Organ, 2006). However, in this case one would expect these structures to lie mediadorsally to the muscle bundles, because tendons attach directly to the bones, whereas the structures

of *Scipionyx* lie in a position usually occupied by a tail muscle, the *M. ilio-ischiocaudalis* (Persons & Currie, 2011). The non-bifurcating pattern of ornithopod tendons is another important character that does not fit with these enigmatic structures of *Scipionyx*.

A third hypothesis was made by Currie (pers. obs., 1999), who observed that the filaments of *Scipionyx* look like the protofeathers of some Chinese compsognathids (e.g., Zhou *et al.*, 2003; Xu, 2006). The position of the filaments is consistent with this interpretation: they might belong to an integumentary external covering be-

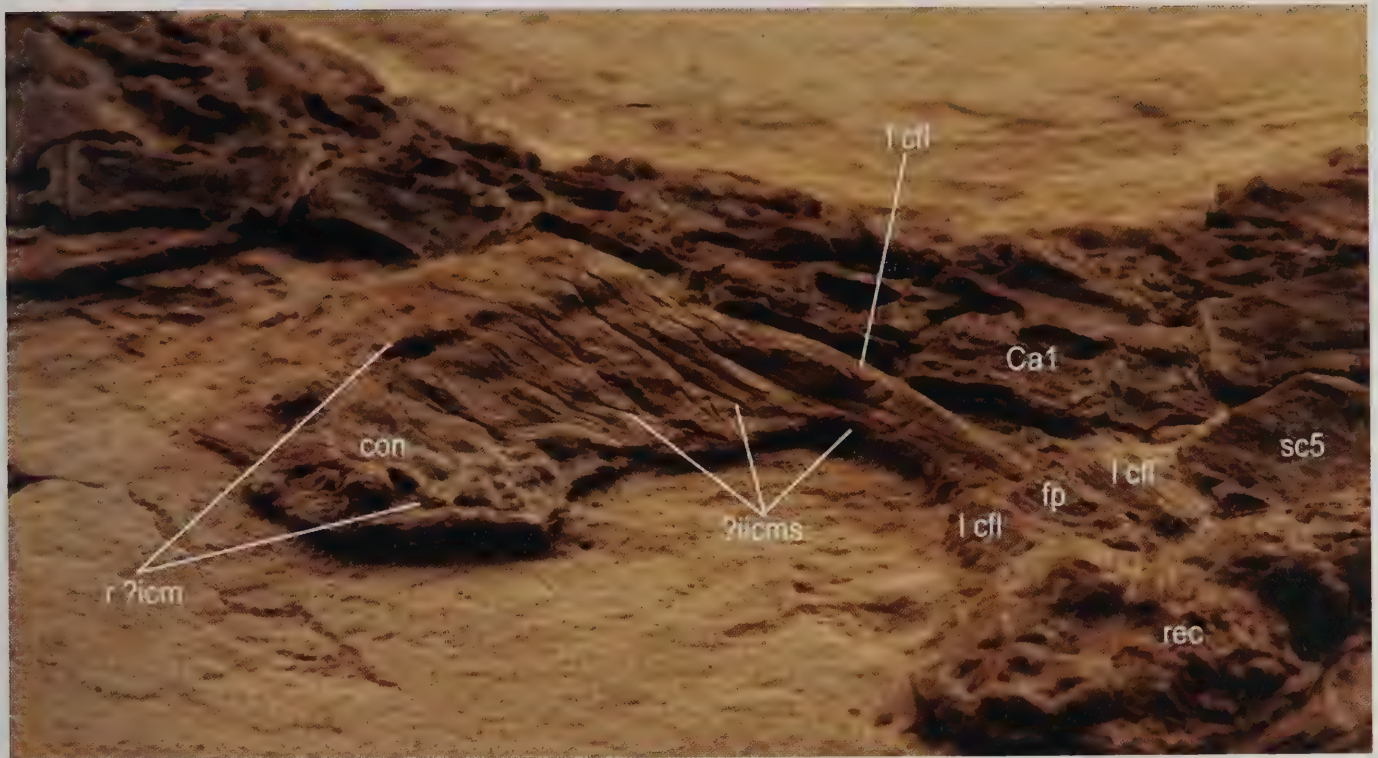


Fig. 158 - A grazing view of the soft tissues fossilised ventral to the tail of *Scipionyx samniticus* highlights the hollow structures possibly related to ileo-ischio-caudal muscle septa. Note also the three-dimensional preservation of the caudofemoral muscle bundles. See Appendix 1 or cover flaps for abbreviations.

Fig. 158 - *Scipionyx samniticus*. Una vista radente dei tessuti molli fossilizzati sotto la coda evidenzia le formazioni cave probabilmente legate ai setti del muscolo ileo-ischio-caudale. Si noti anche la conservazione tridimensionale dei fasci muscolari caudofemorali. Vedi Appendice 1 o risvolti di copertina per le abbreviazioni.



Fig. 159 - The ?ileo-ischio-caudal muscle septa of *Scipionyx samniticus*, seen under ultraviolet-induced fluorescence.

Fig. 159 - I ?setti muscolari ileo-ischio-caudali di *Scipionyx samniticus* visti in fluorescenza indotta da luce ultravioletta.



Fig. 160 - A) ?ileo-ischiocaudal muscle septa of *Scipionyx samniticus* under visible light. B) close-up of some of the hollow, axially-bifurcated traces of the possible septa shown in A, embedded in connective tissue and muscle remains. C) close-up of the septa of the *M. ilio-ischiocaudalis* of a juvenile *Caiman crocodilus* (the arrow points to cranial direction). Scale bars = 2 mm (A), 0.5 mm (B) and 5 mm (C). See Appendix 1 or cover flaps for abbreviations.

Fig. 160 - A) ?setti muscolari ileo-ischiocaudali di *Scipionyx samniticus* fotografati in luce visibile. B) particolare di alcune tracce cave dei probabili setti mostrati in A, che appaiono biforcute lungo l'asse principale e immerse in tessuto connettivo e resti di muscolatura. C) particolare dei setti del *M. ilio-ischiocaudalis* di un giovane *Caiman crocodilus* (la freccia è rivolta in direzione craniale). Scale metriche = 2 mm (A), 0,5 mm (B) e 5 mm (C). Vedi Appendice 1 o risvolti di copertina per le abbreviazioni.

cause they lie some distance from the vertebrae. At first glance, this hypothesis seems supported by superficial similarities, such as that the filaments of *Sinornithosaurus* (Xu *et al.*, 1999) are hollow tubes and that the ones of *Dilong* (Xu *et al.*, 2004) exhibit a roughly comparable branching pattern. Nevertheless, at closer examination also the protofeather hypothesis must be abandoned. In fact, the enigmatic structures of *Scipionyx* gently taper not only in a distal, but also in a proximal, direction, a fact that would be a structural and functional nonsense for any integumentary derivative: the proximal end is for dermal attachment, so needs to be a firm, robust, enlarged base (calamus, hair bulb). According to Xu (pers. comm., 2009), the counterpart-like preservation, as well as the axial bifurcation and irregular tapering shown by the hollow structures of *Scipionyx*, are not consistent with the protofeathers of the Chinese dinosaurs, also because protofeathers are not comparable dimensionally, being thinner and more delicate to the point that they cannot produce any impression in the sediment. Moreover, they branch repeatedly and always from a single central axis.

A fourth hypothesis arose during the present study, after we examined the hollow structures of the abdomen that we then referred to blood vessels of the cranial mesenteric artery. However, the proximal and distal tapering we observe in these enigmatic structures does not make any sense as part of a vessel either, given that a vessel is made to drive a liquid through. Comparison with the blood vessels of the cranial mesenteric artery strengthens our rejection of this hypothesis because, in addition, the hollow structures under the tail are longer, straight rather than wavy, much more strongly coloured and not at all diaphanous. Furthermore, most of them have a greater diameter than the intestinal blood vessels.

The fifth and, in our opinion, most feasible hypothesis, came from an exchange of information that began recently (Persons, pers. comm., 2009, 2010). In a variety of extant reptiles, *M. caudofemoralis* is covered by *M. ilio-ischiocaudalis*, which wraps around the former laterally and ventrally for all its length (e.g., Huchzermeyer, 2003; Persons & Currie, 2011). Consistent with its nomenclature, *M. ilio-ischiocaudalis* is composed of two major muscles: *M. ilio-caudalis* and *M. ischiocaudalis*, with the former origi-

nating from the ilium and the latter from the ischium. *M. ilio-ischiocaudalis* is relatively thin proximally, whereas distally it increases in relative thickness as the thickness of *M. caudofemoralis* decreases. After the latter disappears, *M. ilio-ischiocaudalis* inserts on the full lateral surface of the caudal centra and the haemal arches. Contrary to the caudofemoral muscle, which consists of straight parallel bundles, the ilio-ischiocaudal muscle is partitioned by conical myosepta, that on the surface, or in a longitudinal cross section, produce a pattern of craniocaudally V-oriented bundles. These septa bear a strong resemblance (Fig. 160C; Persons, pers. comm., 2009) to the imbricate V-shaped structures of the enigmatic structures of *Scipionyx* running parallel to the caudofemoral muscle bundles and lying laterally and ventrally, but not medially, to them. The dimensional range of these structures in individuals of extant reptiles of comparable size is also consistent. Therefore, we conclude that the hollow enigmatic structures of *Scipionyx* are most likely ilio-ischiocaudal septa. Specifically, the well-defined septate pattern on the dorsalmost portion might belong to the right *M. iliocaudalis*, whereas the ventral portion, where the pattern is less well-defined, would belong to the right *M. ischiocaudalis*.

In this perspective, the “glued” appearance of the right ilio-ischiocaudal muscle on the left caudofemoral muscle (Fig. 161) might be due to osmosis-driven dehydration that possibly affected the carcass of *Scipionyx* when it sunk in the Pietraraja basin.

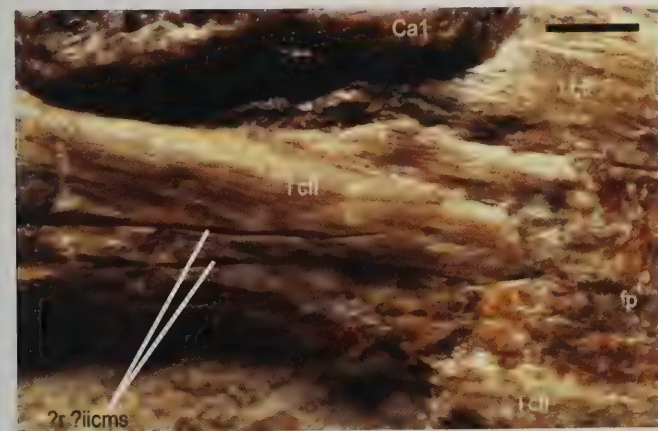


Fig. 161 - Close-up of the contact that seems to exist between the caudal-most bundle of the left caudofemoral muscle and the tapering cranial end of the cranialmost septum of the right ilio-ischiocaudal muscle. Scale bar = 1 mm. See Appendix 1 or cover flaps for abbreviations.

Fig. 161 - Contatto apparente tra il fascio più caudale del muscolo caudofemorale sinistro e la terminazione affusolata del setto muscolare ilio-ischiocaudale destro più craniale. Scala metrica = 1 mm. Vedi Appendice 1 o risvolti di copertina per le abbreviazioni.

Other fragments of pelvic and hindlimb muscles -

At least six relatively loose muscle fragments, composed of parallel myofibres of comparable aspect and size, are preserved in the pelvic and proximal caudal region of *Scipionyx* (Figs. 117, 153). The three cranialmost fragments are superimposed, respectively, on the descending tract of the rectum and on the ascending tract nearby (e.g., Fig. 162). Their distance from the vertebral column as well as the craniocaudal direction of their myofibres are consistent with the position along which the right *M. caudo-*

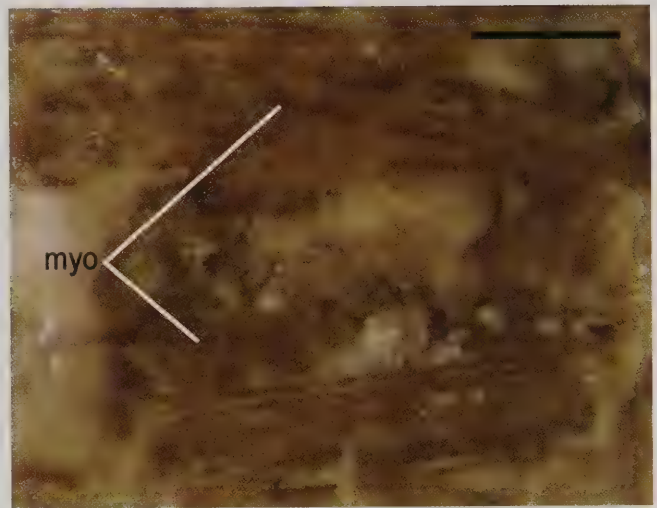


Fig. 162 - Close-up of myofibres covering the rectum of *Scipionyx samniticus*, between the 5th sacral centrum and the ischial feet, tentatively referred to the right caudofemoral muscle. Scale bar = 200 µm. See Appendix 1 or cover flaps for abbreviations.

Fig. 162 - *Scipionyx samniticus*. Particolare di un frammento di tessuto con miofibre, appoggiato sul retto tra il 5° centro vertebrale sacrale e i piedi ischiatici, attribuito tentativamente al muscolo caudofemorale destro. Scala metrica = 200 µm. Vedi Appendice 1 o risvolti di copertina per le abbreviazioni.

femoralis or the right *M. ischiocaudalis* would have run. The former is preferred, as the three fragments lie directly on the surface of the rectum, i.e., in a more medial plane than *M. ischiocaudalis* (e.g., Gatesy, 1990: fig. 3a; Persons & Currie, 2011: fig. 2a). Attribution to *M. adductor femoris II* is unlikely: as already pointed out (Carrano & Hutchinson, 2002), this muscle originates on the caudal edge of the near ischium, but it runs cranioventrally, not caudally, to insert on the femur. *M. ischiotrochantericus* is another possible candidate, but this is improbable because it originates from the medial surface of the ischium, which is only a few millimetres cranial to these fragments. In fact, in crocodylians and other extant reptiles, this muscle also inserts onto the caudolateral surface of the proximal femur, then runs craniodorsally to the ischium, rather than caudally (Carrano & Hutchinson, 2002).

Three other muscle fragments are embedded in the connective tissue including the supposed ilio-ischiocaudal septa (e.g., Fig. 163). All three fragments are found at the level of the 3rd caudal centrum, subequally distant to each other. The most dorsal one seems in line with the left *M. caudofemoralis*, so might represent its caudal continuation; the ventralmost one, and the one in-between the other two, are too ventrally placed to be included in the caudofemoral muscle; thus, they might be remnants of the right ischiocaudal myofibres, for the same reasons we invoked when regarding as possible ischiocaudal septa the nearby mysterious structures.

Caudal hypaxial connective tissue/ligaments

In between the two better exposed chevron bones, which are preserved in an intercentral position between caudal vertebrae 4-5 and 5-6, a small patch of soft tissue can be detected under visible light at medium magnification, and fluorescing under UV light (Fig. 164A). High



Fig. 163 - Close-up of myofibres preserved in between the hollow filamentous traces illustrated in Figs. 159-160, possibly belonging to the right ischiocaudal muscle of *Scipionyx samniticus*. Scale bar = 200 μ m. See Appendix 1 or cover flaps for abbreviations.

Fig. 163 - Particolare di un frammento di tessuto con miofibre conservato fra le tracce filamentose cave illustrate nelle Fig. 159-160, che potrebbe appartenere al muscolo ischiocaudale destro di *Scipionyx samniticus*. Scala metrica = 200 μ m. Vedi Appendice 1 o risvolti di copertina per le abbreviazioni.

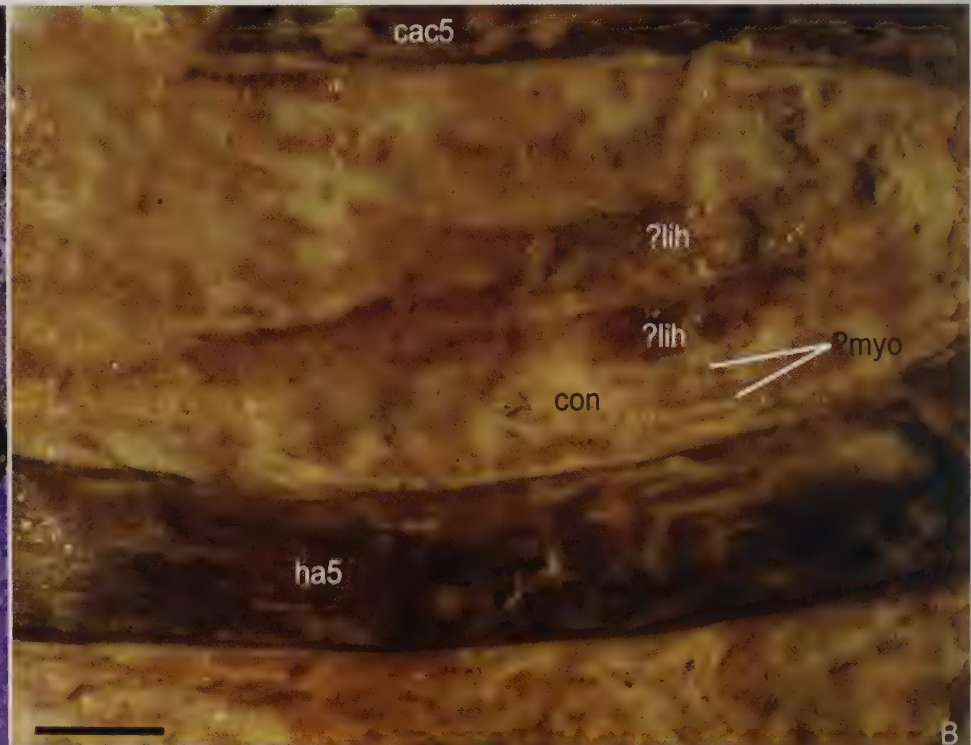


Fig. 164 - Remnants of the caudal hypaxial connective tissue, or ligaments, in *Scipionyx samniticus*, under ultraviolet-induced fluorescence (A) and visible light (B, close-up). Scale bar = 0.5 mm. See Appendix 1 or cover flaps for abbreviations.

Fig. 164 - *Scipionyx samniticus*. Residui del connettivo o dei legamenti ipassiali caudali, fotografati in fluorescenza indotta da luce ultravioletta (A) e in luce visibile (B, particolare). Scala metrica = 0,5 mm. Vedi Appendice 1 o risvolti di copertina per le abbreviazioni.

magnification (Fig. 164B) reveals a number of light brown fibres, possibly myofibres, and a couple of brown coloured, flat, arched structures in the centre of the area, paralleling the curvature of the chevron shafts. These myofibres and arched structures are embedded in a yellowish, amorphous material. The flat, arched structures have a transverse diameter (0.2 mm) which is evidently larger than that of any myofibre preserved here or in other parts of the specimen, and a fibro-laminous aspect which is not even consistent with a bundle of tightly bound myofibres. Rather, such an aspect is compatible with a sheet-like single unit.

According to Persons (pers. comm., 2009), a tendon latticework is expected to run in dinosaurs from haemal arch to haemal arch, medial to the tail muscles but just lateral to the chevron bones, similar to what is seen in extant reptiles. However, the laminae preserved in *Scipionyx* seem to lie just in the medial sagittal plane, and their thin delicate aspect is not at all reminiscent of tendons. So we are confident in referring them to the fibrous connective tissue sheets that separated the counterlateral caudofemoral muscle bundles along the midline, or more likely to the *ligamentum interhaemale* (Frey, 1988; Schwarz-Wings *et al.*, 2009). The amorphous, whitish material surrounding the laminae might belong to loose connective tissue associated with them.

Indeterminate ?connective tissue

Some patches of soft tissue preserved in *Scipionyx* are apparent as a yellowish material embedding myofibres, myosepta and/or fibrous connective tissue. We often describe this material as an amorphous mass, because it does not have any particular structural arrangement under the

optical microscope (e.g., Figs. 129, 159A). The largest areas where this tissue is preserved are found at the base of the neck and at the base of tail – shown in grey-brown shading in the soft tissue general map (Fig. 117).

The possibility that this material represents diagenetically altered adipose tissue cannot be ruled out, because saturated fatty acids are resistant to degradation just like connective tissue (Chin *et al.*, 2003; Killops & Killops, 1993). Nevertheless, fat storage in a hatchling is unlikely, so we have reason to suppose that these tissue patches (especially the one at the base of the tail) have a connective-tissue nature, based on their co-association and intimate connection with myofibres, myosepta and fibrous connec-

tive tissue. Unfortunately, samples of this material were not collected, so at present we cannot test for the presence of the collagen-diagnostic 67 nm banding pattern, given by the peculiar overlap of the molecules composing the collagen fibrils, as conducted by Schweitzer *et al.* (2007, 2008) on dinosaurian soft tissue. Certainly, nothing similar can be seen under the light microscope, and the aspect of this material remains amorphous. This might be due not only to instrumental limits but also to partial decay of the tissue before fossilisation, so that we cannot distinguish whether it was arranged as fibrous or loose connective tissue *in vivo*. For all these reasons, we label this tissue as indeterminate.

EXTERNAL SOFT TISSUES

This section describes integumentary remains, more precisely the horny structures (claws), that from a histological point of view are not a kind of tissue but epidermal derivatives originally composed of keratin. Although keratin is a highly resistant insoluble protein, fossilisation usually takes place after the loss of the skin and its derivatives, so that complete horny claws in fossil vertebrates are found very rarely. Among theropod dinosaurs, the first recording was in *Archaeopteryx* (Ostrom, 1970), but apart from single finds, such as *Rahonavis* (Schweitzer *et al.*, 1999) and *Santanaraptor* (Kellner, 1999), most of the other examples came in recent times from the exceptionally preserved integuments of the “feathered” Yixian dinosaurs (e.g., *Microraptor*, *Protarchaeopteryx*, *Sinornithosaurus*).

Horny claws

All preserved manual ungual phalanges of *Scipionyx* are sheathed by scythe-like, pointed horny claws,

greatly prolonging the curvature of the bony elements (Fig. 165). The horny claws are still well-attached to their bony phalanges. The base attachment is so firm that the horny claws did not detach, even where the pointed apices bent partially (digits II and III of the left manus) or fully (digit I) towards the ventral margin of the bony ungual phalanges (Fig. 166). According to Delfino (pers. comm., 2006), this is evidence of rapid burial, because when the carcasses of extant reptiles are left soaking, the horny claws become quickly detached, together with the skin of the limbs. Therefore, we can deduce that, after *Scipionyx* died, it did not float for any length of time.

The horny tip of the 3rd right digit seems to be in its original apical position by comparison with the other ones. What looks strange is the large horny area embracing it, the size of which seems to fit a base attachment rather than a distal portion of a pointed claw. Actually, this large horny area represents the dorsal and ventral walls of the talon that opened-up *post mortem*, thus exposing their internal surface as an almost flattened table (Fig. 167). As for dimensions, the horny claws of *Scipio-*

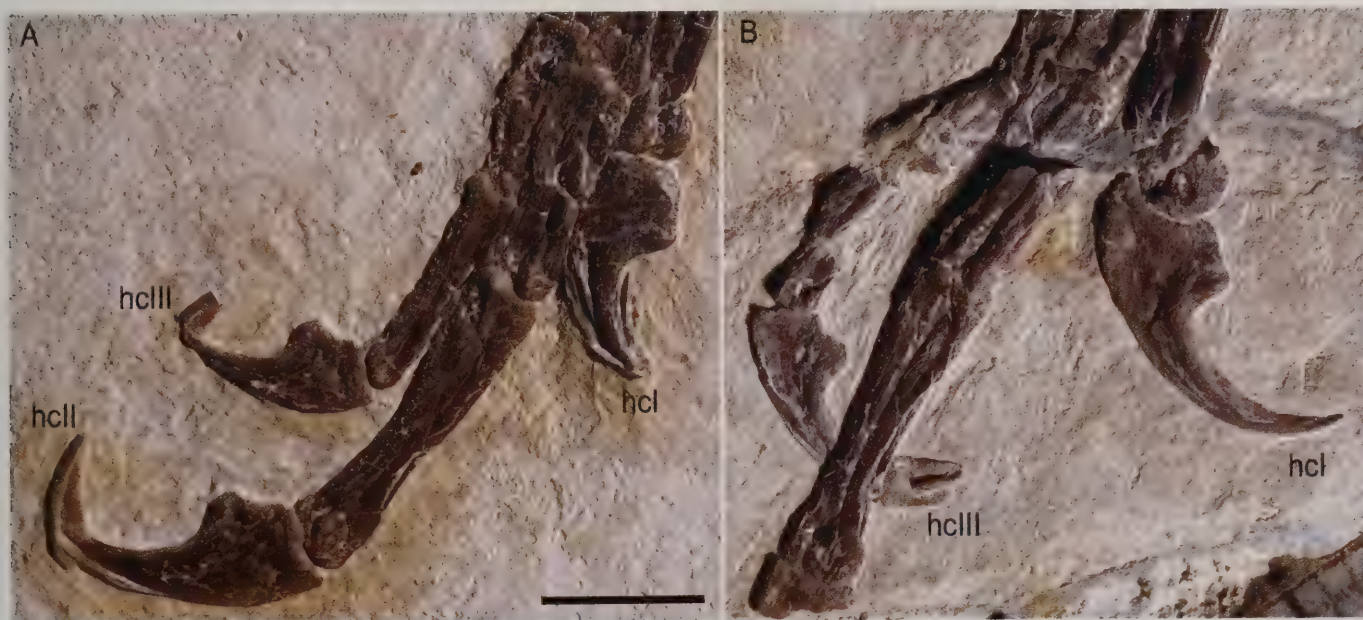


Fig. 165 - Horny claws are still in place on all preserved left (A) and right (B) manual unguals of the holotype of *Scipionyx samniticus*. Scale bar = 5 mm. See Appendix 1 or cover flaps for abbreviations.

Fig. 165 - Gli artigli cornei sono ancora in posto su tutte le falangi ungueali conservate nella mano sinistra (A) e destra (B) dell'olotipo di *Scipionyx samniticus*. Scala metrica = 5 mm. Vedi Appendice 1 o risvolti di copertina per le abbreviazioni.



Fig. 166 - Close-up of the 1st left manual ungual of *Scipionyx samniticus*, showing the pointed apex of the horny claw broken-off and bent-back against the ventral margin of the bone. Scale bar = 0.5 mm. See Appendix 1 or cover flaps for abbreviations.

Fig. 166 - Particolare della 1^a falange ungueale della mano sinistra di *Scipionyx samniticus*, che presenta la punta dell'artiglio corneo ripiegata completamente contro il margine ventrale dell'osso. Scala metrica = 0,5 mm. Vedi Appendice 1 o risvolti di copertina per le abbreviazioni.



Fig. 167 - The unusual state of preservation of the 2nd right horny claw of *Scipionyx samniticus*. Scale bar = 1 mm. See Appendix 1 or cover flaps for abbreviations.

Fig. 167 - L'inusuale modalità di conservazione del 2^o artiglio corneo della mano destra di *Scipionyx samniticus*. Scala metrica = 1 mm. Vedi Appendice 1 o risvolti di copertina per le abbreviazioni.

nyx vary in length from 7.7 mm (linear length of the 2nd left claw) to 6.2 mm (linear length of the 3rd right claw), out-measuring the bony manual phalanges up to 3.2 mm (linear length of the 2nd left claw beyond its bony tip). This means that, when reconstructing the *in vivo* aspect of a theropod hand, the length and the curvature of the fossil bony claws distal to the flexor tubercles should be increased by some 40%.

The preservation of the horny claws of *Scipionyx* is so good that under the light microscope a peculiar semi-transparent, waxy aspect can be seen. No thin sectioning, nor immunohistochemical or mass spectrometric studies were possible, so we were unable to investigate the microstructure and composition of the horny claws of the Italian compsognathid, as has been done on other theropod material (e.g., Schweitzer *et al.*, 1999). Nevertheless, in addition to its waxy and fibrous aspect, it is also evident that the tightly adhering material of the bony claws is arranged in layers, and that the layers composing the dorsal horny talons (unguis) are darker in colour than those composing the ventral horny talons (subunguis). Furthermore, the dark colour of the dorsal horny talons increases towards the tips, becoming almost black (Fig. 168). This feature indicates a higher density of material and, thus, a proportionate mechanical resistance, as is the case in most extant tetrapods in which the unguis is known to have a hard, thick dorsal layer, whereas the subunguis has a soft, thin ventral layer.

Remarkably, a similar colouring is present also in the fossil *Santanaraptor*: like *Scipionyx*, the Brazilian theropod has soft tissue that can be distinguished from the bones by their lighter colours, except near the unguis, where the horny covering is reported to be darker than the bone (Kellner, 1999).



Fig. 168 - Close-up of the 1st right manual horny claw of *Scipionyx samniticus*. Note that the colour of the *unguis* becomes darker towards the pointed apex. Scale bar = 1 mm. See Appendix 1 or cover flaps for abbreviations.

Fig. 168 - Particolare del 1^o artiglio corneo della mano destra di *Scipionyx samniticus*. Si noti la colorazione scura dell'*unguis*, che aumenta in direzione della punta. Scala metrica = 1 mm. Vedi Appendice 1 o risvolti di copertina per le abbreviazioni.

ENDOGENOUS BIOMOLECULAR COMPONENTS

Preservation of endogenous biomolecules has been documented in a variety of vertebrate and invertebrate fossil specimens from varying ages (Schweitzer *et al.*, 1999). Schweitzer *et al.* (2008) demonstrated that, although the almost perfect preservation of form does not guarantee the presence of original organic material, the preservation of endogenous molecules is closely correlated to it. The fossilisation of different types of tissues in different colours also suggests different chemical composition (Schweitzer, pers. comm., 1998); therefore, some endogenous biomolecular components might still be locally present in *Scipionyx*. For instance, highly resistant insoluble keratin molecules might be among the chemical components of the above-mentioned dark portion of the horny claws; some connective tissue patches might contain collagen remains; haem components derived from haemoglobin molecules or their products of decay might be preserved in the reddish pigments of the liver. According to the University of South Florida's endocrinologist David Vesely (pers. comm., 2008), the intestine of *Scipionyx* might even contain atrio-natriuretic peptides, vasodilator hormones which

are usually released by the heart but are also concentrated in the gastrointestinal tissues. Nevertheless, this speculation remains such, as neither chemical analyses (other than SEM element microanalysis) nor molecular analyses were undertaken in this study because the majority of presently used extraction techniques – destruction of macroscopic samples through crushing to a fine powder, with multiple repetitions of the process (Schweitzer *et al.*, 2008) – would cause serious damage to this unique specimen.

Biomolecules have a preservation potential that depends on their size and complexity: for instance, in fossil specimens, macromolecules are found to be more resistant to decay than proteins or nucleic acids (Tegelaar *et al.*, 1989; Briggs, 1993; Schweitzer *et al.*, 2008). The presence in *Scipionyx* of original autogenous DNA should be, anyhow, excluded, given the nature of the deposits from which the fossil comes. Natural biological caskets, like the thick bony wall of a *Tyrannosaurus* femur, have been demonstrated to be much better sites of biomolecular preservation than the laminated limestones, probably because the latter are subjected to intense water permeation (Schweitzer *et al.*, 2007).

Table 3 - Selected measurements of the soft tissues of the holotype of *Scipionyx samniticus*.

Muscles and other soft tissues in the neck	
Neck muscles and other soft tissue remains, length	19.3 mm
Neck muscle and other soft tissue remains, width	12.6 mm
Neck muscle myofibres, minimum diameter	8 μm
Neck muscle myofibres, maximum diameter	13 μm
Neck muscle myofibres, sarcomeric periodicity (length)	2.9 μm
Neck ?collagen bundles, minimum diameter	8 μm
Neck ?collagen bundles, maximum diameter	40 μm

Trachea	
Trachea, length of preserved tract	7 mm
Number of preserved tracheal rings	10-11
Tracheal rings, average diameter of the preserved parts	1 mm
Tracheal rings, average craniocaudal length	0.33 mm
Space between rings, average craniocaudal length	0.17 mm

Oesophagus	
Oesophagus remains, length	5 mm

Liver, and other blood-rich organs	
Reddish halo, diameter (under UV light)	17 mm

Intestine	
Intestine, visible length	173 mm
Intestine, estimated length	300-320 mm
Duodenum, visible length	72 mm
Duodenum, estimated length	105-115mm
Duodenum, maximum diameter	6.5 mm
Duodenum, average diameter	5.2 mm
Number of duodenal folds (<i>plicae circulares</i>) per mm	5-6
Longitudinal visceral (duodenal) myofibres, minimum diameter	7 μm
Longitudinal visceral (duodenal) myofibres, maximum diameter	17 μm
Jejunum, visible length	57 mm
Jejunum, estimated length	85 mm

Jejunum, maximum diameter	5 mm
Jejunum, average diameter	3.5 mm
Number of jejunal folds (<i>plicae circulares</i>) per mm	6
Rectum, visible length	35.5 mm
Rectum, estimated length	55-65 mm
Rectum, maximum diameter	5 mm
Rectum, average diameter	4 mm
Faecal pellet, visible length	5.5 mm
Faecal pellet, estimated length	6-7 mm
Faecal pellet, maximum diameter	2.5 mm
Faecal pellet, average diameter	2.3 mm

Mesenteric blood vessels

Largest blood vessel, length	9-10 mm
Largest blood vessel, minimum diameter	0.04 mm
Largest blood vessel, maximum diameter	0.1 mm

Puboischiofemoral muscle

Muscle remains, length	5 mm
Muscle remains, diameter	2 mm
Myofibres, minimum diameter	10 μ m
Myofibres, maximum diameter	15 μ m

Caudofemoral muscle (*M. caudofemoralis longus*)

Dorsalmost bundle, visible length	6.3 mm
Dorsalmost bundle, diameter	1.6 mm
Dorsalmost bundle myofibres, minimum diameter	13 μ m
Dorsalmost bundle myofibres, maximum diameter	26 μ m
Dorsalmost bundle myofibres, sarcomeric periodicity (length)	2.5 μ m
Ventralmost bundle, visible length	4.3 mm
Ventralmost bundle, diameter	2.2 mm

Ventralmost bundle myofibres, minimum diameter	10 μ m
Ventralmost bundle myofibres, maximum diameter	22 μ m
Distalmost bundle visible, length	9.8 mm
Distalmost bundle, diameter	2.2 mm
Distalmost bundle myofibres, minimum diameter	10 μ m
Distalmost bundle myofibres, maximum diameter	25 μ m

?Ilio-ischiocaudal muscle ?septa

Length of preserved area	17 mm
Width of preserved area	11.5 mm
Smallest element, length	4-5 mm
Largest element, length	9 mm
Smallest element, maximum diameter	0.06 mm
Largest element, maximum diameter	0.16 mm

Horny claws

	Left	Right
Manual digit I horny claw, linear length	7 mm	7.2 mm
Manual digit I horny claw, oversize (linear length beyond bony tip)	3.2 mm	2.8 mm
Manual digit I horny claw, height at bony tip	0.7 mm	0.9 mm
Manual digit II horny claw, linear length	7.5 mm	-
Manual digit II horny claw, oversize (linear length beyond bony tip)	3.3 mm	-
Manual digit II horny claw, height at bony tip	1.1 mm	-
Manual digit III horny claw, linear length	6.7 mm	6.2 mm
Manual digit III horny claw, oversize (linear length beyond bony tip)	2 mm	-
Manual digit III horny claw, height at bony tip	0.8 mm	-

SOFT TISSUE TAPHONOMY

Exceptional preservation of labile soft tissue, such as muscles or loosely connected integumentary structures (see Horny Claws) indicates that diagenetic processes were halted very early after *Scipionyx* died and that mineralisation outpaced degradation (Schweitzer *et al.*, 2008). Briggs (2003) described a peculiar process, that he named authigenic mineralisation, in which microscopic mineral crystals replicate the morphology of a biological structure, driven by the activity of decay bacteria. This process represents the highest taphonomic threshold among the possible stages of soft tissue preservation. According to Briggs (2003), the best known examples are the fish muscle tissue from the Lower Cretaceous Santana Formation of Brazil, which preserve sarcolemma and sarcomere-related banding (Martill, 1988; Briggs *et al.*, 1993). Such details of labile soft tissue may survive as a result of the precipitation of authigenic minerals on the tissues themselves, or on microbial films that cover them. The relevant role of bacterial sealing in the initial stages of fossilisation was confirmed by experimental simulations (Sagemann *et al.*, 1999; Iniesto *et al.*, 2009; Noto, 2009). The quality and fidelity of preservation depends on the composition, form and size of the mineral crystals. Authigenic mineralisation also involves the invasion of tissues by ion-bearing (e.g., phosphorus) pore water.

Scipionyx was preserved in a marine environment. If the model of the shallow lagoon is correct (see Geological Setting), some additional factors, such as reduced vertical water stirring and seasonal overheating, might have favoured low oxygen levels in the Pietraraja deposits (Bravi & Garassino, 1998), slowing down the decay of the dinosaur carcass. Nonetheless, we would like to remark that in aquatic settings, even under normal conditions (i.e., open waters), the oxic-anoxic boundary may be at, or even above, the sediment-water interface, and that underwater, most decay of carcasses is usually anaerobic (Briggs, 2003). Recent experiments confirm this statement and our hypotheses on soft tissue preservation in *Scipionyx* (see below). Noto (2009), for instance, performed a year-long taphonomic experiment investigating the effect of different environmental conditions on the diagenesis of buried bone, observing authigenic mineral formation. Bone was also found to interact with the surrounding sediment, buffering pore water pH changes and contributing to local anoxia.

The major process of organic matter oxidation in marine sediments is bacterial sulphate reduction (Gaillard *et al.*, 1989), which can result in the precipitation of minerals such as calcite, aragonite and apatite. Early cementation is essential for the preservation of soft tissue in three dimensions like we see in *Scipionyx*. In fact, rapid authigenic mineralisation via phosphatisation can occur virtually immediately after death in an appropriate environment (Briggs & Kear, 1993b), preserving cells and subcellular detail faster than they could decay (Butterfield, 2002). Authigenic mineralisation occurs through early infiltration and permeation of labile tissue by mineral-charged water and differs from petrification, which is a replacement process.

In a given specimen, however, these processes do not take place in the same way, at the same time or with the same kinetics. In fact, as well-remarked by Briggs (2003), carcasses are made up of a range of materials with different degrees of resistance to decay, and even at the molecular level, different organic materials have different potential for preservation. Moreover, the precipitation of one mineral or another is linked to labile switches in the chemical reactions. For example, pH is a major determinant in the control of calcium carbonate and calcium phosphate precipitation, operating at the microbial level as an “on” or “off” switch in the different parts of the same carcass (Briggs & Wilby, 1996; Noto, 2009; Sagemann *et al.*, 1999). In our opinion, this is the most likely explanation for preservation of the intestine and decay of the stomach in *Scipionyx*. As we pointed out when describing these two organs, the physiological pH of the abdominal cavity of vertebrates is maintained locally by very diverse homeostatic processes, and probably can persist at diverse levels for a certain time after death. In addition, experiments demonstrate that local shifts in the geochemical gradients develop around a carcass as a result of microbial decay, too, and that these microbially-induced shifts have a profound impact on whether or not minerals form and soft tissues are preserved (Briggs, 2003; Noto, 2009; Sagemann *et al.*, 1999). Other experiments have established that specific bacteria can play a key role in phosphate precipitation. Some bacteria, including the coliform bacterium *Escherichia coli*, appear to facilitate phosphatisation by contributing phosphorus-liberating phosphatases (Chin *et al.*, 2003; Hirschler *et al.*, 1990).

As soft tissues must be replicated before they are destroyed by decay, rapid mineralisation was crucial in *Scipionyx*. Of course, mineralisation relies on the availability of mineral ions. In the case of apatite, laboratory experiments demonstrate that phosphorus may derive from the decaying tissues of the carcasses themselves (Briggs & Kear, 1993a; Noto, 2009) or may derive from the surrounding sediment or pore water (Briggs, 2003). These sources have been also deduced from the fossil occurrences (Wilby & Briggs, 1997). For example, the presence of fossilised soft tissue in several specimens belonging to different taxa in the Solnhofen Limestone reflects the presence of an external, supersaturated source of phosphorus that is available to virtually all carcasses. At Solnhofen, Briggs (2003) observed that fossils with mineralised soft tissue tend to be covered by a thinner lamina of sediment than those without, indicating that they were closer to the sediment-water interface, where adsorbed phosphorus was concentrated.

The Pietraraja Plattenkalk seems to postulate different conditions. In addition to *Scipionyx*, other vertebrate specimens are found to preserve soft tissue remains (Costa, 1853-1864; D’Erasmus, 1914, 1915; Evans *et al.*, 2004), but many other fish and reptile specimens preserve just skeletal parts. Some taxa never show any soft tissue: decapod crustaceans, for instance, do not preserve even traces of gills and muscle attachments (Bravi & Garassino, 1998; Garassino, pers. comm., 2010), which are instead commonly seen at Solnhofen (Garassino &

Schweigert, 2006). At Pietraraja, phosphorus seems to come from the carcasses, not from the sediment - at least in the fossil *Scipionyx*. Our SEM element microanalyses provide compelling evidence that all preserved body parts, bone as well as muscle, cartilage and connective tissue, are phosphorus-rich (Figs. 121A, C; 132B; 143C; 144A, C; 157D), whereas the embedding matrix is completely devoid of it. In fact, the samples of sediment coming from the matrix around the specimen, including the ones taken near the dinosaur's outline and from the same bed (Fig. 10), turned out to be entirely composed of carbonates and silicates, with the former as primary components (Figs. 13A, C). Therefore, as predicted by Noto (pers. comm., 2009), the phosphorus of *Scipionyx* is authigenic.

A survey conducted by Wilby & Briggs (1997) on a range of Mesozoic and Tertiary laminated limestones preserving fossils with phosphatised soft tissues, led to the identification of three kinds of microfibrils. The most spectacular preservation occurs where tissues are phosphatised directly by very small apatite crystallites, often <30nm: this produces a "substrate microfibril" that may preserve details at the cellular or even subcellular level. This is well-documented in *Scipionyx* by the preservation of sarcomere-related banding in the caudofemoral myofibres (e.g., Figs. 157A-C), and indicates that the carcass of the hatching theropod was subjected to very little decay and a rapid mineralisation in the presence of a high concentration of phosphates. This type of soft tissue preservation is microbially induced, even though the microbes themselves do not become mineralised (Briggs, 2003). According to Wilby & Briggs (1997), substrate microfibrils tend to characterise fossil fish, "the thick and toughened dermis of which provides an effective barrier to microbes for a longer period". This statement leads us to infer that the squamous in-

tegument of a dinosaur would provide a comparable, if not tougher, barrier.

On the other hand, where tissues are easily permeated and heavily invaded by microbes during the decay of a carcass, the bacteria themselves may become the site of apatite precipitation, and phosphatised microbes may pseudomorph the gross form of the tissue. This kind of preservation was described by Wilby & Briggs (1997) as a "microbial microfibril". Among the examples given, a microbial microfibril in a fish from the Eocene of Monte Bolca (Wilby & Briggs, 1997: fig. 1a-b) looks very similar to the one we see in all SEM samples from the intestine of *Scipionyx* (Figs. 143A-B; 144B; 149A; 169; 170A). The infill of the intestine of *Scipionyx* is dominated by a phosphatised (Figs. 143C; 144A, C), amorphous matter, characterised by large concretions and many spaces. Notably, a very similar texture, described as "spongy", was found in the intestinal remnants of *Mirischia* (Martill *et al.*, 2000). In *Scipionyx*, this spongy, vacuolar aspect is widespread in the mass embedding the soft tissue remains related to the intestine, and some of the tissue themselves, which are literally full of phosphatised microspheres with an almost constant diameter that never exceeds 2 μm (Figs. 144B; 170). This texture and the order of magnitude of the microspheres are consistent with the tissue having been replaced by pseudomorphed bacteria, many of which are preserved as hollow spheres. We infer from Wilby & Briggs (1997) that in *Scipionyx*, contrary to somatic muscle tissue, such an extensive microbial invasion of the visceral muscles occurred in the intestine thanks to its nature, namely its structurally high permeability. According to Wilby & Briggs (1997), the detail preserved in a microbial microfibril is related to the size of the bacteria, which are normally 1-2 μm in diameter. Such an order of magnitude did not affect the preservation of the middle-gross anatomy of *Scipionyx*, allowing us to observe, after more than 110 million years, the ripples of the mucosa of a dinosaur's intestine (Figs. 140-141).

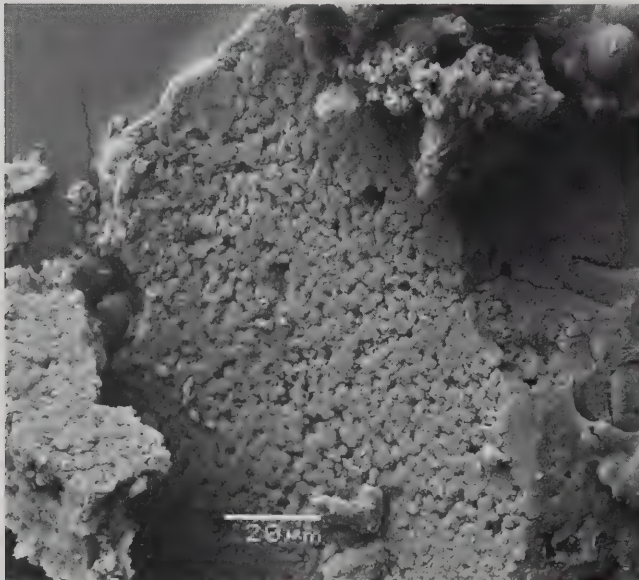


Fig. 169 - SEM image of soft tissue remains and intestinal infill of the duodenum of *Scipionyx samniticus*. The vacuolar aspect may be related to microbial microfibrils (*sensu* Wilby & Briggs, 1997).

Fig. 169 - Immagine al SEM dei resti dei tessuti molli e del riempimento del tubo intestinale a livello del duodeno di *Scipionyx samniticus*. L'aspetto vacuolare dipenderebbe dalle cosiddette "microbial microfibrils" (*sensu* Wilby & Briggs, 1997).

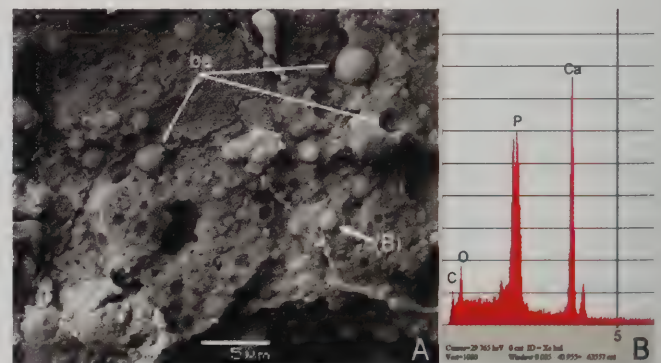


Fig. 170 - A) SEM image of a microsample of the rectum of *Scipionyx samniticus*. The analysed microspheres (B), which in the intestine of the Pietraraja dinosaur are very abundant (see also Figs. 143A-B; 144B; 149A; 169; 170A), could represent phosphatised bacteria. See Appendix 1 or cover flaps for abbreviations.

Fig. 170 - A) immagine al SEM di un microcampione del colon di *Scipionyx samniticus*. L'analisi delle microsferiche (B), che nell'intestino del dinosauro di Pietraraja sono molto abbondanti (vedi anche le Fig. 143A-B; 144B; 149A; 169; 170A), indicherebbe che si tratta di batteri fosfatizzati. Vedi Appendice 1 o risvolti di copertina per le abbreviazioni.

In between these two kinds of preservation is the “intermediate microfabric”, found where microbes are not mineralised and much of the subcellular details are lost. In this kind of preservation, the areas of tissue that survive may preserve cellular traits, but where larger microspheres precipitate, they preserve only the coarsest details. As an example of an intermediate microfabric, Wilby & Briggs (1997: figs. 5b, 6a-b) illustrate muscle fibres replaced by relatively coarse or large agglomerations of apatite crystals, similar in aspect to the muscle fibres we found in *Scipionyx* at the base of the neck. In that area, in fact, the individual myofibres can be resolved but the sarcomeres are more difficult to identify, as their banding is faint (Fig. 132A, C) or lost (Fig. 132D).

Summing up, although substrate-, intermediate- and microbial-microfabrics may occur rarely in the same fossil, from what we can see in *Scipionyx* it is possible that their gross distribution within the specimen reflects the rate at which microbes gained access to the subcutaneous tissues of the organism. This phenomenon was observed in other fossils by Wilby & Briggs (1997), who regarded it just like the tendency of specific microfabrics to be associated with particular taxa and indicating a taxonomic control that is likely to reflect the rate of permeability and resistance to decay of the integument of the different types of animals.

Diagenetic formations possibly related to soft tissues

Three calcite clusters embedded in the same plane of the fossil may be regarded as being related to the decay of the dinosaur carcass because of their proximity to the soft tissue remains, their shape and their consistency, which is definitely different from the surrounding, undisturbed matrix (Fig. 117). The clusters or nodules differ from any other fossil or sedimentary structure seen on the main slab in being homogeneously composed of calcite and in having a cryptocrystalline aspect (Fig. 171), a grey-whitish colour and a high compactness (Dal Sasso & Rampinelli, pers. obs., 1994-2009). The transition to the fine-grained, yellowish and softer micrite is abrupt, so that these nodules have well-delimited margins.

The largest calcite nodule was considered in previous studies (e.g., Ruben *et al.*, 1999; Hillenius & Chinsamy, 2004), and it is re-examined herein in a section devoted to respiratory physiology, because of its improbable bio-

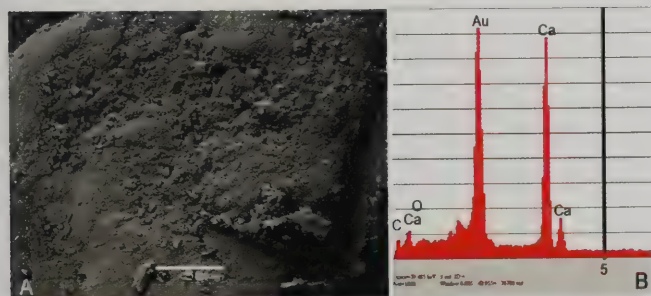


Fig. 171 - SEM image (A) and elemental spectrum (B) of the cranial-most nodule of calcite associated with *Scipionyx samniticus* (Figs. 117, 172). See Appendix 1 or cover flaps for abbreviations.

Fig. 171 - Immagine al SEM (A) e spettro degli elementi (B) del nodule di calcite più craniale associato a *Scipionyx samniticus* (Fig. 117, 172). Vedi Appendice 1 o risvolti di copertina per le abbreviazioni.

logical nature (therefore, we suppose it will become an object of future debate). This nodule, 22.5 mm long and 4.1 mm wide, lies obliquely in the caudal half of the abdomen of *Scipionyx*. Of all calcite nodules, it appears to be the deepest in cross section, and the one with the most irregular surface, being composed of a cluster of large, rounded granules, sub-spherical to drop-shaped and with an average diameter of 0.7 mm each. This original aspect is preserved all along the craniodorsal portion of the nodule, but is lost in its ventral third, which has been polished by preparation tools (Dal Sasso & Rampinelli, pers. obs., 1997; see also Diaphragmatic Muscles).

A second calcite cluster, less extended than the former (around 10.6 mm in diameter), is found between the right humerus and the right radius, and delimited caudally by the reddish halo derived from the blood-rich organs (Figs. 91, 172). This nodule seems quite thin, lying on the exposed bedding plane as an almost flat, roughly subtriangular area. It has a bumpy surface similar to that of the former nodule, but is composed of granules that are more irregular in shape, with an average diameter of 0.8 mm.

The third nodule, slightly more extended than the second one but less exposed because it is hidden by many bones, is visible ventral to and below the cranial dorsal vertebrae and ribs: it is delimited cranially by the scapulae, ventrally by the humeri, and caudally by the reddish macula (Figs. 91, 172). Given its proximity to the second nodule, and that it is covered by large bones and by the reddish macula, we cannot exclude that this nodule might represent a dorsal continuation of the second one. Because of its position, the third nodule has been polished in order to expose the bones (Dal Sasso & Rampinelli, pers. obs., 1997), so that today it displays a smooth surface.

There is a fourth calcite area, which is not properly shaped like a nodule, but is rather a vein that opens gradually between the right ceratobranchial I and the 9th cervical centrum, then runs caudoventrally with an oblique, slightly meandering course, widening to a width of 5.5 mm (Fig. 117). Along this 137 mm-long path, the vein crosses the first two dorsal centra, the neck muscle remains, the left scapular acromion, the right coracoid, the sediment and finally the right manus. The bones crossed by the calcite vein display some horizontal dislocation and vertical deformation (Fig. 172). This indicates that the vein formed early in diagenesis, prior to sediment compression and volume reduction. During this process of heavy compaction, the rigid behaviour of the calcite vein should have mechanically interfered in the nearest parts of the carcass, provoking deformation of the bone and soft-tissue edges where they were crossed by the vein, as both bones and soft tissues acted in a more plastic way. According to Pezzotta (pers. comm., 2009), the syndiagenetic nature of the calcite vein is revealed also by its sinuous, non-angular arrangement. In fact, this indicates that, when infiltration of the calcium carbonate-rich solution occurred, the sediment still had a partially plastic behaviour. Nevertheless, the shape of this vein and its distance from the dinosaur's body prevent us from inferring any relationship with any anatomical structure.

The nature of the three nodules described above is different. According to Pezzotta (pers. comm., 2009), the presence of nodules within the fossil and adjacent to it cannot be fortuitous. The exceptional fossilisation *in situ* of a variety of soft tissues with a chemical diversity in-



Fig. 172 - Oblique view under grazing light of the thorax of *Scipionyx samniticus*, showing the syndiagenetic calcite vein (red arrow; note the dislocated bones), the cranialmost nodule (black arrow), and the polished nodule (white arrow) that might represent a continuation of the latter.

Fig. 172 - Vista obliqua e in luce radente del torace di *Scipionyx samniticus*, che mostra la vena di calcite sindiagenetica (freccia rossa, notare le ossa dislocate), il nodulo in posizione più craniale (freccia nera) e il nodulo levigato (freccia bianca) che potrebbe rappresentare una continuazione dello stesso.

herited from authigenic organic components indicates that during diagenetic processes a rather low chemical mobility was maintained. Thus, as verified through recent observations of experimental taphonomy (Noto, 2009), the chemical diversity of the decomposing tissues would have perturbed and conditioned (in a sense, even polluted) the local fluid chemistry, which generally is as homogenous as a sedimentary layer devoid of inclusions, in the end catalysing the formation of aggregates. That this phenomenon occurred not only at the level of the dinosaur's soft tissues, but also in some areas of the sediment that directly contacted the carcass, is proven by the formation of calcite clusters both inside and outside the fossil of *Scipionyx*.

Likely, the formation of microcrystalline calcite aggregates began at an early diagenetic stage. A concentrated solution of calcite salts accumulated in and around some parts of the carcass because of the above-mentioned local chemical (and probably, textural) inhomogeneities. Parallel to bone and soft-tissue phosphatisation, calcite crystallisation took place in the pseudo-nodules. According to Pezzotta (pers. comm., 2009), chemical and structural inhomogeneities would have conditioned even the crystal texture. One may argue, for example, that the more globular texture of the nodule enclosed in the abdominal area depends on a locally stronger geochemical-structural disturbance. The collapse of the carcass remains and the progress of diagenesis then further deformed and squeezed bone, soft tissue and calcite clusters against each other, rendering them almost flat. Consequently, the calcite precipitation was syndiagenetic.

The calcite of the nodules does not replicate any organic remains; however, on the terms we set out above, it can be related to their presence and, in some cases, po-

sition. For instance, there is reason to suppose that the formation of the nodule cranial to the liver remnants was promoted by the decay of the relevant amount of cartilage composing the sternal plates. Sedimentary nodules are sometimes found to wrap around fossil tetrapod girdles. A well-documented example in the field (Arduini, 1993) is represented by procolophonian parareptiles from Ranohira (SW Madagascar). In that locality, a layer of Upper Permian laminated shales contains dozens of cfr. *Barasaurus* skeletons, that are fully articulated but preserved partly in the layer and partly in nodules. To be more precise, the pectoral girdle and the pelvic girdle of the same specimen are included in two distinct nodules lying side-by-side, with the rest of the skeleton lying in a stratum medial to the nodules' depth. This is *in situ* evidence that the formation of nodules is topographically related to girdle cartilages, the decay of which possibly produced denaturation of chondroitin-4-sulphate, keratan sulphate and hyaluronic acid, setting free groups with a negative valency. The latter would have catalysed agglutination of positive ions within the interstitial water that concentrated around carcasses in the form of nodules during early stages of decay.

The nodules present in the cranialmost portion and in the abdominal portion of the trunk of *Scipionyx* are suggestive of the presence of anatomical virtual spaces, such as lungs, airsacs and yolksacs. However, in the absence of any evidence of anatomical structures in those areas, this idea remains a pure speculation. In fact, as seen for the largest calcite nodule (see Diaphragmatic Muscles), SEM imaging documents that at the ultrastructural level the minor calcite nodules do not replicate soft tissue or any other anatomical structure (Fig. 171A).

PART III - FUNCTIONAL MORPHOLOGY AND PALAEOBIOLOGY

SKELETAL RECONSTRUCTION AND *IN VIVO* RESTORATIONS OF *SCIPIONYX SAMNITICUS*

Although the delicate skeleton of *Scipionyx* was subjected to diagenetic crushing, it has remained beautifully preserved and quite well-articulated (see Skeletal Taphonomy). The presence of unfused skeletal elements, consequent to the early ontogenetic stage of the individual, favoured movement and rotation of the bones, preserving their original shape and limiting the degree of deformation, as not yet tightly fused elements tend to move with respect to one another and to lose contact with the surrounding bones rather than undergo deformation. We re-articulated the disarticulated elements, correcting both diagenetic crushing and the slight distortion suffered by the skeleton, in order to generate the skeletal reconstructions presented herein (Fig. 173). In this section, we will list these corrections and point out the problems encountered during the reconstructions. The unpreserved characters (osteological or otherwise) represented herein were inferred following the methodology proposed by Bryant & Russell (1992), i.e., based on the cladistic distribution of known features in related taxa (primarily the Compsognathidae), when necessary choosing among equivocal or different phylogenetic inferences on the basis of form-function correlation and ecological affinities among the taxa.

Cranial reconstruction - A 3D version of the skull was first reconstructed from thin cardboard on the basis of the (2D) anatomical plates (Figs. 34, 174, 175). The model, scaled 4:1, helped us to verify the interpretation of a number of features.

The skull of *Scipionyx* is almost undisturbed in lateral view. The most relevant corrections were made at the level of the frontoparietal suture and quadrate-quadratojugal

contact. Concerning the former, the rostral margin of the parietal and the caudal margin of the frontal, diverging laterally in the fossil, were realigned, giving a uniform curvature to the cranial vault. The outline we obtained resembles that of the ornithomimosaur *Garudimimus*, which is preserved three-dimensionally (Kobayashi & Barsbold, 2005). The realignment of the parietal and of the frontal also favoured a slight anticlockwise rotation of the postorbital region of the skull, which helped to restore the original contact between the quadrate and the quadratojugal, as clearly indicated by the presence of the quadratojugal facet on the lateral surface of the former (see Quadrate).

The diameter of the scleral rings was reconstructed on the basis of the left one, which is more complete. The estimated minimum number of 16 plates was taken as good for the reconstruction (see Scleral Plates).

As for most theropods, the nasals, prefrontals and frontals of *Scipionyx* must have been partly exposed in both lateral and dorsal views. In particular, as mentioned in the description, the prefrontal of *Scipionyx* is rather large, and it probably formed, together with the lacrimal, a lateral triangular projection in dorsal view. In this view, it is difficult to understand whether a parietal process of the postorbital contacting the parietal was present or not: as the preserved parietal does not show an unequivocal contact surface or process for the parietal, the parietal process of the postorbital was not reconstructed here.

As mentioned above, the ventralmost tip of the pterygoid-ectopterygoid contact, formed by the ventral projections of the caudomedial arm of the ectopterygoid and the ventral bar of the pterygoid, projected from the roof of the mouth and served to maintain the alignment of the mandible.

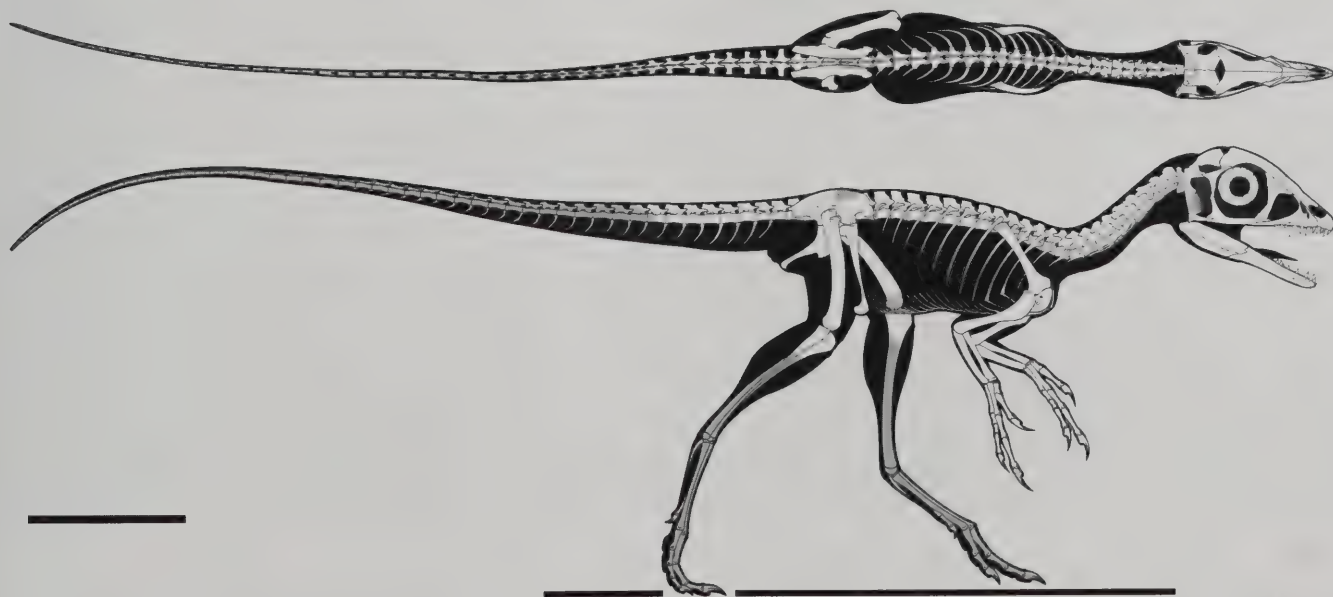


Fig. 173 - Reconstruction of the skeleton of *Scipionyx samniticus* in dorsal and lateral view. Missing bones in light gray. Scale bar = 5 cm.
Fig. 173 - Ricostruzione dello scheletro di *Scipionyx samniticus* in norma dorsale e laterale. In grigio chiaro le ossa mancanti. Scala metrica = 5 cm.

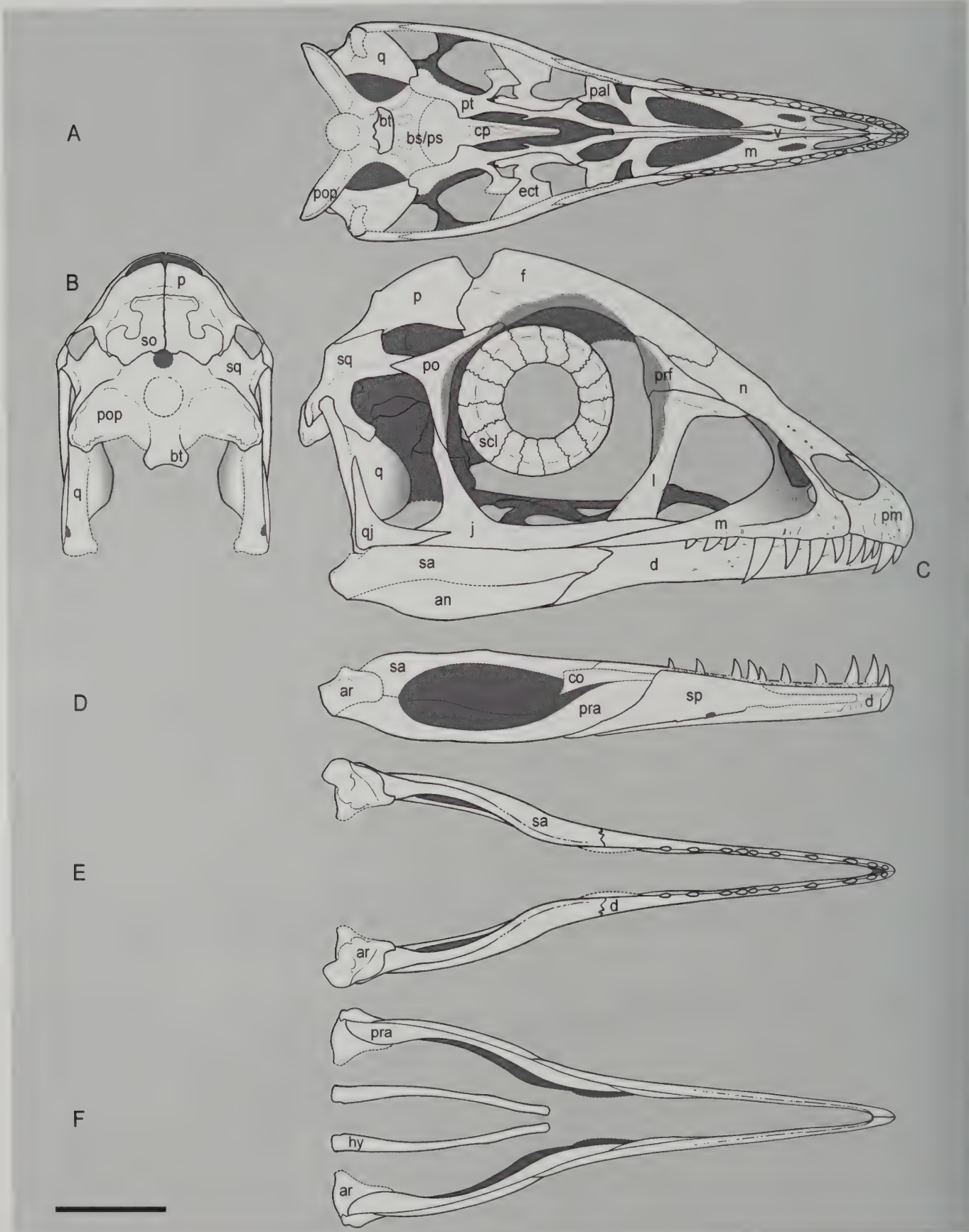


Fig. 174 - Cranial reconstructions of *Scipionyx samniticus* (line drawings). A) skull in ventral (palatal) view; B) skull in caudal (occipital) view; C) articulated skull and mandible with closed jaws in right lateral view; D) left hemimandible in medial view; E) mandible in dorsal view; F) mandible in ventral view. Scale bar = 10 mm. See Appendix 1 or cover flaps for abbreviations.

Fig. 174 - Ricostruzioni del cranio di *Scipionyx samniticus* (disegni al tratto). A) cranio in norma caudale (occipitale); B) cranio in norma ventrale (palatale); C) cranio e mandibola articolati, con bocca chiusa, in norma laterale destra; D) emimandibola sinistra in norma mediale; E) mandibola in norma dorsale; F) mandibola in norma ventrale. Scala metrica = 10 mm. Vedi Appendice 1 o risvolti di copertina per le abbreviazioni.



Fig. 175 - Cranial reconstructions of *Scipionyx samniticus* (shaded drawings). A) articulated skull and mandible in dorsal view; B) articulated skull and mandible with open jaws in right lateral view; C) articulated skull and mandible with closed jaws in left rostradorsolateral view. Scale bar = 10 mm.

Fig. 175 - Ricostruzioni del cranio di *Scipionyx samniticus* (disegni ombreggiati). A) cranio e mandibola articolati, in norma dorsale; B) cranio e mandibola articolati con bocca aperta, in norma laterale destra; C) cranio e mandibola articolati con bocca chiusa, in norma rostradorsolaterale sinistra. Scala metrica = 10 mm.

With closed jaws, the upper dentition was visible in lateral view and passed labially to the lower one, which accommodates medially to the medial walls of the upper tooth-bearing bones, as occurs in toothed theropods (e.g., Weishampel *et al.*, 2004).

In ventral view, the outlines of the jugals and maxillae match both the reconstructed width of the palate based on overall size of palatal bones (primarily palatines and ectopterygoids) and the outline and position of the dorsal skull roof and of the elements of the lateral sides of the skull. As in many theropods, the palatines assumed a steep position in our 3D model, the vomeral processes becoming visible in lateral view through the antorbital fenestra and probably forming a vaulted palate.

The mandibular symphysis in ventral view was reconstructed U-shaped, as suggested by the rostral bending of the left dentary (see Dentary, Skeletal Taphonomy). The retroarticular process, which is shorter than in *Sinosauropteryx* (Currie & Chen, 2001) and *Compsognathus* (Peyer, 2006), was reconstructed bulkier, too, to match the preserved outline of the other post-dentary bones. Finally, the reconstructed skull was articulated to the neck in order to have the upper tooth row on the horizontal plane (i.e., slightly flexed), a position useful to show its full dorsal aspect also in the dorsal view of the whole animal.

Axial skeleton - The neck of *Scipionyx* was reconstructed by articulating the vertebrae with the centra in maximum contact. This resulted in a dorsally deflected base of the neck, an almost vertical mid-cervical region and a slightly ventrally deflected cranial region (Fig. 173). This posture represents the typical sigmoidal curvature visible in the reconstructed neck of many theropods (e.g., Paul, 1988), which is based on the offset cranial and caudal surfaces of the cervical centra. It represents neither the so called “osteological neutral pose”, as some of the vertebrae are not articulated in maximum contact with the zygapophyses, nor the usual orientation *in vivo* of extant amniotes, which usually hold their neck more extended and their head more flexed (Taylor *et al.*, 2009, and reference therein). Also, the reader must bear in mind that in this reconstruction we obviously did not try to restore the unpreserved intervertebral cartilages, which, according to observations on extant animals, enable greater flexibility in the neck than the bones alone suggest (Taylor *et al.*, 2009, and reference therein). However, some osteological evidence does give an idea of the mobility of the neck of *Scipionyx*. In cranial and mid-cervical neural arches, the ventral bending of the rostral half of the convex articular surfaces of the prezygapophyses probably permitted great mobility (in particular flexibility) of the neck, which could have been well-deflected ventrally when the animal drank and explored the ground.

Concerning the dorsal vertebrae, no adjustments were required, except for articulating the disarticulated centra and their respective neural arches.

As already mentioned, the preserved curvature of the shafts of the ribs permitted reconstruction of the shape of the trunk in both dorsal and lateral views. The cranial dorsal ribs have an almost straight mid-

dle tract, indicating a relatively narrow and laterally flattened thoracic region; the caudal dorsal ribs are evenly curved all along their shafts and, thus, delimit an abdominal region more evenly rounded in coronal section than the thoracic one.

The well-preserved gastralia mark the ventral border of the abdominal cavity, which is exactly aligned with the distal margin of the pubis. Thus, the rib cage and the gastralia give a reliable idea of the volume of the body cavity. According to Claessens (2004), this cavity could have been partly enlarged or restricted by the musculature associated with the articulated gastralia, obtaining a function analogous to the diaphragm of the Mammalia (see Gastralia, Respiratory Physiology). The feasibility of these movements in *Scipionyx* is supported by the morphology of the articular surfaces of the medial gastralia, with the sliding surface of the mvf articulating with the mdf of the successive, counterlateral element (Fig. 85). A cartilaginous sternum was also reconstructed, and articulated to the ribs via the cup-like distal ends of the 3rd and 4th dorsal ribs.

Based on the most complete theropod fossils, the tail of *Scipionyx* would have been definitely longer than the presacral region, independent of the ontogenetic stage of the animal (e.g., Kobayashi & Lü, 2003). Moreover, compsognathids are among the longest-tailed theropods: *Sinosauropteryx* has the longest tail, with an estimated number of 64 caudal vertebrae (59 of which are preserved), which is almost twice as long as the presacral region, skull included (Currie & Chen, 2001). We reconstructed the tail of *Scipionyx* with 51 vertebrae, a number close to that (i.e., 49) found in the complete tail of *Sinocallopteryx* (Ji *et al.*, 2007a). Given that the vertebral centra of *Huaxiagnathus* and *Compsognathus* increase in length along the tail up to the distalmost portion, where they start to decrease (Hwang *et al.*, 2004; Peyer, 2006), and that the length of the centra in *Sinosauropteryx* increase only up to the 6th caudal, then steadily decrease (Currie & Chen 2001), we decided to reconstruct the tail of *Scipionyx* maintaining an average length all along the series, with the exception of a decreasing distalmost portion.

Pectoral girdle and forelimb - The coracoids of *Scipionyx* were reconstructed as being closely appressed. Their position can be inferred not only from the taphonomical condition of the specimen (they are found appressed one to the other), but also by articulating the epicleideum of the furcula with the acromion of the scapula. A comparable reconstruction was obtained for *Coelophysis* by Rinehart *et al.* (2007: fig. 3), who demonstrated that the whole furcula closely conforms to the cranial margin of the coracoids. The finding of *Tyrannosaurus* furculae (Larson & Rigby, 2005), together with observations made on other tyrannosaurids (Makovicky & Currie, 1998) and on articulated skeletons of other theropods (Barsbold, 1983; Chure & Madsen, 1996), confirm that the furcula could have articulated with the acromion processes of the scapulae only if the coracoids almost touched along the midline.

The thin distal end of the scapula, which is not completely preserved, was reconstructed as slightly expand-

ed and squared, like in other compsognathids (e.g., Ji *et al.*, 2007a: fig. 1). As the manus of *Scipionyx* could not fold against the forearm in avian fashion on account of the absence of a semilunate carpal (Carpenter, 2002), the angle between forearm and manus was maintained as it is in the fossil. The 1st digit was reconstructed as diverging from the 2nd and 3rd ones, according to the asymmetrical condyles and its position of preservation, the left manus of the fossil showing a mirror-like position of all the three bones composing digit I with respect to digits II and III. The pollex looks like it would have diverged from the second digit during flexion, as is the case in most other theropods, instead of converging (i.e., being in opposition). Divergence would have increased the spread of the fingers, permitting *Scipionyx* to hold larger objects (Gishlick, pers. comm., 2000; Senter, pers. comm., 2007). The suggestion of Currie & Chen (2001) that penultimate phalanges that are longer than the antepenultimate, together with deep, moderately curved unguals that taper to sharp points, might indicate that the hand was adapted for grasping, can be applied also to *Scipionyx*.

Pelvic girdle and hindlimb - After re-articulating and realigning the vertebrae, the ilium, which is fossilised in a slightly anticlockwise-rotated (about 6°) position, was realigned in turn. The angle between the pubis and the ischium resulted slightly increased, from 45° to 60°, after we re-articulated the former to the ilium, according to the shape of their peduncles of contact (Fig. 173).

The difference in size between Sr4 and Sr5, with the latter larger than the former, likely indicates that in *Scipionyx*, as well as in many theropods, the iliac blades diverged at both cranial and caudal ends when seen in dorsal/ventral views, increasing their distance from the vertebral centra.

Only the proximal portions of the tibiae and fibulae of *Scipionyx* are preserved, so the length of the rest of the hindlimbs can only be estimated. Varricchio *et al.* (2002) reported a significant negative allometry of the distal hindlimb segments during growth in the advanced maniraptoran *Troodon*, indicative of longer-limbed hatchlings and juveniles. Tibiae and fibulae are longer than femora in juvenile tyrannosaurids, but the opposite occurs in *Sinornithomimus* (Kobayashi & Lü, 2003). Only few data are available for compsognathids. In *Sinosauropteryx*, the femur/tibia ratio is 87% in the younger and smaller individual NIGP 127586, and 89% in NIGP 127587 (Currie & Chen, 2001). In the French *Compsognathus* the femur/tibia ratio is about 83% (Peyer, 2006); in the German specimen, that ratio is reported to be 76% (Hwang *et al.*, 2004), although this individual is ontogenetically younger than the French one. The femur/tibia ratio is about 90% in *Juravenator*, *Huaxiagnathus* and *Sinocallopteryx*. As there are no fossils of adult *Scipionyx*, and as the femur/tibia ratio is fairly conservative within the Compsognathidae, with a slight increase during ontogeny in those species represented by more than one individual, we tentatively adopted the lowest value recorded for compsognathids (i.e., 76%, in the range of 76-90%) when reconstructing the hindlimb of *Scipionyx*, taking into account that our specimen is an

early hatchling. Based on a similar reasoning, as the range of metatarsus / femur ratios is 67-76% within the Compsognathidae (e.g., Hwang *et al.*, 2004), we adopted the highest value for the metatarsus of *Scipionyx*.

Body length and body mass - According to our reconstruction, the approximate total length of this specimen of *Scipionyx* did not exceed 50 cm. *Contra* Martill *et al.* (2000), the *Scipionyx* fossil is still fairly three-dimensional despite the compression it sustained. After having re-articulated its elements and corrected for the deformation, the pelvis of *Scipionyx* results comparatively slightly narrower mediolaterally than that of *Mirischia*, the three-dimensionally preserved pelvis of which has a width approximately 30 mm wide across the sacrum. The outline of *Scipionyx*'s body (solid black in Fig. 173) has been drawn on the basis of the usual distribution and attachment of the main muscular masses in theropods (e.g., Paul, 1988), adjusting for the size and shape of the bones of *Scipionyx*, and for the bulk of the yolk sac in hatchlings of extant archosaurs (Dal Sasso & Maganuco, pers. obs., 2011). The opening of the cloaca has been placed in proximity to the ischial feet, further ventral to the position in which the preserved faecal pellet is fossilised. If the position of the faecal pellet was considered indicative of the location of the cloaca instead of that of the rectocoprodaeal valve, it would have implied a base of the tail that was not thick enough dorsoventrally, i.e., not consistent with the position of the *M. ilio-ischiocaudalis* and *M. caudofemoralis longus* in *Scipionyx* and in other theropods (see Pelvic And Hindlimb Muscles). A restoration of the whole musculature was not attempted because this is made extremely difficult to carry out by the early ontogenetic stage of the specimen and the consequent lack of clearly visible muscular scars and ligament attachments, which usually develop later during archosaurian ontogeny (e.g., Brochu, 1996). However, comparison with usual body proportions of small extinct and extant coelurosaurs, including birds, permitted us to tentatively estimate a weight in life of no more than 0.2 kg.

Integument - Over the last two decades, several specimens originating from China have provided direct fossil evidence that the body of basal coelurosaurs was extensively covered with "protofeathers" (e.g., Currie & Chen, 2001; Xu *et al.*, 2004; Xu *et al.*, 2006; Ji *et al.*, 2007a, 2007b). Unfortunately, the integument of *Scipionyx* was not preserved (see Description, Ilio-ischiocaudal Muscle Septa). However, based on the results of our phylogenetic analysis, we think that *Scipionyx* would have been protofeathered as well. The pattern of distribution of the protofeathers on the body of compsognathids is not yet clear: for example, the mid part of the tail of *Juravenator* shows a scaly integument composed of small conical and non-imbricated tubercles (Göhlich & Chiappe, 2006). According to these data, all but one of the palaeoartistic restorations presented in the end pages of this monograph incorporate, to various degrees, a proto-feathered coverage for *Scipionyx*.

GUT CONTENTS AND FEEDING CHRONOLOGY

As mentioned beforehand, a variety of allogenous organic remains is found along the path of the digestive tube of *Scipionyx*. Given their intimate relationship with the fossil of the little theropod, these remains can undoubtedly be referred to ingested food items (Fig. 176, see also Fig. 117). Among the osseous remains, the largest are preserved in the stomach region; smaller bones are contained in various portions of the intestinal tract. In this section, we deal also with integumentary remains that are found in the duodenum and in the rectum. Our description follows a craniocaudal direction, which in chronological terms (intake sequence) means from the last meal to the first.

Oesophageal contents

At the level of the right scapular acromion, dorsal to the tracheal tube and somewhat parallel to it, runs a small and elongated cluster of tiny yellowish, flat, sometimes angular, shiny elements (Figs. 135, 177). Their highly reflective surfaces are consistent with smooth integumentary structures, such as tiny reptilian squamae or fish scales. In addition, other very small single elements, which based on their brown colour can be interpreted as bones, are present. At least one of them has an arched shape and may represent a rib or a haemal arch. Given that oesophageal peristalsis is relatively fast (a matter of some seconds), it is statistically improbable that *Scipionyx* would have swallowed food just before its death. The most likely explanations for food being found in the oesophagus would be (agonal) regurgitation during death or the consequence of the relaxation of the gastric sphincters after death – these dynamics are consistent with clinical observations in modern birds

(Huchzermeyer, pers. comm., 2010). The mixture of the oesophageal contents and the high degree of fragmentation support such an interpretation.

Worthy of note is that some scales/squamae along the residual line of the oesophagus display a blackish pigmentation, just like the squamae preserved in the intestine. A similar pigmentation occurs also on the tips of the horny claws of *Scipionyx* and, thus, leads to suspect some sort of correlation in the mode or state of preservation: in other words, it is possible that similar colours reflect analogous chemical compositions (Schweitzer, pers. comm., 1998). To the best of our knowledge, all integumentary derivatives of extant terrestrial vertebrates are made of keratin. As stated above, we do not possess any chemical analysis from any portion of the *Scipionyx* fossil, but this subject would merit deeper examination. In the holotype of *Sino-sauropteryx*, for instance, the integumentary tufts covering the back and the tail are also dark, and very recently they were found to contain fossilised melanosomes, just like the feathers of birds (Zhang *et al.*, 2010).

Gastric contents

A cluster of tiny bones, mostly hidden by the cranial portion of the duodenum, is visible in the middle of the thorax of *Scipionyx* (Figs. 176, 178A-B). Because they look like the ribs of *Scipionyx* in gross position, colour and diameter, at first glance most of these elements might be reasonably referred to the dinosaur's skeleton. However, careful examination finds these tiny bones to be supernumerary and out of specific position with respect to the dinosaur's ribs; under the light microscope, more importantly, they appear rather more complexly shaped than the rod-like bone shafts of the ribs. Most likely, this clus-

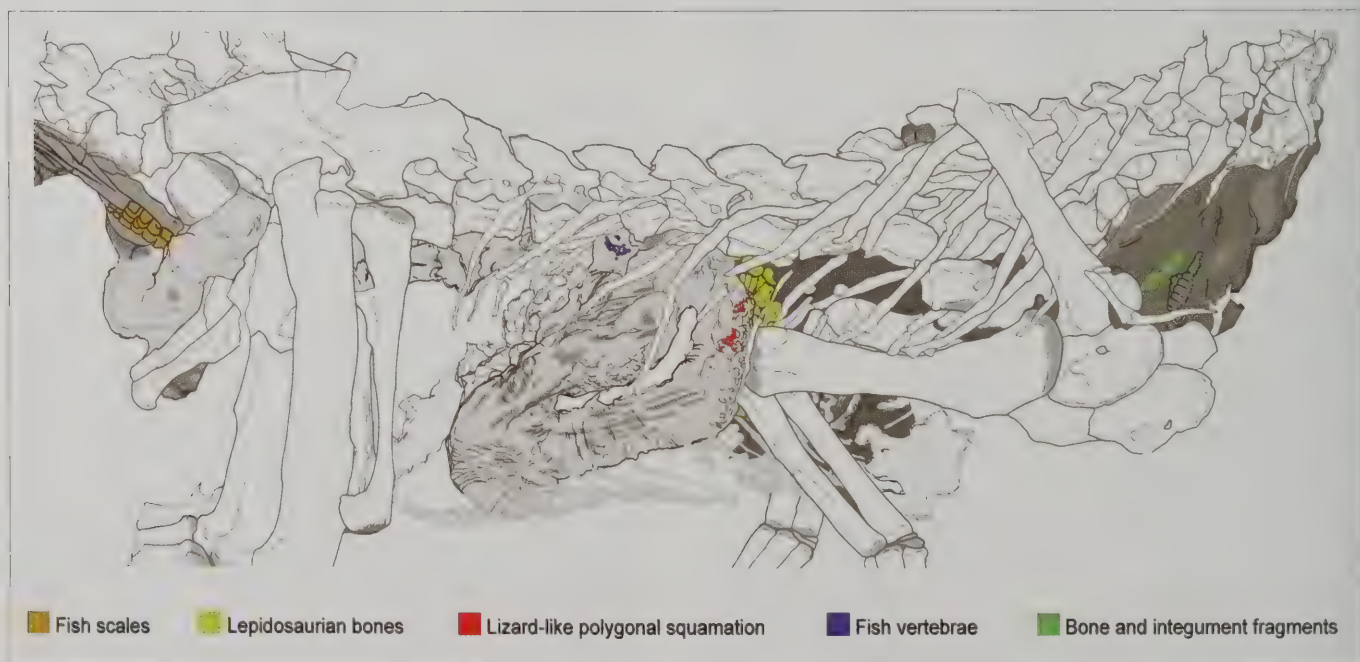


Fig. 176 - Map showing the distribution of the gut contents of *Scipionyx samniticus*.

Fig. 176 - Mappa della distribuzione del contenuto dei visceri di *Scipionyx samniticus*.



Fig. 177 - Oesophageal contents of *Scipionyx samniticus*: close-up of some fragmented scaly/squamous elements (arrows). Scale bar = 0.5 mm.

Fig. 177 - Contenuto esofageo di *Scipionyx samniticus*: particolare di alcuni elementi scagliosi/squamosi frantumati (freccie). Scala metrica = 0,5 mm.

ter of "extra" bones belongs to swallowed prey. In fact, as stated above, the position of the cluster is immediately cranial to, and left of, the duodenum of *Scipionyx*, consistent with the position likely occupied by the dinosaur's stomach within the thoracoabdominal cavity.

Description - Four rod-like bones display side-by-side aligned articular surfaces, with subrectangular blunt-ended shapes. These are appressed to each other, just like metapodial elements of most terrestrial reptiles. We regard these articular surfaces as proximal, given that they face tiny rounded bones reminiscent of mesopodials; moreover, these probable metapodials are more consistent in form, position and proportion with tarsals than with carpals. Therefore, we interpret mesopodium and metapodium as belonging to a still-articulated ankle and pes, with a mediolateral width less than 3 mm.

In particular, we interpret the first three metapodial elements, numbering them from the right 7th dorsal rib of *Scipionyx*, as being metatarsals I, II and III. All of their straight diaphyses disappear under the duodenum, towards the centre of *Scipionyx*'s abdomen. Metatarsal IV diverges slightly from the first three metatarsals, heading towards the right humerus of *Scipionyx*; also, metatarsal IV is the only one that, after passing under a larger bone, reappears to expose its distal end. This seems to possess a ginglymoid distal articulation, exposed in ventral view, which would indicate that the whole ankle and pes are exposed in this aspect and that they are right-side elements. A small bone portion emerges in front of the distal articulation of metatarsal IV, and might belong to a still-articulated phalanx 1 of digit IV. Proximal to metatarsal IV, and seemingly in articulation with the possible distal tarsal 4, is a reniform bone, even more divergent than metatarsal IV, which tapers distally to an oblique truncation. Its surface texture is similar to that of metatarsals I-IV. This element might be an incomplete metatarsal V. This is also supported by its peculiar shape and divergent position, which are consistent with the ankle arrangement of many lepidosaurian reptiles (e.g., Carroll, 1977: fig. 12; Cocude-Michel, 1963: figs. 4B, 21, 39C, 40C).

As the mesopodium is partially covered by the ribs of *Scipionyx*, the exact number of its elements cannot be counted. However, we tentatively identify the triangular portion exposed in between the centrum of the 8th dorsal vertebra and the 7th right dorsal rib of *Scipionyx* as a visible portion of an astragalus or tibia; the tiny bone lying across the proximal end of metatarsals II and III as a distal tarsal 3; the reniform portion of bone appressed to the proximal end of metatarsal IV as a distal tarsal 4 or as the proximal articulation of a metatarsal IV; and the bone area including the relatively large, flat, semicircular element overlapped by the 7th right dorsal rib of *Scipionyx* and surrounded by metatarsal V and distal tarsals 3 and 4 as a calcaneum plus at least one more tarsal.

The bone overlying the diaphysis of metatarsal IV is characterised by the following morphology: a voluminous cylindrical body, grooved by a shallow triangular depression; a hemispherical condylar end; a flattened portion, arising from the central body towards the metatarsals and inclined towards the condylar end; and a markedly concave margin, opposite to the flattened portion, facing the 6th right dorsal rib of *Scipionyx*. We regard this element as a centrum and part of the neural arch of a procoelous vertebra in left lateral view. In particular, the lack of transverse processes, as well as its general morphology, is compatible with a caudal vertebra just distal to the last ones bearing transverse processes. The centrum has no trace of an autotomic septum.

Another allogenous element is present between the shafts of the 6th right and 7th left dorsal ribs of *Scipionyx*, paralleling them and continuing under the right humerus of *Scipionyx*. This long bone has a side with a shallow fossa, elongated towards the midshaft, and a feebly concave, asymmetric articular end facing obliquely towards the same side. Thus, this bone might represent the proximal half of an ulna, with an exposed articular surface for the radius and a well-developed olecranon or, alternatively, the distal portion of a fibula, with an exposed articular surface for the tarsus.

Lastly, ventral to the right elbow of *Scipionyx*, in the corner between the cranial loop of the duodenum and

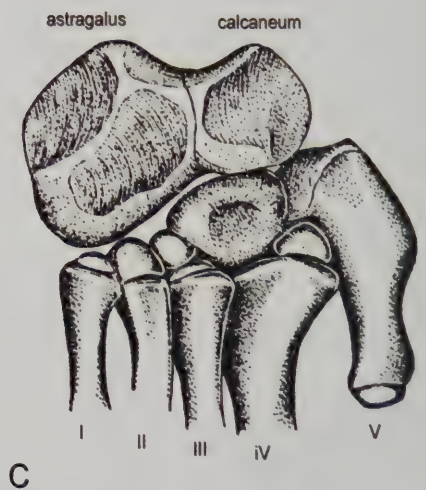
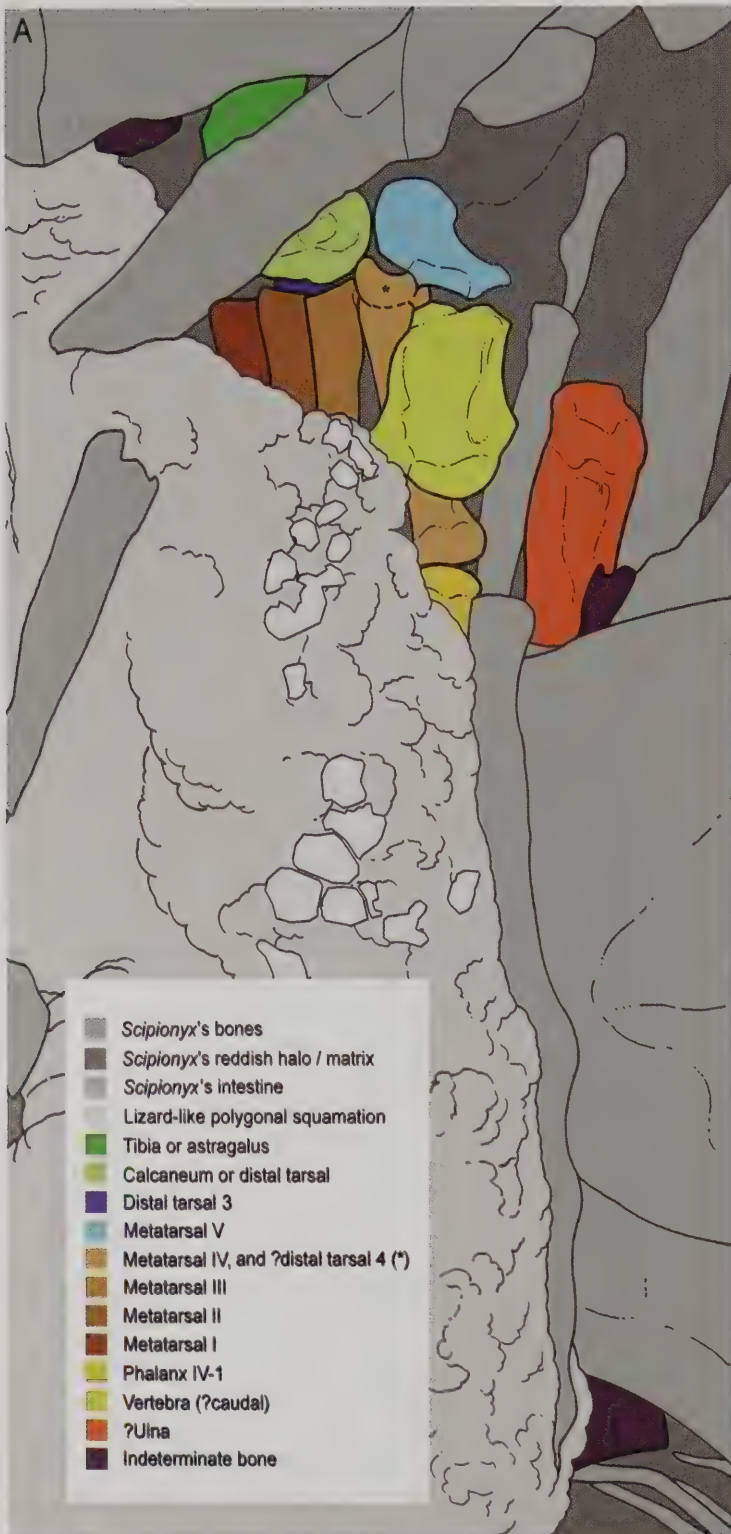


Fig. 178 - Stomach contents of *Scipionyx samniticus*. A) line drawing of all exposed allogenous bones; B) close-up of the main cluster of bones; C) comparison with the ankle of *Iguana* (after Carroll, 1977). For further comparison, see also *Deramosaurus* (Fig. 15). Scale bar = 1 mm.

Fig. 178 - Contenuto stomacale di *Scipionyx samniticus*. A) disegno al tratto di tutte le ossa allogene esposte; B) particolare dell'agglomerato di ossa principale; C) confronto con la caviglia di *Iguana* (da Carroll, 1977). Per confronti ulteriori, vedi anche *Deramosaurus* (Fig. 15). Scala metrica = 1 mm.

the right ulna of the dinosaur, is a triangular bone patch that, despite its small size, does not have anything to do with the thin, delicate gastralia nearby. Given the completeness of *Scipionyx's* forelimbs, this bone cannot possibly belong to the dinosaur. Although it is rela-

tively far from the main cluster of allogenous bones, this element is found in the middle of the dinosaur's abdomen, at the same level as the gastric contents and in a position where the long bones of the swallowed pes are pointing.

Taxonomic affinities - Several genera of reptiles coeval with *Scipionyx* are known at Pietraraja. Unfortunately, these taxa are represented by specimens that are badly or poorly preserved in the skeletal elements homologous to the bones swallowed by the dinosaur. Therefore, we extended our comparison to include related forms from other localities.

Regarding the single vertebra, the combination of a procoelous condition and the lack of an autotomic septum in a caudal element, which is also devoid of a transverse process, prevents us from ascribing it to Rhynchocephalia (e.g., *Derasmosaurus*). Such a vertebra might, on the other hand, be referred to Mesoeucrocodylia (Pol & Norell, 2004), a clade of crocodylians which includes some taxa with procoelous vertebral centra, such as *Araripesuchus* and *Crocodylia*. Actually, in comparison with the vertebra swallowed by *Scipionyx*, an indeterminate mesoeucrocodylian from the Late Cretaceous of Madagascar (MSNM V5632) presents with a condyle which is less pronounced and, more importantly, with a diameter definitely less than that of its own centrum; in addition, its ventral margin is not concave but straight due to the presence of two carinae (Dal Sasso & Maganuco, pers. obs., 2008). Furthermore, if the prey of *Scipionyx* was a crocodylian, the very small size of its vertebra would force our attribution to a rather tiny individual, i.e. a hatchling; unfortunately, the vertebra does not show any neurocentral suture. Most likely, this vertebra belongs to a small squamate lepidosaur which lacked autotomic ability in the tail. This condition is variably distributed, even at the generic level. Among extant taxa, procoelous vertebrae are common in all Squamata except Gekkonidae (Estes *et al.*, 1988; Gauthier *et al.*, 1988). Among basal forms and all forms that cannot be ascribed to living taxa, lack of procoelous vertebrae is reported in *Bavarisaurus*, *Huehucuetzpalli* and *Scandensia*, and in at least two genera sympatric with *Scipionyx*: *Costasaurus* and *Eichstaettisaurus* (Evans *et al.*, 2004). Among the squamates from Pietraraja, only *Chometokadmon* would be a possible candidate, but this character cannot be checked in the type specimen MNP 539 (Dal Sasso & Maganuco, pers. obs., 2008). Among exotic taxa, vertebral procoely is found in *Ardeosaurus* and *Hoyalacerta* as well as in paramacellodids (Evans *et al.*, 2004).

As for the hindlimb bones, the ankle with a non-vestigial metatarsal V would exclude the most advanced Crocodyliformes (e.g., Romer, 1966; Carroll, 1988), including the Pietraraja taxon (Dal Sasso & Maganuco, pers. obs., 2008 on SBA-SA 207240); it is, however, consistent with the Lepidosauria (e.g., Cocude-Michel, 1963). Unfortunately, given the limited exposition of the tiny foot, the potential for further comparison is limited and does not allow taxonomic attribution to a lower hierarchical level. For example, we can tell that metatarsals I and IV seem slightly more robust than metatarsals II and III, so that with respect to this character the ankle swallowed by *Scipionyx* resembles a specimen (MPN A01/82) tentatively ascribed to Rhynchocephalia by Evans *et al.* (2004). On the other hand, we cannot ascertain if like the squamate *Chometokadmon* and unlike the rhynchocephalian *Derasmosaurus* (Dal Sasso & Maganuco, pers. obs., 2008 on MPN 539 e MPN 541) the prey of *Scipionyx* had very elongate metatarsals and phalanges, similar to those of extant lizards.

In conclusion, based on verified morphological affinities we cannot refer all the bones preserved in the stomach of *Scipionyx* to the same taxon with certainty. However, we suggest that they belong to a single individual (and, consequently, to a single taxon) because they are clustered together, like in a single meal, and because the shape and size of the vertebra and the possible ulna/fibula are compatible with the size of the ankle (Cocude-Michel, 1963; Dal Sasso & Maganuco, pers. obs., 2010 on MSNM specimens of extant and extinct diapsid skeletons).

Intestinal contents

Following the winding tangle of the intestinal tube, continuous changes are observed in the aspect of its surface, which goes from smooth to bumpy and from opaque to shiny. Most textural inhomogeneities are likely due to ingested solid food, but where food is deeply embedded, it is impossible to determine its nature. However, remains surface in at least five points of the intestine (Figs. 176, 179, 180) and, thus, some preparation was possible without damaging the intestine itself. Below we describe these contents.

Two adjacent clusters of solid organic remains crop out along the cranialmost side of the descending loop of the duodenum (Figs. 178A, 179A-B). Both are well-preserved and composed of several shiny, polygonal-to-roundish elements, still partly connected and seemingly arranged in non-imbricate contact. This pattern is consistent with the integumentary squamation seen in certain body regions of both extant and fossil Lepidosauria (e.g., Caldwell & Dal Sasso, 2004), so we are confident in referring these remains to a closely related, if not the same, taxon. In several elements of the dorsalmost cluster, the individual edges are blackish in colour (Fig. 179B). As explained above, this is reminiscent of fossilised integumentary structures possibly having a keratinous composition.

A third, apparently allogenous, element surfacing along the descending loop of the duodenum is embedded in a thin layer of longitudinal musculature, about 7 mm caudally to the right elbow of *Scipionyx* (Fig. 179D). It is a single tiny bone, coloured dark brown like the bones of *Scipionyx*. Given its symmetric, asterisk-like shape, we regard it as a fish vertebra in dorsal view. In fact, this is the common aspect of single vertebrae of several bony fish, which are frequently found scattered in many layers of the Pietraraja Plattenkalk.

A fourth area of ingested remains is positioned in the jejunum, adjacent to the cranial face of the 11th dorsal centrum (Fig. 179C). Here, a rounded, 3 mm-diameter cluster of dozens of small cylindrical elements, seemingly devoid of pronounced apophyses, can be seen partial sealed in the intestinal wall: these are likely vertebral centra of a very small fish (see Palaeobiological Significance Of The Gut Contents of *Scipionyx*).

Two even smaller roundish fragments surface along the straight tract of the intestine (jejunum-?ileum), ventral to the centrum of the 1st sacral vertebra (Fig. 179E). These are brown coloured, like all other fossil bones; they are possibly very incomplete vertebrae, but their origin is impossible to determine.

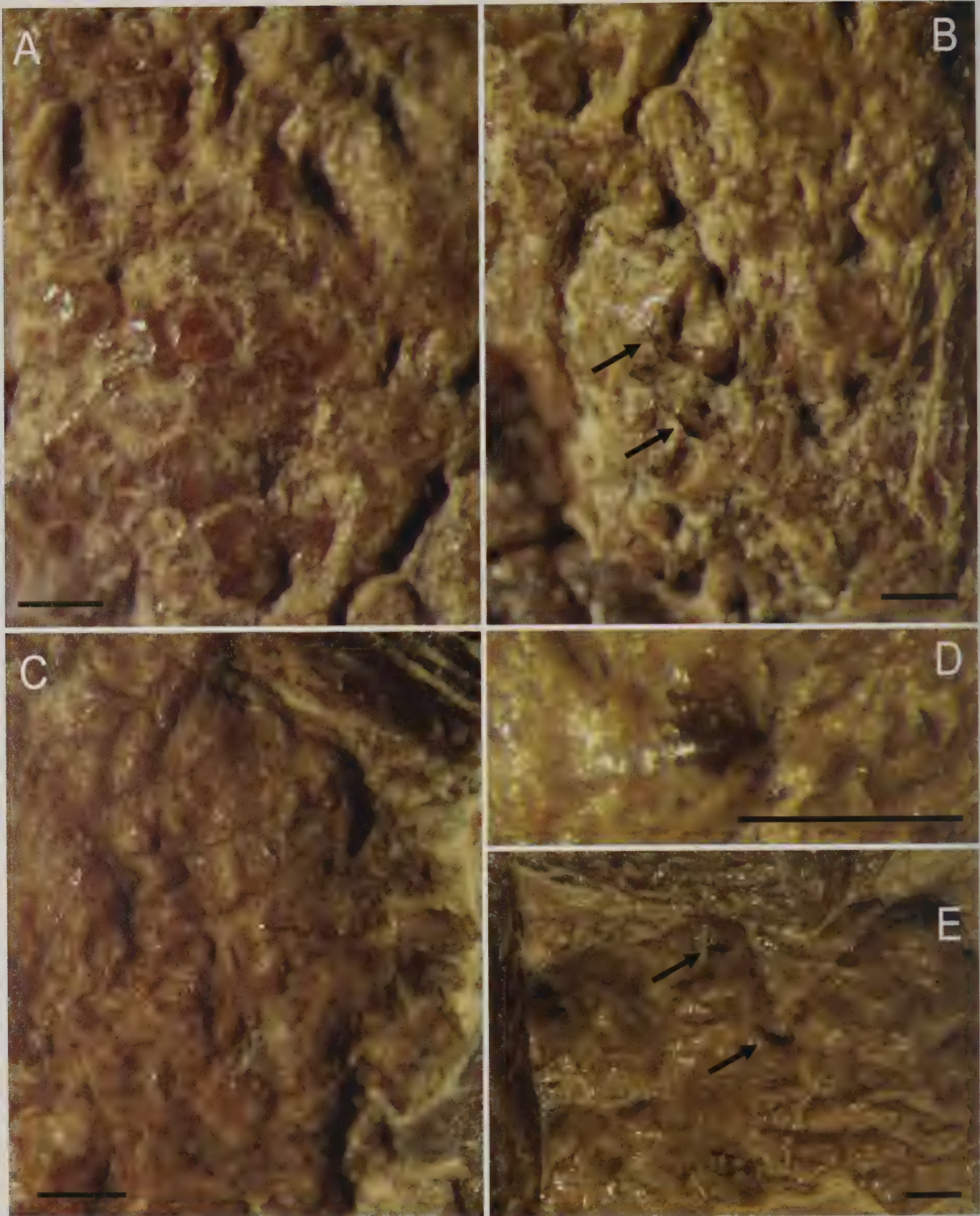


Fig. 179 - Intestinal contents of *Scipionyx samniticus*. A) polygonal squamation in the cranialmost duodenum; B) possible remnants of keratin (arrows) on a second adjacent cluster of integumentary elements; C) cluster of vertebrae in the cranial jejunum; D) isolated vertebra in the descending loop of the duodenum; E) tiny bones (arrows) in the jejunal-ileal region. Scale bars = 0.5 mm.

Fig. 179 - Contenuto intestinale di *Scipionyx samniticus*. A) squame poligonali nel tratto più craniale del duodeno; B) possibili residui di cheratina (freccie) in un secondo agglomerato, adiacente, di elementi tegumentari; C) ammasso di vertebre nel tratto craniale del digiuno; D) vertebra isolata contenuta nell'ansa discendente del duodeno; E) ossa minute nella regione digiuno-ileale. Scale metriche = 0.5 mm.

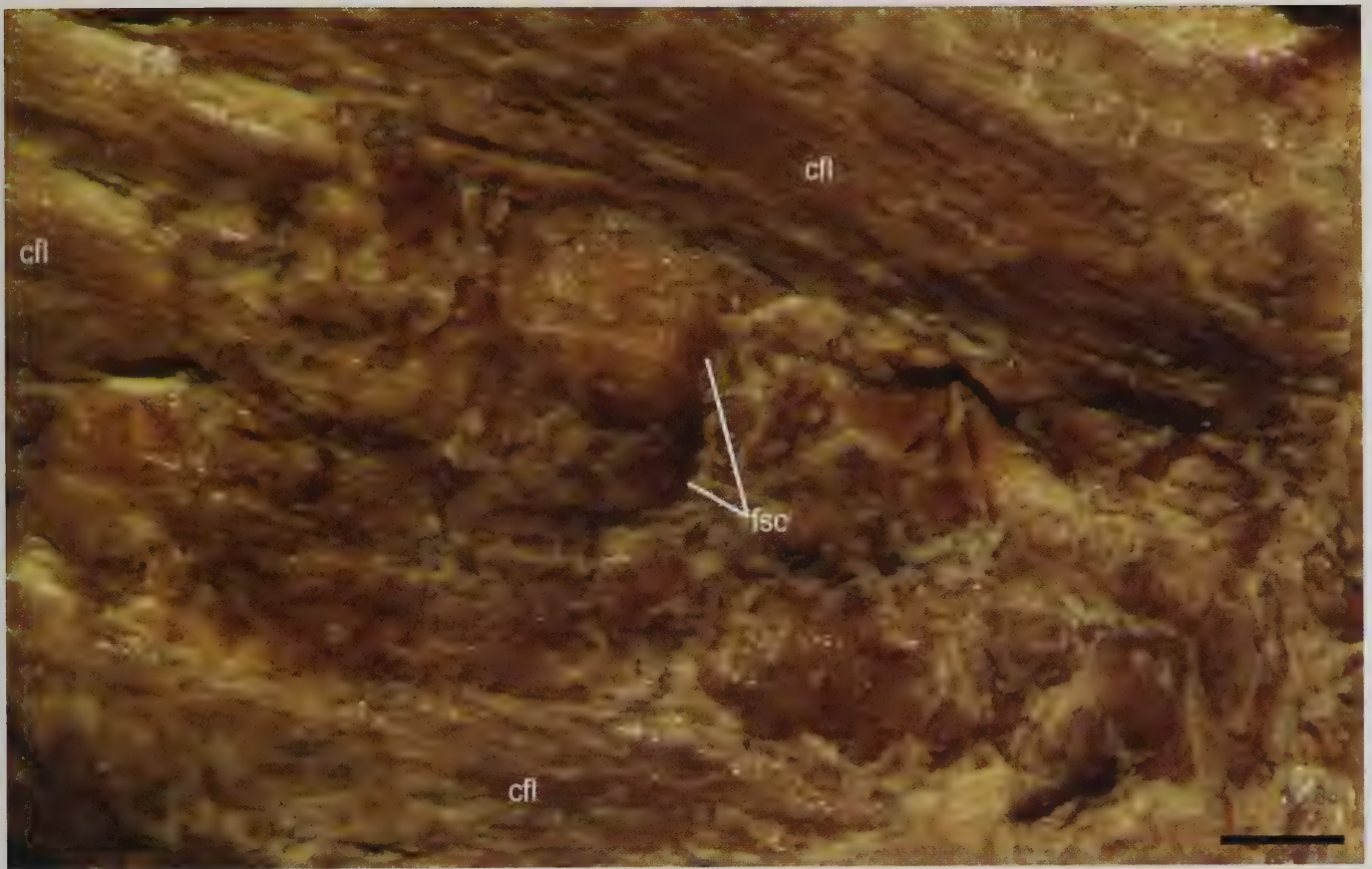


Fig. 180 - Rectal contents of *Scipionyx samniticus*: translucent scales embedded in a faecal mass. Scale bar = 0.5 mm. See Appendix 1 or cover flaps for abbreviations.

Fig. 180 - Contenuto rettale di *Scipionyx samniticus*: scaglie traslucide inglobate in una massa fecale. Scala metrica = 0,5 mm. Vedi Appendice 1 o risvolti di copertina per le abbreviazioni.

Lastly, the rectum of *Scipionyx* contains a faecal pellet with a number of tightly bound, scaly elements paralleling the dorsal and ventral caudofemoral muscle bundles. These elements have a blunt-cornered, sub-rectangular shape; thin, flat edges and seemingly thicker centres; and a highly reflective, yellow-orange semi-transparent surface (Figs. 176, 180). They form 4 partially overlapping rows composed of 4-6 units each; the total count of the exposed scales can be estimated to be at least 17. The arrangement in rows suggests that the dermal tissue connecting the scales had remained almost intact, but it is also possible that the scales became secondarily bound together within the faecal pellet – many more scales are likely hidden within the rectum of *Scipionyx*. SEM imaging highlights that the exposed scales are composed in their entirety of acellular lamellar bone (Fig. 181A-B), characteristic and diagnostic of teleostean fishes (DeLamater & Courtenay, 1974; Meunier, 1984; Bernardo de Sant'Anna, pers. comm., 2010). According to Meunier (pers. comm., 2009), the ornamentation of the scales is reminiscent of the Osteoglossiformes. The shape of the scales suggests that they are of the elasmoid type. At high magnification, the surface of the scales appears acid-etched by digestive enzymes. The presence of 9 growth lines on the natural edge of the scale examined by SEM coincides with the count resulting from the cross-sectioned broken edges (Fig. 181C), documenting that the fish to which the scales belonged had survived for 9 seasons (Bernardo de Sant'Anna, pers. comm., 2010).

Palaeobiological significance of the gut contents of *Scipionyx*

Remains of ingested prey are not uncommon finds in the thoracoabdominal cavity of theropod dinosaurs. Among Compsognathidae, the first record came along with the finding of *Compsognathus longipes*. This German specimen was initially incorrectly described to harbour an embryo (Marsh, 1881). It was then reported to contain a prey (Nopcsa, 1903), an interpretation that was confirmed by Ostrom (1978), who identified the ingested animal as a young individual of the basal squamate *Bavarisaurus*. Bone remnants of several animals, possibly belonging to sphenodontids or lizards, were found also within the gastric area of the French *Compsognathus* (Peyer, 2006). Recent finds in China confirmed the predatory abilities of compsognathid theropods: a specimen of *Sinosauropteryx*, for instance, was recovered with the remains of a lizard skull in its thoracic cavity (Chen *et al.*, 1998); furthermore, the holotype of *Sinocalliopteryx* contains parts of a dromaeosaurid leg (Ji *et al.*, 2007a), and the abdominal cavity of the holotype of *Huaxiagnathus* contains some rounded objects that, given their texture and colour, are likely bone chunks of a partially digested prey (Hwang *et al.*, 2004).

In the light of this well-documented record, *Scipionyx* does not seem to add much to our knowledge. However, at least four features render *Scipionyx* remarkably informative. First, preservation of soft tissues allows us to be absolutely sure that the allogeous remains are situated

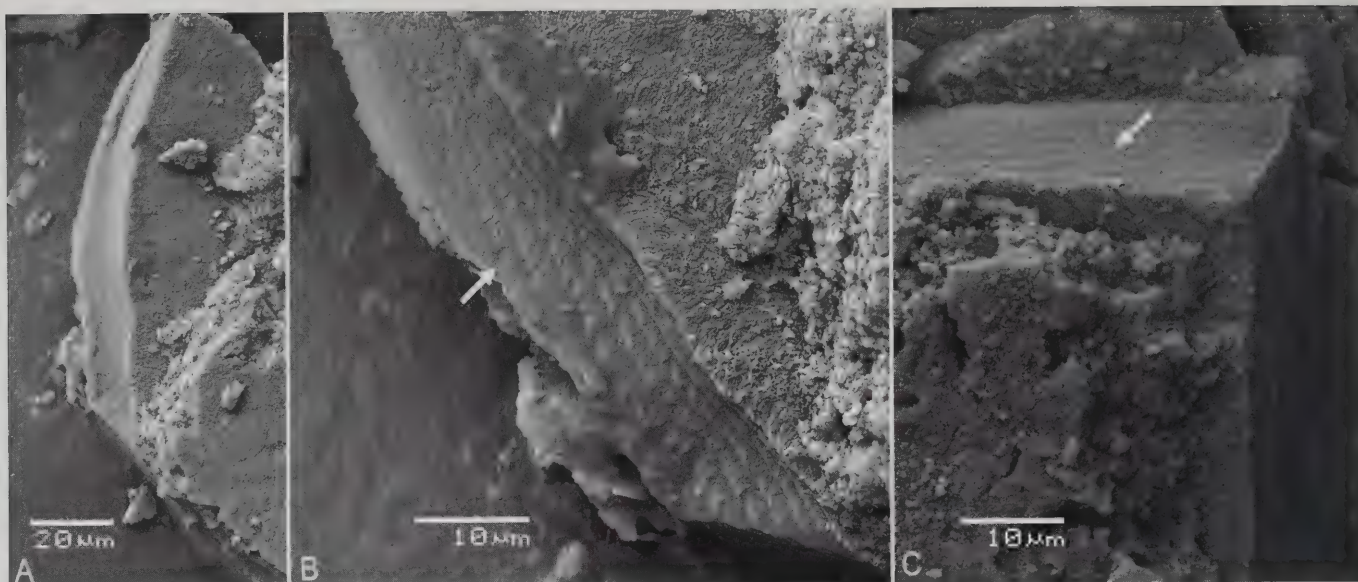


Fig. 181 - A) SEM image of one of the fish scales found in the rectum of *Scipionyx samniticus*. Nine growth lines (arrows) can be counted along natural (B) and broken (C) edges of the scale. Scale bar = 1 mm.

Fig. 181 - A) immagine al SEM di una delle scaglie di pesce trovate nel retto di *Scipionyx samniticus*. Sia lungo i margini naturali (B) che lungo quelli fratturati (C) della scaglia, si possono contare 9 linee di accrescimento (freccie). Scala metrica = 1 mm.

within the digestive tube, so that they can be interpreted unequivocally as ingested prey. Second, being trapped by the gut walls, which became themselves fossilised, the ingested remains did not have the chance to move after the dinosaur died. Consequently, the relative positions of the ingested remains have enabled us to reconstruct a feeding chronology for *Scipionyx* (Fig. 182). This is a remarkable insight, impossible to determine in almost any other fossil specimen. In fact, today we know that *Scipionyx* had fed on at least five different prey. First, one or more teleostean fish, that we estimate to be 4-5 cm long from the size (0.9 mm) of the scales found. A second, certainly distinct meal, was a smaller-sized vertebrate that, given the diameters of the vertebrae (not exceeding 0.5 mm) clustered in the jejunum, we presume to be a clupeomorph-like prey of no more than 2-3 cm in length, after comparison with the *Clupavus* sp. fossilised near *Scipionyx* (Fig. 8) and taking into account a vertebral count of 40-50 elements in similar teleosteans (Murray *et al.*, 2005). A third prey of *Scipionyx* was a lepidosaurian reptile covered with squamae that, based on their size (0.4-0.7 mm in diameter), suggest an animal no more than 10-12 cm long (Dal Sasso & Maganuco, pers. obs., 2010 on MSNM extant reptiles). Fourth came the posterior leg and part of the vertebral column of another reptile, possibly a lizard. Based on Hoffstetter & Gasc (1969), a vertebral length of 2.4 mm and an ankle diameter of 3 mm are indicative of a total body length of 15-40 cm, a size half that of *Scipionyx* and that, in all likelihood, would have prevented the Italian compsognathid from swallowing this prey whole. In addition, hunting a prey half its own size would have been a challenge too hard to face alone and, therefore, such a meal is either indicative of parental feeding or of a scavenging activity. Fifth and last prey items were smaller vertebrates of uncertain affinities.

A third important feature that differentiates *Scipionyx* from other theropod dinosaurs is that the Italian compsognathid had a varied diet, similar to that of the spinosaurid

Baryonyx (Charig & Milner, 1986), consisting of fish and terrestrial vertebrates. Irrespective of whether these prey were captured by a hatchling acting as a primary, active predator or by adult individuals providing food for their hatchlings, *Scipionyx samniticus*, as a species, clearly represents an ecological generalist. Just like the Solnhofen *Bavarisaurus*, the lizard-like squamates of Pietraraja were very fast running, agile prey. Therefore, in all likelihood, *Scipionyx*, like *Compsognathus*, had keen eyesight and was capable of rapid acceleration, high speed and quick reaction and manoeuvrability. Fish might be caught either alive along the shore, most likely while trapped in tide pools, or dead and freshly stranded. Such behaviour seems supported by the frequent finding of theropod-trampled surfaces in shallow marine carbonate platform deposits: for example, in the Cenomanian tracksite of Sezze (Latina, central Italy) facies analysis reveals continuous changes from subtidal to supratidal conditions, and 180 small theropod footprints with multiple crossing orientations on a single surface testify that near-shore environments were often frequented by these animals (Nicosia *et al.*, 2007). Considering the relative richness in food of such environments, it is likely that small-sized theropods searched among beached algae for marine invertebrates or stranded fish when the sea receded. Probably, like present-day shorebirds they were adapted to come and go with each tidal cycle. Such behaviour, as well as the variety of prey revealed by the gut contents of *Scipionyx*, would imply a high level of mobility, either for hunting or for scavenging. Given the early juvenile age of the specimen, this fact strengthens the idea that it was fed, at least in part, by adults (see also Remarks in Ontogenetic Assessment).

Last but not least, the well-preserved gut contents of *Scipionyx* has offered insight into a fourth feature: the number, variety and different localisation of ingested prey has given us the chance to indirectly investigate some aspects of the digestive physiology of theropod dinosaurs. This is discussed in the following chapter.

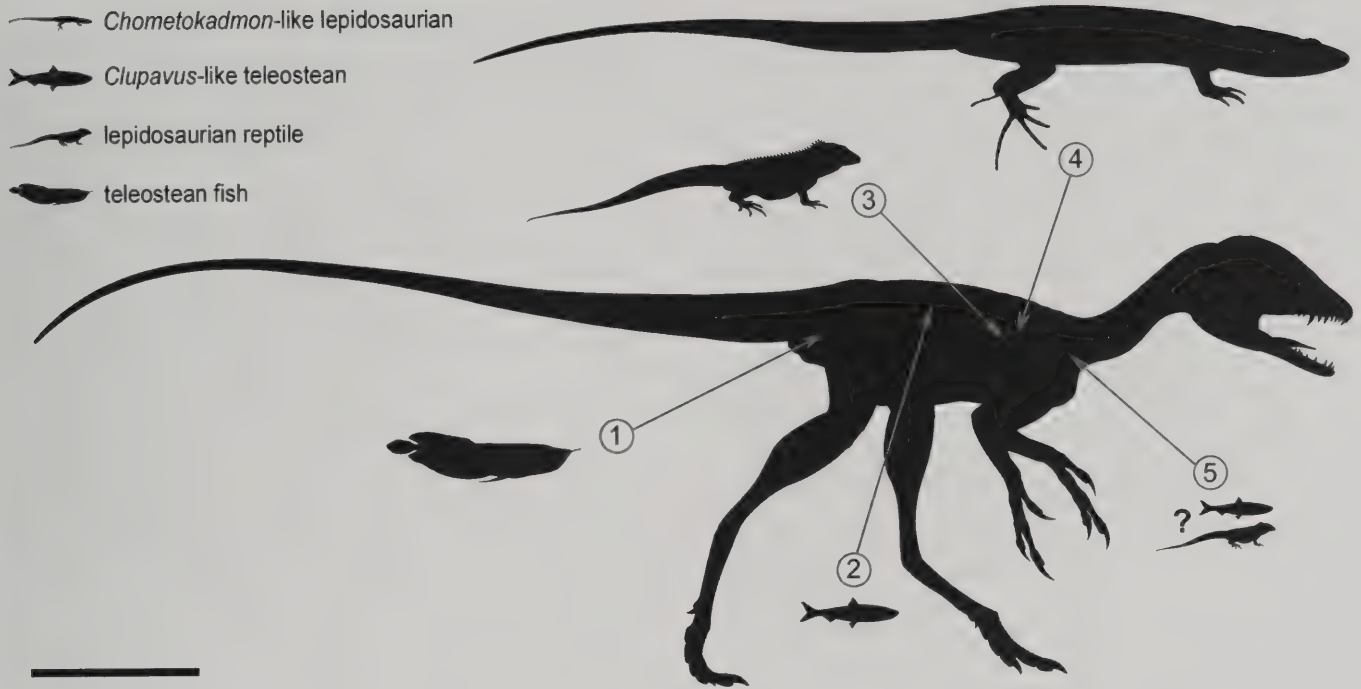


Fig. 182 - The hypothesised prey of *Scipionyx samniticus* (drawn to scale), and sequence of intake (circled numbers), based on the gut contents illustrated in Figs. 176-181. Scale bar = 5 cm.

Fig. 182 - Stima delle prede di *Scipionyx samniticus* (in proporzioni reciproche reali) e ordine di ingestione delle stesse (numeri cerchiati), basato sul contenuto dei visceri illustrato nelle Fig. 176-181. Scala metrica = 5 cm.

REMARKS ON THE PHYSIOLOGY OF *SCIPIONYX*

Digestive physiology

The intestine is the part of the alimentary tract that fulfils the dual task of digestion and absorption of nutritive substances; both are among the most important metabolic functions of an organism. As form and function are correlated with each other, the preservation of the intestine of *Scipionyx* offers a remarkable opportunity for the study of dinosaurian digestive physiology. However, studies on extant vertebrates indicate that physiological processes are influenced by a large number of parameters that cannot be evaluated in a fossil, so the matter requires extreme caution.

Certainly, inference from gross-anatomy is reliable mostly when verified through the well-known, basic bauplans of extant taxa by comparative anatomy and veterinary medicine. For example, the anatomy of the digestive system of extant tetrapods has been demonstrated to be primarily diet-related: the intestines of carnivorous animals tend to be shorter and less complex than those of herbivores, which must be longer and more specialised in order to digest cellulose. This occurs in most taxa, including reptiles (e.g., Skoczylas, 1978), birds (e.g., Ziswiler & Farner, 1972) and mammals (e.g., Kardong, 1997), independently of their metabolic behaviour. Consequently, the short, wide intestine of *Scipionyx* indicates a high absorption rate, and it is an indirect sign of a diet based on animal proteins, which are easily processed, but – unfortunately – this cannot be used to infer endothermy or ectothermy. In other words, an efficient metabolism is not the same thing

as a high metabolic rate. Efficiency, in terms of digestive physiology, is an expression of how completely ingested food is turned into energy for the production of new tissue and the maintenance of all other metabolic functions (McNab, 2002). Therefore, efficiency has nothing to do with how quickly such conversions occur. In the case of *Scipionyx*, we can expect a relatively short intestine to be associated with a slow passage time of the food, in order to allow absorption of most nutrients before the material is egested. Of course the presence of dense, anastomosed plications (*plicae circulares*) on the mucosa of the duodenum greatly increased the surface area of the intestine of *Scipionyx* and gave an important contribution to its absorptional function.

Digestion and absorption times in *Scipionyx* were probably also related to a number of extrinsic and intrinsic factors that, we repeat, cannot be evaluated in the fossil. Skoczylas (1978) and Chin *et al.* (2003), for example, remark that in reptiles the rate at which food is retained and processed is influenced by the frequency of the meals, by the volume, kin, degree of comminution and chemical composition of the food, by the ambient and preferred body temperatures, by the motility capabilities of the gastrointestinal tract and by the physical and mental state of the animal. In extant tetrapods, especially in ectotherms, temperature plays a relevant role, a lowered temperature generally slowing down both time-of-passage and time-of-absorption of nutrients. Diefenbach (1975), for instance, recorded gastrointestinal passage times in *Caiman* ranging from 99 hours, at 30°C, to 315 hours, at 15°C.

Under equal environmental conditions, the persistence of food within the stomach depends on its nature. Hard food resistant to gastric juice (acid-etching), such as bone, may be retained for hours or days before being conveyed to the duodenum. The good preservation of the lepidosaurian bones in the stomach region of *Scipionyx* (articulated ankle; dissociated vertebra and long bone; no acid etching) suggests the meal was recent, probably 12-24 hours before death (see Skoczylas, 1978).

In crocodiles, the pyloric opening of the stomach is so small that it does not allow the passage of undigested bones into the intestine: the faeces are entirely devoid of bones, and, irrespective of the passage time of other food items, bones remain in the stomach until fully dissolved; other accidentally swallowed indigestible items (stones, pieces of wood, nylon netting) remain in the stomach indefinitely, unless they are regurgitated (Huchzermeyer, pers. comm., 2011). An extreme case of stomach retention is that of "turtle" shells, which are found to be frequently swallowed by American alligators (Janes & Gutzke, 2002). At ambient temperatures over the range of 30-35°C, the gastric retention time is demonstrated to increase with the shell size, contrary to prior research claiming that in reptiles larger meals cause shorter permanence in the stomach. It has been suggested that in environments where stones are not available for ingestion, turtle shells may serve as substitute gastroliths, but a real advantage of turtle consumption is the excellent source of calcium provided by the bony shell. This is confirmed by the observation that juvenile saltwater crocodiles, *Crocodylus porosus*, prey extensively on crabs more than adults (Webb *et al.*, 1991). In the calcium/phosphorus ratio, these authors measured a decline from 7/1 in 30-60 cm long juveniles, to 2/1 in 90-120 cm long juveniles, concluding that the higher intake of calcium by the smaller animals is consistent with their immediate need to enhance skeletal development. Similarly, a juvenile *Scipionyx* would have had an intake of calcium higher than that of an adult, which well explains the utility of fish: whole small fish are more digestible than whole reptiles, birds or mammals of the same size, because they contain thinner bones (Klasing, 1998). A second similarity that we may infer for *Scipionyx* comes from data obtained by Webb *et al.* (1991) on predator/prey size. The size of the prey eaten by wild, early juvenile *C. porosus* was found to be strongly bimodal (i.e., a small number of large prey, mainly rats, and a large number of small prey, mainly crustaceans). Similarly, the prey eaten by *Scipionyx* consists of several small fish and small reptiles, and only a single portion of a larger reptile (Fig. 182).

Regarding solid, undemolished food, the digestive tube of *Scipionyx* contains patches of squamose skin in addition to bone remains. Many reptiles consume their relatives, and some reptiles often eat their own sloughed-off skin. Contrary to the calcium obtained from partial bone digestion, keratin is a substrate that is difficult to digest (Skoczylas, 1978), and nothing is known of what might be the alimentary (nutritional) significance of keratophagy, even in extant reptiles. Osseous and chitinous objects are hardly digested by reptiles. Consequently, with the exception of crocodiles (see above), a large variety of undigested material is released by reptiles through their faeces. In snakes, this is mainly fur, hair, squamae, feathers, bird beaks, claws, rattles of rattlesnakes, egg shells,

bone fragments, snail shells and insect remains (Scali, pers. comm., 2010; Skoczylas, 1978); in varanid lizards, the faeces may contain mammalian and reptilian teeth, bones, egg shells, squamae and scutes, fish scales, crustacean carapaces and claws, and insect cuticles (Blamires, 2004). Crocodiles possess particularly strong digestive enzymes and dissolve bones entirely in the stomach (Janes & Gutzke, 2002; Richardson *et al.*, 2000). In this case, it is not the size of the meal but rather the size of the swallowed particles, in particular bone, that determines how long the food remains in the stomach: the larger the pieces of bone, the more time is needed for dissolution by the stomach acid (Huchzermeyer, pers. comm., 2011). There is evidence also in mammals that particle size has a large effect on digestive time and efficiency, but for reptiles and birds, which cannot chew their food, this is a constraint (Carrano, pers. comm., 2010): if bones, squamae, scales, feathers and hair cannot be broken down in the mouth, then they have not enough surface area to be fully digested, even when retention time in the stomach is prolonged.

The hatchling *Scipionyx* was not capable of chewing bones. Therefore, the largest bones in the stomach must have been broken up by the parents feeding it or were broken already when picked up by *Scipionyx*. In the exceptionally "fossil-frozen" digestive tube of *Scipionyx*, we see also that: (a) bones are not fully digested in the stomach; (b) connective tissue connecting small bones remains intact, at least in the stomach; (c) small bones pass whole through the pyloric valve and remain identifiable in the duodenum and in the jejunum; (d) squamous skin (keratine) survives at least to the duodenum; and (e) osseous skin (enamel, dentin) reaches the rectum and, although acid-etched, accumulates in the faecal pellet.

Given that caudal to the pylorus no further digestion of bones takes place in the intestine of extant vertebrates (e.g., Kardong, 1997), the bone fragments in the intestine of *Scipionyx* must have left the stomach in the state in which they arrived in the rectum (Huchzermeyer, pers. comm., 2011). So, after partial gastric dissolution, osseous tissue (bones and scales) swallowed by the hatchling theropod was driven through the intestine and released with the faeces. Similarly, keratinous tissue, reaching the intestine in the form of intact patches, is expected to have been mostly eliminated in the same manner.

Therefore, the digestive physiology of *Scipionyx* seems more like that of extant lepidosaurs than that of extant archosaurs. Crocodiles fully dissolve small- to medium-sized bones and regurgitate large undigested bones (Huchzermeyer, pers. comm., 2011); similarly, carnivorous birds regurgitate bones and other hard prey items within their pellets, producing faeces that are devoid of solid inclusions, as well (Klasing, 1998; Crosta, pers. comm., 2011). Possibly, theropod dinosaurs also regurgitated the largest chunks of bone, but the condition in *Scipionyx* indicates that the swallowed bones were mostly guided through the intestine, like in carnivorous mammals and lepidosaurian reptiles, that have pyloric openings larger than in crocodiles and produce faeces containing bones and other incompletely digested hard tissues. This finding gives important confirmation to the supposedly theropod origin of some bone-bearing coprolites described in recent years (Chin *et al.*, 1998, 2003; Chin & Bishop, 2007).

It is well-demonstrated (e.g. Klasing, 1998) that extant carnivorous and piscivorous vertebrates, by swallowing whole prey, obtain a metabolisable energy reaching 75% of the total available, leaving only 10% of that energy to egested, and 15% to excreted undigested remains. Digestion of bones, even if partial, is crucial to these animals because the ratio of calcium to phosphorus in soft tissues is very poor. The gut contents of *Scipionyx* indicates that theropod dinosaurs, whether having less powerful digestive enzymes than extant crocodiles or not, could take advantage also from hardly digestible food items, even without completely demolishing them.

Respiratory physiology

Except for a short tract of the trachea, there are no remains or imprints of lungs, air sacs or other organs of the respiratory apparatus preserved in *Scipionyx*. Despite this, in recent years the size and position of the liver remnants, as well as the purported presence of diaphragmatic muscles, involved *Scipionyx* in a vivid, though sometimes controversial, debate on the respiratory physiology of dinosaurs. Within the present detailed study, a clarifying state of the art based on our direct observations is needed, and probably expected by many readers.

Liver and diaphragm - Some authors found similarities between the liver of crocodylians, which fills the cranialmost portion of the abdominal cavity, and the soft tissue remains of *Sinosauroptryx* (Ruben *et al.*, 1997) and *Scipionyx* (Ruben *et al.*, 1999). In particular, based on size and position of the possible liver of *Scipionyx*, which under UV light appears particularly large, Ruben *et al.* (1999) concluded that, like in crocodylians, in theropod dinosaurs the liver completely subdivided the visceral cavity into distinct anterior, pleuropericardial and posterior abdominal regions. Together with the purported remnants of diaphragmatic muscles, this suggested that theropods did not have avian-like lungs ventilated by air sacs, but possessed bellows-like septate lungs that were ventilated, at least in part, by a hepatic-piston diaphragm.

Unlike in mammals, the crocodylian diaphragm consists of a sheet of non-muscular connective tissue that adheres tightly to the dome-shaped cranial surface of the liver, while lateral, dorsal and ventral aspects of the caudal portion of the liver serve as sites of insertion for the paired diaphragmatic muscles (Ruben *et al.*, 1997). More precisely, the crocodylian diaphragm is composed of a post-pulmonary septum, as well as a post-hepatic septum (Ruben *et al.*, 2003); the two, in association with the hepatic-piston pump, augment the effectiveness of costal aspiration (Perry, 1998).

According to Ruben *et al.* (1997, 1999, 2003), Jones & Ruben (2001), and Chinsamy & Hillenius (2004), both *Sinosauroptryx* and *Scipionyx* retain preserved outlines of complete thoracic-abdominal separation, defined by “a remarkably crocodylian-like vertically oriented partition coincident with the apparent dome-shaped anterior surface of the liver”. We have not examined the specimen of *Sinosauroptryx* personally, but the describers of the holotype raised some doubts on that conclusion (Currie & Chen, 2001). Careful observations made by Paul (2001, 2002) led him to think that in *Sinosauroptryx*, 60% of the

cranial edge of the carbonised material medial to the ribs consists in breakage of the fossil slab, and the preserved edge is irregularly formed. More remarkably, taking as reference points homologous skeletal elements in *Sinosauroptryx* and *Scipionyx*, Paul (2001, 2002) noted that the position occupied by the carbonised material in the former is occupied by the intestine in the latter. So, above the cranial end of the gastralia in *Sinosauroptryx* there is no liver but an empty space, and the organic remains are most compatible with traces of the stomach and/or intestine.

Paul (2001, 2002) provided relevant information of comparative anatomy also for *Scipionyx*. Among extant tetrapods, livers tend to be largest in growing juveniles, and larger in carnivores than in herbivores. Moreover, liver size can vary within a given species: in some birds, the liver is so large and tall that it almost spans the distance from the sternum to the vertebrae, to the point that it even extends up between the high-set lungs. Experiments on the dynamics of yolk sac resorption and post-hatching development of the gastrointestinal tract in chickens, ducks and geese (Jamroz *et al.*, 2004) indicate that, during the first 21 days of life, the liver and pancreas are the fastest growing organs, increasing rapidly in size. So, the presence of fossil remains of a large liver that, even assuming it as not compressed by *post mortem* burial, spans the entire thoracic cavity and forms a cranially convex arch, is compatible with either a crocodylian- or a bird-like juvenile internal anatomy.

Despite not having examined the fossil directly, Paul (2001, 2002) correctly inferred that no septa are preserved in *Scipionyx*. Our present study of the specimen did not reveal any evidence of either post-hepatic or post-pulmonary septa. Therefore, despite our agreement with Chinsamy & Hillenius (2004) that no significant diagenetic dislocation of the liver occurred, and even assuming that the liver was as large as the halo produced by its decay, one cannot demonstrate that it divided the body into two cavities. We described the reddish matter as a halo (Dal Sasso & Signore, 1998a; Dal Sasso, 2003, 2004; Dal Sasso & Maganuco, this volume), because its shaded-off margins are consistent with a liquid or decay-derived liquefied material that contaminated surrounding elements (including bones) after the animal died (Figs. 137-138). By definition, such a halo would make it impossible to discern any precise physical boundaries. In any case, although the body of *Scipionyx* is more elongate than that of a bird, the proportion of it taken up by the inferred pleural cavity (Ruben *et al.* 1998, 1999) is very small and more bird- than crocodile-like (Huchzermeyer, pers. comm., 2010).

One of the arguments used by the detractors of the theropod-bird link relies on the observation that crocodylians have a diaphragm and birds do not. Actually, some authors (e.g., Ruben *et al.*, 1997) argue that the earliest stages in the derivation of the avian abdominal air sac system from a diaphragm-ventilating ancestor would have necessitated selection for a diaphragmatic hernia in taxa transitional between theropods and birds. Such a “debilitating condition” (*sic*) would have immediately compromised the entire pulmonary ventilatory apparatus and seems unlikely to have been of any selective advantage. We do not see any need of a hernia for a transition from a double abdominal cavity to a single one. Rather, under an

evolutionary perspective we see the diaphragm more likely gradually reducing in size and becoming segregated to a small vestigial cavity, or changing its function, whilst the avian lungs developed, becoming more and more efficient. Actually, Perry (2001) remarks that birds do not lack abdominal septa: during ontogeny, in fact, the thoracic air sacs invade the avian embryonic postpulmonary septum and divide it into two parts: the horizontal septum, which forms the ventral aspect of the lung, and the oblique septum, which abuts the liver. As mentioned above, the diaphragm of crocodylians is partly formed by the postpulmonary septum. Thus, an evolutionary path similar to the one that the avian ontogeny seems to recapitulate has some probability to have been followed by theropod dinosaurs. In any case, our opinion, corroborated by a recent discovery (Farmer & Sanders, 2010; see below), is that even in the presence of a complete diaphragm, primitive avian-like lungs could have worked as well.

Diaphragmatic muscles - As mentioned above, lung ventilation in crocodylians is achieved by costal aspiration in association with a hepatic-piston pump, a derived mechanism utilising a novel respiratory muscle, the *M. diaphragmaticus* (e.g., Brainerd, 1999). This muscle originates from the caudal gastralia and cranial surface of the pubes, and inserts on a collagenous fascia on the caudal surface of the liver: contraction of this muscle pulls the liver and viscera caudally, decreasing the pressure within the thoracic cavity (Carrier & Farmer, 2000). In *Scipionyx*, a calcified area surfacing just cranial to the pubic bones was identified as the possible remnants of a diaphragmatic musculature having an analogous mode of action to that of the *M. diaphragmaticus* (Ruben *et al.*, 1999; Chinsamy & Hillenius, 2004). This assumption was based on compatibility of the position of the purported remnants with a respiratory function, and on the observation that the surface of that area showed, under suitable lighting conditions (e.g., Fig. 185A), longitudinally oriented “imprints” reminiscent of a craniocaudal arrangement of the muscle fibres (Ruben *et al.*, 1999: fig. 3). Actually, our photographs reveal that this calcified area is part of a larger hard nodule, which was partly polished during the preparation of the specimen (Figs. 183-184; Dal Sasso, pers. obs., 1997) and which continues into a bumpy cluster directed craniodorsally in the abdomen, rather than horizontally towards the supposed liver (Fig. 184). Moreover, the longitudinally oriented “imprints” of the nodular surface are an artefact of preparation, produced involuntarily in 1997 by an MSNM collaborator (S. Rampinelli) when trying to weaken and remove the very hard nodule. In addition, comparative SEM imaging and microanalysis revealed that the aspect and the phosphatic composition of the calcite nodule definitely differ from those of the myofibres of *Scipionyx*, even in the areas where the musculature is only moderately preserved, such as in the neck region (Figs. 132, 185). Indeed, this nodule was found to be made in its entirety of an amorphous, cryptocrystalline calcite, just like the nodule found cranial to the right elbow of *Scipionyx* (Fig. 171). Therefore, we conclude that the purported remnants of diaphragmatic musculature are not consistent with the state of preservation of all other muscle tissue in *Scipionyx* and do not show any macroscopic evidence (bundle-like appearance) or microscopic evidence (presence of myofibres) attributable to fossilised muscle. As a

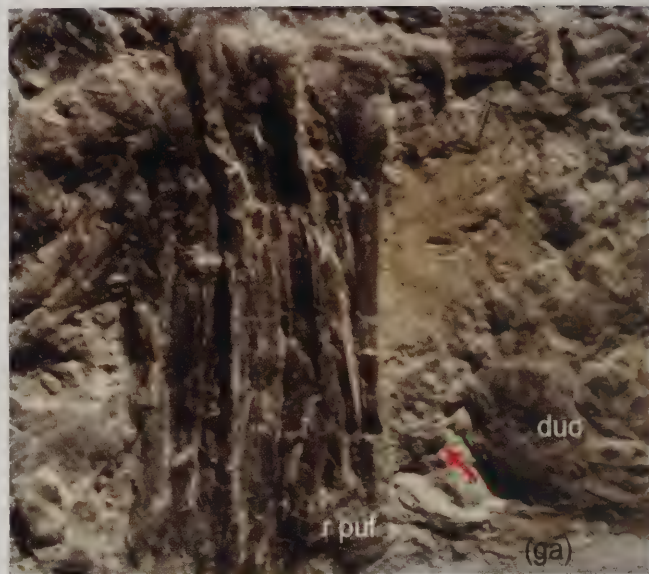


Fig. 183 - This photograph of *Scipionyx samniticus*, taken in 1993, documents the original granular aspect of the nodule of calcite (red arrow) contained in the abdominal region, just cranial to the pubic bones. See Appendix 1 or cover flaps for abbreviations.

Fig. 183 - Questa fotografia di *Scipionyx samniticus*, datata 1993, testimonia che il nodulo di calcite contenuto nella regione addominale, subito cranialmente alle ossa pubiche, aveva in origine un aspetto granulare (freccia rossa). Vedi Appendice 1 o risvolti di copertina per le abbreviazioni.

matter of fact, Huchzermeyer (pers. comm., 2010) points out that the diaphragmatic muscle of crocodiles, albeit strong, is structurally very thin. So, if it was present in *Scipionyx*, it would probably not have been preserved or would have been markedly and definitely thinner than the purported diaphragmatic muscle remnants.

Lungs - Just as we were writing this section of the monograph, a revolutionary discovery in comparative anatomy was published (Farmer & Sanders, 2010). Up to now, the lungs of birds were believed to be unique among vertebrates. The avian respiratory apparatus is composed of two main components – the rigid gas exchanging lungs and the non-vascularised ventilatory air sacs – and air-flow through most of the tubular gas-exchanging bronchi (parabronchi) of the avian lung is unidirectional, air travelling in the same direction during both inspiration and expiration; in contrast, in the lungs of mammals and, presumably, of all other vertebrates, air moves tidally into and out of terminal gas-exchange structures, which are cul-de-sacs. Unidirectional air flow in the avian apparatus was purported to depend exclusively on the bellows-like ventilation of the air sacs, and was thought to have evolved to meet the high aerobic demands needed for sustaining flight. However, Farmer & Sanders (2010) discovered that, despite the different external gross morphology of the respiratory apparatus of birds and crocodylians, the topography of the intrapulmonary bronchus and of the first generation of bronchi is similar in these two taxa, and that air flows unidirectionally through parabronchi in the lungs of the American alligator. This strikingly bird-like respiratory system functions without the presence of air sacs and with a diaphragmatic breathing mechanism. This finding eliminates all the problems raised so far with re-

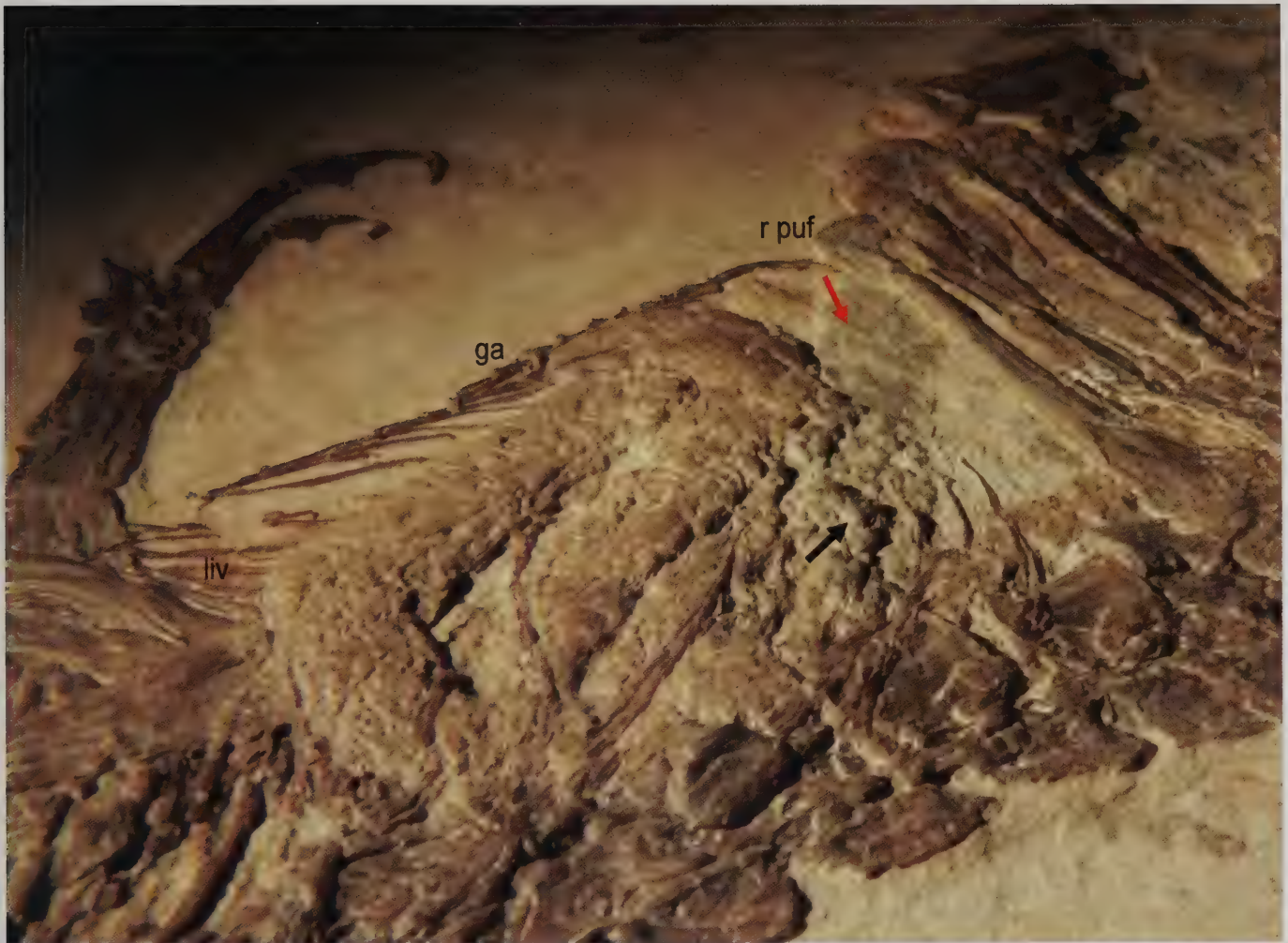


Fig. 184 - Oblique view of the nodule of calcite shown in Fig. 183, as it appears today. The ventralmost portion (red arrow) was polished during preparation in 1997, and then interpreted by some authors as remnants or imprints of diaphragmatic muscles. Actually, its continuity with the craniodorsally directed portion, which retained the original granular texture (black arrow), is still evident. See Appendix 1 or cover flaps for abbreviations.

Fig. 184 - Vista obliqua del nodulo di calcite mostrato in Fig. 183, come appare oggi. La porzione più ventrale (freccia rossa) fu levigata durante la preparazione nel 1997 e in seguito fu interpretata da alcuni autori come residuo o impronta di muscoli diaframmatici. In realtà la sua continuità con la porzione di nodulo diretta craniodorsalmente, che ha mantenuto la tessitura granulare originaria (freccia nera), è ancora evidente. Vedi Appendice 1 o risvolti di copertina per le abbreviazioni.

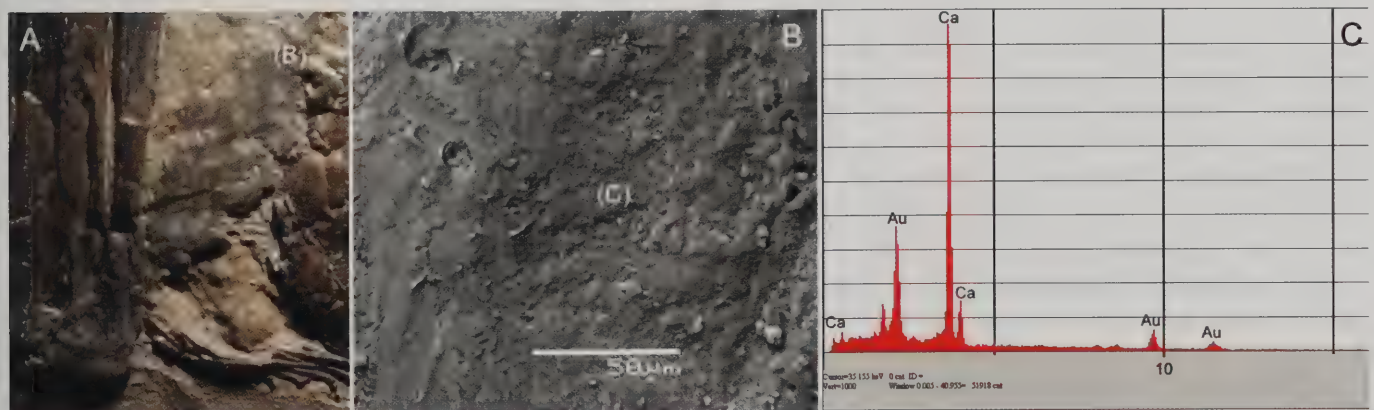


Fig. 185 - Photograph taken under very grazing light (A), SEM imaging (B) and SEM element microanalysis (C) of the purported remnants of diaphragmatic muscles of *Scipionyx samniticus*. These analyses reveal an amorphous cryptocrystalline structure and a composition of calcium carbonate, a result that is incompatible with the mode of preservation of muscle tissue in *Scipionyx* (Figs. 132, 157), but consistent with calcite nodules (Fig. 171). Scale bar = 1 mm. See Appendix 1 or cover flaps for abbreviations.

Fig. 185 - *Scipionyx samniticus*. Le fotografie in luce molto radente (A), le immagini al SEM (B) e la microanalisi degli elementi al SEM (C) degli ipotetici residui di muscoli diaframmatici mostrano una struttura criptocristallina amorfa e una composizione in carbonato di calcio, non compatibili con le modalità di conservazione degli altri tessuti muscolari di *Scipionyx* (Fig. 132, 157), ed equivalenti a quelle degli altri noduli di calcite (Fig. 171). Scala metrica = 1 mm. Vedi Appendice 1 o risvolti di copertina per le abbreviazioni.

gard to the evolutionary transition from a crocodylian-like to a bird-like breathing apparatus and, thus, represents a fundamental advancement in evolutionary biology. It also suggests that unidirectional pulmonary airflow dates back to the basal archosaurs of the Triassic, in that *Alligator* is an ectothermic reptile without air sacs, and that this respiratory modality may well have been present in all cruro-tarsans as well as in ornithomirans, dinosaurs included.

Trachea - Ruben *et al.* (1999, 2003) and Chinsamy & Hillenius (2004) drew attention to the ventral position of the trachea in *Scipionyx*: the preserved tract of the trachea, found in the caudal cervical region, is well-distant from the vertebral column and immediately cranial to the scapulocoracoid complex. These authors suggested that this position was evidence of a crocodylian-like, dorsoventrally deep lung, contrasting with the location of the caudal portion of the avian cervical trachea, which is usually more dorsal, i.e. adjacent to the ventral margin of the vertebral centra, in order to facilitate entry of the trachea into the dorsally attached parabronchi (McLelland, 1989). Paul (2001, 2002) ascribed some ventral displacement of the trachea of *Scipionyx* to the 10th cervical vertebra, but in our opinion this element is too distant, at least from the preserved tract of trachea, to infer any cause-and-effect dependence (Fig. 129). However, according to Paul (2001, 2002), the position of the trachea in *Scipionyx* is consistent with both crocodylian-like and bird-like respiratory systems. In fact, although it is common for the trachea of birds to run just below the cervicodorsal vertebrae, as described by Ruben *et al.* (1999, 2003) and Chinsamy & Hillenius (2004), in some birds, especially those with long necks, the trachea runs more ventrally and is remarkably mobile. Indeed, tracheal position may change with the position of the neck at any given moment even in the same individual, and the air passage may drop well-below the vertebral column, just cranial to the shoulder girdle (McLelland, 1989: fig. 2.8a). Also, this position is not immediately adjacent to the lung entrance, so we tend to agree with Paul (2001, 2002) that the fossil-frozen position of the trachea in *Scipionyx* does not offer definitive evidence regarding lung depth.

Abdominal air sacs - In *Scipionyx*, the duodenum seems to be slightly displaced cranially, while a more anomalous displacement appears to have moved the rectum caudally. These two parts of the digestive tract have left a large, potentially empty space within the pelvic cavity in front of the pubic bones. According to some authors (Martill *et al.*, 2000; Paul, 2001, 2002), this space is suggestive of the presence of avian-like abdominal air sacs. *Contra* Ruben *et al.* (1999: fig. 2; 2003: fig. 11), the intimate attachment of the intestine to the vertebral column in *Scipionyx* is not an evidence against the presence of air sacs, as in extant birds the intestine does not have to hang loose in the abdomen to accommodate them (Huchzermeyer, pers. comm., 2010). Although it is true that the dorsal position of the rectum in *Scipionyx* is like that of crocodylians and mammals, nobody has shown to date that dorsally placed recta are not found in tetrapods that do not use the hepatic-piston pump (Paul, 2001, 2002). In any case, avian-like archosaurian lungs do not necessarily require avian-like air sacs, as strikingly demonstrated recently by Farmer & Sanders (2010).

Although carnivorous dinosaurs have pneumatised bones, to date there is no direct evidence for theropod air sacs in the fossil record. The only case in which something similar appears to be seen is that of the Brazilian compsognathid *Mirischia*, the pelvis of which was found well-preserved in three dimensions inside a nodular concretion from the Chapada do Araripe fossil site. According to Martill *et al.* (2000), the large empty space impressed in the sediment caudal to the pubic shafts was left by an abdominal air sac. Such an air sac could have been ventilated by a dorsal pneumatic duct passing between the sacrum and the pubes, and a ventral one passing through the distal opening in the pubic apron. However, observations on extant birds (Huchzermeyer, pers. comm., 2010; McLelland, 1989) show that the walls of air sacs are very thin, and that the air sacs of dead animals are only virtual spaces. Air sacs do not displace abdominal organs cranially, and after death of the animal they do not leave any evidence: as written by Paul (2001, 2002), “fossilising the air sacs of a bird is as improbable as fossilising a balloon”. Also, the majority of the air sacs lie lateral to the internal organs, so organ-free areas will not necessarily mark the sites of air sacs in a laterally flattened specimen. In this respect, the alternative yolk-sac hypothesis, that we discussed while describing the rectum, fits better with the displacement of the intestine and the empty space seen in the abdominopelvic cavity of *Scipionyx*.

Osteological correlates: pneumatic bones - Among extant tetrapods, pneumatic postcranial bones are only present in birds and are the osteological correlates of the pulmonary air sacs. The air sacs serve as air storage chambers and ventilatory bellows, which generate airflow through the rigid lungs (Scheid & Piiper, 1989). Extrapulmonary diverticula of the air sac system invade the postcranial skeleton of birds, resulting in the pneumaticity of variable portions of both the axial and appendicular skeleton (O'Connor, 2006). A recent study on the avian vertebral column (Wedel, 2009) demonstrates that this invasion takes place during ontogeny following a predominantly craniocaudal order, with diverticula of different sources (cervical air sacs, lungs, abdominal air sacs) pneumatising their respective skeletal domains at different times. Wedel (2009) observed that this sequence in bird ontogeny recapitulates the evolution of pneumaticity in theropods and sauropodomorphs. In extant birds, Wedel (2009) also found apneumatic vertebrae that are bordered cranially and caudally by pneumatic vertebrae. These hiatuses are produced if the diverticula from the different parts of the respiratory system do not meet. Similarly, the presence of pneumatic hiatuses in dinosaurs suggests that vertebral diverticula developed from different, specific air sacs. Likely, as found in the postcranial skeleton of *Majungasaurus* (O'Connor & Claessens, 2005) and proven in extant birds (Schachner *et al.*, 2009), the cervical and cranial dorsal vertebrae of theropods were pneumatised by diverticula of cervical air sacs; the middle dorsal vertebrae were pneumatised by diverticula of the lung; and diverticula of the abdominal air sac pneumatised the caudal dorsal, sacral and proximalmost caudal vertebrae.

Based on the distribution of pneumatic foramina in the vertebrae (see Postcranial Axial Skeleton), *Scipionyx* has at least two evident hiatuses: a cervicodorsal hiatus

and a dorsocaudal hiatus. The reason for the amplitude of the pneumatic hiatuses in the axial skeleton of *Scipionyx* could likely be the immaturity of the specimen, but what is important here is that these hiatuses exist.

The diverticula pneumatizing the skeleton of saurischian dinosaurs might have evolved before they could have become extra-osseous air sacs functional to lung ventilation, producing useful exaptations like lightening of the skeleton and the body mass. Under this perspective, postcranial pneumaticity may have facilitated the evolution of unprecedented body sizes. In fact, the pneumatic diverticula of extant birds do not just replace bone tissue, they also fill up space that in mammals are otherwise occupied by fat. Sereno *et al.* (2008), for instance, described several pneumatized gastralia in the tetanuran theropod *Aerosteon*, suggesting that diverticula of the air sac system were present also in surface tissues of the thorax.

Osteological correlates: morphology of ribs and vertebrae - The lungs of birds are rigid and do not change volume during breathing. Each lung is positioned in the craniodorsal region of the thoracic cavity, with the costal surface tightly attached to the ribs, and the vertebral (medial) surface adhering to adjacent vertebral bodies (Duncker, 1972). Because of this intimate connection, the vertebral and costal surfaces of bird lungs are deeply incised by the proximal section of each rib; as the ribs are strongly bicipitate, composed of distinctly separate capitula and tubercula, approximately one-fifth to one-third of the lung tissue is located in between the neighbouring thoracic ribs (Maina, 2005). A recent report on living and extinct archosaurs, studying thoracic rib morphology and the position of the diapophysis and parapophysis of dorsal vertebrae, suggests that most nonavian theropods were similar to birds in that they possessed lungs that were dorsally attached to the vertebral column and that were deeply incised by the adjacent bicipitate thoracic ribs (Schachner *et al.*, 2009): this functionally constrained the lungs as rigid, non-expansive organs that had to be ventilated by nonvascularised accessory air sacs.

Like in most theropods, parapophyses and diapophyses are completely separated along most of the dorsal vertebrae in *Scipionyx*. Paralleling their vertebral articulations, almost all the dorsal ribs are bicipitate, the capitulum and the tuberculum of each being well-distinct (Figs. 60, 76A, 77). In crocodylians, on the other hand, the parapophyses of almost all dorsal vertebrae are shifted along the transverse process towards the diapophyses, so much so that the two articulations form almost a single surface. The result of this shift is a thoracic cavity with a very flat and smooth ceiling caudal to the first two ribs. According to Schachner *et al.* (2009), this facilitates the cranial and caudal movement of the lungs when inflated and deflated by the hepatic-piston pump. Based on this, we remark that, as in most theropods, the manner in which the bicipitate ribs of *Scipionyx* articulated with their corresponding vertebrae generated a rigid ribcage around lungs with a limited mobility compared to those of crocodylians. Moreover, the corrugated ceiling resulting from this arrangement of the axial skeleton would have greatly inhibited the inflation of the lungs by a crocodylian hepatic-piston mechanism. This mechanism likely would not function with lungs that were in-

cised and fixed in place by the thoracic ribs and, thus, the axial osteology of *Scipionyx* and most nonavian theropods contradicts the hypothesis that they may have had a hepatic-piston pump mechanism of ventilation.

Osteological correlates: gastralia - Because the complex rib-sternum complex seen in birds did not evolve in the nonavian theropods, Schachner *et al.* (2009) hypothesised that the protoavian lung must have been ventilated in a different manner, possibly by gastralia or pelvic aspiration. In contrast to the reduction of the gastralia seen in other amniote groups, theropod gastralia show elaborate modifications. The imbricating articulations observed in theropods, including the peculiar morphology we describe for the gastralia heads of *Scipionyx* (Figs. 82, 85; see Gastralia), unite the individual gastralia into a single functional unit. As remarked by Claessens (2004), no significant movement of individual gastralia can take place without affecting the position of other components. The mid-ventral articulations limit movement to a single plane. Effectively, retraction and protraction of the gastralia system narrows and widens the ventrolateral dimensions of the theropod trunk. Thus, the anatomy of the gastralia system in theropod dinosaurs indicates a more active function than merely abdominal support or protection. A plausible function for active retraction and protraction of the gastralia system is lung ventilation. According to Claessens (2004), the gastralia may have functioned as an accessory component of the aspiration pump, increasing tidal volume. Moreover, if the caudal region of the lungs in some theropods had differentiated to form abdominal air-sacs, the gastralia might have ventilated them. Gastralia aspiration may have been linked to the generation of small pressure differences between potential cranial and caudal lung diverticula, which may have been important for the evolution of the more specialised unidirectional airflow lung of birds.

Skeletal adaptations consistent with an avian-like aspiration pump are already present in basal neotheropods (O'Connor & Claessens, 2005). In the thoracic ribcage, the vertical arrangement of the diapophyses and parapophyses ensures a rigid and relatively incompressible skeletal framework around the pleural cavity. As already stated, also in *Scipionyx* the orientation of the vertebrocostal articulations changes to a horizontal position in the caudalmost elements. This shift allows lateral excursion of the last dorsal ribs, which, along with movements of the gastralia apparatus, may provide relevant volumetric changes in the caudal half of the trunk.

According to Sereno *et al.* (2008), the evolution of a primitive costosternal pump took place only in maniraptoriform theropods with osteological correlates that *Scipionyx* lacks, such as ossified sternal ribs and sternum, and specialised joints between vertebral ribs, sternal ribs and sternum. Hypapophyses and uncinat processes are other key osteological characters used as evidence for a more advanced protoavian respiratory system (Codd *et al.*, 2007).

Osteological correlates: pelvic girdle - The hepatic-piston hypothesis, suggested by some authors for the theropod respiratory physiology and partly discussed above, relies also on controversial osteological homologies in the pelvic girdle, which led to putative similari-

ties between theropods and extant crocodylians (Ruben *et al.*, 1997, 1998, 1999). Actually, the pelvis of crocodylians is highly derived and modified in relation to the basal archosaurian condition in that the pubis articulates only with the ischium, forming a mobile joint that is correlated with the action of *M. diaphragmaticus* (Carrier & Farmer, 2000). On the other hand, the pubes were certainly immobile in theropods (*Scipionyx* included) and most other non-crocodyliform archosauromorphs. According to Hutchinson (2001), this feature weakens the inference that any theropods had such a ventilatory mechanism. Ruben *et al.* (2003) replied that experimental data falsify this assertion, because alligators with surgically fixed pubes exhibit no alteration in intra-abdominal pressures during exercise-induced periods of enhanced lung ventilation, although caudal, inhalatory rotation of the liver and lung tidal volume are reduced by about 15% in these animals.

Hutchinson (2001) casted doubt on the inference of *M. diaphragmaticus* in any noncrocodyliform archosaur, arguing that the crocodylian pubic foot is a vestige of the ancestral archosauriform pubic apron, whereas in tetanuran theropods the pubic foot is an expansion of the lateral surface of the distal pubic symphysis. Furthermore, he remarks that Ruben *et al.* (1997) compared crocodylian pubes with theropod pubes in lateral view, but these are not homologous lateral bone surfaces because the crocodylian bone surface shown is caudal, not lateral, and is occupied primarily by the origin of the *M. puboischiofemoralis externus*, not the *M. diaphragmaticus* (Hutchinson, 2001: fig. 14). Ruben *et al.* (2003) replied that in crocodylians the pubic rami are not major sites of origin for the diaphragmatic musculature; instead, the large, ventral portion of *M. diaphragmaticus* attaches primarily to the last pair of gastralia; some portions of this muscle may originate directly from the pubis, but these attach to the cranio-lateral edge of the distal part of the pubis, ventrally adjacent to the sites of attachment of the puboischiofemoral muscles. Whereas the presence of diaphragmatic muscles in theropods remains to be demonstrated, it does not preclude air sac development, as recently observed by Farmer & Sanders (2010) and first discussed by Perry (2001). The latter author found that hypothesis particularly interesting, because under the perspective of a costal breathing mechanism aided by actively kinetic gastralia (Claessens, 2004), the main function of a diaphragmatic-like muscle, if present in a pre-

avian theropod abdomen, could have been to fix the liver dynamically during inspiration and, thereby, to increase the efficiency of costogastral ventilation. According to Perry (2001), a ventrally oriented contraction would prevent dorsal movement of the liver, assuming it to lie ventral to the lungs, as in birds and in fetal crocodylians, and as we infer from *Scipionyx*. It would also explain the presence of the post-hepatic septum as a relic structure in birds. This septum stabilises the liver piston and attaches the liver to the dorsal body wall in crocodylians, but lacks a compelling function in birds.

Nevertheless, a significant flaw in a theropod dinosaur with a hepatic-piston mechanism identical to that of extant crocodylians, as hypothesised for *Scipionyx* and *Sinosauropteryx* (e.g., Ruben *et al.*, 1999; Chinsamy & Hillenius, 2004), concerns the basic biomechanics of bipedal locomotion. All theropods are obligatory bipeds, whereas all crocodylians are obligatory quadrupeds. When the abdominal viscera shift cranially and caudally by the action of the diaphragmatic muscles in crocodylians, the centre of mass also shifts (Farmer, 2006). This is not a problem for a quadrupedal sprawling animal with a low centre of mass, but it may create an equilibrium problem for a parasagittally erect biped by shifting of the centre of mass cranially and caudally with every breath, disrupting balance and agility (Schachner *et al.*, 2009). Despite the arguments for the presence of a hepatic-piston based respiratory apparatus in theropods, both the biomechanics of bipedalism and the osteology of the theropod axial skeleton make this hypothesis extremely weak from a functional point of view.

Finally, we like to repeat a conclusive remark made by O'Connor & Claessens (2005): "recent studies of non-avian theropod dinosaurs have documented several features once thought solely to characterize living birds, including the presence of feather-like integumentary specializations (Xu *et al.*, 2004), rapid, avian-like growth rates (Padian *et al.*, 2001; Erickson *et al.*, 2001), and even bird-like behaviours captured in the fossil record (Norell *et al.*, 1995; Xu & Norell, 2004). Either implicitly or explicitly, these studies have linked anatomical, physiological or behavioural inferences with an increased metabolic potential, suggesting that if not bird-like in metabolism, theropods were at least "more similar" to birds than to reptiles".

CONCLUDING REMARKS

Scipionyx samniticus represents not only the most complete predatory dinosaur from the middle to Late Cretaceous of Europe, but also the dinosaur with the best preserved internal anatomy ever found so far in the world. It is a key fossil specimen, which deserved a long and detailed examination. We did our best to accomplish this, but we are aware that some subjects could be more thoroughly studied. For example, even though the whole osteology of the specimen has been revised bone by bone, addressing our knowledge of the anatomy of the species and of the Compsognathidae as well, it remains difficult to determine to what extent the basal phylogenetic position of *Scipionyx* within the Compsognathidae is due to its generally plesiomorphic condition or to its immaturity.

Further finds, desirably including a growth series of the species, are needed to support any postnatal trajectory in *Scipionyx* and to improve our understanding of what can be observed in other compsognathids as well as of the phylogeny of the group.

New skeletal reconstructions of the holotype of *Scipionyx samniticus* have been made based on its overall skeletal anatomy. Besides skeletal reconstructions, a gallery of artwork by several Italian palaeoartists has been included herein, livening up the end pages of this monograph.

A summary of the biodiversity of the coeval flora and fauna from the Lower Cretaceous (Albian) of Pietraraja, as well as a short review of the present knowledge about

the depositional environment of the Pietraraja Plattenkalk and the paleogeography of southern Italy at that time confirmed that *Scipionyx samniticus* inhabited a coastal environment under a tropical-subtropical climate.

The preservation of a variety of ingested allochthonous remains in the gut of *Scipionyx* has provided a rare glimpse of trophic biology in a Lower Cretaceous ecosystem. Based on the nature of those animals, we now have compelling evidence that *Scipionyx* fed on both lizards and fish, with the latter being regular, non-occasional, meals. This confirms and extends a hypothesis by Naish *et al.* (2004), who found ecological similarities between the Solnhofen and the Santana lagoons, with a variety of theropods, including compsognathids, acting as generalist carnivores, scavenging at the shoreline and fishing in shallow waters. Given how immature the holotypic individual of *Scipionyx* was at the time of death (probably less than three weeks old, maybe only three days old), it is fair to state that the presence of gut contents might be evidence of parental care and feeding. Parental care means protection of the offspring (in birds it also includes keeping the hatchlings warm) and guiding to food sources, i.e., teaching the offspring how to obtain food and which food to eat; parental feeding implicates also provision of bits of food.

In any case, the most striking result of the present study is that it documents a unique variety of fossilised soft tissues, which at present renders this specimen of *Scipionyx* the most remarkably preserved dinosaur known, the Liaoning feathered examples notwithstanding. Investigation of the taphonomy of the specimen led to the conclusion that the dinosaur's carcass was exquisitely preserved because it had undergone very little decay and a rapid mineralisation process in the presence of high concentrations of phosphates. Through detailed examination under optical microscopy, ultraviolet-induced fluorescence photography and scanning electron microscopy coupled with el-

ement microanalysis, we have demonstrated that the soft tissues of *Scipionyx samniticus* are mineralised in three dimensions, and that their preservation is exceptional even at cellular and subcellular levels. We presume that future examinations of *Scipionyx* with more advanced, hopefully non-invasive, techniques will uncover further remarkable information.

Perhaps the most relevant results in terms of the contribution to the debate on dinosaur physiology have arisen from new studies on the reddish halo preserved in the thorax of *Scipionyx* and on the "diaphragmatic muscles" purported by some authors. That the reddish halo is referred to the liver, and likely also to the decay of the heart and the spleen, has been confirmed by its haematic origin, but unfortunately there have been no insights into either the original structure of the organ or to a link to any sort of diaphragm. The remnants of "diaphragmatic musculature", on the other hand, turned out to be an amorphous calcite nodule with a structure that is inconsistent with that of the preserved muscles in *Scipionyx*. So, the hypothesis of a hepatic-piston-assisted breathing mechanism in theropods does not receive any support from this study of the Italian compsognathid.

We think that the present description and the supporting figures, allowing the comparison of the soft-tissue morphology from a relevant extinct taxon with the analogous biological structures of extant vertebrates, may interest a broad community of scientists, including palaeontologists, evolutionary biologists, functional morphologists, comparative anatomists, biologists, veterinarians, herpetologists and ornithologists. In addition, given the popular appeal of dinosaurs, we also feel that a non-scientific audience will be interested in such unusual "palaeo-autopsy", as well as the media will be fascinated by the amount of information provided by such a tiny, single fossil specimen on the life and death of a hatchling predatory dinosaur.

ACKNOWLEDGEMENTS

We wish to thank all the people who helped us in the study of *Scipionyx*, especially in the last 4-5 years. During this period, five superintendents succeeded to the head of the present Soprintendenza per i Beni Archeologici di Salerno, Avellino, Benevento e Caserta: Giuliana Tocco (1986-2007), Angelo Maria Ardovino (2007-2008), Mario Pagano (2008), Maria Luisa Nava (2008-2010) and Adele Campanelli (2010-present). We are grateful to all of them for having always met our needs in the examination of the fossil *Scipionyx*, ensuring the continuity of our research. Continuity was guaranteed also by the tenure of Leonardo Vitola, the person responsible for the Department of Photography. In photographing *Scipionyx* over the years, he got very keen on any new finds, just like the authors of this monograph, and, thus, contributed greatly in increasing the value of this unique fossil specimen.

Without the sharp eye of the person who collected the tiny specimen in the Pietraraja quarry, nothing of what is documented herein could have been imagined. Giovanni Todesco, but also those who first recognised the scientific meaning of the first Italian dinosaur (Giovanni Pasini and Giorgio Teruzzi), paved the way with crucial decisions and actions. The 1993 editorial staff of *Oggi*

magazine (Paolo Occhipinti, Pino Aprile and Franco Capone) helped the return of the specimen to the competent authorities. Sergio Rampinelli performed a superb preparation of the fossil from 1994 to 1997. Giuseppe Leonardi and Marco Signore were former fellow travellers with one of us (CDS). In more recent years, Mariella del Re and her collaborators at the Museo di Paleontologia, Università di Napoli "Federico II", provided access to the historical specimens collected at Pietraraja by Costa, D'Erasmus and others.

Three referees patiently read and reviewed this monograph according to their field of research: Karin Peyer (Muséum national d'Histoire naturelle, Paris), an expert in fossil compsognathids, focused on osteology; Matt Carrano (Smithsonian Institution, Washington DC) kindly commented on soft tissue anatomy, physiology and taphonomy; and Fritz Huchzermeyer (Onderstepoort Veterinary Institute) offered his valuable help with a truly "fresh" observational perspective with respect to traditional vertebrate palaeontology – as a veterinary pathologist, Fritz has dissected thousands of crocodiles and ostriches, experiencing in the best way the comparative anatomy of extant archosaurs.

At the end of the review process, Mike Latronico quickly revised our (too approximate) English syntax. We are also grateful to our colleagues Anna Alessandrello and Michela Mura for the editing of this huge volume, and to Claudio Pagliarin and Graziella Perini for scanning many photographs.

Fundamental technical support, which greatly improved our knowledge of *Scipionyx*, was given by the following persons and institutions:

Michele Zilioli (Laboratorio di Microscopia Elettronica, MSNM) operated the SEM for hours and captured all the SEM images and SEM element microanalyses published herein; Paolo Gentile (Dipartimento di Scienze Geologiche e Geotecnologie, Università degli Studi di Milano-Bicocca) gold-coated the microsamples for SEM; Roberto Appiani (Gruppo Mineralogico Lombardo) took all the photos under UV light and many other photos under visible light; Armando Cioffi (Computerized Tomography, Healthcare Sector Imaging, Siemens S.p.A., Milano) optimised the CT scan images, after operating with the equipment given at our disposal by Piero Biondetti (U.O. Radiologia, Fondazione Ospedale Maggiore IRCCS, Milano); Stefano Torricelli (SPES, Biostratigraphy & Sedimentology, ENI S.p.A., Exploration & Production Division, San Donato Milanese) and Paola Maffioli (Laboratorio di Micropaleontologia e Paleoecologia, Dipartimento di Scienze Geologiche e Geotecnologie, Università degli Studi di Milano-Bicocca) searched for microfossils in our sedimentological samples; Fabrizio Rigato and Maurizio Pavesi (Sezione di Entomologia, MSNM) assisted us in getting micro-measurements with the optical micrometer; Ermano Bianchi (Laboratorio di Tassidermia, MSNM) dissected some alligator hatchlings and birds for comparative anatomical observations; Stefany Potze and Lemmy Mashinini (Department of Herpetology, Transvaal Museum, Pretoria, South Africa) arranged the shipping of the Nile crocodile hatchling bones collected by Fritz Huchzermeyer (Onderstepoort Veterinary Institute).

Our very special, heartfelt thanks go to Marco Auditore, who passionately drew all the anatomical drawings of *Scipionyx*, improving them dozens of times according to our continuous new interpretations. Marco's boss, Fulvio Montaldo (Cantieri Navali di Sestri s.r.l., Genova), patiently endured the days off that Marco took in order to travel to the MSNM and study the specimen almost like us. In addition to Marco, who also worked with Arianna Nicora, many thanks are due to all other palaeoartists who accepted our proposal to produce their artwork free of charge, specifically for the present monograph: Davide Bonadonna, Paolo Cinquemani, Fabio Fogliazza, Lukas Panzarin, Fabio Pastori, Tullio Perentin, Loana Riboli, Emiliano "Troco" and Renzo Zanetti.

For helpful discussions we are grateful to a number of researchers (here listed in alphabetical order): Amy Balanoff, Vivianne Bernardo de Sant'Anna, Paulo Brito, Chris Brochu, Mauro Buttafava, Matt Carrano, Andrea Cau, Luis Chiappe, Dan Chure, Leon Claessens, Phil Currie, Massimo Delfino, Mike D'Emic, Cinzia Domeneghini, Greg Erickson, Alessandro Garassino, Stephen Gatesy, Alan Gishlick, Ursula Göhlich, Tom Holtz, Fritz Huchzermeyer, John Hutchinson, Alex Kellner, Dave Martill, Jesús Marugan, Francesco Mascarello, Octavio Matéus, François Meunier, Umberto Nicosia, Gregory Paul, Scott Persons, Fabio Petti, Karin Peyer, Federico Pezzotta, Stefano Scali, Mary Schweitzer, Giorgio Teruzzi, David Vesely, Larry Witmer and Xu Xing.

Among others, Phil Currie (University of Alberta, Edmonton) and Giorgio Teruzzi (MSNM) encouraged us in the past years to carry on with the study of the Pietraraja theropod; with the same aim, Stefania Nosotti (MSNM) translated for us some literature published in German.

Our bibliographic database improved with the help of Marco Auditore, Derek Briggs, Andrea Cau, Fulvio Gandolfi, Paola Livi, Lukas Panzarin, Mary Schweitzer and many others; Giorgio Chiozzi, Nicolai Christiansen, Lorenzo Crosta, and Luigi Scaccabarozzi provided useful references; Karen Gariboldi and Daniela Cipollone assisted us in arranging the paper-based, and the electronic archive.

Last but not least, we wish to thank also all persons who helped us in various ways in the past years, apologising if we have overlooked anybody: Enza Braca, Sergio Bravi, Cesare Brizio, Luigi Cagnolaro, Luigi Cazzaro, Maria Fariello, Fabio Fogliazza, Giovanna Gange mi, Henry Gee, Antonio Giannattasio, David Govoni, Eva Koppelhus, Anastasios Kotsakis, Peter Makovicky, Giuseppe Marramà, Rodolfo Martini, Ralph Molnar, Ermanno Montanara, Ferdinando Moretti Foggia, Franco Nodo, Mark Norell, Michael Novacek, Renato Pollini, Antonella Russo, Gianni Tafuni, Silvo Tassinari and Franco Valoti.

Special thanks

This monograph was written and published with the financial support of the Società Italiana di Scienze Naturali, the Museo di Storia Naturale di Milano and the following additional sponsors, painstakingly made aware of the importance of our work by our colleague Ilaria Vinassa Guaraldi de Regny: Bocconi Traverso & Partners; Beth Campbell Lasio, Giovanni Lasio and their friends; Cinehollywood S.r.l.; Hasbro Inc., IMCD Italia S.r.l.

REFERENCES

- AA.VV., 2005 – Nomina Anatomica Veterinaria. *The Editorial Committee*.
- Agnolin F. D., Ezcurra M. D., Pais D. F. & Salisbury S. W., 2010 – A reappraisal of the Cretaceous non-avian dinosaur faunas from Australia and New Zealand: evidence for their Gondwanan affinities. *Journal of Systematic Palaeontology*, 8 (2): 257-300.
- Andreassi G., Claps M., Sarti M., Nicosia U. & Ventura D., 1999 – The late Cretaceous Dinosaur tracksite near Altamura (Bari), Southern Italy. *Geitalia 1999, 2° Forum Italiano di Scienze della Terra. Riassunti*, 1: 28.
- Arduini P., 1993 – Research on Upper Permian Reptiles of Sakamena Formation (Madagascar). In: Evolution, ecology and biogeography of the Triassic Reptiles. Mazin J. M. & Pinna G. (eds.). *Paleontologia Lombarda*, N. Ser., II: 5-8.
- Avanzini M., Leonardi G., Masetti D. & Mietto P., 2000 – Conclusioni. In: Dinosauri in Italia. Le orme giurassiche dei Lavinini di Marco (Trentino) e gli altri resti fossili italiani. Leonardi G. & Mietto P. (eds.). *Accademia Editoriale*: 393-398.
- Azuma Y. & Currie P. J., 2000 – A new carnosaur (Dinosauria: Theropoda) from the Lower Cretaceous of Japan. *Canadian Journal of Earth Sciences*, 37: 1735-1753.
- Balanoff A. M. & Rowe T., 2007 – Osteological description of an embryonic skeleton of the extinct elephant bird, *Aepyornis* (Palaeognathae: Ratitae). *Society of Vertebrate Paleontology Memoir*, 9: 1-53.
- Balanoff A. M., Norell M. A., Grellet-Tinner G. & Lewin M. R., 2008 – Digital preparation of a probable neoceratopsian preserved within an egg, with comments on microstructural anatomy of ornithischian eggshells. *Naturwissenschaften*, 95: 493-500.
- Balanoff A. M., Xu X., Kobayashi Y., Matsufune Y. & Norell M. A., 2009 – Cranial Osteology of the Theropod Dinosaur *Incisivosaurus gauthieri* (Theropoda: Oviraptorosauria). *American Museum Novitates*, 3651: 1-35.
- Barbera C. & La Magna G., 1999 – Finding of ammonites in the ittiolithic limestones at Pietraraja. In: Third International Symposium on Lithographic Limestones. Renesto S. (ed.). *Rivista del Museo Civico di Scienze Naturali "E. Caffi"*, 20: 23-24.
- Barbera C. & Macuglia L., 1988 – Revisione dei tetrapodi del Cretacico inferiore di Pietraraja (Matese orientale, Benevento) appartenenti alla collezione Costa del Museo di Paleontologia dell'Università di Napoli. *Memorie della Società Geologica Italiana*, 41: 567-574.
- Barbera C. & Macuglia L., 1991 – Cretaceous herpetofauna of Pietraraja. In: Symposium on the Evolution of Terrestrial Vertebrates. Ghiara G. (ed.). *Unione Zoologica Italiana, Selected Symposia and Monographs*, 4: 421-429.
- Barsbold R., 1983 – Carnivorous dinosaurs from the Cretaceous of Mongolia. *Trudy Sovmestnoi Sovetsko-Mongolskoi Paleontologicheskoi Ekspeditsii*, 19: 1-117. [In Russian].
- Barsbold R. & Osmólska H., 1999 – The skull of *Velociraptor* (Theropoda) from the Late Cretaceous of Mongolia. *Acta Paleontologica Polonica*, 44: 189-219.
- Barsbold R. & Perle A., 1984 – The first record of a primitive ornithomimosaur from the Cretaceous of Mongolia. *Paleontological Journal*, 1984: 118-120.
- Barsbold R., Maryanska T. & Osmólska H., 1990 – Oviraptorosauria. In: The Dinosauria. Weishampel D. B., Dodson P. & Osmólska H. (eds.). *University of California Press*: 249-258.
- Bartirolo A., Barone Lumaga M. R. & Bravi S., 2006 – First finding of a fossil fern (Matoniaceae) in the paleontological site of Pietraraja (Benevento, Southern Italy). *Bollettino della Società Paleontologica Italiana*, 45 (1): 29-34.
- Bassani F., 1885 – Risultati ottenuti dallo studio delle principali ittiofaune cretatiche. *Rendiconti dell'Istituto Lombardo*, 18: 513-535.
- Baumel J. J. & Raikow R. J., 1993 – Arthrologia. In: Handbook of Avian Anatomy: Nomina Anatomica Avium. Baumel J. J., King A. S., Breazile J. E., Evans H. E. & Vanden Berge J. C. (eds.). *Nuttall Ornithological Club*: 133-187.
- Baumel J. J., King A. S., Breazile J. E., Evans H. E. & Vanden Berge J. C., 1993 – Handbook of Avian Anatomy: Nomina Anatomica Avium. *Nuttall Ornithological Club*.
- Bellairs A. & Jenkins C. R., 1960 – The skeleton of birds. In: Biology and comparative physiology of birds. Marshall A. J. (ed.). *Academic Press*: 241-300.
- Bennett S. C., 1993 – The ontogeny of *Pteranodon* and other pterosaurs. *Paleobiology*, 19: 92-106.
- Benson R. B. J., Carrano M. T. & Brusatte S. L., 2010 – A new clade of archaic large-bodied predatory dinosaurs (Theropoda: Allosauroidae) that survived to the latest Mesozoic. *Naturwissenschaften*, 97: 71-78.
- Benton M. J., Cook E., Grigorescu D., Popa E. & Tallódi E., 1997 – Dinosaurs and other tetrapods in an Early Cretaceous bauxite-filled fissure, northwestern Romania. *Palaogeography, Palaeoclimatology, Palaeoecology*, 130: 275-292.
- Berger A. J., 1960 – The musculature. In: Biology and comparative physiology of birds. Marshall A. J. (ed.). *Academic Press*: 301-344.
- Bever G. S. & Norell M. A., 2009 – The perinate skull of *Byronosaurus* (Troodontidae) with observations on the cranial ontogeny of paravian theropods. *American Museum Novitates*, 3657: 1-51.
- Biur K. & Thapliyal J. P., 1972 – Cranial Pneumatization in the Indian Weaver Bird, *Ploceus philippinus*. *The Condor*, 74 (2): 198-200.
- Blamires S. J., 2004 – Habitat Preferences of Coastal Goannas (*Varanus panoptes*): Are They Exploiters of Sea Turtle Nests at Fog Bay, Australia? *Copeia*, 2: 370-377.
- Bonaparte J. F., Novas F. E. & Coria R. A., 1990 – *Carnotaurus sastrei* Bonaparte, the horned, lightly built carnosaur from the Middle Cretaceous of Patagonia. *Natural History Museum of Los Angeles County, Contributions in Science*, 416: 1-42.
- Bosellini A., 2002 – Dinosaurs "re-write" the geodynamics of the eastern Mediterranean and the paleogeography of the Apulia Platform. *Earth Science Review*, 59: 211-234.
- Botte V. & Pelagalli G. V., 1982 – Anatomia funzionale degli uccelli domestici. *Edizioni Ermes*.
- Bottjer D. J., Etter W., Hagadorn J. W., Tang C. M. (eds.), 2002 – Exceptional fossil preservation. *Columbia University Press*.
- Brainerd E. L., 1999 – New perspectives on the evolution of lung ventilation mechanisms in vertebrates. *Experimental Biology Online*, 4: 11-28.
- Bravi S., 1987 – Contributo allo studio del giacimento ad ittioliti di Pietraraja (Benevento). *Dipartimento di Paleontologia, Università degli Studi di Napoli "Federico II", unpublished degree thesis*.
- Bravi S., 1988 – Contributo allo studio del giacimento ad Ittioliti di Pietraraja (Benevento). I. *Pleuropholis decastroi* n. sp. (Pisces, Actinopterygii, Pholidophoriformes). *Memorie della Società Geologica Italiana*, 41 (I): 575-586.
- Bravi S., 1994 – New observations on the Lower Cretaceous fish *Notagogus pentlandi* Agassiz (Actinopterygii, Halecostomi, Macrosemiidae). *Bollettino della Società Paleontologica Italiana*, 33: 51-70.

- Bravi S., 1999 – A tentative reassessment of the fauna and flora from the Pietraraja plattenkalk (Bn). In: Third International Symposium on Lithographic Limestones. Renesto S. (ed.). *Rivista del Museo Civico di Scienze Naturali "E. Caffi"*, 20: 39-41.
- Bravi S., & De Castro P., 1995 – The Cretaceous fossil fishes level of Capo d'Orlando, near Castellammare di Stabia (NA). Biostratigraphy and depositional environment. *Memorie di Scienze Geologiche*, 47: 45-72.
- Bravi S. & Garassino A., 1998 – New biostratigraphic and paleoecological observations on the Plattenkalk of the Lower Cretaceous (Albian) of Pietraraja (Benevento, S. Italy), and its decapod crustacean assemblage. *Atti della Società Italiana di Scienze Naturali e del Museo Civico di Storia Naturale di Milano*, 138/1997 (I-II): 119-171.
- Breislak S., 1798 – Topografia fisica della Campania. *Stamperia Antonio Brazzini*.
- Briggs D. E. G., 2003 – The role of decay and mineralization in the preservation of soft-bodied fossils. *Annual Review of Earth and Planetary Sciences*, 31: 275-301.
- Briggs D. E. G. & Kear A. J., 1993a – Fossilization of soft tissue in the laboratory. *Science*, 259: 1439-1442.
- Briggs D. E. G. & Kear A. J., 1993b – Decay and preservation of polychaetes: taphonomic thresholds in soft-bodied organisms. *Paleobiology*, 19: 107-135.
- Briggs D. E. G. & Wilby P. R., 1996 – The role of the calcium carbonate-calcium phosphate switch in the mineralization of soft-bodied fossils. *Journal of Geological Society*, 153: 665-668.
- Briggs D. E. G., Kear A. J., Martill D. M. & Wilby P. R., 1993 – Phosphatization of soft tissue in experiments and fossils. *Journal of the Geological Society*, 150: 1035-1038.
- Briggs D. E. G., Wilby P. R., Pérez-Moreno B. P., Sanz J. L. & Martínez M. F., 1997 – The mineralization of dinosaur soft tissue in the Lower Cretaceous of Las Hoyas, Spain. *Journal of the Geological Society*, 154 (4): 587-588.
- Britt B. B., 1991 – Theropods of Dry Mesa Quarry (Morrison Formation, Late Jurassic), Colorado, with emphasis on the osteology of *Torvosaurus tanneri*. *Brigham Young University Geology Studies*, 37: 1-72.
- Britt B. B. & Naylor B. G., 1994 – An embryonic *Camarasaurus* (Dinosauria, Sauropoda) from the Upper Jurassic Morrison Formation (Dry Mesa Quarry, Colorado). In: Dinosaur eggs and babies. Carpenter K., Hirsch K. F. & Horner J. R. (eds.). *Cambridge University Press*: 256-264.
- Brochu C. A., 1996 – Closure of neurocentral sutures during crocodylian ontogeny: implications for maturity assessment in fossil archosaurs. *Journal of Vertebrate Paleontology*, 16: 49-62.
- Brochu C. A., 2003 – Osteology of *Tyrannosaurus rex*: insights from a nearly complete skeleton and high-resolution computed tomographic analysis of the skull. *Society of Vertebrate Paleontology Memoir*, 7: 1-138.
- Bryant H. N. & Russell A. P., 1992 – The role of phylogenetic analysis in the inference of unpreserved attributes of extinct taxa. *Philosophical Transactions of the Royal Society, Series B*, 337: 405-418.
- Brusatte S. L., Carr T. D., Erickson G. M., Bever G. S. & Norell M. A., 2009 – A long-snouted, multihorned tyrannosaurid from the Late Cretaceous of Mongolia. *Proceedings of the National Academy of Sciences of the United States of America*, 106 (41): 17261-17266.
- Burnham D. A., Derstler K. L., Currie P. J., Bakker R. T., Zhou Z-H. & Ostrom J. H., 2000 – Remarkable new birdlike dinosaur (Theropoda: Maniraptora) from the Upper Cretaceous of Montana. *University of Kansas Paleontological Contributions, New Series*, 13: 1-14.
- Butler J. R. & Upchurch P., 2007 – Highly incomplete taxa and the phylogenetic relationships of the theropod dinosaur *Juravenator starki*. *Journal of Vertebrate Paleontology*, 27 (1): 253-256.
- Butterfield N. J., 2002 – *Leaenchoilia* guts and the interpretation of three-dimensional structures in Burgess Shale-type fossils. *Paleobiology*, 28: 155-171.
- Caldwell M. W. & Dal Sasso C., 2004 – Soft-tissue preservation in a 95 million year old marine lizard: form, function, and aquatic adaptation. *Journal of Vertebrate Paleontology*, 24 (4): 980-985.
- Canudo J. I., Barco J. L., Pereda-Suberbiola X., Ruiz-Omeñaca J. I., Salgado L., Fernández-Balador F. T. & Gasulla J. M., 2009 – What Iberian dinosaurs reveal about the bridge said to exist between Gondwana and Laurasia in the Early Cretaceous. *Bulletin de la Société Géologique de France*, 180 (1): 5-11.
- Carannante G., D'Argenio B., Dello Iacovo B., Ferreri V., Mindszenty A. & Simone L., 1988 – Studi sul carsismo cretacico dell'Appennino Campano. *Memorie della Società Geologica Italiana*, 41: 733-759.
- Carannante G., Pugliese A., Simone L. & Vigorito M., 2004 – A Cretaceous tectonically controlled carbonate margin: the case history of the Matese Mountains, central-southern Apennines, Italy. *23rd IAS Meeting of Sedimentology, Coimbra. Abstract Volume*: 79.
- Carannante G., Signore M. & Vigorito M., 2006 – Vertebrate-rich Plattenkalk of Pietraraja (Lower Cretaceous, Southern Apennines, Italy): a new model. *Facies*, 52: 555-577.
- Carpenter K., 1994 – Baby *Dryosaurus* from the Upper Jurassic Morrison Formation of Dinosaur National Monument. In: Dinosaur eggs and babies. Carpenter K., Hirsch K. F. & Horner J. R. (eds.). *Cambridge University Press*: 288-297.
- Carpenter K., 1999 – Eggs, nests, and baby dinosaurs. A look at dinosaur reproduction. *Indiana University Press*.
- Carpenter K., 2002 – Forelimb biomechanics of nonavian theropod dinosaurs in predation. *Senckenbergiana lethaea*, 82 (1): 59-76.
- Carpenter K., Miles C., & Cloward K., 2005a – New small theropods from the upper Jurassic Morrison Formation of Wyoming. In: The Carnivorous Dinosaurs. Carpenter K. (ed.). *Indiana University Press*: 23-48.
- Carpenter K., Miles C., Ostrom J. H. & Cloward K., 2005b – Redescription of the small maniraptoran theropods *Ornitholestes* and *Coelurus* from the Upper Jurassic Morrison Formation of Wyoming. In: The Carnivorous Dinosaurs. Carpenter K. (ed.). *Indiana University Press*: 49-71.
- Carr T. D. & Williamson T. E., 2004 – Diversity of late Maastrichtian Tyrannosauridae (Dinosauria: Theropoda) from western North America. *Zoological Journal of the Linnean Society*, 142: 479-523.
- Carrano M. T. & Hutchinson J. R., 2002 – Pelvic and Hindlimb Musculature of *Tyrannosaurus rex* (Dinosauria: Theropoda). *Journal of Morphology*, 253: 207-228.
- Carrano M. T. & Sampson S. D., 2008 – The phylogeny of Ceratosauria. *Journal of Systematic Palaeontology*, 6 (2): 183-236.
- Carrano M. T., Sampson S. D. & Forster C. A., 2002 – The osteology of *Masiakasaurus knopfleri*, a small abelisauroid (Dinosauria: Theropoda) from the Late Cretaceous of Madagascar. *Journal of Vertebrate Paleontology*, 22: 510-534.
- Carrano M. T., Hutchinson J. R. & Sampson S. D., 2005 – New information on *Segisaurus halli*, a small theropod dinosaur from the Early Jurassic of Arizona. *Journal of Vertebrate Paleontology*, 25: 835-849.
- Carrier D. R. & Farmer C. G., 2000 – The evolution of pelvic aspiration in archosaurs. *Paleobiology*, 26: 271-293.

- Carroll R. L., 1977 – The origin of lizards. In: Problems in vertebrate evolution. Andrews S. M., Miles R. S. & Walker A. D. (eds.). *Linnean Society Symposium Series no. 4, Academic Press*: 359-396.
- Carroll R. L., 1988 – Vertebrate Paleontology and Evolution. *John Wiley & Sons*.
- Catenacci E. & Manfredini M., 1963 – Osservazioni stratigrafiche sulla Civita di Pietrarroia (Benevento). *Bollettino della Società Geologica Italiana*, 82: 65-92.
- Cati A., Sartorio D. & Venturini S., 1989 – Carbonate platforms in the subsurface of the Northern Adriatic Area. *Memorie della Società geologica Italiana*, 40: 295-308.
- Cavitt L. C., Youm G. W., Meullenet J. F., Owens C. M. & Xiong R., 2004 – Prediction of poultry meat tenderness using razor blade shear, allo-Kramer shear, and sarcomere length. *Journal of Food Science*, 69 (1): 1-8.
- Channel J. E. T., D'Argenio B. & Horwath F., 1979 – Adria, the African Promontory, in Mesozoic Mediterranean Paleogeography. *Earth Science Reviews*, 15: 213-292.
- Charig A. J. & Milner A. C., 1986 – *Baryonyx*, a remarkable new theropod dinosaur. *Nature*, 324: 359-361.
- Chen P. J., Dong Z. & Zhen S., 1998 – An exceptionally well-preserved theropod dinosaur from the Yixian Formation of China. *Nature*, 391: 147-152.
- Chiappe L. M., Norell M. A. & Clark J. M., 2002 – The Cretaceous, short-armed Alvarezsauridae: *Mononykus* and its kin. In: Mesozoic birds: above the heads of dinosaurs. Chiappe L. M. & Witmer L. M. (eds.). *University of California Press*: 87-119.
- Chin K. & Bishop J., 2007 – Exploited twice: bored bone in a theropod coprolite from the Jurassic Morrison Formation of Utah, USA. In: Sediment-Organism Interactions: A Multifaceted Ichnology. Bromley R. G., Buatois L. A., Mángano M. G., Genise J. F. & Melchor R. N. (eds.). *SEPM Special Publications*, 88: 379-387.
- Chin K., Tokaryk T. T., Erickson G. M. & Calk L. C., 1998 – A king-sized theropod coprolite. *Nature*, 393: 680-682.
- Chin K., Eberth D. A., Schweitzer M. H., Rando T. A., Sloboda W. J. & Horner J. R., 2003 – Remarkable preservation of undigested muscle-tissue within a late Cretaceous tyrannosaurid coprolite from Alberta, Canada. *Palaos*, 18 (3): 286-294.
- Chinsamy A. & Hillenius W. J., 2004 – Physiology of nonavian dinosaurs. In: The Dinosauria. 2nd edition. Weishampel D. B., Dodson P. & Osmólska H. (eds.). *University of California Press*: 643-659.
- Choiniere J. N., Clark J. M., Forster C. A. & Xu X., 2010 – A basal coelurosaur (Dinosauria: Theropoda) from the Late Jurassic (Oxfordian) of the Shishugou Formation in Wucuiwan, People's Republic of China. *Journal of Vertebrate Paleontology*, 30 (6): 1773-1796.
- Chure D. J., 2001 – The wrist of *Allosaurus* (Saurischia: Theropoda), with observations on the carpus in theropods. In: New perspectives on the origin and early evolution of birds: proceedings of the International Symposium in Honor of John H. Ostrom. Gauthier J. & Gall L. F. (eds.). *Peabody Museum of Natural History, Yale University*: 283-300.
- Chure D. J. & Madsen J. H., 1996 – On the presence of furculae in some nonmaniraptoran theropods. *Journal of Vertebrate Paleontology*, 16: 63-66.
- Cillari A., Di Stefano P., Guzzetta D., Nicosia U., Petti F. M. & Zarcone G., 2009 – Back to Adria, the African Promontory: geological and palaeontological constraints from central and southern Italy. *International Conference on Vertebrate Palaeobiogeography and continental bridges across Tethys, Mesogea, and Mediterranean Sea. Museo Geologico Giovanni Capellini, Dipartimento di Scienze della Terra e Geologico-Ambientali (28–29 September 2009). Abstract Book*: 28-30.
- Claessens L. P. A. M., 2004 – Dinosaur gastralia; origin, morphology, and function. *Journal of Vertebrate Paleontology*, 24 (1): 89-106.
- Clark J. M., Perle A., & Norell M. A., 1994 – The skull of *Erlingosaurus andrewsi*, a Late Cretaceous “segnosaur” (Theropoda: Therizinosauridae) from Mongolia. *American Museum Novitates*, 3115: 1-39.
- Clark J. M., Norell M. A. & Chiappe L., 1999 – An oviraptorid skeleton from the Late Cretaceous of Ukhaa Tolgod, Mongolia, preserved in an avian-like brooding position over an oviraptorid nest. *American Museum Novitates*, 3265: 1-36.
- Clark J. M., Norell M. A. & Barsbold R., 2001 – Two new oviraptorids (Theropoda: Oviraptorosauria) Late Cretaceous Djadokhta Formation, Ukhaa Tolgod, Mongolia. *Journal of Vertebrate Paleontology*, 21: 209-213.
- Clark J. M., Norell M. A. & Rowe T., 2002 – Cranial Anatomy of *Citipati osmolskai* (Theropoda, Oviraptorosauria), and a reinterpretation of the holotype of *Oviraptor philoceratops*. *American Museum Novitates*, 3364: 1-26.
- Cocude-Michel M., 1963 – Les Rhynchocephales et les Sauriens des Calcaires Lithographiques (Jurassique-Superieur) d'Europe Occidentale. *Nouvelles Archives du Museum d'Histoire Naturelle de Lyon*, 7: 1-187.
- Codd J. R., Manning P. L., Norell M. A. & Perry S. F., 2007 – Avian-like breathing mechanics in maniraptoran dinosaurs. *Proceeding of the Royal Society B*, 1233: 1-5.
- Colbert E. H., 1989 – The Triassic dinosaur *Coelophysis*. *Museum of Northern Arizona Bulletin*, 57: 1-160.
- Colbert E. H. & Russell D. A., 1969 – The small Cretaceous dinosaur *Dromaeosaurus*. *American Museum Novitates*, 2380: 1-49.
- Conti M. A., Morsilli M., Nicosia U., Sacchi E., Savino V., Wagensommer A., Di Maggio L. & Gianolla P., 2005 – Jurassic Dinosaur Footprints From Southern Italy: Footprints as Indicators of Constraints in Paleogeographic Interpretation. *Palaos*, 20 (6): 534-550.
- Coombs Jr. W. P., 1982 – Juvenile specimens of the ornithischian dinosaurs *Psittacosaurus*. *Palaontology*, 25: 89-107.
- Coria R. A. & Currie P. J., 2006 – A new carcharodontosaurid (Dinosauria, Theropoda) from the Upper Cretaceous of Argentina. *Geodiversitas*, 28 (1): 71-118.
- Costa O. G., 1851 – Cenni intorno alle scoperte fatte nel Regno riguardante la Paleontologia. *Il Filiale Sebezio*, 21: 40-46.
- Costa O. G., 1853-1864 – Paleontologia del Regno di Napoli, I-III. *Atti Accademia Pontaniana*, 5, 7, 8.
- Costa O. G., 1865 – Studi sopra i terreni ad Ittioliti delle Provincie napolitane diretti a stabilire l'età geologica de' medesimi. Parte II: Calcarea stratosia di Pietrarroja. *Atti dell'Accademia delle Scienze Fisiche e Matematiche di Napoli*, s. 2, 2 (16): 1-33.
- Costa O. G., 1866 – Nuove osservazioni e scoperte intorno ai fossili della calcarea ad ittioliti di Pietrarroja. *Atti dell'Accademia delle Scienze Fisiche e Matematiche di Napoli*, s. 1, 2 (22): 1-12.
- Cross H. R., West R. L. & Dutson T. R., 1981 – Comparison of methods for measuring sarcomere length in beef semitendinosus muscle. *Meat Science*, 5: 261-266.
- Currie P. J., 1995 – New information on the anatomy and relationships of *Dromaeosaurus albertensis* (Dinosauria: Theropoda). *Journal of Vertebrate Paleontology*, 15: 576-591.
- Currie P. J., 2003 – Cranial anatomy of tyrannosaurid dinosaurs from the Late Cretaceous of Alberta, Canada. *Acta Palaeontologica Polonica*, 48 (2): 191-226.
- Currie P. J. & Chen P. J., 2001 – Anatomy of *Sinosauropteryx prima* from Liaoning, northeastern China. *Canadian Journal of Earth Sciences*, 38: 1705-1727.

- Currie P. J. & Dong Z., 2001 – New information on Cretaceous troodontids (Dinosauria, Theropoda) from the People's Republic of China. *Canadian Journal of Earth Sciences*, 38: 1753-1766.
- Currie P. J. & Russell D. A., 1988 – Osteology and relationships of *Chirostenotes pergracilis* (Saurischia, Theropoda) from the Judith River (Oldman) Formation of Alberta, Canada. *Canadian Journal of Earth Sciences*, 25: 972-986.
- Currie P. J. & Zhao X. J., 1993a – A new carnosaur (Dinosauria, Theropoda) from the Jurassic of Xinjiang, People's Republic of China. *Canadian Journal of Earth Sciences*, 30: 2037-2081.
- Currie P. J. & Zhao X. J., 1993b – A new troodontid (Dinosauria, Theropoda) braincase from the Dinosaur Park Formation (Campanian) of Alberta. *Canadian Journal of Earth Sciences*, 30: 2231-2247.
- Currie P. J., Hurum J. H. & Sabath K., 2003 – Skull structure and evolution in tyrannosaurid dinosaurs. *Acta Palaeontologica Polonica*, 48 (2): 227-234.
- Dalla Vecchia F. M., 2001 – The Mesozoic Periadriatic Carbonate Platforms as terrestrial ecosystems: the vertebrate evidence. *VII International Symposium on Mesozoic Terrestrial Ecosystems, Buenos Aires, 26 September-1 October 1999, Abstracts*: 20-21.
- Dalla Vecchia F. M., 2002 – Cretaceous dinosaurs in the Adriatic-Dinaric Carbonate Platform (Italy and Croatia): paleoenvironmental implications and paleogeographical hypotheses. *Memorie della Società Geologica Italiana*, 57 (1): 89-100.
- Dalla Vecchia F. M., 2005 – Between Gondwana and Laurasia: Cretaceous Sauropods in an Intraoceanic Carbonate Platform. In: *Thunder Lizards: The Sauropodomorph Dinosaurs*. Carpenter K. & Tidwell V. (eds.). *Indiana University Press*: 395-429.
- Dalla Vecchia F. M., 2009 – *Tethyshadros insularis*, a new hadrosauroid dinosaur (Ornithischia) from the Upper Cretaceous of Italy. *Journal of Vertebrate Paleontology*, 29 (4): 1100-1116.
- Dalla Vecchia F. M., Tarlao A., Tunis G. & Venturini S., 2000 – New dinosaur track sites in the Albian (Early Cretaceous) of the Istrian Peninsula (Croatia). *Memorie di Scienze Geologiche*, 52: 193-292.
- Dalla Vecchia F. M., Tarlao A., Tunis G. & Venturini S., 2001 – Dinosaur track sites in the upper Cenomanian (Late Cretaceous) of the Istrian peninsula (Croatia). *Bollettino della Società Paleontologica Italiana*, 40: 25-54.
- Dal Sasso C., 2001 – Dinosauri italiani. *Marsilio Editore*.
- Dal Sasso C., 2002 – Update on Italian dinosaurs: witnesses of a terrestrial, epicontinental ecosystem. *8th International Symposium on Mesozoic Terrestrial Ecosystems, Cape Town (South Africa), 21-26 July 2002, Abstract Book*: 24.
- Dal Sasso C., 2003 – Les dinosaures d'Italie. In: *Les dinosaures d'Europe/European Dinosaurs*. Padian K., de Ricqlès A. & Taquet T. (eds.). *Comptes Rendus Palevol, Académie des Sciences de Paris*, 2 (1): 45-66.
- Dal Sasso C., 2004 – Dinosaurs of Italy. *Indiana University Press*.
- Dal Sasso C. & Maganuco S., 2009 – Osteology, ontogenetic assessment, phylogeny, paleobiology, and soft-tissue anatomy of *Scipionyx sammiticus*. *Journal of Vertebrate Paleontology*, 29 (3, suppl.): 84A.
- Dal Sasso C. & Signore M., 1998a – Exceptional soft-tissue preservation in a theropod dinosaur from Italy. *Nature*, 392: 383-387.
- Dal Sasso C. & Signore M., 1998b – *Scipionyx sammiticus* (Theropoda, Coelurosauria) and its exceptionally preserved internal organs. *Journal of Vertebrate Paleontology*, 18 (3, suppl.): 37A.
- D'Argenio B., 1963 – I calcari ad ittioliti del Cretacico inferiore del Matese. *Atti dell'Accademia delle Scienze Fisiche e Matematiche*, 4 (3): 1-63.
- D'Argenio B., 1976 – Le piattaforme carbonatiche periadriatiche. Una rassegna di problemi nel quadro geodinamico mesozoico dell'area mediterranea. *Memorie della Società Geologica Italiana*, 13 (2, suppl.): 137-159.
- D'Argenio B., Pescatore T. & Scandone P., 1973 – Schema geologico dell'Appennino Meridionale (Campania, Lucania). *Accademia Nazionale dei Lincei, Quaderno*, 183: 49-72.
- D'Emic M., 2009 – The evolution of tooth replacement rates in sauropod dinosaurs. *Journal of Vertebrate Paleontology*, 29 (3, suppl.): 84A.
- D'Erasmo G., 1914 – La fauna e l'età dei calcari ad ittioliti di Pietraroia (Prov. di Benevento). *Palaeontographia italiana*, 20: 29-86.
- D'Erasmo G., 1915 – La fauna e l'età dei calcari ad ittioliti di Pietraroia (Prov. di Benevento). *Palaeontographia italiana*, 21: 1-53.
- de Klerk W. J., Forster C. A., Sampson S. D., Chinsamy A. & Ross C. F., 2000 – A new coelurosaurian dinosaur from the Early Cretaceous of South Africa. *Journal of Vertebrate Paleontology*, 20: 324-332.
- DeLamater E. D. & Courtenay W. R. Jr., 1974 – Fish scales as seen by scanning electron microscopy. *Florida Scientist*, 37: 141-149.
- Dercourt J., Ricou L. E. & Vrielynck B., 1993 – Atlas Tethys Palaeoenvironmental Maps. *P. Gauthier-Villars*.
- Dercourt J., Gaetani M., Vrielynck B., Barriere E., Biju-Duval B., Brunet M. F., Cadet J. P., Crasquin S. & Sandulescu M. E., 2000 – Atlas Peri-Tethys, Palaeogeographical Maps. *Carte Géologique du Monde / Commission for the Geologic Map of the World*.
- de Ricqlès A. J., Padian K., Horner J. R. & Francillon-Viellet H., 2000 – Paleohistology of the bones of pterosaurs (Reptilia: Archosauria): anatomy, ontogeny, and biomechanical implications. *Zoological Journal of the Linnean Society*, 129: 349-385.
- Diefenbach C., 1975 – Gastric function in *Caiman crocodilus* (Crocodylia: Reptilia). I. Rate of gastric digestion and gastric motility as a function of temperature. *Comparative Biochemistry and Physiology*, 51A: 259-265.
- D'Orazi Porchetti S., Conti M. A., Nicosia U., Mariotti N., Petti F. M., Sacchi E. & Valentini M., 2008 – Italian Vertebrate Ichnology Reference List. *Studi Trentini di Scienze Naturali, Acta Geologica*, 83: 335-347.
- Dunham R. J., 1962 – Classification of carbonate rocks according to depositional texture. In: *Classification of carbonate rocks*. Ham W. E. (ed.). *American Association of Petroleum Geologists, Memoir*, 1: 108-121.
- Duncker H. R., 1972 – Structure of the avian lungs. *Respiration Physiology*, 14 (1-2): 44-63.
- Edmund A. G., 1969 – Dentition. In: *Biology of the Reptilia*, Vol. 1: Morphology A. Gans C., Bellairs A. & Parson T. S. (eds.). *Academic Press*: 117-200.
- Elzanowski A., 2002 – Archaeopterygidae (Upper Jurassic of Germany). In: *Mesozoic birds: above the heads of dinosaurs*. Chiappe L. M. & Witmer L. M. (eds.). *University of California Press*: 129-159.
- Erickson G. M., 1996a – Daily deposition of dentine in juvenile *Alligator* and assessment of tooth replacement rates using incremental line counts. *Journal of Morphology*, 228: 189-194.
- Erickson G. M., 1996b – Incremental lines of von Ebner in dinosaurs and the assessment of tooth replacement rates using growth line counts. *Proceedings of the National Academy of Science*, 93: 14623-14627.

- Erickson G. M., Curry-Rogers K. & Yerby S. A., 2001 – Dinosaurian growth patterns and rapid avian growth rates. *Nature*, 412: 429-433.
- Estes R., 1983 – Sauria Terrestria, Amphisbaenia. In: *Handbuch der Paläoherpertologie 10A*. Wellnhofer P. (ed.). *Gustav Fischer Verlag*.
- Estes R., de-Queiroz K. & Gauthier J. A., 1988 – Phylogenetic relationships within Squamata. In: *Phylogenetic relationships of the lizard families*. Estes R. & Pregill G. (eds.). *Stanford University Press*: 119-282.
- Evans S. E., Raia P. & Barbera C., 2004 – New lizards and rhynchocephalians from the Lower Cretaceous of southern Italy. *Acta Palaeontologica Polonica*, 49 (3): 393-408.
- Evans S. E., Raia P. & Barbera C., 2006 – The Lower Cretaceous lizard genus *Chometokadmon* from Italy. *Cretaceous Research*, 27: 673-683.
- Farmer C. G., 2006 – On the origin of avian air sacs. *Respiratory Physiology & Neurobiology*, 154: 89-106.
- Farmer C. G. & Sanders K., 2010 – Unidirectional Airflow in the Lungs of Alligators. *Science*, 327: 338-340.
- Finetti I. R., 2005 – Ionian and Alpine Neotethyan Ocean opening. In: *CROP PROJECT: Deep Seismic Exploration of the Central Mediterranean and Italy*. Finetti I. R. (ed.). *Elsevier*: 103-107.
- Fisher P. E., Russell D. A., Stoskopf M. K., Barrick R. E., Hammer M. & Kuzmitz A. A., 2000 – Cardiovascular Evidence for an Intermediate or Higher Metabolic Rate in an Ornithischian Dinosaur. *Science*, 288: 503-505.
- Freels D., 1975 – Plattenkalk-Becken bei Pietraroia (Prov. Benevento, S-Italien) als Voraussetzung einer Fossilagerstätten-Bildung. *Neues Jahrbuch für Geologie und Paläontologie, Abhandlungen*, 148: 320-352.
- Frey E., 1988 – Anatomie des Körperstammes von *Alligator mississippiensis* Daudin. *Stuttgarter Beiträge zur Naturkunde A*, 24: 1-106.
- Frey E., Tischlinger H., Buchy M.-C. & Martill D. M., 2003 – New specimens of Pterosauria (Reptilia) with soft parts with implications for pterosaurian anatomy and locomotion. In: *Evolution and Palaeobiology of Pterosaurs*. Buffetaut E. & Mazin J.-M. (eds.). *Geological Society Special Publications*, 217: 233-266.
- Galton P. M., 1990 – Basal Sauropodomorpha-Prosauropoda. In: *The Dinosauria*. Weishampel D. B., Dodson P. & Osmólska, H. (eds.). *University of California Press*: 320-344.
- Garassino A. & Schweigert G., 2006 – The Upper Jurassic Solnhofen decapod crustacean fauna: review of the types from old descriptions. Part I. Infraorders Astacidea, Thalassinidea, and Palinura. *Memorie della Società Italiana di Scienze Naturali e del Museo Civico di Storia Naturale di Milano*, 34 (1): 3-44.
- Garilli V., Klein N., Buffetaut E., Sander P. M., Pollina F., Galletti L., Cillari A. & Guzzetta D., 2009 – First dinosaur bone from Sicily identified by histology and its paleobiogeographical implications. *Neues Jahrbuch für Geologie und Paläontologie, Abhandlungen*, 252 (2): 207-216.
- Gatesy S. M., 1990 – Caudofemoral musculature and the evolution of theropod locomotion. *Paleobiology*, 16: 170-186.
- Gauthier J., 1986 – Saurischian monophyly and the origin of birds. In: *The Origin of Birds and the Evolution of Flight*. Padian K. (ed.). *Memoirs of the Californian Academy of Sciences*, 8: 1-55.
- Gauthier J. A., Estes R. & de-Queiroz K., 1988 – A phylogenetic analysis of Lepidosauromorpha. In: *Phylogenetic relationships of the lizard families*. Estes R. & Pregill G. (eds.). *Stanford University Press*: 15-98.
- Geist N. R. & Jones D. G., 1996 – Juvenile skeletal structure and the reproductive habits of dinosaurs. *Science*, 272: 712-714.
- George J. C. & Berger A. J., 1966 – Avian myology. *Academic Press*.
- Gianolla P., Morsilli M. & Bosellini A., 2000a – First discovery of Early Cretaceous dinosaur footprints in the Gargano Promontory (Apulia carbonate platform, southern Italy). In: *Quantitative Models on Cretaceous Carbonates and the Eastern Margin of the Apulia Platform*. Global Sedimentary Geology Program (GSGP), Cretaceous Resources Events and Rhythms (CRER) Working Group 4 (eds.). Vieste, Gargano, Italy. September 25th-28th 2000, *Abstract Book*: 9.
- Gianolla P., Morsilli M., Dalla Vecchia F. M., Bosellini A. & Russo A., 2000b – Impronte di dinosauri nel Cretaceo inferiore del Gargano (Puglia, Italia Meridionale): nuove implicazioni paleogeografiche. *80^a Riunione Estiva della Società Geologica Italiana, Trieste, 6-8 settembre 2000. Riassunti*: 265-266.
- Gianolla P., Morsilli M. & Bosellini A., 2001 – Impronte di dinosauri nel Gargano. In: *Cenni di Geologia e itinerari geologici. Il Promontorio del Gargano*. Bosellini A. & Morsilli M. (eds.). Box 1.2.
- Gishlick A. D. & Gauthier J. A., 2007 – On the manual morphology of *Compsognathus longipes* and its bearing on the diagnosis of Compsognathidae. *Zoological Journal of the Linnean Society*, 149: 569-581.
- Godfrey S. J. & Currie P. J., 2004 – A theropod (Dromaeosauridae, Dinosauria) sternal plate from the Dinosaur Park Formation (Campanian, Upper Cretaceous) of Alberta, Canada. In: *Feathered Dragons*. Currie P. J., Koppelhus E. B., Shugar M. A. & Wright J. L. (eds.). *Indiana University Press*: 144-149.
- Göhlich U. B. & Chiappe L. M., 2006 – A new carnivorous dinosaur from the Late Jurassic Solnhofen archipelago. *Nature*, 440: 329-332.
- Göhlich U. B., Tischlinger H. & Chiappe L. M., 2006 – *Jurave-nator starki* (Reptilia, Theropoda), ein neuer Raubdinosaurier aus dem Oberjura der südlichen Frankenalb (Süddeutschland): Skelettanatomie und Weichteilbefunde. *Archaeopteryx*, 24: 1-26.
- Goodwin M. B., Clemens W. A., Horner J. R. & Padian K., 2006 – The smallest known *Triceratops* skull: new observations on ceratopsid cranial anatomy and ontogeny. *Journal of Vertebrate Paleontology*, 26: 103-112.
- Gradstein F. M., Ogg J. G. & Smith A. G. (eds.), 2004 – A Geologic Time Scale 2004. *Cambridge University Press*.
- Grigorescu D., Venczel N., Csiki Z. & Limborea R., 1999 – New latest Cretaceous microvertebrate fossil assemblages from the Hateg basin (Romania). *Geologie en Mijnbouw*, 78: 310-314.
- Hirschler A., Lucas J. & Hubert J.-C., 1990 – Bacterial involvement in apatite genesis. *FEMS Microbiology Ecology*, 73: 211-220.
- Hoffstetter R. & Gasc J. P., 1969 – Vertebrae and ribs of modern reptiles. In: *Biology of the Reptilia*. Gans C. (ed.). *Academic Press*, 1: 201-310.
- Holliday C. M., 2009 – New insights into dinosaur jaw muscle anatomy. *Anatomical Record*, 292: 1246-1265.
- Holtz T. R. Jr., 1994 – The phylogenetic position of the Tyrannosauridae: implication for theropod systematics. *Journal of Paleontology*, 68: 1100-1117.
- Holtz T. R. Jr., 1996 – Phylogenetic taxonomy of the Coelurosauria (Dinosauria: Theropoda). *Journal of Paleontology*, 70: 536-538.
- Holtz T. R. Jr., 2000 – A new phylogeny of the carnivorous dinosaurs. *Gaia*, 15: 5-61.
- Holtz T. R. Jr., 2004 – Tyrannosauroidae. In: *The Dinosauria* (2nd edition). Weishampel D. B., Dodson P. & Osmólska H. (eds.). *University of California Press*: 111-136.

- Holtz T. R. Jr., Molnar R. E. & Currie P. J., 2004 – Basal Tetanurae. In: *The Dinosauria* (2nd edition). Weishampel D. B., Dodson P. & Osmólska H. (eds.). *University of California Press*: 71-110.
- Hone D. W. E., Tischlinger H., Xu X. & Zhang F., 2010 – The Extent of the Preserved Feathers on the Four-Winged Dinosaur *Microraptor gui* under Ultraviolet Light. *PLoS ONE*, 5 (2): e9223.
- Horner J. R. & Currie P. J., 1994 – Embryonic and neonatal morphology and ontogeny of a new species of *Hypacrosaurus* (Ornithischia, Lambeosauridae) from Montana and Alberta. In: *Dinosaur eggs and babies*. Carpenter K., Hirsch K. F. & Horner J. R. (eds.). *Cambridge University Press*: 312-337.
- Horner J. R., de Ricqlès A. & Padian K., 2000 – Long bone histology of the hadrosaurid dinosaur *Maiasaura peeblesorum*: growth dynamics and physiology based on an ontogenetic series of skeletal elements. *Journal of Vertebrate Paleontology*, 20 (1): 115-129.
- Huchzermeyer F. W., 2000 – Le patologie dello struzzo e degli altri ratiti. *Papi Editore*.
- Huchzermeyer F. W., 2003 – Crocodiles: Biology, Husbandry and Diseases. *Centre for Agricultural Bioscience International Publishing*.
- Hutchinson J. R., 2001 – The evolution of femoral osteology and soft tissues on the line to extant birds (Neornithes). *Zoological Journal of the Linnean Society*, 131: 169-197.
- Hutchinson J. R. & Gatesy S. M., 2000 – Adductors, abductors, and the evolution of archosaur locomotion. *Paleobiology*, 26: 734-751.
- Hutt S., Martill D. A. & Barker M. J., 1996 – The first European allosaurid dinosaur (Lower Cretaceous, Wealden Group, England). *Neues Jahrbuch für Geologie und Paläontologie, Monatshefte*, 1996 (10): 635-644.
- Hwang S. H., Norell M. A., Qiang J. & Keqin G., 2002 – New specimens of *Microraptor zhaoianus* (Theropoda: Dromaeosauridae) from northeastern China. *American Museum Novitates*, 3381: 1-44.
- Hwang S. H., Norell M. A., Qiang J. & Keqin G. A., 2004 – Large compsognathid from the Early Cretaceous Yixian Formation of China. *Journal of Systematic Paleontology*, 2 (1): 13-30.
- Iniesto M., Lopez-Archilla A., Buscalioni A. D., Penalver E., Fregenal-Martinez M. A. & Guerrero M. C., 2009 – Experimental simulation of initial stages of fossilisation by bacterial sealing. Implications for the formation of Las Hoyas Konservat-Lagerstätte (Lower Cretaceous, Iberian Ranges, Spain). In: 5th International Symposium on Lithographic Limestone and Plattenkalk. Billon-Bruyat J. P., Marty D., Costeur L., Meyer C.A. & Thuring B. (eds.). *Actes 2009 bis de la Société Jurassienne d'émulation*: 46-47.
- Jamroz D., Wartecki T., Wilczkiewicz A., Orda J., & Skrupinska J., 2004 – Dynamics of yolk sac resorption and post-hatching development of the gastrointestinal tract in chickens, ducks and geese. *Journal of Animal Physiology and Animal Nutrition*, 88 (5-6): 239-250.
- Janes D. & Gutzke W. H. N., 2002 – Factors Affecting Retention Time of Turtle Scutes in Stomachs of American Alligators, *Alligator mississippiensis*. *American Midland Naturalist*, 148 (1): 115-119.
- Ji Q., Currie P. J., Norell M. A. & Ji S. A., 1998 – Two feathered dinosaurs from North-eastern China. *Nature*, 393: 753-761.
- Ji Q., Norell M. A., Makovicky P. J., Gao K., Ji S. & Yuan C., 2003 – An early ostrich dinosaur and implication for ornithomimosaur phylogeny. *American Museum Novitates*, 3420: 1-19.
- Ji Q., Ji S., Lü J. & You H., 2005 – First avialian bird from China, *Jinfengopteryx elegans* gen. et sp. nov. *Geological Bulletin of China*, 24 (3): 197-210.
- Ji Q., Ji S., Lü J. & Yuan C., 2007a – A New Giant Compsognathid Dinosaur with Long Filamentous Integuments from Lower Cretaceous of Northeastern China. *Acta Geologica Sinica*, 81: 8-15.
- Ji S., Gao C., Liu J., Meng Q. & Ji Q., 2007b – New Material of *Sinosauropteryx* (Theropoda: Compsognathidae) from Western Liaoning, China. *Acta Geologica Sinica*, 81: 177-182.
- Jianu C.-M. & Weishampel D. B., 1999 – The smallest of the largest. A new look at possible dwarfing in sauropod dinosaurs. *Geologie en Mijnbouw*, 78: 335-343.
- Kadler K. E., Holmes D. F., Trotter J. A. & Chapman J. A., 1996 – Collagen fibril formation. *Biochemical Journal*, 316: 1-11.
- Kardong K.V., 1997 – Vertebrates: Comparative Anatomy, Function, Evolution. *McGraw-Hill*.
- Kellner A. W. A., 1996a – Remarks on Brazilian dinosaurs. *Memoirs of the Queensland Museum*, 39: 611-626.
- Kellner A. W. A., 1996b – Fossilised theropod soft-tissue. *Nature*, 379: 32.
- Kellner A. W. A., 1999 – Short note on a new dinosaur (Theropoda, Coelurosauria) from the Santana Formation (Romualdo Member, Albian), Northeastern Brazil. *Boletim do Museu Nacional, N.S.*, 49: 1-8.
- Killops S. D. & Killops V. J., 1993 – An Introduction to Organic Geochemistry. *Longman Scientific and Technical*.
- Kirkland J. I. & Wolfe D. G., 2001 – First definitive therizinosaurid (Dinosauria: Theropoda) from North America. *Journal of Vertebrate Paleontology*, 21: 410-414.
- Kirkland J. I., Britt B. B., Whittle C. H., Madsen S. K. & Burge D. L., 1998 – A small coelurosaurian theropod from the Yellow Cat Member of the Cedar Mountain Formation (Lower Cretaceous, Barremian) of eastern Utah. In: *Lower and Middle Cretaceous Ecosystems*. Lucas S. G., Kirkland J. I. & Estep J. W. (eds.). *New Mexico Museum of Natural History and Science Bulletin*, 14: 239-248.
- Kirkland J. I., Zanno L. E., Sampson S. D., Clark J. M. & DeBlieux D. D., 2005 – A primitive therizinosaurid dinosaur from the Early Cretaceous of Utah. *Nature*, 7038: 84-87.
- Kitching I. J., Forey P. L., Humphries C. J., & Williams D. M., 1998 – Cladistics. Second Edition. The Theory and Practice of Parsimony Analysis. *Oxford University Press*: 1-228.
- Klasing K. C., 1998 – Comparative avian nutrition. *Centre for Agricultural Bioscience International Publishing*.
- Kobayashi Y. & Barsbold R., 2005 – Reexamination of a primitive ornithomimosaur, *Garudimimus brevipes* Barsbold, 1981 (Dinosauria: Theropoda), from the Late Cretaceous of Mongolia. *Canadian Journal of Earth Sciences*, 42: 1501-1521.
- Kobayashi Y. & Lü J.-C., 2003 – A new ornithomimid dinosaur with gregarious habits from the Late Cretaceous of China. *Acta Palaeontologica Polonica*, 48 (2): 235-259.
- Kuchel L. J. & Franklin C. E., 2000 – Morphology of the cloaca in the estuarine crocodile, *Crocodylus porosus*, and its plastic response to salinity. *Journal of Morphology*, 245 (2): 168-176.
- Kundrát M., Cruickshank A. R. I., Manning T. W. & Nudds J., 2008 – Embryos of therizinosaurid theropods from the Upper Cretaceous of China: diagnosis and analysis of ossification patterns. *Acta Zoologica*, 88: 231-251.
- Lambe L. M., 1917 – The Cretaceous carnivorous dinosaur *Gorgosaurus*. *Geological Survey of Canada, Memoir*, 100: 1-84.
- Langer M. C., 2004 – Basal Saurischia. In: *The Dinosauria* (2nd edition). Weishampel D. B., Dodson P. & Osmólska H. (eds.). *University of California Press*: 25-46.
- Larson P. & Rigby J. K. Jr., 2005 – Furcula of *Tyrannosaurus rex*. In: *The Carnivorous Dinosaurs*. Carpenter K. (ed.). *Indiana University Press*: 247-255.
- Leahy G., 2000 – Noses, Lungs, and Guts. In: *The Scientific American Book of Dinosaurs*. Paul G. (ed.). *Byron Preiss Visual Publications & Scientific American*: 52-63.

- Leonardi G., 2008 – Vertebrate ichnology in Italy. *Studi Trentini di Scienze Naturali, Acta Geologica*, 83: 213-221.
- Leonardi G. & Avanzini M., 1994 – Dinosauri in Italia. *Le Scienze (Quaderni)*, 76: 69-81.
- Leonardi G. & Lanzinger M., 1992 – Dinosauri nel Trentino: venticinque piste fossili nel Liassico di Rovereto (Trento, Italia). *Paleocronache*, 1: 13-24.
- Leonardi G. & Mietto P., 2000 – Le piste liassiche di dinosauri dei Lavini di Marco. In: Dinosauri in Italia. Le orme giurassiche dei Lavini di Marco (Trentino) e gli altri resti fossili italiani. Leonardi G. & Mietto P. (eds.). *Accademia Editoriale*: 169-247.
- Leonardi G. & Teruzzi G., 1993 – Prima segnalazione di uno scheletro fossile di dinosauro (Theropoda, Coelurosauria) in Italia (Cretacico di Pietrarroia, Benevento). *Paleocronache*, 1: 7-14.
- Li D., Norell M. A., Gao K.-Q., Smith N. D. & Makovicky P. J., 2009 – A longirostrine tyrannosauroid from the Early Cretaceous of China. *Proceedings of the Royal Society of London, B*, 277: 183-190.
- Lindgren J., Currie P. J., Siverson M., Rees J., Cederström P. & Lindgren F., 2007 – The first neoceratopsian dinosaur remains from Europe. *Palaeontology*, 50 (4): 929-937.
- Lingham-Soliar T. & Wesley-Smith J., 2008 – First investigation of the collagen D-band ultrastructure in fossilized vertebrate integument. *Proceedings of the Royal Society of London, B*, 275: 2207-2212.
- Lipkin C., Sereno P. C. & Horner J. R., 2007 – The furcula in *Suchomimus tenerensis* and *Tyrannosaurus rex* (Dinosauria: Theropoda: Tetanurae). *Journal of Paleontology*, 81 (6): 1523-1527.
- Long, J. A. & McNamara K. J., 1997 – Heterochrony. In: Encyclopedia of dinosaurs. Currie P. J. & Padian K. (eds.). *Academic Press*: 311-317.
- Longrich N. R. & Currie P. J., 2009 – *Albertonykus borealis*, a new alvarezsaur (Dinosauria: Theropoda) from the Early Maastrichtian of Alberta, Canada: Implications for the systematics and ecology of the Alvarezsauridae. *Cretaceous Research*, 30: 239-252.
- Lyman R. L., 1994 – Vertebrate Taphonomy. *Cambridge University Press*.
- Madsen J. R. Jr., 1976 – *Allosaurus fragilis*: a revised osteology. *Utah Geological Survey Bulletin*, 109: 1-163.
- Madsen J. H. Jr. & Welles S. P., 2000 – *Ceratopsaurus* (Dinosauria, Theropoda): a revised osteology. *Miscellaneous Publications of the Utah Geological Survey*, 2: 1-80.
- Maganuco S., Cau A. & Pasini G., 2005 – First description of theropod remains from the Middle Jurassic (Bathonian) of Madagascar. *Atti della Società Italiana di Scienze Naturali e del Museo Civico di Storia Naturale in Milano*, 146 (II): 165-202.
- Maganuco S., Steyer J. S., Pasini G., Boulay M., Lorrain S., Bénéteau A. & Audatore M., 2009 – An exquisite specimen of *Edingerella madagascariensis* (Temnospondyli) from the Lower Triassic of NW Madagascar: cranial anatomy, phylogeny and restorations. *Memorie della Società Italiana di Scienze Naturali e del Museo Civico di Storia Naturale di Milano*, XXXVI (II): 1-72.
- Maina J. N., 2005 – The lung-air sac system of birds: development, structure, and function. *Springer-Verlag*.
- Makovicky P. J., 1995 – Phylogenetic aspects of the vertebral morphology of Coelurosauria (Dinosauria: Theropoda). *Master's Thesis, Copenhagen University*.
- Makovicky P. J., 1997 – Postcranial axial skeleton, comparative anatomy. In: Encyclopedia of dinosaurs. Currie P. J. & Padian K. (eds.). *Academic Press*: 579-590.
- Makovicky P. J. & Currie P. J., 1998 – The presence of a furcula in tyrannosaurid theropods, and its phylogenetic and functional implications. *Journal of Vertebrate Paleontology*, 18: 143-149.
- Makovicky P. J. & Norell M. A., 1998 – A partial ornithomimid braincase from Ukhaa Tolgod (Upper Cretaceous, Mongolia). *American Museum Novitates*, 3247: 1-16.
- Makovicky P. J. & Norell M. A., 2004 – Troodontidae. In: The Dinosauria (2nd edition). Weishampel D. B., Dodson P. & Osmólska H., (eds.). *University of California Press*: 184-195.
- Makovicky P. J., Norell M. A., Clark J. M. & Rowe T., 2003 – Osteology and Relationships of *Byronosaurus jaffei* (Theropoda: Troodontidae). *American Museum Novitates*, 3402: 1-32.
- Makovicky P. J., Kobayashi Y. & Currie P. J., 2004 – Ornithomimosauria. In: The Dinosauria (2nd edition). Weishampel D. B., Dodson P. & Osmólska H. (eds.). *University of California Press*: 137-150.
- Manning P. L., 2008 – Grave secrets of dinosaurs. Soft tissues and hard science. *National Geographic Books*.
- Marsh O. C., 1881 – Jurassic birds and their allies. *American Journal of Science*, 3rd ser., 22: 337-340.
- Martill D. M., 1988 – Preservation of fish in the Cretaceous Santana formation of Brazil. *Palaeontology*, 31: 1-18.
- Martill D. M., Frey E., Sues H-D. & Cruickshank A. R. I., 2000 – Skeletal remains of a small theropod dinosaur with associated soft structures from the Lower Cretaceous Santana Formation of northeast Brazil. *Canadian Journal of Earth Sciences*, 37 (6): 891-900.
- Martin R. E., 1999 – Taphonomy: a process approach. *Cambridge University Press*.
- Martinez R. D. & Novas F. E., 2006 – *Aniksosaurus darwini* gen. et sp. nov., a new coelurosaurian theropod from the Early Late Cretaceous of Central Patagonia, Argentina. *Revista del Museo Argentino de Ciencias Naturales, n.s.* 8 (2): 243-259.
- Mateus O., 1998 – *Lourinhanosaurus antunesi*, a new Upper Jurassic Allosauroid (Dinosauria: Theropoda) from Lourinhã, Portugal. *Memórias de Academia de Ciências das Lisboa*, 37: 111-124.
- Mateus I., Mateus H., Antunes M. T., Mateus O., Taquet P., Ribeiro V. & Manuppella G., 1998 – Upper Jurassic theropod dinosaur embryos from Lourinhã (Portugal). *Memórias de Academia de Ciências das Lisboa*, 37: 101-110.
- McGowan G. J., 2002 – Albanerpetontid amphibians from the Lower Cretaceous of Spain and Italy: a description and reconsideration of their systematics. *Zoological Journal of the Linnean Society*, 135: 1-32.
- McGowan G. & Evans S. E., 1995 – Albanerpetontid amphibians from the Cretaceous of Spain. *Nature*, 373: 143-145.
- McLelland J., 1989 – Anatomy of lungs and air sacs. In: Form and Function in Birds. Vol. 4. King A. S. & McLelland J. (eds.). *Academic Press*: 221-279.
- McLelland J., 1990 – A colour atlas of avian anatomy. *Wolfe Publishing*.
- McNab B. K., 2002 – The Physiological Ecology of Vertebrates: A View from Energetics. *Cornell University Press*.
- Meunier F., 1984 – Structure et minéralisation des écailles de quelques Osteoglossidae (Osteichthiens, Téléostéens). *Annales des Sciences Naturelles, Zoologie, 3 Sér.*, 6: 111-124.
- Mezga A. & Bajraktarević Z., 1999 – Cenomanian dinosaur tracks on the islet of Fenoliga in southern Istria, Croatia. *Cretaceous Research*, 20: 735-746.
- Mezga A., Meyer C. A., Cvetko Tešović B., Bajraktarević Z. & Gušić I., 2006 – The first record of dinosaurs in the Dalmatian part (Croatia) of the Adriatic-Dinaric carbonate platform (ADCP). *Cretaceous Research*, 27: 735-742.

- Mezga A., Cvetko Tešović B. & Bajraktarević Z., 2007 – First record of dinosaurs in the late Jurassic of the Adriatic-Dinaric Carbonate Platform (Croatia). *Palaios*, 22 (2): 188-199.
- Mietto P., 1988 – Piste di dinosauri nella Dolomia Principale (Triassico superiore) del Monte Pelmetto (Cadore). *Memorie della Società Geologica Italiana*, 30: 307-310.
- Mindszenty A., D'Argenio B. & Aiello G., 1995 – Lithospheric bulges recorded by regional unconformities. The case of Mesozoic-Tertiary Apulia. *Tectonophysics*, 252: 137-161.
- Mortimer M., 2004-2010 – Theropod Database. <http://home.comcast.net/~eoraptor/Home.html>
- Muhl Z. F., Grimm A. F. & Glick P., 1976 – Technique for measurements of sarcomere length of striated muscle. *Journal of Dental Research*, 55 (1): 170.
- Murphy N. L., Trexler D. & Thompson M., 2007 – “Leonardo”, a mummified *Brachylophosaurus* (Ornithischia: Hadrosauridae) from the Judith River Formation of Montana. In: Horns & Beaks. Ceratopsian and Ornithopod Dinosaurs. Carpenter K. (ed.). *Indiana University Press*: 117-133.
- Murray A. M., Simons E. L. & Attiac Y. S., 2005 – A new clupeid fish (Clupeomorpha) from the Oligocene of Fayum, Egypt, with notes on some other fossil clupeomorphs. *Journal of Vertebrate Paleontology*, 25 (2): 300-308.
- Naish D. W., Hutt S., & Martill D. M., 2001 – Saurischian dinosaurs: Theropods. In: Dinosaurs of the Isle of Wight. Field Guides to Fossils 10. Martill D. M. & Naish D. W. (eds.). *Palaeontological Association*: 242-309.
- Naish D., Martill D. M. & Frey E., 2004 – Ecology, systematics and biogeographical relationships of dinosaurs, including a new theropod, from the Santana Formation (?Albian, Early Cretaceous) of Brazil. *Historical Biology*, 16: 57-70.
- Nesbitt S. J., Turner A. H., Spaulding M., Conrad J. L. & Norell M. A., 2009 – The theropod furcula. *Journal of Morphology*, 270 (7): 856-879.
- Nicholls E. L. & Russell A. P., 1981 – A new specimen of *Struthiomimus altus* from Alberta, with comments on the classificatory characters of Upper Cretaceous ornithomimids. *Canadian Journal of Earth Sciences*, 18: 518-526.
- Nicosia U., Marino M., Mariotti N., Muraro C., Panigutti S., Petti F. M. & Sacchi E., 2000a – The Late Cretaceous dinosaur tracksite near Altamura (Bari, southern Italy). I Geological framework. *Geologica Romana*, 35 (1999): 231-236.
- Nicosia U., Marino M., Mariotti N., Muraro C., Panigutti S., Petti F. M. & Sacchi E., 2000b – The Late Cretaceous dinosaur tracksite near Altamura (Bari, southern Italy). II *Apulosauripus federicianus* new ichnogen. and new ichnosp. *Geologica Romana*, 35 (1999): 237-247.
- Nicosia U., Avanzini M., Barbera C., Conti M. A., Dalla Vecchia F., Dal Sasso C., Gianolla P., Leonardi G., Loi M., Mariotti N., Mietto P., Morsilli M., Paganoni A., Petti F. M., Piubelli D., Raia P., Renesto S., Sacchi E., Santi G. & Signore M., 2005 – I vertebrati continentali del Paleozoico e Mesozoico. In: Paleontologia dei vertebrati in Italia. Evoluzione biologica, significato ambientale e paleogeografia. Bonfiglio L. (ed.). *Memorie del Museo Civico di Storia Naturale di Verona*, 2^a serie, sezione Scienze della Terra, 6: 41-66.
- Nicosia U., Petti F. M., Perugini G., D'Orazi Porchetti S., Sacchi E., Conti M. A., Mariotti N. & Zarattini A., 2007 – Dinosaur Tracks as Paleogeographic Constraints: New Scenarios for the Cretaceous Geography of the Periadriatic Region. *Ichnos*, 14: 69-90.
- Nopcsa F., 1903 – Neues über *Compsognathus*. *Neues Jahrbuch für Geologie und Paläontologie*, 16: 476-494.
- Norell M. A. & Makovicky P. J., 1997 – Important features of the dromaeosaur skeleton: information from a new specimen. *American Museum Novitates*, 3215: 1-28.
- Norell M. A. & Makovicky P. J., 1999 – Important features of the dromaeosaur skeleton, II. Information from newly collected specimens of *Velociraptor mongoliensis*. *American Museum Novitates*, 3282: 1-45.
- Norell M. A. & Makovicky P. J., 2004 – Dromaeosauridae. In: The Dinosauria (2nd edition). Weishampel D. B., Dodson P. & Osmólska H. (eds.). *University of California Press*: 196-209.
- Norell M. A., Clark J. M., Dashzeveg D., Barsbold R., Chiappe L. M., Davidson A. R., McKenna M. C., Perle A. & Novacek M. J., 1994 – A theropod dinosaur embryo and the affinities of the Flaming Cliffs dinosaur eggs. *Science*, 266: 779-782.
- Norell M. A., Clark J. M., Chiappe L. M. & Dashzeveg D., 1995 – A nesting dinosaur. *Nature*, 378: 774-776.
- Norell M. A., Makovicky P. J. & Clark J. M., 1997 – A *Velociraptor* wishbone. *Nature*, 389: 447.
- Norell M. A., Makovicky P. J. & Clark J. M., 2000 – A new troodontid theropod from Ukhaa Tolgod, Mongolia. *Journal of Vertebrate Paleontology*, 20: 7-11.
- Norell M. A., Clark J. M. & Chiappe L. M., 2001 – An embryonic oviraptorid (Dinosauria: Theropoda) from the Upper Cretaceous of Mongolia. *American Museum Novitates*, 3315: 1-17.
- Norell M. A., Makovicky P. J., Bever G. S., Balanoff A. M., Clark J. M., Barsbold R., & Rowe T., 2009 – A Review of the Mongolian Cretaceous Dinosaur *Saurornithoides* (Troodontidae: Theropoda). *American Museum Novitates*, 3654: 1-63.
- Noto C., 2009 – The potential utility of authigenic minerals on modern and fossil bones for environmental and taphonomic analysis. *Journal of Vertebrate Paleontology*, 29 (3, suppl.): 156A.
- Novas F. E., Ezcurra M. D. & Lecuona A., 2008a – *Orkoraptor burkei* nov. gen. et sp., a large theropod from the Maastrichtian Pari Aike Formation, Southern Patagonia, Argentina. *Cretaceous Research*, 29: 468-480.
- Novas F. E., Pol D., Canale J. I., Porfiri J. D. & Calvo J. O., 2008b – A bizarre Cretaceous theropod dinosaur from Patagonia and the evolution of Gondwanan dromaeosaurids. *Proceedings of the Royal Society B*, 276 (1659): 1101-1107.
- O'Connor P. M., 2006 – Postcranial pneumaticity: an evaluation of soft-tissue influences on the postcranial skeleton and the reconstruction of pulmonary anatomy in archosaurs. *Journal of Morphology*, 267: 1199-1226.
- O'Connor P. M., 2007 – The postcranial axial skeleton of *Majungasaurus crenatissimus* (Theropoda: Abelisauridae) from the Late Cretaceous of Madagascar. *Society of Vertebrate Paleontology Memoir*, 8: 127-162.
- O'Connor P. M. & Claessens L. P., 2005 – Basic avian pulmonary design and flow-through ventilation in non-avian theropod dinosaurs. *Nature*, 436: 253-256.
- Organ C. L., 2006 – Biomechanics of ossified tendons in ornithomimid dinosaurs. *Paleobiology*, 32 (4): 652-665.
- Osborn H. F., 1916 – Skeletal adaptations of *Ornitholestes*, *Struthiomimus*, *Tyrannosaurus*. *Bulletin of the American Museum of Natural History*, 35: 733-771.
- Ósi A., Butler R. J. & Weishampel D. B., 2010 – A Late Cretaceous ceratopsian dinosaur from Europe with Asian affinities. *Nature*, 456: 466-468.
- Osmólska H., Maryanska T. & Barsbold R., 1972 – A new dinosaur, *Gallimimus bullatus* n. gen., n. sp. (Ornithomimidae) from the Upper Cretaceous of Mongolia. *Palaeontologia Polonica*, 27: 103-143.
- Osmólska H., Currie P. J. & Barsbold R., 2004 – Oviraptorosauria. In: The Dinosauria (2nd edition). Weishampel D. B., Dodson P. & Osmólska H. (eds.). *University of California Press*: 165-183.

- Ostrom J. H., 1969 – Osteology of *Deinonychus anthyropus*, an unusual theropod from the Lower Cretaceous of Montana. *Bulletin of the Peabody Museum of Natural History*, 30: 1-165.
- Ostrom J. H., 1970 – *Archaeopteryx*: Notice of a “New” Specimen. *Science*, 170: 537-538.
- Ostrom J. H., 1978 – The osteology of *Compsognathus longipes* Wagner. *Zitteliana*, 4: 73-118.
- Padian K., 2004 – Basal Avialae. In: The Dinosauria (2nd edition). Weishampel D. B., Dodson P. & Osmólska H. (eds.). *University of California Press*: 210-231.
- Padian K., de Ricqlès A. J. & Horner J. R., 2001 – Dinosaurian growth rates and bird origins. *Nature*, 412: 405-408.
- Page R. D. M., 1996 – TREEVIEW: An application to display phylogenetic trees on personal computers. *Computer Application in the Biosciences*, 12: 357-358.
- Page R. D. M., 2001 – NEXUS Data Editor. 0.5.0. <http://taxonomy.zoology.gla.ac.uk/rod/NDE/nde.html>.
- Panchangam A., Claffin D. R., Palmer M. L. & Faulkner J. A., 2008 – Magnitude of Sarcomere Extension Correlates with Initial Sarcomere Length during Lengthening of Activated Single Fibers from Soleus Muscle of Rats. *Biophysical Journal*, 95 (4): 1890-1901.
- Patacca E. & Scandone P., 2004 – A geological transect across the Southern Apennines along the seismic line CROP 04. In: Field Trip Guide Books. Post Congress P20, 32nd IGC Florence, 20-28 August 2004. Guerrieri L., Rischia I. & Serva L. (eds.). *Memorie Descrittive della Carta Geologica d'Italia*, 63 (4): 14-36.
- Patacca E. & Scandone P., 2007 – Geology of the Southern Apennines. *Bollettino della Società Geologica Italiana, Volume speciale*, 7: 75-119.
- Paul G. S., 1988 – Predatory Dinosaurs of the World: A Complete Illustrated Guide. *Simon & Schuster*: 1-464.
- Paul G. S., 2001 – Were the respiratory complexes of predatory dinosaurs like crocodylians or birds? In: New Perspectives on the Origin and Early Evolution of Birds. Proceedings of the International Symposium in Honor of John H. Ostrom. Gauthier J. A. & Gall L. F. (eds.). *Peabody Museum of Natural History*: 463-482.
- Paul G. S., 2002 – Dinosaurs of the air: the evolution and loss of flight in dinosaurs and birds. *The John Hopkins University Press*: 1-460.
- Pérez-Moreno B. P., Sanz J. L., Buscalioni A. D., Moratalla J. J., Ortega F. & Rasskin-Gutman D., 1994 – A unique multi-toothed ornithomimosaur dinosaur from the Lower Cretaceous of Spain. *Nature*, 370: 363-367.
- Perry S. F., 1998 – Lungs: comparative anatomy, functional morphology, and evolution. In: Biology of the Reptilia, Volume 19, Morphology G, Visceral Organs. Gans C. & Gaunt A. S. (eds.). *Society for the Study of Amphibians and Reptiles*: 1-92.
- Perry S. F., 2001 – Functional morphology of the reptilian and avian respiratory system and its implications for theropod dinosaurs. In: New Perspectives on the Origin and Early Evolution of Birds. Proceedings of the International Symposium in Honor of John H. Ostrom. Gauthier J. A. & Gall L. F. (eds.). *Peabody Museum of Natural History*: 429-441.
- Persons W. S. & Currie P. J., 2011 – The tail of *Tyrannosaurus*: reassessing the size and locomotive importance of the *M. caudofemoralis* in non-avian theropods. *Anatomical Record*, 294: 119-131.
- Petti F. M., Conti M. A., D’Orazi Porchetti S., Morsilli M., Nicosia U. & Gianolla P., 2008a – A theropod dominated ichnocoenosis from late Hauterivian-early Barremian of Borgo Celano (Gargano Promontory, Apulia, southern Italy). *Rivista Italiana di Paleontologia e Stratigrafia*, 14 (1): 3-17.
- Petti F. M., D’Orazi Porchetti S., Conti M. A., Nicosia U., Perugini G. & Sacchi E., 2008b – Theropod and sauropod footprints in the Early Cretaceous (Aptian) Apenninic Carbonate Platform (Esperia, Lazio, Central Italy): a further constraint on the palaeogeography of the Central Mediterranean area. *Studi Trentini di Scienze Naturali, Acta Geologica*, 83: 323-334.
- Peyer K., 2004 – A reevaluation of the French *Compsognathus* of the Tithonian of southeastern France and its phylogenetic relationship with other compsognathids and coelurosaurs. *PhD Thesis, Muséum national d’Histoire naturelle, Paris*.
- Peyer K., 2006 – A reconsideration of *Compsognathus* from the Upper Tithonian of Canjuers, Southeastern France. *Journal of Vertebrate Paleontology*, 26 (4): 879-896.
- Pinto e Silva C. J. R., Martins M. R. F. B. & Guazzelli Filho J., 2008 – Study on cranial and caudal mesenteric arteries in opossum (*Didelphis albiventris*). *International Journal of Morphology*, 26 (3): 635-637.
- Pol D. & Norell M. A., 2004 – A new gobiosuchid crocodyliform taxon from the Cretaceous of Mongolia. *American Museum Novitates*, 3458: 1-31.
- Pol D. & Powell J. E., 2007 – Skull anatomy of *Mussaurus patagonicus* (Dinosauria: Sauropodomorpha) from the Late Triassic of Patagonia. *Historical Biology*, 19 (1): 125-144.
- Poyato-Ariza F. J. & Wenz S., 2002 – A new insight into pycnodontiform fishes. *Geodiversitas*, 24 (1): 139-248.
- Raath M. A., 1985 – The theropod *Syntarsus* and its bearing on the origin of birds. In: The beginnings of birds: Proceedings of the International *Archaeopteryx* Conference, Eichstätt 1984. Hecht M. K., Ostrom J. H., Viohl G. & Wellnhofer P. (eds.). *Freunde des Jura- Museums*: 219-227.
- Rauhut O. W. M., 2003 – The interrelationships and evolution of basal theropod dinosaurs. *Special Papers in Palaeontology*, 69: 1-213.
- Rauhut O. W. M. & Fechner R., 2005 – Early development of the facial region in a non-avian theropod dinosaur. *Proceedings of the Royal Society of London B*, 272: 1179-1183.
- Rauhut O. W. M. & Xu X., 2005 – The small theropod dinosaurs *Tugulusaurus* and *Phaedrolosaurus* from the Early Cretaceous of Xinjiang, China. *Journal of Vertebrate Paleontology*, 25: 107-118.
- Rauhut O. W. M., Milner A. C. & Moore-Fay S., 2009 – Cranial osteology and phylogenetic position of the theropod dinosaur *Proceratosaurus bradleyi* (Woodward, 1910) from the Middle Jurassic of England. *Zoological Journal of the Linnean Society*: 1-41.
- Reisz R. R., Scott D., Sues H.-D., Evans D. C. & Raath M. A., 2005 – Embryos of an early Jurassic prosauropod dinosaur and their evolutionary significance. *Science*, 309: 761-764.
- Richardson K., Webb G. & Manolis C., 2000 – Crocodiles: Inside and Out. *Surrey Beatty and Sons*.
- Rieppel O., 1992a – Studies on skeleton formation in reptiles. I. The post-embryonic development of the skeleton in *Cyrtodactylus pubisulcus* (Reptilia: Gekkonidae). *Journal of Zoology*, 227: 87-100.
- Rieppel O., 1992b – Studies on skeleton formation in reptiles. III. Patterns of ossification in the skeleton of *Lacerta vivipara* Jacquin (Reptilia, Squamata). *Fieldiana: Zoology*, 68: 1-25.
- Rieppel O., 1993 – Studies on skeleton formation in reptiles: patterns of ossification in the skeleton of *Chelydra serpentina* (Reptilia, Testudines). *Journal of Zoology*, 231: 487-509.
- Rinehart L. F., Lucas S. G. & Hunt A. P., 2007 – Furculae in the Late Triassic theropod dinosaur *Coelophysis bauri*. *Paläontologische Zeitschrift*, 81 (2): 174-180.
- Romer A. S., 1966 – Vertebrate paleontology. *University of Chicago Press*.

- Romer A. S. & Parsons T. S., 1977 – The Vertebrate Body. *Holt-Saunders International*.
- Rosenbaum G., Lister G. & Duboz C., 2004 – The Mesozoic and Cenozoic motion of Adria (central Mediterranean): a review of constraints and limitations. *Geodinamica Acta*, 17 (2): 125-139.
- Rowe T., 1989 – A new species of the theropod dinosaur *Syntarsus* from the Early Jurassic Kayenta Formation of Arizona. *Journal of Vertebrate Paleontology*, 9 (2): 125-136.
- Rowe T., McBride E. F. & Sereno P. C., 2001 – Technical comment: dinosaur with a heart of stone. *Science*, 291 (5505): 783.
- Ruben J. A., Jones T. D., Geist N. R. & Hillenius W. J., 1997 – Lung structure and ventilation in theropod dinosaurs and early birds. *Science*, 278: 1267-1270.
- Ruben J. A., Jones T. D., Geist N. R. & Hillenius W. J., 1998 – Letter in response to criticisms of Ruben *et al.*, 1997. *Science*, 281: 47-48.
- Ruben J. A., Dal Sasso C., Geist N. R., Hillenius W. J., Jones T. D. & Signore M., 1999 – Pulmonary function and metabolic physiology of theropod dinosaurs. *Science*, 283: 514-516.
- Ruben J. A., Jones T. D. & Geist N. R., 2003 – Respiratory and reproductive paleophysiology of dinosaurs and early birds. *Physiological and Biochemical Zoology*, 76: 141-164.
- Russell D. A. & Dong Z., 1993 – A nearly complete skeleton of a new troodontid dinosaur from the Early Cretaceous of the Ordo Basin, Inner Mongolia, People's Republic of China. *Canadian Journal of Earth Sciences*, 30: 2163-2173.
- Sacchi E., Conti M. A., D'Orazi Porchetti S., Nicosia U., Perugini G., Petti F. M. & Logoluso A., 2006 – A new diverse dinosaur footprint association from the Calcare di Bari (Lower Cretaceous, Apulia, southern Italy): implication for paleoecology and paleogeography. *Giornate di Paleontologia 2006. Abstracts*: 78.
- Sacchi E., Conti M. A., D'Orazi Porchetti S., Logoluso A., Nicosia U., Perugini G. & Petti F. M., 2009 – Aptian dinosaur footprints from the Apulian platform (Bisceglie, Southern Italy) in the framework of periadriatic ichnosites. *Palaeogeography, Palaeoclimatology, Palaeoecology*, 271: 104-116.
- Sagemann J., Bale S. J., Briggs D. E. G. & Parkes R. J., 1999 – Controls on the formation of authigenic minerals in association with decaying organic matter: an experimental approach. *Geochimica et Cosmochimica Acta*, 63: 1083-1095.
- Saladin K. S., 2010 – Anatomy & Physiology: A Unity of Form and Function (5th Edition). *McGraw-Hill*.
- Salgado L., Coria R. A., & Chiappe L. M., 2005 – Osteology of the sauropod embryos from the Upper Cretaceous of Patagonia. *Acta Palaeontologica Polonica*, 50 (1): 79-92.
- Sampson S. D. & Witmer L. M., 2007 – Craniofacial anatomy of *Majungasaurus crenatissimus* (Theropoda: Abelisauridae) from the Late Cretaceous of Madagascar. *Society of Vertebrate Paleontology, Memoir*, 8: 32-102.
- Sander M. P., Mateus O., Laven T. & Knötschke N., 2006 – Bone histology indicates insular dwarfism in a new Late Jurassic sauropod dinosaur. *Nature*, 441: 739-741.
- Sanz J. L., Chiappe L. M., Perez-Moreno B. P., Moratalla J. J., Hernández Carrasquilla F., Buscalioni A. D., Ortega F., Poyato-Ariza F., Rasskin-Gutman D. & Martín-Delclòs X., 1997 – A nestling bird from the Lower Cretaceous of Spain: implications for avian skull and neck evolution. *Science*, 276: 1543-1546.
- Schachner E. R., Lyson T. R. & Dodson P., 2009 – Evolution of the Respiratory System in Nonavian Theropods: Evidence from Rib and Vertebral Morphology. In: *Unearthing the Anatomy of Dinosaurs: New Insights into their Functional Morphology and Paleobiology*. Dodson P. (ed.). *The Anatomical Record: Advances in Integrative Anatomy and Evolutionary Biology, Special Issue*, 292 (9): 1501-1513.
- Schaffner F., 1998 – The liver. In: *Biology of Reptilia*. Gans C. & Gaunt A. S. (eds.). *Society for the Study of Amphibians and Reptiles Press*, 19: 297-374.
- Scheid P. & Piiper J., 1989 – Respiratory mechanics and air flow in birds. In: *Form and function in birds*. Vol. 4. King A. S. & McLelland J. (eds.). *Academic Press*: 369-391.
- Schettino A. & Scotese C., 2002 – Global kinematic constraints to the tectonic history of the Mediterranean region and surrounding areas during the Jurassic and Cretaceous. In: *Reconstruction of the evolution of the Alpine-Himalayan Orogen*. Rosenbaum G. & Lister G. S. (eds.). *Journal of the Virtual Explorer*, 8: 149-168.
- Schwarz D., Ikejiri T., Breithaupt B. H., Sander P. M. & Klein N., 2007a – A nearly complete skeleton of an early juvenile diplodocid (Dinosauria: Sauropoda) from the lower Morrison Formation (Late Jurassic) of north central Wyoming and its implications for early ontogeny and pneumaticity in sauropods. *Historical Biology*, 19: 225-253.
- Schwarz D., Wings O. & Meyer C. A., 2007b – Super sizing the giants: first cartilage preservation at a sauropod dinosaur limb joint. *Journal of the Geological Society*, 164: 61-65.
- Schwarz D., Frey E. & Meyer C. A., 2007c – Pneumaticity and soft-tissue reconstructions in the neck of diplodocid and dicraeosaurid sauropods. *Acta Palaeontologica Polonica*, 52 (1): 167-188.
- Schwarz-Wings D., Frey E. & Martin T., 2009 – Reconstruction of the bracing system of the trunk and tail in Hyposaurine Dyrosaurids (Crocodylomorpha; Mesoeucrocodylia). *Journal of Vertebrate Paleontology*, 29 (2): 453-472.
- Schweitzer M. H., Watt J. A., Avci R., Forster C. A., Krause D. W., Knapp L., Rogers R. R., Beech I. & Marshall M., 1999 – Keratin immunoreactivity in the Late Cretaceous bird *Rahonavis ostromi*. *Journal of Vertebrate Paleontology*, 10 (4): 712-722.
- Schweitzer M. H., Wittmeyer J. L. & Horner J. R., 2007 – Soft tissue and cellular preservation in vertebrate skeletal elements from the Cretaceous to the present. *Proceeding of the Royal Society B*, 274: 183-197.
- Schweitzer M. H., Avci R., Collier T. & Goodwin M. B., 2008 – Microscopic, chemical and molecular methods for examining fossil preservation. In: *Paléogénétique en Paléontologie, Archéologie et Paléoanthropologie: Contributions et Limites*. Vigne J.-D. & Darlu P. (eds.). *Comptes Rendus Palevol*, 7 (2-3): 159-184.
- Seilacher A., 1970 – Begriff und Bedeutung der Fossil-Lagerstätten. *Neues Jahrbuch Geol. Paläontol. Abh.*, 1970: 34-39.
- Senter P., 2007 – A new look at the phylogeny of the Coelurosauria (Dinosauria: Theropoda). *Journal of Systematic Palaeontology*, 1-35.
- Sereno P. C., 2001 – Alvarezsaurids: birds or ornithomimosaurs? In: *New Perspectives on the Origin and Early Evolution of Birds: Proceedings of the International Symposium in Honor of John H. Ostrom*. Gauthier J. & Gall L. F. (eds.). *Peabody Museum of Natural History*: 69-98.
- Sereno P. C. & Arcucci A. B., 1994 – Dinosaurian precursors from the Middle Triassic of Argentina: *Marasuchus lilloensis*, gen. nov. *Journal of Vertebrate Paleontology*, 14: 53-73.
- Sereno P. C., Forster C. A., Rogers R. R., & Monetta A. M., 1993 – Primitive dinosaur skeleton from Argentina and the early evolution of Dinosauria. *Nature*, 361: 64-66.
- Sereno P. C., Wilson J. A., Larsson H. C. E., Duthiel D. B. & Sues H. D., 1994 – Early Cretaceous dinosaurs from the Sahara. *Science*, 265: 267-271.

- Sereno P. C., Martinez R. N., Wilson J. A., Varricchio D. J., Alcover O. A. & Larsson H. C. E., 2008 – Evidence for avian intrathoracic air sacs in a new predatory dinosaur from Argentina. *PLoS ONE*, 3 (9), e3303.
- Sereno P. C., Tan L., Brusatte S. L., Kriegstein H. J., Zhao X. & Cloward K., 2009 – Tyrannosaurid Skeletal Design First Evolved at Small Body Size. *Scienceexpress*, 17 September 2009.
- Serventy D. L., Nicholls C. A. & Farner D. S., 1966 – Pneumatization of the cranium of the zebra finch *Taeniopygia castanotis*. *Ibis*, 190 (4): 570-578.
- Signore M., 1995 – Il teropode del Plattenkalk della Civita di Pietraroia (Cretaceo inferiore, BN). *Dipartimento di Paleontologia, Università degli Studi di Napoli "Federico II"*. unpublished degree thesis.
- Signore M., 2004 – Sample excavations in Pietraroia (lower Cretaceous, Southern Italy) in 2001 and notes on the Pietraroia paleoenvironment. *PalArch*, 2: 13-22.
- Signore M., Barbera C., DeVita S. & La Magna G., 2001 – Tetrapod Fauna of Pietraroia Plattenkalk (Benevento, Southern Italy). *6th European Workshop on Vertebrate Paleontology. Florence and Montevarchi (Italy), September 19-22, 2001. Abstract book*: 53.
- Signore M., Bucci E., Pede C. & Barbera C., 2005 – A new ichthyodectid fish from the Lower Cretaceous of Pietraroia (Southern Italy). *PalArch*, 5: 25-29.
- Signore M., Pede C., Bucci E. & Barbera C., 2006 – First report of the genus *Cladocyclus* in the Lower Cretaceous of Pietraroia (Southern Italy). *Bollettino della Società Paleontologica Italiana*, 45 (1): 141-146.
- Skoczylas R., 1978 – Physiology of the digestive tract. In: *Biology of the Reptilia*, Vol 8: Physiology B. Gans C. (ed.). *Academic Press*: 589-717.
- Smith J. W., 1968 – Molecular pattern in native collagen. *Nature*, 219: 157-158.
- Smith J. B. & Dodson P., 2003 – A proposal for a standard terminology of anatomical notation and orientation in fossil vertebrate dentitions. *Journal of Vertebrate Paleontology*, 23 (1): 1-12.
- Stampfli G. M., 2005 – Plate tectonics of the Apulia-Adria Microcontinents. In: *CROP PROJECT: Deep Seismic Exploration of the Central Mediterranean and Italy*. Finetti I. R. (ed.). *Elsevier*: 747-776.
- Stein K., Csiki Z., Curry-Rogers K., Weishampel D. B., Redelstorff R., Carballido J. L. & Sander P. M., 2010 – Small body size and extreme cortical bone remodeling indicate phyletic dwarfism in *Magyarosaurus dacus* (Sauropoda: Titanosauria). *Proceedings of the National Academy of Sciences*.
- Steyer J. S., 2003 – A revision of the Early Triassic "Capitosaurs" (Stegocephali, Stereospondyli) from Madagascar, with remarks on their comparative ontogeny. *Journal of Vertebrate Paleontology*, 23: 544-555.
- Sues H.-D., 1977 – The skull of *Velociraptor mongoliensis*, a small Cretaceous theropod dinosaur from Mongolia. *Paläontologische Zeitschrift*, 51 (3/4): 173-184.
- Swofford D. L., 2002 – PAUP*. Phylogenetic Analysis Using Parsimony (*and other methods). Version 4. *Sinauer Associates*.
- Taylor M. P., Wedel M. J. & Naish D., 2009 – Head and neck posture in sauropod dinosaurs inferred from extant animals. *Acta Palaeontologica Polonica*, 54 (2): 213-220.
- Tegelaar E. W., de Leeuw J. W., Derenne S. & Largeau C., 1989 – A reappraisal of kerogen formation. *Geochimica et Cosmochimica Acta*, 53: 3103-3106.
- Tischlinger H., 2002 – Der Eichstätter *Archaeopteryx* im langwelligeren UV-Licht. [The Eichstätt specimen of *Archaeopteryx* under longwave ultraviolet light]. *Archaeopteryx*, 20: 21-38.
- Turco E., Schettino A., Nicosia U., Santantonio M., Di Stefano P., Iannace A., Cannata D., Conti M. A., Deiana G., D'Orazi Porchetti S., Felici F., Liotta D., Mariotti N., Milia A., Petti F. M., Pierantoni P. P., Sacchi E., Sbrescia V., Tommasetti K., Valentini M., Zamparelli V. & Zarcione G., 2007 – Mesozoic Paleogeography of the Central Mediterranean Region. *Geoitalia 2007. VI Forum Italiano di Scienze della Terra, Epitome*, 2: 108.
- Tykoski R. S., 2005 – Anatomy, Ontogeny, and Phylogeny of Coelophysoid Theropods. *PhD Thesis, University of Texas, Austin*.
- Tykoski R. S. & Rowe T., 2004 – Ceratosauria. In: *The Dinosauria* (2nd edition). Weishampel D. B., Dodson P., & Osmólska H. (eds.). *University of California Press*: 47-70.
- Tykoski R. S., Forster C. A., Rowe T., Sampson S. D., & Muniyihwa D., 2002 – A furcula in the coelophysoid theropod *Syntarsus*. *Journal of Vertebrate Paleontology*, 22: 728-733.
- Varricchio D. J., 1997 – Growth and embryology. In: *Encyclopedia of dinosaurs*. Currie P. J. & Padian K. (eds.). *Academic Press*: 282-288.
- Varricchio D. J., 2001 – Gut contents from a Cretaceous tyrannosaurid: implications for theropod dinosaur digestive tracts. *Journal of Paleontology*, 75: 401-406.
- Varricchio D. J., Horner J. R. & Jackson F. D., 2002 – Embryos and eggs for the Cretaceous theropod dinosaur *Troodon formosus*. *Journal of Vertebrate Paleontology*, 22: 564-576.
- Vigorito M., Simone L. & Carannante G., 2003 – Tectonically controlled carbonate channelized slope complexes: a Cretaceous-Miocene case-history from Matese Mountains (Central-Southern Apennines, Italy). *Slope 2003-Submarine Slope Systems: Processes, Products and Prediction. April 28-29, 2003, Liverpool, Abstracts*: 95.
- Webb G. J. W., Hollis G. J. & Manolis S. C., 1991 – Feeding, growth, and food conversion rates of wild juvenile saltwater crocodiles (*Crocodylus porosus*). *Journal of Herpetology*, 25: 462-473.
- Wedel M. J., 2009 – Evidence for bird-like air sacs in saurischian dinosaurs. *Journal of Experimental Zoology*, 311A (8): 611-628.
- Weishampel D. B., Dodson P. & Osmólska H., 2004 – Introduction. In: *The Dinosauria* (2nd edition). Weishampel D. B., Dodson P. & Osmólska H. (eds.). *University of California Press*: 1-3.
- Welles S. P., 1984 – *Dilophosaurus wetherilli* (Dinosauria, Theropoda). Osteology and comparisons. *Palaeontographica Abt. A*, 185: 85-180.
- Wellnhofer P., 1985 – Remarks on the digit and pubis problems of *Archaeopteryx*. In: *The beginnings of birds: proceedings of the International Archaeopteryx Conference*, Eichstätt 1984. Hecht M. K., Ostrom J. H., Viohl G. & Wellnhofer P. (eds.). *Freunde des Jura- Museums*: 113-122.
- Westergaard B. & Ferguson M. W. J., 1990 – Development of dentition in *Alligator mississippiensis*: upper jaw dental and craniofacial development in embryos, hatchlings and young juveniles, with a comparison to lower jaw development. *The American Journal of Anatomy*, 187: 393-421.
- Wheeler T. L. & Koohmaraie M., 1994 – Prerigor and postrigor changes in tenderness of ovine longissimus muscle. *Journal of Animal Science*, 72: 1232-1238.
- Wilby P. R. & Briggs D. E. G., 1997 – Taxonomic trends in the resolution of detail preserved in fossil soft tissues. *Geobios*, 20: 493-502.

- Wilkinson M., 2001a – TAXEQ3: software and documentation. *Department of Zoology, The Natural History Museum.*
- Wilkinson M., 2001b – REDCON 3.0: software and documentation. *Department of Zoology, The Natural History Museum.*
- Wilson J. A., 1999 – A nomenclature for vertebral laminae in sauropods and other saurischian dinosaurs. *Journal of Vertebrate Paleontology*, 19: 639-653.
- Witmer L. M., 1995 – The extant phylogenetic bracket and the importance of reconstructing soft tissues in fossils. In: Functional morphology in vertebrate paleontology. Thomason J. J. (ed.). *Cambridge University Press*: 19-33.
- Witmer L. M., 1997 – The evolution of the antorbital cavity in archosaurs: a study in soft-tissue reconstruction in the fossil record with an analysis of the function of pneumaticity. *Journal of Vertebrate Paleontology, Memoir 3*: 1-73.
- Woodward A. S., 1910 – On a skull of *Megalosaurus* from the Great Oolite of Minchinhempton (Gloucestershire). *Quarterly Journal of the Geological Society*, 66: 111-115.
- Xu X., 2006 – Feathered dinosaurs from China and the evolution of major avian characters. *Integrative Zoology*, 1: 4-11.
- Xu X., 2010 – Horned dinosaurs venture abroad. *Nature*, 465: 431-432.
- Xu X. & Norell M. A., 2004 – A new troodontid dinosaur from China, with avian-like sleeping posture. *Nature*, 431: 838-841.
- Xu X. & Norell M. A., 2006 – Non-Avian dinosaur fossils from the Lower Cretaceous Jehol Group of western Liaoning, China. *Geological Journal*, 41: 419-417.
- Xu X. & Wu X.-C., 2001 – Cranial morphology of *Sinornithosaurus millenii* Xu et al. 1999 (Dinosauria: Theropoda: Dromaeosauridae) from the Yixian Formation of Liaoning, China. *Canadian Journal of Earth Sciences*, 38: 1939-1752.
- Xu X., Zhou Z. & Wang X., 2000 – The smallest known non-avian theropod dinosaur. *Nature*, 408: 705-708.
- Xu X., Wang X.-L. & You H.-L., 2001 – A juvenile ankylosaur from China. *Naturwissenschaften*, 88: 297-300.
- Xu X., Cheng Y. N., Wang X. L. & Chang C. H., 2002a – An unusual oviraptorosaurian dinosaur from China. *Nature*, 419: 291-293.
- Xu X., Norell M. A., Wang X. L., Makovicky P. J. & Wu X. C., 2002b – A basal troodontid from the Early Cretaceous of China. *Nature*, 415: 780-784.
- Xu X., Norell M. A., Kuang X., Wang X., Zhao Q. & Jia C., 2004 – Basal tyrannosauroids from China and evidence for protofeathers in tyrannosauroids. *Nature*, 431: 680-684.
- Xu X., Clark J. M., Forster C. A., Norell M. A., Erickson G. M., Eberth D. A., Jia C. & Zhao Q., 2006 – A basal tyrannosauroid from the Late Jurassic of China. *Nature*, 439: 715-718.
- Xu X., Wang K. B., Zhao K. J. & Li D. J., 2010 – First ceratopsid dinosaur from China and its biogeographical interpretation. *Chinese Science Bulletin*, 55: 1631-1635.
- Yates A. M. & Warren A. A., 2000 – The phylogeny of the “higher” temnospondyls (Vertebrata: Choanata) and its implications for the monophyly and origins of Stereospondyli. *Zoological Journal of the Linnean Society*, 128: 77-121.
- Yilmaz P. O., Norton I. O., Leary D. & Chuchla J., 1996 – Tectonic evolution and paleogeography of Europe. In: Peri-Tethys Memoir 2: Structure and Prospects of Alpine Basins and Forelands. Ziegler P. A. & Horváth F. (eds.). *Memoires du Muséum d'Histoire Naturelle*, 170: 47-60.
- Zanno L. E., 2006 – The pectoral girdle and forelimb of the primitive therizinosauroid *Falcarius utahensis* (Theropoda, Maniraptora): analyzing evolutionary trends within Therizinosauroidea. *Journal of Vertebrate Paleontology*, 26: 636-650.
- Zanno L. E., 2010 – Osteology of *Falcarius utahensis* (Dinosauria: Theropoda): characterizing the anatomy of basal therizinosauroids. *Zoological Journal of the Linnean Society*, 158: 196-230.
- Zappaterra E., 1990 – Carbonate paleogeographic sequences of the periadriatic region. *Bollettino della Società Geologica Italiana*, 109: 5-20.
- Zappaterra E., 1994 – Source rock distribution model of the Periadriatic Region. *American Association of Petroleum Geologists Bulletin*, 78: 333-354.
- Zarcone G. & Di Stefano P., 2008 – Mesozoic discontinuities in the Panormide Carbonate Platform: constraints on the palaeogeography of the central Mediterranean. *Rendiconti Online della Società Geologica Italiana*, 2: 191-194.
- Zhang F., Kearns S. L., Orr P. J., Benton M. J., Zhou Z., Johnson D., Xu X. & Wang X., 2010 – Fossilized melanosomes and the colour of Cretaceous dinosaurs and birds. *Nature*, 463: 1075-1078.
- Zhang X.-H., Xu X., Zhao X.-J., Sereno P. C., Kuang X.-W. & Tan L., 2001 – A long-necked therizinosauroid dinosaur from the Upper Cretaceous Iren Dabasu Formation of Nei Mongol, People's Republic of China. *Vertebrata Palasiatica*, 10: 282-290.
- Zheng X., Xu X., You H., Zhao Q. & Dong Z., 2009 – A short-armed dromaeosaurid from the Jehol Group of China with implications for early dromaeosaurid evolution. *Proceedings of the Royal Society B*, 277: 211-217.
- Zhou Z.-H., Wang X.-L., Zhang F.-C. & Xu X., 2000 – Important features of *Caudipteryx* - evidence from two nearly complete new specimens. *Vertebrata Palasiatica*, 10: 241-254.
- Zhou Z., Barrett P. M. & Hilton J., 2003 – An exceptionally preserved Lower Cretaceous ecosystem. *Nature*, 421: 807-811.
- Zinke J., 1998 – Small theropod teeth from the Upper Jurassic coal mine of Guimarães (Portugal). *Paläontologische Zeitschrift*, 72: 179-189.
- Ziswiler V. & Farner D. S., 1972 – Digestion and the digestive system. In: Avian Biology, Volume II. Farner D. S. & King J. R. (eds.). *Academic Press*: 343-430.

Cristiano Dal Sasso

Museo Civico di Storia Naturale di Milano, Sezione di Paleontologia dei Vertebrati, Corso Venezia 55, 20121 Milano, Italia.
e-mail: cdalsasso@yahoo.com

Simone Maganuco

Museo Civico di Storia Naturale di Milano, Sezione di Paleontologia dei Vertebrati, Corso Venezia 55, 20121 Milano, Italia.
e-mail: simonemaganuco@iol.it

NOTE ADDED IN PROOF

Very recently, the anatomy of *Juravenator* was re-described [Chiappe L. & Göhlich U., December 2010 – Anatomy of *Juravenator starki* (Theropoda: Coelurosauria) from the Late Jurassic of Germany. *Neues Jahrbuch für Geologie und Paläontologie, Abhandlungen*, 258 (3): 257-296]. Given that this taxon is closely related to *Scipionyx* and frequently mentioned throughout the present monograph, and also that *Scipionyx* is frequently mentioned by Chiappe & Göhlich (2010), we thought it necessary to add the following comparative remarks.

Nasal and lacrimal foramina – No nasal foramina are reported in *Juravenator*, but the presence of at least two of them is suggested by a UV photograph published by Chiappe & Göhlich (2010: fig. 8B). Consistent with the position they occupy in *Scipionyx* (Figs. 23-24, 27), these foramina look to be craniocaudally aligned at the centre of the nasals of *Juravenator*.

On the other hand, Chiappe & Göhlich (2010) confirm in writing a previous personal communication that *Juravenator*, unlike *Scipionyx*, has a lacrimal foramen (pneumatopore), not a simple depression.

Palatal bones – From the illustrations published by Chiappe & Göhlich (2010: fig. 8A-C) it can be seen that some unnamed cranial bones, visible through the right infratemporal, orbital and antorbital fenestrae of *Juravenator*, are nearly in the same position as similarly shaped bones that we identified in the skull of *Scipionyx* (Figs. 23-26), and likely represent homologous elements (e.g., right ectopterygoid).

Diastema – Chiappe & Göhlich (2010) contradict themselves in writing that *Scipionyx* does (p. 263) and does not (p. 268) possess a premaxillary-maxillary diastema. We confirm that such a diastema is present (Figs. 29, 44).

Tooth count and shape – Although Chiappe & Göhlich (2010) estimate a dentary tooth count for *Scipionyx* that is wrong (12-14 *contra* 10; see Fig. 44), what is important is that their estimate for *Juravenator* “did not exceed 11”. In fact, a low number of dentary teeth, approaching that present in *Scipionyx*, is consistent with the low number of maxillary teeth in these two taxa (see also Low Number Of Lateral Teeth in Ontogenetic Assessment).

With regard to tooth shape, we have well-documented (see Heterodonty) that, *contra* Chiappe & Göhlich (2010), the teeth of *Scipionyx* are not “more homogenous in shape”. Rather, like in *Juravenator*, the “maxillary and posterior dentary teeth are more recurved than the premaxillary teeth”.

Cervical pneumaticity – In the present monograph we generically mention the presence of cervical pleurocoels in *Juravenator*, having inferred this from the data matrix of Göhlich & Chiappe (2006). In their redescription of the specimen, Chiappe & Göhlich (2010) specify that “the third cervical in front of the first dorsal exhibits a small, round foramen piercing the center of the centrum – this is the only possible evidence of pneumaticity in the cervical series”. This position, relative to both the bone and

the vertebral series, is consistent with what is observed in other basal coelurosaurs (see Cervical Vertebrae; Figs. 49-50, 53-54).

Neurocentral sutures – The lack of fusion between sacral vertebrae and the presence of open neurocentral sutures, visible on many caudal vertebrae of *Juravenator* (Chiappe & Göhlich, 2010), is further evidence that in compsognathids, as well as in other nonavian theropods, the closure of the neurocentral sutures proceeds from the cervical vertebrae in a caudal direction (see Incomplete Ossification Of The Vertebral Column in Ontogenetic Assessment).

Furcula – In the new description of *Juravenator*, the furcula is reported as “unfused” clavicles. The hatchling *Scipionyx*, which is certainly more juvenile than the specimen of *Juravenator*, unquestionably has two firmly sutured elements (Figs. 87-89). Chiappe & Göhlich (2010) mention this condition of *Scipionyx* and illustrate the clavicles of *Juravenator* as clearly asymmetric (Chiappe & Göhlich, 2010: fig. 17). This, and their observation that one of the two elements “exhibits a hook-like end that is possibly a preservational artifact”, suggest that the furcula of *Juravenator*, rather than being unfused, may have been not only deformed but also broken by the diagenetic processes.

Carpal bones – According to Chiappe & Göhlich (2010), *Juravenator* does not have any carpal bone, probably because not ossified yet – “another indication of the juvenile/immature age of the specimen”. Seeing that ossified tarsal elements are present in the hindlimb of the same specimen (Chiappe & Göhlich, 2010), and that well-formed (radiale) and even co-ossified (dc1+2) carpal bones are present in the *Scipionyx* hatchling (Figs. 93-95), we wonder if the unlabelled osseous elements seen under visible and UV light in the well-articulated forelimb of *Juravenator* (Chiappe & Göhlich, 2010: fig. 20) may in fact be carpals.

Manual phalanges – In the present monograph (see Manual Phalanges) we report that, according to Göhlich & Chiappe (2006, suppl. info., table I), digits I and III of the manus of *Juravenator* are subequal in length, with the latter digit slightly shorter than (i.e., 95% of the length of) the former. In the new table of measurements (Chiappe & Göhlich, 2010), the manual ungual of digit I is now longer, so that digit III is now about 10% shorter than digit I. This increases the difference between *Juravenator* and *Scipionyx* in a character that may be autapomorphic for *Scipionyx* (manual digit III markedly longer than digit I is included in our emended diagnosis).

Reconstructions of *Scipionyx* – The new paper on *Juravenator* contains three reconstructions of *Scipionyx* that are based on Dal Sasso & Signore (1998a) and, consequently, that are not up to date. Referring the reader to the reconstructions included in this monograph, we would like to point out that in the skull of *Scipionyx* redrawn by Chiappe & Göhlich (2010: figs. 9-10) there are portions that in actual fact are not missing; that the mandibular foramen (i.e., the external mandibular fenestra) should be omitted – correctly following the main text (Chiappe &

Göhlich, 2010: p. 272); and that the small foramen in the centre of the maxillary medial wall is actually a depression, not a perforation. Moreover, in the reconstruction of *Scipionyx*'s forelimb (Chiappe & Göhlich, 2010: fig. 19), the scapular acromion should be notched. In fact, in the type specimen two patches of soft tissue overlap the cranial margins of the left and right scapulae in a similar manner, thus hiding scapular necks that gently merge into the acromia (Figs. 87-88, 129).

Horny claws – The preservation of all the horny claws, firmly attached to the manual and pedal ungual phalanges of *Juravenator*, is remarkable and gives us the opportunity to compare them with the homologous elements in *Scipionyx*. The UV photographs published by Chiappe & Göhlich (2010: fig. 20) show that the horny claws of *Juravenator* have very similar shape, structure, curvature and relative length to those of *Scipionyx*.

Internal soft tissue – Although the mode of preservation of *Juravenator* is different from that of *Scipionyx*, we think that some remnants of internal soft tissue in the two specimens may be homologous. Chiappe & Göhlich (2010: fig. 24B) observe vertical strips in between the chevrons of *Juravenator* and suggest that they reflect segmentation of the tail. In our opinion, if these structures really lay on the medial sagittal plane, they are very likely homologous to the similarly shaped laminae preserved between the chevrons of *Scipionyx*, that we refer to the *ligamentum interhaemale* (Fig. 164). On the other hand, pending more detailed illustrations, we provisionally agree with Chiappe & Göhlich (2010: fig. 24A) that the structures paralleling the axis of the tail ventral to the chevrons in *Juravenator* might be remnants of the septa of the *M. ilio-ischiocaudalis*, although not so well-preserved as in *Scipionyx* (Figs. 158-161).

APPENDIX 1

Anatomical abbreviations used in text and figures
Abbreviazioni anatomiche riportate nel testo e nelle figure

l r	when preceding abbreviation, refer to left and right elements davanti ad una abbreviazione, indicano rispettivamente elementi del lato sinistro e destro
()	when including abbreviation, refer to elements overlain by others quando racchiudono una abbreviazione, indicano elementi sottostanti
—	bold lines: visible limits of a given anatomical element linee spesse: limiti visibili di un dato elemento anatomico
—	thin lines: anatomical structures within a given element linee sottili: strutture anatomiche all'interno di un dato elemento
---	hatched lines: estimated limits of an element overlain by others linee tratteggiate: limiti stimati di un elemento sottostante
<i>Italic</i>	latin names
<i>Corsivo</i>	nomi in latino

Cranial skeleton / Cranio

af	adductor fossa fossa degli adduttori	f	frontal frontale
an	angular angolare	feo	<i>fenestra ovalis</i> (oval fenestra finestra ovale)
aofe	antorbital fenestra finestra antorbitale	fln	fossa for <i>ligamentum nuchae</i> fossa del legamento nucale
aof	antorbital fossa fossa antorbitale	fpf	frontoparietal fontanelle fontanella frontoparietale
apm	ascending process of maxilla processo ascendente del mascellare	hy	hyoid ioide
ar	articular articolare	idp	interdental plates piastre interdentali
bs/ps	basisphenoid/parasphenoid basisfenoide/parasfenoide	if	inner (ventral) wall of frontal parete interna (ventrale) del frontale
bt	basal tuber tubero basale	ifb	interfenestral bar barra interfenestratale
capsq	caudal process of squamosal processo caudale dello squamoso	im	inner (lingual) wall of maxilla parete interna (linguale) del mascellare
cif	<i>cresta interfenestralis</i> (interfenestral crest cresta interfenestratale)	in	inner (ventromedial) wall of nasal parete interna (ventromediale) del nasale
cp	cultriform process processo cultriforme	inb	internarial bar barra internasale
cpppt	caudal palatine process of pterygoid processo palatino caudale dello pterigoide	iptv	interpterygoid vacuity spazio interpterigoideo
d	dentary dentale	itfe	infratemporal fenestra finestra infratemporale
d1-10	dentary teeth 1-10 denti 1-10 del dentale	j	jugal giugale
dent	tooth denticles denticoli dei denti	jpect	jugal process of ectopterygoid processo giugale dell'ectopterigoide
dmaf	dorsal margin of adductor fossa margine dorsale della fossa degli adduttori	jpm	jugal process of maxilla processo giugale del mascellare
dtr	dorsal tympanic recess recesso timpanico dorsale	jppal	jugal process of palatine processo giugale del palatino
ect	ectopterygoid ectopterigoide	l	lacrimal lacrimale
en	<i>apertura nasi ossea</i> (external naris narice esterna)	lbn	longitudinal bar of maxilla barra longitudinale del mascellare
epcpt	epipterygoid contact of pterygoid contatto epipterigoideo dello pterigoide	lcq	lateral condyle of quadrate condilo laterale del quadrato
eppt	ectopterygoid process of pterygoid processo ectopterigoideo dello pterigoide	lppt	lateral process of pterygoid processo laterale dello pterigoide
ept	epipterygoid epipterigoide	ls	laterosphenoid laterosfenoide

lv	lacrimal vacuity cavità lacrimale	pro	prootic prootico
m	maxilla mascellare	prs	promaxillary strut puntello promascellare
m1-7	maxillary teeth 1-7 denti mascellari 1-7	pt	pterygoid pterigoide
mcq	medial condyle of quadrate condilo mediale del quadrato	ptaq	pterygoid ala of quadrate ala pterigoidea del quadrato
mfe	maxillary fenestra finestra mascellare	ptect	pterygoid process of ectopterygoid processo pterigoideo dell'ectopterigoide
mfo	maxillary foramina forami mascellari	ptpal	pterygoid process of palatine processo pterigoideo del palatino
mg	Meckelian groove solco di Meckel	ptppv	pterygopalatine process of vomer processo pterigopalatino del vomere
mgar	medial glenoid of articular glenoide mediale dell'articolare	q	quadrate quadrato
mmw	maxillary medial wall parete mediale del mascellare	qapt	quadrate ala of pterygoid ala quadratica dello pterigoide
mn	mylohyoid notch incisura miloioidea	qcsq	quadrate cotyle of squamosal cotilo quadratico dello squamoso
mppal	maxillary process of palatine processo mascellare del palatino	qh	quadrate head testa del quadrato
ms	mandibular symphysis sinfisi mandibolare	qj	quadratojugal quadratojugale
n	nasal nasale	qjcq	quadratojugal contact of quadrate contatto quadratojugale del quadrato
nfo	nasal foramina forami nasali	qjpsq	quadratojugal process of squamosal processo quadratojugale dello squamoso
ofe	orbital fenestra finestra orbitale	rarp	retroarticular process processo retroarticolare
os	orbitosphenoid orbitosfenoide	rrm	rostral ramus of maxilla ramo rostrale del mascellare
p	parietal parietale	sa	surangular soprangolare
pal	palatine palatino	sbtfe	subtemporal fenestra finestra sottotemporale
pm	premaxilla premascellare	scl	scleral plates placche della sclera
pm1-5	premaxillary teeth 1-5 denti premascellari 1-5	snf	subnarial foramen forame sottonasale
pmfo	premaxillary foramina forami premascellari	so	supraoccipital sopraoccipitale
pmpv	premaxillary process of vomer processo premascellare del vomere	sofe	suborbital fenestra finestra sottorbitale
po	postorbital postorbitale	sp	splenic spleniale
pop	paroccipital process processo paroccipitale	spfe	subsidiary palatal fenestra finestra palatale sussidiaria
popp	postorbital process of parietal processo postorbitale del parietale	sq	squamosal squamoso
popsq	postorbital process of squamosal processo postorbitale dello squamoso	srsf	sinusoidal ridge of supratemporal fossa cresta sinusoidale della fossa sopratemporale
pppt	posteromedial process of pterygoid processo posteromediale dello pterigoide	ss	sagittal suture sutura sagittale
ppsq	parietal process of squamosal processo parietale dello squamoso	stfe	supratemporal fenestra finestra sopratemporale
pqf	paraquadrate foramen forame paraquadratico	subn	subnarial process of nasal processo sottonasale del nasale
pra	prearticular prearticolare	subpm	subnarial process of premaxilla processo sottonasale del premascellare
prf	prefrontal prefrontale	suppm	supranarial process of premaxilla processo sopranasale del premascellare
prfe	promaxillary fenestra finestra promascellare	tncp	transverse nuchal crest of parietal cresta nucale trasversale del parietale

trso	transverse ridge of supraoccipital cresta trasversale del supraoccipitale	dna	dorsal neural arch arco neurale dorsale
v	vomer vomere	dp	diapophysis diapofisi
vcd	entrance of <i>vena capitis dorsalis</i> ingresso della vena dorsale del capo	Dr	dorsal rib costola dorsale
vfect	ventral fossa of ectopterygoid fossa ventrale dell'ectopterigoide	ep	epiphysis epifofisi
vmaf	ventral margin of adductor fossa margine ventrale della fossa degli adduttori	ga	gastralia
vppal	vomer process of palatine processo vomerale del palatino	ha	haemal arch (chevron) arco emale
vppt	vomer process of pterygoid processo vomerale dello pterigoide	ila	interspinal ligament attachment inserzione dei legamenti interspinali
wmfe	osseous wall of maxillary fenestra parete ossea della fenestra mascellare	ipofs	infrapostzygapophyseal fossa fossa infrapostzigapofisaria
Axial skeleton / Scheletro assiale		lga	lateral gastralium gastralium laterale
asil	articular surface for ilium superficie articolare per l'ileo	mdf	mediodorsal facet faccetta mediodorsale
assr	articular surface for sacral rib superficie articolare per la costola sacrale	mga	medial gastralium gastralium mediale
ati	atlantal intercentrum intercentro dell'atlante	mvf	medioventral facet faccetta medioventrale
atn	atlantal neurapophysis neurapofisi dell'atlante	nc	neural canal canale neurale
axi	axial intercentrum intercentro dell'epistrofeo	ncs	neurocentral suture sutura neurocentrale
axns	axial neural spine spina neurale dell'epistrofeo	ncas	neurocentral articular surface superficie articolare neurocentrale
C	cervical vertebra vertebra cervicale	ns	neural spine spina neurale
Ca	caudal vertebra vertebra caudale	pcdl	posterior centrodiapophyseal lamina lamina centrodiapofisaria posteriore
caaf	caudal articular facet faccetta articolare caudale	pn	pneumatopore pneumatoporo
cac	caudal centrum centro caudale	podl	postzygodiapophyseal lamina lamina postzigodiapofisaria
cana	caudal neural arch arco neurale caudale	poz	postzygapophysis postzigapofisi
cap	capitulum capitello	ppdl	paradiapophyseal lamina lamina paradiapofisaria
cc	cervical centrum centro cervicale	prdl	prezygodiapophyseal lamina lamina prezigodiapofisaria
cg	costal groove solco costale	prel	prezygoepipophyseal lamina lamina prezigoeipofisaria
clp	craniolateral process processo craniolaterale	prpl	prezygoparapophyseal lamina lamina prezigoparapofisaria
cons	concavity of the neural spine concavità della spina neurale	prz	prezygapophysis prezigapofisi
Cr	cervical rib costola cervicale	S	sacral vertebra vertebra sacrale
craf	cranial articular facet faccetta articolare craniale	sc	sacral centrum centro sacrale
crpr	cranial process processo craniale	sna	sacral neural arch arco neurale sacrale
csga	cranial chevron-shaped gastralium gastralium craniale a forma di V	Sr	sacral rib costola sacrale
ctw	capitulotubercular web membrana capitello-tuberculare	tp	transverse process processo trasverso
D	dorsal vertebra vertebra dorsale	tpolf	intrapostzygapophyseal fossa fossa intrapostzigapofisaria
dc	dorsal centrum centro dorsale	tpolp	intrapostzygapophyseal pneumatopore pneumatoporo intrapostzigapofisario

tu tuberculum
tubercolo
wemvfv wing-like expansion of the medioventral facet
espansione ad ala della faccetta medioventrale

Appendicular skeleton / Scheletro appendicolare

I-III first to third digit
dito dal primo al terzo
1-4 first to fourth phalanx
falangi dalla prima alla quarta
ac acromion
actil acetabular portion of ilium
porzione acetabolare dell'ileo
actis acetabular portion of ischium
porzione acetabolare dell'ischio
bf *brevis fossa*
ca carpals
carpali
cabil caudal blade of ilium
lama caudale dell'ileo
ccil cranial concavity of ilium
concavità craniale dell'ileo
clf fossa of collateral ligament
fossa del legamento collaterale
cn cnemial crest
cresta cnemiale
co coracoid
coracoide
cof coracoid foramen
forame coracoideo
cot coracoid tubercle
tubercolo del coracoide
erbil cranial blade of ilium
lama craniale dell'ileo
cvp cranioventral process
processo cranioventrale
dc1+2 distal carpals 1+2
carpali distali 1+2
dpc deltopectoral crest
cresta deltopettorale
epc *epicleideum*
exp extensor pit
fossa dell'estensore
fe femur
femore
fi fibula
fic fibular condyle
condilo fibulare
ft flexor tubercle
tubercolo del flessore
fu furcula
fus symphysis of furcula
sinfisi della furcula
gl glenoid fossa
fossa glenoidea
gt greater trochanter
trocantere maggiore
hh humeral head
testa dell'omero
hpil hooked process of ilium
processo uncinato dell'ileo
hu humerus
omero
hyc *hypocleideum*

il ilium
ileo
ilis iliac process of ischium
processo iliaco dell'ischio
ilpu iliac process of pubis
processo iliaco del pube
inc internal condyle
condilo interno
is ischium
ischio
isf ischial foot
piede ischiatico
ismf ischial medial facet
faccetta mediale dell'ischio
isp ischial peduncle
peduncolo ischiatico
iti *incisura tibialis*
lec lateral epicondyle
epicondilo laterale
lt lesser trochanter
trocantere minore
mc metacarpal
metacarpale
mec medial epicondyle
epicondilo mediale
mfi medial fossa of fibula
fossa mediale della fibula
obn obturator notch
incisura otturatoria
obp obturator process
processo otturatore
olp olecranon process
processo olecranico
pfo popliteal fossa
fossa poplitea
phar phalangeal articulation
articolazione della falange
pu pubis
pube
pua pubic apron
grembiule pubico
puf pubic foot
piede pubico
pufo pubic foramen
forame pubico
pup pubic peduncle
peduncolo pubico
ra radius
radio
rae radiale
rc radial condyle
condilo radiale
sac supracetabular crest
cresta sopracetabolare
sca scapula
scapola
scono scapulocoracoidal notch
incisura scapolocoracoidea
si *spatium interosseum*
ti tibia
uc ulnar condyle
condilo ulnare
ul ulna

Soft anatomy / Tessuti molli

Ab	A band banda A	jej	jejunum digiuno
aduo	ascending loop of the duodenum ansa ascendente del duodeno	lam	lamella
ait	amorphous indeterminate tissue tessuto amorfo indeterminato	lih	<i>ligamentum interhaemale</i> (interhaemal ligament legamento interemale)
ana	anastomoses anastomosi	liv	liver and other blood-rich organs fegato e altri organi ricchi di sangue
apa	apatite crystallites cristalliti di apatite	lu	lumen lume
atrar	dorsal apexes of one tracheal ring apici dorsali di un anello tracheale	mead	<i>muscularis externa</i> and/or <i>adventitia</i> tonaca muscolare esterna e/o avventizia
ba	bacteria batteri	mes	mesenteric connection connessione mesenterica
bv	blood vessel vaso sanguigno	myo	myofiber miofibra
bvb	branch of blood vessel ramificazione del vaso sanguigno	ncarc	neurocentral articular cartilage cartilagine articolare neurocentrale
bvw	blood vessel wall parete del vaso sanguigno	ol	osteocyte lacuna lacuna osteocitaria
can	canaliculi canalicoli	pifm	puboischiofemoral muscle muscolo puboischiofemorale
cfl	<i>M. caudofemoralis longus</i> (caudofemoral muscle muscolo caudofemorale)	plci	<i>plicae circulares</i> (circular folds pieghe circolari)
cob	collagen bundles fasci di collagene	psila	posterior sacroiliac ligament attachment inserzione del legamento sacroiliaco posteriore
con	connective tissue tessuto connettivo	rec	rectum retto
dduo	descending loop of the duodenum ansa discendente del duodeno	sar	sarcomere sarcomero
duo	duodenum duodeno	sto	stomach contents contenuto stomacale
ensa	endomysium and sarcolemma endomio e sarcolemma	sun	<i>subunguis</i>
eso	oesophagus esofago	tra	trachea
fac	fibrous articular cartilage cartilagine articolare fibrosa	trar	tracheal ring anello tracheale
fp	faecal pellet massa fecale	ts	transverse section sezione trasversa
fsc	fish scales squame di pesce	un	<i>unguis</i>
hac	hyaline articular cartilage cartilagine articolare ialina	Chemical elements / Elementi chimici	
hc	horny claw artiglio corneo	Al	<i>Aluminium</i> (aluminium alluminio)
Ib	I band banda I	Au	<i>Aurum</i> (gold oro)
icm	<i>M. ischiocaudalis</i> (ischiocaudal muscle muscolo ischiocaudale)	C	<i>Carbonium</i> (carbon carbonio)
iicm	<i>M. ilio-ischiocaudalis</i> (ilio-ischiocaudal muscle muscolo ileo-ischiocaudale)	Ca	<i>Calcium</i> (calcium calcio)
iicms	ilio-ischiocaudal muscle septa setti del muscolo ileo-ischiocaudale	Fe	<i>Ferrum</i> (iron ferro)
ile	ileum ileo	Na	<i>Natrium</i> (sodium sodio)
ill	interlamellar line linea interlamellare	O	<i>Oxygenum</i> (oxygen ossigeno)
int	intestine intestino	P	<i>Phosphorus</i> (phosphorus fosforo)
ipam	hypaxial musculature muscolatura ipoassiale	Si	<i>Silicium</i> (silicon silicio)

APPENDIX 2

Modifications to the character list of Senter (2007)

The characters of Senter (2007; and references therein) are not repeated here, except where changes to the character definitions have been made or character states have been added/deleted. Details of the former description are provided in square brackets, with accompanying explanations for changes where needed.

ch27. Pronounced accessory antorbital fenestra absent (0) or present (1) [Formerly: Pronounced, round accessory antorbital fenestra absent (0) or present (1). Reworded according to the observation that in some taxa the accessory antorbital fenestra is not round].

ch28. Accessory antorbital fenestra situated at rostral border of antorbital fossa (0) or situated caudal to rostral border of fossa (1) [Formerly: Accessory antorbital fossa situated at rostral border of antorbital fossa (0) or situated caudal to rostral border of fossa (1)].

ch32. Postorbital process of the jugal: well-developed, taller than half orbit (0) or reduced/absent (1) [Formerly: Jugal and postorbital contribute equally to postorbital bar (0) or ascending process of jugal reduced and descending process of postorbital ventrally elongate (1). In the data matrix of Senter (2007) there were no taxa coded (1), so that the previous character was uninformative].

ch45. Frontal edge smooth in region of lacrimal suture (or prefrontal suture, where the contact is with this bone) (0) or edge notched (1) [Formerly: Frontal edge smooth in region of lacrimal suture (0) or edge notched (1). Reworded according to the observation that in *Scipionyx* the frontal edge contacts the prefrontal. *Scipionyx* is coded (0), the edge forming a faint, unnotched concavity].

ch48. Descending process of squamosal nearly parallels quadrate shaft (0) or nearly perpendicular to quadrate shaft (1) [Formerly: Descending process of squamosal parallels quadrate shaft (0) or nearly perpendicular to quadrate shaft (1)].

ch63. Palatine and ectopterygoid separated by pterygoid or making point contact, at most (0) or contact (1) [Formerly: Palatine and ectopterygoid separated by pterygoid (0) or contact (1). In *Scipionyx*, palatine and ectopterygoid make point contact, but they can be considered as separated].

ch73. External mandibular fenestra oval (0), subdivided by a spinous rostral process of the surangular (1), or absent (2) [Formerly: External mandibular fenestra oval (0) or subdivided by a spinous rostral process of the surangular (1). We added the character state (2), several taxa lacking a mandibular fenestra].

ch74. Internal mandibular fenestra absent or small and slit-like (0) or large and rounded (1) [Formerly: Internal mandibular fenestra small and slit-like (0) or large and rounded (1). Reworded according to the observation

that in some taxa (e.g., *Compsognathus*) the internal mandibular fenestra can be considered as absent; this absence potentially represents a new derived character state, however, it can not be ascertained pending new, more complete specimens, and new studies on the known ones].

ch77. Coronoid ossification present (0) or absent (1) [Formerly: Coronoid ossification large (0) or only a thin splint (1) or absent (2). The coronoid is the complex supradyratory-coronoid (e.g., Holtz *et al.*, 2004)].

ch101. Cervical and cranial trunk vertebrae amphiplatyan to platycoelous (0) or strongly opisthocelous (1) [Formerly: Cervical and anterior trunk vertebrae amphiplatyan (0) or opisthocelous (1)].

ch106. Dorsal vertebrae not pneumatic (0) or pneumatic (1) [Formerly: Middle and posterior dorsal vertebrae not pneumatic (0) or pneumatic (1)].

ch109. Scars for interspinal ligaments terminate at apex of neural spine in dorsal vertebrae (0) or terminate below apex of neural spine (1), or interspinal ligament attachments in form of beak-like processes below apex of neural spine (2) [Formerly: Scars for interspinal ligaments terminate at apex of neural spine in dorsal vertebrae (0) or terminate below apex of neural spine (1). Character state (2) has been added to reflect the condition visible in some basal coelurosaurus, *Scipionyx* included].

ch154. Ventral edge of cranial ala of ilium straight or gently curved (0) or ventral edge hooked cranially (1) [Formerly: Ventral edge of anterior ala of ilium straight or gently curved (0) or ventral edge hooked anteriorly (1) or very strongly hooked (2). Character state (2) has been deleted because there are no taxa showing that character state in the present data set].

ch168. Obturator process of ischium contacts pubis in the distal half (1) or not (0) [Formerly: Obturator process does not contact pubis (0) or contacts pubis (1)].

ch169. Craniocaudal length of the caudal process of the pubic foot: process absent (0); process present but shorter than 1/5 of the proximodistal length of the pubis (1); process present and long more than 1/5 but less than 1/3 of the proximodistal length of the pubis (2); process present and longer than 1/3 of the proximodistal length of the pubis (3) (Modified from Holtz, 2000; following Cau, pers. comm., 2009). [Formerly: Length of pubic boot $\leq 30\%$ of length of pubis (0) or $\geq 40\%$ (1). There are some taxa (e.g., *Sinocalliopteryx*) showing intermediate values that render impossible the application of the character as proposed by Senter (2007), and render difficult, at the same time, to define new values for separating the character states; for this reason we have preferred to focus our attention on the caudal process of the pubic foot, and to change the whole character].

ch205. Foot symmetrical (0), asymmetrical with slender mt II and very robust mt IV (1), or asymmetrical with mt IV reduced in mediolateral width (2) [Formerly: Foot symmetrical (0), or asymmetrical with slender mt II and very robust mt IV (1). Character state (2) has been introduced to describe the condition in some taxa, such as *Nqwebasaurus* and *Aniksosaurus*].

ch207. Shaft diameter of phalanx I-1 less (0) or equal/greater (1) than shaft diameter of radius [Reworded because there are some taxa in which phalanx I-1 is equal to the shaft diameter of the radius, resulting more similar to the condition in which phalanx I-1 is greater than the shaft diameter of the radius, than to the opposite condition. Formerly: Shaft diameter of phalanx I-1 less (0) or greater (1) than shaft diameter of radius].

ch231. Dentary teeth do not (0) or do (1) increase in size rostrally [Formerly: Dentary teeth do not (0) or do increase in size rostrally, becoming more conical in shape (1). Senter (2007) commented: "Character reworded to refer only to tooth size". He maintained, however, a reference to the tooth shape; we completely deleted any reference to the tooth size to avoid confusion - e.g., *Compsognathus* should be coded (0) for tooth size and (1) for tooth shape].

ch235. Cranial concavity of the preacetabular blade of the ilium in lateral view: absent (0); present and slightly developed (1); present and craniocaudally expanded (2) [Formerly: Snout does not (0) or does taper to an anterior point (1). This character from Senter (2007) has been excluded because equivocal: for example, it is not clear in which view the snout is intended to taper, and why *Archaeopteryx* is coded (1) and *Compsognathus* (0) in the Senter (2007) data matrix. The new character focusses on the cranial concavity of the preacetabular blade of the ilium seen in several basal coelurosaurs; the same concavity is described as "craniodorsal" in Rauhut (2003), and "anterodorsal" in Xu *et al.* (2004); although it is virtually cranioventral in position (Carpenter *et al.*, 2005b: fig. 3.10), the concavity shown by *Ornitholestes* was coded (1), supposing it as homologous].

ch239. Rostral portion of the maxillary antorbital fossa: small, from 10% to less than 40% of the rostrocaudal length of the antorbital cavity (0), large, greater than 40% of the rostrocaudal length of the antorbital cavity (1) [Formerly: Maxillary antorbital fossa: small, from 10% to less than 40% of the rostrocaudal length of the antorbital cavity (0), large, greater than 40% of the rostrocaudal length of the antorbital cavity (1)].

ch240. Maxillary fenestra large and round (0), a large, craniocaudally elongate oblong (1), a small, craniocaudally elongate slit, not dorsally displaced (2), a small, dorsally displaced opening (3), or a small and round, not dorsally displaced opening (4) [Formerly: ch240. Maxillary fenestra large and round (0), a large, craniocaudally elongate oblong (1), a small, craniocaudally elongate slit, not dorsally displaced (2), or a small, dorsally displaced opening (3). Character state (4) has been added to reflect the condition in *Juravenator* and *Huaxiagnathus*].

ch270. Acromion process does not match any of the following descriptions (0), rectangular with its dorsal edge forming a 90° angle with the dorsal edge of the scapular blade (1) or a quarter-circle in shape (2) or triangular, with apex pointing away from and subparallel to scapular blade (3) [Formerly: Acromion process does not match any of the following descriptions: (0) rectangular with its dorsal edge forming a 90° angle with the dorsal edge of the scapular blade (1) or a quarter-circle in shape (2) or triangular, with apex pointing away from and subparallel to scapular blade (3)].

APPENDIX 3

Major changes in character codings with respect to the data matrix of Senter (2007)

ch40. This has been coded (2) for most of the ornithomimids in which the character can be scored (see Data matrix in Appendix 6), with the only exception of *Pelecanimimus polyodon*. This is *contra* Senter (2007), in which the character state for most ornithomimids is (0).

ch47. The codings have been checked for all the taxa, with the following additions: *Harpymimus okladnikovi* (0); *Caudipteryx* (1); *Oviraptor philoceratops* (1); and *Epidendrosaurus ningchengensis* (1).

ch51. The codings have been checked for all the taxa, with the following additions: *Eotyrannus lengi* (0); *Gorgosaurus libratus* (0); *Garudimimus brevipes* (0); *Erlikosaurus andrewsi* (0); *Protarchaeopteryx robusta* (0); *Epidendrosaurus ningchengensis* (0); *Confuciusornis sanctus* (1); and *Yanornis martini* (1).

ch255. This character has been coded as inapplicable (-) in taxa lacking an external mandibular fenestra.

ch258. This character has been coded as inapplicable (-) in taxa lacking mesial denticles, including the troodontids *Byronosaurus jaffei* and *Troodon formosus*, which formerly were coded (1).

Huxiagnathus orientalis

Additions: ch37(0); ch73(2); ch85(0/2); ch96(0); ch107(0); ch109(2); ch116(0); ch117(0); ch121(0/1); ch187(0); ch192(0); ch204(0); ch268(0); ch282(1); ch346(1); ch357(0).

Changes: ch42(2); ch115(0); ch126(0); ch142(0/1); ch175(1); 202(?); ch236(?); ch240(4); ch251(?); ch255(-); ch258(-); ch263(1); ch283(1); ch284(1); ch286(1); ch299(1); ch360(-).

Compsognathus longipes

Additions: ch20(0); ch22(0); ch28(1); ch29(1); ch31(0); ch32(0); ch33(1); ch34(1); ch41(1); ch42(2); ch45(0); 48(0); 49(0); 50(0); 51(0); 52(0); 73(2); 74(0); 76(0); 77(0); 78(0); 80(0); ch101(1); ch107(0); ch109(2); ch110(0); ch127(0); ch134(0); ch138(0); ch141(0); ch146(1); ch148(0); ch149(0); ch150(0); ch152(0); ch153(0); ch154(0); ch156(0); ch174(0); ch192(0); ch193(0); ch194(1); ch210(0); ch214(0); ch218(0); ch225(0); ch226(0); ch227(0); ch241(0); ch256(0); ch257(0/1); ch260(0); ch268(0); ch280(0); ch282(1); ch283(0); ch284(1); ch285(0); ch286(1); ch287(0); ch288(1); ch289(0); ch290(0); ch291(0); ch292(1); ch293(0); ch298(1); ch328(0); ch337(0); ch344(0); ch345(0); ch354(0); ch360(-).

Changes: ch71(0); ch96(0); ch115(0); ch126(0); ch135(?); ch181(0); ch182(0); ch184(0); ch233(1); ch255(-); ch258(-); ch263(1); ch275(1).

Sinosauropteryx prima

Additions: ch33(0); ch69(0); ch76(0); ch109(2); ch160(0); ch204(0); ch226(1); ch227(0).

Changes: ch73(2); ch96(0); ch126(0); ch175(1); ch202(?); ch255(-); ch258(-); ch263(1).

Dilong paradoxus

Additions: ch51(1); ch256(1).

Changes: ch72(1).

Tanycolagreus topwilsoni

Additions: ch146(1); ch211(0).

Changes: ch148(0); ch271(0); ch310(1).

Ornitholestes hermanni

Additions: ch84(1).

Changes: ch109(2); ch117(1); ch152(?); ch173(0); ch235(1); ch314(0).

Coelurus fragilis

Additions: ch117(1).

Changes: ch100(0/1); ch169(?); ch263(0/1); ch310(1).

Bambiraptor feinbergi

Changes: 135(?); 241(?).

APPENDIX 4

Comments on selected characters of Senter (2007)

ch43. Anterior emargination of supratemporal fossa on frontal straight or slightly curved (0) or strongly sinusoidal and reaching onto postorbital process (1). In *Scipionyx* the fossa is confined to the lateral part of the skull roof, showing a limited mediolateral extension; the caudal margin of the frontal, however, forms a sinusoidal emargination reaching the postorbital process in correspondence with the fossa and well-extended medially, farther than the medial extension of the fossa. Taking into account the whole sinusoidal emargination, and not only its portion in correspondence with the fossa, *Scipionyx* is coded (1).

ch89. Dentary teeth evenly spaced (0) or rostral dentary teeth smaller, more numerous and more closely appressed than those in middle of tooth row (1). The dentary teeth of *Scipionyx* are evenly spaced from each other but slightly more closely appressed than those in the middle of the tooth row. Nevertheless, they are neither more numerous nor smaller, being rather larger than those in the middle of the tooth row. Therefore, *Scipionyx* can be coded (0).

ch108. Neural spines of dorsal vertebrae not expanded distally (0) or expanded to form a "spine table" (1). In *Scipionyx* the apex of the neural spine in dorsal vertebrae 2, 3 and 6 is feebly expanded, but in our opinion it cannot be considered a true spine table and *Scipionyx* has been coded (0). However, this character should be more clearly quantified.

ch142. Olecranon process weakly developed (0) or distinct and large but not hypertrophied (1) or hypertrophied (2). Character state (2) is clearly referred to the hypertrophied olecranon process of alvarezsaurids. On the other hand, distinction between character states (0) and (1) is not so clear in certain cases, some taxa showing "intermediate" conditions, and the state (1), as it is, includes a large variability of development of the olecranon process. For example, *Scipionyx*, as well as *Sinosauropteryx* and *Compsognathus*, can be coded (1). However, the olecranon process of *Sinosauropteryx* is comparatively more developed than that of *Scipionyx* and *Compsognathus*, being sometimes described as "hypertrophied", although it is not as hypertrophied as in alvarezsaurids. This degree of variability would require more states for this character, more clearly separated and, possibly, well-quantified.

ch148. Distal carpals 1+2 well-developed, covering all of proximal ends of metacarpals I and II (0) or small, cover about half of base of metacarpals I and II (1) or cover bases of all metacarpals (2). *Scipionyx* can be coded (1), although it shows a particular condition (see Forelimb) in which most of the proximal end of McI is covered. *Huaxiagnathus* and *Sinocalliopteryx* have been coded (1) as well, their distal carpals 1+2 contacting both McI and McII, although covering less than half of the two bones.

ch206. Neural spines on caudal dorsal vertebrae in lateral view rectangular or square (0) or craniocaudally expanded distally, fan-shaped (1). *Scipionyx* has been coded (1), but see description (Dorsal Vertebrae) about the use of the term "fan-shaped".

APPENDIX 5

Comments on the coding of character states possibly affected by juvenile ontogenetic stage

ch2. Orbit round in lateral or dorsolateral view (0) or dorsoventrally elongate (1). Among basal coelurosaurs, a dorsoventrally elongate orbit is present only in the adults of the large-sized tyrannosaurids *Tyrannosaurus* and *Gorgosaurus*. All the other taxa maintain a round orbit in all growth stages; therefore, *Scipionyx* has been coded (0).

ch38. Supraorbital crests on lacrimal in adult individuals absent (0) or dorsal crest above orbit (1) or lateral expansion rostral and dorsal to orbit (2). Dorsal crests and rugosities above orbit and lateral to it are often present in allosauroids, but are uncommon in coelurosaurs (e.g., Holtz *et al.*, 2004). A lateral expansion rostral and dorsal to the orbit is present in the ornithomimosaur *Garudimimus* and *Pelecanimimus*, and in the troodontids *Troodon*, *Byronosaurus* and *Zanabazar*. All these taxa are known from adult individuals. In *Scipionyx*, the lacrimal closely resembles that of other basal coelurosaurs, both juveniles and adults. For this reason, we have coded *Scipionyx* (0), pending adult material.

ch46. Dorsal surface of parietals flat, lateral ridge borders supratemporal fenestra (0) or parietals dorsally convex with very low sagittal crest along midline (1) or dorsally convex with well-developed sagittal crest (2). Parietal crests are very low or absent in various small-sized theropods not strictly related to each other, such as coelophysoids, *Compsognathus*, ornithomimosaur and oviraptorosaurs. In ornithomimosaur (Makovicky *et al.*, 2004), the sagittal crest is absent in both juveniles and adults. A sharp but rather low sagittal ridge is present in some adult oviraptorosaurs (Osmólska *et al.*, 2004) but is totally absent in early ontogenetic stages of *Citipati* and cf. *Rinchenia* (Auditore, pers. comm., 2009), in which, however, the parietals are already convex dorsally. A well-developed sagittal crest is present in both tyrannosauroids and some troodontids. In tyrannosaurids the sagittal crest is already well-developed in juveniles (Carr & Williamson, 2004). Tykoski (2005) did not include this character in the list of the maturity-dependent characters deleted from the analysis. In all the above mentioned taxa, the parietal does not vary noticeably in curvature during ontogeny. Concerning *Scipionyx*, the sagittal crest is absent, and the dorsal surface of the parietal is almost flat (see Parietal), with lateral ridges bordering extensively the supratemporal fenestra. Based on all these data, we provisionally coded *Scipionyx* (0), pending adult material.

ch47. Parietals separate (0) or fused (1). In *Scipionyx* the parietals are separated. However, this character is often indicated as a maturity-dependent character (e.g., Tykoski, 2005). For this reason it has been coded (?).

ch65. Suborbital fenestra similar in length to orbit (0) or about half or less than half orbital length (1) or absent (2). The orbit in *Scipionyx* is very large, more than four times the length of the suborbital fenestra. However, the size of the orbit is clearly maturity-dependent, as is often the case in extant vertebrates. For this reason, *Scipionyx* is coded (0/1).

ch85. Dentary and maxillary teeth large, less than 25 in dentary (0) or large number of small teeth (25 or more in dentary) (1) or small number of dentary teeth (≤ 11) (2) or dentary without teeth (3). *Scipionyx* has 10 dentary teeth. However, as the formation of new tooth positions would be expected during growth (see Ontogenetic assessment), *Scipionyx* has been coded (?).

ch135. Scapula and coracoid separate (0) or fused into scapulocoracoid (1). According to Tykoski (2005), scapula and coracoid fuse in adults. For this reason, *Scipionyx*, *Juravenator*, *Compsognathus* and *Bambiraptor* have been scored (?).

ch139. Scapula longer than humerus (0) or humerus longer than scapula (1). As the girdles are comparatively small in size in immature theropods (see Ontogenetic Assessment), *Scipionyx* has been coded (?).

ch169. Craniocaudal length of the caudal process of the pubic foot: process absent (0); process present but shorter than 1/5 of the proximodistal length of the pubis (1); process present and long more than 1/5 but less than 1/3 of the proximodistal length of the pubis (2); process present and longer than 1/3 of the proximodistal length of the pubis (3). According to Tykoski (2005) this character is maturity-dependent. In *Scipionyx* a caudal process of the pubic foot is present, and it is craniocaudally shorter than 1/5 of the proximodistal length of the pubis. However, we cannot exclude that during ontogeny it would have become longer. For this reason *Scipionyx* is coded (1/3).

ch232. Length of skull more than 90% of femoral length (0) or less than 80% (1). Most basal coelurosaurs have a skull length that is more than 90% of the femoral length. In *Scipionyx* the skull length is 130% of the femoral length. The skull is longer than the femur also in *Juravenator* and in the large, more mature compsognathids *Sinocallipteryx* and *Huaxiagnathus*, and it approximates femoral length in *Compsognathus*. In both juveniles and adults of *Tyrannosaurus* (Brochu, 2003; Mortimer, 2004-2010) the skull is almost as long as the femur. In juveniles and adults of *Sinornithomimus* (Kobayashi & Lü, 2003) the skull is 61% and 69% of the femoral length, respectively. Taking into account those examples, it is very unlikely to suppose that in *Scipionyx* the skull, starting from 130%, would have become shorter than 80% of the femoral length during growth. For this reason *Scipionyx* is coded (0).

ch236. Area of antorbital fenestra greater than that of orbit (0) or less than that of orbit (1). In non-tyrannosauroid basal coelurosaurs the area of the antorbital fenestra measures less than the orbital area. In *Scipionyx* the snout should have become more than three times longer than it is, in order to have an area of antorbital fenestra comparable to that of the orbit. For this reason *Scipionyx* is coded (1).

ch239. Rostral portion of the maxillary antorbital fossa: small, from 10% to less than 40% of the rostrocaudal length of the antorbital cavity (0), large, greater than 40% of the rostrocaudal length of the antorbital cavity (1). The rostral portion of the maxillary antorbital fossa is very small in *Scipionyx*, due to the shortness of the snout. As this character is clearly maturity-dependent, the Italian compsognathid has been coded (?).

ch240. Maxillary fenestra large and round (0), a large, craniocaudally elongate oblong (1), a small, craniocaudally elongate slit, not dorsally displaced (2), a small, dorsally displaced opening (3), or a small and round, not dorsally displaced opening (4). The snout in *Scipionyx* is very short craniocaudally and steeply inclined, leaving little space for the maxillary fenestra. We cannot exclude that the small, dorsally displaced opening of *Scipionyx* would have changed in shape and position during growth, therefore this taxon has been coded (?).

ch241. Nasal fusion: absent, nasals separate (0) or present, nasals fused together (1). According to Tykoski (2005) this character is maturity-dependent, and has been coded (?) in taxa not represented by adult individuals (e.g., *Scipionyx*, *Juravenator*, *Compsognathus* and *Bambiraptor*). The only exception is *Dilong*, in which the nasal fusion occurred prior to maturity (Xu *et al.*, 2004), so that it has been coded (1).

ch244. Nasals at least as long as frontals (0) or shorter than frontals (1). In *Scipionyx* the nasal is shorter than the frontal (1). However, the condition in all likelihood reflects the early ontogenetic stage of the individual (see Ontogenetic Assessment).

Taxa	Characters	61	62	63	64	65	66	67	68	69	70	71	72	73	74	75
<i>Allosaurus fragilis</i>		0	0	0	0	0	0	0	0	0	0	0	0	0	0	1
<i>Sinraptor</i>		0	0	0	0	?	0	0	0	0	0	0	0	0	?	1
<i>Dilong paradoxus</i>		?	?	?	?	?	0	0	0	?	0	0	1	?	?	0
<i>Eotyrannus lengi</i>		?	?	?	?	?	0	0	?	?	0	?	0	?	?	?
<i>Tyrannosaurus rex</i>		?	0	0	0	0	0	0	0	0	0	0	0	0	0	1
<i>Gorgosaurus libratus</i>		?	?	?	?	0	0	0	0	0	0	0	0	0	0	1
<i>Tanycolagreus topwilsoni</i>		?	?	?	?	?	?	?	?	?	?	?	?	?	?	?
<i>Coelurus fragilis</i>		?	?	?	?	?	?	2	?	?	0	0	1	?	?	?
<i>Ornitholestes hermanni</i>		?	?	?	?	?	0	0	0	0	0	0	0	0	0	0
<i>Guanlong wucaii</i>		?	?	?	?	?	0	1	0	0	0	0	1	0	?	0
<i>Aniksosaurus darwini</i>		?	?	?	?	?	?	?	?	?	?	?	?	?	?	?
<i>Nedcolbertia justinhoffmani</i>		?	?	?	?	?	?	?	?	?	?	?	?	?	?	?
<i>Nqwebasaurus thwazi</i>		?	?	?	?	?	?	?	?	?	?	?	?	?	?	?
<i>Santanaraptor placidus</i>		?	?	?	?	?	?	?	?	?	?	?	?	?	?	?
<i>Orkoraptor burkei</i>		?	?	?	?	?	?	?	?	?	?	?	?	?	?	?
<i>Juravenator starki</i>		?	0	?	0	0	1	?	0	0	0	0	1	0	2	?
<i>Mirischia asymmetrica</i>		?	?	?	?	?	?	?	?	?	?	?	?	?	?	?
<i>Compsognathus longipes</i>		?	0	?	?	0	1	0	0	0	0	0	0	2	0	0
<i>Sinocalliopteryx gigas</i>		?	0	?	?	0	1	0	0	?	0	0	0	2	?	?
<i>Huaxiagnathus orientalis</i>		?	?	?	?	?	0	0	?	0	0	1	0	2	?	?
<i>Sinosauropteryx prima</i>		?	?	?	?	?	0	0	0	0	0	1	?	2	?	?
<i>Scipionyx samniticus</i>		?	0	0	0	0	1	0	0	0	0	0	0	2	?	?
<i>Deinocheirus mirificus</i>		?	?	?	?	?	?	?	?	?	?	?	?	?	?	?
<i>Harpymimus okladnikovi</i>		?	?	?	?	?	0	2	0	0	0	0	?	0	0	0
<i>Pelecanimimus polyodon</i>		?	?	?	?	?	0	0	0	?	0	0	0	0	?	0
<i>Shenzhousaurus orientalis</i>		?	?	?	0	?	0	0	0	0	0	0	0	0	?	?
<i>Archaeornithomimus asiaticus</i>		?	?	?	?	?	?	?	?	?	?	?	?	?	?	?
<i>Garudimimus brevipes</i>		?	?	1	?	?	0	0	0	0	0	0	0	0	0	0
<i>Anserimimus planinychus</i>		?	?	?	?	?	?	?	?	?	?	?	?	?	?	?
<i>Ornithomimus edmontonicus</i>		?	?	?	?	?	0	0	0	0	0	0	0	0	0	1
<i>Struthiomimus altus</i>		?	0	1	?	?	0	0	0	0	0	0	0	0	0	1
<i>Gallimimus bullatus</i>		?	0	1	0	1	0	0	0	0	0	0	0	0	0	1
<i>Falcarius utahensis</i>		?	?	?	?	?	?	0	?	?	0	0	0	?	?	?
<i>Beipiaosaurus inexpectus</i>		?	?	?	?	?	?	2	?	?	1	?	?	?	?	?
<i>Alxasaurus elesitaiensis</i>		?	?	?	?	?	2	2	0	?	1	0	0	?	?	?
<i>Nothronychus mckinleyi</i>		?	?	?	?	?	?	?	?	?	?	?	?	?	?	?
<i>Erliaosaurus bellamanus</i>		?	?	?	?	?	?	?	?	?	?	?	?	?	?	?
<i>Nanshiungosaurus brevispinus</i>		?	?	?	?	?	?	?	?	?	?	?	?	?	?	?
<i>Neimongosaurus yangi</i>		?	?	?	?	?	2	1	?	?	?	?	0	?	?	?
<i>Segnosaurus galbiensis</i>		?	?	?	?	?	?	2	?	?	1	0	?	0	0	0
<i>Erlikosaurus andrewsi</i>		?	1	1	1	1	2	2	0	0	1	0	0	0	0	0
<i>Therizinosaurus cheloniformis</i>		?	?	?	?	?	?	?	?	?	?	?	?	?	?	?
<i>Alvarezsaurus calvoi</i>		?	?	?	?	?	?	?	?	?	?	?	?	?	?	?
<i>Patagonykus puertai</i>		?	?	?	?	?	?	?	?	?	?	?	?	?	?	?
<i>Mononykus olecranus</i>		?	?	?	?	?	?	?	?	?	?	?	?	?	?	?
<i>Shuvuuia deserti</i>		?	1	?	1	1	0	0	0	1	0	0	0	0	0	0
<i>Incisivosaurus gauthieri</i>		0	1	1	1	1	2	0	0	1	0	0	0	0	1	0
<i>Protarchaeopteryx robusta</i>		?	?	?	?	?	?	0	?	?	0	0	0	?	?	?

Taxa / Characters	76	77	78	79	80	81	82	83	84	85	86	87	88	89	90
<i>Allosaurus fragilis</i>	0	0	0	0	0	0	0	0	0	0	1	0	1	0	1
<i>Sinraptor</i>	0	?	0	0	0	0	0	0	0	0	1	0	1	0	1
<i>Dilong paradoxus</i>	?	?	?	0	0	0	0	0	0	0	1	0	1	0	?
<i>Eotyrannus lengi</i>	?	?	?	?	?	0	0	0	0	?	1	0	?	?	0
<i>Tyrannosaurus rex</i>	0	0	1	0	0	0	0	0	0	0	1	0	1	0	1
<i>Gorgosaurus libratus</i>	0	0	1	0	0	0	0	0	0	0	1	0	1	0	1
<i>Tanycolagreus topwilsoni</i>	?	?	0	0	0	0	0	?	?	?	?	?	1	?	?
<i>Coelurus fragilis</i>	?	?	?	?	?	?	?	?	?	0	?	?	?	?	1
<i>Ornitholestes hermanni</i>	0	?	0	0	0	0	0	0	1	0	1	0	1	0	0
<i>Guanlong wucaii</i>	0	?	0	0	0	0	0	0	0	0	1	0	1	0	?
<i>Aniksosaurus darwini</i>	?	?	?	?	?	?	?	?	?	?	?	?	?	?	?
<i>Nedcolbertia justinhoffmani</i>	?	?	?	?	?	?	?	?	?	?	?	?	?	?	?
<i>Nqwebasaurus thwazi</i>	?	?	?	?	?	?	?	?	?	?	?	?	?	?	?
<i>Santanaraptor placidus</i>	?	?	?	?	?	?	?	?	?	?	?	?	?	?	?
<i>Orkoraptor burkei</i>	?	0	?	?	?	?	?	0	1	?	1	0	1	?	?
<i>Juravenator starki</i>	0	?	?	?	?	0	0	0	0	2	1	0	1	0	?
<i>Mirischia asymmetrica</i>	?	?	?	?	?	?	?	?	?	?	?	?	?	?	?
<i>Compsognathus longipes</i>	0	0	0	0	0	0	0	0	1	0	1	0	1	0	1
<i>Sinocalliopteryx gigas</i>	?	?	0	0	0	0	0	0	1	0	2	1	0	1	0
<i>Huaxiagnathus orientalis</i>	?	?	?	0	?	0	0	0	1	0	2	1	0	1	0
<i>Sinosauropteryx prima</i>	0	?	?	0	?	0	0	0	1	0	1	0	1	0	?
<i>Scipionyx samniticus</i>	0	0	0	0	?	0	1	0	1	2	1	0	1	0	1
<i>Deinocheirus mirificus</i>	?	?	?	?	?	?	?	?	?	?	?	?	?	?	?
<i>Harpymimus okladnikovi</i>	0	?	?	?	?	1	?	1	2	2	?	?	?	?	0
<i>Pelecanimimus polyodon</i>	0	?	?	0	?	0	0	0	2	1	?	?	0	0	0
<i>Shenzhousaurus orientalis</i>	0	?	?	0	?	1	?	1	2	2	?	?	1	?	?
<i>Archaeornithomimus asiaticus</i>	?	?	?	?	?	?	?	?	?	?	?	?	?	?	?
<i>Garudimimus brevipes</i>	0	1	0	0	0	1	?	1	?	3	?	?	?	?	?
<i>Anserimimus planinychus</i>	?	?	?	?	?	?	?	?	?	?	?	?	?	?	?
<i>Ornithomimus edmontonicus</i>	0	?	?	0	0	1	?	1	?	3	?	?	?	?	?
<i>Struthiomimus altus</i>	0	1	0	0	0	1	?	1	?	3	?	?	?	?	?
<i>Gallimimus bullatus</i>	0	1	0	0	0	1	?	1	?	3	?	?	?	?	?
<i>Falcarius utahensis</i>	?	?	?	?	?	?	?	0	0	1	1	0	0	0	0
<i>Beipiaosaurus inexpectus</i>	?	?	?	?	?	?	?	?	0	1	0	0	0	0	1
<i>Alxasaurus elesitaiensis</i>	?	?	?	?	?	?	?	?	0	1	0	0	0	0	1
<i>Nothronychus mckinleyi</i>	?	?	?	?	?	?	?	0	0	1	0	0	0	?	?
<i>Erliansaurus bellamanus</i>	?	?	?	?	?	?	?	?	?	?	?	?	?	?	?
<i>Nanshiungosaurus brevispinus</i>	?	?	?	?	?	?	?	?	?	?	?	?	?	?	?
<i>Neimongosaurus yangi</i>	?	?	?	?	?	?	?	?	0	?	0	0	0	?	1
<i>Segnosaurus galbiensis</i>	0	?	0	0	0	?	?	?	0	1	0	0	0	0	1
<i>Erlikosaurus andrewsi</i>	0	1	0	0	0	1	?	0	0	1	0	0	0	0	1
<i>Therizinosaurus cheloniformis</i>	?	?	?	?	?	?	?	?	?	?	?	?	?	?	?
<i>Alvarezsaurus calvoi</i>	?	?	?	?	?	?	?	?	?	?	?	?	?	?	?
<i>Patagonykus puertai</i>	?	?	?	?	?	?	?	?	?	?	?	?	?	?	?
<i>Mononykus olecranus</i>	?	?	?	?	?	?	?	?	2	?	?	?	0	?	?
<i>Shuvuuia deserti</i>	0	1	1	0	0	0	?	0	2	1	?	?	0	0	0
<i>Incisivosaurus gauthieri</i>	0	0	?	1	?	0	2	0	2	2	?	?	0	0	0
<i>Protarchaeopteryx robusta</i>	?	?	?	?	?	0	2	0	2	2	?	?	0	0	0

Taxa	Characters	91	92	93	94	95	96	97	98	99	100	101	102	103	104	105
<i>Allosaurus fragilis</i>		0	0	1	0	0	0	0	0	0	0	1	0	0	1	0
<i>Sinraptor</i>		0	0	1	0	0	0	0	0	0	0	1	0	0	1	0
<i>Dilong paradoxus</i>		1	?	?	?	0	0	?	0	1	0	1	?	?	?	?
<i>Eotyrannus lengi</i>		1	?	?	?	0	0	?	?	1	?	1	?	?	?	?
<i>Tyrannosaurus rex</i>		1	0	1	0	0	0	0	0	0	0	1	0	0	1	0
<i>Gorgosaurus libratus</i>		1	0	1	0	0	0	0	0	0	?	?	0	0	1	0
<i>Tanycolagreus topwilsoni</i>		0	?	?	?	?	?	?	?	?	?	?	?	0	1	0
<i>Coelurus fragilis</i>		?	?	?	?	0	0	0	0	1	0	1	0	?	0	1
<i>Ornitholestes hermanni</i>		0	?	?	?	0	0	0	1	1	?	1	1	0	1	1
<i>Guanlong wucaii</i>		1	0	?	?	?	?	?	?	1	0	0	?	?	1	?
<i>Aniksosaurus darwini</i>		?	?	?	?	0	?	?	0	1	?	0	?	?	?	?
<i>Nedcolbertia justinhoffmani</i>		?	?	?	?	?	?	?	?	?	0	?	?	?	?	?
<i>Nqwebasaurus thwazi</i>		?	?	?	?	0	?	?	1	1	?	?	?	?	?	?
<i>Santanaraptor placidus</i>		?	?	?	?	?	?	?	?	?	?	?	?	?	?	?
<i>Orkoraptor burkei</i>		?	?	?	?	?	?	?	?	?	?	?	?	?	?	?
<i>Juravenator starki</i>		0	0	0	?	?	?	?	?	1	0	?	?	?	?	?
<i>Mirischia asymmetrica</i>		?	?	?	?	?	?	?	?	?	?	?	?	?	?	?
<i>Compsognathus longipes</i>		0	0	0	?	0	0	0	?	1	0	1	0	?	?	?
<i>Sinocalliopteryx gigas</i>		0	0	?	?	?	0	?	?	1	?	1	?	?	?	?
<i>Huaxiagnathus orientalis</i>		0	0	?	?	0	0	?	?	1	?	?	?	?	?	?
<i>Sinosauropteryx prima</i>		0	0	?	?	0	0	?	?	1	0	0	?	?	?	?
<i>Scipionyx samniticus</i>		0	0	1	1	0	0	?	0	1	0	1	?	0	?	?
<i>Deinocheirus mirificus</i>		?	?	?	?	?	?	?	?	?	?	?	?	?	?	?
<i>Harpymimus okladnikovi</i>		?	0	?	?	?	0	0	?	1	1	0	0	0	1	?
<i>Pelecanimimus polyodon</i>		1	?	?	?	1	0	0	1	1	?	0	0	?	?	?
<i>Shenzhousaurus orientalis</i>		?	?	?	?	?	?	?	?	?	?	0	?	?	?	?
<i>Archaeornithomimus asiaticus</i>		?	?	?	?	?	0	0	0	1	1	0	0	0	1	0
<i>Garudimimus brevipes</i>		?	?	0	1	1	0	0	?	?	?	0	0	0	?	?
<i>Anserimimus planinychus</i>		?	?	?	?	?	?	?	?	?	?	?	?	?	?	0
<i>Ornithomimus edmontonicus</i>		?	0	0	1	?	0	0	1	1	0	0	0	0	1	0
<i>Struthiomimus altus</i>		?	0	0	1	?	1	0	1	1	0	0	0	0	1	0
<i>Gallimimus bullatus</i>		?	0	0	1	1	0	0	1	1	0	0	0	0	1	0
<i>Falcarius utahensis</i>		?	?	?	?	1	0	?	0	1	1	0	1	?	1	0
<i>Beipiaosaurus inexpectus</i>		?	?	?	?	?	?	?	?	1	?	?	?	?	?	?
<i>Alxasaurus elesitaiensis</i>		?	?	?	?	?	?	?	?	?	?	0	?	0	1	?
<i>Nothronychus mckinleyi</i>		?	?	?	?	0	0	0	0	1	1	0	1	?	?	1
<i>Erliansaurus bellamanus</i>		?	?	?	?	?	?	?	?	?	?	?	1	?	?	?
<i>Nanshiungosaurus brevispinus</i>		?	?	?	?	?	?	?	?	?	?	0	0	0	1	?
<i>Neimongosaurus yangi</i>		?	1	?	?	1	0	0	1	1	?	0	1	0	1	?
<i>Segnosaurus galbiensis</i>		?	?	?	?	?	?	?	?	?	?	?	?	?	?	?
<i>Erlikosaurus andrewsi</i>		?	?	?	?	?	?	?	?	?	?	?	?	?	?	?
<i>Therizinosaurus cheloniformis</i>		?	?	?	?	?	?	?	?	?	?	?	?	?	?	?
<i>Alvarezsaurus calvoi</i>		?	?	?	?	1	?	?	?	1	0	0	?	?	?	?
<i>Patagonykus puertai</i>		?	?	?	?	?	?	?	?	?	?	?	?	1	1	1
<i>Mononykus olecranus</i>		?	?	?	?	?	0	1	?	1	?	1	1	1	0	1
<i>Shuvuuia deserti</i>		?	?	0	1	1	1	1	1	1	0	1	1	1	0	1
<i>Incisivosaurus gauthieri</i>		2	?	?	?	?	?	?	?	?	?	?	?	?	?	?
<i>Protarchaeopteryx robusta</i>		2	?	?	?	?	0	0	?	1	?	?	?	?	?	?

Taxa / Characters	106	107	108	109	110	111	112	113	114	115	116	117	118	119	120
<i>Allosaurus fragilis</i>	0	0	0	0	0	0	0	0	0	1	?	0	1	0	0
<i>Sinraptor</i>	0	0	0	0	0	0	0	0	0	1	?	0	?	?	?
<i>Dilong paradoxus</i>	0	?	?	?	?	?	?	?	?	1	?	?	?	?	0
<i>Eotyrannus lengi</i>	?	?	?	?	?	?	?	?	?	?	?	?	?	?	?
<i>Tyrannosaurus rex</i>	1	0	0	0	0	0	0	1	0	1	?	0	0	0	0
<i>Gorgosaurus libratus</i>	1	0	0	0	0	0	0	1	0	1	?	0	0	0	0
<i>Tanycolagreus topwilsoni</i>	0	0	0	?	?	?	?	?	?	?	?	0	?	?	0
<i>Coelurus fragilis</i>	0	0	0	?	?	?	?	?	?	?	?	1	0	0	2
<i>Ornitholestes hermanni</i>	0	0	0	2	?	?	1	0	0	?	?	1	0	1	0
<i>Guanlong wucaii</i>	0	0	0	?	0	?	?	0	1	?	?	?	?	2	0
<i>Aniksosaurus darwini</i>	?	?	?	?	?	?	?	?	?	?	?	2	0	?	?
<i>Nedcolbertia justinhoffmani</i>	1	?	?	?	?	?	0	0	?	?	?	0	?	?	?
<i>Nqwebasaurus thwazi</i>	?	?	?	?	?	?	?	?	?	?	?	?	?	?	?
<i>Santanaraptor placidus</i>	?	?	?	?	?	?	?	?	?	?	?	?	?	?	?
<i>Orkoraptor burkei</i>	?	?	?	?	?	?	?	?	?	?	?	?	0	?	?
<i>Juravenator starki</i>	?	0	0	?	?	?	0	1	0	0	0	0	?	0	?
<i>Mirischia asymmetrica</i>	?	?	?	?	?	0	0	1	0	?	?	?	?	?	?
<i>Compsognathus longipes</i>	0	0	0	2	0	?	?	?	0	0	0	?	0	?	2
<i>Sinocalliopteryx gigas</i>	0	0	0	?	?	?	?	?	?	0	0	?	0	?	2
<i>Huaxiagnathus orientalis</i>	?	0	0	2	?	?	?	?	?	0	0	0	0	?	2
<i>Sinosauropteryx prima</i>	0	?	0	2	0	?	?	?	?	1	?	?	1	1	2
<i>Scipionyx samniticus</i>	?	0	?	2	0	?	?	?	0	?	0	1	1	?	?
<i>Deinococheirus mirificus</i>	?	?	?	?	?	?	?	?	?	?	?	?	?	?	?
<i>Harpymimus okladnikovi</i>	0	0	0	0	1	?	1	0	0	0	0	?	0	0	0
<i>Pelecanimimus polyodon</i>	?	0	?	?	?	?	?	?	?	?	?	?	?	?	?
<i>Shenzhousaurus orientalis</i>	0	?	?	?	0	?	?	?	0	0	0	0	0	?	?
<i>Archaeornithomimus asiaticus</i>	0	0	0	0	1	?	1	0	0	0	0	0	0	0	0
<i>Garudimimus brevipes</i>	0	?	0	0	1	?	?	0	?	?	?	?	?	?	?
<i>Anserimimus planinychus</i>	?	?	?	?	?	?	?	?	?	?	?	?	?	?	?
<i>Ornithomimus edmontonicus</i>	0	0	0	0	1	0	1	0	0	0	0	0	0	0	0
<i>Struthiomimus altus</i>	0	0	0	0	1	0	1	0	0	0	0	0	0	0	0
<i>Gallimimus bullatus</i>	0	0	0	0	1	?	1	0	0	0	0	0	0	0	0
<i>Falcarius utahensis</i>	1	?	0	0	0	?	1	1	0	0	1	1	1	0	2
<i>Beipiaosaurus inexpectus</i>	?	?	?	?	?	?	?	?	?	?	?	?	?	?	?
<i>Alxasaurus elesitaiensis</i>	0	0	0	0	0	?	1	?	0	0	1	?	?	0	2
<i>Nothronychus mckinleyi</i>	0	0	0	0	1	?	?	?	?	?	?	1	?	?	?
<i>Erliaosaurus bellamanus</i>	0	?	?	?	?	?	?	?	?	?	?	?	0	?	?
<i>Nanshiungosaurus brevispinus</i>	0	0	?	?	0	?	?	?	0	?	?	?	?	?	?
<i>Neimongosaurus yangi</i>	0	?	0	?	1	?	?	2	?	0	1	0	0	0	2
<i>Segnosaurus galbiensis</i>	?	?	?	?	?	?	?	?	0	?	?	?	?	?	?
<i>Erlikosaurus andrewsi</i>	?	?	?	?	?	?	?	?	?	?	?	?	?	?	?
<i>Therizinosaurus cheloniformis</i>	?	?	?	?	?	?	?	?	?	?	?	?	?	?	?
<i>Alvarezsaurus calvoi</i>	?	?	?	?	?	?	2	?	1	?	?	2	?	1	2
<i>Patagonykus puertai</i>	?	?	?	?	?	?	?	?	1	?	?	2	?	?	?
<i>Mononykus olecranus</i>	0	0	1	1	?	?	?	?	1	?	?	2	?	?	?
<i>Shuvuuia deserti</i>	?	0	?	?	1	?	2	0	1	?	?	2	0	1	2
<i>Incisivosaurus gauthieri</i>	?	?	?	?	?	?	?	?	?	?	?	?	?	?	?
<i>Protarchaeopteryx robusta</i>	?	?	?	?	?	?	?	?	?	0	1	?	?	?	?

Taxa / Characters	121	122	123	124	125	126	127	128	129	130	131	132	133	134	135
<i>Allosaurus fragilis</i>	0	0	0	0	0	0	1	?	?	?	?	0	0	0	0
<i>Sinraptor</i>	?	?	?	?	?	?	?	1	?	0	0	?	0	?	0
<i>Dilong paradoxus</i>	?	0	?	0	?	1	?	0	?	?	?	?	?	?	0
<i>Eotyrannus lengi</i>	?	?	?	?	?	?	?	?	?	?	?	?	0	?	0
<i>Tyrannosaurus rex</i>	0	0	0	0	?	?	1	?	?	?	?	0	0	0	0
<i>Gorgosaurus libratus</i>	0	0	0	0	0	0	1	?	?	?	?	0	0	0	0
<i>Tanycolagreus topwilsoni</i>	?	?	?	?	?	?	?	?	?	?	?	?	0	0	0
<i>Coelurus fragilis</i>	?	?	?	?	?	?	?	?	?	?	?	?	0	?	0
<i>Ornitholestes hermanni</i>	?	?	1	?	?	?	?	?	?	?	?	?	?	?	?
<i>Guanlong wucaii</i>	?	0	?	?	0	?	?	?	?	?	?	?	0	0	0
<i>Aniksosaurus darwini</i>	?	?	?	?	?	?	?	?	?	?	?	?	?	?	?
<i>Nedcolbertia justinhoffmani</i>	?	0	?	?	?	?	?	?	?	?	?	?	?	?	0
<i>Nqwebasaurus thwazi</i>	?	?	?	?	?	?	?	?	?	?	?	?	0	0	0
<i>Santanaraptor placidus</i>	?	?	?	?	?	?	?	?	?	?	?	?	?	?	?
<i>Orkoraptor burkei</i>	?	0	?	?	?	?	?	?	?	?	?	?	?	?	?
<i>Juravenator starki</i>	0	0	?	0	1	0	0	0	?	0	0	?	0	0	?
<i>Mirischia asymmetrica</i>	?	?	?	?	?	?	?	?	?	?	?	?	?	?	?
<i>Compsognathus longipes</i>	0	0	0	0	0	0	1	?	?	?	?	?	0	0	?
<i>Sinocalliopteryx gigas</i>	0	0	0	0	0	0	0	?	?	?	?	0	0	0	0
<i>Huaxiagnathus orientalis</i>	0	1	0	0	0	0	0	?	?	?	?	0	0	0	0
<i>Sinosauropteryx prima</i>	0	0	0	0	0	0	0	0	?	?	?	?	0	0	0
<i>Scipionyx samniticus</i>	?	0	?	0	0	0	1	?	?	?	?	1	0	0	?
<i>Deinocheirus mirificus</i>	?	?	?	?	?	?	?	?	?	?	?	?	?	?	1
<i>Harpymimus okladnikovi</i>	0	0	?	1	?	?	?	?	?	?	?	?	0	?	0
<i>Pelecanimimus polyodon</i>	?	?	?	?	?	?	?	0	1	0	0	?	?	?	0
<i>Shenzhousaurus orientalis</i>	?	0	?	?	?	?	?	?	?	?	?	?	?	?	?
<i>Archaeornithomimus asiaticus</i>	?	0	?	?	?	?	?	?	?	?	?	?	0	1	0
<i>Garudimimus brevipes</i>	?	?	?	?	?	?	?	?	?	?	?	?	?	?	?
<i>Anserimimus planinychus</i>	?	?	0	?	?	?	?	?	?	?	?	?	?	1	?
<i>Ornithomimus edmontonicus</i>	?	0	0	1	0	0	1	?	?	?	?	?	0	1	1
<i>Struthiomimus altus</i>	0	0	0	1	0	0	1	?	?	?	?	?	0	1	1
<i>Gallimimus bullatus</i>	0	0	0	1	0	0	?	?	?	?	?	?	0	1	1
<i>Falcarius utahensis</i>	?	0	1	1	?	?	?	?	?	?	?	?	?	0	0
<i>Beipiaosaurus inexpectus</i>	1	?	?	?	?	?	?	?	?	?	?	0	?	?	?
<i>Alxasaurus elesitaiensis</i>	?	0	?	1	?	?	?	?	?	?	?	?	?	?	?
<i>Nothronychus mckinleyi</i>	1	?	?	?	?	?	?	?	?	?	?	?	0	?	0
<i>Erliaosaurus bellamanus</i>	?	?	?	?	?	?	?	?	?	?	?	?	?	?	?
<i>Nanshiungosaurus brevispinus</i>	?	?	?	?	?	?	?	?	?	?	?	?	?	?	?
<i>Neimongosaurus yangi</i>	1	0	?	1	?	?	?	?	?	?	?	0	0	0	1
<i>Segnosaurus galbiensis</i>	?	?	?	?	?	?	?	?	?	?	?	?	0	?	1
<i>Erlikosaurus andrewsi</i>	?	?	?	?	?	?	?	?	?	?	?	?	?	?	?
<i>Therizinosaurus cheloniformis</i>	?	?	?	?	?	?	?	?	?	?	?	?	0	0	1
<i>Alvarezsaurus calvoi</i>	?	?	?	?	?	?	?	?	?	?	?	?	0	?	0
<i>Patagonykus puertai</i>	?	?	?	?	?	?	?	?	?	?	?	?	?	0	0
<i>Mononykus olecranus</i>	?	?	?	1	?	?	?	1	0	0	0	?	0	0	0
<i>Shuvuuia deserti</i>	0	0	0	1	0	0	?	1	0	0	0	?	0	0	0
<i>Incisivosaurus gauthieri</i>	?	?	?	?	?	?	?	?	?	?	?	?	?	?	?
<i>Protarchaeopteryx robusta</i>	1	0	?	?	?	?	?	0	?	?	?	0	?	?	?

Taxa / Characters	136	137	138	139	140	141	142	143	144	145	146	147	148	149	150
<i>Allosaurus fragilis</i>	0	0	0	0	0	0	1	0	0	0	1	0	1	0	0
<i>Sinraptor</i>	?	?	0	0	?	?	?	?	?	?	?	?	?	?	0
<i>Dilong paradoxus</i>	2	0	?	1	0	?	?	?	?	?	?	0	?	0	0
<i>Eotyrannus lengi</i>	?	0	?	0	0	0	?	?	?	?	?	?	?	?	0
<i>Tyrannosaurus rex</i>	0	0	0	0	1	0	1	0	0	?	?	0	?	0	1
<i>Gorgosaurus libratus</i>	0	0	0	0	1	0	1	0	0	0	0	0	1	0	1
<i>Tanycolagreus topwilsoni</i>	0	0	0	0	0	0	1	0	0	?	1	0	0	0	0
<i>Coelurus fragilis</i>	?	?	0	?	0	0	1	0	0	?	?	0	1	?	0
<i>Ornitholestes hermanni</i>	?	?	?	?	0	?	0	0	0	?	?	?	?	?	?
<i>Guanlong wucaii</i>	?	?	?	0	0	?	0	0	?	?	1	0	1	0	0
<i>Aniksosaurus darwini</i>	?	?	?	?	0	0	?	0	?	?	?	?	?	?	?
<i>Nedcolbertia justinhoffmani</i>	?	?	?	?	?	?	?	?	?	?	?	?	?	?	?
<i>Nqwebasaurus thwazi</i>	0	0	0	0	0	?	1	?	?	-	0	0	1	1	0
<i>Santanaraptor placidus</i>	?	?	?	?	?	?	?	?	?	?	?	?	?	?	?
<i>Orkoraptor burkei</i>	?	?	?	?	?	?	?	?	?	?	?	?	?	?	?
<i>Juravenator starki</i>	?	?	0	0	0	?	0	0	?	?	?	0	?	0	0
<i>Mirischia asymmetrica</i>	?	?	?	?	?	?	?	?	?	?	?	?	?	?	?
<i>Compsognathus longipes</i>	0	0	0	0	0	0	1	0	?	?	1	0	0	0	0
<i>Sinocalliopteryx gigas</i>	0	?	0	0	0	?	0	0	?	?	1	0	1	0	0
<i>Huaxiagnathus orientalis</i>	0	0	0	0	0	?	0	1	0	?	?	1	0	1	0
<i>Sinosauropteryx prima</i>	0	0	?	0	0	?	1	0	?	?	1	0	1	0	0
<i>Scipionyx samniticus</i>	0	?	0	1	0	0	1	0	?	-	1	0	1	0	0
<i>Deinocheirus mirificus</i>	?	0	0	0	0	0	1	0	0	?	?	0	?	1	0
<i>Harpymimus okladnikovi</i>	?	0	?	0	0	0	1	0	0	1	0	0	1	0	0
<i>Pelecanimimus polyodon</i>	2	?	?	?	2	?	1	0	?	?	0	0	1	1	0
<i>Shenzhousaurus orientalis</i>	?	?	?	?	?	?	?	?	?	?	?	?	?	?	0
<i>Archaeornithomimus asiaticus</i>	2	0	1	?	2	0	1	0	0	?	?	0	?	1	0
<i>Garudimimus brevipes</i>	?	?	?	?	?	?	?	?	?	?	?	?	?	?	?
<i>Anserimimus planinychus</i>	?	?	1	?	2	?	?	?	?	0	0	0	1	1	0
<i>Ornithomimus edmontonicus</i>	2	0	1	0	2	0	1	0	0	0	0	0	?	1	0
<i>Struthiomimus altus</i>	2	0	1	0	2	0	1	0	0	0	0	0	1	1	0
<i>Gallimimus bullatus</i>	2	0	1	0	2	0	1	0	0	0	?	0	1	1	0
<i>Falcarius utahensis</i>	?	1	0	0	0	1	1	0	1	1	0	0	0	0	0
<i>Beipiaosaurus inexpectus</i>	0	?	?	?	?	?	?	?	?	?	0	0	?	0	0
<i>Alxasaurus elesitaiensis</i>	?	?	?	0	0	0	?	0	?	1	0	0	0	0	0
<i>Nothronychus mckinleyi</i>	?	?	?	?	0	1	1	0	0	?	?	?	?	?	?
<i>Erliaosaurus bellamanus</i>	?	?	?	0	0	?	1	0	?	?	?	0	?	0	0
<i>Nanshiungosaurus brevispinus</i>	?	?	?	?	?	?	?	?	?	?	?	?	?	?	?
<i>Neimongosaurus yangi</i>	0	0	0	0	0	0	?	?	?	?	?	?	?	?	?
<i>Segnosaurus galbiensis</i>	0	?	1	?	0	0	?	?	?	?	?	?	?	?	0
<i>Erlikosaurus andrewsi</i>	?	?	?	?	0	?	?	?	?	?	?	?	?	?	?
<i>Therizinosaurus cheloniformis</i>	0	0	0	?	0	?	0	0	?	?	0	0	1	0	0
<i>Alvarezsaurus calvoi</i>	?	0	?	?	?	?	?	?	?	?	?	?	?	?	?
<i>Patagonykus puertai</i>	2	0	?	?	3	0	2	1	0	?	1	1	0	?	?
<i>Mononykus olecranus</i>	2	0	0	0	3	0	2	1	0	?	1	1	2	2	?
<i>Shuvuuia deserti</i>	2	0	?	0	3	0	2	1	?	?	1	1	2	2	0
<i>Incisivosaurus gauthieri</i>	?	?	?	?	?	?	?	?	?	?	?	?	?	?	?
<i>Protarchaeopteryx robusta</i>	1	?	?	?	?	?	0	0	?	?	1	0	1	0	0

Taxa / Characters	136	137	138	139	140	141	142	143	144	145	146	147	148	149	150
<i>Avimimus portentosus</i>	?	0	0	0	1	0	0	?	?	?	1	1	0	?	?
<i>Caudipteryx</i>	1	0	0	0	1	?	0	0	?	?	1	0	0	0	0
<i>Microvenator celer</i>	0	0	?	?	0	1	0	0	0	?	?	?	?	?	?
<i>Elmisaurus rarus</i>	?	?	?	?	?	?	?	?	?	?	?	0	?	?	0
<i>Chirostenotes pergracilis</i>	1	?	?	?	?	?	?	?	?	?	?	?	?	?	0
<i>Caenagnathus collinsi</i>	?	?	?	?	?	?	?	?	?	?	?	?	?	?	?
<i>Oviraptor philoceratops</i>	?	0	?	0	0	0	0	0	1	?	1	1	0	?	0
<i>Rinchenia mongoliensis</i>	?	?	0	0	0	0	0	?	?	?	1	?	0	?	?
<i>Citipati osmolskae</i>	1	0	0	0	0	1	0	0	?	1	1	0	0	0	0
Zamyn Khondt oviraptorine	1	0	0	0	0	?	0	?	?	?	1	0	0	0	0
<i>Ingenia yanshini</i>	1	?	0	0	0	0	0	0	?	?	1	0	0	0	0
<i>Conchoraptor gracilis</i>	1	0	0	0	0	1	0	?	?	?	?	?	?	?	?
<i>Khaan mckennai</i>	1	0	0	0	0	?	0	0	?	1	1	0	0	0	0
<i>Heyuannia huangi</i>	1	0	?	0	0	?	1	0	?	?	1	1	1	0	?
<i>Sinovenator changii</i>	1	1	1	?	0	?	?	?	?	?	?	?	?	?	?
<i>Mei long</i>	1	1	?	1	0	?	0	?	1	?	1	0	0	0	0
<i>Byronosaurus jaffei</i>	?	?	?	?	?	?	?	?	?	?	?	?	?	?	?
<i>Sinornithoides youngi</i>	1	1	?	?	0	?	0	0	?	?	1	0	0	0	0
IGM 100/44	?	?	?	?	?	?	?	?	?	?	1	0	0	0	0
<i>Troodon formosus</i>	?	?	?	?	0	1	0	?	?	?	?	0	?	?	?
<i>Saurornithoides mongoliensis</i>	?	?	?	?	?	?	?	?	?	?	?	?	?	?	?
<i>Zanabazar junior</i>	?	?	?	?	?	?	?	?	?	?	?	?	?	?	?
<i>Unenlagia</i>	?	?	1	?	0	1	?	?	?	?	?	?	?	?	?
<i>Buitreraptor gonzalezorum</i>	1	1	1	1	0	1	0	?	1	?	1	0	0	?	0
<i>Rahonavis ostromi</i>	?	?	1	1	?	?	0	0	0	?	?	?	?	?	?
<i>Bambiraptor feinbergi</i>	1	1	1	1	0	?	0	0	1	?	1	0	1	0	0
<i>Sinornithosaurus millenii</i>	3	1	1	1	0	?	0	0	?	?	?	0	?	0	0
<i>Microaptor zhaoianus</i>	?	1	?	1	0	1	0	0	?	1	1	0	1	0	0
NGMC91	3	1	?	1	0	?	0	0	?	?	1	?	1	0	0
IGM 100 1015	?	?	?	?	?	?	?	?	?	?	?	?	?	?	?
<i>Adasaurus mongoliensis</i>	1	?	1	?	?	?	?	?	?	?	?	?	?	?	?
<i>Velociraptor mongoliensis</i>	1	1	1	1	0	1	0	0	1	1	1	0	0	0	0
<i>Saurornitholestes langstoni</i>	1	?	1	?	?	?	?	?	?	?	1	0	?	?	0
<i>Deinonychus antirrhopus</i>	1	1	1	1	0	1	0	0	1	1	1	0	0	0	0
<i>Achillobator giganticus</i>	1	?	?	?	?	?	?	?	?	?	?	?	?	?	0
<i>Dromaeosaurus albertensis</i>	?	?	?	?	?	?	?	?	?	?	?	?	?	?	?
<i>Utahraptor ostrommaysi</i>	1	?	?	?	?	?	?	?	?	?	?	?	?	?	?
<i>Atrociraptor marshalli</i>	?	?	?	?	?	?	?	?	?	?	?	?	?	?	?
<i>Epidendrosaurus ningchengensis</i>	1	1	?	1	0	?	0	0	?	?	1	0	1	0	0
<i>Archaeopteryx lithographica</i>	1	1	1	1	0	0	0	0	?	1	1	0	0	0	0
<i>Wellnhoferia grandis</i>	1	1	1	1	0	?	0	?	?	?	?	0	?	0	0
<i>Jeholornis prima</i>	3	?	1	1	0	?	0	0	?	?	1	1	0	0	0
<i>Sapeornis chaoyangensis</i>	1	1	1	1	0	?	0	0	?	?	1	1	2	0	0
<i>Confuciusornis sanctus</i>	3	1	1	1	4	0	0	0	1	1	1	1	1	0	0
<i>Protopteryx fengningensis</i>	3	1	?	1	0	0	0	0	?	?	1	1	2	0	0
<i>Yanornis martini</i>	3	1	?	1	0	?	0	0	?	?	1	1	2	0	?
<i>Hagryphus giganteus</i>	?	?	?	?	?	?	?	?	?	?	1	0	0	0	0

Taxa	/	Characters	151	152	153	154	155	156	157	158	159	160	161	162	163	164	165
<i>Allosaurus fragilis</i>			0	1	0	1	0	0	0	0	0	0	1	0	0	0	0
<i>Sinraptor</i>			0	?	?	1	0	0	0	0	?	0	1	0	0	?	0
<i>Dilong paradoxus</i>			0	0	0	0	0	0	?	1	?	?	?	?	?	?	0
<i>Eotyrannus lengi</i>			0	0	?	?	?	?	?	?	?	?	?	?	?	?	?
<i>Tyrannosaurus rex</i>			0	0	0	1	0	0	1	0	0	0	1	0	0	0	0
<i>Gorgosaurus libratus</i>			0	0	0	1	0	0	1	0	0	0	1	0	0	0	0
<i>Tanycolagreus topwilsoni</i>			0	1	0	?	?	?	?	?	?	?	?	?	?	?	?
<i>Coelurus fragilis</i>			?	?	?	?	?	?	?	?	?	?	?	?	?	?	?
<i>Ornitholestes hermanni</i>			0	?	0	1	0	0	0	1	?	?	0	1	0	?	0
<i>Guanlong wucaii</i>			0	0	0	1	0	0	0	1	0	0	?	0	1	0	1
<i>Aniksosaurus darwini</i>			0	?	?	?	?	?	1	0	1	?	?	?	1	0	?
<i>Nedcolbertia justinhoffmani</i>			0	1	0	?	?	?	?	?	?	?	?	?	?	?	?
<i>Nqwebasaurus thwazi</i>			1	1	0	?	?	?	?	?	?	?	?	?	?	?	?
<i>Santanaraptor placidus</i>			?	?	?	?	?	?	?	?	?	?	?	?	?	?	0
<i>Orkoraptor burkei</i>			?	?	?	?	?	?	?	?	?	?	?	?	?	?	?
<i>Juravenator starki</i>			0	0	0	0	0	0	?	0	?	0	0	0	?	0	0
<i>Mirischia asymmetrica</i>			?	?	?	1	?	0	?	?	?	?	?	0	0	0	0
<i>Compsognathus longipes</i>			0	0	0	0	0	0	?	?	?	0	?	?	?	?	0
<i>Sinocalliopteryx gigas</i>			0	0	0	1	0	0	?	0	?	0	?	?	1	0	1
<i>Huaxiagnathus orientalis</i>			0	0	0	0	0	0	2	0	?	0	?	?	1	0	0
<i>Sinosauropteryx prima</i>			0	1	0	0	0	0	2	0	?	0	?	?	?	?	0
<i>Scipionyx samniticus</i>			0	0	0	1	0	0	1	0	?	0	?	?	1	0	1
<i>Deinocheirus mirificus</i>			0	0	0	?	?	?	?	?	?	?	?	?	?	?	?
<i>Harpymimus okladnikovi</i>			2	0	0	1	0	?	?	0	0	0	1	1	?	?	?
<i>Pelecanimimus polyodon</i>			2	0	0	?	?	?	?	?	?	?	?	?	?	?	?
<i>Shenzhousaurus orientalis</i>			2	0	0	1	0	0	0	0	?	?	1	1	0	?	0
<i>Archaeornithomimus asiaticus</i>			1	0	0	?	?	?	0	0	0	?	1	1	0	0	0
<i>Garudimimus brevipes</i>			?	?	?	1	0	0	0	0	0	0	1	1	0	0	?
<i>Anserimimus planinychus</i>			1	0	0	?	?	?	?	?	?	?	?	?	?	?	?
<i>Ornithomimus edmontonicus</i>			1	0	0	1	0	0	0	0	0	0	1	1	0	0	0
<i>Struthiomimus altus</i>			1	0	0	1	0	0	0	0	0	0	1	1	0	0	0
<i>Gallimimus bullatus</i>			1	0	0	1	0	0	0	0	0	0	1	1	0	0	0
<i>Falcarius utahensis</i>			0	0	0	1	0	0	?	1	1	0	0	1	0	1	0
<i>Beipiaosaurus inexpectus</i>			0	0	?	1	0	0	?	?	?	?	?	?	?	?	?
<i>Alxasaurus elesitaiensis</i>			0	0	0	1	0	0	2	1	?	0	0	?	?	1	0
<i>Nothronychus mckinleyi</i>			?	?	?	?	?	?	?	?	?	?	?	?	?	?	0
<i>Erliansaurus bellamanus</i>			0	1	0	?	?	?	?	1	?	?	?	1	?	?	?
<i>Nanshiungosaurus brevispinus</i>			?	?	?	1	?	0	?	?	?	0	?	?	?	2	0
<i>Neimongosaurus yangi</i>			?	?	?	1	?	?	2	1	1	0	0	?	?	2	?
<i>Segnosaurus galbiensis</i>			?	?	?	1	0	0	2	1	1	0	0	1	?	2	0
<i>Erlikosaurus andrewsi</i>			?	?	?	?	?	?	?	?	?	?	?	?	?	?	?
<i>Therizinosaurus cheloniformis</i>			0	?	0	?	?	?	?	?	?	?	?	?	?	?	?
<i>Alvarezsaurus calvoi</i>			1	?	?	?	0	0	1	1	1	?	0	?	?	2	?
<i>Patagonykus puertai</i>			1	1	0	?	?	?	?	?	?	?	?	1	?	?	?
<i>Mononykus olecranus</i>			1	1	0	0	?	?	1	?	?	?	?	1	?	?	0
<i>Shuvuuia deserti</i>			1	1	0	0	0	?	1	?	1	0	1	1	?	2	0
<i>Incisivosaurus gauthieri</i>			?	?	?	?	?	?	?	?	?	?	?	?	?	?	?
<i>Protarchaeopteryx robusta</i>			0	0	0	0	0	2	?	1	?	?	?	?	?	?	?

Taxa / Characters	166	167	168	169	170	171	172	173	174	175	176	177	178	179	180
<i>Allosaurus fragilis</i>	0	1	0	2	0	0	0	0	0	0	0	0	0	0	0
<i>Sinraptor</i>	0	1	0	2	0	0	0	0	0	0	1	0	0	0	0
<i>Dilong paradoxus</i>	?	1	0	3	?	0	?	1	?	?	1	?	0	?	?
<i>Eotyrannus lengi</i>	?	?	?	?	?	?	?	?	?	?	?	?	?	?	?
<i>Tyrannosaurus rex</i>	0	1	0	3	1	0	1	1	0	1	0	0	0	0	0
<i>Gorgosaurus libratus</i>	0	1	0	3	1	0	0	1	0	1	0	0	0	0	0
<i>Tanycolagreus topwilsoni</i>	?	?	?	2 3	?	?	?	?	?	?	1	0	0	0	0
<i>Coelurus fragilis</i>	?	?	?	3	?	?	?	?	?	1	1	0	0	0	0
<i>Ornitholestes hermanni</i>	0	1	0	?	0	0	0	0	0	1	?	1	0	0	0
<i>Guanlong wucaii</i>	0	1	0	3	1	0	0 1	0	0	1	0	0	0	0	?
<i>Aniksoosaurus darwini</i>	?	1	?	?	0	?	?	?	0	?	?	?	?	?	0
<i>Nedcolbertia justinhoffmani</i>	?	?	0	2	0	?	?	0	?	0	1	0	0	0	?
<i>Nqwebasaurus thwazi</i>	?	?	0	1	?	?	?	?	?	0	0	0	0	0	?
<i>Santanaraptor placidus</i>	0	1	0	?	0	?	?	1	0	?	?	?	?	?	?
<i>Orkoraptor burkei</i>	?	?	?	?	?	?	?	?	?	?	?	?	?	?	?
<i>Juravenator starki</i>	0	1	0	?	?	?	0 1	?	0	0	?	?	?	?	?
<i>Mirischia asymmetrica</i>	0	1	0	3	0	?	0 1	?	0	0	1	1	0	0	?
<i>Compsognathus longipes</i>	0	1	0	3	?	1	0	0	0	0	1	?	0	?	?
<i>Sinocalliopteryx gigas</i>	1	1	0	2	?	0	0 1	0	0	1	0 1	?	0	?	?
<i>Huaxiagnathus orientalis</i>	0	1	0	2	?	0	0	0	0	1	1	?	0	?	?
<i>Sinosauropteryx prima</i>	0	1	0	2	?	1	0	0	?	1	1	?	0	?	?
<i>Scipionyx samniticus</i>	0	1	0	1 3	?	0	0	0	?	1	1	0	0	0	?
<i>Deinocheirus mirificus</i>	?	?	?	?	?	?	?	?	?	?	?	?	?	?	?
<i>Harpymimus okladnikovi</i>	0	?	?	?	?	?	?	?	?	?	?	?	0	0	?
<i>Pelecanimimus polyodon</i>	?	?	?	?	?	?	?	?	?	?	?	?	?	?	?
<i>Shenzhousaurus orientalis</i>	0	1	0	1	?	0	0	0	0	0	0	1	0	0	?
<i>Archaeornithomimus asiaticus</i>	1	1	0	?	1	?	0	0	?	0	0	1	0	0	0
<i>Garudimimus brevipes</i>	?	?	?	2	?	?	?	?	?	0	0	?	0	0	0
<i>Anserimimus planinychus</i>	?	?	?	?	?	?	?	?	?	?	?	?	?	?	?
<i>Ornithomimus edmontonicus</i>	1	1	0	2	1	0	0	0	0	0	0	1	0	0	0
<i>Struthiomimus altus</i>	1	1	0	2	1	0	0	0	0	0	0	0	0	0	0
<i>Gallimimus bullatus</i>	1	1	0	2	1	0	0	0	0	0	0	1	0	0	0
<i>Falcarius utahensis</i>	2	2	0	1	0	1	?	1	0	1	0	1	0	0	0
<i>Beipiaosaurus inexpectus</i>	?	?	?	?	?	?	?	?	?	?	?	?	?	?	?
<i>Alxasaurus elesitaiensis</i>	0	2	1	1 2	?	0	?	1	?	2	?	?	?	?	?
<i>Nothronychus mckinleyi</i>	0	2	1	2	0	?	1	1	0	?	?	?	?	?	?
<i>Erliaosaurus bellamanus</i>	?	?	?	?	?	?	?	?	?	?	?	?	?	?	0
<i>Nanshiungosaurus brevispinus</i>	0	2	0	?	0	?	0	1	0	2	?	?	?	?	?
<i>Neimongosaurus yangi</i>	?	?	?	?	?	?	?	?	?	?	?	?	?	?	0
<i>Segnosaurus galbiensis</i>	0	2	1	0	?	0	?	1	0	2	0	?	0	?	?
<i>Erlikosaurus andrewsi</i>	?	?	?	?	?	?	?	?	?	?	?	?	?	?	?
<i>Therizinosaurus cheloniformis</i>	?	?	?	?	?	?	?	?	?	?	?	?	?	?	?
<i>Alvarezsaurus calvoi</i>	?	?	?	?	?	?	?	?	?	?	?	?	?	?	?
<i>Patagonykus puertai</i>	?	?	?	2	?	?	?	?	?	1	0	?	0	0	?
<i>Mononykus olecranus</i>	0	0	?	?	?	?	?	?	?	3	?	?	0	?	0
<i>Shuvuuia deserti</i>	0	0	?	0	0	0	2	1	0	3	2	?	0	?	?
<i>Incisivosaurus gauthieri</i>	?	?	?	?	?	?	?	?	?	?	?	?	?	?	?
<i>Protarchaeopteryx robusta</i>	2	2	0	1	?	1	?	1	?	?	?	?	0	0	?

Taxa / Characters	196	197	198	199	200	201	202	203	204	205	206	207	208	209	210
<i>Allosaurus fragilis</i>	0	0	0	0	0	0	0	0	0	0	0	0	0	0	0
<i>Sinraptor</i>	0	0	0	0	0	0	0	0	0	0	0	?	1	0	0
<i>Dilong paradoxus</i>	?	?	?	1	0	0	?	0	?	?	0	0	?	?	0
<i>Eotyrannus lengi</i>	0	0	?	?	?	?	?	?	?	?	?	?	?	?	0
<i>Tyrannosaurus rex</i>	0	0	0	0	2	0	0	0	0	0	0	0	1	0	0
<i>Gorgosaurus libratus</i>	0	0	0	0	2	0	0	0	0	0	0	0	1	0	0
<i>Tanycolagreus topwilsoni</i>	0	0	0	0	0	0	?	0	0	0	0	0	?	?	0
<i>Coelurus fragilis</i>	0	0	?	0	?	?	?	?	?	?	0	0	?	?	0
<i>Ornitholestes hermanni</i>	0	0	0	0	0	?	?	?	?	0	0	0	0	0	?
<i>Guanlong wucaii</i>	?	0	?	?	0	0	0	0	0	0	0	?	1	?	0
<i>Aniksosaurus darwini</i>	0	0	0	0	0	?	0	1	0	0	2	?	?	?	?
<i>Nedcolbertia justinhoffmani</i>	0	0	0	0	1	0	1	?	0	0	?	?	?	?	?
<i>Nqwebasaurus thwazi</i>	0	0	0	0	0	?	1	0	1	2	?	1	?	?	0
<i>Santanaraptor placidus</i>	?	?	?	?	0	?	?	?	?	0	?	?	?	?	?
<i>Orkoraptor burkei</i>	?	?	?	?	?	?	?	?	?	?	?	?	?	?	?
<i>Juravenator starki</i>	0	0	?	?	0	0	0	0	0	0	1	1	?	?	0
<i>Mirischia asymmetrica</i>	?	?	?	?	?	?	?	?	?	0	1	?	?	?	?
<i>Compsognathus longipes</i>	0	0	0	0	0	0	0	0	0	0	1	1	0	0	0
<i>Sinocalliopteryx gigas</i>	0	0	?	?	0	0	0	0	?	0	1	1	?	?	0
<i>Huaxiagnathus orientalis</i>	0	0	0	0	0	0	?	0	0	0	1	1	?	?	0
<i>Sinosauropteryx prima</i>	0	0	0	0	0	0	?	0	0	0	1	1	?	?	0
<i>Scipionyx samniticus</i>	?	?	?	?	?	?	?	?	?	?	1	1	?	?	0
<i>Deinocheirus mirificus</i>	?	?	?	?	?	?	?	?	?	?	?	?	?	?	0
<i>Harpyimimus okladnikovi</i>	0	0	0	0	1	0	?	?	0	0	0	0	?	1	0
<i>Pelecanimimus polyodon</i>	?	?	?	?	?	?	?	?	?	?	?	0	0	1	0
<i>Shenzhousaurus orientalis</i>	?	?	?	?	?	?	?	?	?	?	0	?	?	1	?
<i>Archaeornithomimus asiaticus</i>	0	0	0	0	1	?	3	?	0	0	0	0	?	?	0
<i>Garudimimus brevipes</i>	0	0	0	0	1	?	?	0	0	0	0	?	0	1	?
<i>Anserimimus planinychus</i>	0	0	0	0	2	?	3	?	0	0	?	?	?	?	1
<i>Ornithomimus edmontonicus</i>	0	0	0	0	2	0	3	?	0	0	0	0	1	1	1
<i>Struthiomimus altus</i>	0	0	0	0	2	0	3	?	0	0	0	0	1	1	1
<i>Gallimimus bullatus</i>	0	0	0	0	2	0	3	?	0	0	0	0	0	1	1
<i>Falcarius utahensis</i>	0	0	0	0	0	0	?	0	0	0	0	0	?	?	0
<i>Beipiaosaurus inexpectus</i>	0	0	?	?	?	?	?	0	?	?	?	?	?	?	?
<i>Alxasaurus elesitaiensis</i>	?	0	0	0	0	0	2	?	0	0	0	0	?	?	0
<i>Nothronychus mckinleyi</i>	?	?	0	?	?	?	?	?	?	?	?	?	?	?	0
<i>Erliaosaurus bellamanus</i>	?	?	?	?	?	?	?	?	?	?	?	?	?	?	0
<i>Nanshiungosaurus brevispinus</i>	?	?	?	?	?	?	?	?	?	?	?	?	?	?	?
<i>Neimongosaurus yangi</i>	0	0	0	0	0	?	2	0	1	0	0	?	?	?	?
<i>Segnosaurus galbiensis</i>	?	0	0	0	0	?	2	1	?	0	?	?	0	0	?
<i>Erlikosaurus andrewsi</i>	0	?	0	0	?	0	2	1	?	?	?	?	0	0	?
<i>Therizinosaurus cheloniformis</i>	?	?	?	?	?	?	?	?	?	?	?	?	?	?	0
<i>Alvarezsaurus calvoi</i>	0	0	0	0	0	0	?	?	?	0	?	?	?	?	?
<i>Patagonykus puertai</i>	?	0	?	?	0	?	?	?	?	?	0	1	?	?	0
<i>Mononykus olecranus</i>	0	0	0	0	2	0	?	0	0	0	0	1	?	?	0
<i>Shuvuuia deserti</i>	0	0	0	0	2	0	1	0	0	0	?	1	1	0	0
<i>Incisivosaurus gauthieri</i>	?	?	?	?	?	?	?	?	?	?	?	?	0	0	?
<i>Protarchaeopteryx robusta</i>	?	0	?	?	?	0	0	0	?	0	0	0	?	?	?

Taxa	Characters	211	212	213	214	215	216	217	218	219	220	221	222	223	224	225
<i>Allosaurus fragilis</i>		0	0	1	0	0	0	0	0	0	0	0	0	0	0	0
<i>Sinraptor</i>		?	0	0	0	?	0	0	?	0	0	0	0	0	0	?
<i>Dilong paradoxus</i>		?	0	?	?	?	?	0	?	0	?	?	?	?	0	?
<i>Eotyrannus lengi</i>		?	0	?	?	?	?	0	0	?	?	?	?	?	?	0
<i>Tyrannosaurus rex</i>		0	0	0	0	0	0	0	0	0	0	0	0	1	0	0
<i>Gorgosaurus libratus</i>		0	0	0	0	0	0	0	0	0	0	?	0	1	0	0
<i>Tanycolagreus topwilsoni</i>		0	?	?	?	1	?	?	0	0	0	?	?	?	?	0
<i>Coelurus fragilis</i>		?	?	?	?	0	?	0	?	?	0	?	?	?	0	0
<i>Ornitholestes hermanni</i>		0	0	1	0	?	0	0	?	0	?	0	0	?	0	0
<i>Guanlong wucaii</i>		0	0	0	0	?	0	0	0	0	?	?	0	?	0	?
<i>Aniksosaurus darwini</i>		0	?	?	1	0	?	?	?	?	?	?	?	?	?	0
<i>Nedcolbertia justinhoffmani</i>		?	?	?	?	?	?	?	?	?	?	?	?	?	?	?
<i>Nqwebasaurus thwazi</i>		0	?	?	?	?	?	?	?	?	?	?	?	?	?	0
<i>Santanaraptor placidus</i>		?	?	?	?	?	?	?	?	?	?	?	?	?	?	?
<i>Orkoraptor burkei</i>		?	?	?	?	?	?	0 1	?	?	?	?	?	?	?	?
<i>Juravenator starki</i>		0	0	?	0	?	?	0	0	?	0	?	?	?	0	0
<i>Mirischia asymmetrica</i>		?	?	?	?	?	?	?	?	?	?	?	?	?	?	?
<i>Compsognathus longipes</i>		0	0	?	0	?	?	0	0	0	?	?	?	?	0	0
<i>Sinocalliopteryx gigas</i>		0	0	?	?	?	?	0	0	0	?	?	?	?	0	?
<i>Huaxiagnathus orientalis</i>		0	0	?	?	?	?	0	0	?	0	?	?	?	0	?
<i>Sinosauropteryx prima</i>		0	0	0	?	0	0	0	0	0	0	?	?	?	0	?
<i>Scipionyx samniticus</i>		0	0	1	0	0	0	0	0	?	0	?	?	?	0	0
<i>Deinocheirus mirificus</i>		?	?	?	?	?	?	?	0	?	0	?	?	?	?	0
<i>Harpymimus okladnikovi</i>		1	1	0	?	?	?	1	?	0	0	?	?	?	0	0
<i>Pelecanimimus polyodon</i>		1	0	?	?	?	?	1	?	1	?	?	?	?	0	?
<i>Shenzhousaurus orientalis</i>		?	1	?	0	0	1	1	?	?	?	?	?	?	0	?
<i>Archaeornithomimus asiaticus</i>		1	?	?	1	0	?	?	1	?	1	?	?	?	?	0
<i>Garudimimus brevipes</i>		?	1	1	1	0	?	?	1	1	?	0	0	1	0	?
<i>Anserimimus planinychus</i>		1	?	?	1	0	?	?	1	?	1	?	?	?	?	?
<i>Ornithomimus edmontonicus</i>		1	1	1	1	0	1	?	1	1	1	0	0	?	0	0
<i>Struthiomimus altus</i>		1	1	1	1	0	1	?	1	1	1	0	0	1	0	0
<i>Gallimimus bullatus</i>		1	1	1	1	0	1	?	1	1	1	0	0	1	0	0
<i>Falcarius utahensis</i>		?	?	?	1	0	?	0	0	?	0	?	0	1	1	1
<i>Beipiaosaurus inexpectus</i>		?	?	?	?	?	?	0	?	?	?	?	?	?	1	1
<i>Alxasaurus elesitaiensis</i>		?	?	?	1	?	?	0	0	?	0	?	?	?	1	1
<i>Nothronychus mckinleyi</i>		?	?	?	?	?	?	0	?	?	?	?	?	0	?	1
<i>Erliaosaurus bellamanus</i>		?	?	?	?	?	?	?	?	?	?	?	?	?	?	1
<i>Nanshiungosaurus brevispinus</i>		?	?	?	?	?	?	?	?	?	?	?	?	?	?	?
<i>Neimongosaurus yangi</i>		?	0	?	1	?	?	?	0	?	0	?	?	?	?	1
<i>Segnosaurus galbiensis</i>		?	?	?	1	?	?	0	?	0	?	?	?	?	1	1
<i>Erlikosaurus andrewsi</i>		?	0	1	?	?	0	0	?	0	?	0	0	0	1	1
<i>Therizinosaurus cheloniformis</i>		?	?	?	?	?	?	?	0	?	0	?	?	?	?	1
<i>Alvarezsaurus calvoi</i>		?	?	?	1	?	?	?	0	?	?	?	?	?	?	?
<i>Patagonykus puertai</i>		?	?	?	1	?	?	?	0	?	?	?	?	?	?	0
<i>Mononykus olecranus</i>		0	?	?	?	1	?	?	0	?	0	?	?	?	?	0
<i>Shuvuuia deserti</i>		0	0	0	1	1	0	0	0	0	0	0	1	0	0	0
<i>Incisivosaurus gauthieri</i>		?	0	0	?	?	0	0	?	0	?	?	0	0	0	?
<i>Protarchaeopteryx robusta</i>		1	0	?	?	?	?	?	?	0	?	?	?	?	0	0

Taxa / Characters	226	227	228	229	230	231	232	233	234	235	236	237	238	239	240	
<i>Allosaurus fragilis</i>	0	0	0	0	0	0	0	0	0	0	0	0	0	0	0	
<i>Sinraptor</i>	?	0	0	0	0	0	0	0	0	0	0	0	0	0	0	
<i>Dilong paradoxus</i>	?	?	0	?	0	0	0	0	0	1	2	0	0	0	1	3
<i>Eotyrannus lengi</i>	0	?	?	?	0	0	?	?	0	?	?	0	0	?	?	
<i>Tyrannosaurus rex</i>	0	1	0	0	0	0	0	0	0	2	0	0	0	1	0	
<i>Gorgosaurus libratus</i>	0	1	0	0	0	0	0	0	0	2	0	0	0	1	0	
<i>Tanycolagreus topwilsoni</i>	0	?	?	?	?	?	?	?	?	?	?	0	?	?	?	
<i>Coelurus fragilis</i>	0	?	?	?	?	?	?	?	?	?	?	?	?	?	?	
<i>Ornitholestes hermanni</i>	0	1	0	0	0	0	1	0	0	1	1	0	0	1	0	
<i>Guanlong wucaii</i>	0	1	?	0	0	0	1	0	0	2	0	1	0	1	0	
<i>Aniksosaurus darwini</i>	0	?	?	0	?	?	?	?	?	?	?	?	?	?	?	
<i>Nedcolbertia justinhoffmani</i>	0	0	?	?	?	?	?	?	?	?	?	?	?	?	?	
<i>Nqwebasaurus thwazi</i>	?	?	?	?	?	?	?	?	?	?	?	?	?	?	?	
<i>Santanaraptor placidus</i>	?	0	?	?	?	?	?	?	?	?	?	?	?	?	?	
<i>Orkoraptor burkei</i>	?	?	0	?	0	?	?	?	?	?	?	?	?	?	?	
<i>Juravenator starki</i>	0	?	0	0	0	0	0	1	0	0	1	1	0	0	4	
<i>Mirischia asymmetrica</i>	?	0	?	0	?	?	?	?	?	1	?	?	?	?	?	
<i>Compsognathus longipes</i>	0	0	0	0	0	0	0	1	0	?	1	1	0	1	0	
<i>Sinocalliopteryx gigas</i>	0	0	0	0	0	0	0	?	0	1	1	1	0	1	?	
<i>Huaxiagnathus orientalis</i>	?	?	0	0	0	0	0	0	0	0	?	1	0	1	4	
<i>Sinosauropteryx prima</i>	1	0	0	0	0	0	0	0	0	0	1	1	0	1	0	
<i>Scipionyx samniticus</i>	0	0	?	0	1	0	1	0	1	0	1	1	0	?	?	
<i>Deinocheirus mirificus</i>	?	?	?	?	?	?	?	?	?	?	?	?	?	?	?	
<i>Harpymimus okladnikovi</i>	0	?	1	?	2	0	1	1	0	0	1	1	0	1	?	
<i>Pelecanimimus polyodon</i>	?	?	1	?	1	0	?	1	0	?	1	1	0	0	2	
<i>Shenzhousaurus orientalis</i>	?	0	1	0	2	0	?	1	0	0	?	?	0	?	1	
<i>Archaeornithomimus asiaticus</i>	0	0	?	?	?	?	?	?	?	?	?	?	?	?	?	
<i>Garudimimus brevipes</i>	?	?	?	0	?	?	1	1	0	0	1	1	0	1	2	
<i>Anserimimus planinychus</i>	?	?	?	?	?	?	?	?	?	?	?	?	?	?	?	
<i>Ornithomimus edmontonicus</i>	0	?	?	0	?	?	1	1	0	0	1	1	0	1	2	
<i>Struthiomimus altus</i>	0	?	?	0	?	?	1	1	0	0	1	1	0	1	2	
<i>Gallimimus bullatus</i>	0	0	?	0	?	?	1	1	0	0	1	1	0	1	2	
<i>Falcarius utahensis</i>	1	1	1	1	1	1	?	?	?	0	?	?	?	?	?	
<i>Beipiaosaurus inexpectus</i>	1	?	?	?	1	?	?	?	?	0	?	?	?	?	?	
<i>Alxasaurus elesitaiensis</i>	?	?	1	1	1	1	?	?	?	?	?	?	?	?	?	
<i>Nothronychus mckinleyi</i>	1	1	1	?	1	?	?	?	?	?	?	?	?	?	?	
<i>Erliaosaurus bellamanus</i>	1	?	?	?	?	?	?	?	?	?	?	?	?	?	?	
<i>Nanshiungosaurus brevispinus</i>	?	?	?	2	?	?	?	?	?	0	?	?	?	?	?	
<i>Neimongosaurus yangi</i>	1	?	1	2	1	?	?	?	?	?	?	?	?	?	?	
<i>Segnosaurus galbiensis</i>	1	0	1	2	1	1	1	?	?	0	?	?	?	?	?	
<i>Erlikosaurus andrewsi</i>	1	?	1	?	1	1	?	0	0	?	1	0	0	1	?	
<i>Therizinosaurus cheloniformis</i>	1	?	?	?	?	?	?	?	?	?	?	?	?	?	?	
<i>Alvarezsaurus calvoi</i>	?	?	?	0	?	?	?	?	?	0	?	?	?	?	?	
<i>Patagonykus puertai</i>	1	0	?	?	?	?	?	?	?	?	?	?	?	?	?	
<i>Mononykus olecranus</i>	1	?	?	0	0	0	?	?	?	?	?	?	0	?	?	
<i>Shuvuuia deserti</i>	1	?	1	?	?	0	?	1	0	0	1	1	0	?	?	
<i>Incisivosaurus gauthieri</i>	?	?	0	0	1	0	?	0	0	?	1	0	?	1	0	
<i>Protarchaeopteryx robusta</i>	?	?	1	?	1	0	1	?	?	0	?	0	?	?	?	

Taxa / Characters	256	257	258	259	260	261	262	263	264	265	266	267	268	269	270
<i>Allosaurus fragilis</i>	1	0	0	0	0	0	0	0	0	0	0	0	0	0	0
<i>Sinraptor</i>	1	0	0	0	0	0	0	0	1	0	0	?	?	0	0
<i>Dilong paradoxus</i>	1	1	1	0	?	0	0	0	1	1	0	0	?	0	0
<i>Eotyrannus lengi</i>	1	1	1	?	0	0	?	0	?	?	?	?	?	0	0
<i>Tyrannosaurus rex</i>	1	1	0	0	0	0	0	0	0	0	0	0	0	0	1
<i>Gorgosaurus libratus</i>	1	1	0	0	0	0	0	0	0	0	0	0	0	0	1
<i>Tanycolagreus topwilsoni</i>	?	1	?	?	?	?	?	?	1	1	0	?	?	0	0
<i>Coelurus fragilis</i>	?	?	?	?	?	?	1	1	1	1	0	?	?	0	0
<i>Ornitholestes hermanni</i>	0	0	?	0	0	0	0	1	1	1	0	?	?	?	?
<i>Guanlong wucaii</i>	0	0	1	0	?	0	0	?	1	1	?	?	?	0	0
<i>Aniksosaurus darwini</i>	?	?	?	?	?	?	?	0	?	?	?	?	?	?	?
<i>Nedcolbertia justinhoffmani</i>	?	?	?	?	?	?	?	?	?	?	?	1	?	?	?
<i>Nqwebasaurus thwazi</i>	?	?	?	?	?	?	?	1	?	?	?	?	?	0	0
<i>Santanaraptor placidus</i>	?	?	?	?	?	?	?	?	?	?	?	?	?	?	?
<i>Orkoraptor burkei</i>	?	?	-	?	?	?	?	?	?	?	?	?	?	?	?
<i>Juravenator starki</i>	?	0	-	0	?	?	0	?	1	?	?	1	0	0	0
<i>Mirischia asymmetrica</i>	?	?	?	?	?	?	?	?	?	?	?	?	?	?	?
<i>Compsognathus longipes</i>	0	0	1	-	0	0	0	1	1	1	0	0	0	0	0
<i>Sinocalliopteryx gigas</i>	0	1	?	0	?	0	0	1	1	1	0	0	?	0	0
<i>Huaxiagnathus orientalis</i>	?	1	-	0	?	0	0	1	1	1	?	0	0	0	0
<i>Sinosauropteryx prima</i>	?	0	-	0	?	0	0	1	1	1	0	1	?	0	0
<i>Scipionyx samniticus</i>	?	0	-	0	?	0	0	1	1	1	0	0	0	0	0
<i>Deinocheirus mirificus</i>	?	?	?	?	?	?	?	?	?	?	?	?	?	?	0
<i>Harpymimus okladnikovi</i>	0	?	?	?	0	0	0	0	1	1	0	?	?	0	0
<i>Pelecanimimus polyodon</i>	0	0	-	0	1	0	0	0	1	?	?	?	?	?	?
<i>Shenzhousaurus orientalis</i>	?	?	?	?	?	0	?	?	1	1	0	0	?	?	?
<i>Archaeornithomimus asiaticus</i>	?	?	?	?	?	?	?	1	1	1	0	?	?	0	0
<i>Garudimimus brevipes</i>	0	?	?	?	?	?	1	1	1	1	0	?	?	?	?
<i>Anserimimus planinychus</i>	?	?	?	?	?	?	?	?	?	?	?	?	?	?	?
<i>Ornithomimus edmontonicus</i>	?	?	?	?	?	?	1	?	1	1	0	0	?	0	0
<i>Struthiomimus altus</i>	0	?	?	?	?	?	1	1	1	1	0	0	0	0	0
<i>Gallimimus bullatus</i>	0	?	?	?	?	?	1	1	1	1	0	0	?	0	0
<i>Falcarius utahensis</i>	?	?	?	0	0	0	1	?	1	1	?	?	?	0	?
<i>Beipiaosaurus inexpectus</i>	?	?	?	?	?	?	?	?	?	?	?	?	0	?	?
<i>Alxasaurus elesitaiensis</i>	?	?	0	?	0	1	1	1	1	1	?	?	?	?	?
<i>Nothronychus mckinleyi</i>	?	?	0	?	?	?	1	0	1	?	0	?	?	?	0
<i>Erliaosaurus bellamanus</i>	?	?	?	?	?	?	?	?	?	?	?	?	?	?	?
<i>Nanshiungosaurus brevispinus</i>	?	?	?	?	?	?	1	?	0	1	0	?	?	?	?
<i>Neimongosaurus yangi</i>	?	?	?	?	0	1	1	1	1	1	0	0	0	0	?
<i>Segnosaurus galbiensis</i>	?	?	?	?	0	1	?	?	?	?	?	?	?	0	2
<i>Erlikosaurus andrewsi</i>	0	0	0	0	0	1	?	?	?	?	?	?	?	?	?
<i>Therizinosaurus cheloniformis</i>	?	?	?	?	?	?	?	?	?	?	?	?	?	0	2
<i>Alvarezsaurus calvoi</i>	?	?	?	?	?	?	1	1	1	1	1	0	?	?	0
<i>Patagonykus puertai</i>	?	?	?	?	?	?	?	?	1	?	1	?	?	?	?
<i>Mononykus olecranus</i>	?	?	?	?	?	?	0	?	1	1	1	?	?	0	0
<i>Shuvuuia deserti</i>	0	?	?	0	?	0	?	?	?	?	?	?	?	0	0
<i>Incisivosaurus gauthieri</i>	0	?	-	0	0	1	?	?	?	?	?	?	?	?	?
<i>Protarchaeopteryx robusta</i>	?	?	?	?	0	1	0	?	1	1	?	0	0	0	0

Taxa / Characters	271	272	273	274	275	276	277	278	279	280	281	282	283	284	285
<i>Allosaurus fragilis</i>	0	0	0	0	0	0	0	0	0	0	0	0	0	0	0
<i>Sinraptor</i>	?	0	?	?	?	?	?	?	?	0	?	0	0	?	?
<i>Dilong paradoxus</i>	0	1	0	1	1	?	1	?	?	0	0	?	1	0	0
<i>Eotyrannus lengi</i>	?	?	?	?	1	1	?	0	?	?	0	?	?	1	?
<i>Tyrannosaurus rex</i>	0	1	0	0	0	0	0	0	?	0	0	1	1	1	0
<i>Gorgosaurus libratus</i>	1	1	0	0	0	0	0	0	0	0	0	1	1	0	0
<i>Tanycolagreus topwilsoni</i>	0	0	0	1	1	1	1	0	0	0	0	1	1	1	0
<i>Coelurus fragilis</i>	?	?	?	1	1	1	1	0	0	?	?	1	?	1	?
<i>Ornitholestes hermanni</i>	?	?	?	1	1	0	1	0	?	0	?	?	?	?	?
<i>Guanlong wucaii</i>	0	1	0	1	1	?	1	0	1	0	0	0	1	0	0
<i>Aniksosaurus darwini</i>	?	?	?	?	0	?	?	?	?	?	?	?	?	?	?
<i>Nedcolbertia justinhoffmani</i>	?	?	?	?	?	?	?	?	?	?	?	?	?	?	?
<i>Nqwebasaurus thwazi</i>	?	1	0	0	1	0	1	0	?	0	0	1	0	1	0
<i>Santanaraptor placidus</i>	?	?	?	?	?	?	?	?	?	?	?	?	?	?	?
<i>Orkoraptor burkei</i>	?	?	?	?	?	?	?	?	?	?	?	?	?	?	?
<i>Juravenator starki</i>	0	1	?	0	0	0	0	0	0	0	?	?	?	0	0
<i>Mirischia asymmetrica</i>	?	?	?	?	?	?	?	?	?	?	?	?	?	?	?
<i>Compsognathus longipes</i>	0	1	0	1	1	0	1	0	0	0	?	1	0	1	0
<i>Sinocalliopteryx gigas</i>	0	1	0	0	1	0	1	0	0	0	?	0	1	1	0
<i>Huaxiagnathus orientalis</i>	0	0	0	1	0	0	1	0	0	0	0	1	1	1	0
<i>Sinosauropteryx prima</i>	0	1	0	0	0	0	0	0	0	0	0	?	0	0	0
<i>Scipionyx samniticus</i>	0	?	0	1	1	0	1	0	0	0	0	1	0	1	0
<i>Deinocheirus mirificus</i>	?	0	?	?	1	0	?	0	?	?	1	1	0	0	0
<i>Harpymimus okladnikovi</i>	?	0	?	?	1	0	?	0	0	0	0	1	0	0	0
<i>Pelecanimimus polyodon</i>	?	?	0	?	1	0	?	0	0	?	1	1	0	0	0
<i>Shenzhousaurus orientalis</i>	?	?	?	?	?	?	?	?	?	0	?	?	0	?	?
<i>Archaeornithomimus asiaticus</i>	?	?	0	?	1	0	?	0	?	?	1	1	0	?	0
<i>Garudimimus brevipes</i>	?	?	?	?	?	?	?	?	?	?	?	?	?	?	?
<i>Anserimimus planinychus</i>	?	1	?	?	?	0	?	?	0	?	1	?	0	0	0
<i>Ornithomimus edmontonicus</i>	1	1	0	1	1	0	1	0	?	0	1	?	0	0	0
<i>Struthiomimus altus</i>	1	0	0	1	1	0	1	0	0	0	1	1	0	0	0
<i>Gallimimus bullatus</i>	?	0	0	1	1	0	1	0	0	0	1	1	0	0	0
<i>Falcarius utahensis</i>	?	?	?	?	1	1	?	0	1	?	0	1	1	1	0
<i>Beipiaosaurus inexpectus</i>	?	?	0	?	?	?	?	0	1	0	0	?	1	1	0
<i>Alxasaurus elesitaiensis</i>	?	0	?	1	0	0	1	0	1	?	0	1	1	?	?
<i>Nothronychus mckinleyi</i>	?	0	?	?	0	0	?	?	?	?	?	?	?	?	?
<i>Erliansaurus bellamanus</i>	?	0	?	1	0	0	1	0	?	0	0	1	1	1	0
<i>Nanshiungosaurus brevispinus</i>	?	?	?	?	?	?	?	?	?	?	?	?	?	?	?
<i>Neimongosaurus yangi</i>	?	?	0	1	0	?	1	?	?	?	?	?	?	?	?
<i>Segnosaurus galbiensis</i>	1	?	0	?	0	?	?	0	?	?	?	?	?	?	?
<i>Erlikosaurus andrewsi</i>	?	?	?	?	0	?	?	?	?	?	?	?	?	?	?
<i>Therizinosaurus cheloniformis</i>	?	?	0	?	0	0	?	?	0	?	0	1	1	?	?
<i>Alvarezsaurus calvoi</i>	?	?	?	?	?	?	?	?	?	?	?	?	?	?	?
<i>Patagonykus puertai</i>	?	?	?	?	?	?	?	0	0	?	0	?	?	?	?
<i>Mononykus olecranus</i>	?	0	0	0	0	0	0	0	0	?	0	1	0	0	0
<i>Shuvuuia deserti</i>	1	?	0	0	0	0	0	?	?	0	?	?	?	0	0
<i>Incisivosaurus gauthieri</i>	?	?	?	?	?	?	?	?	?	?	?	?	?	?	?
<i>Protarchaeopteryx robusta</i>	?	0	0	1	1	1	1	0	0	0	?	?	0	1	0

Taxa	/	Characters	271	272	273	274	275	276	277	278	279	280	281	282	283	284	285
<i>Avimimus portentosus</i>			?	?	?	1	1	1	?	?	1	?	?	?	?	?	?
<i>Caudipteryx</i>			?	0	0	0	1	1	1	0	1	0	0	?	0	1	0
<i>Microvenator celer</i>			?	?	0	1	1	1	1	0	?	?	0	?	?	?	?
<i>Elmisaurus rarus</i>			?	?	?	?	?	?	?	?	?	?	0	?	?	?	?
<i>Chirosstenotes pergracilis</i>			?	?	0	?	?	?	?	?	?	0	0	?	?	?	?
<i>Caenagnathus collinsi</i>			?	?	?	?	?	?	?	?	?	?	?	?	?	?	?
<i>Oviraptor philoceratops</i>			?	0	0	?	1	1	?	0	1	?	?	1	0	1	0
<i>Rinchenia mongoliensis</i>			?	?	?	1	?	?	?	?	?	?	?	?	?	?	?
<i>Citipati osmolskae</i>			?	0	0	1	0	1	1	0	1	0	0	1	0	1	0
Zamyn Khondt oviraptorine			?	0	0	1	0	1	1	?	1	0	0	?	0	1	0
<i>Ingenia yanshini</i>			?	0	0	1	0	1	1	0	1	0	0	1	0	1	0
<i>Conchoraptor gracilis</i>			?	?	?	1	?	1	?	?	?	?	0	1	0	?	0
<i>Khaan mckennai</i>			?	0	0	1	0	1	1	0	1	0	0	1	0	1	0
<i>Heyuannia huangi</i>			?	0	0	?	0	1	?	0	1	0	0	0	0	1	0
<i>Sinovenator changii</i>			1	0	0	?	?	?	?	?	?	?	?	?	?	?	?
<i>Mei long</i>			1	0	0	1	1	1	1	0	?	0	?	?	0	?	?
<i>Byronosaurus jaffei</i>			?	?	?	?	?	?	?	?	?	?	?	?	?	?	?
<i>Sinornithoides youngi</i>			?	?	0	1	1	1	1	0	1	0	0	1	0	1	0
IGM 100/44			?	?	?	?	?	?	?	?	1	?	0	1	0	1	0
<i>Troodon formosus</i>			?	?	?	?	?	1	?	0	1	?	0	?	?	?	?
<i>Saurornithoides mongoliensis</i>			?	?	?	?	?	?	?	?	?	?	?	?	?	?	?
<i>Zanabazar junior</i>			?	?	?	?	?	?	?	?	?	?	?	?	?	?	?
<i>Unenlagia</i>			?	0	?	1	1	?	?	?	?	?	?	?	?	?	?
<i>Buitreraptor gonzalezorum</i>			1	0	0	1	1	1	2	0	?	?	?	?	?	?	?
<i>Rahonavis ostromi</i>			?	0	?	?	?	1	3	0	?	?	?	?	?	?	?
<i>Bambiraptor feinbergi</i>			?	0	0	1	1	1	2	0	1	0	1	1	0	1	0
<i>Sinornithosaurus millenii</i>			1	0	0	1	1	1	2	1	?	0	0	1	0	1	1
<i>Microraptor zhaoianus</i>			1	0	0	1	1	1	2	1	1	0	?	?	0	1	1
NGMC91			?	0	0	1	1	1	2	1	1	0	?	?	0	1	1
IGM 100 1015			?	?	?	?	?	?	?	?	?	?	?	?	?	?	?
<i>Adasaurus mongoliensis</i>			?	0	?	?	?	?	?	?	?	?	?	?	?	?	?
<i>Velociraptor mongoliensis</i>			1	0	0	1	1	1	1	0	1	0	0	1	0	1	0
<i>Saurornitholestes langstoni</i>			1	0	0	?	?	?	?	?	1	?	?	?	?	?	?
<i>Deinonychus antirrhopus</i>			?	?	0	1	1	1	1	0	1	0	0	1	0	1	0
<i>Achillobator giganticus</i>			?	?	0	?	?	?	1	?	?	?	?	?	?	?	?
<i>Dromaeosaurus albertensis</i>			?	?	?	?	?	?	?	?	?	?	?	?	?	?	?
<i>Utahraptor ostrommaysi</i>			?	?	?	?	?	?	?	?	?	?	?	?	?	?	?
<i>Atrociraptor marshalli</i>			?	?	?	?	?	?	?	?	?	?	?	?	?	?	?
<i>Epidendrosaurus ningchengensis</i>			?	0	0	2	1	0	2	0	1	0	?	?	0	1	0
<i>Archaeopteryx lithographica</i>			?	0	1	2	1	1	3	0	1	1	0	?	0	1	0
<i>Wellnhoferia grandis</i>			1	0	?	2	1	1	3	0	?	1	0	?	0	1	1
<i>Jeholornis prima</i>			1	0	1	2	1	1	3	0	1	1	?	?	0	1	1
<i>Sapeornis chaoyangensis</i>			1	0	1	2	1	1	3	1	1	1	?	1	0	1	1
<i>Confuciusornis sanctus</i>			1	0	1	2	1	1	2	1	1	1	0	1	0	1	0
<i>Protopteryx fengningensis</i>			?	0	1	2	1	1	3	1	1	1	?	?	0	1	1
<i>Yanornis martini</i>			?	0	1	2	1	1	3	1	1	1	?	?	0	1	1
<i>Hagryphus giganteus</i>			?	?	?	?	?	?	?	?	0	?	0	1	1	1	0

Taxa / Characters	286	287	288	289	290	291	292	293	294	295	296	297	298	299	300
<i>Allosaurus fragilis</i>	0	0	0	0	0	0	1	0	0	0	0	0	0	0	0
<i>Sinraptor</i>	0	0	?	0	?	?	?	?	?	?	?	?	0	0	?
<i>Dilong paradoxus</i>	0	0	1	0	0	0	1	0	0	0	0	0	0	0	0
<i>Eotyrannus lengi</i>	0	?	0	?	?	0	?	0	?	?	0	?	0	0	?
<i>Tyrannosaurus rex</i>	0	0	1	0	0	0	?	0	?	0	0	?	0	?	?
<i>Gorgosaurus libratus</i>	1	0	1	0	0	0	?	0	?	0	0	0	0	0	0
<i>Tanycolagreus topwilsoni</i>	0	0	1	0	0	0	1	0	0	0	1	0	0	0	0
<i>Coelurus fragilis</i>	?	?	?	0	0	0	1	0	0	0	?	?	?	?	?
<i>Ornitholestes hermanni</i>	?	?	?	0	?	?	?	?	?	0	0	0	1	0	0
<i>Guanlong wucaii</i>	0	0	1	0	0	0	1	0	0	0	0	0	0	1	0
<i>Aniksosaurus darwini</i>	?	?	?	?	?	?	?	?	?	?	0	?	0	?	?
<i>Nedcolbertia justinhoffmani</i>	?	?	?	?	?	?	?	?	?	?	?	?	?	?	?
<i>Nqwebasaurus thwazi</i>	0	0	?	0	0	1	0	0	0	0	0	?	1	1	0
<i>Santanaraptor placidus</i>	?	?	?	?	?	?	?	?	?	?	?	?	?	?	?
<i>Orkoraptor burkei</i>	?	?	?	?	?	?	?	?	?	?	?	?	?	?	?
<i>Juravenator starki</i>	?	?	1	0	0	0	1	0	0	0	0	0	1	1	0
<i>Mirischia asymmetrica</i>	?	?	?	?	?	?	?	?	?	?	?	?	?	?	?
<i>Compsognathus longipes</i>	1	0	1	0	0	0	1	0	?	0	0	0	1	1	0
<i>Sinocalliopteryx gigas</i>	1	?	0	0	0	0	1	0	0	0	0	0	0	1	0
<i>Huaxiagnathus orientalis</i>	1	0	1	0	0	0	1	0	?	0	0	0	0	1	0
<i>Sinosauropteryx prima</i>	0	0	1	0	0	0	1	0	0	0	0	0	0	1	0
<i>Scipionyx samniticus</i>	0	0	1	0	0	0	1	0	0	0	0	0	1	1	0
<i>Deinocheirus mirificus</i>	0	0	1	0	0	0	0	0	0	0	0	0	0	0	0
<i>Harpymimus okladnikovi</i>	0	0	1	0	0	0	0	0	0	0	0	0	0	1	0
<i>Pelecanimimus polyodon</i>	1	1	1	0	0	0	0	1	0	0	0	0	1	2	0
<i>Shenzhousaurus orientalis</i>	0	?	1	0	?	0	0	1	0	?	0	0	1	0	?
<i>Archaeornithomimus asiaticus</i>	0	0	1	0	0	0	?	1	?	?	0	0	1	2	0
<i>Garudimimus brevipes</i>	?	?	?	?	?	?	?	?	?	?	?	?	?	?	?
<i>Anserimimus planinychus</i>	1	1	1	0	0	0	1	0	0	0	0	0	2	2	0
<i>Ornithomimus edmontonicus</i>	1	1	1	0	0	0	1	1	0	0	0	0	2	2	0
<i>Struthiomimus altus</i>	0	1	1	0	0	0	0	1	0	0	0	0	1	1	0
<i>Gallimimus bullatus</i>	0	0	1	0	0	0	0	1	0	0	0	0	1	1	0
<i>Falcarius utahensis</i>	0	0	1	0	0	0	1	0	0	0	0	0	0	0	1
<i>Beipiaosaurus inexpectus</i>	0	0	1	0	?	0	1	0	?	0	?	1	0	0	?
<i>Alxasaurus elesitaiensis</i>	0	0	?	1	?	?	?	?	?	?	1	1	0	0	1
<i>Nothronychus mckinleyi</i>	?	?	?	?	?	?	?	?	?	?	?	?	0	0	0
<i>Erliansaurus bellamanus</i>	0	0	0	1	0	1	0	0	0	0	1	1	0	0	0
<i>Nanshiungosaurus brevispinus</i>	?	?	?	?	?	?	?	?	?	?	?	?	?	?	?
<i>Neimongosaurus yangi</i>	?	?	?	?	?	?	?	?	?	?	?	?	?	?	?
<i>Segnosaurus galbiensis</i>	?	?	?	?	?	?	?	?	?	?	?	?	?	?	?
<i>Erlikosaurus andrewsi</i>	?	?	?	?	?	?	?	?	?	?	?	?	?	?	?
<i>Therizinosaurus cheloniformis</i>	0	0	0	1	0	1	?	0	?	?	?	1	?	1	0
<i>Alvarezsaurus calvoi</i>	?	?	?	?	?	?	?	?	?	?	0	?	1	?	?
<i>Patagonykus puertai</i>	?	?	?	0	?	?	?	?	?	0	0	?	1	?	?
<i>Mononykus olecranus</i>	1	0	0	0	?	?	?	?	?	0	0	?	1	?	?
<i>Shuvuuia deserti</i>	1	?	0	0	0	?	?	0	?	0	0	0	1	1	0
<i>Incisivosaurus gauthieri</i>	?	?	?	?	?	?	?	?	?	?	?	?	?	?	?
<i>Protarchaeopteryx robusta</i>	?	?	1	0	?	0	1	0	0	0	1	0	0	0	0

Taxa / Characters	286	287	288	289	290	291	292	293	294	295	296	297	298	299	300
<i>Avimimus portentosus</i>	0	?	?	?	?	?	?	?	?	?	?	?	?	?	?
<i>Caudipteryx</i>	0	0	0	0	0	0	1	0	?	0	0	0	1	1	0
<i>Microvenator celer</i>	?	?	?	?	?	?	?	?	?	?	?	0	?	0	?
<i>Elmisaurus rarus</i>	?	?	0	0	0	0	1	0	0	0	0	?	0	?	?
<i>Chiostenotes pergracilis</i>	?	?	0	0	0	0	1	0	?	0	?	1	0	0	1
<i>Caenagnathus collinsi</i>	?	?	?	?	?	?	?	?	?	?	?	?	?	?	?
<i>Oviraptor philoceratops</i>	0	0	0	0	0	0	0	0	0	0	0	0	0	0	1
<i>Rinchenia mongoliensis</i>	?	?	?	?	?	?	?	?	?	?	?	?	?	?	?
<i>Citipati osmolskae</i>	0	0	0	0	0	0	0	0	0	0	0	0	0	0	1
Zamyn Khondt oviraptorine	0	0	1	?	0	0	0	0	0	0	0	0	0	0	1
<i>Ingenia yanshini</i>	0	0	0	0	0	1	0	0	0	0	0	0	0	1	1
<i>Conchoraptor gracilis</i>	?	?	?	0	?	0	0	?	0	0	0	0	1	1	1
<i>Khaan mckennai</i>	0	0	0	0	0	0	0	0	0	0	0	0	0	1	1
<i>Heyuannia huangi</i>	0	0	0	0	0	1	?	0	?	0	0	?	0	1	?
<i>Sinovenator changii</i>	?	?	?	0	?	?	?	?	?	0	0	0	0	0	0
<i>Mei long</i>	?	?	?	0	?	?	?	?	?	?	0	0	0	0	0
<i>Byronosaurus jaffei</i>	?	?	?	?	?	?	?	?	?	?	?	?	?	?	?
<i>Sinornithoides youngi</i>	0	0	1	0	0	0	0	0	0	0	0	0	0	0	0
IGM 100/44	0	0	?	0	0	0	?	?	?	?	0	0	0	0	0
<i>Troodon formosus</i>	?	?	?	?	?	?	?	?	?	?	?	?	?	?	?
<i>Saurornithoides mongoliensis</i>	?	?	?	?	?	?	?	?	?	?	?	?	?	?	?
<i>Zanabazar junior</i>	?	?	?	?	?	?	?	?	?	?	?	?	?	?	?
<i>Unenlagia</i>	?	?	?	?	?	?	?	?	?	?	1	?	0	?	?
<i>Buitreraptor gonzalezorum</i>	?	?	?	?	?	?	?	?	?	?	?	?	?	?	?
<i>Rahonavis ostromi</i>	?	?	?	?	?	?	?	?	?	?	?	?	?	?	?
<i>Bambiraptor feinbergi</i>	0	0	1	0	0	0	0	0	1	0	1	1	0	0	1
<i>Sinornithosaurus millenii</i>	0	0	0	0	1	0	0	0	1	1	1	1	0	0	0
<i>Microraptor zhaoianus</i>	0	0	0	0	1	0	0	0	1	1	1	1	0	0	1
NGMC91	0	0	0	?	1	0	0	0	1	1	0	1	0	0	1
IGM 100 1015	?	?	?	?	?	?	?	?	?	?	?	?	?	?	?
<i>Adasaurus mongoliensis</i>	?	?	?	?	?	?	?	?	?	?	?	?	?	?	?
<i>Velociraptor mongoliensis</i>	0	0	1	0	0	0	0	0	0	0	1	1	0	0	1
<i>Saurornitholestes langstoni</i>	?	?	?	?	?	?	?	?	?	?	1	1	0	0	1
<i>Deinonychus antirrhopus</i>	0	0	1	0	0	0	0	0	0	0	1	1	0	0	1
<i>Achillobator giganticus</i>	?	?	?	0	?	?	?	?	?	0	1	?	0	?	?
<i>Dromaeosaurus albertensis</i>	?	?	?	?	?	?	?	?	?	?	?	?	?	?	?
<i>Utahraptor ostrommaysi</i>	?	?	?	?	?	?	?	?	?	?	?	?	?	?	?
<i>Atrociraptor marshalli</i>	?	?	?	?	?	?	?	?	?	?	?	?	?	?	?
<i>Epidendrosaurus ningchengensis</i>	0	0	1	0	0	0	0	0	0	0	0	0	0	0	0
<i>Archaeopteryx lithographica</i>	0	0	1	0	0	0	1	0	0	0	0	1	0	0	1
<i>Wellnhoferia grandis</i>	0	0	1	0	0	0	1	0	0	0	0	1	0	0	1
<i>Jeholornis prima</i>	0	0	0	?	1	1	0	0	1	1	0	0	0	0	0
<i>Sapeornis chaoyangensis</i>	1	0	0	?	1	1	1	0	0	1	1	1	0	0	?
<i>Confuciusornis sanctus</i>	0	0	0	0	1	0	1	0	1	0	1	1	0	0	1
<i>Protopteryx fengningensis</i>	0	0	0	?	1	1	0	0	1	0	1	1	0	0	0
<i>Yanornis martini</i>	0	?	0	0	1	1	?	0	?	1	1	1	1	1	0
<i>Hagryphus giganteus</i>	0	0	0	0	0	0	1	0	0	0	1	?	0	0	1

Taxa / Characters	301	302	303	304	305	306	307	308	309	310	311	312	313	314	315
<i>Allosaurus fragilis</i>	0	0	0	0	0	0	0	0	0	0	0	0	0	0	0
<i>Sinraptor</i>	?	?	0	2	0	0	0	0	0	0	0	0	0	0	1
<i>Dilong paradoxus</i>	0	1	?	0	0	0	1	0	1	0	?	1	0	1	1
<i>Eotyrannus lengi</i>	?	?	?	?	?	?	?	?	?	?	?	?	?	?	?
<i>Tyrannosaurus rex</i>	?	?	0	1	0	0	1	0	0	1	0	1	0	1	1
<i>Gorgosaurus libratus</i>	?	?	0	1	0	0	1	0	0	1	0	1	0	1	1
<i>Tanycolagreus topwilsoni</i>	0	1	?	?	?	?	?	0	1	1	0	1	0	1	1
<i>Coelurus fragilis</i>	?	?	?	?	?	?	?	0	1	1	?	1	0	1	?
<i>Ornitholestes hermanni</i>	?	?	0	1	0	0	1	0	?	0	?	1	0	0	?
<i>Guanlong wucaii</i>	0	1	0	0	0	0	1	0	1	1	?	1	?	1	1
<i>Aniksosaurus darwini</i>	?	?	?	?	?	?	?	?	1	1	?	1	?	1	?
<i>Nedcolbertia justinhoffmani</i>	?	?	?	0 2	?	0	?	0	?	1	0	1	?	0	?
<i>Nqwebasaurus thwazi</i>	0	0	?	?	?	?	?	?	1	?	?	1	?	1	?
<i>Santanaraptor placidus</i>	?	?	?	?	1	0	1	?	?	1	?	1	?	1	?
<i>Orkoraptor burkei</i>	?	?	?	?	?	?	?	?	?	?	0	?	?	?	?
<i>Juravenator starki</i>	0	0	0	?	?	?	?	?	1	?	?	1	?	?	1
<i>Mirischia asymmetrica</i>	?	?	?	1	0	0	0	0	?	1	?	?	?	?	?
<i>Compsognathus longipes</i>	?	?	0	1	0	0	1	0	1	?	?	1	0	1	1
<i>Sinocalliopteryx gigas</i>	0	1	0	1	0	0	1	0	1	?	?	1	0	1	1
<i>Huaxiagnathus orientalis</i>	0	?	0	1	0	0	1	0	1	?	?	1	0	1	1
<i>Sinosauropteryx prima</i>	0	0	0	1	0	0	1	0	1	0	?	1	?	1	1
<i>Scipionyx samniticus</i>	0	1	0	0	0	0	1	0	?	?	0	?	?	?	?
<i>Deinocheirus mirificus</i>	0	1	?	?	?	?	?	?	?	?	?	?	?	?	?
<i>Harpymimus okladnikovi</i>	0	2	0	?	?	?	?	0	?	?	?	?	0	1	?
<i>Pelecanimimus polyodon</i>	0	2	?	?	?	?	?	?	?	?	?	?	?	?	?
<i>Shenzhousaurus orientalis</i>	0	2	0	0	?	0	?	0	?	0	?	?	?	?	?
<i>Archaeornithomimus asiaticus</i>	0	?	?	0	0	0	1	0	1	0	0	?	1	1	?
<i>Garudimimus brevipes</i>	?	?	0	?	?	?	?	0	1	0	1	1	0	1	1
<i>Anserimimus planinychus</i>	0	1	?	?	?	?	?	?	?	?	?	?	?	1	?
<i>Ornithomimus edmontonicus</i>	0	2	0	0	0	0	1	0	1	0	?	1	1	1	?
<i>Struthiomimus altus</i>	0	2	0	0	0	0	1	0	1	0	?	1	1	1	1
<i>Gallimimus bullatus</i>	0	2	0	0	0	0	1	0	1	0	1	1	1	1	?
<i>Falcarius utahensis</i>	0	0	0	2	1	?	1	0	1	?	?	?	?	0	?
<i>Beipiaosaurus inexpectus</i>	0	?	1	?	?	?	?	?	1	1	?	0	?	?	?
<i>Alxasaurus elesitaiensis</i>	?	?	1	?	0	0	1	?	?	?	0	0	?	?	?
<i>Nothronychus mckinleyi</i>	?	?	?	?	0	0	1	?	0	?	?	?	?	?	?
<i>Erliaosaurus bellamanus</i>	0	1	?	?	?	?	?	?	0	1	?	?	?	?	?
<i>Nanshiungosaurus brevispinus</i>	?	?	1	0	0	1	1	?	?	?	?	?	?	?	?
<i>Neimongosaurus yangi</i>	?	?	?	?	?	?	?	?	0	1	0	0	0	0	?
<i>Segnosaurus galbiensis</i>	?	?	1	0	0	0	1	0	0	?	?	0	?	0	1
<i>Erlikosaurus andrewsi</i>	?	?	?	?	?	?	?	?	?	?	?	0	?	0	?
<i>Therizinosaurus cheloniformis</i>	?	?	?	?	?	?	?	?	?	?	?	?	?	?	?
<i>Alvarezsaurus calvoi</i>	?	?	0	?	?	?	?	?	?	?	?	?	?	1	?
<i>Patagonykus puertai</i>	?	?	?	?	?	?	?	?	?	1	1	?	?	1	?
<i>Mononykus olecranus</i>	?	?	?	?	?	?	?	?	1	1	1	?	?	1	?
<i>Shuvuuia deserti</i>	?	?	?	0	?	?	?	?	1	?	?	1	1	1	?
<i>Incisivosaurus gauthieri</i>	?	?	?	?	?	?	?	?	?	?	?	?	?	?	?
<i>Protarchaeopteryx robusta</i>	0	0	0	0	0	0	1	0	1	1	?	1	?	1	?

Taxa / Characters	316	317	318	319	320	321	322	323	324	325	326	327	328	329	330
<i>Allosaurus fragilis</i>	0	0	0	0	0	0	0	0	0	0	0	0	0	0	0
<i>Sinraptor</i>	0	?	0	0	0	0	0	0	0	?	?	0	?	0	0
<i>Dilong paradoxus</i>	0	0	0	0	0	0	0	0	0	0	0	1	0	?	?
<i>Eotyrannus lengi</i>	?	?	?	?	?	?	?	?	?	?	?	?	1	?	?
<i>Tyrannosaurus rex</i>	0	?	0	0	0	0	0	0	0	?	?	?	0	0	0
<i>Gorgosaurus libratus</i>	0	0	0	0	0	0	0	0	0	?	?	?	0	0	0
<i>Tanycolagreus topwilsoni</i>	0	0	0	0	0	0	0	0	0	0	0	1	1	?	?
<i>Coelurus fragilis</i>	0	?	?	?	?	?	?	?	?	?	?	1	1	?	?
<i>Ornitholestes hermanni</i>	0	?	?	?	?	?	?	?	0	?	?	?	?	0	0
<i>Guanlong wucaii</i>	0	?	?	?	2	1	0	?	0	0	0	0	0	?	0
<i>Aniksosaurus darwini</i>	0	?	0	0	0	1	?	0	?	?	?	?	?	?	0
<i>Nedcolbertia justinhoffmani</i>	0	?	0	?	0	0	?	0	0	?	?	?	?	?	?
<i>Nqwebasaurus thwazi</i>	0	0	0	0	0	0	?	0	0	1	1	0	0	?	?
<i>Santanaraptor placidus</i>	0	?	?	?	?	?	?	?	?	?	?	?	?	0	0
<i>Orkoraptor burkei</i>	?	?	?	?	?	?	?	?	?	?	?	?	?	?	?
<i>Juravenator starki</i>	?	0	0	0	0	1	0	0	0	0	0	0	0	?	?
<i>Mirischia asymmetrica</i>	?	?	?	?	?	?	?	?	?	?	?	?	?	?	0
<i>Compsognathus longipes</i>	0	0	0	0	0	0	0	0	0	?	?	0	0	0	0
<i>Sinocalliopteryx gigas</i>	0	0	0	0	0	0	?	?	0	0	0	0	0	0	0
<i>Huaxiagnathus orientalis</i>	0	0	0	0	0	0	0	?	0	0	0	1	0	0	0
<i>Sinosauropteryx prima</i>	0	0	0	0	0	0	0	0	0	0	?	1	0	0	0
<i>Scipionyx samniticus</i>	?	?	?	?	?	?	?	?	?	0	0	0	0	0	0
<i>Deinocheirus mirificus</i>	?	?	?	?	?	?	?	?	?	1	1	0	0	?	?
<i>Harpymimus okladnikovi</i>	0	?	?	?	0	0	0	0	0	0	1	0	0	0	0
<i>Pelecanimimus polyodon</i>	?	?	?	?	?	?	?	?	?	1	1	0	0	?	?
<i>Shenzhousaurus orientalis</i>	?	?	?	?	?	?	?	?	?	1	0	0	?	0	?
<i>Archaeornithomimus asiaticus</i>	0	?	?	?	?	?	?	?	?	?	?	0	0	0	0
<i>Garudimimus brevipes</i>	0	0	1	0	?	?	?	0	0	?	?	?	?	?	?
<i>Anserimimus planinychus</i>	0	?	?	?	?	?	?	?	?	?	1	0	0	?	?
<i>Ornithomimus edmontonicus</i>	0	?	?	?	1	0	0	0	0	1	1	0	0	0	0
<i>Struthiomimus altus</i>	0	?	?	?	1	0	0	0	0	1	1	0	0	0	0
<i>Gallimimus bullatus</i>	0	?	?	?	1	0	0	0	0	1	1	0	0	0	0
<i>Falcarius utahensis</i>	0	?	0	?	0	0	?	0	0	0	0	1	0	?	?
<i>Beipiaosaurus inexpectus</i>	?	0	?	1	?	?	?	?	?	0	?	0	0	?	?
<i>Alxasaurus elesitaiensis</i>	?	?	?	?	0	0	0	0	0	?	?	0	?	1	?
<i>Nothronychus mckinleyi</i>	?	?	?	?	?	?	?	?	1	?	?	?	?	1	1
<i>Erliansaurus bellamanus</i>	?	?	?	?	?	?	?	?	?	0	1	0	0	?	?
<i>Nanshiungosaurus brevispinus</i>	?	?	?	?	?	?	?	?	?	?	?	?	?	?	0
<i>Neimongosaurus yangi</i>	0	0	?	?	0	0	0	0	?	?	?	?	?	?	?
<i>Segnosaurus galbiensis</i>	0	0	1	1	?	?	?	0	1	?	?	?	?	?	?
<i>Erlikosaurus andrewsi</i>	0	0	1	1	0	0	0	0	1	?	?	?	?	?	?
<i>Therizinosaurus cheloniformis</i>	?	?	?	?	?	?	?	?	?	?	?	?	?	?	?
<i>Alvarezsaurus calvoi</i>	?	?	?	?	0	0	0	?	0	?	?	?	?	?	?
<i>Patagonykus puertai</i>	?	?	?	0	?	?	?	?	?	?	?	?	?	?	?
<i>Mononykus olecranus</i>	?	0	0	0	0	0	0	0	0	?	?	?	?	0	?
<i>Shuvuuia deserti</i>	0	0	0	?	0	0	1	0	0	1	1	0	0	0	?
<i>Incisivosaurus gauthieri</i>	?	?	?	?	?	?	?	?	?	?	?	?	?	?	?
<i>Protarchaeopteryx robusta</i>	0	0	0	0	0	0	?	?	0	0	0	0	0	?	?

Taxa / Characters	316	317	318	319	320	321	322	323	324	325	326	327	328	329	330
<i>Avimimus portentosus</i>	0	?	?	?	0	0	0	0	0	?	?	?	?	1	0
<i>Caudipteryx</i>	0	0	0	0	0	0	0	0	0	?	?	?	0	1	0
<i>Microvenator celer</i>	?	?	?	?	?	?	?	?	?	?	?	?	?	?	?
<i>Elmisaurus rarus</i>	0	?	0	0	0	0	0	1	0	?	?	1	1	?	?
<i>Chiurostenotes pergracilis</i>	0	0	0	0	0	0	0	1	0	0	0	1	1	1	0
<i>Caenagnathus collinsi</i>	?	?	?	?	?	?	?	?	?	?	?	?	?	?	?
<i>Oviraptor philoceratops</i>	?	?	?	?	?	?	?	?	?	1	0	0	0	?	?
<i>Rinchenia mongoliensis</i>	?	?	?	?	?	?	?	?	?	?	?	?	?	?	?
<i>Citipati osmolskae</i>	0	0	0	0	0	0	0	1	0	1	1	0	0	1	0
Zamyn Khondt oviraptorine	0	?	?	?	0	0	0	0	0	1	1	0	0	1	0
<i>Ingenia yanshini</i>	0	0	?	?	?	?	?	0	0	1	0	0	0	1	0
<i>Conchoraptor gracilis</i>	0	?	?	?	?	?	?	?	0	?	0	0	0	1	0
<i>Khaan mckennai</i>	0	0	0	0	0	0	0	0	0	1	0	0	0	1	0
<i>Heyuannia huangi</i>	0	?	0	0	0	1	0	0	0	?	?	?	0	1	0
<i>Sinovenator changii</i>	1	?	?	?	0	0	1	1	?	?	0	?	?	1	0
<i>Mei long</i>	1	0	0	?	1	?	1	?	?	0	0	0	?	1	1
<i>Byronosaurus jaffei</i>	?	?	?	?	?	1	1	?	?	?	?	?	?	?	?
<i>Sinornithoides youngi</i>	1	0	0	0	1	1	1	1	1	0	0	0	0	1	0
IGM 100/44	?	?	0	?	1	1	1	1	?	?	?	?	0	?	?
<i>Troodon formosus</i>	1	0	1	0	1	1	1	1	0	?	?	?	?	?	?
<i>Saurornithoides mongoliensis</i>	?	0	1	0	1	1	1	1	0	?	?	?	?	1	0
<i>Zanabazar junior</i>	?	?	?	?	?	?	?	?	?	?	?	?	?	1	?
<i>Unenlagia</i>	?	?	?	?	?	?	?	1	?	?	?	?	?	1	2
<i>Buitreraptor gonzalezorum</i>	0	?	?	?	0	?	2	?	?	?	?	?	?	1	2
<i>Rahonavis ostromi</i>	0	1	?	1	0	0	2	1	?	?	?	?	?	1	1
<i>Bambiraptor feinbergi</i>	0	0	0	1	0	0	1	1	0	0	?	0	0	1	2
<i>Sinornithosaurus millenii</i>	0	0	0	1	2	0	1	?	0	0	0	0	0	1	2
<i>Microraptor zhaoianus</i>	0	0	0	1	2	0	1	1	1	0	0	0	0	0	2
NGMC91	?	0	0	1	2	0	1	1	1	0	0	0	0	?	?
IGM 100 1015	?	?	?	?	?	?	?	?	?	?	?	?	?	?	?
<i>Adasaurus mongoliensis</i>	0	0	0	1	0	1	1	1	0	?	?	?	?	1	2
<i>Velociraptor mongoliensis</i>	0	0	0	0	0	1	1	1	0	0	0	0	0	1	2
<i>Saurornitholestes langstoni</i>	?	?	?	?	?	?	?	1	?	?	0	0	?	1	?
<i>Deinonychus antirrhopus</i>	0	0	0	1	0	1	1	1	0	0	0	0	0	1	2
<i>Achillobator giganticus</i>	?	?	?	?	?	1	1	?	?	?	?	?	?	1	0
<i>Dromaeosaurus albertensis</i>	?	?	?	?	0	1	1	1	?	?	?	?	?	?	?
<i>Utahraptor ostrommaysi</i>	?	?	?	?	?	?	?	?	?	?	?	?	?	1	0
<i>Atrociraptor marshalli</i>	?	?	?	?	?	?	?	?	?	?	?	?	?	?	?
<i>Epidendrosaurus ningchengensis</i>	0	1	1	0	2	0	0	0	0	1	1	0	0	?	?
<i>Archaeopteryx lithographica</i>	0	1	1	1	2	0	0	1	0	0	0	0	0	1	0
<i>Wellnhoferia grandis</i>	0	1	1	1	2	0	0	?	0	0	0	0	0	1	?
<i>Jeholornis prima</i>	0	1	1	1	2	0	0	0	1	0	0	1	0	1	?
<i>Sapeornis chaoyangensis</i>	0	1	1	1	?	?	?	?	1	?	?	1	0	1	?
<i>Confuciusornis sanctus</i>	0	1	1	1	2	0	0	0	1	0	1	1	0	1	?
<i>Protopteryx fengningensis</i>	0	1	1	1	2	0	0	?	0	?	?	1	0	?	?
<i>Yanornis martini</i>	0	1	?	?	2	0	0	0	0	?	?	?	0	?	?
<i>Hagryphus giganteus</i>	?	?	?	?	?	?	?	?	?	0	?	1	1	?	?

Taxa / Characters	331	332	333	334	335	336	337	338	339	340	341	342	343	344	345
<i>Allosaurus fragilis</i>	0	0	0	0	0	0	0	0	0	0	0	0	0	0	0
<i>Sinraptor</i>	0	0	0	0	0	?	0	0	?	?	0	0	0	?	?
<i>Dilong paradoxus</i>	?	0	?	0	1	?	0	0	?	?	0	?	0	?	0
<i>Eotyrannus lengi</i>	?	?	?	?	1	?	?	0	0	0	?	?	0	?	0
<i>Tyrannosaurus rex</i>	1	0	0	0	0	0	0	0	0	0	0	0	0	1	0
<i>Gorgosaurus libratus</i>	1	0	0	0	1	0	0	0	0	0	0	0	0	1	0
<i>Tanycolagreus topwilsoni</i>	1	?	0	?	1	?	?	0	0	0	0	0	?	0	0
<i>Coelurus fragilis</i>	1	?	0	?	1	?	?	?	0	0	?	?	0	0	?
<i>Ornitholestes hermanni</i>	0	0	0	0	1	0	0	0	0	0	?	?	0	?	?
<i>Guanlong wucaii</i>	?	0	0	0	1	?	0	0	?	?	0	0	0	0	0
<i>Aniksosaurus darwini</i>	?	0	0	?	1	?	0	0	0	0	0	0	?	?	?
<i>Nedcolbertia justinhoffmani</i>	0	?	?	?	1	0	?	0	?	0	?	0	?	?	?
<i>Nqwebasaurus thwazi</i>	?	?	?	?	1	?	?	0	0	0	?	0	?	0	1
<i>Santanaraptor placidus</i>	?	?	?	0	1	?	?	?	?	?	?	?	?	?	?
<i>Orkoraptor burkei</i>	?	?	?	?	?	?	?	?	?	?	?	?	?	?	?
<i>Juravenator starki</i>	?	0	0	?	?	0	0	0	0	0	0	0	0	0	0
<i>Mirischia asymmetrica</i>	0	?	?	0	?	?	?	?	?	?	?	?	?	?	?
<i>Compsognathus longipes</i>	?	0	0	0	1	0	0	0	0	0	0	0	0	0	0
<i>Sinocalliopteryx gigas</i>	?	0	?	0	1	0	0	0	0	0	0	?	0	0	0
<i>Huaxiagnathus orientalis</i>	?	0	0	0	1	0	0	0	0	0	0	0	0	0	0
<i>Sinosauropteryx prima</i>	0	?	?	0	1	0	0	0	0	0	0	0	0	0	1
<i>Scipionyx samniticus</i>	0	0	?	0	?	?	0	?	0	0	?	?	0	0	0
<i>Deinocheirus mirificus</i>	?	?	?	?	?	?	?	?	0	0	?	?	?	1	1
<i>Harpymimus okladnikovi</i>	?	0	0	?	1	?	0	0	0	0	?	0	0	0	0
<i>Pelecanimimus polyodon</i>	?	0	?	0	?	?	?	?	?	?	?	?	0	1	1
<i>Shenzhousaurus orientalis</i>	?	0	?	0	?	0	0	?	?	?	?	?	0	?	?
<i>Archaeornithomimus asiaticus</i>	?	0	0	0	1	0	0	?	0	0	?	?	?	1	1
<i>Garudimimus brevipes</i>	0	0	0	?	1	0	0	0	?	?	0	0	0	?	?
<i>Anserimimus planinychus</i>	?	?	?	?	2	?	?	?	0	0	?	?	?	1	1
<i>Ornithomimus edmontonicus</i>	?	0	0	0	2	0	0	0	0	0	?	0	0	1	1
<i>Struthiomimus altus</i>	?	0	0	0	2	0	0	0	0	0	?	0	0	1	1
<i>Gallimimus bullatus</i>	0	0	0	0	2	0	0	0	0	0	?	0	0	1	1
<i>Falcarius utahensis</i>	?	0	0	0	0	0	0	0	0	0	0	0	0	?	0
<i>Beipiaosaurus inexpectus</i>	?	?	?	?	?	?	1	?	?	?	0	?	0	?	0
<i>Alxasaurus elesitaiensis</i>	?	0	0	0	?	0	1	0	0	0	1	?	0	?	?
<i>Nothronychus mckinleyi</i>	?	?	?	1	?	?	?	?	0	0	?	?	?	?	?
<i>Erliaensaurus bellamanus</i>	?	?	?	?	?	?	1	?	0	0	?	?	?	0	0
<i>Nanshiungosaurus brevispinus</i>	?	?	?	0	?	?	1	?	?	?	1	?	?	?	?
<i>Neimongosaurus yangi</i>	?	0	?	?	0	0	1	1	1	0	1	0	0	?	?
<i>Segnosaurus galbiensis</i>	?	0	0	1	?	?	1	1	?	0	1	?	0	?	?
<i>Erlikosaurus andrewsi</i>	?	?	?	?	0	?	?	1	1	1	1	0	0	?	?
<i>Therizinosaurus cheloniformis</i>	?	?	?	?	?	?	?	?	1	1	?	?	?	0	?
<i>Alvarezsaurus calvoi</i>	?	0	?	?	1	0	0	0	?	?	?	0	?	?	?
<i>Patagonykus puertai</i>	?	?	?	?	?	?	?	?	?	1	?	?	?	?	?
<i>Mononykus olecranus</i>	?	0	0	?	?	?	0	0	1	1	0	0	?	1	?
<i>Shuvuuia deserti</i>	0	0	0	0	2	?	0	0	1	1	0	0	0	1	2
<i>Incisivosaurus gauthieri</i>	?	?	?	?	?	?	?	?	?	?	?	?	0	?	?
<i>Protarchaeopteryx robusta</i>	0	0	0	0	1	0	0	?	0	0	0	0	0	0	0

APPENDIX 7

List of the sampling points for SEM analysis (Fig. 186)

1. Microsample of somatic musculature from the base of the neck of *Scipionyx*, between the centrum of D2 and the shaft of Dr1. It is likely a cortical (peripheral) slice, as other layers underlay it.
2. Bone fragment of *Scipionyx*, coming from the dorsal wall of the shaft of Dr3, just cranial to the cranial margin of the right scapular blade.
3. Dome-shaped element (whose elliptical base has been left in place), belonging to the nodule of calcite grains that form a cluster in the ventral portion of the thoracic region of *Scipionyx*.
4. Red macula in the thorax of *Scipionyx*: encrustations on the shaft of the left radius, and on the matrix bordering the cranial margin of the diaphysis of the right humerus, provided 6 microsamples.
5. Cranial tract of the descending loop of the duodenum of *Scipionyx*: microsample from the dorsocaudal section of the tube, at the level of the right elbow.
6. Fold of the mucosa from the internal curve (cranial margin) of the U-turn linking the descending and the ascending loop of the duodenum of *Scipionyx*. In a microsample from this point, even fragments of mesenteric and pancreatic tissue might be potentially included.
7. Drop-shaped granule, positioned as the most caudoventral untouched element of the calcite cluster that in the abdomen of *Scipionyx* parallels the ascending loop of the duodenum, between D12 and S1. As for sampling n. 3, the element has been cut at the base.
8. Microsample from a right lateral section of the descending loop of the rectum of *Scipionyx*, located between the centrum of S5 and the ischial feet. Given the irregular preserved surface of the tube in this region, part of the intestinal contents may be included in the sampling.
9. Fragment of one of the fish scales contained in the faecal pellet that fills the end of the rectum of *Scipionyx*, at the level of the caudal margin of the right ilium.
10. Microsample from the dorsal bundle of the left caudofemoral muscle of *Scipionyx*. More precisely, it comes from its dorsal margin, where it faces the cranial articular surface of the centrum of Ca1.
11. Sample of sediment from the granular bed emerging below *Scipionyx*, at the level of the right tibia.
12. Sample of sediment from the granular bed emerging below *Scipionyx*, at the level of the right femur.
13. Sample of sediment from the granular bed emerging below *Scipionyx*, at the level of the left manus.

SUPPLEMENTARY INFORMATION

Character change list (ACCTTRAN and DELTRAN) related to the data matrix published in Appendix 6 is available on the website

<http://www.scienzeaturali.org/riviste/memorie/37sup.html>



Fig. 186 - Map of the sampling points (numbered dots) selected for the SEM analyses published in this study.

Fig. 186 - Mappa dei punti di campionamento (pallini numerati) scelti per le analisi al SEM pubblicate in questo studio.



Marco Auditore & Arianna Nicora, *L'ultima cena* (*The last supper*), Genova 2010. Matita su carta e Photoshop (Crayon on paper and Photoshop).



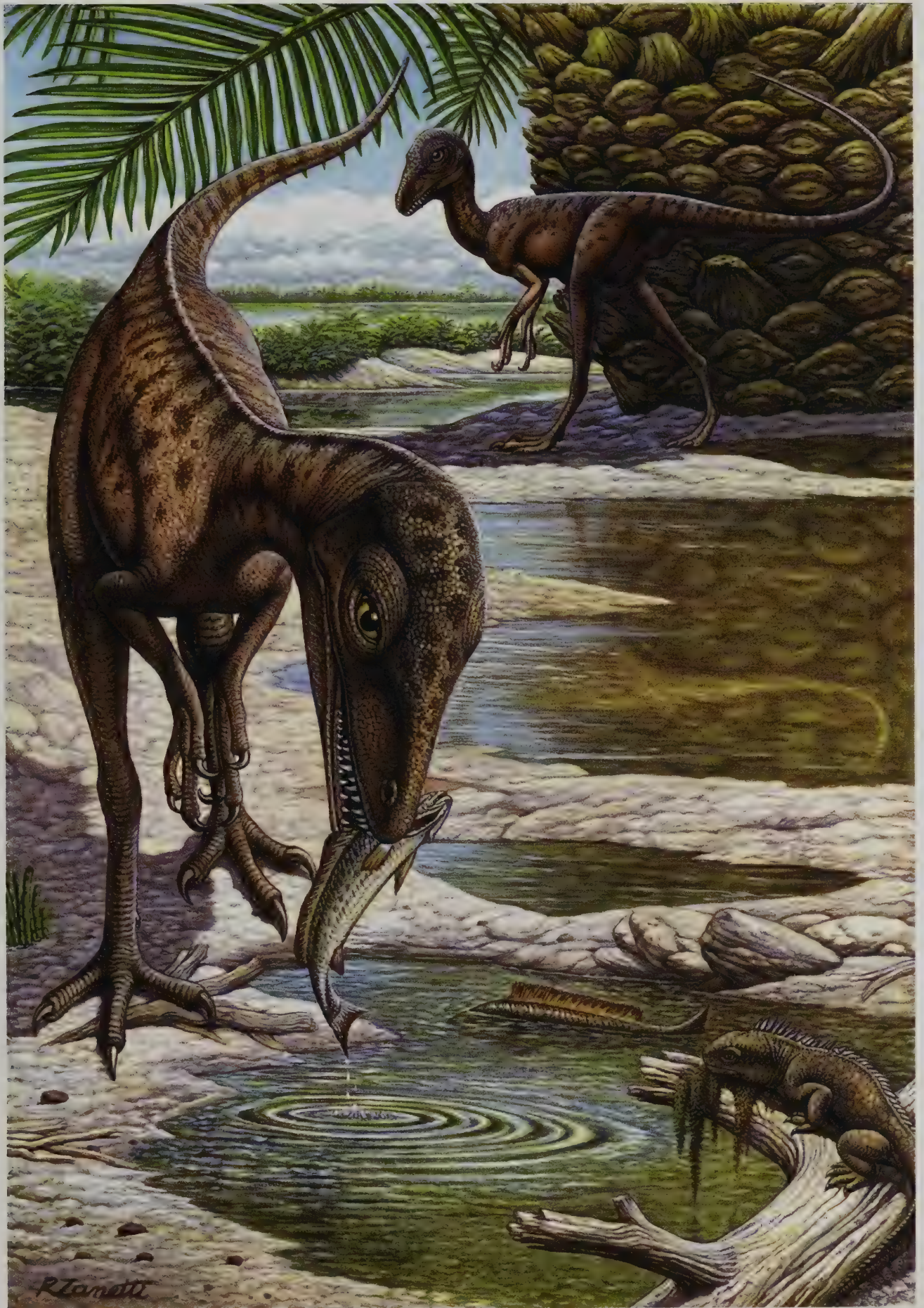
Davide Bonadonna, *Scipionyx samniticus* a caccia di un *Eichstaettisaurus* (*Scipionyx samniticus* chasing *Eichstaettisaurus*), Segrate 2010. Tempera su carta e Photoshop (Tempera on paper and Photoshop).



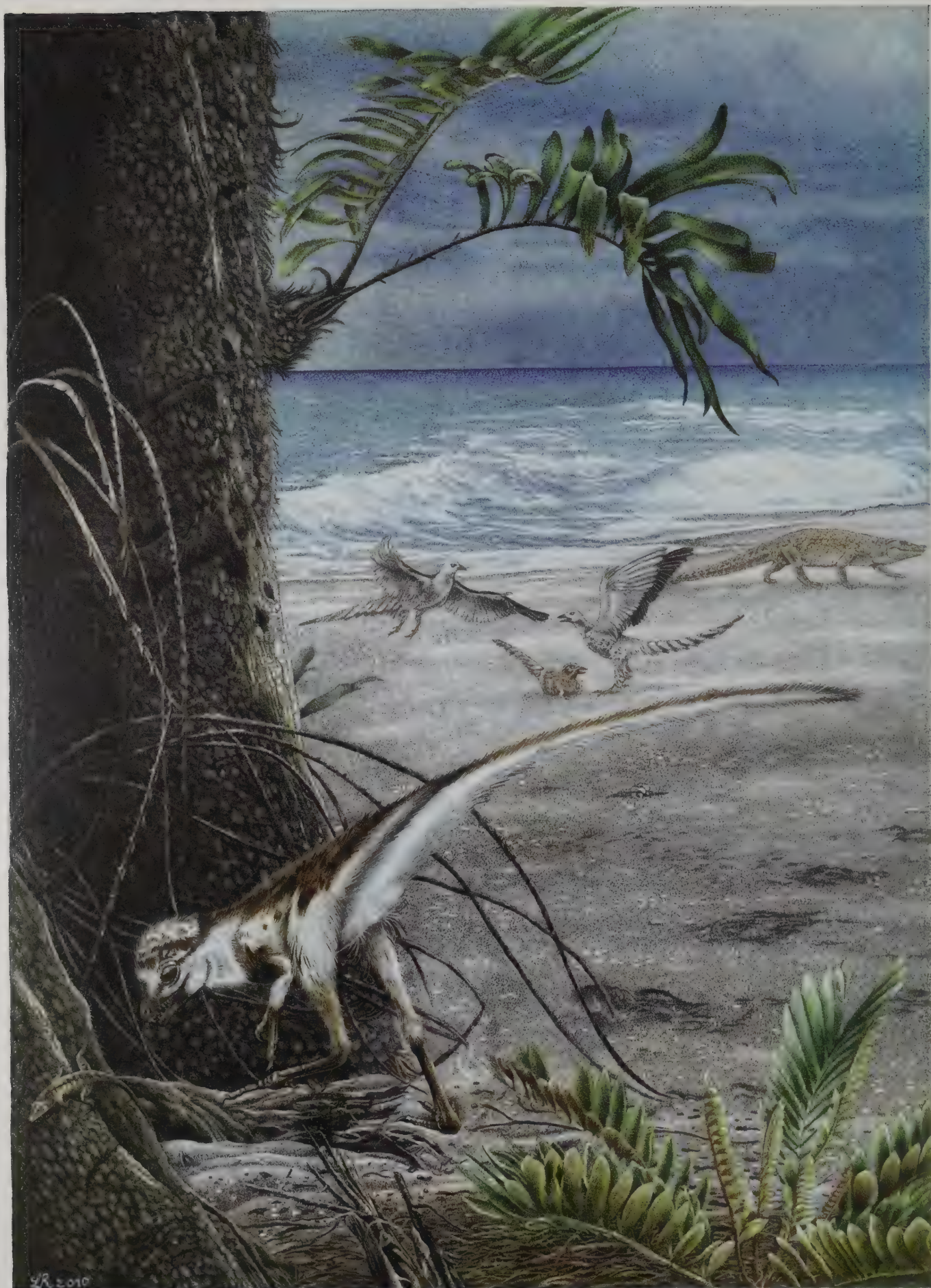
Paolo Cinquemani, *Ciro nuota* (*Ciro swims*), Trieste 2010. Acrilico su tela (Acrylic on canvas).



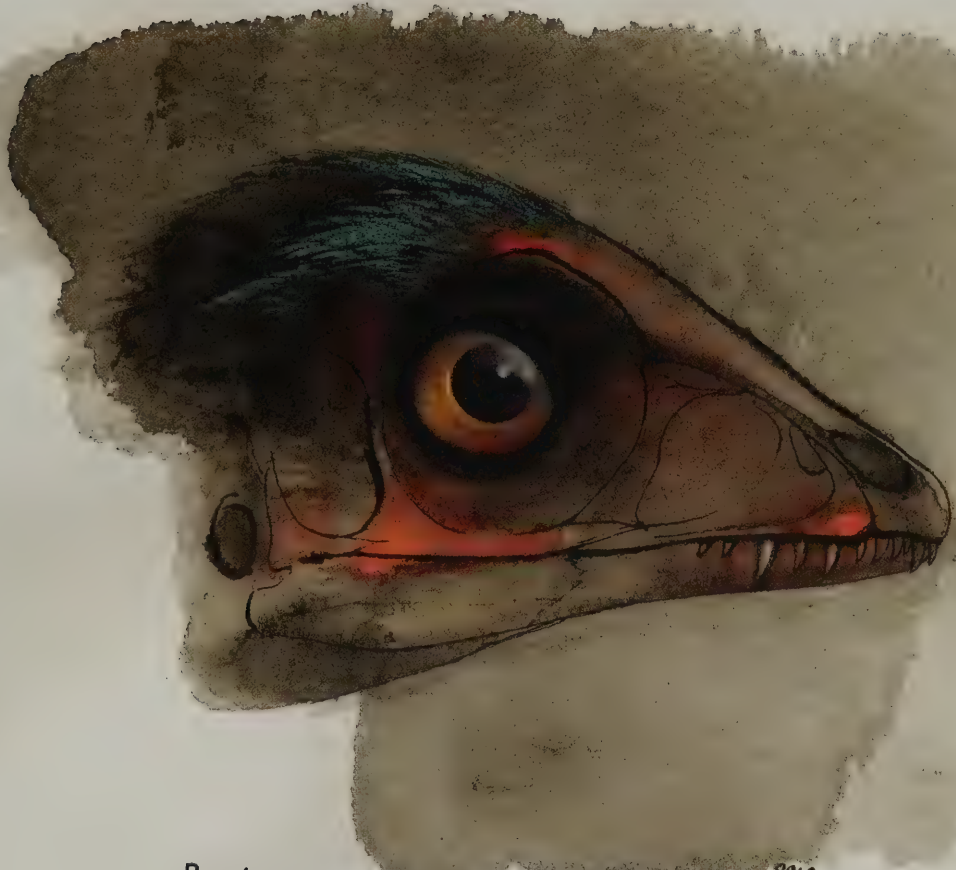
Fabio Pastori, *Il secondo pasto* (*The second lunch*), Milano 2010. Acrilico su cartoncino (Acrylic on cardboard).



Renzo Zanetti, *A caccia nelle pozze (Hunting in pools)*, Monteveglio 2010. Acquarello e pastello su carta (Watercolor and crayon on paper).



Loana Riboli, *All'ombra della Zamites (Under the Zamites tree)*, Crema 2010. Tecnica mista su carta (Mixed technique on paper).



Ricostruzione testa *Scipionyx samniticus* 2010

F.F.



Lukas Panzarin, *Il buongiorno si vede dal mattino* (*You can tell a good day from the morning*), Torre di Mosto 2010. Acrilico su carta (Acrylic on paper).



Tullio Perentin, *Cinque piccoli ruffiani* (*Five little panders*), Trieste 2010. Matita su lucido (Pencil on tracing paper).



Troco, *Ciro e cicadeoidea* (*Ciro and cycadoid*), Venezia 2010. Olio su tela (Oil on canvas).

TABLE OF CONTENTS

INTRODUCTION	Pag. 6	Type locality	Pag. 34
GEOLOGICAL SETTING	Pag. 7	Type horizon and age	Pag. 34
The locality	Pag. 7	Emended diagnosis	Pag. 34
Historical background	Pag. 9	Remarks	Pag. 34
Geological framework	Pag. 10	OSTEOLOGICAL DESCRIPTION AND	
Lithology, stratigraphy, and sedimentology	Pag. 12	COMPARISONS	
Stratigraphic position of <i>Scipionyx</i>	Pag. 12	General features	Pag. 34
Macroscopic aspect of the embedding sediment	Pag. 14	SKULL AND MANDIBLE	
Microscopic aspect and chemical composition of the embedding sediment	Pag. 15	Cranial openings	Pag. 35
Depositional environment	Pag. 15	Apertura nasi ossea	Pag. 35
Lagoon model	Pag. 16	Antorbital fossa	Pag. 36
Slope/shallow basin model	Pag. 16	Antorbital fenestra	Pag. 36
Submarine channel model	Pag. 16	Maxillary fenestrae	Pag. 36
The fossil assemblage and palaeoenvironment .	Pag. 17	Orbit	Pag. 37
Microfossils	Pag. 17	Supratemporal fossa	Pag. 37
Plants	Pag. 18	Supratemporal fenestra	Pag. 37
Invertebrates	Pag. 18	Infratemporal fenestra	Pag. 37
Fishes	Pag. 19	Palatal fenestrae	Pag. 37
Tetrapods	Pag. 19	Foramen magnum	Pag. 37
Palaeogeography	Pag. 20	Scleral plates	Pag. 37
Evidence from central and southern Italian dinosaur tracksites	Pag. 21	Dermal skull roof	Pag. 38
Palaeobiogeographical remarks	Pag. 22	Premaxilla	Pag. 38
MATERIAL	Pag. 24	Maxilla	Pag. 39
METHODS	Pag. 24	Nasal	Pag. 41
Preparation	Pag. 24	Lacrima	Pag. 41
Optical microscopy	Pag. 25	Prefrontal	Pag. 42
Photographs and drawings	Pag. 25	Postorbital	Pag. 42
Measurements	Pag. 25	Jugal	Pag. 42
UV light analysis	Pag. 25	Quadratojugal	Pag. 42
CT scan analysis	Pag. 26	Squamosal	Pag. 43
SEM analysis	Pag. 26	Frontal	Pag. 44
Anatomical terms	Pag. 27	Parietal	Pag. 45
Systematic terms	Pag. 27	Braincase	Pag. 45
Anatomical abbreviations	Pag. 27	Supraoccipital	Pag. 45
Institutional abbreviations	Pag. 27	Exoccipital	Pag. 46
PART I - OSTEOLOGY	Pag. 34	Prootic	Pag. 46
Systematic Palaeontology	Pag. 34	Basioccipital-Basisphenoid	Pag. 46
Type and only species	Pag. 34	Basisphenoid-Parasphenoid	Pag. 46
Etymology	Pag. 34	Laterosphenoid	Pag. 47
Holotype	Pag. 34	Orbitosphenoid	Pag. 47
		Palatoquadrate complex	Pag. 47
		Vomer	Pag. 47

Palatine	Pag. 47	Pelvic girdle	Pag. 97
Pterygoid	Pag. 48	Ilium	Pag. 97
Epipterygoid	Pag. 49	Pubis	Pag. 101
Ectopterygoid	Pag. 49	Ischium	Pag. 103
Quadrate	Pag. 50	Hindlimb	Pag. 104
Mandible	Pag. 50	Femur	Pag. 104
Mandibular openings	Pag. 51	Tibia	Pag. 105
Dentary	Pag. 51	Fibula	Pag. 106
Supradentary-coronoid	Pag. 52	ONTOGENETIC ASSESSMENT	Pag. 110
Splenic	Pag. 52	Introduction	Pag. 110
Surangular	Pag. 52	Gut contents	Pag. 110
Angular	Pag. 53	Scarred bone surfaces	Pag. 110
Prearticular	Pag. 53	Large skull	Pag. 111
Articular	Pag. 53	Orbital foramina rounded and proportionally very large and antorbital region short and deep	Pag. 111
Dentition	Pag. 54	Position of the maxillary fenestra	Pag. 112
Premaxillary teeth	Pag. 54	Rostral ramus of the maxilla	Pag. 112
Maxillary teeth	Pag. 55	Unfused interdental plates	Pag. 112
Dentary teeth	Pag. 57	Nasals shorter than frontals	Pag. 112
Heterodonty	Pag. 58	Position of the caudal margin of the apertura nasi ossea	Pag. 112
Hyoid apparatus	Pag. 58	Shape of the lacrimal	Pag. 113
POSTCRANIAL AXIAL SKELETON	Pag. 59	Large prefrontals, with descending lateral process well-exposed in lateral view	Pag. 113
Vertebrae	Pag. 59	Sublacrimal expansion of the jugal	Pag. 113
Cervical vertebrae	Pag. 59	Frontoparietal fontanelle open	Pag. 113
Dorsal vertebrae	Pag. 64	Elements of the braincase in loose contact ..	Pag. 113
Sacral vertebrae	Pag. 70	Vomers unfused to each other all along their length	Pag. 114
Caudal vertebrae	Pag. 71	Craniocaudal length of the dentary	Pag. 114
Haemal arches	Pag. 75	Angular moved dorsally	Pag. 114
Ribs	Pag. 76	Symmetrical tooth crown height in counterlateral tooth rows	Pag. 114
Cervical ribs	Pag. 76	Low number of lateral teeth	Pag. 114
Dorsal ribs	Pag. 78	Teeth with few denticles	Pag. 115
Sacral ribs	Pag. 80	Denticle size and density	Pag. 115
Gastralia	Pag. 80	Incomplete ossification of the vertebral column	Pag. 115
APPENDICULAR SKELETON	Pag. 84	Cervical ribs not fused to the corresponding vertebrae	Pag. 117
Pectoral girdle	Pag. 84	Unfused girdle elements	Pag. 117
Scapula	Pag. 85	Relative size of the girdle elements	Pag. 117
Coracoid	Pag. 88	Degree of ossification of the ilium	Pag. 117
Furcula	Pag. 89	Non-ossified sternal plates	Pag. 118
Forelimb	Pag. 89	Limb proportions	Pag. 118
Humerus	Pag. 90	Carpal count and ossification	Pag. 118
Radius	Pag. 91		
Ulna	Pag. 92		
Carpus	Pag. 92		
Metacarpus	Pag. 95		
Manual phalanges	Pag. 96		

Elongation of the manus Pag. 118

Development of the fourth trochanter Pag. 118

Remarks Pag. 119

PHYLOGENETIC ANALYSIS Pag. 121

Modification of the data matrix Pag. 121

Terminal taxa Pag. 121

Characters Pag. 121

Results Pag. 122

Comments Pag. 123

SKELETAL TAPHONOMY Pag. 127

PART II - SOFT TISSUE ANATOMY Pag. 129

Introduction Pag. 129

INTERNAL SOFT TISSUES Pag. 129

Soft tissue within the bones Pag. 133

Periosteal remains Pag. 135

Axial ligaments Pag. 136

Axial articular cartilages Pag. 137

Appendicular articular cartilages Pag. 137

Muscles, connective tissue and other soft tissues in the neck Pag. 138

Trachea Pag. 141

Oesophagus and stomach Pag. 142

Dorsal epaxial muscles Pag. 143

Liver and other blood-rich organs Pag. 143

Intestine Pag. 145

 Duodenum Pag. 147

 Jejunum Pag. 148

 Ileum Pag. 149

 Rectum Pag. 150

 Faecal pellet Pag. 151

Mesenteric blood vessels Pag. 153

Pelvic and hindlimb muscles Pag. 155

 Puboischiofemoral muscle Pag. 155

 Caudofemoral muscles Pag. 156

 Ilio-ischiocaudal muscle septa Pag. 157

 Other fragments of pelvic and hindlimb muscles Pag. 161

Caudal hypaxial connective tissue/ligaments Pag. 161

Indeterminate ?connective tissue Pag. 162

EXTERNAL SOFT TISSUES Pag. 163

Horny claws Pag. 163

ENDOGENOUS BIOMOLECULAR COMPONENTS Pag. 165

SOFT TISSUE TAPHONOMY Pag. 167

Diagenetic formations possibly related to soft tissues Pag. 169

PART III - FUNCTIONAL MORPHOLOGY AND PALAEOBIOLOGY Pag. 171

SKELETAL RECONSTRUCTION AND IN VIVO RESTORATIONS OF SCIPIONYX SAMNITICUS Pag. 171

 Cranial reconstruction Pag. 171

 Axial skeleton Pag. 174

 Pectoral girdle and forelimb Pag. 174

 Pelvic girdle and hindlimb Pag. 175

 Body length and body mass Pag. 175

 Integument Pag. 175

GUT CONTENTS AND FEEDING CHRONOLOGY Pag. 176

Oesophageal contents Pag. 176

Gastric contents Pag. 176

 Description Pag. 177

 Taxonomic affinities Pag. 179

Intestinal contents Pag. 179

Palaeobiological significance of the gut contents of *Scipionyx* Pag. 181

REMARKS ON THE PHYSIOLOGY OF SCIPIONYX Pag. 183

Digestive physiology Pag. 183

Respiratory physiology Pag. 185

 Liver and diaphragm Pag. 185

 Diaphragmatic muscles Pag. 186

 Lungs Pag. 186

 Trachea Pag. 188

 Abdominal air sacs Pag. 188

 Osteological correlates: pneumatic bones Pag. 188

 Osteological correlates: morphology of ribs and vertebrae Pag. 189

 Osteological correlates: gastralia Pag. 189

 Osteological correlates: pelvic girdle Pag. 189

CONCLUDING REMARKS Pag. 190

ACKNOWLEDGEMENTS Pag. 191

Special thanks Pag. 192

REFERENCES Pag. 193

NOTE ADDED IN PROOF Pag. 205

APPENDIX 1 Pag. 207

APPENDIX 2 Pag. 212

APPENDIX 3 Pag. 214

APPENDIX 4 Pag. 215

APPENDIX 5 Pag. 216

APPENDIX 6 Pag. 218

APPENDIX 7 Pag. 266

SUPPLEMENTARY INFORMATION Pag. 266

- II - MONTANARI L., 1969 - Aspetti geologici del Lias di Gozzano (Lago d'Orta), pp. 23-92, 42 figg., 4 tavv. n.t.
- III - PETRUCCI F., BORTOLAMI G. C. & DAL PIAZ G. V., 1970 - Ricerche sull'anfiteatro morenico di Rivoli-Avigliana (Prov. Torino) e sul suo substrato cristallino, pp. 93-169, con carta a colori al 1:40.000, 14 figg., 4 tavv. a colori e 2 b.n.

Volume XIX

- I - CANTALUPPI G., 1970 - Le *Hilodoceratidae* del Lias medio delle regioni mediterranee - Loro successione e modificazioni nel tempo. Riflessi biostratigrafici e sistematici, pp. 5-46, 2 tabb. n.t.
- II - PINNA G. & LEVI-SETTI F., 1971 - I *Dactyloceratidae* della Provincia Mediterranea (*Cephalopoda Ammonoidea*), pp. 47-136, 21 figg., 12 tavv.
- III - PELOSIO G., 1973 - Le ammoniti del Trias medio di Asklepion (Argolide, Grecia) - I. Fauna del «calcare a *Psychites*» (Anisot sup.), pp. 137-168, 3 figg., 9 tavv.

Volume XX

- I - CORNAGGIA CASTIGLIONI O., 1971 - La cultura di Remedello. Problematologia ed ergologia di una facies dell'Eneolitico Padano, pp. 5-80, 2 figg., 20 tavv.
- II - PETRUCCI F., 1972 - Il bacino del Torrente Cinghio (Prov. Parma). Studio sulla stabilità dei versanti e conservazione del suolo, pp. 81-127, 37 figg., 6 carte tematiche.
- III - CERETTI E. & POLUZZI A., 1973 - Briozoi della bioalcalarenite del Fosso di S. Spirito (Chieti, Abruzzi), pp. 129-169, 18 figg., 2 tavv.

Volume XXI

- I - PINNA G., 1974 - I crostacei della fauna triassica di Cene in Val Seriana (Bergamo), pp. 5-34, 16 figg., 16 tavv.
- II - POLUZZI A., 1975 - I Briozoi Cheilostomi del Pliocene della Val d'Arda (Piacenza, Italia), pp. 35-78, 6 figg., 5 tavv.
- III - BRAMBILLA G., 1976 - I Molluschi pliocenici di Viallervia (Alessandria), I. Lamellibranchi, pp. 79-128, 4 figg., 10 tavv.

Volume XXII

- I - CORNAGGIA CASTIGLIONI O. & CALEGARI G., 1978 - Corpus delle pintaderas preistoriche italiane. Problematologia, schede, iconografia, pp. 5-30, 6 figg., 13 tavv.
- II - PINNA G., 1979 - Osteologia dello scheletro di *Kritosaurus notabilis* (Lambe, 1914) del Museo Civico di Storia Naturale di Milano (*Ornithischia Hadrosauridae*), pp. 31-56, 3 figg., 9 tavv.
- III - BIANCOTTI A., 1981 - Geomorfologia dell'Alta Langa (Piemonte meridionale), pp. 57-104, 28 figg., 12 tabb., 1 carta f.t.

Volume XXIII

- I - GIACOBINI G., CALEGARI G. & PINNA G., 1982 - I resti umani fossili della zona di Arena Po (Pavia). Descrizione e problematica di una serie di reperti di probabile età paleolitica, pp. 5-44, 4 figg., 16 tavv.
- II - POLUZZI A., 1982 - I Radiolari quaternari di un ambiente idrotermale del Mar Tirreno, pp. 45-72, 3 figg., 1 tab., 13 tavv.
- III - ROSSI F., 1984 - Ammoniti del Kimmeridgiano superiore-Berriasiano inferiore del Passo del Furlo (Appennino Umbro-Marchigiano), pp. 73-138, 9 figg., 2 tabb., 8 tavv.

Volume XXIV

- I - PINNA G., 1984 - Osteologia di *Drepanosaurus unguicaudatus*, lepidosauro triassico del sottordine *Lacerilia*, pp. 5-28, 12 figg., 2 tavv.
- II - NOSOTTI S. & PINNA G., 1989 - Storia delle ricerche e degli studi sui rettili Placodonti. Parte prima 1830-1902, pp. 29-86, 24 figg., 12 tavv.

Volume XXV

- I - CALEGARI G., 1989 - Le incisioni rupestri di Taouardei (Gao, Mali). Problematologia generale e repertorio iconografico, pp. 1-14, 9 figg., 24 tavv.
- II - PINNA G. & NOSOTTI S., 1989 - Anatomia, morfologia funzionale e paleoecologia del rettile placodonte *Psephoderma alpinum* Meyer, 1858, pp. 15-50, 20 figg., 9 tavv.
- III - CALDARA R., 1990 - Revisione Tassonomica delle specie paleartiche del genere *Tychius* Germar (Coleoptera Curculionidae), pp. 51-218, 575 figg.

Volume XXVI

- I - PINNA G., 1992 - *Cyamodus hildegardis* Peyer, 1931 (Reptilia, Placodontia), pp. 1-21, 23 figg.
- II - CALEGARI G. a cura di, 1993 - L'arte e l'ambiente del Sahara preistorico: dati e interpretazioni, pp. 25-556, 647 figg.
- III - ANDRI E. & ROSSI F., 1993 - Genesi ed evoluzione di frangenti, cinte, barriere ed atolli. Dalle stromatoliti alle comunità di scogliera moderne, pp. 559-610, 49 figg., 1 tav.

Volume XXVII

- I - PINNA G. and GHISELIN M. edited by, 1996 - Biology as History. N. 1. Systematic Biology as an Historical Science, pp. 1-133, 68 figs.
- II - LEONARDI C. & SASSI D. a cura di, 1997 - Studi geobotanici ed entomofaunistici nel Parco Regionale del Monte Barro, pp. 135-266, 122 figg., 23 tabb.

Volume XXVIII

- I - BANFI E. & GALASSO G., 1998 - La flora spontanea della città di Milano alle soglie del terzo millennio e i suoi cambiamenti a partire dal 1700, pp. 267-388, 71 figg., 30 tabb.

Volume XXIX

- I - CALEGARI G., 1999 - L'arte rupestre dell'Eritrea. Repertorio ragionato ed esegesi iconografica, pp. 1-174, 268 figg.

Volume XXX

- I - PEZZOTTA F. edited by, 2000 - Mineralogy and petrology of shallow depth pegmatites. Paper from the First International Workshop, pp. 1-117, 30 figs., 19 tabs.
- II - PARISI B., FRANCHINO A. & BERTIA. con la collaborazione di POTENZA B. & RUBINI D., 2000 - La Società Italiana di Scienze Naturali 1855 - 2000. Percorsi storici, pp. 1-163, 199 figg.
- III - DE ANGELIA. & GARASSINO A., 2002 - Galatheid, chirostylid and porcellanid decapods (Crustacea, Decapoda, Anomura) from the Eocene and Oligocene of Vicenza (N Italy), pp. 1-31, 21 figs., 9 pls.

Volume XXXI

- I - NOSOTTI S. & RIEPPEL O., 2002 - The braincase of *Placodus* Agassiz, 1833 (Reptilia, Placodontia), pp. 1-18, 15 figs.
- II - MARTORELLI G., 2002 - Monografia illustrata degli uccelli di rapina in Italia. (1895). Riedizione a cura di Fausto Barbagli, pp. [XX] 1-216, [14] 46 figg., 4 tavv.
- III - NOSOTTI S. & RIEPPEL O., 2003 - *Eusauropsargis dalsassoi* n. gen. n. sp., a new, unusual diapsid reptile from the Middle Triassic of Besano (Lombardy, N Italy), pp. 1-33, 19 figs., 1 tab., 3 pls.

Volume XXXII

- I - ALESSANDRELLO A., BRACCHI G. & RIOU B., 2004 - Polychaete, sipunculan and enteropneust worms from the Lower Callovian (Middle Jurassic) of La Vouille-sur-Rhône (Ardèche, France), pp. 1-16, 9 figs., 1 pl.
- II - RIEPPEL O. & HEAD J. J., 2004 - New specimens of the fossil snake genus *Eupodophis* Rage & Escuillie, from Cenomanian (Late Cretaceous) of Lebanon, pp. 1-26, 13 figs., 1 tab.
- III - BRACCHI G. & ALESSANDRELLO A., 2005 - Paleodiversity of the free-living polychaetes (Annelida, Polychaeta) and description of new taxa from the Upper Cretaceous *Lagersätten* of Haql, Hadjula and Al-Namoura (Lebanon), pp. 1-48, 8 figs., 1 tab., 16 pls.

Volume XXXIII

- I - BOESI A. & CARDI F. edited by, 2005 - Wildlife and plants in traditional and modern Tibet: conception, exploration and conservation, pp. 1-88, 30 figs., 9 tabs.
- II - BANFI E., BRACCHI G., GALASSO G. & ROMANI E., 2005 - *Agrostologia Placentina*, pp. 1-80, 7 figs., 1 tab.
- III - LIVI P. a cura di 2005 - I fondi speciali della Biblioteca del Museo Civico di Storia Naturale di Milano. La raccolta di stampe antiche del Centro Studi Archeologia Africana, pp. 1-250, 389 figs.

Volume XXXIV

- I - GARASSINO A. & SCHWEIGERT G., 2006 - The Upper Jurassic Solnhofen decapod crustacean fauna: review of the types from old descriptions. Part I. Infraorders Astacidea, Thalassinidea and Palinura, pp. 1-64, 12 figs., 20 pls.
- II - FUCHS D., 2006 - Morphology, taxonomy and diversity of vampyropod Coleoids (Cephalopoda) from the Upper Cretaceous of Lebanon, pp. 1-28, 9 figs., 9 pls.
- III - CALDWELL M. W., 2006 - A new species of *Pontosaurus* (Squamata, Pythonomorpha) from the Upper Cretaceous of Lebanon and a phylogenetic analysis of Pythonomorpha, pp. 1-42, 18 figs., 1 pl.

Volume XXXV

- I - DE ANGELIA. & GARASSINO A., 2006 - Catalog and bibliography of the fossil Stomatopoda and Decapoda from Italy, pp. 1-95.
- II - GARASSINO A., FELDMANN R.M. & TERUZZI G., edited by, 2007 - 3rd Symposium on Mesozoic and Cenozoic Decapod Crustaceans. Museo di Storia Naturale di Milano May 23-25, 2007, pp. 1-104, 38 figs., 6 tabs.
- III - NOSOTTI S., 2007 - *Tamystropheus longobardicus* (Reptilia, Protosauira): re-interpretations of the anatomy based on new specimens from the Middle Triassic of Besano (Lombardy, N Italy), pp. 1-88, 67 figs., 4 pls., 9 tabs.

Volume XXXVI

- I - GALASSO G., CHIOZZI G., AZUMA M. & BANFI E., a cura di, 2008 - Le specie alloctone in Italia: censimenti, invasività e piani di azione. Milano, 27-28 Novembre 2008, pp. 1-96.
- II - MAGANUCO S., STEYER J. S., PASINI G., BOULAY M., LORRAIN S., BENETEAU A. & AUDITORE A., 2009 - An exquisite specimen of *Edingerella madagascariensis* (Temnospondyli) from the Lower Triassic of NW Madagascar; cranial anatomy, phylogeny, and restorations, pp. 1-72, 32 figs., 1 tab., 4 appendix.
- III - GARASSINO A., 2009 - The thoracic sternum and spermatheca in the extant genera of the family Homolidae De Haan, 1839 (Crustacea, Decapoda, Brachyura), pp. 1-80, 2 figs., 18 pls., 1 tab.

dna	dorsal neural arch arco neurale dorsale	actis	acetabular portion of ischium porzione acetabolare dell'ischio
dp	diapophysis diapofisi	bf	<i>brevis fossa</i>
Dr	dorsal rib costola dorsale	ca	carpals carpali
ep	epiphysis epipofisi	cabil	caudal blade of ilium lama caudale dell'ileo
ga	gastralia	ccil	cranial concavity of ilium concavità craniale dell'ileo
ha	haemal arch (chevron) arco emale	clf	fossa of collateral ligament fossa del legamento collaterale
ila	interspinal ligament attachment inserzione dei legamenti interspinali	cn	cnemial crest cresta cnemiale
ipofs	infrapostzygopophysal fossa fossa infrapostzigopofisaria	co	coracoid coracoide
lga	lateral gastralium gastralium laterale	cof	coracoid foramen forame coracoideo
mdf	mediodorsal facet facetta mediodorsale	cot	coracoid tubercle tubercolo del coracoide
mga	medial gastralium gastralium mediale	crbil	cranial blade of ilium lama craniale dell'ileo
mvf	medioventral facet facetta medioventrale	cvp	cranioventral process processo cranioventrale
nc	neural canal canale neurale	dc1+2	distal carpals 1+2 carpali distali 1+2
ncs	neurocentral suture sutura neurocentrale	dpc	deltpectoral crest cresta deltopettorale
ncas	neurocentral articular surface superficie articolare neurocentrale	epc	<i>epicleidum</i>
ns	neural spine spina neurale	exp	extensor pit fossa dell'estensore
pcdl	posterior centrodiapophyseal lamina lamina centrodiapofisaria posteriore	fe	femur femore
pn	pneumatopore pneumatoporo	fi	fibula
podl	postzygodiapophyseal lamina lamina postzigodiapofisaria	fic	fibular condyle condilo fibulare
poz	postzygopophysis postzigopofisi	ft	flexor tubercle tubercolo del flessore
ppdl	paradiapophyseal lamina lamina paradiapofisaria	fu	furcula
prdl	prezygodiapophyseal lamina lamina prezigodiapofisaria	fus	symphysis of furcula sinfisi della furcula
prel	prezygoepiphysal lamina lamina prezigoeipofisaria	gl	glenoid fossa fossa glenoidea
prpl	prezygoparapophysal lamina lamina prezigoparapofisaria	gt	greater trochanter trocantere maggiore
prz	prezygopophysis prezigopofisi	hh	humeral head testa dell'omero
S	sacral vertebra vertebra sacrale	hpl	hooked process of ilium processo uncinato dell'ileo
sc	sacral centrum centro sacrale	hu	humerus omero
sna	sacral neural arch arco neurale sacrale	hyc	<i>hypocleidum</i>
Sr	sacral rib costola sacrale	il	ilium ileo
tp	transverse process processo trasverso	ilis	iliac process of ischium processo iliaco dell'ischio
tpolf	intrapostzygopophysal fossa fossa infrapostzigopofisaria	ilpu	iliac process of pubis processo iliaco del pube
tpolp	intrapostzygopophysal pneumatopore pneumatoporo infrapostzigopofisario	inc	internal condyle condilo interno
tu	tuberculum tubercolo	is	ischium ischio
wenvf	wing-like expansion of the medioventral facet espansione ad ala della facetta medioventrale	isf	ischial foot piede ischiatico
		ismf	ischial medial facet facetta mediale dell'ischio
		isp	ischial peduncle peduncolo ischiatico
		iti	<i>incisura tibialis</i>
		lec	lateral epicondyle epicondilo laterale
		lt	lesser trochanter trocantere minore
I-III	first to third digit dito dal primo al terzo	mc	metacarpal metacarpale
1-4	first to fourth phalanx falangi dalla prima alla quarta	mec	medial epicondyle epicondilo mediale
ac	acromion	mfi	medial fossa of fibula fossa mediale della fibula
actil	acetabular portion of ilium porzione acetabolare dell'ileo		

Appendicular skeleton / Scheletro appendicolare

Le Memorie sono disponibili presso la Segreteria della Società Italiana di Scienze Naturali,
Museo Civico di Storia Naturale, Corso Venezia 55 - 20121 Milano
Pubblicazione disponibile al cambio